PYRIDINE DIAMIDE COMPLEXES OF EARLY TRANSITION METALS: ACTIVATION OF SMALL ORGANIC MOLECULES

by

FRÉDÉRIC GUÉRIN

B.Sc. Université du Québec à Chicoutimi, 1992

M.Sc. The University of Ottawa, 1994

A THESIS SUBMITTED IN PARTIAL FULFILLMENT OF

THE REQUIREMENTS FOR THE DEGREE OF

DOCTOR OF PHILOSOPHY

in

THE FACULTY OF GRADUATE STUDIES

Department of Chemistry

We accept this thesis as conforming to the required standard

THE UNIVERSITY OF BRITISH COLUMBIA

November 1997

In presenting this thesis in partial fulfilment of the requirements for an advanced degree at the University of British Columbia, I agree that the Library shall make it freely available for reference and study. I further agree that permission for extensive copying of this thesis for scholarly purposes may be granted by the head of my department or by his or her representatives. It is understood that copying or publication of this thesis for financial gain shall not be allowed without my written permission.

Department of Chemistry

The University of British Columbia
Vancouver, Canada

Date 15 Jan 98

DE-6 (2/88)

Abstract

Titanium complexes bearing a pyridine-diamide ligand $[2,6\text{-}(RNCH_2)_2NC_5H_3]^{2-}$ (R = 2,6-diisopropylphenyl (BDPP); R = 2,6-dimethylphenyl (BDMP)) have been synthesized. The dichloride complexes $[2,6\text{-}(RNCH_2)_2NC_5H_3]TiCl_2$ are prepared in high yield from $\{2,6\text{-}[(Me_3Si)RNCH_2]_2NC_5H_3\}$ and $TiCl_4$ via the elimination of 2 equiv of $ClSiMe_3$. Monoalkyl and bis(alkyl) complexes are prepared from $[2,6\text{-}(RNCH_2)_2NC_5H_3]TiCl_2$ and various Grignard reagents. Reduction of the dichloride precursors $(BDPP)TiCl_2$ and $(BDMP)TiCl_2$ with excess 1% Na/Hg amalgam in the presence of >2 equiv of internal (PhC≡CPh, EtC≡CEt, PrC≡CPr) or terminal ($HC{\equiv}CSiMe_3$, PhC≡CH) alkynes yields metallacyclopentadiene derivatives in good yield No cyclotrimerization of alkyne is observed. Ligand activation is observed in certain cases for complexes bearing the BDMP ligand.

In a similar way, the reaction of $\{2,6\text{-}[(Me_3Si)RNCH_2]_2NC_5H_3\}$ with $TaCl_5$ yields the complex, *mer*-$(BDPP)TaCl_3$, and two equiv of $ClSiMe_3$. The reduction of the trichloride complex with excess Na/Hg in the presence of alkynes yields the pseudo 5-coordinate Ta(III) derivatives, $(BDPP)Ta(\eta^2\text{-}RC{\equiv}CR')Cl$ (R = R' = Pr, Et, Ph; R = Ph, R' = H). The 4-octyne compound reacts with $LiC{\equiv}CR$ to give the acetylide octyne derivatives $(BDPP)Ta(\eta^2\text{-}PrC{\equiv}CPr)(C{\equiv}CR)$ (R = Ph, Bu, $SiMe_3$, *o*-$Me_3SiC_6H_4$). The phenylacetylide complex reacts with phenylacetylene to give the metallacyclic derivative $(BDPP)Ta[(\eta^2\text{-}PhC{\equiv}C)PrC{=}CPrHC{=}CPh]$. Similarly, $(BDPP)Ta(\eta^2\text{-}PrC{\equiv}CPr)(C{\equiv}CBu)$ and $(BDPP)Ta(\eta^2\text{-}PrC{\equiv}CPr)(C{\equiv}CSiMe_3)$ react with $HC{\equiv}CBu$ and $HC{\equiv}CSiMe_3$ to give the expected metallacycles. $(BDPP)Ta(\eta^2\text{-}PrC{\equiv}CPr)(C{\equiv}CBu)$ reacts with HC≡CPh to give $(BDPP)Ta[(\eta^2\text{-}BuC{\equiv}C)PrC{=}CPrHC{=}CPh]$ only, establishing that the starting acetylide is retained in the final product.

Zirconium complexes bearing a pyridine-diamide ligand $[2,6\text{-}(RNCH_2)_2\text{-}NC_5H_3]^{2-}$ (R = 2,6-diisopropylphenyl (BDPP); R = 2,6-diethylphenyl (BDEP); R = 2,6-dimethylphenyl (BDMP); R = ^{i}Pr (iPAP); R = Cy (CyAP); R = 2,4-dimethyl-3-pentylamine (LiAP); R = ^{t}Bu

(tBAP)) have been synthesized. The mixed amide complexes [2,6-$(RNCH_2)_2$-NC_5H_3]$Zr(NMe_2)_2$ are prepared in high yield from [2,6-$(RHNCH_2)_2$-NC_5H_3] and $Zr(NMe_2)_4$. The mixed amides react with excess $ClSiMe_3$ to afford the dichlorides [2,6-$(RNCH_2)_2$-NC_5H_3]$ZrCl_2$ in nearly quantitative yield. Dimethyl complexes are prepared from [2,6-$(RNCH_2)_2$-NC_5H_3]$ZrCl_2$ and 2 equiv of MeMgBr. The frontier orbitals of a model of the fragment (BDEP)Zr are very similar the those of Cp_2Zr.

A similar protocol has been used to prepare [2,6-$(RNCH_2)_2NC_5H_3$]ZrX_2 (X = NMe_2, Cl, Me; R = 2-PhC_6H_4 (BPhP); 2-$^iPrC_6H_4$ (BMPP); 2-$^tBuC_6H_4$ (BMBP), 2-^{i}Pr-6-MeC_6H_3 (MPPP)). NMR spectroscopy has been used to identify rotameric isomers derived from restricted rotation about the N-C_{ipso} bond of the ligand. The aryl groups in (BPhP)ZrX_2 complexes freely rotate at all temperatures (-80°C to +80°C) while (BMPP)ZrX_2 (X = NMe_2, Cl, Me) derivatives adopt *meso* and *rac* rotamers at low temperatures. In contrast, (BMBP)ZrX_2 and (MPPP)ZrX_2 (X = NMe_2, Cl, Me) compounds are locked at all temperatures. (BMBP)$ZrCl_2$ is isolated as a single isomer, likely the *meso* rotamer, while (MPPP)$ZrCl_2$ is a near statistical mixture of *meso* and *rac* isomers.

Table of Contents

List of Tables

List of Figures

List of Schemes

List of Abbreviations

Å	Angstrom	MO	molecular orbital
Anal. Calcd	analysis calculated	NMR	nuclear magnetic resonance
atm	atmosphere	NOE	nuclear Overhauser effect
br	broad	OEt_2	diethylether
Bu	butyl	Ph	phenyl
COSY	correlated spectroscopy	ppm	parts per million
Cp	cyclopentadiene	Pr	propyl
Cy	cyclohexyl	Py	pyridine
deg	degrees	^{t}Bu	*tert*-butyl
DME	1,2-dimethoxyethane	sbp	square-base pyramid
EI	electron ionization	tbp	trigonal bipyramid
equiv	equivalent(s)	THF	tetrahydrofuran
Et	ethyl		
^{i}Pr	*iso*-propyl		
HETCOR	heteronuclear correlation		
ind	indenyl		
IR	infra-Red		
LLDPE	linear low density polyethylene		
Lut	lutidine		
M	molar		
MAO	methylaluminoxane		
Me	methyl		
mL	millilitre		
mmol	millimole		

Acknowledgements

I would like to thank Prof. David H. McConville for his support and enthusiasm over the last four years. Thank you for keeping me "on track".

I would also like to thank past and present group members.

I would like to thank J. J. Vittal, N.C. Payne, G. P. Yap. and D. Stephan for solving the crystal structures presented in this manuscript.

I also want to thank the support staff at UWO (Bruce Artwood and the mech shop guys) and UBC (Steve Rak, Peter Borda, mass spectrometry, electronic and mech shop staff).

Finally, I would like to thank NSERC, Union Carbide Canada Inc., the University of Western Ontario and the University of British Columbia for their financial support.

"... I find that a great part of the information I have was acquired by looking up something and finding something else on the way... "
Franklin P. Adams

Introduction

1 Generalities

In 1951 a compound of formula $(C_5H_5)_2Fe$ was reported and was subsequently shown to have a unique "sandwich" structure in which the metal lies between two planar cyclopentadienyl rings. As a result of the η^5 coordination, a cyclopentadienyl ligand acts like a 6-electron donor. The stabilizing effects of the two cyclopentadienyl ligands were rapidly realized. The organometallic chemistry of the transition metals has since been dominated by complexes bearing cyclopentadienyl ligands[1].

Cyclopentadienyl based complexes such as Cp_2TiPh_2, Cp_2ZrPh_2 or Cp_2ZrCl_2[2] have been used as homogeneous models for Ziegler-Natta olefin polymerization. It is believed that a cationic alkyl in the +4 oxidation state is the active catalytic species (Figure 1). These systems are very efficient catalysts for the polymerization of ethylene but do not polymerize α-olefins very efficiently.

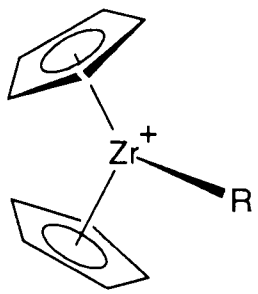

Figure 1. Cationic Cp_2MR^+

The investigation of simple metallocene systems gave way to ingeniously designed bridged-metallocene complexes: for example, Figure 2a, *rac*-ethylenebis(η^5-tetrahydroindenyl)$ZrCl_2$[3]; Figure 2b, *rac*-dimethylsilylbis(η^5-indenyl)$ZrMe_2$[4]; and Figure 2c, isopropyl(η^5-Cp-1-η^5-fluorenyl)$ZrCl_2$[5]. Linking the two Cp ligands together results in a more

References start on page 18

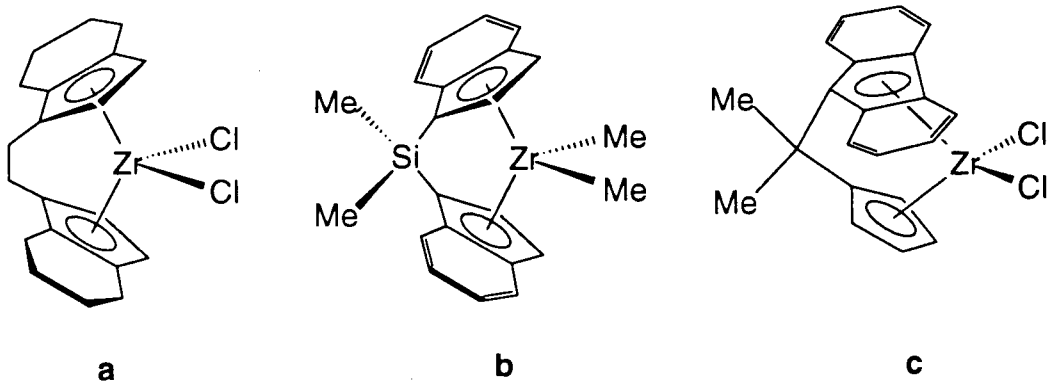

Figure 2. Some bridged metallocene catalysts

open metal centre and as a result these catalysts polymerize α-olefins better than unbridged species.

Amide ligands, like alkoxide ligands, are generally viewed as hard donors. This is an important difference when compared to a soft cyclopentadienyl donor. Moreover, amide ligands are formally 4 electron ligands, two less than a Cp group. These ligands can be viewed as electron deficient cyclopentadienyl equivalents. As a result, a transition metal surrounded by amide ligands is more electrophilic than when it is bound to an equal number of cyclopentadienyl ligands.

In an attempt to create more electrophilic species, complexes where one of the cyclopentadienyl has been replaced were synthesized. Complexes that contain a linked cyclopentadienyl-amide ligand (e.g., η^5-$C_5Me_4SiMe_2(NCMe_3)ML_n$, M = Ti, Zr, Hf[6-8] or Sc[9]; L halide or alkyl) (Figure 3) were synthesized and used for the copolymerization of ethylene and α-olefins (eq. 1).

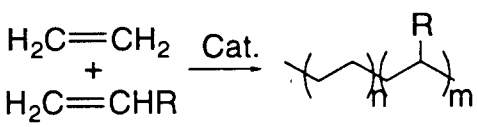

(1)

References start on page 18

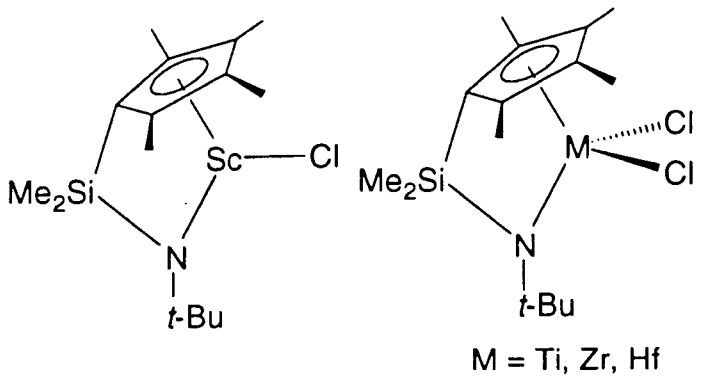

Figure 3. Linked Cp-amide complexes

Unlike the metallocene-based catalysts, which do not incorporate α-olefins very well, these complexes are very efficient at incorporating α-olefins in the polymer chain. This is probably a result of the reduced steric crowding around the active catalytic centre and the increased electrophilicity of the metal.

The next logical extension would be to replace both Cp ligands with amides or alkoxides. Recently, complexes that contain a chelating diamide[10] {Figure 4(I)} or bis(alkoxide)[11] {Figure 4(II)} functionality have been reported.

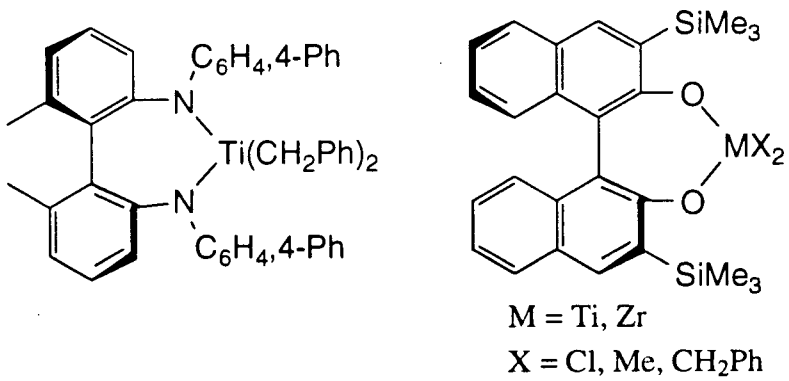

Figure 4. Linked bis(amide) and bis(alkoxide) complexes

References start on page 18

2 Historical Background

A metal amide is defined as a compound which contains one or more M–NR_2 (R = H, alkyl, aryl, e.g., ^-NHMe, $^-NMe_2$, $^-NPh_2$ or $^-N(SiMe_3)_2$) moieties. These are generally molecular compounds having the general structural unit shown in Figure 5.

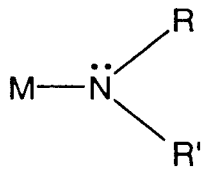

Figure 5. Structural unit

However, some larger aggregates have been observed for small metals such as lithium. The first metal amide, zinc-bis(dimethylamide), was prepared in 1856 by Frankland[12]. The first transition metal dialkylamide complex was reported by Dermer and Fernelius[13] in 1935. They showed that the metathesis reaction of an excess of potassium diphenylamide and titanium tetrachloride formed tetrakis(diphenylamido)titanium. In 1959, Bradley and Thomas[14] explored the use of lithium dialkylamides as reagents for the synthesis of early transition metal amides. Amide complexes for almost all the elements have since been synthesized. They are very common for early transition metals, however, they are rare for the later metals. Amide ligands can be found in homoleptic, i.e., $M(NRR')_n$, or heteroleptic complexes, i.e., Me_3SnNMe_2 or $Cp_2Ti(NMe_2)_2$.

Finally, is its important to note that transition–metal amide complexes also have an important role in biological systems. Naturally occurring molecules such as chlorophyll (Figure 6) and vitamin B_{12} coenzyme (Cobalt based) contain M–N fragments.

References start on page 18

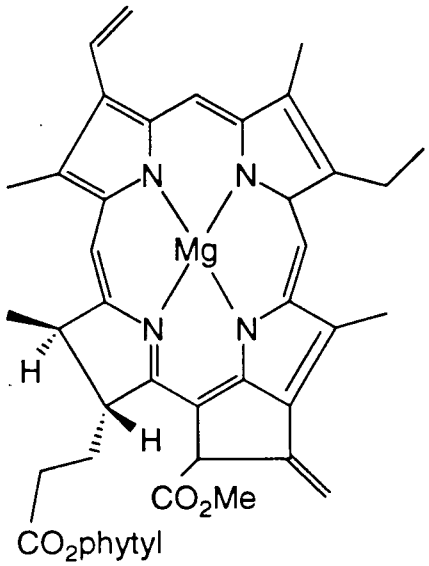

Figure 6. Structure of Chlorophyll

3 Synthesis

3.1 Transmetallation

The most common route to transition metal amide is via transmetallation (e.g., eq. 2).

$$MCl_n + n\,LiNR_2 \longrightarrow M(NR_2)_n + n\,LiCl \qquad (2)$$

This synthetic procedure has since been employed to prepare a wide variety of transition metal amide complexes. This methodology generally affords the homoleptic amide complex in the same oxidation state as the starting material. However, in some cases steric effects or disproportionation of the first formed homoleptic amide yields unexpected products (examples are in eq. 3[15], eq. 4[16,17] and eq. 5[17]).

$$MoCl_5 + 5\,LiNMe_2 \longrightarrow Mo(NMe_2)_4 + LiCl + \text{other products} \qquad (3)$$

$$TaCl_5 + 5\,LiNMe_2 \longrightarrow Ta(NMe_2)_5 \qquad (4)$$

References start on page 18

$$TaCl_5 + 5\,LiNEt_2 \longrightarrow Ta(NEt_2)_3(NEt) \qquad (5)$$

3.2 Elimination of amine hydrohalide

The elimination of $[NR_3H]^+Cl^-$ has been used for many years as a synthetic approach to metal amide complexes (eq. 6). This methodology has been employed with the higher oxidation states of the early transition metals (for examples: Ti^{IV} 18,19, V^{IV} 20, Nb^{V} 21, Ta^{V} 22, W^{IV} 23, W^{V} 23, W^{VI} 23-25).

$$TiCl_4 + 8\,HNMe_2 \longrightarrow Ti(NMe_2)_4 + 4\,[Me_2NH_2]^+Cl^- \qquad (6)$$

The main drawback with this method is the possible formation of a donor complex, for example, $MoCl_3(NHMe_2)(NMe_2)_2$[26]. The use of sterically demanding groups on the nitrogen can prevent coordination of the amine donor.

3.3 Elimination of alkane

The elimination of a simple alkane can also be used as a synthetic approach to metal-amide bonds. This route was used by Frankland to synthesis the first metal-amide, $Zn(NR_2)_2$[12](eq. 7).

$$ZnEt_2 + 2\,HNR_2 \longrightarrow Zn(NR_2)_2 + 2\,C_2H_6 \qquad (7)$$

This technique has one major advantage over the elimination of hydrohalide approach. There is no formation of amine which could potentially remain coordinated to the metal centre. Nevertheless, this method has not been widely employed due to the lack of stable metal alkyl complexes.

3.4 Transamination

Transamination reactions are strongly dependent on steric factors. The steric requirements of the substituents on the incoming amine dictate the degree of substitution that is obtained as illustrated in Scheme 1[27].

References start on page 18

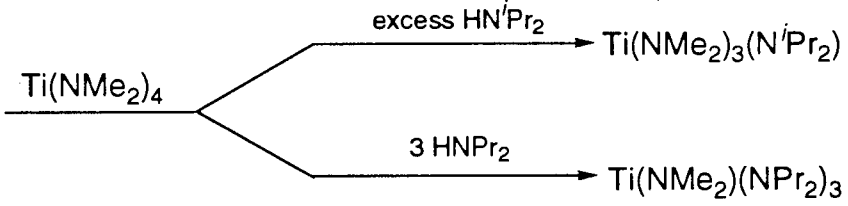

Scheme 1. Steric effect on transamination reactions

The more volatile amine is generally displaced. This procedure is particularly appealing if the eliminated amine is $HNMe_2$. In this case, the desired complex is the only non-gaseous product.

4 Characterization

4.1 Nuclear Magnetic Resonance Spectroscopy

^1H and ^{13}C NMR spectroscopy have been used extensively to determine the presence and nature of transition metal amide complexes. The methyl groups in dimethylamine are observed at 2.18 ppm in the ^1H NMR (δ, in C_6D_6). A shift to lower field strength is observed when the amide group is bound to a transition–metal. For example, the ^1H NMR spectra of $Ti(NMe_2)_4$[28-31] and $Zr(NMe_2)_4$[14,29,30,32] show resonances at 3.04 ppm and 2.90 ppm (δ, in C_6D_6), respectively. Heteroleptic complexes also exhibit a similar chemical shift variation by ^1H NMR spectroscopy. For example, $Ti(NMe_2)_2Cl_2$[33,34] displays a signal at 3.14 ppm (δ, in C_6D_6). A downfield shift of the methyl carbons is also observed by $^{13}C\{^1H\}$ NMR spectroscopy.

Another important use of ^1H NMR spectroscopy is in the elucidation of fluxional processes. Through variable temperature experiments, it is possible to observe the different species in equilibrium. One such example is the Ti^{III} dimeric complex $[Ti(NMe_2)_3]_2$[35]. The ^1H NMR spectrum in D_8-toluene shows a sharp singlet at room temperature. However, at -80°C, two distinct resonances 2.2 Hz apart are observed in approximately a 2:1 ratio. This is consistent

References start on page 18

with a dimeric structure at low temperature (Figure 7). There are four distinct terminal NMe_2 groups and two bridging moieties. At higher temperature, interconversion between the different sites is fast and a time averaged spectrum is obtained.

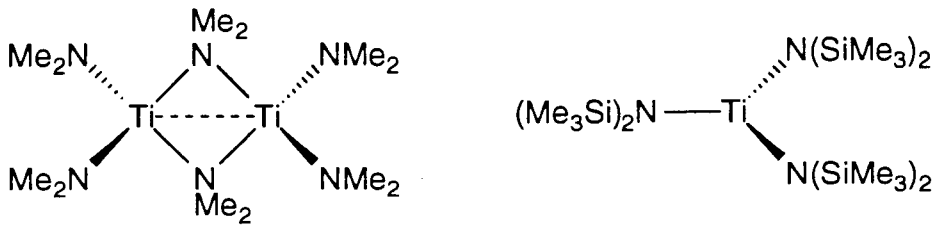

Figure 7. Dimeric $[Ti(NMe_2)_3]_2$ vs monomeric $Ti[N(SiMe_3)_2]_3$

^{14}N (I = 1) NMR has not yet been used to any significant extent for the identification of metal amide complexes. This is in part due to the quadrupolar moment of ^{14}N. ^{15}N (I = 1/2) has proven quite useful in determinig the diference between NH, NH_2 and N functionalities[93-95].

5 Bonding Considerations

There are three possible metal-nitrogen interactions for an amido ligand. The first case involves only a σ-bond between the metal and nitrogen. It this case the nitrogen has a pyramidal geometry and approximately sp^3 hybridization (Figure 8 I). Figure 8 II illustrates π-bonding between the nitrogen atom and the metal centre.

It is useful to compare the bonding interaction of a metal amide versus a metal alkyl. First, a σ bond is formed by the overlap of the nitrogen sp^2 orbital (or sp^3 orbital in the case of a pyramidal nitrogen) with a suitable σ-type orbital on the metal. Second, the lone pair of electrons on nitrogen can overlap with a suitable π-type metal orbital rendering the amide a four-electron donor (Figure 8 II). On the other hand, alkyl ligands can only donate two electrons.

References start on page 18

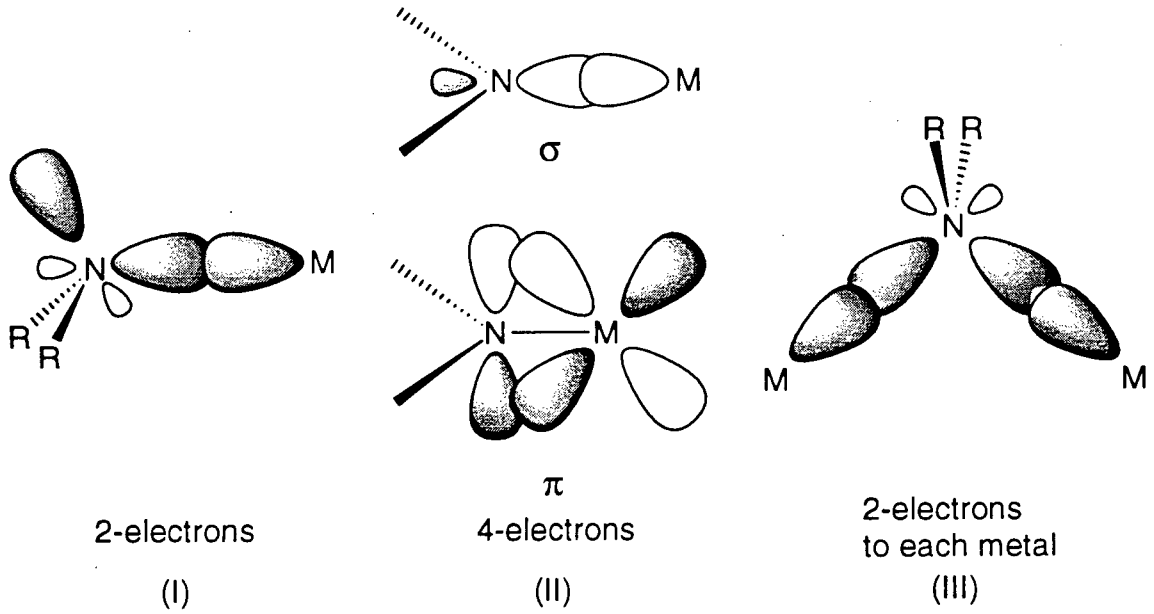

Figure 8. Metal-amide orbital interactions

In the third type of interaction, the amide ligand behaves as a bridging moiety (Figure 8 III). It is generally possible to preclude such bonding by employing bulky substituents on nitrogen. For example, $Ti(NMe_2)_3$ is dimeric and its structure (Figure 7) shows two bridging and four terminal amide ligands[35,36]. On the other hand, $Ti[N(SiMe_3)_2]_3$ has a monomeric structure[37].

In some cases orbital availability may prevent metal-amide multiple bonding. For example, in the compound $\{(R_3SiNCH_2CH_2)_3N\}ML$[38,39]; R = Me, Ph, Cy, *t*-Bu; M = Ta, V (Figure 9), the geometry of the complex does not allow simultaneous π bonding between the three amide nitrogens and the metal. The result is a ligand centred non-bonding pair of electrons. This type of bonding can be viewed as a hybrid of the first two bonding possibilities.

References start on page 18

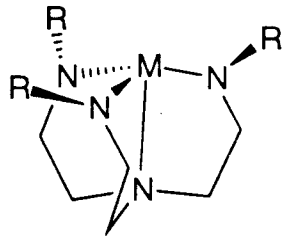

Figure 9. N_3N ligand

Consequently, the ligand can only be considered as a 12-electron donor and not 14 (three M–N double bonds {4 electrons each} and a M–N single bond {2 electrons}) as one might expect.

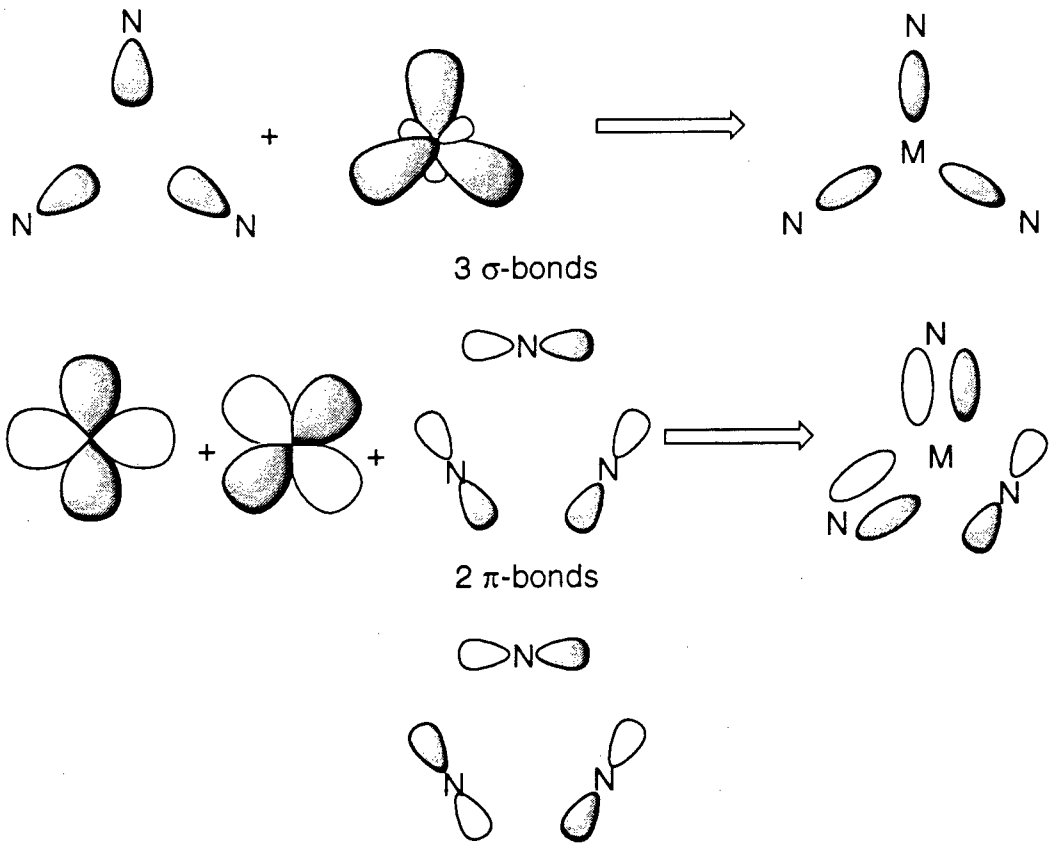

Figure 10. Bonding of the N_3N ligand

References start on page 18

5.1 X-ray crystallography

The increased availability and reduced cost of single crystal X-ray diffraction analysis have made this an invaluable tool in the characterization of transition–metal complexes. This technique has allowed accurate measurement of the metal-nitrogen bond distances in many complexes (Table 1). Some arguments relating the degree of N->M π-bonding to the bond distance have been proposed.

Table 1. Metal-nitrogen bond distances in selected complexes

Compounds	M–N(amide) (Angstrom)	Reference
$Cr[N(SiMe_3)_2]_3(NO)$	1.790	40
$TiCl_3(NEt_2)$	1.852	41
$Ni[N(SiMe_3)_2](PPh_3)_2$	1.870	42
$TiCl_2[N(SiMe_3)_2]$	1.89	43
$Fe[N(SiMe_3)_2]_3$	1.918	44
$Co[N(SiMe_3)_2](PPh_3)_2$	1.924	42
$W_2(NMe_2)_6$	1.97	45
$Mo_2(NMe_2)_6$	1.98	46
$Sc[N(SiMe_3)_2]_3$	2.049	47
$Eu[N(SiMe_3)_2]_3$	2.259	47
$Co[N(SiMe_3)_2]_2(PPh_3)$	1.934 and 1.917	42

6 Chemical Properties of a M–N Bond

The reactivity of a transition metal amide bond generally depends on its polarity and bond strength. The chemistry of metal amides can be compared with the isoelectronic alkyls, alkoxides and fluorides. They have much more in common with alkyls and alkoxides than fluorides. Bond

References start on page 18

polarities ($M^{\delta+}$-$X^{\delta-}$) and bond strengths increase in the sequence M–R < M–NRR' < M–OR < M–F. This follows the same trend as the electronegativity, C < N < O < F.

6.1 Insertion reactions

Insertion reactions are one of the most common organometallic reactions. Two conditions must be met in order for an insertion to take place. The reagent must be susceptible to attack by a nucleophile and the M–NR_2 bond must be polarized. The proposed concerted mechanism for this reaction is shown in Scheme 2.

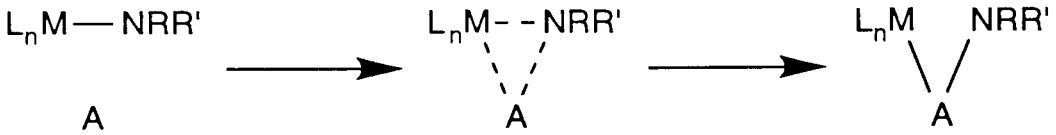

Scheme 2. Mechanism of Insertion

6.1.1 Insertion reactions of an alkene or alkyne

As a result of the lack of polarity in the C-C multiple bond, simple internal olefins or alkynes do not react with a metal amide. However, strongly electron withdrawing groups facilitate the insertion. For example, $Ti(NMe_2)_4$ and $Zr(NMe_2)_4$ both react with MeOOCC≡CCOOMe[48] to form $Ti[C(CONMe_2)=C(COOMe)NMe_2](NMe_2)_2OMe$ and $Zr[C(CONMe_2)=C(COOMe)NMe_2]_2(OMe)_2$, respectively.

6.1.2 Insertion of RNCX (X = O, S, NR)

These insertion reactions of RNCX (X = O, S, NR) are normally carried out at room temperature. The yields are generally quantitative; for example, $Ti(NMe_2)_4$ reacts with PhNCO to form 1:2 (Figure 11I) or 1:4 (Figure 11II) complexes depending on the stoichiometry[48]. On the other hand, the zirconium and hafnium derivatives only afford the 1:4 complexes. The driving force for these reactions is provided by the strong metal-oxygen bond.

References start on page 18

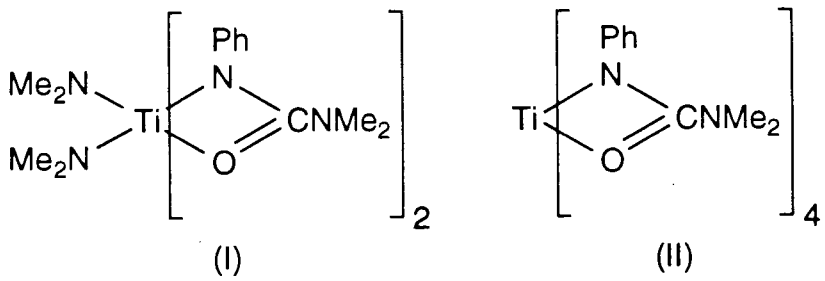

(I) (II)

Figure 11. Insertion products from PhNCO and $Ti(NMe_2)_4$

6.1.3 Insertion of CO_2, CS_2 and SO_2

The insertion of CO_2 or CS_2 into a L_nM–NRR' bond generally yields the corresponding carbamate L_nM–OCONRR' (e.g., eq. 8[28]) or sulfamate L_nM–SCSNRR' (e.g., eq. 9[35,49]). However, in some cases, a change in the oxidation state of the metal together with redistribution of the ligands affords unexpected products (e.g., eq. 10[35,49]).

$$Ti(NMe_2)_4 + CO_2 \longrightarrow Ti(OCONMe_2)_4 \qquad (8)$$

$$Ti(NMe_2)_4 + CS_2 \longrightarrow Ti(SCSNMe_2)_4 \qquad (9)$$

$$\underset{(Ti^{III})}{\{Ti(NMe_2)_3\}_2} + CS_2 \longrightarrow \underset{(Ti^{IV})}{Ti(SCSNMe_2)_4} \qquad (10)$$

The reaction between a metal amide and SO_2 rarely affords the expected product. In most cases, the loss of thionyl or sulfuryl amide results in the formation of compounds having a M=O or M–O–M bonds (eq. 11[50,51]). This is undoubtedly the result of the high thermodynamic stability of a metal-oxygen bond and the relatively weak S–O bond.

$$Ti(NMe_2)_2 + SO_2 \longrightarrow Ti(O)(OSONMe_2)_2 + OS(NMe_2)_2 \qquad (11)$$

6.2 Reactions with protic compounds (protonolysis)

The high susceptibility of transition metal amides to protic reagents has allowed the use of amide ligands as protecting groups for the synthesis of more complex molecules (eq. 12). The transamination reaction described earlier is considered a protonolysis reaction.

References start on page 18

$$L_nM\text{–}NR_2 \;+\; HA \longrightarrow L_nM\text{–}A \;+\; HNR_2 \qquad (12)$$

It this type of reaction, the metal amide, M–NR_2, behaves as a base. The steric congestion around the nitrogen is of great importance in this type of reaction. The availability of a suitable orbital on the metal is also an important factor. A good example of the steric effect on the protonolysis of a metal amide bond is given with $W(NMe_2)_6$. The ease of alcoholysis follows the sequence MeOH > EtOH > PrOH > ^{t}BuOH, Me_3CCH_2OH, while Et_3SiOH does not react at room temperature[52].

A wide variety of protic sources can be used: inorganic and organic acids, alcohols, terminal alkynes (eq. 13)[53] or even cyclopentadiene (eq. 14)[54].

$$Zr(\eta\text{-}C_5H_5)_2(NMe_2)_2 \xrightarrow[-\,2\,HNMe_2]{+2\,HC\equiv CPh} Zr(\eta\text{-}C_5H_5)_2(C\equiv CPh)_2 \qquad (13)$$

$$Ti(NR_2)_4 \;+\; C_5H_6 \longrightarrow Ti(\eta\text{-}C_5H_5)(NR_2)_3 \;+\; HNR_2 \qquad (14)$$

6.3 Miscellaneous reactions

6.3.1 Disproportionation reactions

The disproportionation of a metal amide involves a change in the formal oxidation state at the metal centre. It is a bimolecular internal redox reaction in which two products, oxidized and reduced derivatives of the original complex, are formed. The reaction generally occurs upon heating of a lower oxidation state metal amide. This type of reaction is common for early transition elements (eq. 16[35], eq. 16[28] and eq. 17[55]).

$$\{Ti(NMe_2)_2X\}_2 \longrightarrow Ti(NMe_2)_4 \;+\; 1/n\,\{TiX_2\}_n \qquad (15)$$

$$X = NMe_2,\ NEt_2,\ N^iPr_2 \text{ or } Cl$$

$$VCl_3 \xrightarrow{3\,LiNEt_2} \left[\, V(NEt_2)_3 \,\right] \longrightarrow V(NEt_2)_4 + 1/n\,\{V(NEt_2)_2\}_n \qquad (16)$$

References start on page 18

$$CrCl_3 \xrightarrow{3\ LiNEt_2} \left[Cr(NEt_2)_3 \right] \longrightarrow Cr(NEt_2)_4 + 1/n\ \{Cr(NEt_2)_2\}_n \qquad (17)$$

6.3.2 Elimination reactions

This type of reaction involves the elimination of a small stable molecule to afford a compound which may either contain a multiple M=N bond or the product of its oligomerization. The driving force for these reactions includes the facile removal of an amine or a trimethylhalogenosilane and the high standard free energies of the products.

The elimination of trimethylchlorosilane has been reported for some transition metal complexes (eq. 18)[56,57].

$$TiCl_4 + N(SiMe_3)_3 \longrightarrow TiCl_3\{N(SiMe_3)_2\} + ClSiMe_3$$
$$\downarrow \qquad (18)$$
$$1/n\{TiCl_2N(SiMe_3)\}_n + ClSiMe_3$$

7 Project Proposal

The bent metallocene fragment is one of the most intensely studied moieties in early-transition-metal chemistry. As a result, complexes that contain one or even no cyclopentadienyl groups have received increasing attention. Polyfunctional amide[38,58-70] and alkoxide[71-79] ligands have been studied in this context. These ligands can be viewed as electron deficient cyclopentadienyl equivalents.

It was demonstrated that enhanced kinetic protection of the metal centre can be obtained by linking the amide donors[80-83]. Moreover, the introduction of a donor functionality in the ligand can be used to modify the electronic properties of the metal centre and to provide rigidity to the ligand framework[84-87]. For example, the amide donors can be incorporated into a pyridine

References start on page 18

backbone that significantly reduces the flexibility of the ligand, enforcing a meridional coordination (Figure 12)[88].

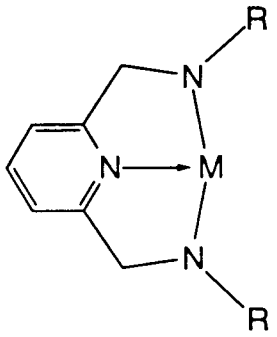

Figure 12. Pyridine diamide ligand

With this in mind, we decided to vary the size of the R–groups attached to nitrogen, thus altering the steric environment about the metal.

The synthesis and characterization of some early transition metal complexes of this pyridine diamide ligand are described in the proceeding chapters[89-92].

References start on page 18

8 References

(1) Bochmann, M., *Comprehensive Organometallic Chemistry II*; Bochmann, M., Ed.; Elsevier Science Ltd.: New York, 1995; Vol. 4.

(2) Ewen, J. A. *J. Am. Chem. Soc.* **1984**, *106*, 6355.

(3) Kaminsky, W.; Kulper, K.; Brintzinger, H. H.; Wild, F. R. W. P. *Angew. Chem., Int. Ed. Engl.* **1985**, *24*, 507.

(4) Bochmann, A.; Lancaster, S. J. *Angew. Chem., Int. Ed. Engl.* **1994**, *33*, 1634.

(5) Ewan, J. A.; Jones, R. L.; Razavi, A. *J. Am. Chem. Soc.* **1988**, *110*, 6255.

(6) Canich, J. A. ; Canich, J. A., Ed., European Patent Application EP-420-436-A1; Vol. April 4, 1991.

(7) Canich, J. A.; Turner, H. W. ; Canich, J. A.; Turner, H. W., Ed., W. PCT Int. Appl. WO 92/12162; Vol. filing date December 26, 1991.

(8) Stevens, J. C.; Timmers, F. J.; Wilson, D. R.; Schmidt, G. F.; Nickias, P. N.; Rosen, R. K.; Knight, G. W.; Lai, S. Y. ; Stevens, J. C.; Timmers, F. J.; Wilson, D. R.; Schmidt, G. F.; Nickias, P. N.; Rosen, R. K.; Knight, G. W.; Lai, S. Y., Ed., European Patent Application EP-416-815-A2; Vol. March 13, 1991.

(9) Shapiro, P. J.; Bunel, E.; Schaefer, W. P.; Bercaw, J. E. *Organometallics* **1990**, *9*, 867.

(10) Cloke, F. G. N.; Geldbach, T. J.; Hitchcock, P. B.; Love, J. B. *J. Organomet. Chem.* **1996**, *506*, 343.

(11) van der Linden, A.; Schaverien, C. J.; Meijboom, N.; Ganter, C.; Orpen, A. G. *J. Am. Chem. Soc.* **1995**, *117*, 3008.

(12) Frankland, E. *Proc. Roy. Soc.* **1856-7**, *8*, 502.

(13) Dermer, D. C.; Fernelius, W. C. *Z. Anorg. Chem.* **1935**, *221*, 83.

References start on page 18

(14) Bradley, D. C.; Thomas, I. M. *Chemical Society London. Proceedings* **1959**, 225.

(15) Bradley, D. C.; Chisholm, M. H. *J. Chem. Soc. (A)* **1971**, 2741.

(16) Burger, H. *Monatsh.* **1964**, *95*, 671.

(17) Bradley, D. C.; Gitlitz, M. H. *J. Chem. Soc. (A)* **1969**, 1894.

(18) Drake, J. E.; Fowles, G. W. A. *J. Chem. Soc.* **1960**, 1498.

(19) Cowdell, R. T.; Fowles, G. W. A. *J. Chem. Soc.* **1960**, 2522.

(20) Fowles, G. W. A.; Pleass, C. M. *J. Chem. Soc.* **1957**, 1674.

(21) Fowles, G. W. A.; Pleass, C. M. *J. Chem. Soc.* **1957**, 2078.

(22) Fuggle, J. C.; Sharp, D. W. A.; Winfield, J. M. *J. Chem. Soc., Dalton Trans.* **1972**, 1766.

(23) Brisdon, B. J.; Fowles, G. W. A.; Osborne, B. P. *J. Chem. Soc.* **1962**, 1330.

(24) Majid, A.; McLean, R. R.; Sharp, D. W. A.; Winfield, J. M. *Z. Anorg. Chem.* **1971**, *385*, 65.

(25) Majid, A.; Sharp, D. W. A.; Winfield, J. M.; Hanby, I. *J. Chem. Soc., Dalton Trans.* **1973**, 1876.

(26) Edwards, D. A.; Fowles, G. W. A. *J. Chem. Soc.* **1961**, 24.

(27) Bradley, D. C.; Thomas, I. M. *J. Chem. Soc.* **1960**, 3857.

(28) Alyea, E. C.; Bradley, D. C.; Lappert, M. F.; Sanger, A. R. *J. Chem. Soc., Chem. Commun.* **1969**, 1064.

(29) Bradley, D. C.; Gitlitz, M. H. *J. Chem. Soc. (A)* **1969**, 980.

(30) Gibbins, S. G.; Lappert, M. F.; Pedley, J. B.; Sharp, G. J. *J. Chem. Soc., Dalton Trans.* **1975**, 72.

(31) Bürger, H.; Kluess, C.; Neese, H.-J. *Z. Anorg. Chem.* **1971**, *381*, 198.

References start on page 18

(32) Bradley, D. C.; Thomas, I. M. *J. Chem. Soc.* **1960**, 3857.

(33) Bürger, H.; Neese, H.-J. *Z. Anorg. Chem.* **1969**, *365*, 243.

(34) Benzing, E. P.; Kornicker, W. A. *Chem. Ber.* **1961**, *94*, 2263.

(35) Lappert, M. F.; Sanger, A. R. *J. Chem. Soc. (A)* **1971**, 874.

(36) Alyea, E. C.; Bradley, D. C.; Copperthwaite, R. G. *J. Chem. Soc., Dalton Trans.* **1972**, 1580.

(37) Bradley, D. C.; Copperthwaite, R. G. *J. Chem. Soc., Chem. Commun.* **1971**, 764.

(38) Cummins, C. C.; Schrock, R. R.; Davis, W. M. *Organometallics* **1992**, *11*, 1452.

(39) Cummins, C. C.; Lee, J.; Schrock, R. R. *Angew. Chem., Int. Ed. Engl.* **1992**, *31*, 1501.

(40) Bradley, D. C.; Hursthouse, M. B.; Newing, C. W.; Welch, A. J. *J. Chem. Soc., Chem. Commun.* **1972**, 567.

(41) Fayos, J.; Mootz, D. *Z. Anorg. Chem.* **1971**, *380*, 196.

(42) Bradley, D. C.; Hursthouse, M. B.; Smallwood, R. J.; Welch, A. J. *J. Chem. Soc., Chem. Commun.* **1972**, 872.

(43) Alcock, N. M.; Pierce-Butler, M.; Willey, G. R. *J. Chem. Soc., Chem. Commun.* **1974**, 627.

(44) Bradley, D. C.; Hursthouse, M. B.; Rodesiler, P. F. *J. Chem. Soc., Chem. Commun.* **1969**, 14.

(45) Chisholm, M. H.; Exxtine, M. W.; Cotton, F. A.; Stults, B. R. *J. Am. Chem. Soc.* **1976**, *98*, 4477.

(46) Chisholm, M. H.; Cotton, F. A.; Frenz, B. A.; Shive, L. *J. Chem. Soc., Chem. Commun.* **1974**, 480.

(47) Bradley, D. C.; Ghotra, J. S.; Hart, F. A. *J. Chem. Soc., Dalton Trans.* **1973**, 1021.

References start on page 18

(48) Chandra, G.; Jenkins, A. D.; Lappert, M. F.; Sricastava, R. C. *J. Chem. Soc. (A)* **1970**, 2550.

(49) Lappert, M. F.; Sanger, A. R. *J. Chem. Soc. (A)* **1971**, 1314.

(50) Nöth, H.; Schweizer, P. *Chem. Ber.* **1964**, *97*, 1464.

(51) Chandra, G.; George, T. A.; Lappert, M. F. *J. Chem. Soc. (A)* **1969**, 2565.

(52) Bradley, D. C.; Chisholm, M. H.; Extine, M. W.; Stager, M. E. *Inorg. Chem.* **1977**, *16*, 1794.

(53) Jenkins, A. D.; Lappert, M. F.; Srivastava, R. C. *J. Organomet. Chem.* **1970**, *23*, 165.

(54) Anderson, H. H. *J. Am. Chem. Soc.* **1953**, *75*, 1576.

(55) Basi, J. S.; Bradley, D. C.; Chisholm, M. H. *J. Chem. Soc. (A)* **1971**, 1433.

(56) Alcock, N. W.; Pierce-Butler, M.; Willey, G. R. *J. Chem. Soc., Dalton Trans.* **1976**, 707.

(57) Akiyama, M.; Chisholm, M. H.; Cotton, F. A.; Extine, M. W.; Murillo, C. A. *Inorg. Chem.* **1977**, *16*, 2407.

(58) Aoyagi, K.; Gantzel, P. K.; Kalai, K.; Tilley, T. D. *Organometallics* **1996**, *15*, 923.

(59) Berno, P.; Minhas, R.; Hao, S.; Gambarotta, S. *Organometallics* **1994**, *13*, 1052.

(60) Cai, S.; Schrock, R. R. *Inorg. Chem.* **1991**, *30*, 4106.

(61) Warren, T. H.; Schrock, R. R.; Davis, W. M. *Organometallics* **1996**, *15*, 562.

(62) tom Dieck, H.; Rieger, H. J.; Fendesak, G. *Inorg. Chim. Acta* **1990**, *177*, 191.

(63) Planalp, R. P.; Andersen, R. A.; Zalkin, A. *Organometallics* **1983**, *2*, 16.

(64) Okuda, J. *Chem. Ber.* **1990**, *123*, 1649.

(65) Dick, D. G.; Duchateau, R.; Edema, J. J. H.; Gamborotta, S. *Inorg. Chem.* **1993**, *32*, 1959.

References start on page 18

(66) Bürger, H.; Betersdorf, D. *Z. Anorg. Allg. Chem.* **1979**, *459*, 111.

(67) Bradley, D. C.; Chudzynska, H.; Backer-Dirks, J. D. J.; Hursthouse, M. B.; Ibrahim, A. A.; Motevalli, M.; Sullivan, A. C. *Polyhedron* **1990**, *9*, 1423.

(68) Bradley, D. C. *Inorg. Syn.* **1978**, *18*, 112.

(69) Tsuie, B.; Swenson, D. C.; Jordan, R. F. *Organometallics* **1997**, *16*, 1392.

(70) Male, N. A. H.; Thornton-Pett, M.; Bochmann, M. *J. Chem. Soc., Dalton Trans.* **1997**, 2487.

(71) Jones, R. A.; Hefner, J. G.; Wright, T. C. *Polyhedron* **1984**, *3*, 1124.

(72) Balaich, G. L.; Hill, J. E.; Waratuke, S. A.; Fanwick, P. E.; Rothwell, I. P. *Organometallics* **1995**, *14*, 656 and references therein.

(73) Lubben, T. V.; Wolczanski, P. T.; Van Duyne, G. D. *Organometallics* **1984**, *3*, 977.

(74) Duff, A. W.; Kamarudin, R. A.; Lappert, M. F.; Norton, R. J. *J. Chem. Soc., Dalton Trans.* **1986**, 489.

(75) Floriani, C.; Corazza, F.; Lesueur, W.; Chiesi-Villa, A.; Guestini, C. *Angew. Chem., Int. Ed. Engl.* **1989**, *28*, 66.

(76) Durfee, L. D.; Hill, J. E.; Fanwick, P. E.; Rothwell, I. P. *Organometallics* **1990**, *9*, 75.

(77) Berg, J. M.; Clark, D. L.; Huffman, J. C.; Morris, D. E.; Sattelberger, A. P.; Streib, W. E.; Van Der Sluys, W. G.; Watkin, J. G. *J. Am. Chem. Soc.* **1992**, *114*, 10811.

(78) McLain, S. J.; Ford, T. M.; Drysdale, N. E. **1992**, 463-464.

(79) McLain, S. J.; Drysdale, N. E. *Polymer Preprints* **1992**, *33*, 463.

(80) Brauer, D. J.; Bürger, H.; Weigel, K. *J. Organomet. Chem.* **1978**, *150*, 215.

(81) Bürger, H.; Dämmgen, U. *Z. Anorg. Chem.* **1977**, *429*, 173.

References start on page 18

(82) Bürger, H.; Weigel, K. *J. Organomet. Chem.* **1977**, *124*, 279.

(83) Bradley, D. C.; Torrible, E. G. *Can. J. Chem.* **1962**, *41*, 134.

(84) Fuhrmann, H.; Bernner, S.; Arndt, P.; Kempe, R. *Inorg. Chem.* **1996**, *35*, 6742.

(85) Friedrich, S.; Gade, L. H.; Edwards, A. J.; McPartlin, M. *J. Chem. Soc., Dalton Trans.* **1993**, 2861.

(86) Schubart, M.; O'Dwyer, L.; Gade, L. H.; Li, W.-S.; McPartlin, M. *Inorg. Chem.* **1994**, *33*, 3893.

(87) Baumann, R.; Davis, W. M.; Schrock, R. R. *J. Am. Chem. Soc.* **1997**, *119*, 3830.

(88) Cai, S.; Schrock, R. R. *Inorg. Chem.* **1991**, *30*, 4105.

(89) Guérin, F.; McConville, D. H.; Vittal, J. *Organometallics* **1995**, *14*, 3154.

(90) Guérin, F.; McConville, D. H.; Vittal, J. J. *Organometallics* **1996**, *15*, 5586.

(91) Guérin, F.; McConville, D. H.; Payne, N. C. *Organometallics* **1996**, *15*, 5085.

(92) Guérin, F.; McConville, D. H.; Vittal, J. J.; Yap, G. P. *Organometallics* **1997**, Submited for publication.

(93) Banaszak Holl, M. M.; Wolczanski, P. T. *J. Am. Chem. Soc.* **1990**, *112*, 7989.

(94) Banaszak Holl, M. M.; Wolczanski, P. T. *J. Am. Cham. Soc.* **1992**, *114*, 3854.

(95) Banaszak Holl, M. M.; Wolczanski, P. T.; Proserpio, D.; Bielecki, A.; Zax, D. B. *Chem. Mater.*, **1996**, *8*, 2468.

References start on page 18

"... As a general rule, the shorter the interval that separates us from our planned objective the longer it seems to us, because we apply to it a more minute scale of measurement, or simply because it occurs to us to measure it..."

Marcel Proust

Chapter One. Titanium Complexes

1 Introduction

1.1 Titanium amide complexes: history and recent advances

Of all the transition elements, homoleptic and heteroleptic titanium amide complexes have been studied in the greatest detail[1-3]. Many amide complexes of Ti^{III} and Ti^{IV} are known but there are few examples of Ti^{I} or Ti^{II}.

The only Ti^{I} compound that has been reported is $TiNMe_2$[4]. Low oxidation state complexes are generally obtained by disproportionation of Ti^{III} or Ti^{IV} complexes. For example, the Ti^{III} complexes $[Ti(NMe_2)_3]_2$ disproportionate to the Ti^{IV} complex $Ti(NMe_2)_4$ and the Ti^{II} complexes $[Ti(NMe_2)_2]_m$[5,6]. Similar reactivity has been observed for the halide complexes[7,8]. The structures of the low valent titanium amide complexes are polymeric with bridging NR_2 groups.

Many Ti^{III} amide complexes have been synthesized. Homoleptic complexes of the general formula $Ti(NR_2)_3$ are known for NR_2 = NMe_2[5,6,9], NEt_2[5,6,9], NPh_2[10], $N(SiMe_3)_2$[11-13] or cyclopropamide[6]. Heteroleptic amide complexes $Ti(NR_2)_x(NR'_2)_{3-x}$ (e.g., $Ti(NMe_2)_2(NEt_2)$[6]) and $TiL_x(NR_2)_{3-x}$ (where L = η–C_5H_5 or alkyl and R = alkyl) (e.g., $Cp_2Ti(NMe_2)$ or $CpTi(NMe_2)_2(NEt_2)$[5,6,9]) are also known.

Recently, Ti^{III} and Ti^{IV} alkyl complexes stabilized by a linked cyclopentadienyl-amide ligand (Figure 1- 1) have been synthesized and their use for the polymerization of olefins demonstrated[14-16].

References start on page 80

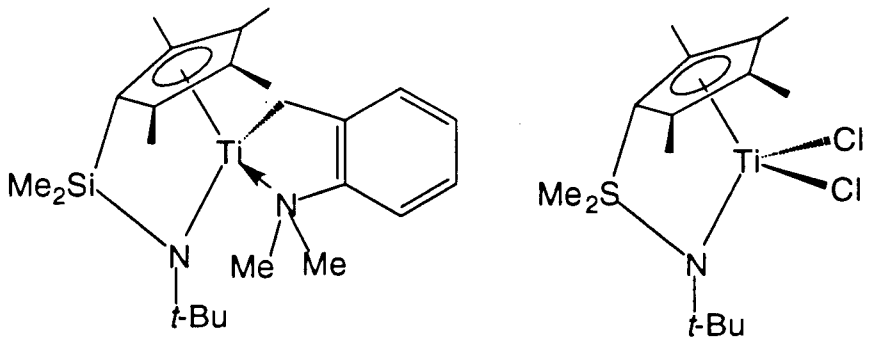

Figure 1- 1. Linked Cp-amide complex titanium

Of the four oxidation states, Ti^{IV} forms the most numerous amide complexes. Homoleptic complexes of formula $Ti(NR_2)_4$ are known for NMe_2,[17-19] NEt_2[17-21], NPr_2[17], N^iPr_2[22], NBu_2[17], NPh_2[23] etc. Heteroleptic compounds have also been prepared. For example, the mixed amide complexes (e.g., $Ti(NMe_2)_3(N^iPr_2)$[24]), amide-alkyl complexes (e.g., $Cp_2Ti(NMe_2)_2$[25,26], $(PhCH_2)_2Ti(NMe_2)_2$[27] or $Me_2Ti(NMe_2)_2$[27]) or amide-halide complexes (e.g., $Cl_3Ti(NMe_2)$[28], $Cl_2Ti(NMe_2)_2$[28,29], $ClTi(NMe_2)_3$[29]) have been reported.

It has been shown that the bulky dicyclohexylamide ligand can stabilize a highly reactive Ti^{IV} methylene complex (Figure 1- 2)[30]. In comparison, the cyclopentadienyl complexes

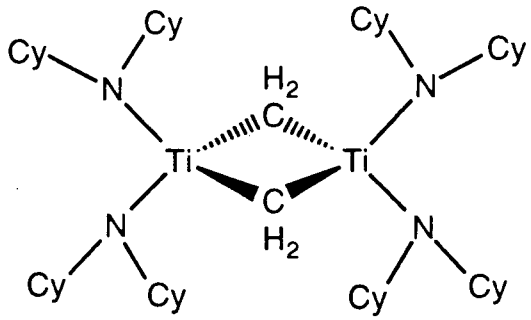

Figure 1- 2. $[(Cy_2N)_2Ti(\mu\text{-}CH_2)]_2$

References start on page 80

$[Cp_2Ti(\mu\text{-}CH_2)]_2$[31] and $Cp_2Ti(=CH_2)PMe_3$[32] have only been characterized on the basis of spectroscopic data.

Polyfunctional amide complexes of Ti^{III} and Ti^{IV} have also been synthesized. Many different linking group have been designed taking advantage of the chelate effect to offer enhanced stereorigidity of the metal centre (for example: three-atom bridge, Figure 1- 3(1)[33] and (2) (R = Me, ^{i}Pr, $SiMe_3$)[34]; two-atom bridge, Figure 1- 3(3)[35,36]; single-atom bridge, Figure 1- 3(4)[37]).

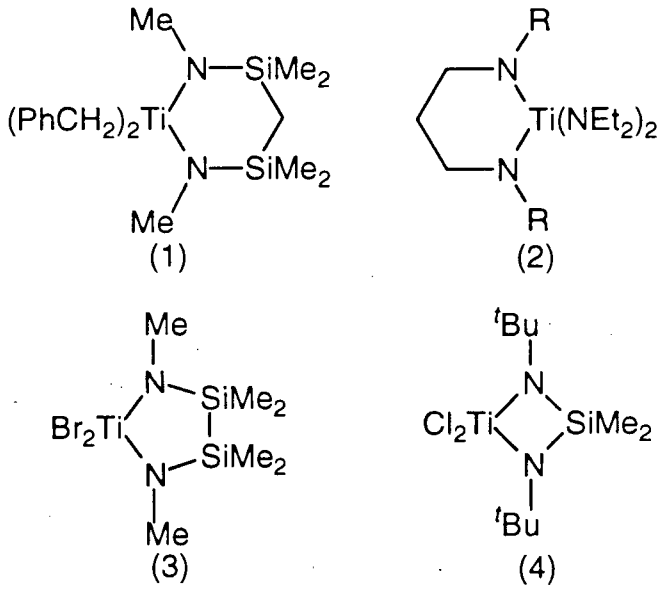

Figure 1- 3. Chelating diamide complexes

Recently, attempts to alter the electrophilicity of the metal centre by changing the electronic properties of the diamide ligands have been reported. For example, the use of a strongly π-accepting boryl group on the amide has been reported (Figure 1- 4)[38]. The electron accepting properties of the boron reduce the ability of the nitrogen to donate π-electron density to the metal centre. As a result, the metal centre should be more electrophilic than the corresponding alkyl or arylamide complexes.

References start on page 80

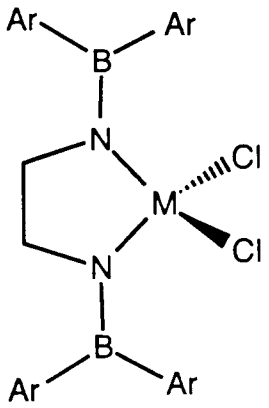

Ar = 2,4,6-trimethylphenyl

Figure 1- 4. Boron substituted amide ligand

The introduction of a donor functionality in amide ligands has been used to modify the electronic properties of the metal centre and the rigidity of the complex. Following this approach, bipodal mono(amide) {Figure 1- 5(1)[39]}, tripodal di(amide) {Figure 1- 5(2)[40]} and tetrapodal tri(amide) {Figure 1- 5(3)[41]} complexes of titanium(IV) have been reported.

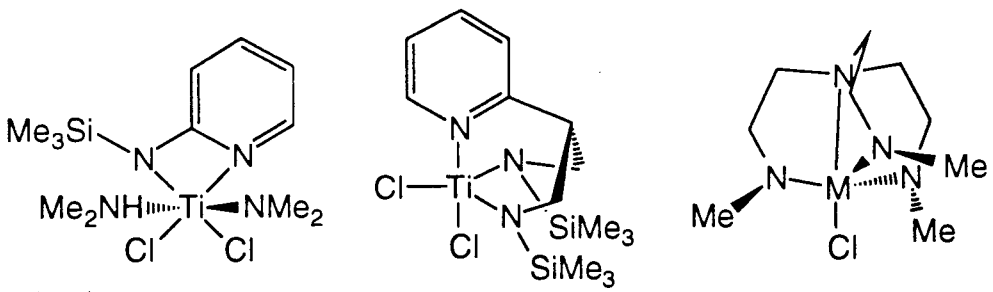

(1) (2) (3)

Figure 1- 5. Multipodal amide/amine ligands

References start on page 80

1.2 Alkyne cyclotrimerization mediated by transition metal complexes

Catalytic cyclotrimerization of alkynes leading to substituted arenes can be accomplished with a variety of transition metal complexes such as Ti[42,43], Zr[44,45], Nb[46-49], Ta[47-52], Rh[53,54], Pd[55,56], Co[57] and Ir[58]. This type of reaction has been used for the synthesis of organic molecules. For example, rhodium assisted cyclotrimerization has been used in the synthesis of *C*-arylglycoside (an antitumor agent)[53].

The mechanism of cyclotrimerization of alkynes by transition metal complexes has been debated extensively in the literature[47,59-75]. The cyclization of alkynes most often proceeds by an intermediate metallacyclopentadiene complex (**A**, Scheme 1- 1). The point of contention involves the intermediates involved in the reaction of a metallacyclopentadiene with 1 equiv of alkyne to generate the uncomplexed arene product.

Two mechanisms have been proposed for the addition of a third alkyne. In the first mechanism the addition proceeds through a metallacycloheptatriene complex (**B**-path 1, Scheme 1- 1) and the two new carbon-carbon bonds are formed in a stepwise fashion. The second mechanism involves the concerted formation of the two carbon-carbon bonds via the formation of the Diels-Alder "7-metallanorbornadiene" adduct (**C**-path 2, Scheme 1- 1).

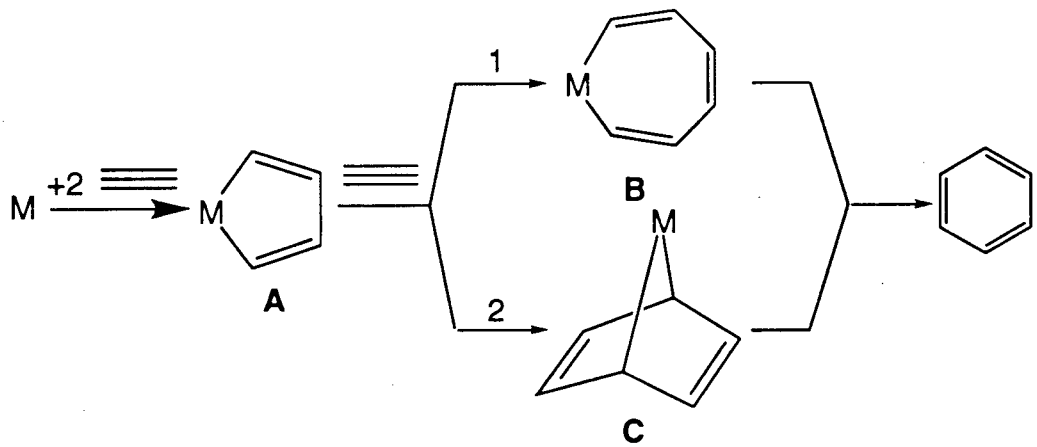

Scheme 1- 1. Mechanism of cyclotrimerization

References start on page 80

Recent work by Wigley and co-workers has shed some light on the mechanism operative in the alkyne cyclotrimerization reactions using early transition metal complexes[52,76]. The two-electron reduction of $(DIPP)_2TaCl_3(OEt_2)$ (DIPP = 2,6-diisopropylphenoxide) in the presence of 2-butyne affords $(DIPP)_2Ta(\eta^6\text{-}C_6Me_6)Cl$. The molecular structure of $(DIPP)_2Ta(\eta^6\text{-}C_6Me_6)Cl$ (Figure 1- 6) shows striking resemblance to the proposed Diels-Alder intermediate (**C**, Scheme 1-1). Related studies on an iridacyclopentadiene complex also favor a concerted pathway[77].

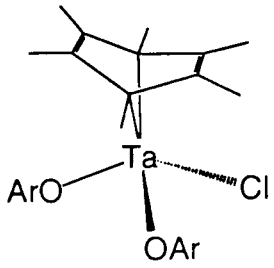

Figure 1- 6. $(DIPP)_2Ta(\eta^6\text{-}C_6Me_6)Cl$

Cyclization reactions are highly dependent on the steric and electronic properties of the ancillary ligands [78-81]. Under similar conditions, the more sterically hindered complex, $(DIPP)_3TaCl_2(OEt_2)$ (DIPP = 2,6-diisopropylphenoxide), does not lead to the formation of hexaethylbenzene, and only the metallacyclopentadiene complex $(DIPP)_3Ta(C_4Et_4)$[82,83] is obtained.

In contrast, various metallocene-based metallacyclopentadiene complexes undergo facile alkyne insertion to yield the corresponding metallacycloheptatriene[84] or metallacyclononatetraenes[85]. There are however no reports of catalytic oligomerization or polymerization of alkynes using metallocene complexes.

References start on page 80

2 Results and Discussion

2.1 Synthesis of aryl substituted pyridine diamines

2,6-Bis(bromomethyl)pyridine[86] was treated with two equivalents of LiNRH to yield the diamine compounds {$(BDPP)H_2$ (**1a**), R = 2,6 diisopropylphenyl; $(BDMP)H_2$ (**1b**), R = 2,6 dimethylphenyl} (eq. 1) in 50-80% yield.

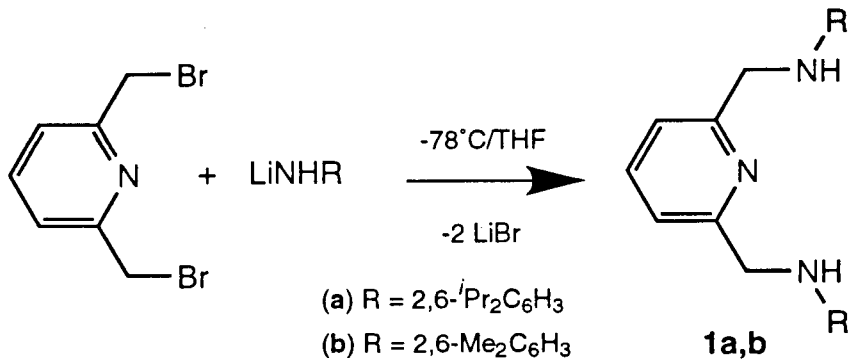

(1)

Surprisingly, no reaction occurs between the diamine $2,6\text{-}(RHNCH_2)_2NC_5H_3$ and $Ti(NMe_2)_4$ or $Ti(NMe_2)_2Cl_2$, even at elevated temperatures (110 °C). Moreover, attempts to deprotonate the diamine to form the diamide derivatives were unsuccessful. Deprotonation using *n*-BuLi only yielded strongly coloured decomposition products. KH did not react with $(BDPP)H_2$ or $(BDMP)H_2$. The pyridine nitrogen atom stabilizes negative charges at the benzylic positions, thus abstraction of the benzylic protons is favoured and decomposition occurs. An alternative route to diamide complexes of titanium was necessary.

The addition of 2 equivalents of $LiNR(SiMe_3)$ to a DME solution of 2,6-bis(bromomethyl)pyridine at -30 °C affords the white crystalline silylated diamines $2,6\text{-}\{(Me_3Si)RNCH_2\}_2NC_5H_3$ (**2a,b**) in moderate yield (eq. 2).

References start on page 80

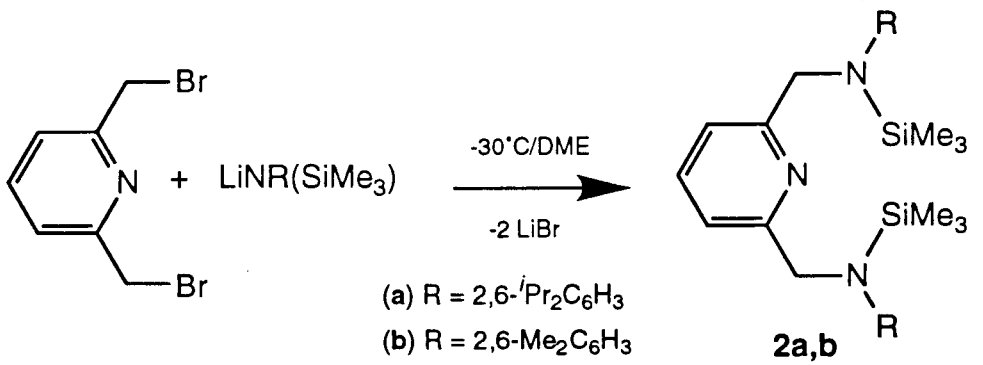

(2)

2.2 Synthesis of alkyl substituted pyridine diamines

The reaction of 2 equivalents of $LiNR(SiMe_3)$ (R = Cy, ^{i}Pr or ^{t}Bu)} with 2,6-bis(bromomethyl)pyridine does not afford the expected silylated diamines. A white insoluble polymeric material is isolated after workup. This is probably a result of the lack of steric protection at the nitrogen centre. Nucleophilic attack on a CH_2Br functionality by a newly formed $CH_2NR(SiMe_3)$ group is a possible reaction pathway (eq. 3) for the formation of polymer.

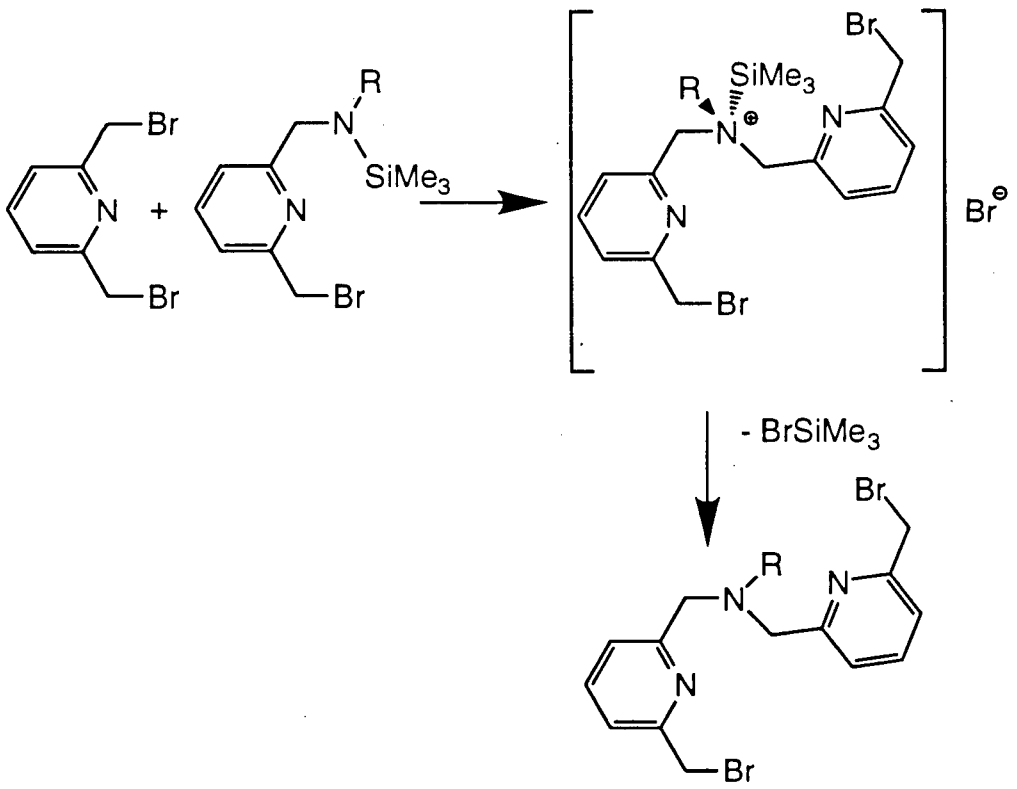

(3)

References start on page 80

Similarly, the reaction of 2 equivalents of LiNHR (R = Cy, ^{i}Pr or ^{t}Bu) with 2,6-bis(bromomethyl)pyridine does not yield the expected diamines. The proposed reaction mechanism is similar to the one above and involves the attack on a CH_2Br group by a CH_2NRH group to afford the ammonium salt $CH_2NHR^+Br^-$ (eq. 4).

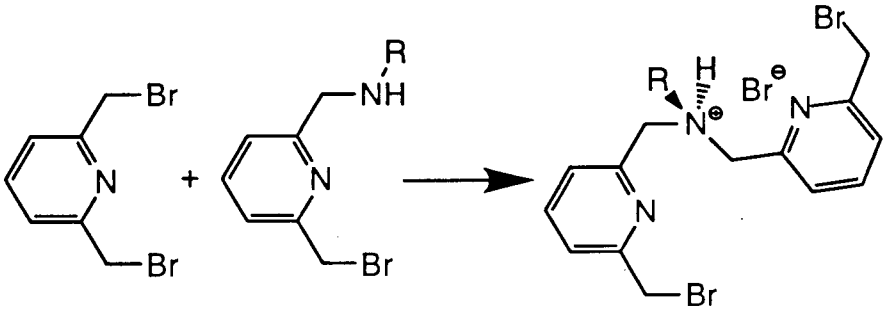

(4)

The addition of solid 2,6-bis(bromomethyl)pyridine to a large excess of H_2NR (R = Cy, ^{i}Pr or ^{t}Bu) in hexanes at room temperature affords the oily diamines 2,6-$(HRNCH_2)_2NC_5H_3$ {(CyAP)H_2 (**1c**) R = Cy; (iPAP)H_2 (**1d**) R = ^{i}Pr; (tBAP)H_2 (**1e**) R= ^{t}Bu} in quantitative yield after workup (eq. 5). Compounds **1c,d,e** can be prepared on a scale of 10-15 g and can be purified by distillation under full vacuum to afford colourless oils.

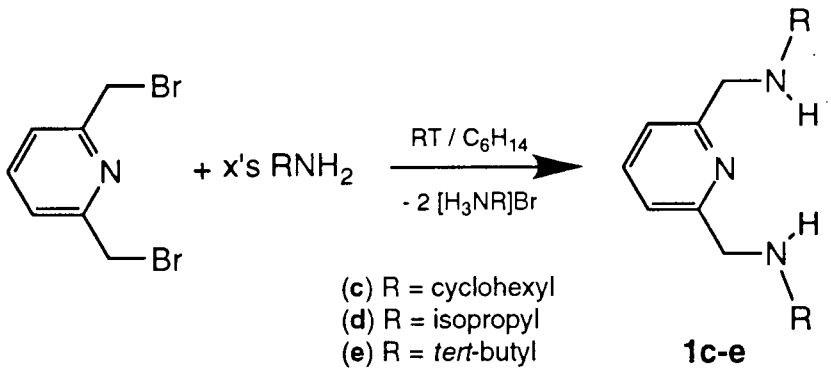

(5)

The addition of 2 equivalents of halotrimethylsilane to a diethyl ether solution of **1c-e** at ambient temperature results in the rapid formation of a white precipitate. The complexed hydrogen halide formed in the reaction can then be removed by quenching with an excess of Et_3N (eq. 6). The silylated compounds **2c-e** can be prepared on a large scale in high yield using this synthetic method.

References start on page 80

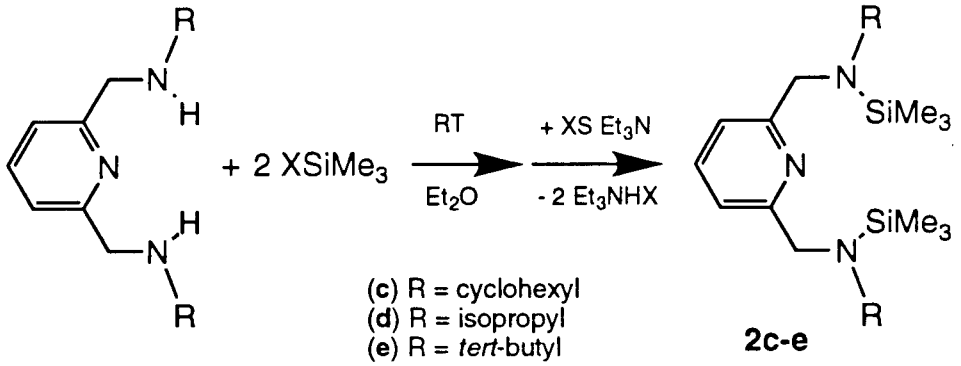

(6)

2.3 Synthesis of the titanium dichloride complexes

The silylated diamines **2a,b** react cleanly with $TiCl_4$ to give 2 equivalents of $ClSiMe_3$ (confirmed by ^1H NMR spectroscopy) and the red dichloride complexes (**3a,b**) in >85% yield (eq. 7).

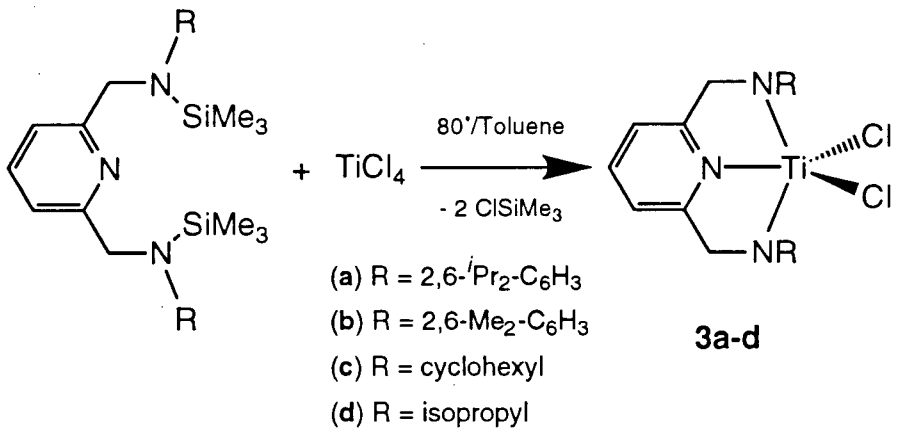

(7)

Compounds **2c,d** also react with $TiCl_4$ to give the red dichloride complexes (**3c,d**) in 50% and 72% yield, respectively. However, a green insoluble product is also formed during the reaction. A similar green solid (**3e**) is the major product of the reaction between $TiCl_4$ and compound **2e**. It can be isolated in approximately 80% yield from the reaction mixture. Complex **3e** is soluble in dichloromethane from which dark green needles can be obtained. The ^1H NMR spectrum (CD_2Cl_2) of complex **3e** is very broad and remains unchanged at 50 °C. The determination of the magnetic susceptibility using Evans method[87] showed that complex **3e** is diamagnetic in solution. Attempts to isolate a suitable crystal for single crystal X-ray analysis

References start on page 80

were thwarted by rapid loss of solvent molecules from the lattice. The ^{1}H NMR spectrum of the hydrolysis product from complex **3e** confirmed the presence of solvent in the crystal lattice. The nature of this green complex is uncertain but might be dimeric.

The ^{1}H NMR spectra of complexes **3a-d** exhibit a singlet at approximately 5.8 ppm due to the ligand methylene protons (CH_2N). This is consistent with the C_{2v} symmetry and a meridional coordination of the ligand. A facial coordination of the ligand would yield a complex with C_s symmetry. In this case, the methylene (CH_2N) protons would appear as an AB pattern in the ^{1}H NMR spectrum. In contrast, a facial coordination geometry as been observed for [CH(2-C_5H_4N)(CH_2NSiMe_3)$_2$]$TiBr_2$ [40]. The isopropyl methyl groups of complex **3a** are diastereotopic. This has been interpreted as a consequence of restricted rotation about the N-Aryl C_{ipso} bond (i.e. the methyl groups can not be made equivalent if the aryl can not rotate freely, Figure 1- 7). The proton NMR spectrum remains unchanged at 80 °C. It is not possible to determine by spectroscopic means if the same restricted rotation is present in compound **3b**.

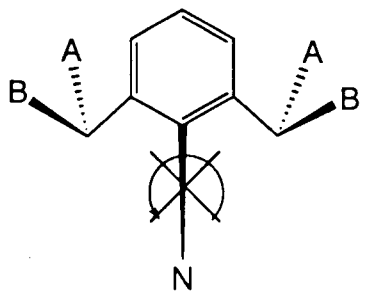

Figure 1- 7. Restricted rotation of the aryl

The isopropyl methine protons of complex **3d** appear at an unusually high chemical shift (δ 5.97 ppm) in the ^{1}H NMR spectrum. Comparatively, the ^{1}H NMR spectrum of the diamine **2d** displays a septet at 3.26 ppm for the isopropyl methine protons. In a similar way, the cyclohexyl methine protons in the dichloride complex **3c** appear as a broad triplet of triplets at 5.54 ppm compared to 2.82 ppm for the diamine **2c**.

References start on page 80

The consequence of the rigid coordination of the ligand is the enforced location of the substituents on the nitrogen. The type of protection afforded by the ligand is thus a function of the nature of these groups. With aryl substituents, a "pocket" opposite the pyridine ring is created and the metal is protected about the N_3 plane. On the other hand, alkyl substituents protect the site trans to the pyridine and the faces (either sides of the N_3 plane) are left open.

2.4 Synthesis of alkyl complexes

Complexes **3a,b,d** can be alkylated using various alkylating reagents (Scheme 1- 2). The addition of 2 equivalents of MeMgBr to ether suspensions of **3a,b,d** at -78 °C affords the dimethyl derivatives **4a,b,d** in good yield. Compounds **4a,b,d** are thermally sensitive in the absence of coordinating ligands; for example, they can be crystallized readily from ether or THF but decompose slowly in toluene or benzene. Titanium dimethyl derivatives bearing amide ligands are believed to form transient methylidene species via α-elimination[30]. Attempts to trap a methylidene complex by heating the dimethyl complexes in the presence of PMe_3 were unsuccessful and no reaction was observed.

The addition of 2.2 equivalents of MeMgBr or $PhCH_2MgCl$ to ether suspensions of complex **3e** only gave small amounts (20-30% yield) of the corresponding Ti^{IV} bis(alkyl) complex, (tBAP)$TiMe_2$ and (tBAP)$Ti(CH_2Ph)_2$ (detected by ^1H NMR spectroscopy). No attempt was made to isolate these species. Moreover, the diamine **2e** reacts very slowly with $Ti(CH_2SiMe_3)_4$[89] at 80 °C to give (tBAP)$Ti(CH_2SiMe_3)_2$ (< 5 % after 5 days) while rapid decomposition of the titanium tetra(alkyl) starting material is observed at higher temperature[90,91].

References start on page 80

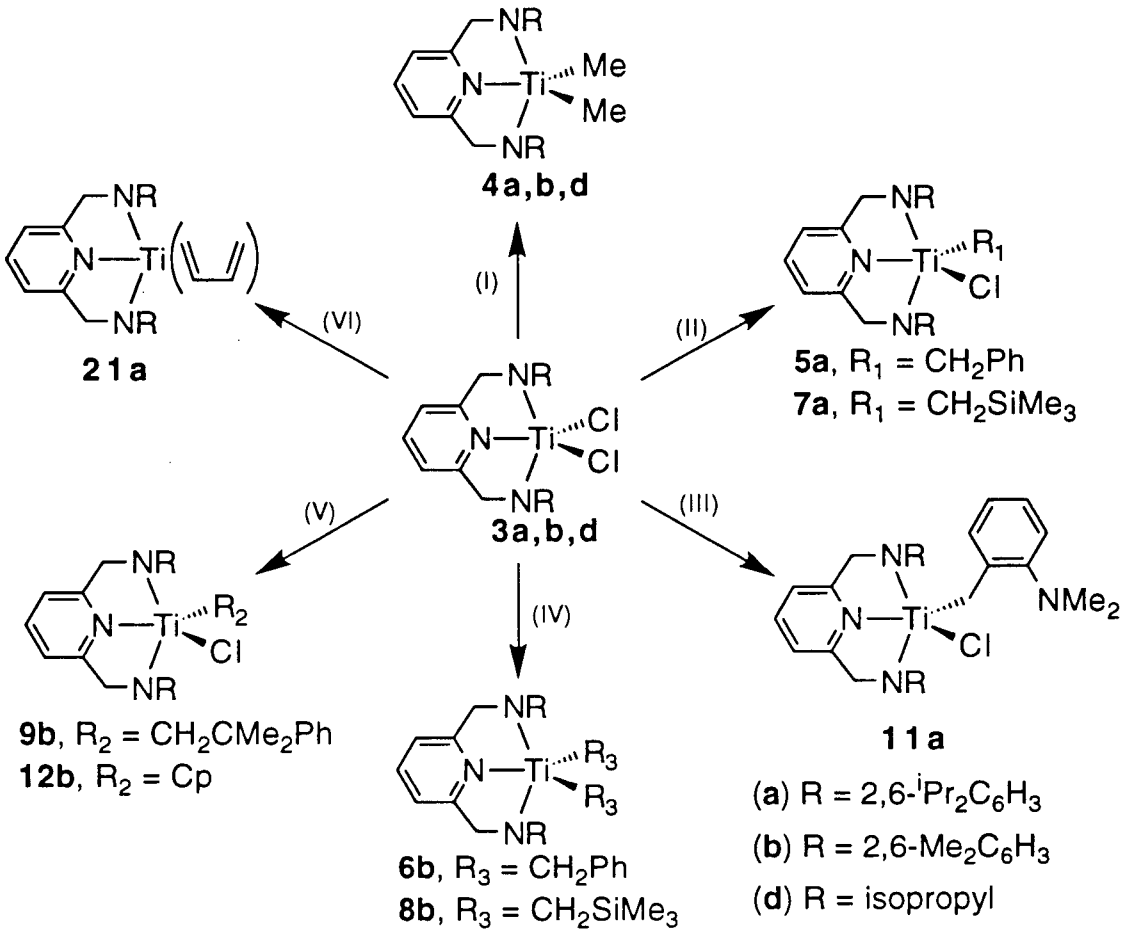

Scheme 1- 2. Alkylation of complexes ***2a,b,d***[¥]

[¥] Reagents and conditions. (I) 2 equivalents MeMgBr, Et_2O, -78 °C; (II) 1 equivalent $PhCH_2MgCl$ or $LiCH_2SiMe_3$, Et_2O, 22 °C; (III) 1.2 equivalents $LiCH_2C_6H_4$-*o*-NMe_2, Et_2O, -78 °C; (IV) 2 equivalents $PhCH_2MgCl$ or $LiCH_2SiMe_3$, Et_2O, 22 °C; (V) 1 equivalent NaCp•DME or $PhMe_2CCH_2MgCl$, Et_2O, -30 °C; (VI) 1.2 equivalents $(C_4H_6)Mg \bullet 2THF$, Et_2O, -78 °C.

The ^1H NMR spectra of complexes **4a,b,d** are similar to those obtained for compound **3a,b,d** and are consistent with C_{2v} symmetry. Additional resonances for the Ti–CH_3 group are

References start on page 80

observed at 1.06, 1.08 and 0.81 ppm, respectively. The diastereotopic isopropyl methyl resonances observed in the ^{1}H NMR spectrum of complex **4a** indicates that restricted rotation about the N-aryl C_{ipso} bond is retained upon alkylation.

The addition of 1.2 equivalents of $(C_4H_6)Mg•2THF$[92] to an ether suspension of compound **3a** at -78°C affords a mixture of the 1,3-butadiene complex **21a** and black byproducts. It was not possible to isolate complex **21a** from the impurities via crystallization. The ^{1}H NMR spectrum of complex **21a** displays two singlets at δ 5.19 and 4.98 ppm consistent with two inequivalent methylene groups (NCH_2) on the ligands. This is interpreted as a result of asymmetry about the NMX_2 plane (Figure 1- 8 II) and a complex with C_s symmetry. Two resonances at δ 5.28 ppm and 2.78 ppm are attributable to the butadiene fragment. It is not possible to discern the third butadiene resonance due to the resonances of the byproduct. Moreover, the difficulties associated with the purification of complex **21a** prevented its characterization by ^{13}C NMR spectroscopy. As a result, it is not possible to established the mode of coordination of the butadiene fragment.

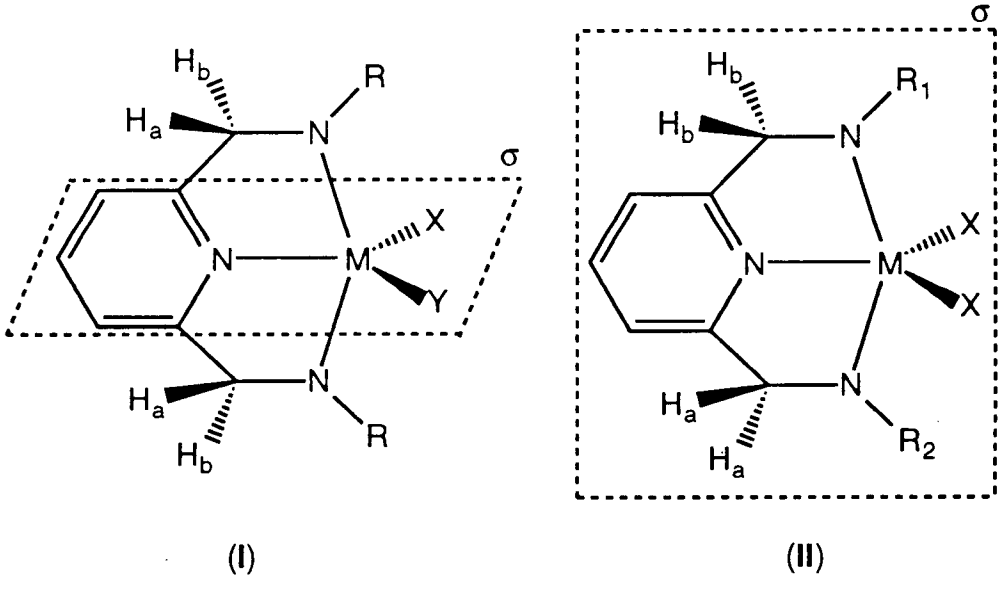

Figure 1- 8. Mirror planes in complexes with C_s symmetry

References start on page 80

The addition of 1 equivalent of $PhCH_2MgCl$, $LiCH_2SiMe_3$ or $LiCH_2C_6H_4$-*o*-NMe_2 to an ether suspension of the dichloride complex **3a** at 22 °C yields the mono(alkyl) derivatives (BDPP)Ti(CH_2Ph)Cl (**5a**), (BDPP)Ti(CH_2SiMe_3)Cl (**7a**) and (BDPP)Ti($CH_2C_6H_4$-*o*-NMe_2)Cl (**11a**), respectively (Scheme 1- 2). The ligand methylene protons (CH_AH_BN) appear as AB quartet patterns in the ^1H NMR spectra of complexes **5a**,**7a** and **11a**. This indicates asymmetry about the N_3 plane (Figure 1- 8 I). Moreover, two isopropyl methine and four isopropyl methyl resonances are observed for complexes **5a**, **7a** and **11a**, which is in agreement with the C_s symmetry of the complexes and the restricted rotation of the N-C_{ipso} bond.

Certain Ti^{III} complexes containing a $CH_2C_6H_4$-*o*-NMe_2 group are active catalysts for the polymerization of olefins[93]. Attempts to generate a Ti^{III} complex by reduction of **11a** were unsuccessful yielding intractable materials.

The addition of 2 equivalents of $PhCH_2MgCl$ or $LiCH_2SiMe_3$ to an ether suspension of **3b** at 22 °C yields the bis(alkyl) derivatives (BDMP)Ti(CH_2Ph)$_2$ (**6b**) and (BDMP)Ti(CH_2SiMe_3)$_2$ (**8b**), respectively (Scheme 1- 2). The ^1H NMR spectra of complexes **6b** and **8b** display a singlet for the methylene protons (NCH_2) of the ligand. This is in agreement with the expected C_{2v} symmetry of the complexes. The addition of 1 equivalent of alkylating reagent in CH_2Cl_2 at -78 °C affords a 50% yield (by ^1H NMR spectroscopy) of compounds **6b** and **8b**, respectively. The resonances attributable to the starting dichloride complexes (**3a,b**) are also observed.

The addition of 1 equivalent of NaCp•DME to complex **3b** in ether at -30 °C affords the η^5-cyclopentadienyl derivative **12b**. No reaction is observed between the bulkier dichloride compound **3a** and NaCp•DME. The ^1H NMR spectrum of compound **12b** is characteristic for a molecule with C_s symmetry. Rotation around the N-C_{ipso} bond of the ligand is hindered by the presence of the Cp group resulting in two inequivalent arene methyl environments. Attempts to substitute the remaining chloride group using MeMgBr were unsuccessful. No reaction was observed between Mg metal and complex **12b**. The use of stronger reducing agent such as Na or K metal or Na/K alloy yielded intractable materials.

References start on page 80

The mono(alkyl) complex (BDMP)Ti(CH_2CMe_2Ph)Cl (**9b**) is obtained by the reaction of 2 equivalents of $PhMe_2CCH_2MgCl$ with complex **3b** and not the expected bis(neophyl) derivative. The ^1H NMR spectrum (Figure 1- 9) of complex **9b** displays an AB quartet pattern for the methylene protons (CH_AH_BN) (①) and the two distinct aryl methyl (②/③) resonances. This is consistent with asymmetry about the MN_3 plane in a complex with C_s symmetry (Figure 1- 8 I) and restricted rotation about the N-C_{ipso} bond. No evidence of N-C_{ipso} bond rotation is observed at 80 °C.

Attempts to grow X-ray quality crystals of complex **9b** were unsuccessful. However, the bromide analogue **10b** does provide suitable crystals. The bromide complex can be synthesized from complex **9b** and $MgBr_2(Et_2O)$ in ether (eq. 8).

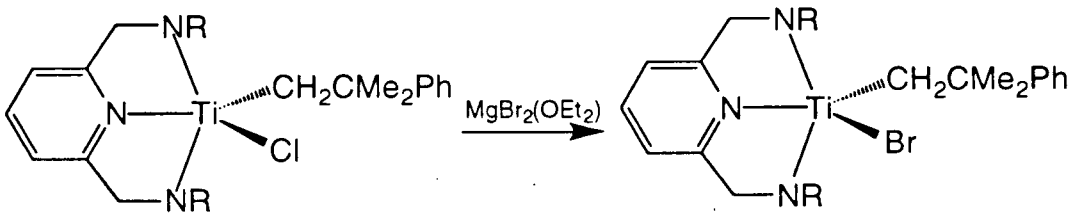

9b **10b** **(8)**

In fact, complex **10b** was originally formed from the reaction of the dichloride derivative **3b** and $PhMe_2CCH_2MgCl$ contaminated with $MgBr_2(OEt_2)$. The $MgBr_2(OEt_2)$ was formed during the activation of the Mg turnings with 1,2-dibromoethane in the preparation of the Grignard reagent.

The solid-state structure of **10b**•C_6H_6 was determined by X-ray crystallography. The full crystallographic data can be found in the appendix. The molecular structure of complex **10b** is shown in Figure 1- 10 and selected bond distances and angles in Table 1- 1.

References start on page 80

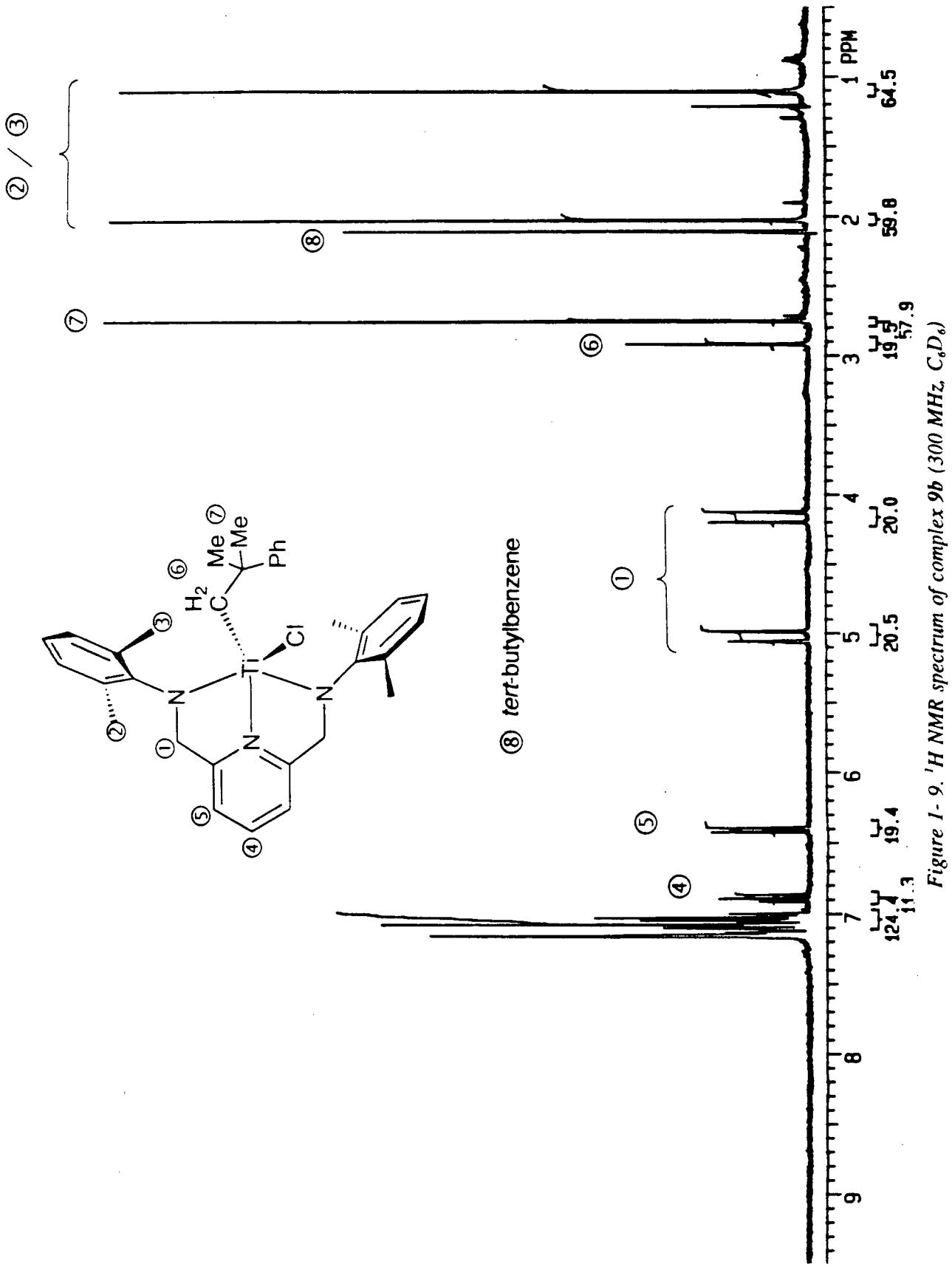

*Figure 1- 9. ^1H NMR spectrum of complex **9b** (300 MHz, C_6D_6)*

References start on page 80

Table 1- 1. Selected Bond Distances (Å) and Angles (deg) for 8b•C_6H_6

Bond Distances			
Ti-Br	2.399(2)	Ti-N(1)	1.979(5)
Ti-N(2)	2.126(6)	Ti-N(3)	1.977(6)
Ti-C(8)	2.121(7)		
Bond Angles			
N(1)-Ti-N(3)	1412.1(2)	Br-Ti-N(3)	100.3(2)
C(8)-Ti-Br	102.8(2)	Br-Ti-N(1)	98.1(2)
C(8)-Ti-N(2)	101.4(3)	Br-Ti(N(2)	155.8(2)
C(8)-Ti-N(1)	102.7(3)	C(8)-Ti-N(3)	105.1(3)

The structure is best described as a distorted square pyramid with the neophyl carbon {C(8)} occupying the apical position (Figure 1- 10). The titanium atom is located about 0.48 Å above the basal plane formed by the bromide, the two amides and pyridine nitrogen. The Ti-amide distances {1.979(5) and 1.977 (6)} Å are comparable to those observed in other titanium amide complexes[30,37,40,94-97]. The amide nitrogens are nearly sp^2-hybridized as evidenced by the sum of the angles about each nitrogen atom {N(1) = 359.1° and N(3) = 359.3°}. The complex probably adopts a square based pyramidal structure over a trigonal bipyramid structure to minimize steric interactions between the neophyl group and the 2,6-dimethylphenyl substituents of the ligand.

The rigid coordination of the ligand and the location of the aryl methyl groups create a protective "pocket" opposite the pyridine. The bromide is located in this "pocket" and is laterally shielded from incoming alkylating agents. This may explain the lack of reactivity of this compound with reagents such as MeMgBr. However, a small molecule such as $H_{2(g)}$ might be able to access the "pocket" and react.

References start on page 80

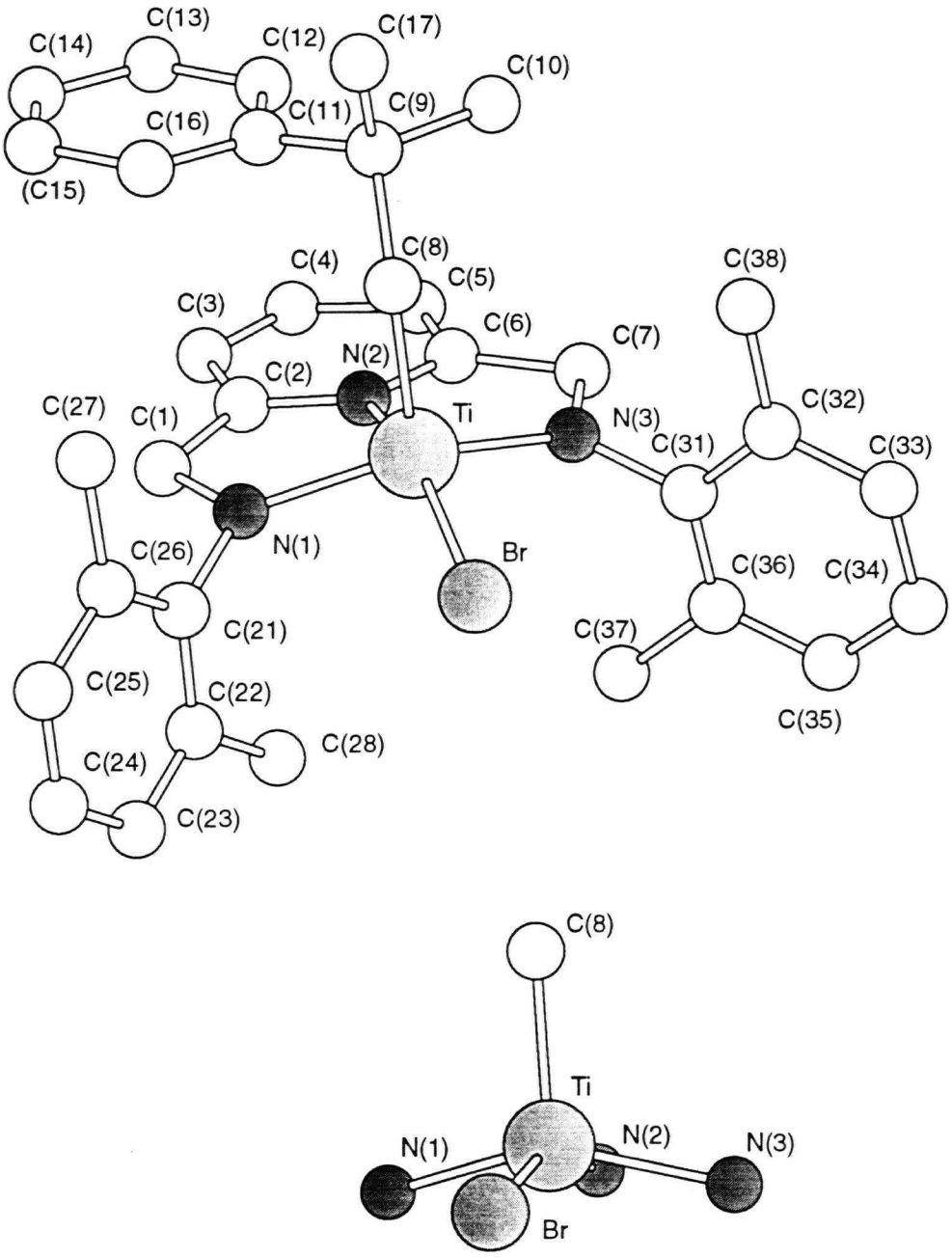

Figure 1- 10. Top: Chem 3D™ drawing of the molecular structure of ***8b***•C_6H_6 *(The benzene molecule is not shown.) Bottom: Chem 3D™ drawing of the core of* ***8b***•C_6H_6.

References start on page 80

In order to test this hypothesis, complexes **7a** and **9b** were exposed to approximately 3 atm of $H_{2(g)}$ (in C_6D_6) for 12 hours at ambient temperature. In both cases, a white solid precipitated from solution after a few hours. The insoluble materials were removed by centrifugation and the soluble products were characterized by ^1H NMR spectroscopy.

The ^1H NMR spectrum of the solution obtained with compound **7a** showed resonances characteristic of the parent dichloride complex (**3a**) as well as Me_4Si and free pyridine diamine (**1a**). Attempts to dissolve the white solid formed in the reaction in various solvents were unsuccessful (CD_2Cl_2, Pyridine-d_5, THF-d_8). A possible pathway for this reaction is shown in Scheme 1- 3. The first step involves the hydrogenolysis of the Ti-C bond to form one equivalent of Me_4Si and the transient mono(hydride) complex. The unstable mono(hydride) complex then decomposes to form 1/2 equivalent of the dichloride **3a**, 1/2 equivalent of the diamine **1a** (Scheme 1- 3, step A) and insoluble products.

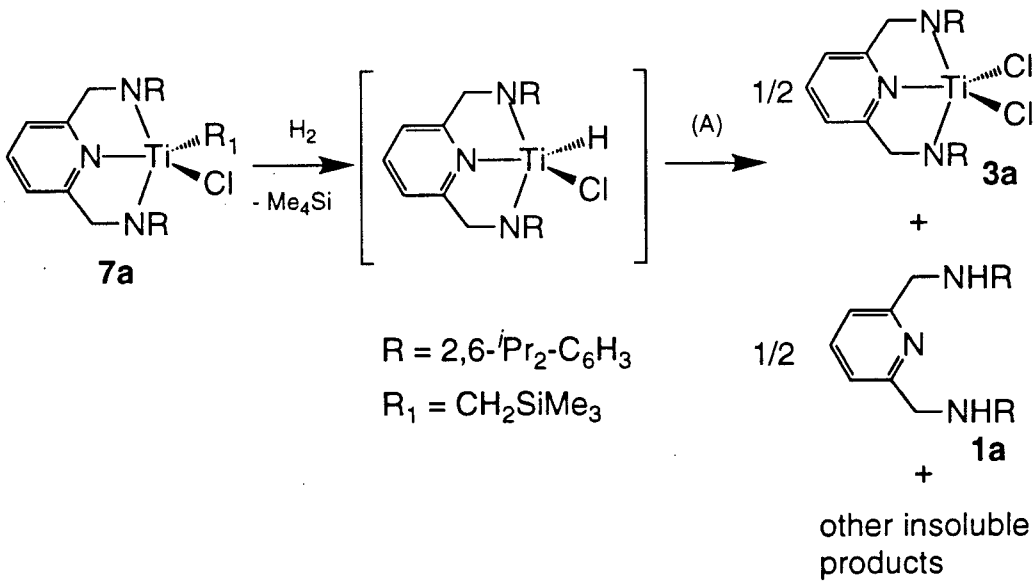

*Scheme 1- 3. Proposed mechanism for the hydrogenation of complex **7a***

References start on page 80

The reaction between $H_{2(g)}$ and complex **9b** gave similar results. The ^1H NMR spectrum of the soluble products displays resonances characteristic for free pyridine diamine (**1b**) and *tert*-butylbenzene. A similar pathway is proposed for this reaction (Scheme 1- 4). First, hydrogenolysis of the Ti-C bond affords one equivalent of *tert*-butylbenzene. The transient mono(hydride) complex then decomposes to give free pyridine diamine (**1b**) and insoluble Ti compounds.

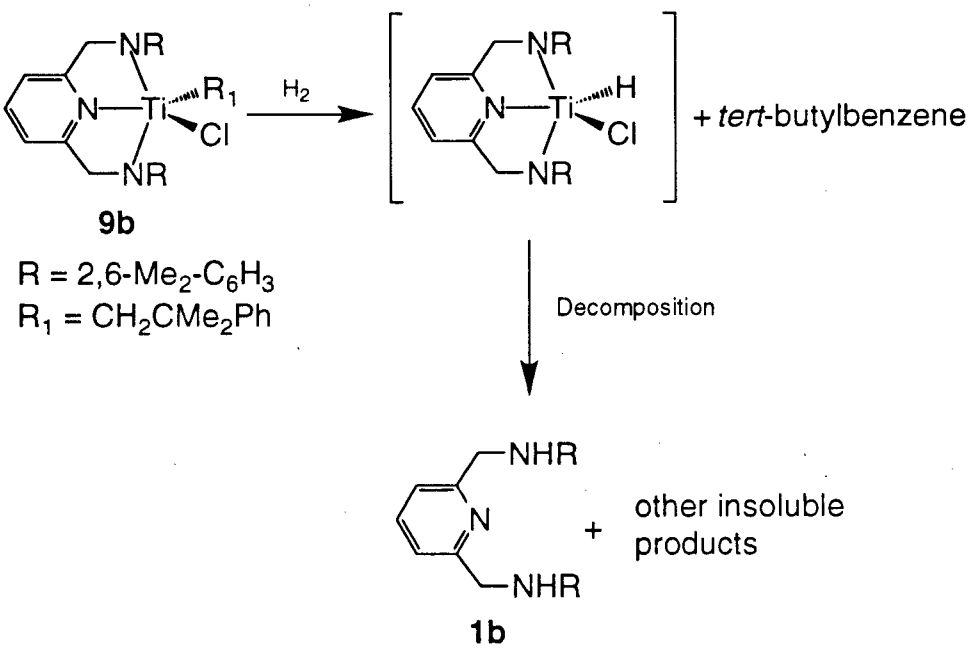

*Scheme 1- 4. Proposed mechanism for the hydrogenation of complex **9b***

References start on page 80

2.5 Reduction of $TiCl_2$ complexes: Metallacycle formation

2.5.1 Metallacyclopentadiene complexes derived from internal alkynes

The reduction of the dichloride complexes **3a,b** with excess Na/Hg amalgam (1%) in toluene in the presence of >2 equivalents of internal alkyne (Scheme 1- 5) yields the tetrasubstituted metallacyclopentadiene complexes **13a**, **14a** and **15a,b**.

Complexes **13a**, **14a** and **15a,b** can be recrystallized from pentane in good yield

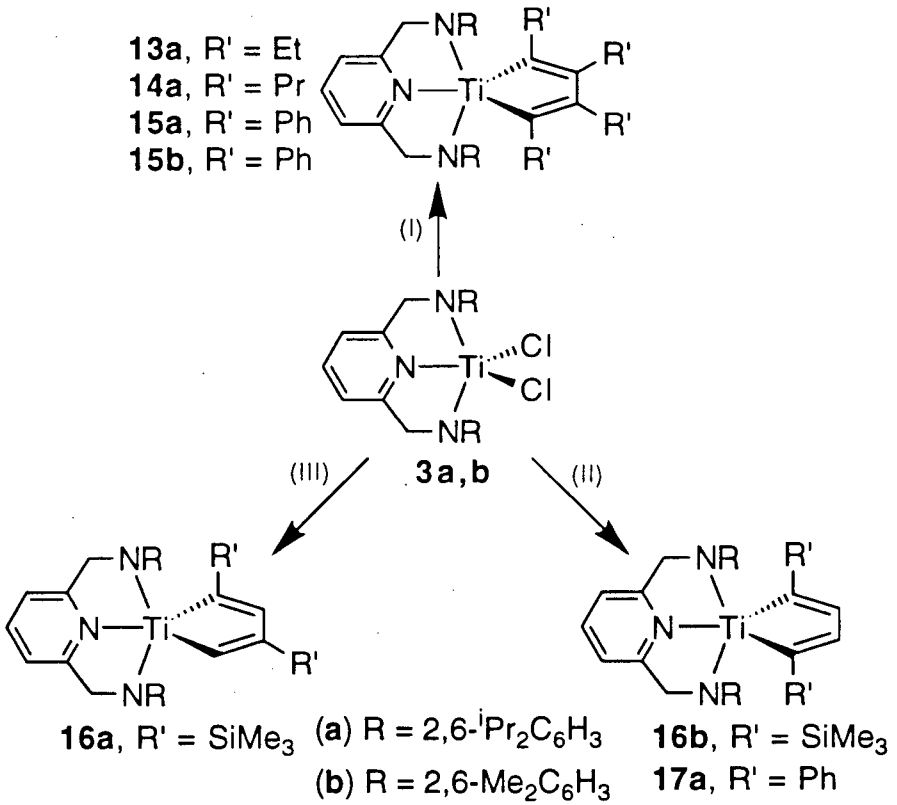

Scheme 1- 5. Preparation of Titanacyclopentadiene derivatives[¥]

[¥]Reagents and conditions: toluene, 23 °C, excess Na/Hg amalgam, > 2 equivalents alkyne. (I) R'C≡CR', R' = Et, Pr, Ph. (II) R'C≡CH, R' = $SiMe_3$, Ph. (III) R'C≡CH, R' = $SiMe_3$.

References start on page 80

(≈65%). Attempts to isolate the titanacyclopentadiene complexes **13b** {(BDMP)Ti(C_4Et_4)} and **14b** {(BDMP)Ti(C_4Pr_4)} (not shown) were unsuccessful. They were observed by ^{1}H NMR spectroscopy but they proved too soluble to be separated from the byproducts of the reaction.

The ^{1}H NMR spectra of complexes **13a**, **14a** and **15a,b** are consistent with a meridional coordination of the ligand and mirror symmetry about the N_3-plane as evidenced by a singlet observed for the ligand methylene (NCH_2) protons. The low-fields resonances (> 190 ppm) observed for the α-carbons of the metallacycle in the ^{13}C{^{1}H} NMR spectra are similar to previously reported values[43,98,99]. The low-field resonance observed for the α-carbon atom in complex **15b** (δ 221.7 ppm) is downfield from the one obtained for the metallocene analogue $Cp_2Ti(C_4Ph_4)$ (δ 202.1 ppm). Comparatively, the α-carbon atoms in (Ar"O)$_2$Ti(C_4Ph_4) (Ar" = 2,6-diphenylphenoxide) are observed at 225.0 ppm. Chemically inequivalent ethyl and propyl substituents (α and β positions) are observed for compounds **13a** and **14a,** respectively. The ^{1}H NMR spectrum of compound **15a**, however, is quite broad at 23 °C. A stacked plot of the ligand methylene (CH_2N) region at various temperatures is shown in Figure 1- 11.

The low temperature limiting spectrum (-20 °C) shows an AB quartet (①) ($^2J_{HH}$ = 20.6 Hz) for the ligand methylene (CH_AH_BN) protons and resonances at 4.99 ppm (②) and 2.79 ppm (not shown) attributable to two inequivalent isopropyl methine protons. As the temperature is increased, the isopropyl methine resonances coalesce to a single resonance at 3.88 ppm (not shown) while the resonance at 5.47 ppm (③) shifts to lower field. The high temperature limiting spectrum (80 °C) shows a single broad resonance for the ligand methylene protons at about 5.05 ppm (④). This exchange process is interpreted as a result of synchronized restricted rotation of the phenyl rings of the titanacycle eq. 9. Using eq. 10[100] it is possible to calculate an approximate value for $\Delta G^{\ddagger}$ of 14.7(5) kcal mol^{-1}.

References start on page 80

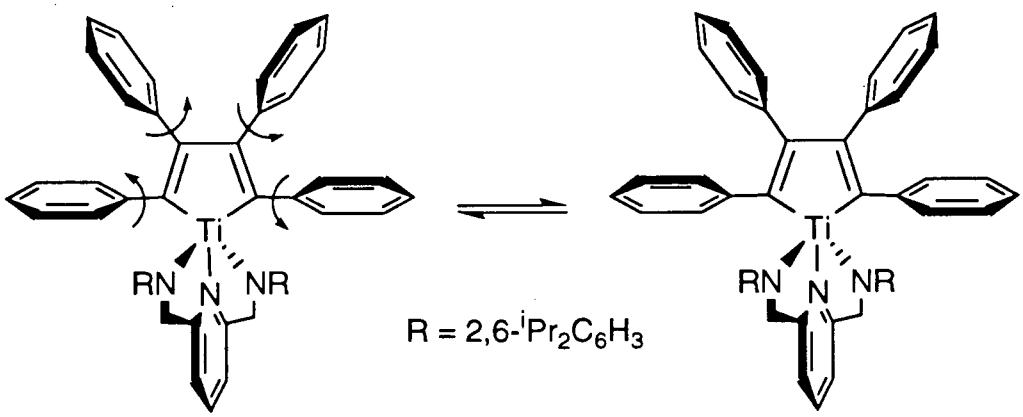

(9)

$$\Delta G^{\ddagger} = -RT_c \ln\left(\frac{\pi(\delta\upsilon)}{\sqrt{2}} \times \frac{h}{kT_c}\right) \quad (10)$$

T_c = coalescence temperature
$\delta\upsilon$ = distance between the peaks at slow exchange (Hz)
h = Planck constant
k = Boltzmann constant

Rotation of the phenyl rings in the α and α' positions is hampered by the bulky 2,6-diisopropylphenyl substituents which in turn affects the orientation of the phenyl groups in the β and β' positions of the titanacycle. The low temperature spectrum would be characteristic of a complex with C_2 symmetry. Alternatively, the high temperature structure would have C_{2v} symmetry. Comparatively, the less bulky titanacyclopentadiene complex **15b** (R = 2,6-$Me_2C_6H_3$) shows no restricted rotation at -80 °C. The solid-state structure of $Cp_2Ti(C_4Ph_4)$ shows a propeller arrangement of the phenyl rings as proposed here[101].

Attempt to achieve cyclotrimerization using the titanacyclopentadiene complexes **13a**, **14a** and **15a,b** were fruitless. These complexes do no react with excess alkyne or acetonitrile even at elevated temperatures (110 °C, 24 h).

References start on page 80

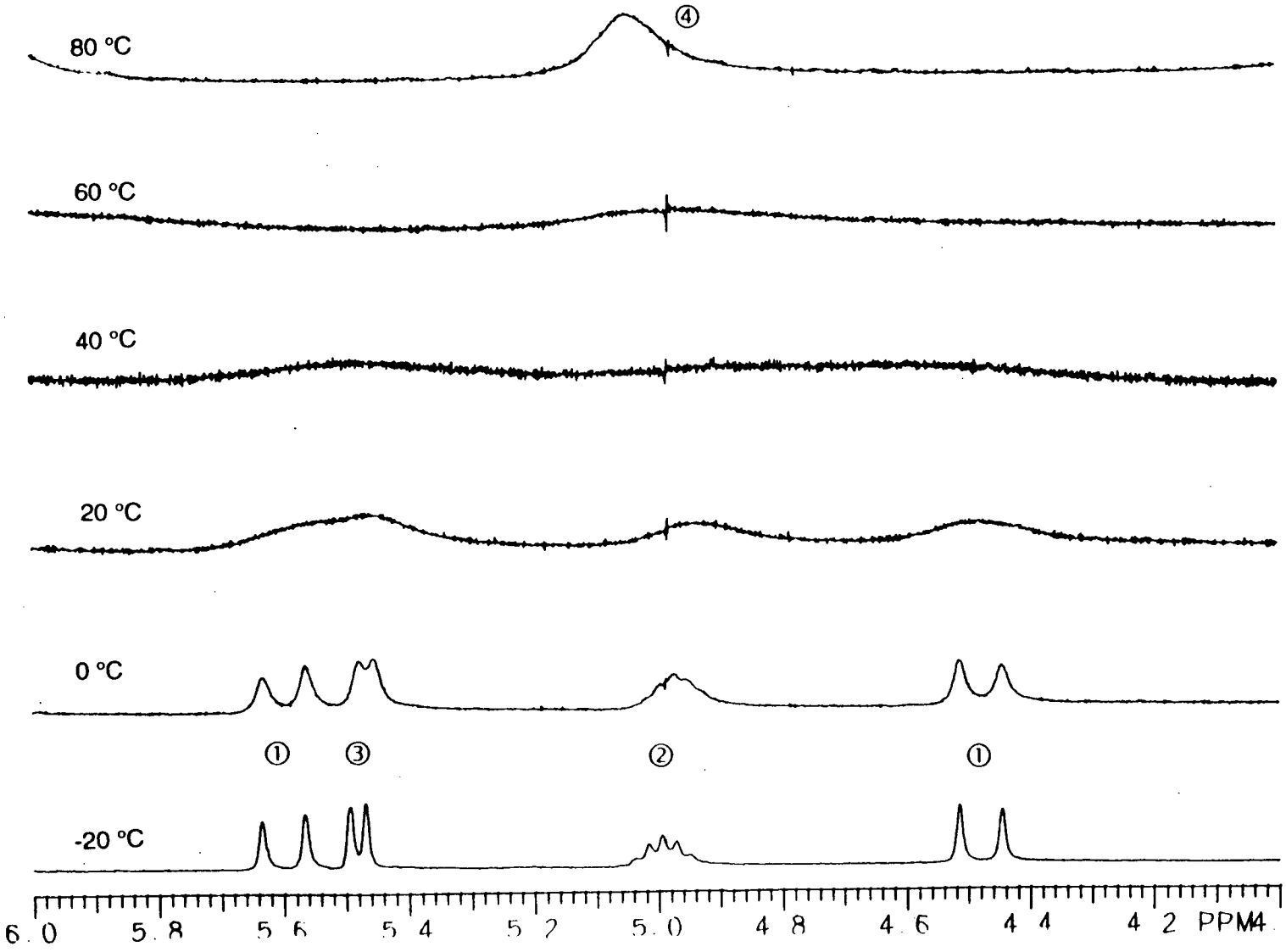

Figure 1- 11. Variable-temperature ^1H NMR spectra of the ligand methylene (CH_2N) region of coupound ***15a*** *(300MHz, $CD_3C_6D_5$)*

References start on page 80

2.5.2 Metallacyclopentadiene complexes derived from terminal alkynes

The reduction of the dichloride complexes **3a,b** in the presence of terminal alkynes affords the metallacyclopentadiene complexes **16a,b** and **17a** (Scheme 1- 5). It is possible to rationalize the regiochemistry by assuming that the formation of compounds **16a,b** and **17a** proceeds via a common mono(alkyne) intermediate (Scheme 1- 6, compound **I**).

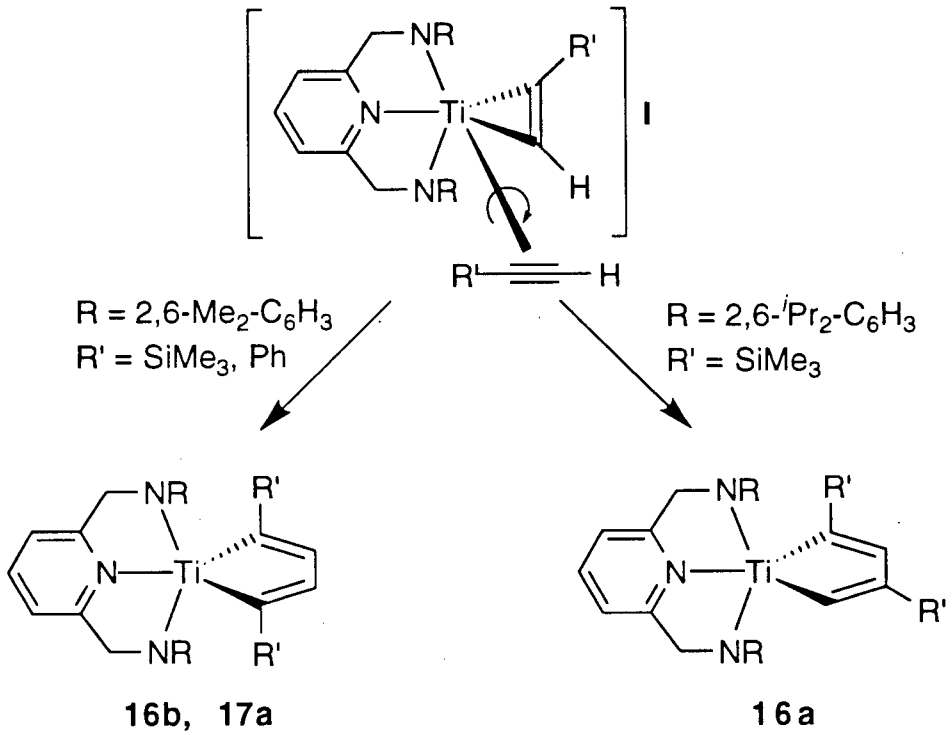

Scheme 1- 6. Regiochemistry of the insertion

Steric interactions with the R' substituent (Ph or $SiMe_3$) inhibit back-side attack of the second alkyne to the intermediate **I**. The incoming alkyne must then approach from the front. When the pyridine ligand bears the larger 2,6-diisopropylphenyl groups on nitrogen and the alkyne substituent is bulky (Me_3Si), steric interactions between the R and R' groups direct the bulk of the alkyne away from the isopropyl group of the ligand and the α,β' product is obtained

References start on page 80

(**16a**). When the incoming alkyne is relatively small (HC≡CPh), the more favorable α,α' product is obtained (**17a**). Comparatively, with the smaller 2,6-dimethylphenyl substituents on the ligand, the alkyne inserts with the R' group pointing towards the ligand giving rise to the α,α' titanacycle(**16b**). Similar steric effects have been observed for related systems. For example, the phenyl groups in $Cp_2Ti(C_4H_2Ph_2)$ are in the α and β' positions while the an α,α' arrangement of methyl substituents is obtained with $Cp_2Ti(C_4H_2Me_2)$[101]. Rothwell and co-workers reported[43,99] that in some cases α,β substituted titanacyclopentadiene can rearrange to the more thermodynamically favored α,α' isomer. Compounds **16a,b** and **17a** do not isomerize when heated to 80 °C in benzene.

The solid-state structure of complex **16a** was determined by X-ray crystallography. Complete crystallographic data can be found in the appendix. The molecular structure of complex **16a** is shown in Figure 1- 12 and selected bond distances and angles in Table 1- 2.

*Table 1- 2. Selected Bond Distances (Å) and Angles (deg) for Complex **16b***

Bond Distances			
Ti(1)-C(1)	2.046(11)	Ti(1)-C(4)	2.070(10)
Ti(1)-N(1)	1.989(8)	Ti(1)-N(2)	2.009(8)
Ti(1)-N(3)	2.172(8)	C(1)-C(2)	1.348(13)
C(2)-C(3)	1.553(14)	C(3)-C(4)	1.357(13)
Bond Angles			
N(2)-Ti(1)-N(3)	74.1(3)	C(1)-Ti(1)-C(4)	100.7(4)
N(2)-Ti(1)-N(1)	141.5(3)	N(3)-Ti(1)-N(1)	73.6(3)
Ti(1)-N(3)-C(1)	155.6(4)	Ti(1)-N(3)-C(4)	103.6(4)
C(30)-N(1)-C(17)	109.8(7)	C(18)-N(2)-C(11)	112.3(7)
C(17)-N(1)-Ti(1)	121.8(6)	Ti(1)-N(2)-C(11)	122.1(6)
Ti(1)-N(1)-C(30)	128.3(6)	Ti(1)-N(2)-C(18)	125.3(6)

References start on page 80

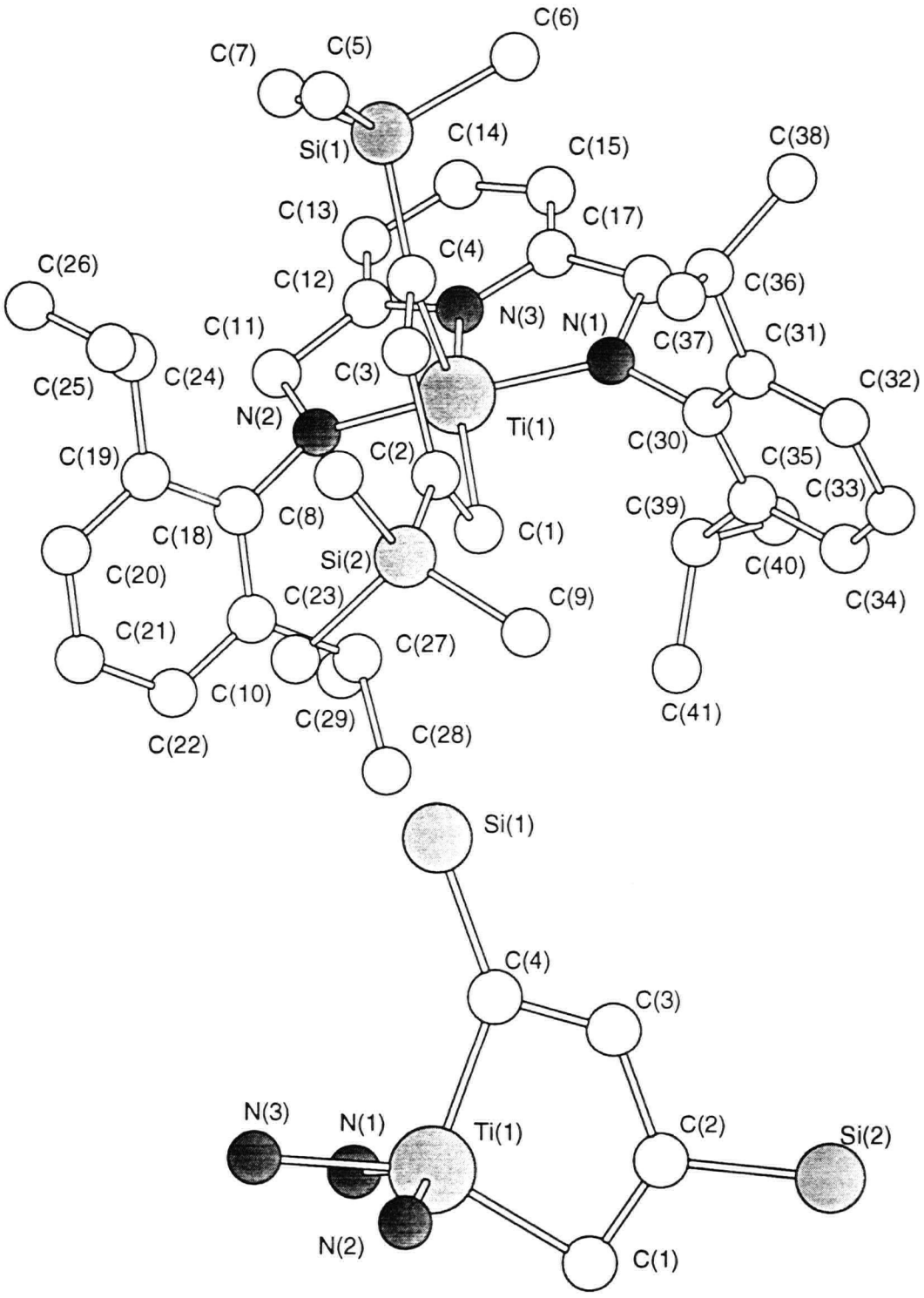

Figure 1- 12. Top: Chem 3D™ representation of the molecular structure of ***16b****.*

Bottom: Chem 3D™ representation of the core of ***16b***

References start on page 80

As previously noted for compound **9b**, the structure of the titanacyclopentadiene complex **16a** is also best described as a distorted square base pyramid with the metallacycle carbon C(4) occupying the apical position. The titanium lies approximately 0.45 Å above the basal plane defined by the three nitrogen atoms and C(1). The Ti-amide distances are comparable to those observed in complex **9b**. Finally, the short-long-short {1.348(13)-1.553(14)-1.357(13)} bond distances and the planarity of the metallacycle are consistent with its diene formulation. Similar geometrical parameters have been reported for titanacyclopentadienes supported by alkoxide[99] or cyclopentadienyl[101] ligands.

It has been proposed that the mechanism for the cyclotrimerization of alkyne using early transition metal complexes proceeds through a Diels-Alder "7-metallanorbornadiene" adduct[83]. This type of intermediate requires attack of the incoming alkyne on one of the two faces of the metallacyclopentadiene. The structure of complex **16a** (Figure 1- 12) demonstrates the steric congestion created by the 2,6-diisopropylphenyl group about the N_3 plane. Approach of a third alkyne on either face of the metallacycle is thwarted by the sterically demanding ligand. This may explain the lack of insertion chemistry observed with this complex.

Unlike compounds **13-17a** and **15b** which do not react with excess alkyne (110 °C, 24 h), compound **16b** reacts with excess alkyne at 80 °C to give the asymmetric metallacycle derivatives **18b** and **19b** in quantitative yield by ^{1}H NMR spectroscopy (eq. 11). The ^{1}H NMR spectrum of compound **18b** is shown in Figure 1- 13.

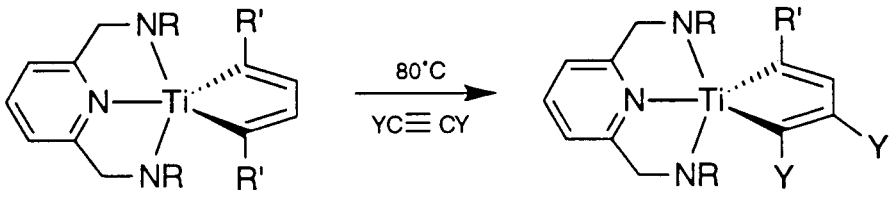

16b → **18b**, Y = Et; **19b**, Y = Pr

R = 2,6-$Me_2C_6H_3$
R' = $SiMe_3$

(11)

References start on page 80

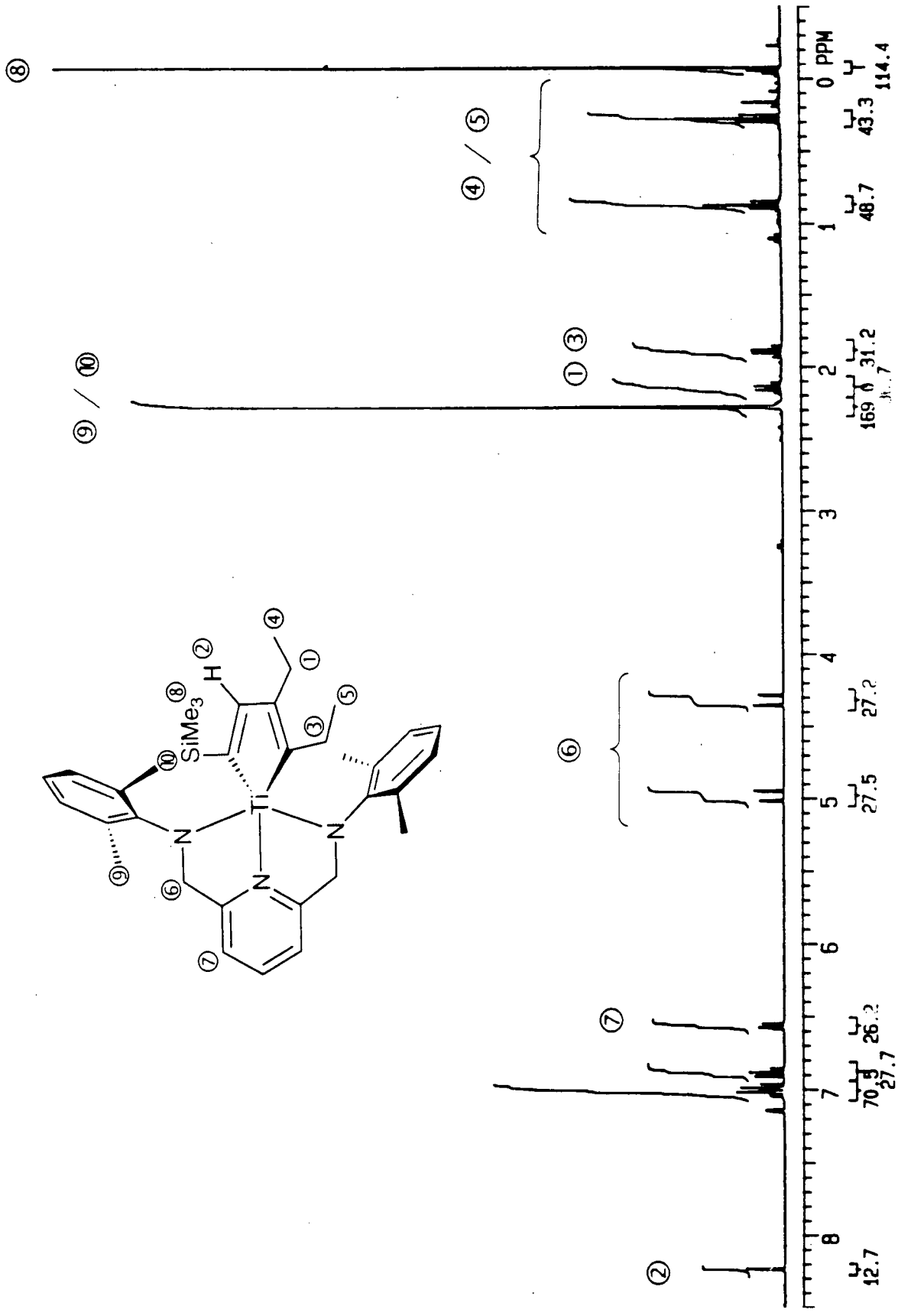

*Figure 1- 13. ^1H NMR spectrum of complex **18b** (300 MHz, C_6D_6)*

References start on page 80

The substitution pattern of the metallacycle was established based on the results of NOE experiments. For example, irradiation of the CH_2Me signal at 2.14 ppm (Figure 1- 13 ①) caused the enhancement of the metallacycle proton resonance at 8.23 ppm (Figure 1- 13 ②). Irradiation of other groups was consistent with this assignment. This is in agreement with the metallacycle proton being in proximity to one of the ethyl groups.

Two mechanisms have been proposed for the substitution of alkynes in metallacyclopentadiene complexes. The fragmentation of the metallacycle to an intermediate bis(alkyne) complex has been proposed to explain the exchange of alkyne in $(Ar"O)_2Ti(C_4Et_4)$[43,99] (Scheme 1- 7, path A). The other approach involves the dissociation of the metallacycle into a mono(alkyne) adduct and free alkyne (Scheme 1- 7, path B). This pathway has been proposed for alkyne exchange in tantalum alkoxide systems[52].

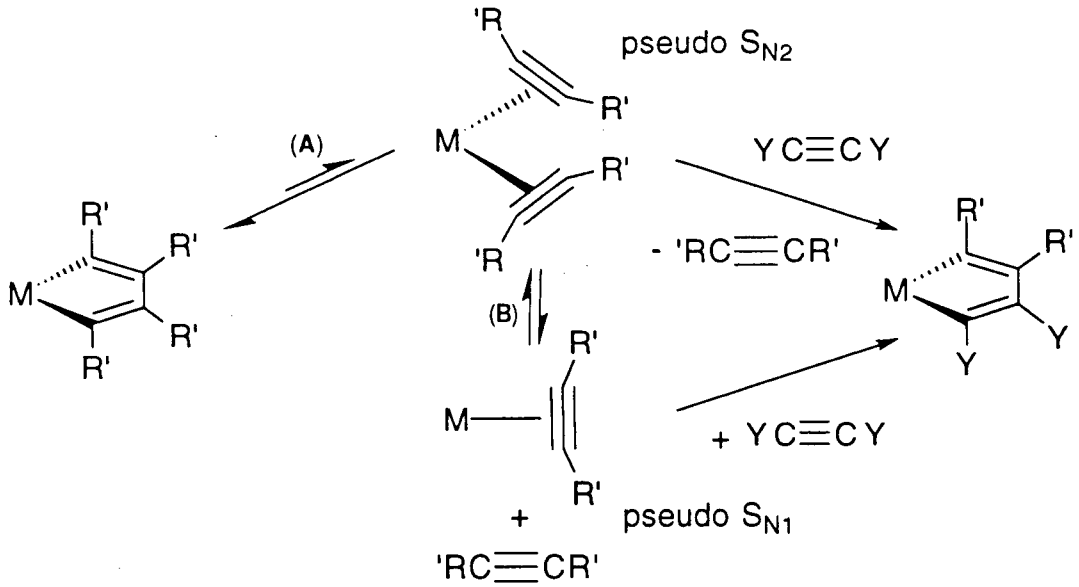

Scheme 1- 7. Proposed mechanisms for alkyne exchange

It is not possible to distinguish which mechanism is operative in the formation of complexes **18b** and **19b**. It is, however, important to note that only one of the original alkynes is substituted. The steric congestion of the tri-substituted metallacycle obtained might explain the

References start on page 80

lack of further exchange. Furthermore, with the more sterically imposing 2,6-diisopropylphenyl ligand, no evidence of alkyne exchange was observed.

2.6 Reduction of titanium dichloride complexes: ligand C-H bond activation

As mentioned above, the reduction of complex **3b** in the presence of 3-hexyne or 4-octyne yields a mixture of compounds from which the desired metallacycle can be observed by spectroscopic means. However, when the reduction is performed in the presence of MeC≡CPh, the side product (**20b**) is formed in high yield and can be isolated.

The ^{1}H NMR spectrum of compound **20b** as well as the signal assignments are shown in Figure 1- 14. The spectrum displays two AB quartet patterns for the ligand methylene protons (③ ,NCH_AH_B). This indicates that all four protons are inequivalent and that the complex has C_1 symmetry. Moreover only three resonances attributable to the ligand aryl methyl groups are observed (⑨). A combination of ^{1}H homonuclear decoupling experiments (Figure 1- 15) and ^{1}H-^{13}C heteronuclear correlation spectroscopy (Figure 1- 16) were used in proposing a structure for complex **20b**. The quartet at 3.64 ppm (③) collapses to a singlet upon irradiation of the doublet at 1.97 ppm (⑦) (Figure 1- 15). These signals are attributable to a vinyl moiety resulting from the insertion of MeC≡CPh into a Ti-H bond (Ti–C(Ph)=CHMe). A coupling of 6.2 Hz is observed between the vinylic C-H and the methyl group, characteristic for this type of fragment[102].

The proposed mechanism for the formation of complex **20b** is shown in Scheme 1- 8. In the first step, the Ti^{IV} dichloride precursor is reduced to a Ti^{II} complex (**A**). This intermediate then activates the methyl group of the arene to yield a Ti-H complex (**B**). Presumably, the isopropyl methine in complex **3a** is well protected by the isopropyl methyl groups and this activation does not occur. A molecule of PhC≡CMe is then inserted into the newly formed titanium-hydride bond to generate the vinyl moiety shown in **C.**

References start on page 80

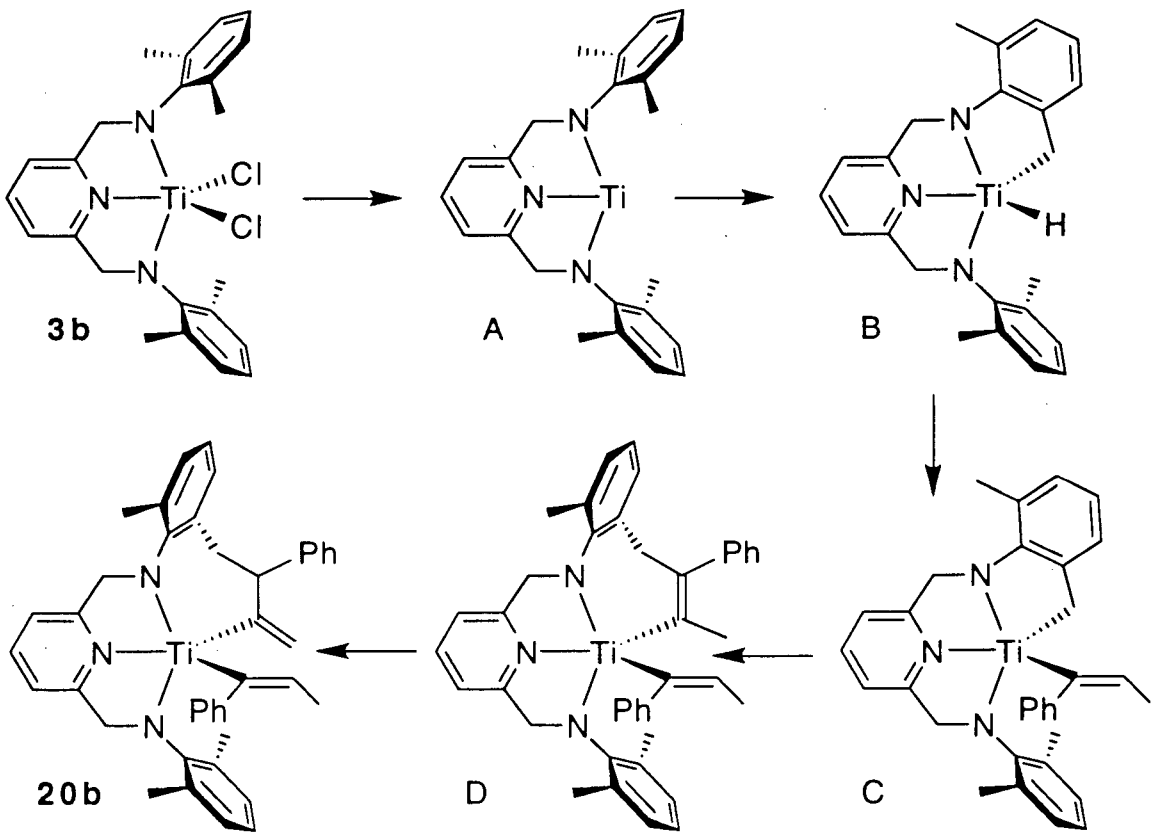

Scheme 1- 8. Proposed mechanism for the formation of complex 20b

Insertion of a second equivalent of PhC≡CMe into the Ti-C bond of complex **C** followed by a 1,3-hydrogen shift yields the final product **20b**. The proton shift may occur in an attempt to relieve ring strain.

Attempts to isolate a Ti^{II} complex by the reduction of complex **3a,b** in the presence of a donor ligand such as PMe_3 or pyridine were unsuccessful. It is not clear why this ligand-activated complex forms in such high yield with certain alkynes. There is no evidence of the formation of a similar product when the dichloride complex **3b** is reduced in the presence of diphenylacetylene or trimethylsilylacetylene. This type of ligand activation may prove to be one of the major drawback in the use of these complexes for the catalytic cyclization of alkynes since Ti^{II} species are key intermediates.

References start on page 80

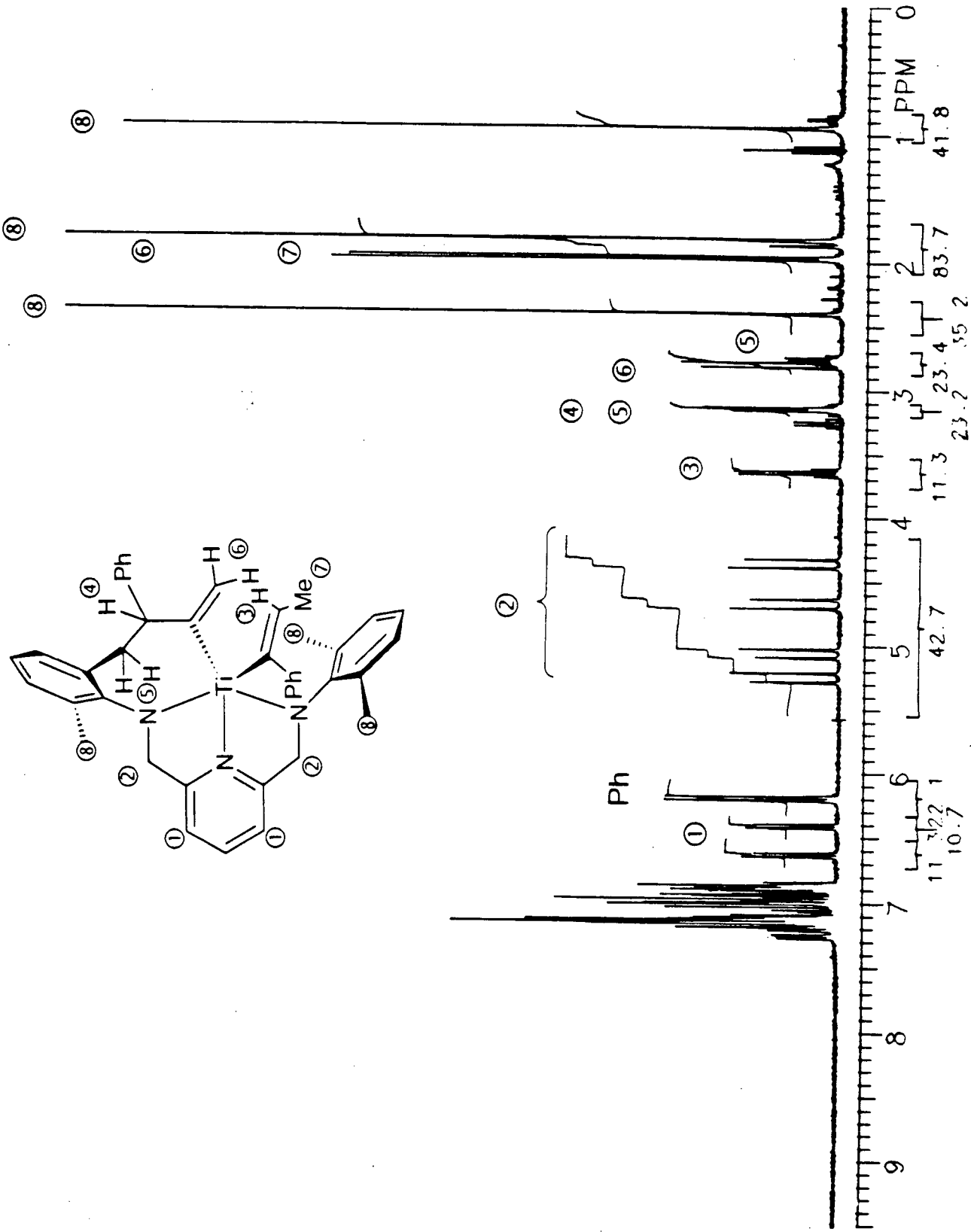

*Figure 1- 14. ^1H NMR spectrum of complex **20b** (300 MHz, C_6D_6)*

References start on page 80

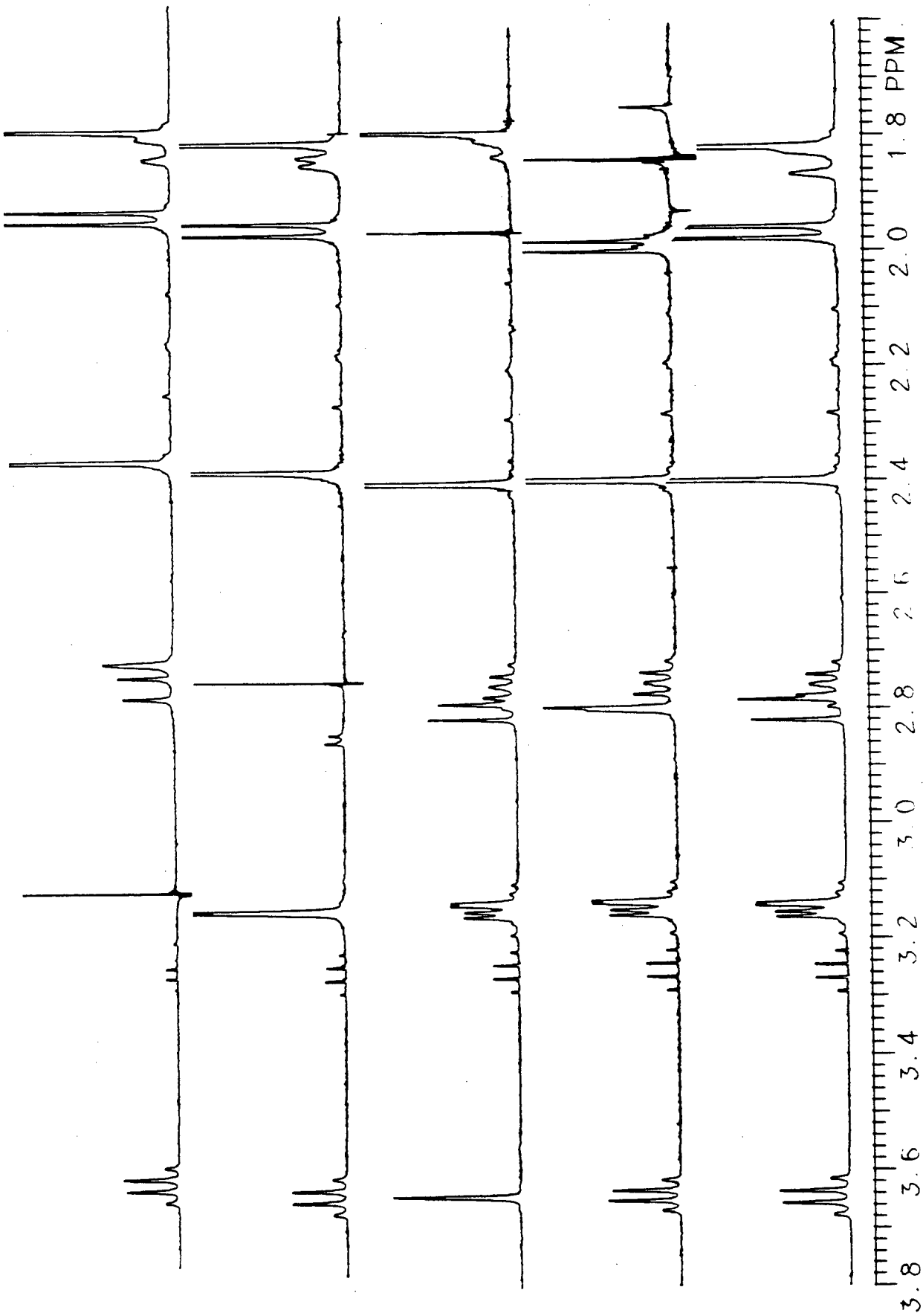

Figure 1- 15. ^1H Homonuclear decoupling spectra of complex ***20b*** *(300 Mhz, C_6D_6)*

References start on page 80

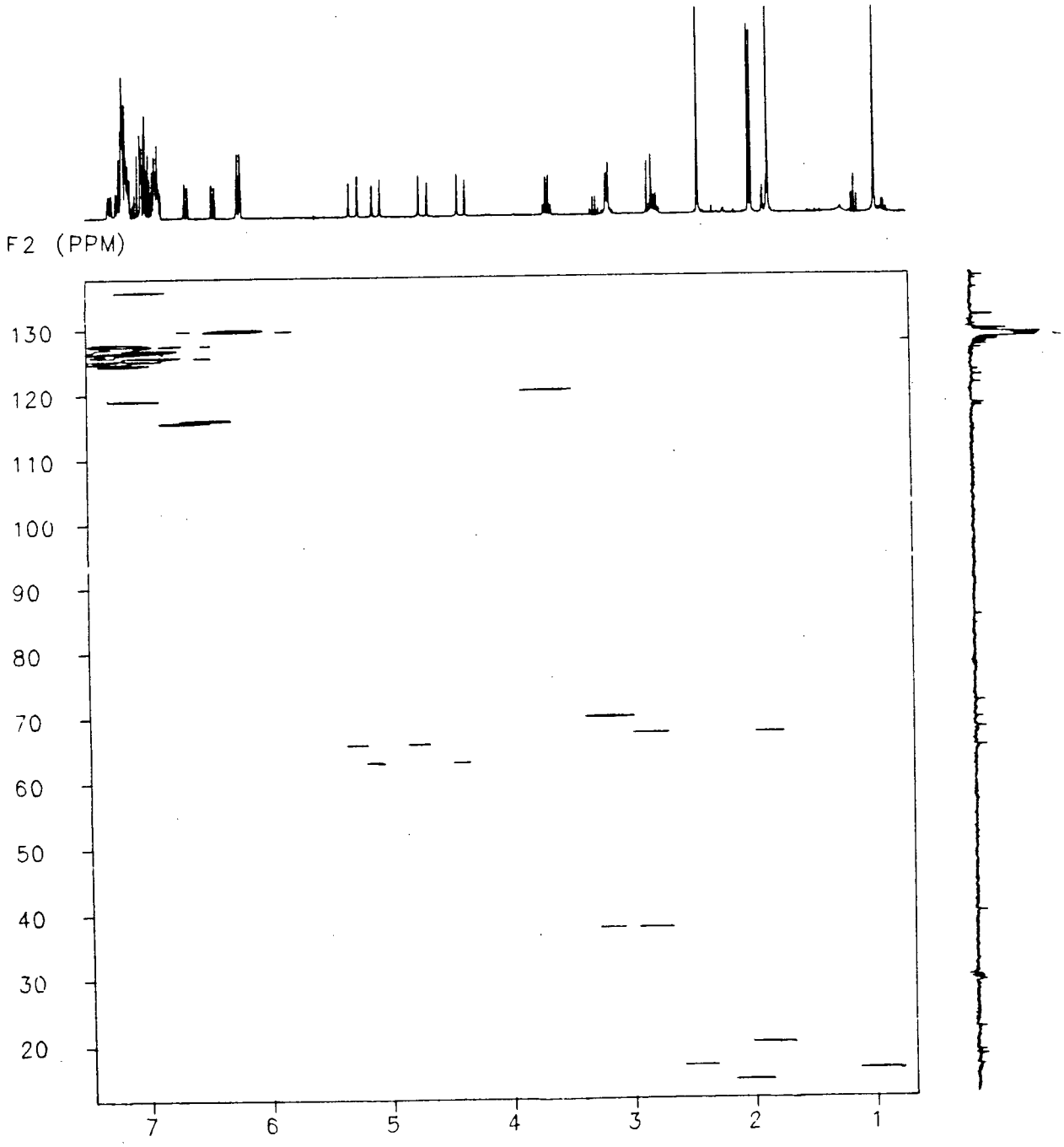

Figure 1- 16. ^{1}H ^{13}C HETCOR spectrum of complex ***20b*** *(300 MHz, C_6D_6)*

References start on page 80

2.7 Zwitterionic complex and reaction with olefins.

The reaction of complex **16a** with 1 equivalent of $B(C_6F_5)_3$ in pentane at low temperature results in the formation of the zwitterionic complex eq. 12).

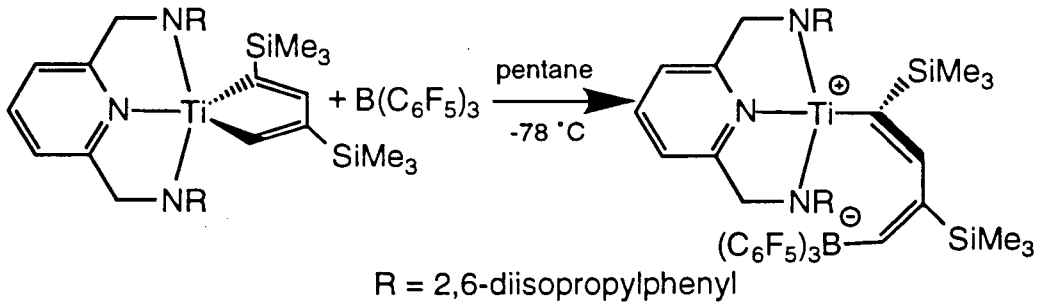

(12)

R = 2,6-diisopropylphenyl

16a **22a**

Restricted rotation about the Ti–vinyl bond is advanced to account for the observed C_s symmetric geometry. This is consistent with the AB pattern observed for the ligand methylene protons (CH_2N) in the ^1H NMR spectrum of compound **22a** . Four isopropyl methine and eight isopropyl methyl resonances are observed as a consequence of restricted rotation about the N-C_{ipso}. Two low field resonances (9.29 and 8.07 ppm) are assigned to the two dienyl protons (C*H*). The resonance at 9.29 ppm appears as a multiplet possibly a result of long range coupling to ^{19}F. This is consistent with the borane attacking the least substituted α-carbon of the metallacycle complex. In the absence of ^{19}F NMR data, it is not possible to establish with certainty the nature of complex **22a** but a similar titanocene-based complex has been structurally characterized[103]. Erker and co-worker[104] reported the unusual reactivity of $B(C_6F_5)_3$ with the metallacyclopentadiene derivative $Cp_2Zr(C_4Me_4)$. They showed that the borane did not attack the α-carbon atoms of the metallacycle but one of the carbon of the Cp rings to form a zirconocene-betaine system. The steric protection offered by the 2,6-diisopropylphenyl group of the ligand in complex **16a** may explain the difference in reactivity. The amide groups are sterically protected and the borane can only attack the α-carbon atoms of the metallacycle.

References start on page 80

Attempts to generate a similar compound from metallacycle **16b** and $B(C_6F_5)_3$ were unsuccessful. This might be a result of both α-carbons being protected by the large $SiMe_3$ groups.

No reaction is observed upon addition of excess 1-hexene or ca. 3 atm. of ethylene to complex **22a** in pentane or toluene. Similarly, no reaction is observed when complex **16a** is heated to 60 °C in the presence of 1-hexene. However, a small amount of a white insoluble material is obtained when complex **16b** is heated to 60 °C in the presence of 3 atm. of ethylene. The insolubility of the white material prevented its identification by ^1H NMR spectroscopy. It has already been shown that $[(ArO)_2Ti(C_4Et_4)]$ (Ar = 2,6-diphenylphenoxide) reacts with ethylene to produce $[(ArO)_2Ti(C_4H_8)]$ along with 1 equiv of a substituted 1,3-cyclohexadiene (eq. 13)[105]. We see no evidence for the formation of $(BDMP)Ti(C_4H_8)$ or 1,3-bis(trimethylsilyl)1,3-hexadiene. Complex **16b** did not react with 1-hexene.

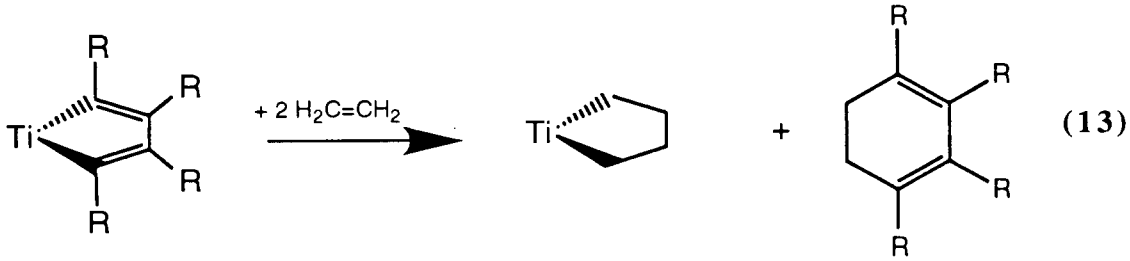

(13)

References start on page 80

3 Conclusions

Pyridine diamide complexes of titanium can be synthesized in high yield from $TiCl_4$ and the silylated compound **2a,b** using the elimination of Me_3SiCl as a driving force for the reaction. Both mono(alkyl) and bis(alkyl) complexes are stabilized by this pyridine diamide ligand system. However, the dimethyl derivatives are thermally unstable.

The dichloride complexes can be reduced in the presence of internal and terminal alkynes to give the corresponding metallacyclopentadiene derivatives in good yield. No reaction is observed between the titanacyclopentadiene complexes **13-17a**, and **15b** and excess alkyne or acetonitrile. On the other hand, alkyne exchange has been observed with complex **16b**. The symmetrical metallacycles ($L_nTiC_4R_4$, R = Et, Pr) are formed in low yield. The activation of the methyl groups of the ligand appears to compete with the formation of the desired metallacycle. The bulkier 2,6-diisopropylphenyl ligand does not engage in ligand activation. However, the steric bulk of the ligand precludes further reactivity of the metallacyles.

References start on page 80

4 Experimental Details

General Details. All experiments were performed under a dry dinitrogen atmosphere using standard Schlenk techniques or in an Innovative Technology Inc. glovebox. Solvents were distilled from sodium/benzophenone ketyl (DME, THF, hexanes, diethylether and benzene) or molten sodium (toluene) under argon and stored over activated 4Å molecular sieves. Titanium(IV) chloride and methylmagnesium bromide were purchased from Aldrich and used as received. Phenylacetylene, diphenylacetylene, 1-phenylpropyne, 3-hexyne, 4-octyne, trimethylsylilacetylene, 2,6-diisopropylaniline, 2,6-dimethylaniline, cyclohexylamine, *iso*-propylamine, *tert*-butylamine, triethylamine, chlorotrimethylsilane, bromotrimethylsilane were purchased from Aldrich and distilled before use. A CH_2Cl_2 solution of 2,6-bis(bromomethyl)pyridine•HBr[86] was extracted with $NaHCO_3$ to yield 2,6-bis(bromomethyl)pyridine. LiNR($SiMe_3$) (R = 2,6-^{i}Pr$_2$C$_6$H$_3$, 2,6-$Me_2C_6H_3$) was prepared as noted in the literature[106]. $MgBr_2$•$2Et_2O$ was made from Mg and $BrCH_2CH_2Br$ in ether. The Me_3SiCH_2Li[107], $Li(CH_2C_6H_4$-*o*-$NMe_2)$[108], $Mg(C_4H_6)$•2THF[92] and NaC_5H_5•DME[109] were prepared using previously reported syntheses. Proton (300 MHz) and carbon (75.46 MHz) NMR spectra were recorded in C_6D_6 at approximately 22 °C on a Varian Gemini-300 or 300-XL spectrometer. The proton chemical shifts were referenced to internal C_6D_5H (δ = 7.15 ppm) and the carbon resonances to C_6D_6 (δ = 128.0 ppm). The elemental analysis were performed using sealed tin cups on a Fisons Instruments model 1108 elemental analyzer by Mr. Peter Borda of UBC or by Oneida Research Services Inc., Whitesboro, NY.

2,6-$(RHNCH_2)_2$-NC_5H_3, (R = 2,6-diisopropylphenyl), $(BDPP)H_2$ (1a). A THF (150 mL) solution of LiNHR (12.226 g, 66.77 mmol) was added slowly to a THF (100 mL) solution of 2,6-bis(bromomethyl)pyridine (8.842 g, 33.37 mmol) at -78 °C. The mixture was allowed to warm to room temperature and stirred for 12 h. The solution was quenched with a saturated $NaHCO_3$ solution (100 ml) and extracted with diethyl ether. The solvent was removed

References start on page 80

in *vacuo* to yield a yellow-brown viscous liquid. The oil was then dissolved in hot hexanes and cooled to -30 °C. White crystalline **1a** was isolated by filtration and dried under vaccum (7.792 g, 17.02 mmol, 51%). ^{1}H NMR δ 7.20-7.10 (m, 6H, Ar), 7.12 (t, 1H, py), 6.84 (d, 2H, py), 4.24 (s, 4H, NCH_2), 4.21 (br s, 2H, N*H*), 3.53 (sept, 4H, C*H*Me$_2$), 1.24 (d, 24H, CH*Me*$_2$). ^{13}C{^{1}H} NMR δ 158.21, 154.18, 143.27, 137.25, 125.12, 124.17, 121.16, 57.02, 28.24, 24.62. MS (EI) *m/z* 457.346 (M^+). Calcd for $C_{31}H_{43}N_3$: 457.346

2,6-(RHNCH$_2$)$_2$-NC$_5$H$_3$, (R = 2,6-dimethylphenyl), (BDMP)H$_2$ (1b). The preparation of compound **1b** is identical to that of **1a**. LiNHR (2.879 g, 22.65 mmol) and 2,6-bis(bromomethyl)pyridine (3.000 g, 11.32 mmol) yield a yellow-brown viscous liquid (3.105 g, 8.987 mmol, 79%). ^{1}H NMR δ 7.05-6.95 (m, 5H, Ar and py), 6.86 (m, 2H, Ar), 6.67 (d, 2H, py), 4.21 (br s, 2H, N*H*), 4.15 (s, 4H, NCH_2), 2.25 (s, 12H, Me). ^{13}C{^{1}H} NMR δ 159.04, 146.88, 136.72, 18.50, 129.24, 122.18, 120.24, 53.93, 18.87. MS (EI) *m/z* 345.220 (M^+). Calcd for $C_{23}H_{27}N_3$: 345.220.

2,6-(RHNCH$_2$)$_2$-NC$_5$H$_5$ (R = cyclohexyl) (CyAP)H$_2$ (1c). Solid 2,6-bis(bromomethyl)pyridine (5.000 g, 18.87 mmol) was added to a solution of cyclohexylamine (10.00 g, 100.8 mmol) in hexanes (50 mL). The solution got warm and a white solid started to form within minutes. The solution was stired for 12 hours at 23 °C and was quenched with 100 mL of a saturated aqueous $NaHCO_3$ solution and extracted with CH_2Cl_2. The solvent was removed in *vacuo* to yield a light yellow liquid **1c** (4.800 g, 15.92 mmol, 84 %). ^{1}H NMR δ 7.23 (t, 1H, py), 7.04 (d, 2H, py), 3.90 (s, 4H, NCH_2), 2.39 (br m, 2H, NC*H*(CH$_2$)$_2$), 1.81 (br m, 4H, Cy), 1.61 (br m, 4H, Cy), 1.12 (br m, 2H, Cy), 1.04 (br m, 8H, Cy). ^{13}C {^{1}H} NMR δ 160.88, 136.38, 120.00, 56.68 ($^1J_{CH}$ = 131 Hz), 53.00, 34.00, 26.70, 25.18. MS (EI) *m/z* 300.243 {$(M-1)^+$}. Calcd. for $C_{19}H_{30}N_3$: 300.244.

2,6-(RHNCH$_2$)$_2$-NC$_5$H$_5$ (R = *iso*-propyl) (iPAP)H$_2$ (1d). The preparation of compound **1d** is identical to that of **1c**. 2,6-bis(bromomethyl)pyridine (5.000 g, 18.87 mmol) and cyclohexylamine (10.00 g, 169.2 mmol) yield a yellow liquid **1d** (7.820 g, 18.75 mmol, 99

References start on page 80

%). ^{1}H NMR δ 7.20 (t, 1H, py), 7.02 (d, 2H, py), 3.86 (s, 4H, NCH_2), 2.70 (sept, 2H, CHMe$_2$), 1.56 (br s, 2H, NH), 0.97 (s, 12H, CHMe_2). ^{13}C {^{1}H} NMR δ 160.65, 136.34, 119.99, 53.45, 48.64 ($^1J_{CH}$ = 130 Hz), 23.27. MS (EI) *m/z* 221.187 (M)$^+$. Calcd. for $C_{13}H_{23}N_3$: 221.189.

2,6-(RHNCH$_2$)$_2$-NC$_5$H$_5$ (R = *tert*-butyl) (tBAP)H$_2$ (1e). The preparation of compound **1e** is identical to that of **1c**. 2,6-bis(bromomethyl)pyridine (5.000 g, 18.87 mmol) and *t*-butylamine (10.00 g, 136.7 mmol) in hexanes (50mL) yield a light yellow liquid **1e** (4.580 g, 18.36 mmol, 97 %). ^{1}H NMR δ 7.16 (m, 1H, py), 7.14 (d, 2H, py), 3.89 (s, 4H, NCH_2), 1.55 (br s, 2H, NH), 1.05 (s, 18H, *t*-Bu). ^{13}C {^{1}H} NMR δ 161.07, 135.44, 120.10, 50.35, 49.09, 29.23. MS (EI) *m/z* 249.221 (M$^+$). Calcd. for $C_{15}H_{27}N_3$: 249.221.

2,6-[RN(SiMe$_3$)CH$_2$]$_2$-NC$_5$H$_3$(R = 2,6-diisopropylphenyl), (BDPP)(SiMe$_3$)$_2$ (2a). A DME (150 mL) solution of LiNR(SiMe$_3$) (8.820 g, 35.53 mmol) was added slowly to a DME (100 mL) solution of 2,6-bis(bromomethyl)pyridine (4.621 g, 17.44 mmol) at -30 °C. The mixture was allowed to warm to room temperature and stirred for 12 h. The solvent was removed in *vacuo* and the resulting solid extracted with hexanes (3 × 100 mL) and filtered through Celite. The volume of the filtrate was reduced to 50 mL and cooled to -30 °C for 12 h. A white crystalline solid was isolated by filtration and dried under vacuum (4.530 g, 7.502 mmol, 44%). ^{1}H NMR δ 7.15 (t, 2H, Ar), 7.02 (d, 4H, Ar), 6.48 (t, 1H, py), 6.47 (d, 2H, py), 4.28 (s, 4H, NCH_2), 3.31 (sept, 4H, CHMe$_2$), 1.17 (d, 12H, CHMe_2), 0.90 (d, 12H, CHMe_2), 0.27 (s, 18H, SiMe_3). ^{13}C{^{1}H} NMR δ 159.88, 148.69, 143.40, 135.88, 126.30, 124.24, 122.28, 58.78, 27.94, 25.18, 1.06. MS (EI) *m/z* 601.423 (M$^+$). Calcd for $C_{37}H_{59}N_3Si_2$: 601.424.

2,6-[RN(SiMe$_3$)CH$_2$]$_2$-NC$_5$H$_3$, (R = 2,6-dimethylphenyl) (BDMP)(SiMe$_3$)$_2$ (2b). The preparation of compound **2b** is identical to that of compound **2a**. LiNR(SiMe$_3$) (4.500 g, 23.30 mmol) and 2,6-bis(bromomethyl)pyridine (3.083 g, 11.73 mmol) gave a white crystalline solid (**2b**) (2.389 g, 4.882 mmol, 42%). ^{1}H NMR δ 6.98-6.88 (t, 6H, Ar), 6.72 (t, 1H, py), 6.34 (d, 2H, py), 4.18 (s, 4H, NCH_2), 2.01 (s, 12H, Me), 0.23 (s, 18H, SiMe_3).

References start on page 80

$^{13}C\{^1H\}$ NMR δ 159.89, 146.32, 138.22, 135.54, 128.74, 125.09, 121.51, 56.50, 19.30, 0.87. MS (EI) *m/z* (M^+) 489.300. Calcd for $C_{29}H_{43}N_3Si_2$: 489.300.

2,6-[RN(SiMe$_3$)CH$_2$]$_2$-NC$_5$H$_3$, (R = cyclohexyl) (CyAP)(SiMe$_3$)$_2$ (2c). $ClSiMe_3$ (3.243 g, 29.85 mmol) was added dropwise to a diethylether solution (50 mL) of $(CyAP)H_2$ (3.000 g, 9.951 mmol). The reaction mixture was stired at room temperature for 12 hours. A solution of Et_3N (5.035 g, 49.76 mmol) in diethylether (50 mL) was added to the reaction mixture which was stirred for 12 hours. The solvent was removed in *vacuo*. The white solid was then extracted with hexanes (500 mL). The volume of the solution was reduced to 25 mL and the solution cooled to -30 °C for 12 hours. White crystalline **2c** was isolated by filtration and dried in *vacuo* (3.987 g, 8.943 mmol, 90 %). ^1H NMR δ 7.30 (m, 3H, py), 4.28 (s, 4H, NCH_2), 2.82 (tt, 2H, NC*H*), 1.28 (m, 8H, Cy), 1.40 (m, 6H, Cy), 1.09 (m, 4H, Cy), 0.85 (m, 2H, Cy), 0.17 (s, 18H, SiMe_3). $^{13}C\{^1H\}$ NMR δ 164.56, 135.95, 118.57, 57.59, 50.20, 33.99, 26.88, 26.00, 0.84. MS (EI) *m/z* $(M-1)^+$ 444.323. Calcd for $C_{25}H_{46}N_3Si_2$: 444.323.

2,6-[RN(SiMe$_3$)CH$_2$]$_2$-NC$_5$H$_3$, (R = isopropyl) (iPAP)(SiMe$_3$)$_2$ (2d). The preparation of compound **2d** is similar to that of compound **2c**. $(iPAP)H_2$ (2.000 g, 9.036 mmol), $BrSiMe_3$ (4.565 g, 29.82 mmol) and Et_3N (4.574 g, 45.20 mmol) gave a white low melting solid (**2d**) (3.250 g, 8.887 mmol, 98 %). ^1H NMR δ 7.28 (t, 1H, py), 7.19 (d, 2H, py), 4.14 (s, 4H, NCH_2), 3.28 (sept, 2H, NC*H*Me$_2$), 0.94 (d, 12H, NCHMe_2), 0.12 (s, 18H, SiMe_3). $^{13}C\{^1H\}$ NMR δ 164.35. 135.89. 118.50. 48.89. 48.03. 22.94. 0.62. MS (EI) *m/z* (M^+) 365.265. Calcd for $C_{19}H_{39}N_3Si_2$: 365.268.

2,6-[RN(SiMe$_3$)CH$_2$]$_2$-NC$_5$H$_3$, (R = t-butyl) (tBAP)(SiMe$_3$)$_2$ (2e). The preparation of compound **2e** is identical to that of compound **2c**. $(tBAP)H_2$ (2.500 g, 10.02 mmol), $BrSiMe_3$ (5.064 g, 33.08 mmol) and Et_3N (5.060 g, 50.00 mmol) gave a white crystalline solid (**2e**) (3.895 g, 9.894 mmol, 99 %). ^1H NMR δ 7.33 (m, 4H, py), 4.32 (s, 4H, NCH_2), 1.11 (s, 18H, CMe_3), 0.21 (s, 18H, SiMe_3). $^{13}C\{^1H\}$ NMR δ 162.28, 136.08, 118.02, 54.69, 51.92, 30.88, 4.10. MS (EI) *m/z* (M^+) 393.298. Calcd for $C_{21}H_{43}N_3Si_2$: 393.300.

References start on page 80

(BDPP)$TiCl_2$ (3a). Liquid $TiCl_4$ (1.850 g, 9.752 mmol) was added in small portions to a toluene (50 mL) solution of BDPP($SiMe_3$)$_2$ (5.880 g, 9.737 mmol) at -40 °C. The solution immediately turned bright red and was heated to 80 °C for 12 h. The solution was filtered through Celite and the solvent removed in *vacuo*. The resulting solid was washed with cold hexanes (3 × 50 mL) to yield a bright red powder (4.450 g, 7.747 mmol, 80%). ^{1}H NMR δ 7.14 (m, 6H, Ar), 6.75 (t, 1H, py), 6.27 (d, 2H, py), 4.87 (s, 4H, NCH_2), 3.75 (sept, 4H, CHMe$_2$), 1.53 (d, 12H, CHMe_2), 1.19 (d, 12H, CHMe_2). ^{13}C{^{1}H} NMR δ 161.58, 154.08, 142.83, 138.88, 124.80, 117.56, 103.30, 70.60, 28.58, 26.33, 25.12. Anal. calcd. for $C_{31}H_{41}N_3TiCl_2$: C, 64.81; H, 7.19; N, 7.31. Found: C, 64.35; H, 7.08; N, 6.95.

(BDMP)$TiCl_2$ (3b). The preparation of compound **3b** is identical to that for compound **3a**. $TiCl_4$ (2.35 mL , 1.04 M, 2.444 mmol) and compound **2b** (1.088 g, 2.223 mmol) gave a bright red solid (**2b**) (0.839 g, 1.815 mmol, 82%). ^{1}H NMR δ 7.05-6.95 (m, 6H, Ar), 6.85 (t, 1H, py), 6.36 (d, 2H, py), 4.52 (s, 4H, NCH_2), 2.42 (s, 12H, Me). ^{1}H NMR (CD_2Cl_2) δ 8.09 (t, 1H, py), 7.58 (d, 2H, py), 7.15-7.00 (m, 6H, Ar), 5.8 (s, 4H, NCH_2), 2.32 (s, 12H, Me). ^{13}C{^{1}H} NMR (CD_2Cl_2) δ 163.51, 154.50, 140.29, 133.54, 129.22, 126.91, 118.96, 69.13 (CH_2N), 19.48.

(CyAP)$TiCl_2$ (3c). The preparation of compound **3c** is identical to that for compound **3a**. $TiCl_4$ (0.247 g, 1.302 mmol) and compound **2c** (0.580 g, 1.301 mmol) gave an orange crystalline solid (**3c**) (0.273 g, 0.653 mmol, 50 %) when recrystalized from CH_2Cl_2 at -30 °C. ^{1}H NMR δ 7.06 (t, 1H, py), 6.58 (d, 2H, py), 5.54 (tt, 2H, NCH), 4.42 (s, 4H, NCH_2), 2.30 (d, 4H, Cy), 1.80 (d, 4H, Cy), 1.55 (m, 6H, Cy), 1.10 (m, 6H, Cy). ^{13}C{^{1}H} NMR δ 164.60, 137.63, 117.51, 62.79, 61.27, 30.50, 26.94, 26.49.

(iPAP)$TiCl_2$ (3d). The preparation of compound **3d** is identical to that for complex **3a**. $TiCl_4$ (1.073 g, 5.656 mmol) and compound **2d** (1.880 g, 5.140 mmol) gave bright orange crystalline **3d** (1.257 g, 3.717 mmol, 72 %). ^{1}H NMR δ 6.95 (t, 1H, py), 6.47 (d, 2H, py),

References start on page 80

5.97 (sept, 2H, NC*H*Me$_2$), 4.31 (s, 4H, NC*H*$_2$), 1.22 (d, 12H, NCH*Me*$_2$). $^{13}C\{^1H\}$ NMR δ 164.58, 137.46, 117.51, 59.61, 53.80, 19.57.

(tBAP)TiCl (3e). Liquid $TiCl_4$ (0.096 g, 0.506 mmol) was added in small portions to a toluene (50 mL) solution of (tBAP)$(SiMe_3)_2$ (0.200 g, 0.508 mmol) at -40 °C. The solution immediately turned bright red then green and was heated to 80 °C for 12 h. The solution was filtered through Celite and the solvent removed in *vacuo*. The resulting solid was washed with cold hexanes (3 × 50 mL) to yield a green powder. The green powder was dissolved in a minimum ammount of CH_2Cl_2 and cooled to -30 °C. Compound **3e** was isolated by filtration as a dark green crystalline solid and dried under vaccum (0.183 g, 0.405 mmol, 80 % based on the formulation (tBAP)$TiCl_2 \bullet CH_2Cl_2$).

(BDPP)TiMe$_2$ (4a). To a diethyl ether (25 mL) suspension of compound **3a** (0.500 g, 0.870 mmol) was added 2 equiv of MeMgBr (0.58 mL, 3.0 M, 1.7 mmol) at -78 °C. The solution changed from orange to dark red within minutes and was stirred for 12 h. The solvent was removed in *vacuo*. The resulting solid was extracted with toluene (3 × 10 mL) and filtered through Celite to give a red-brown solution. The solvent was removed in vacuo, the solid dissolved in a minimum amount of diethyl ether, and cooled to -30 °C for 12 h. Bright yellow crystalline **4a** was isolated by filtration and dried under vacuum (0.314 g, 0.461 mmol, 53%). The solid is thermally and photolytically sensitive and was stored at -40 °C in the dark to prevent decomposition. ^1H NMR δ 7.02 (m, 6H, Ar), 6.76 (t, 1H, py), 6.30 (d, 2H, py), 4.98 (s, 4H, NC*H*$_2$), 3.69 (sept, 4H, C*H*Me$_2$), 1.28 (d, 12H, CH*Me*$_2$), 1.11 (d, 12H, CH*Me*$_2$), 1.06 (s, 6H, Ti*Me*). $^{13}C\{^1H\}$ NMR δ 162.93, 145.41, 137.87, 129.29, 126.33, 124.51, 117.03, 68.33, 64.40 (Ti*C*H$_3$), 28.11, 28.04, 24.35.

(BDMP)TiMe$_2$ (4b). The preparation of complex **4b** is identical to that of compound **4a**. Complex **3b** (0.100 g, 0.216 mmol) and MeMgBr (0.2 mL, 2.40 M, 0.48 mmol) gave a bright yellow crystalline solid (**4b**) (0.072 g, 0.171 mmol, 79%). The solid is thermally and photolytically sensitive and was stored at -40 °C in the dark to prevent decomposition. ^1H NMR δ

References start on page 80

7.21 (d, 4H, Ar), 7.08 (t, 2H, Ar), 6.91 (t, 1H, py), 6.47 (d, 2H, py), 4.73 (s, 4H, NCH_2), 2.38 (s, 12H, Me), 1.08 (s, 6H, Ti*Me*). $^{13}C\{^1H\}$ NMR d 163.49, 153.08, 137.50, 135.09, 129.09, 125.41, 117.13, 65.96, 62.28, 18.62.

(iPAP)TiMe$_2$ (4d). The preparation of complex **4d** is identical to that of compound **4a**. Complex **3d** (0.250 g, 0.739 mmol) and MeMgBr (0.62 mL, 3.0 M, 1.9 mmol) gave a bright yellow crystalline solid (**4d**) (0.152 g, 0.511 mmol, 69 %). The solid is thermally and photolytically sensitive and was stored at -40 °C in the dark to prevent decomposition. ^1H NMR δ 6.92 (t, 1H, py), 6.53 (d, 2H, py), 5.92 (sept, 2H, NC*H*Me$_2$), 4.59 (s, 4H, NCH_2), 1.44 (d, 12H, NCH*Me*$_2$), 0.81 (s, 6H, Ti*Me*). $^{13}C\{^1H\}$ NMR δ 164.52, 136.37, 116.91, 57.00, 50.36 ($^1J_{CH}$ = 133 Hz), 45.12, 21.17.

(BDPP)Ti(CH$_2$Ph)Cl (5a). To a diethyl ether (30 mL) suspension of compound **3a** (0.500 g, 0.870 mmol) was added 1 equiv of PhCH$_2$MgCl (0.62 mL, 1.4 M, 0.87 mmol) at 23 °C. The solution changed from orange to dark red within minutes and was stirred for 12 h. The solvent was removed in *vacuo*. The resulting solid was extracted with toluene (3 × 10 mL) and filtered through Celite to give a red-brown solution. The solvent was removed in vacuo, the solid dissolved in a minimum amount of hot hexanes, and cooled to -40 °C for 12 h. Dark red crystalline **5a** was isolated by filtration and dried under vacuum (0.418 g, 0.663 mmol, 75%). ^1H NMR δ 7.30-7.17, 6.90, 6.80 and 6.54 (Ar and CH$_2$*Ph*), 6.69 (t, 1H, py), 6.19 (d, 2H, py), 4.92 (AB quartet, $^2J_{HH}$ = 22.7 Hz, 4H, NCH_2), 4.71 (sept, 2H, C*H*Me$_2$), 3.72 (s, 2H, CH_2Ph), 3.09 (sept, 2H, C*H*Me$_2$), 1.60 (d, 6H, CH*Me*$_2$), 1.52 (d, 6H, CH*Me*$_2$), 1.30 (d, 6H, CH*Me*$_2$), 1.06 (d, 6H, CH*Me*$_2$). $^{13}C\{^1H\}$ NMR δ 161.57, 154.84, 149.49, 143.83, 142.69, 138.27, 127.52, 126.66, 125.30, 124.52, 124.39, 121.81, 117.04, 79.89, 69.41, 28.87, 26.17, 25.79, 24.96, 24.81. Anal. Calcd for $C_{38}H_{45}N_3TiCl \cdot C_6H_{14}$: C, 73.78; H, 8.72; N, 5.87. Found: C, 73.98; H, 8.42; N, 5.90.

(BDMP)Ti(CH$_2$Ph)$_2$ (6b). To a diethyl ether (30 mL) suspension of compound **3b** (0.100 g, 0.216 mmol) was added 2.2 equiv of PhCH$_2$MgCl (2.2 mL, 0.22 M, 0.48 mmol) at 23

References start on page 80

°C. The solution changed from orange to dark red within minutes and was stirred for 12 h. The solvent was removed in *vacuo*. The resulting solid was extracted with toluene (3 × 10 mL) and filtered through Celite to give a red-brown solution. The volume of the solvent was reduced (5 mL) and the solution cooled to -40 °C. Dark red crystalline **6b** was isolated by filtration (0.089 g, 0.124 mmol, 72%). ^{1}H NMR δ 7.17 (d, 4H, Ar), 7.05 (m, 2H, Ar), 6.88 (t, 4H, CH_2*Ph*), 6.77 (t, 1H, py), 6.62 (t, 2H, CH_2*Ph*), 6.60 (d, 4H, CH_2*Ph*), 6.25 (d, 2H, py), 4.59 (s, 4H, NCH_2), 2.62 (s, 4H, CH_2Ph), 2.46 (s, 12H, Me). ^{13}C{^{1}H} NMR δ 161.85, 156.88, 145.89, 137.83, 134.43, 129.26, 128.63, 125.49, 124.81, 122.31, 118.16, 116.83, 65.49, 19.92.

(BDPP)Ti(CH_2SiMe_3)Cl (7a). To a diethyl ether (30 mL) suspension of compound **3a** (0.500 g, 0.870 mmol) was added 1 equiv of $LiCH_2SiMe_3$ (0.082 g, 0.871 mmol) at 23 °C. The solution changed from orange to yellow within minutes and was stirred for 12 h. The solvent was removed in *vacuo*. The resulting solid was extracted with toluene (3 × 10 mL) and filtered through Celite. The solvent was removed in vacuo, the solid dissolved in a minimum amount of diethyl ether and cooled to -40 °C for 12 h. Yellow crystalline **7a** was isolated by filtration and dried under vacuum (0.430 g, 0.687) mmol, 79%). ^{1}H NMR δ 7.25-7.15 (Ar), 6.83 (t, 1H, py), 6.38 (d, 2H, py), 5.07 (AB quartet, $^2J_{HH}$ = 22.0 Hz, 4H, NCH_2), 4.39 (sept, 2H, C*H*Me$_2$), 3.25 (sept, 2H, C*H*Me$_2$), 2.89 (s, 2H, CH_2Si), 1.54 (d, 6H, CH*Me*$_2$), 1.45 (d, 6H, CH*Me*$_2$), 1.40 (d, 6H, CH*Me*$_2$), 1.11 (d, 6H, CH*Me*$_2$), -0.18 (s, 9H, Si(CH_3)$_3$). ^{13}C{^{1}H} NMR δ 162.76, 154.21, 143.74, 142.95, 138.62, 127.00, 126.52, 124.77, 124.35, 117.31, 83.70, 69.47, 38.83, 27.66, 26.81, 26.34, 25.28, 24.63, 2.34. Anal. Calcd for $C_{35}H_{52}N_3SiTiCl$: C, 67.13; H, 8.37; N, 6.71. Found: C, 67.08; H, 8.44; N, 5.79.

(BDMP)Ti(CH_2SiMe_3)$_2$ (8b). To a diethyl ether (30 mL) suspension of compound **3b** (0.100 g, 0.216 mmol) was added 2.2 equiv of $LiCH_2SiMe_3$ (0.045 g, 0.476 mmol) at -40 °C. The solution changed from orange to yellow within minutes and was stirred for 12 h. The solvent was removed in *vacuo*. The resulting solid was extracted with toluene (3 × 10 mL) and filtered through Celite. The solvent was removed in vacuo, the solid dissolved in a minimum

References start on page 80

amount of hexanes and cooled to -40 °C for 12 h. Yellow crystalline **8b** was isolated by filtration and dried under vacuum (0.112 g, 0.198 mmol, 92%). ^{1}H NMR δ 7.17 (d, 4H, Ar), 7.03 (m, 2H, Ar), 6.89 (t, 1H, py), 6.45 (d, 2H, py), 4.76 (s, 4H, NCH_2), 2.52 (s, 12H, Me), 1.84 (s, 4H, CH_2Si), -0.19 (s, 18H, Si(CH_3)$_3$). ^{13}C{^{1}H} NMR δ 162.64, 156.36, 138.17, 134.07, 129.35, 125.29, 117.10, 83.16, 66.23, 19.62, 2.38.

(BDMP)Ti(CH$_2$CMe$_2$Ph)Cl (9b). To a diethyl ether (30 mL) suspension of compound **3b** (0.400 g, 0.865 mmol) was added 1.1 equiv of PhCMe$_2$CH$_2$MgCl (1.09 mL, 0.867 M, 0.952 mmol) at -40 °C. The solution changed from orange to dark red within minutes and was stirred for 12 h. The solvent was removed in *vacuo*. The resulting solid was extracted with toluene (3 × 10 mL) and filtered through Celite. The solvent was removed in vacuo, the solid dissolved in a minimum amount of a 20:1 mixture of THF/benzene and cooled to -40 °C for 12 h. Red crystalline **9b** was isolated by filtration and dried under vacuum (0.400 g, 0.627 mmol, 72%). ^{1}H NMR δ 7.19-6.98 (m, 11H, Ar and Ph), 6.89 (t, 1H, py), 6.39 (d, 2H, py), 4.59 (AB quartet, $^2J_{HH}$ = 21.98 Hz, 4H, NCH_2), 2.92 (s, 2H, CH_2CMe$_2$), 2.75 (s, 6H, Me), 2.10 (s, 6H, Me), 1.10 (s, 6H, CH$_2$CMe_2). ^{13}C{^{1}H} NMR δ 163.38, 157.73, 152.96, 138.26, 133.36, 132.50, 128.99, 128.87, 125.55, 125.42, 125.22, 117.35, 97.42, 66.33, 46.33, 32.05, 20.67, 18.50. Anal. Calcd for $C_{33}H_{38}N_3TiCl \cdot C_6H_6$: C, 73.40; H, 6.95; N, 6.58. Found: C, 73.60; H, 7.26; N, 6.16.

(BDMP)Ti(CH$_2$CMe$_2$Ph)Br (10b). To a diethyl ether (30 mL) solution of compound **9b** (0.400 g, 0.714 mmol) was added 10 equiv of $MgBr_2 \cdot 2Et_2O$ (2.373 g, 7.14 mmol) at room temperature. The solution was stirred for 12 h. The solvent was removed in *vacuo*. The resulting solid was extracted with toluene (3 × 10 mL) and filtered through Celite. The solvent was removed in vacuo, the solid dissolved in a minimum amount of a 20:1 mixture of THF/benzene and cooled to -40 °C for 12 h. Red crystalline **10b** was isolated by filtration and dried under vacuum (0.356 g, 0.522 mmol, 73%). ^{1}H NMR δ 7.19-6.98 (m, 11H, Ar and Ph), 6.86 (t, 1H, py), 6.36 (d, 2H, py), 4.59 (AB quartet, $^2J_{HH}$ = 21.98 Hz, 4H, NCH_2), 2.95 (s,

References start on page 80

2H, CH_2CMe_2), 2.80 (s, 6H, Me), 2.03 (s, 6H, Me), 1.08 (s, 6H, CH_2CMe_2). $^{13}C\{^1H\}$ NMR δ 163.36, 158.33, 152.80, 138.22, 133.34, 132.51, 129.03, 128.88, 125.53, 125.51, 125.25, 117.28, 102.03, 66.50, 46.89, 31.96, 20.78, 19.66. Anal. Calcd for $C_{33}H_{38}N_3TiBr \cdot C_6H_6$: C, 68.62; H, 6.50; N, 6.16. Found: C, 68.61; H, 6.69; N,. 5.76

(BDPP)Ti($CH_2C_6H_4$-*o*-NMe_2)Cl (11a). To a diethyl ether (25 mL) suspension of complex **3a** (0.250 g, mmol) was added 1.2 equiv. of Li($CH_2C_6H_4$-*o*-NMe_2) (0.074 g, mmol) at -78 °C. The solution changed from yellow to black within minutes and was stirred for 12 h. The solvent was removed in *vacuo*. The resulting solid was extracted with toluene (3 × 10 mL) and filtered through Celite. Attempt to separate complex **11a** from the reaction mixture were unsuccessul. ^1H NMR δ 7.29 (dd, 1H, $CH_2C_6H_4$), 7.22 (t, 2H, Ar), 7.18 (d, 4H, Ar), 6.77 (td, 1H, $CH_2C_6H_4$), 6.68 (t, 1H, py), 6.63 (td, 1H, $CH_2C_6H_4$), 6.49 (dd, 1H, $CH_2C_6H_4$), 6.19 (d, 2H, py), 4.88 (AB quartet, $^2J_{HH}$ = 22.0 Hz, 4H, NCH_2), 4.72 (sept, 2H, $CHMe_2$), 3.62 (s, 2H, $CH_2C_6H_4$), 2.90 (sept, 2H, $CHMe_2$), 2.28 (s, 6H, NMe_2), 1.65 (d, 6H, $CHMe_2$), 1.49 (d, 6H, $CHMe_2$), 1.22 (d, 6H, $CHMe_2$), 1.03 (d, 6H, $CHMe_2$).

(BDMP)Ti(η^5-C_5H_5)Cl (12b). To a diethyl ether (30 mL) suspension of compound **3b** (0.100 g, 0.216 mmol) was added 1.3 equiv of NaC_5H_5•DME (0.049 g, 0.275 mmol) at -40 °C. The solution changed from orange to yellow within minutes and was stirred for 12 h. The solvent was removed in *vacuo*. The resulting solid was extracted with toluene (3 × 10 mL) and filtered through Celite. The solvent was removed in *vacuo*, the solid dissolved in a minimum amount of diethyl ether and cooled to -40 °C for 12 h. Orange crystalline **12b** was isolated by filtration and dried under vacuum (0.097 g, 0.197 mmol, 77%). ^1H NMR δ 7.17-7.00 (m, 7H, Ar and py), 6.50 (d, 2H, py), 6.02 (s, 5H, Cp), 4.47 (AB quartet, $^2J_{HH}$ = 21.83 Hz, 4H, NCH_2), 2.44 (s, 6H, Me), 1.80 (s, 6H, Me). $^{13}C\{^1H\}$ NMR δ163.98, 159.76, 136.62, 133.44, 130.99, 129.29, 128.52, 124.53, 119.63 (Cp), 116.15, 69.26, 18.65.

(BDPP)Ti(C_4Et_4) (13a). A toluene (30 mL) solution of compound **3a** (0.100 g, 0.174 mmol) and 3-hexyne (0.035 g, 0.426 mmol) was added to an excess of 1% Na/Hg

References start on page 80

amalgam (0.074 g Na, 3.22 mmol; 7.40 g Hg). The mixture was stirred for 12 h. The solution was decanted from the amalgam and filtered through a medium porosity frit with the aid of Celite. The solvent was removed in *vacuo* to yield an orange-brown solid. Due to its high solubility, compound **13a** was not isolated in crystalline form. ^{1}H NMR 7.25–7.10 (m, 6H, Ar), 6.93 (t, 1H, py), 6.48 (d, 2H, py), 5.02 (s, 4H, NCH_2), 3.62 (sept, 4H, CHMe$_2$), 2.13 (m, 8H, α,β CH_2Me), 1.35 (d, 12H, CHMe_2), 1.28 (d, 12H, CHMe_2), 0.92 and 0.39 (t, 6H each, α,β CH$_2$$Me$). ^{13}C{^{1}H} NMR δ 229.33 (C$_\alpha$), 162.35, 154.12, 143.72, 137.97, 124.90, 123.78, 116.65, 68.72 (NCH_2), 28.86, 28.37, 28.16, 26.73, 24.49, 24.29, 22.20, 15.96.

(BDPP)Ti(C$_4$Pr$_4$) (14a). The preparation of compound **14a** is identical to that of compound **13a**. Compound **3a** (0.250 g, 0.435 mmol), 4-octyne (0.120 g, 1.09 mmol) and excess 1% Na/Hg amalgam (0.30 g Na, 13.0 mmol; 30.0 g Hg) gave dark red **14a** (0.213 g, 0.294 mmol, 68%) when recrystallized from diethylether at -30 °C. ^{1}H NMR 7.25–7.10 (m, 6H, Ar), 6.93 (t, 1H, py), 6.46 (d, 2H, py), 5.05 (br s, 4H, NCH_2), 3.64 (br sept, 4H, CHMe$_2$), 2.21 and 2.11 (m, 8H, α,β CH_2CH$_2$Me), 1.38 (d, 12H, CHMe_2), 1.24 (d, 12H, CHMe_2), 0.90 (m, 12H, α,β CH$_2$CH$_2$$Me$), 0.71 (br m, 8H, α,β CH$_2$CH_2Me). ^{13}C{^{1}H} NMR δ 229.33 (C$_\alpha$), 162.22, 154.06, 143.80, 137.86, 124.94, 123.80, 116.57, 68.69 (NCH_2), 68.73, 39.09, 32.35, 28.42, 26.71, 25.05, 24.38, 23.25, 15.24. Anal. Calcd for C$_{47}$H$_{69}$N$_3$Ti: C, 77.97 ; H, 9.61; N, 5.80. Found: C, 78.18; H, 9.49; N, 6.20.

(BDPP)Ti(C$_4$Ph$_4$) (15a). The preparation of compound **15a** is identical to that of complex **13a**. Compound **3a** (0.500 g, 0.870 mmol), diphenylacetylene (0.310 g, 1.74 mmol) and excess 1% Na/Hg amalgam (0.60 g Na, 26.1 mmol; 60.0 g Hg) gave red crystalline **15a** (0.423 g, 0.620 mmol, 71%) when recrystallized from diethylether at -30 °C. ^{1}H NMR (23 °C) δ 7.2-6.1 (br m, Ar, Ph, py), 6.27 (d, 2H, py), 5.56 (br m, 2H, CH_2N), 4.95 (br m, 2H, CHMe$_2$), 4.51 (br m, 2H, CH_2N), 2.83 (br m, 2H, CHMe$_2$), 1.87 (br m, 6H,CHMe_2), 1.53 (br m, 6H, CHMe_2), 0.87 (br m, 12H, CHMe_2). ^{1}H NMR (-20 °C, d$_8$-toluene) δ 7.4-6.5 (m, Ar, Ph and py), 6.22 (d, py, 2H), 5.47 (d, 2H, Ph$_o$), 5.03 (AB quartet, $^2J_{HH}$ = 20.63 Hz, 4H, NCH_2),

References start on page 80

4.99 (sept, 2H, C*H*Me$_2$), 2.79 (sept, 2H, C*H*Me$_2$), 1.93 (d, 6H, CH*Me*$_2$), 1.62 (d, 6H, CH*Me*$_2$), 0.91 (d, 6H, CH*Me*$_2$), 0.82 (d, 6H, CH*Me*$_2$). ^{13}C{^{1}H} NMR (-40 °C, d_8-toluene) δ 161.16, 152.28, 146.88, 138.03, 131.89, 131.60 (br), 131.78, 129.95, 127.27, 126.57, 126.17, 125.74, 124.23 (br), 123.19, 116.59, 69.21, 29.75 (br), 28.40 (br), 27.26 (br), 25.84 (br), 23.75. Anal. Calcd for $C_{59}H_{61}N_3Ti$: C, 82.40; H, 7.15; N, 4.89. Found: C, 82.37; H, 7.21; N, 5.13.

(BDMP)Ti(C_4Ph_4) (15b). The preparation of compound **15b** is identical to that of compound **13a**. Compound **3b** (0.500 g, 1.08 mmol), diphenylacetylene (0.482 g, 2.70 mmol) and excess 1% Na/Hg (0.25 g Na, 10.9 mmol; 24.9 g Hg) gave red crystalline **15b** (0.497 g, 0.665 mmol, 62%) when recrystallized from diethylether at -30 °C. ^{1}H NMR δ 7.21 (d, 4H, Ar), 7.08 (t, 2H, Ar), 6.92 (m, 4H, Ph), 6.76 (m, 8H, Ph), 6.66 (m, 5H, Ph and py), 6.34 (d, 2H, py), 5.96 (m, 4H, Ph), 4.71 (s, 4H, C*H*$_2$N), 2.52 (s, 12H, Me). ^{13}C {^{1}H} NMR δ 221.66 (C_α), 161.72, 153.74, 146.02, 143.66, 140.22, 137.99, 134.07, 131.91, 130.48, 129.25, 127.08, 126.98, 125.80, 125.36, 123.31, 116.88, 66.16 (NC*H*$_2$), 19.24.

(BDPP)Ti[α,β'-$C_4H_2(SiMe_3)_2$] (16a). The preparation of compound **16a** is identical to that of compound **13a**. Compound **3a** (0.200 g, 0.348 mmol), $Me_3SiC{\equiv}CH$ (0.088 g, 0.696 mmol) and excess 1% Na/Hg amalgam (0.240 g Na, 10.4 mmol; 24.0 g Hg) gave yellow crystalline **16a** (0.157 g, 0.224 mmol, 64%) when recrystallized from pentane at -30 °C. ^{1}H NMR δ 8.68, 8.66 (s, 1H each, α,β'-C*H*), 7.15-7.05 (m, 6H, Ar), 6.95 (t, 1H, py), 6.53 (d, 2H, py), 4.92 (AB quartet, $^2J_{HH}$ = 21.15 Hz, 4H, NC*H*$_2$), 3.66 (sept, 2H, C*H*Me$_2$), 3.46 (sept, 2H, C*H*Me$_2$), 1.43 (d, 6H, CH*Me*$_2$), 1.28 (d, 6H, CH*Me*$_2$), 1.24 (d, 6H, CH*Me*$_2$), 1.15 (d, 6H, CH*Me*$_2$), 0.04 and -0.15 (s, 9H each, α,β'-Si*Me*$_3$). ^{13}C{^{1}H} NMR δ 218.81 (α-*C*H), 215.04 (α-*C*SiMe$_3$), 163.12, 153.33, 144.06, 142.71, 138.14 (β-*C*H), 137.63, 128.59, 124.94, 124.20, 123.64, 117.25, 67.35, 28.72, 27.10, 26.65, 26.41, 24.87, 23.78, -0.38, -1.86. Anal. Calcd for $C_{41}H_{61}N_3Si_2Ti$: C, 70.35; H, 8.78; N, 6.00. Found: C, 69.97; H, 8.94; N, 6.02.

References start on page 80

(BDMP)Ti[α,α'-$C_4H_2(SiMe_3)_2$] (16b). The preparation of compound 16b is identical to that of compound 13a. Compound 3b (0.100 g, 0.216 mmol), $Me_3SiC{\equiv}CH$ (0.047 g, 0.476 mmol) and excess Na/Hg amalgam (0.074 g Na, 3.22 mmol; 7.40 g Hg) gave yellow crystalline 16b (0.431 g, 0.609 mmol, 70%) when recrystallized from pentane at -30 °C. ^{1}H NMR δ 8.50 (s, 2H, β,β'-C*H*), 7.03 (d, 4H, Ar), 6.94 (t, 1H, py), 6.91 (m, 2H, Ar), 6.55 (d, 2H, py), 4.59 (s, 4H, NCH_2), 2.27 (s, 12H, *Me*), -0.23 (s, 18H, α,α'-SiMe_3). ^{13}C{^{1}H} NMR δ 228.41 (*C*$SiMe_3$), 163.15, 156.02, 138.25, 133.72, 132.26, 124.70, 117.43, 65.45, 20.10, -0.28. Anal. Calcd for $C_{33}H_{45}N_3Si_2Ti$: C, 67.43; H, 7.72; N, 7.15. Found: C, 67.83; H, 7.93; N, 7.29.

(BDPP)Ti[α,β'-$C_4H_2Ph_2$] (17a). The preparation of compound **17a** is identical to that of compound **13a**. Compound **3a** (0.500 g, 0.870 mmol), phenylacetylene (0.267 g, 2.61 mmol) and excess Na/Hg amalgam (0.60 g Na, 26.0 mmol; 60.0 g Hg) gave dark-red crystalline **17a** (0.431 g, 0.609 mmol, 70%) when isolated from diethylether at -30 °C. ^{1}H NMR δ 7.45 (s, 2H, β,β'-C*H*), 7.21 (m, 6H, Ar), 7.00 (t, 4H, Ph), 6.89 (m, 3H, Ph and py), 6.41 (d, 2H, py), 6.18 (d, 4H, Ph), 4.99 (s, 4H, NCH_2), 2.65 (sept, 4H, C*H*Me_2), 1.18 (d, 12H, CHMe_2), 1.20 (d, 12H, CHMe_2). ^{13}C {^{1}H} NMR δ 220.77 (α–*C*Ph), 161.88, 153.74, 148.02 (β–*C*H), 143.50, 138.18, 125.65, 125.39, 125.25, 124.46, 124.16, 117.23, 68.32, 28.04, 26.70, 23.37. Anal. Calcd for $C_{47}H_{53}N_3Ti$: C, 79.75; H, 7.55; N, 5.94. Found: C, 79.35; H, 7.91; N, 5.99.

(BDMP)Ti[C_4α-($SiMe_3$)Et_2H] (18b). A benzene (5 mL) solution containing complex **16b** (0.025 g, 0.043 mmol) and 3-hexyne (0.030 g, 0.365 mmol) was heated to 80 °C for 12 h. The solvent was removed in *vacuo* and the sample dissolved in C_6D_6. Quantitative yield by ^{1}H NMR spectroscopy. ^{1}H NMR δ 8.23 (s, 1H, β'-C*H*), 7.05-6.95 (m, 5H, Ar and py), 6.88 (t, 2H, Ar), 6.55 (d, 2H, py), 4.65 (AB quartet, $^2J_{HH}$ = 21.1 Hz, CH_2N), 2.28 (s, 12H, Me), 2.14 and 1.89 (q, 2H each, CH_2Me), 0.87 and 0.27 (t, 3H each, CH_2*Me*), -0.08 (s, 9H,

References start on page 80

Si*Me*$_3$). $^{13}C\{^1H\}$ NMR δ 228.35, 221.93, 162.96, 155.30, 137.74, 135.44, 134.60, 134.00, 132.73, 123.88, 117.01, 64.99, 31.87, 27.82, 19.84, 19.11, 12.80, 12.63, -0.38.

(BDMP)Ti[C_4α-(SiMe$_3$)Pr$_2$H] (19b). A benzene (5 mL) solution containing complex **16b** (0.025 g, 0.043 mmol) and 4-octyne (0.030 g, 0.272 mmol) was heated to 80 °C for 12 h. The solvent was removed in *vacuo* and the sample dissolved in C_6D_6. Quantitative yield by ^1H NMR spectroscopy. ^1H NMR δ 8.29 (s, 1H, β'-C*H*), 7.10-6.95 (m, 5H, Ar and py), 6.90 (t, 2H, Ar), 6.57 (d, 2H, py), 4.66 (AB quartet, $^2J_{HH}$ = 21.1 Hz, C*H*$_2$N), 2.30 (s, 12H, Me), 2.8 and 1.85 (m, 2H each, C*H*$_2$CH$_2$Me, 1.38 (m, 2H, CH$_2$C*H*$_2$Me), 0.82 and 0.70 (t, 3 each, CH$_2$CH$_2$*Me*), 0.58 (m, 2H, CH$_2$C*H*$_2$Me), -0.07 (s, 9H, Si*Me*$_3$). $^{13}C\{^1H\}$ NMR δ 228.64, 221.78, 162.95, 155.36, 137.78, 134.66, 133.90, 132.84, 129.25, 127.24, 127.04, 124.76, 123.95, 122.24, 120.20, 117.03, 65.18,41.40, 37.94, 22.04, 21.64, 19.86, 19.08, 15.28, 14.68, -0.34.

Activated ligand complex (20b). A THF (30 mL) solution of compound **3b** (0.500 g, 1.08 mmol) and 1-phenylpropyne (0.314 g, 2.70 mmol) were added to an excess of Mg (0.250 g, 10.3 mmol). The mixture was stirred for 12 h. The solution was decanted from the magnesium and filtered through Celite. The solvent was removed in *vacuo* to yield an dark brown solid. The solid was dissolved in a minimum amount of diethylether and cooled to -30 °C for 12 h. Dark red crystalline **20b** was isolated by filtration and dried under vacuum (0.371 g, 0.595 mmol, 55%). ^1H NMR δ 7.20-6.80 (m, 15H, Ph, Ar and py), 6.63 and 6.41 (d, 1H each, py), 6.19 (m, 2H, Ph), 4.96 (AB quartet, $^2J_{HH}$ = 21.3 Hz, 2H, C*H*$_2$N), 4.71 (AB quartet, $^2J_{HH}$ = 19.9 Hz, 2H C*H*$_2$N), 3.65 (q, 1H, C=C*H*Me), 3.13 (m, 2H), 2.78 (m, 2H), 2.40 (s, 3H, ArMe), 1.97 (d, 3H, C=CH*Me*), 1.85 (m, 1H), 1.82 (s, 3H, ArMe), 0.94 (s, 3H, ArMe). $^{13}C\{^1H\}$ δ 166.32, 162.63, 154.66, 148.25, 147.98, 142.48, 141.40, 140.49, 137.30, 136.85, 135.47, 131.20, 129.01, 128.73, 127.44, 147.21, 126.93, 126.82, 126.53, 126.00, 122.62, 121.81, 120.62, 117.51, 117.09, 84.78, 71.57, 69.09, 67.55, 64.73, 39.54, 21.64, 18.10, 17.47, 15.96.

References start on page 80

(BDPP)Ti(C_4H_6) (21a). To a diethyl ether (30 mL) suspension of compound **3a** (0.100 g, 0.216 mmol) was added 1.3 equiv of $Mg(C_4H_6)$ • 2THF (0.062 g, 0.279 mmol) at -40 °C. The solution changed from orange to black within minutes and was stirred for 12 h. The solvent was removed in *vacuo*. The resulting solid was extracted with toluene (3 × 10 mL) and filtered through Celite. The solvent was removed in *vacuo* to give a black oily solid (0.058 g, 0.104 mmol, 48 %). The high solubility of complex **21b** prevented its isolation from the reaction mixture. ^{1}H NMR δ 7.17-7.00 (m, 7H, Ar and py), 6.65 (d, 2H, py), 5.28 (m, 2H, C_4H_6), 5.19 (s, 2H, NCH_2), 4.98 (s, 2H, NCH_2), 3.80 (sept, 2H, CHMe$_2$), 3.61 (m, 2H, C_4H_6), 2.78 (sept, 2H, CHMe$_2$), 1.38 (d, 6H, CHMe_2), 1.21 (d, 6H, CHMe_2), 1.18 (d, 6H, CHMe_2), 1.00 (d, 6H, CHMe_2). The remaining butadiene resonance is undiscernable from the resonances due to impurities.

(BDPP)Ti$^+${C(SiMe$_3$)=CHC(SiMe$_3$)=CHB$^-${C$_6$F$_5$}$_3$ (22a). To a pentane solution (5 mL) of $B(C_6F_5)_3$ (0.073 g, 0.143 mmol) was added a pentane solution (5 mL) of complex **16a** (0.100 g, 0.143 mmol) at -30°C. The solution was stirred for 30 minutes and the solvent removed *in vacuo*. The yellow oily solid (**22a**) was then dissolved in C_6D_6 and characterized by ^{1}H NMR spectroscopy. ^{1}H NMR δ 9.29 (m, 1H, CHB), 8.07 (s, 2H, CHC), 7.52 (d, 2H, py), 7.48 (t, 1H, py), 6.97 (m, 4H, Ar), 6.79 (m, 2H, Ar), 4.88 (AB quartet, $^2J_{HH}$ = 21.0 Hz, 4H, NCH_2), 3.12 (sept, 1H, CHMe$_2$), 2.49 (sept, 1H, CHMe$_2$), 2.37 (sept, 1H, CHMe$_2$), 1.81 (sept, 1H, CHMe$_2$), 1.39 (d, 3H, CHMe_2), 1.13 (d, 3H, CHMe_2), 1.11 (d, 3H, CHMe_2), 0.98 (d, 3H, CHMe_2), 0.86 (d, 3H, CHMe_2), 0.85 (d, 3H, CHMe_2), 0.82 (d, 3H, CHMe_2), 0.74 (d, 3H, CHMe_2), -0.12 (s, 9H, SiMe_3), -0.48 (s, 9H, SiMe_3).

X-ray Crystallographic Analysis of complex 10b. A suitable crystal of **10b** was grown from a saturated THF/benzene solution at room temperature. Complete crystal data may be found in the appendix. Data were collected on a Enraf-Nonius CAD4F diffractometer using CAD4F software[110]. Intensity data were recorded in ω-2θ scan mode at variable scan speeds within a maximum time per datum of 45s. Moving background estimates were made at 25% scan extensions on each side. Standard reflections were monitored every 180 min of X-ray

References start on page 80

exposure time. Lorentz, polarization and decay corrections were applied. Crystal faces were identified by optical goniometry, and a Gaussian absorption correction made to the data, which were averaged to yield 6115 unique data for structure solution and refinement. The structure was solved by a combination of SHELXS and difference Fourier syntheses using SHELXL-93 software[111]. Anisotropic thermal parameters were refined for all non-hydrogen atoms. All phenyl hydrogen atoms were located by difference Fourier methods, placed in calculated positions (C-H = 0.9Å), and included in the structure factor calculations. The four methyl groups C(27), C(28), C(37), and C(38) showed disorder. The idealized tetrahedral groups were assigned 0.5 multiplicities. The benzene solvent molecule showed considerable thermal motion, but refined well to an acceptable geometry.

X-ray Crystallographic Analysis of complex 16a. A suitable crystal of **16a** was grown from a saturated hexane solution at -30 °C. Complete crystal data may be found in appendix. A preliminary investigation showed that the crystals were weakly diffracting. Data were collected on a Siemans P4 diffractometer with the XSCANS software package.[112] The Laue symmetry 2/m was determined by merging symmetry equiv positions. A total of 6646 data were collected in the range of θ = 1.9-22.0° ($-1 \le h \le 11$, $-1 \le k \le 38$, $-12 \le l \le 12$). Three standard reflections monitored at the end of every 297 reflections collected showed no decay of the crystal. In the shell $38 \le 2\theta \le 44°$ only 3% of the reflections were found to be significant. The data processing, solution and refinement were done using *SHELXTL-PC* programs.[113] The methyl carbons attached to Si(2) were found to have two different orientations with occupancies of 0.6 and 0.4. Similarly, the two methyl carbon atoms of the isopropyl group attached to C(27) were found to occupy two positions (occupancy 0.5 and 0.5). Common isotropic thermal parameters were refined for these disordered carbon atoms. An empirical absorption correction was applied to the data using the ψ scans data. No attempt was made to locate hydrogen atoms and were placed in calculated positions. The phenyl groups were constrained to be regular hexagons with C-C distances of 1.395Å. In the final difference Fourier synthesis the electron density fluctuates in the range 0.385 to -0.346 e Å^3.

References start on page 80

5 References

(1) Lappert, M. F.; Power, P. P.; Sanger, A. R.; Srivastava, R. C. *Metal and Metalloid amides: Synthesis, Structures and Physical and Chemical Properties*; John Wiley & Sons: Chichester, 1980.

(2) Bürger, H.; Neese, H.-J. *Chimia* **1970**, *35*, 209.

(3) Bradley, D. C.; Chisholm, M. H. *Acc. Chem. Res.* **1976**, *9*, 273.

(4) Kornicker, W. A. *U.S. Patent 3,318,932* **1967**.

(5) Alyea, E. C.; Bradley, D. C.; Lappert, M. F.; Sanger, A. R. *J. Chem. Soc., Chem. Commun.* **1969**, 1064.

(6) Lappert, M. F.; Sanger, A. R. *J. Chem. Soc. (A)* **1971**, 874.

(7) Alyea, E. C.; Bradley, D. C. *J. Chem. Soc. (A)* **1969**, 2330.

(8) Alyea, E. C.; Bradley, D. C.; Copperthwaite, R. G. *J. Chem. Soc., Dalton Trans.* **1972**, 1580.

(9) Lappert, M. F.; Sanger, A. R. *J. Chem. Soc. (A)* **1971**, 1314.

(10) Chien, J. C. W.; Kruse, W. *Inorg. Chem.* **1970**, *9*, 2615.

(11) Bradley, D. C.; Copperthwaite, R. G. *J. Chem. Soc., Chem. Commun.* **1971**, 764.

(12) Alyea, E. C.; Bradley, D. C.; Copperthwaite, R. G. *J. Chem. Soc., Dalton Trans.* **1973**, 185.

(13) Alyea, E. C.; Bradley, D. C.; Copperthwaite, R. G. *J. Chem. Soc., Dalton Trans.* **1972**, 1580.

(14) Canich, J. A. ; Canich, J. A., Ed., European Patent Application EP-420-436-A1; Vol. April 4, 1991.

(15) Canich, J. A.; Turner, H. W. ; Canich, J. A.; Turner, H. W., Ed., W. PCT Int. Appl. WO 92/12162; filing date December 26, 1991.

(16) Stevens, J. C.; Timmers, F. J.; Wilson, D. R.; Schmidt, G. F.; Nickias, P. N.; Rosen, R. K.; Knight, G. W.; Lai, S. Y. ; Stevens, J. C.; Timmers, F. J.; Wilson, D. R.; Schmidt, G. F.;

References start on page 80

Nickias, P. N.; Rosen, R. K.; Knight, G. W.; Lai, S. Y., Ed., European Patent Application EP-416-815-A2; March 13, 1991.

(17) Bradley, D. C.; Gitlitz, M. H. *J. Chem. Soc. (A)* **1969**, 980.

(18) Bürger, H.; Kluess, C.; Neese, H.-J. *Z. Anorg. Chem.* **1971**, *381*, 198.

(19) Gibbins, S. G.; Lappert, M. F.; Pedley, J. B.; Sharp, G. J. *J. Chem. Soc., Dalton Trans.* **1975**, 72.

(20) Bradley, D. C.; Gitlitz, M. H. *J. Chem. Soc. (A)* **1969**, 1152.

(21) Bradley, D. C.; Gitlitz, M. H. *J. Chem. Soc., Chem. Commun.* **1965**, 289.

(22) Airoldi, C.; Bradley, D. C. *Inorg. Nucl. Chem. Letters* **1975**, *11*, 155.

(23) Dermer, D. C.; Fernelius, W. C. *Z. Anorg. Chem.* **1935**, *221*, 83.

(24) Bradley, D. C.; Thomas, I. M. *J. Chem. Soc.* **1960**, 3857.

(25) Chandra, G.; Lappert, M. F. *Inorg. Nucl. Chem., Letters* **1965**, *1*, 83.

(26) Chandra, G.; Lappert, M. F. *J. Chem. Soc. (A)* **1968**, 1940.

(27) Bürger, H.; Kluess, C. *J. Organomet. Chem.* **1976**, *108*, 69.

(28) Bürger, H.; Neese, H.-J. *Z. Anorg. Chem.* **1969**, *365*, 243.

(29) Benzing, E. P.; Kornicker, W. A. *Chem. Ber.* **1961**, *94*, 2263.

(30) Scoles, L.; Minhas, R.; Duchateau, R.; Jubb, J.; Gambarotta, S. *Organometallics* **1994**, *13*, 4978.

(31) Ott, K. C.; Grubbs, R. H. *J. Am. Chem. Soc.* **1981**, *103*, 5922.

(32) Meinhart, J. D.; Anslyn, E. V.; Grubbs, R. H. *Organometallics* **1989**, *8*, 583.

(33) Brauer, D. J.; Bürger, H.; Weigel, K. *J. Organomet. Chem.* **1978**, *150*, 215.

(34) Bürger, H.; Dämmgen, U. *Z. Anorg. Chem.* **1977**, *429*, 173.

(35) Bürger, H.; Weigel, K. *J. Organomet. Chem.* **1977**, *124*, 279.

(36) Bradley, D. C.; Torrible, E. G. *Can. J. Chem.* **1962**, *41*, 134.

(37) Jones, R. A.; Seeberger, M. H.; Atwood, J. L.; Hunter, W. E. *J. Organomet. Chem.* **1983**, *247*, 1.

References start on page 80

(38) Warren, T. H.; Schrock, R. R.; Davis, W. M. *Organometallics* **1996**, *15*, 562.

(39) Fuhrmann, H.; Bernner, S.; Arndt, P.; Kempe, R. *Inorg. Chem.* **1996**, *35*, 6742.

(40) Friedrich, S.; Gade, L. H.; Edwards, A. J.; McPartlin, M. *J. Chem. Soc., Dalton Trans.* **1993**, 2861.

(41) Schubart, M.; O'Dwyer, L.; Gade, L. H.; Li, W.-S.; McPartlin, M. *Inorg. Chem.* **1994**, *33*, 3893.

(42) Hubert, A. J.; Dale, J. *J. Chem. Soc.* **1965**, 3160.

(43) Hill, J. E.; Balaich, G.; Fanwick, P. E.; Rothwell, I. P. *Organometallics* **1993**, *12*, 2911.

(44) Takahashi, T.; Kotora, M.; Xi, Z. *J. Chem. Soc., Chem. Commun.* **1995**, 361.

(45) van der Linden, A.; Schaverien, C. J.; Meijboom, N.; Ganter, C.; Orpen, A. G. *J. Am. Chem. Soc.* **1995**, *117*, 3008.

(46) Williams, A. C.; Sheffels, P.; Sheenan, D.; Livinghouse, T. *Organometallics* **1989**, *8*, 1566.

(47) Masuda, T.; Deng, Y.-X.; Higashimura, T. *Bull. Chem. Soc. Jpn.* **1983**, *56*, 2798.

(48) Masuda, T.; Deng, Y.-X.; Higashimura, T. *Bull. Chem. Soc. Jpn.* **1980**, *53*, 1152.

(49) Cotton, F. A.; Hall, W. T.; Cann, K. J.; Karol, F. J. *Macromolecules* **1981**, *14*, 233.

(50) Strickler, J. R.; Bruck, M. A.; Wigley, D. E. *J. Am. Chem. Soc.* **1990**, *112*, 2814.

(51) Gambarotta, S.; Wielstra, Y.; Meetsma, A.; Boer, J. L. d. *Organometallics* **1989**, *11*, 1275.

(52) Smith, D. P.; Strickler, J. R.; Gray, S. D.; Bruck, M. A.; Holmes, R. S.; Wigley, D. E. *Organometallics* **1992**, *11*, 1275.

(53) McDonald, F. E.; Zhu, H. Y. H.; Holmquist, C. R. *J. Am. Chem. Soc.* **1995**, *117*, 6605.

(54) Taber, D. F.; Rahimizadeg, M. *Tetrahedron Lett.* **1994**, *35*, 9139.

(55) Yokota, T.; Sakurai, Y.; Skaguchi, S.; Ishii, Y. *Tetrahedron Lett.* **1997**, *38(22)*, 3923.

(56) Jhingan, A. K.; Maier, W. F. *J. Org. Chem.* **1987**, *52*, 1161.

(57) Tyler, D. R.; Mao, F.; Shut, D. M. *Organometallics* **1996**, *15*, 4770.

(58) Bianchini, C.*Organometallics* **1994**, *13*, 2010.

References start on page 80

(59) Calderazzo, F.; Marchetti, F.; Pampaloni, G.; Hiller, W.; Antropiusová, H.; Mach, K. *Chem. Ber.* **1989**, *122*, 2229.

(60) Canziani, F.; Allevi, C.; Garlaschelli, L.; Malatesta, M. C.; Albinati, A.; Ganazolli, F. *J. Chem. Soc., Dalton Trans.* **1984**, 2637.

(61) Chiusoli, G. P.; Pallini, L.; Terenchi, G. *Trans. Met. Chem.* **1983**, *8*, 189.

(62) Collman, J. P.; Kang, J. W.; Little, W. F.; Sullivan, M. F. *Inorg. Chem.* **1968**, *7*, 1298.

(63) Cotton, F. A.; Hall, W. T.; Cann, K. J.; Karol, F. J. *Macromolecules* **1981**, *14*, 233.

(64) Grigg, R.; Scott, R.; Stevenson, P. *Tetrahedron Lett.* **1982**, *23*, 2691.

(65) Halterman, R. L.; Nguyen, N. H.; Vollhardt, K. P. C. *J. Am. Chem. Soc.* **1985**, *107*, 1379.

(66) Jhingan, A. K.; Maier, W. F. *J. Org. Chem.* **1987**, *52*, 1161.

(67) Lachmann, G.; DuPlessis, J. A. K.; DuTort, C. J. *J. Mol. Catal.* **1987**, *42*, 151.

(68) Maitlis, P. M. *J. Organomet. Chem.* **1980**, *200*, 161.

(69) Mantovani, A.; Marcomini, A.; Belluco, U. *J. Mol. Catal.* **1985**, *30*, 73.

(70) McAlister, D. R.; Bercaw, J. E.; Bergman, R. G. *J. Am. Chem. Soc.* **1977**, *99*, 1666.

(71) Schönfelder, W.; Snatzke, G. *Chem. Ber.* **1980**, *113*, 1855.

(72) Shore, N. E. *Chem. Rev.* **1988**, *88*, 1081.

(73) Ville, G. A.; Vollhardt, K. P. C.; Winter, M. J. *Organometallics* **1984**, *3*, 1177.

(74) Vollhardt, K. P. C. *Angew. Chem., Int. Ed. Engl.* **1984**, *23*, 539.

(75) Winter, M. J., *Mechanism of cyclotrimerization*; Winter, M. J., Ed.; Wiley: Chichester, U.K., 1985; Vol. 3, pp Chapter 5.

(76) Strickler, J. R.; Wexler, P. A.; Wigley, D. E. *Organometallics* **1988**, 2067.

(77) Bianchini, C.; Caulton, K. G.; Chardon, C.; Eisenstein, O.; Folting, K.; Johnson, T. J.; Meli, A.; Peruzzini, M.; Rauscher, D. J.; Streib, W. E.; Vizza, F. *J. Am. Chem. Soc.* **1991**, *113*, 5127.

(78) Labinger, J. A.; Schwartz, J.; Townsend, T. M. *J. Am. Chem. Soc.* **1974**, *96*, 4009.

References start on page 80

(79) Green, M. L. H.; Jousseaume, B. *J. Organomet. Chem.* **1980**, *193*, 339.

(80) Gibson, V. C.; Parkin, G.; Bercaw, J. *Organometallics* **1991**, *10*, 220.

(81) Chao, Y.-W.; Wexler, P. A.; Wigley, D. E. *Inorg. Chem.* **1989**, *28*, 3860.

(82) Bruck, M. A.; Copenhaver, A. S.; Wigley, D. E. *J. Am. Chem. Soc.* **1987**, *109*, 6525.

(83) Strickler, J. R.; Wexler, P. A.; Wigley, D. E. *Organometallics* **1991**, *10*, 118.

(84) Sikora, D. J.; Rausch, M. D. *J. Organomet. Chem.* **1984**, *276*, 21.

(85) Famili, A.; Farona, M. F.; Thanedar, S. *J. Chem. Soc., Chem. Commun.* **1983**, 435.

(86) Haeg, M. E.; Whitlock, B. J.; Whitlock Jr., H. W. *J. Am. Chem. Soc.* **1989**, *111*, 692.

(87) Evans, D. F.; Fazakerley, G. V.; Phillips, R. F. *J. Chem. Soc. (A)* **1971**, 1931.

(88) .

(89) Collier, M. R.; Lappert, M. F.; Pierce, R. *J. Chem. Soc., Dalton Trans.* **1973**, 445.

(90) Zucchini, U.; Albizatti, E.; Giannini, U. *J. Organomet. Chem.* **1971**, *26*, 357.

(91) Thiele, K. H.; Köhler, E.; Adler, B. *J. Organomet. Chem.* **1973**, *50*, 153.

(92) Fujita, K.; Ohnuma, Y.; Yasuda, H.; Tani, H. *J. Organomet. Chem.* **1976**, *113*, 201.

(93) Rosen, R. K. *Addition polymerization catalysts comprising reduced oxidation state metal complexes*; Rosen, R. K., Ed.; (DOW) US Patent WO 93/19104 PCT/US93/02584, 1993.

(94) Herrmann, W. A.; Denk, M.; Albach, R. W.; Behm, J.; Herdtweck, E. *Chem. Ber.* **1991**, *124*, 683.

(95) Cummins, C. C.; Schrock, R. R.; Davis, W. M. *Organometallics* **1992**, *11*, 1452.

(96) Aoyagi, K.; Gantzel, P. K.; Kalai, K.; Tilley, T. D. *Organometallics* **1996**, *15*, 923.

(97) Clark, H. C. S.; Cloke, F. G. N.; Hitchcock, P. B.; Love, J. B.; Wainwright, A. P. *J. Organomet. Chem.* **1995**, *501*, 333.

(98) Alt, H. G.; Englehardt, H. E.; Rausch, M. D.; Kool, L. B. *J. Am. Chem. Soc.* **1985**, *107*, 3717.

(99) Hill, J. E.; Fanwick, P. E.; Rothwell, I. P. *Organometallics* **1990**, *9*, 2211.

References start on page 80

(100) McCLure, *NMR Spectroscopy Techniques*; Second Edition, Revised and Expanded ed.; Marcel Dekker Inc.: New York, 1996; Vol. 21, pp 269.

(101) Atwood, J. L.; Hunter, W. E.; Alt, H.; Rausch, M. D. *J. Am. Chem. Soc.* **1976**, *98*, 2454.

(102) Silverstein, R. M.; Bassler, G. C.; Morrill, T. C., *Spectrometric Identification of Organic Compounds*; Fourth ed.; Silverstein, R. M.; Bassler, G. C.; Morrill, T. C., Ed.; John Wiley & Sons: New York, 1981, pp 235.

(103) Eisch, J. J.; Piotrowski, A. M.; Brownstein, S. K.; Gabe, E. J.; Lee, F. L. *J. Am. Chem. Soc.* **1985**, *107*, 7219.

(104) Ruwwe, J.; Erker, G.; Fröhlich, R. *Angew. Chem., Int. Ed. Engl.* **1996**, *35(1)*, 80.

(105) Hill, J. E.; Fanwick, P.; Rothwell, I. P. *Organometallics* **1991**, *10*, 15.

(106) Kennepohl, D. K.; Brooker, S.; Sheldrick, G. M.; Roesky, H. W. *Chem. Ber.* **1991**, *124*, 2223.

(107) Schrock, R. R.; Fellmann, J. D. *J. Am. Chem. Soc.* **1978**, *100*, 3359.

(108) Manzer, L. E. *J. Am. Chem. Soc.* **1978**, *100*, 8068.

(109) Smart, J. C.; Curtis, C. J. *Inorganic Chemistry* **1977**, *16*, 1788.

(110) Enraf-Nonius *Enraf-Nonius Data Collection Package*; V5.0 ed.; Enraf-Nonius, Ed.; Enraf-Nonius: Delft, The Netherlands, 1984.

(111) Sheldrick, G. M. *SHELXL-93*; Sheldrick, G. M., Ed.; Institute fuer Anorg. Chemie: Goettingen, Germany, 1993.

(112) *XSCANS*; Siemens Analytical X-Ray Instruments Inc.: Madison, 1990.

(113) Sheldrick, G. M. *SHELXTL-PC*; V4.1 ed.; Sheldrick, G. M., Ed.; Siemens Analytical X-Ray Instruments Inc.: Madison, WI, U.S.A., 1990.

References start on page 80

"When you sit with a nice girl for two hours, you think it's only a minute. But when you sit on a hot stove for a minute, you think it's two hours. That's relativity!"

Albert Einstein

Chapter Two. Zirconium Complexes

1 Introduction

1.1 Generalities of zirconium amide complexes

Amide complexes of Zr^{IV} are prepared by similar methods to those used for Ti^{IV}. Homoleptic {i.e., $Zr(NR_2)_4$: R = Me[1-4], Et[1-4], Pr[3], ^{i}Pr[5], Bu[3], ^{i}Bu[3]] and heteroleptic {i.e., $Cp_2Zr(NR_2)_2$: R = Me[6,7], Et[6]; $LZr(NR_2)_3$: L = Cp[6], R = Me; L = Ind[6], R = Me; L = Cl[8], Me[9], R = $SiMe_3$} amide complexes of zirconium are known. Chelating diamide complexes of Zr^{IV} have also been reported (Figure 2- 1)[10,11].

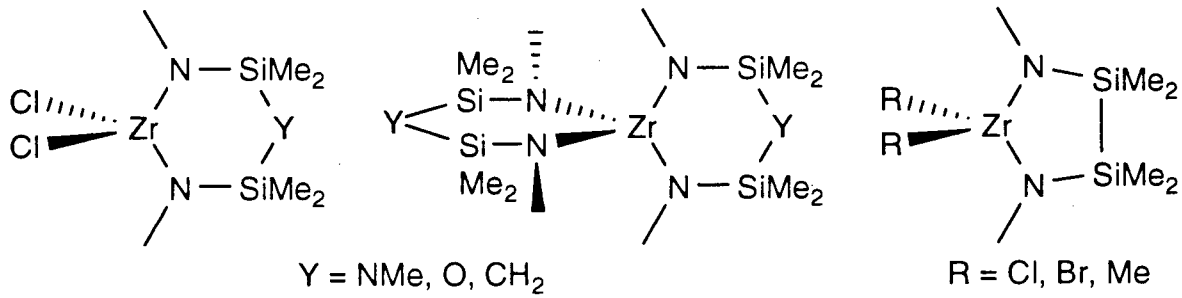

Figure 2- 1. Chelating diamide complexes of Zr^{IV}

1.2 Ziegler-Natta olefin polymerization

Karl Ziegler was the first to report the polymerization of ethylene at ambient pressure using the $TiCl_4/AlEt_3$ catalyst system[12,13]. At about the same period, Giulio Natta reported the discovery of the stereoselective polymerization of α-olefins[14-16]. These systems are, however, heterogeneous and the active species is believed to be a neutral Ti^{III} or cationic Ti^{IV} complex. The proposed mechanism involves the insertion of a C=C molecule into a metal-alkyl bond.

References on page 191

The desire to elucidate the mechanism of heterogeneous polymerization catalysts led to metallocene-catalyzed olefin polymerization. Cyclopentadienyl based systems such as Cp_2TiPh_2, Cp_2ZrPh_2 or Cp_2ZrCl_2[17-20] were used as models for Ziegler-Natta catalysis.

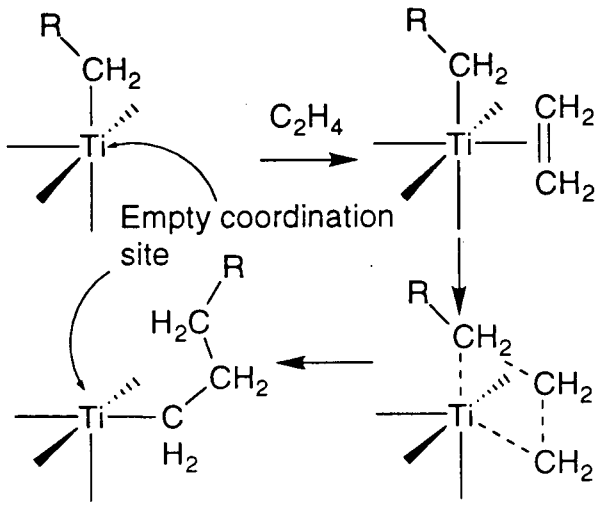

Figure 2- 2. Cossee-Arlman ethylene polymerization mechanism

Around 1986, the tetraphenylborate salts of cations such as $Cp_2ZrMe(THF)^+$ and $Cp_2Zr(CH_2Ph)(THF)^+$ (Figure 2- 3) were isolated and their ability to polymerize ethylene without addition of any activator demonstrated[21-31]. These and related findings in other groups[32-43] lent general acceptance to the proposal that (alkyl)metallocene cations are key intermediates in homogeneous polymerization catalysis.

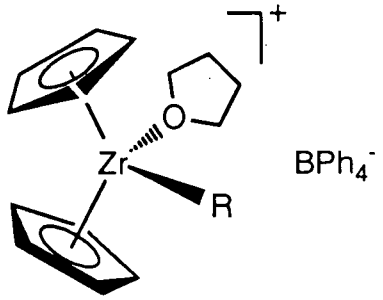

Figure 2- 3. Cationic Cp_2ZrR

References on page 190

The study of simple metallocenes led the way to homogeneous catalysts suitable for the polymerization of propylene and higher α-olefins[44]. Following this discovery, chiral metallocene catalysts capable of polymerizing α-olefins in a stereoregular fashion were reported {i.e. *rac*-ethylenebis(η^5-indenyl)$TiCl_2$ (Figure 2- 4, **a**), *rac*-ethylenebis(η^5-tetrahydroindenyl)$TiCl_2$ (Figure 2- 4, **b**)[45-53] and *rac*-dimethylsilylbis(η^5-indenyl)$TiMe_2$ (Figure 2- 4, **c**)[54,55]}. When activated with MAO, these ingeniously designed *ansa*-metallocenes[a] catalysts polymerize propylene and other α-olefins to give highly isotactic polymers[46,57,58].

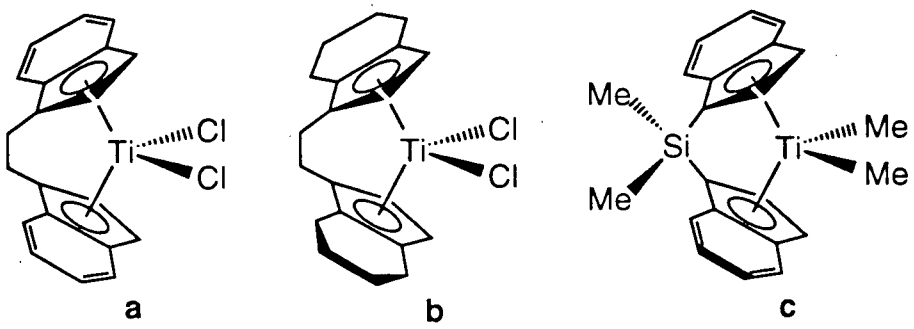

Figure 2- 4. Some bridged metallocene complexes

The structures of the metallocene and the polymers are in accord with chain migratory insertion being the predominant mechanism of chain growth and with stereochemical control being provided by an asymmetric cationic mono(alkyl) species (Figure 2- 5).

An unbridged chiral zirconocene, (1-methylfluorenyl)$_2ZrCl_2$, that produces isotactic polypropylene was recently described[59-61]. As a result of strong steric interactions between the two fluorenyl ligands, mutual rotation is hindered and the enantiomers of this complex do not interconvert during the growth of the polymer chain.

---

[a] The prefix *ansa* (lat. ansa = bent, handle), first used for compounds with an alkane bridge across an arene ring, was adopted as a short notation for metallocene derivatives with an interannular bridge[56].

References on page 190

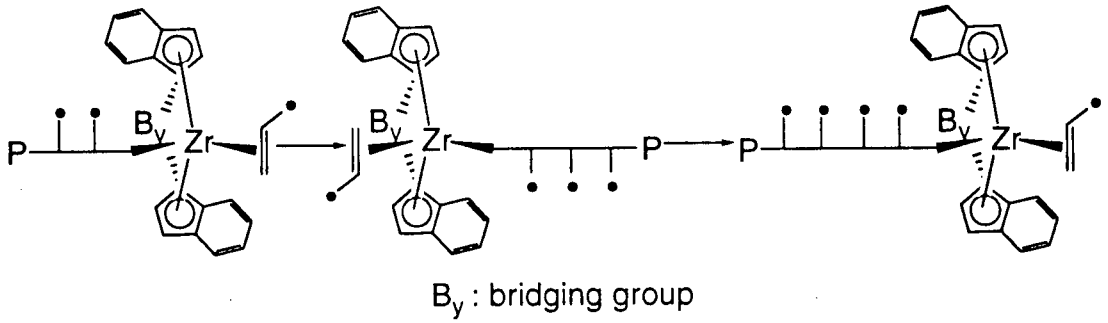

Figure 2- 5. Isospecific catalysts, alternating handedness polymerization

The unbridged zirconocene-based catalyst (2-phenylindenyl)$_2$ZrCl$_2$/MAO yields a highly stretchable atactic-isotactic stereoblock polypropylene[62]. As a result of restricted rotation about the Zr-indenyl (centroid) bond, the complex appears to isomerize between chiral and achiral coordination geometries during chain growth. The chiral-like complex generates isotactic polypropylene while the achiral-like species affords atactic polypropylene (Figure 2- 6).

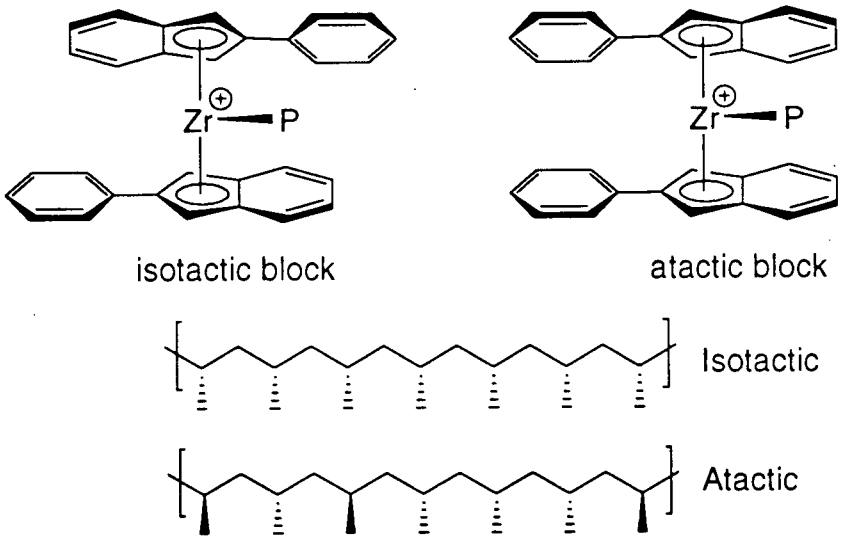

Figure 2- 6. Waymouth's catalyst, bis(2-phenyl-indenyl)ZrCl$_2$

The relationship between catalyst structure and stereoselectivity was elegantly delineated in a series of studies on Me$_2$C-bridged fluorenyl complexes (Figure 2- 7). For example the C_s-symmetric complex Me$_2$C(Cp)(9-fluorenyl)-ZrCl$_2$ produces highly syndiotactic polypropylene in the presence of MAO[63-65]. This particular tacticity arises from alternating enantiofacial

References on page 190

orientation of subsequent olefin insertions. The two coordination sites in this C_s-symmetric complex are no longer homotopic, as in a complex with C_2 -symmetry, but enantiotopic[66].

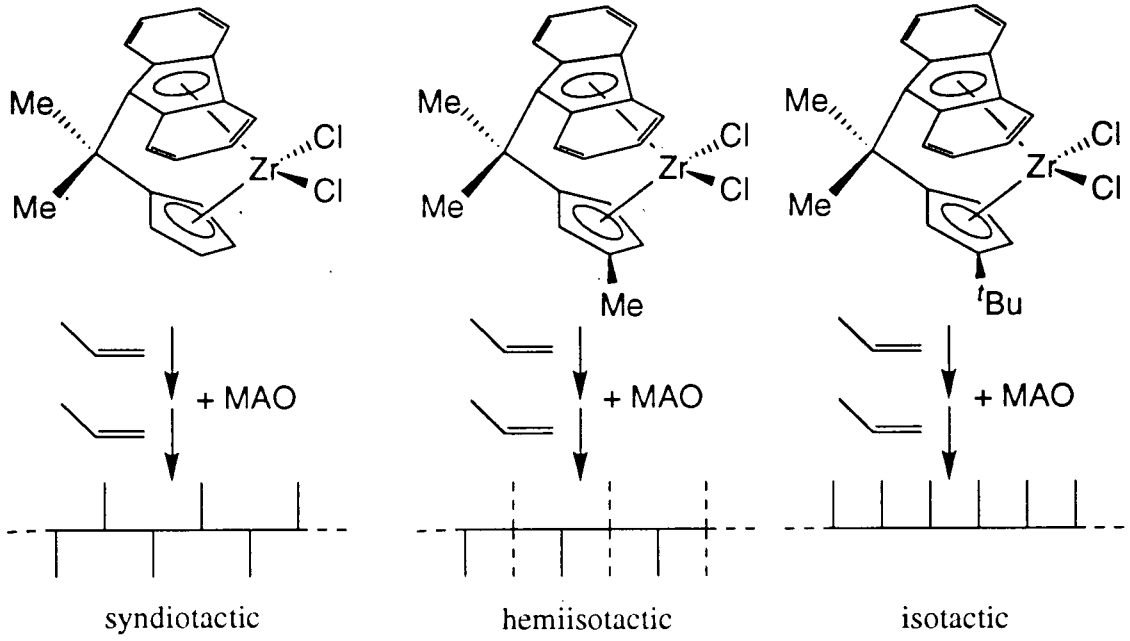

Figure 2- 7. Relationship between catalyst structure and stereoselectivity

A new stereoisomer of polypropylene is formed with MAO-activated $Me_2C(2\text{-}MeC_5H_3)$-(9-fluorenyl)$ZrCl_2$[67]. This catalyst, with one coordination site blocked by one β-substituent and one by two β-substituents (Figure 2- 7), produces hemiisotactic polypropylene. In this type of polypropylene, every other repeat unit is of identical configuration while the remaining units are randomly configurated. Isotactic polypropylene is obtained when one of the coordination sites in the catalyst $Me_2C(2\text{-}^tBuC_5H_3)$-(9-fluorenyl)$ZrCl_2$/MAO is blocked with a *tert*-butyl group[68].

The copolymerization characteristics of metallocene-based catalysts vary with the metallocene complex used[69,70]. However, in most cases the incorporation of α-olefins remains low. Recently, catalysts that contain a dimethylsilyl-bridged amidocyclopentadienyl ligand have been synthesized[71-74] (Figure 2- 8). These catalysts yield ethylene/α-olefin copolymers with a high degree of α-olefin incorporation including long-chain branching. In contrast, metallocene-

References on page 190

based catalysts only afford linear polyethylene with a low degree of α-olefin insertion. A related dimethylsilylene-linked amido-fluorenyl ligand has also been prepared[75].

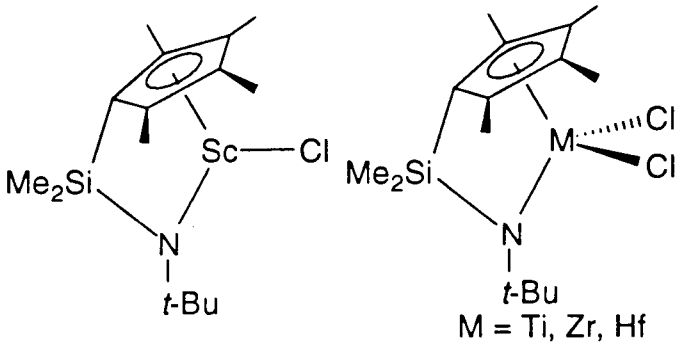

Figure 2- 8. Linked Cp-amide complexes

Finally, complexes that do not incorporate a cyclopentadienyl ligand have been reported. For example, a series of titanium and zirconium complexes bearing sterically hindered chelating binaphtolates and biphenolates have been synthesized and used for the polymerization of α-olefins (Figure 2- 9)[76]. This class of L_2MCl_2 systems can be regarded as being analogous to the well-documented group IV metallocenes. These complexes in the presence of MAO are active for the polymerization of α-olefins. As a result of the chiral structure, stereoregular polymerization of 1-hexene is observed and high molecular weight isotactic polyhexene is obtained.

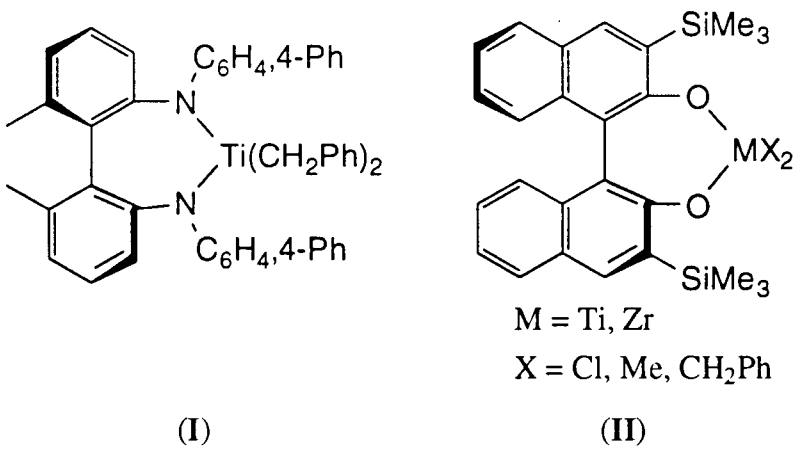

Figure 2- 9. Non-Cp metal complexes

References on page 190

2 Results and Discussion

2.1 2,6-disubstituted and 2,4-6-trisubstituted aryl diamido complexes

As described in chapter one, the reaction of two equivalents of LiNHR (R = 2,6-diisopropylphenyl, 2,6-diethylphenyl, 2,6-dimethylphenyl, 2,4,6-trichlorophenyl or 2,4,6-tribromophenyl) with 2,6-bis(bromomethyl)pyridine[77] yields the diamine $(BDPP)H_2$ (**1a**), $(BDEP)H_2$ (**1b**), $(BDMP)H_2$ (**1c**), $(TCPP)H_2$ (**1d**) or $(TBPP)H_2$ (**1e**) (eq. 1). Compounds **1a,d,e** can be isolated as white crystalline solids while the diamines **1b,c** are viscous oils. All five compounds can be prepare in 50-80% yield on a scale of 5-10 g.

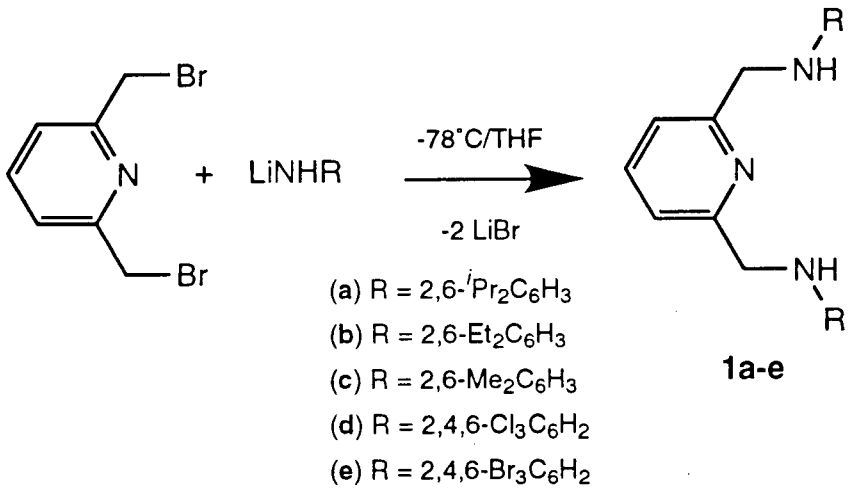

(1)

The diamines **1a-e** react cleanly with $Zr(NMe_2)_4$[1] to give two equivalents of $HNMe_2$ and the yellow crystalline mixed amide complexes **2a-e** in greater than 90 % yield (eq. 2).

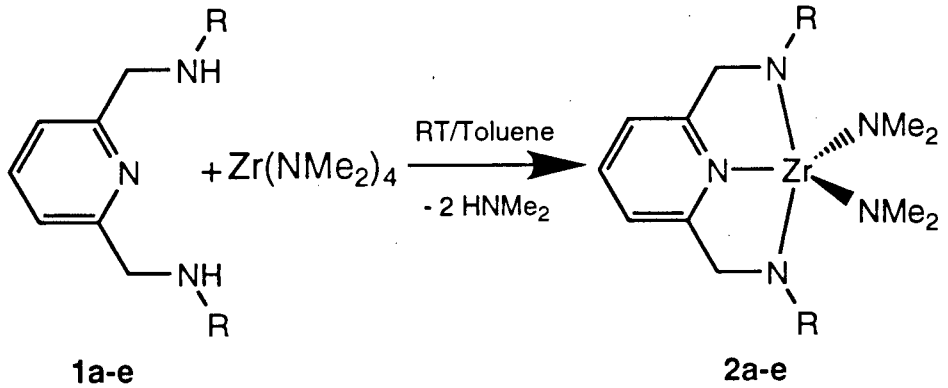

(2)

References on page 190

The room temperature ^{1}H NMR spectra of complexes **2a-e** display a sharp singlet for the ligand methylene protons (NCH_2) consistent with a meridional coordination mode of the ligand. Moreover, the isopropyl methyl groups of complex **2a** and the ethyl methylene protons of complex **2b** are diastereotopic, which is interpreted as a consequence of restricted rotation about the N–C_{ipso} bond. There is no direct spectroscopic means to determine if the same restricted rotation exists for complexes **2b,d,e**, however, modeling[78] studies indicate that the barrier to rotation is high.

Chloride derivatives were desired as precursors to alkyl derivatives. The addition of $(Me_2NH_2)Cl$, (PyH)Cl or (LutH)Cl to complex **2a** results in protonolysis of the BDPP ligand to yield the diamine **1a**. Similar reactivity has been observed for other chelating amide derivatives of zirconium[79]. The aryl substituents in the 2,6-position do not seem to kinetically protect the ligand from proton attack. In contrast, a highly selective reaction between compounds **2a-e** and excess $ClSiMe_3$ affords the white crystalline dichloride derivatives in nearly quantitative yield (eq. 3).

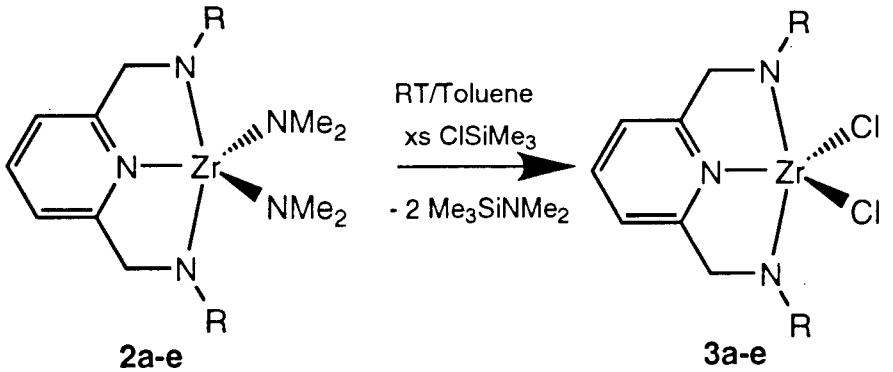

2a-e **3a-e** (3)

The dichloride complexes **3a-e** are very soluble in THF, CH_2Cl_2 and $CHCl_3$, soluble in aromatic solvents, and insoluble in aliphatic solvents. The ^{1}H NMR spectra of complexes **3a-e** indicates that the meridional coordination of the pyridine-diamide ligand and restricted rotation about the N–C_{ipso} bond are retained upon chlorination.

In an attempt to generate the dichloride derivative **3a** in a single step, compound **1a** was reacted with $ZrCl_2[N(SiMe_3)_2]_2$[80] in toluene at room temperature (eq. 4). A yellow oily solid (**4a**) was isolated by evaporation of the solvent. The ^{1}H NMR spectrum of complex **4a** displays

References on page 190

an AB quartet for the ligand methylene protons (NCH_2) indicating asymmetry about the N_3Zr plane. The two isopropyl methine and the four isopropyl methyl resonances are also consistent with meridional coordination of the ligand and restricted rotation about the $N–C_{ipso}$ bond. Moreover, the two $SiMe_3$ singlets (δ 0.27 and 0.16 ppm) indicate the presence of one equivalent of coordinated $HN(SiMe_3)_2$ and one equivalent of free $NH(SiMe_3)_2$. A cis arrangement of the $HN(SiMe_3)_2$ relative to the pyridine is proposed based on the observed asymmetry. It is noteworthy that there is no evidence of coordination of $Me_2N(SiMe_3)$ in the products obtained in eq. 3.

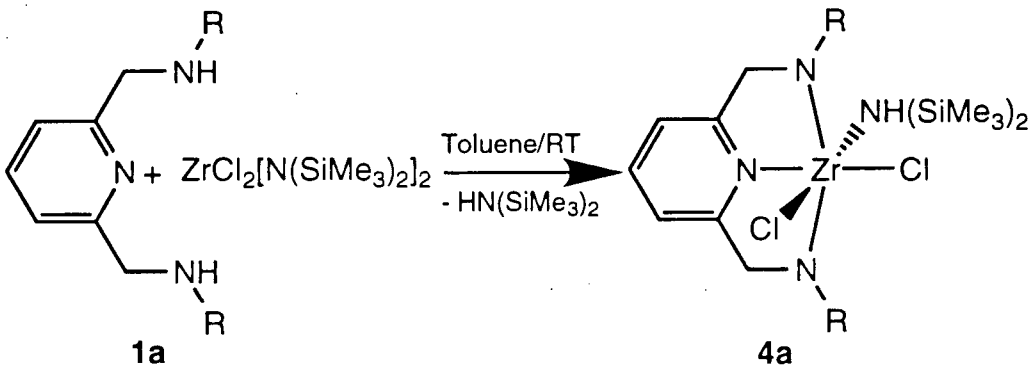

(4)

The reaction of the dichloride **3a-e** with two equivalents of MeMgBr affords the white crystalline dimethyl derivatives **5a-e** in 80-90 % yield (eq. 5).

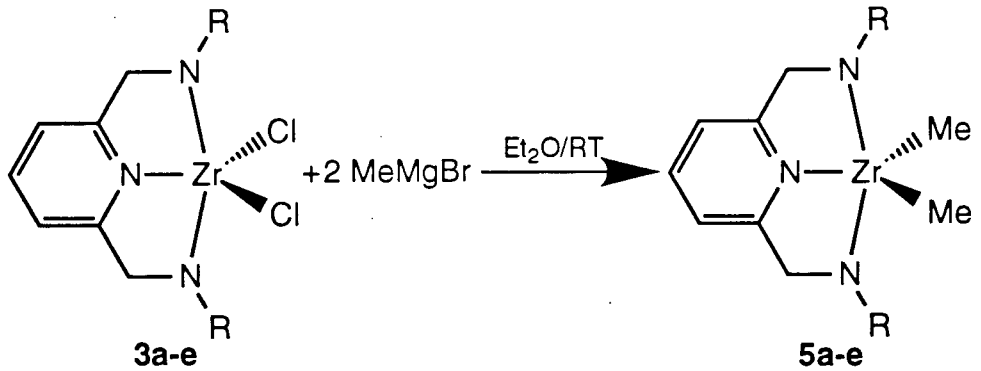

(5)

The ^1H and $^{13}C\{^1H\}$ NMR spectra for complexes **5a-e** are very similar to those obtained for complexes **3a-e** with additional resonances for the $Zr–CH_3$ group ($Zr–CH_3$, ca. 0.50 ppm; $Zr–CH_3$, ca. 45 ppm). These data are comparable to literature values for other zirconium methyl derivatives[23,80-83].

References on page 190

The solid state structure of complex **5b** was determined by X-ray crystallography. The molecular structure of complex **5b** can be found in Figure 2- 10 and relevant bond distances and angles in Table 2- 1. The complete data set can be found in the Appendix.

*Table 2- 1. Selected Bond Distances (Å) and Angles (deg) for **5b***

Bond Distances			
Zr(1) - C(1)	2.248(7)	Zr(1) - C(2)	2.243(6)
Zr(1) - N(1)	2.325(4)	Zr(1) - N(2)	2.101(4)
Zr(1) - N(3)	2.104(5)		
Bond Angles			
N(2) - Zr(1) - N(3)	139.6(2)	C(1) - Zr(1) - C(2)	102.4(3)
N(2) - Zr(1) - N(1)	70.0(2)	N(3) - Zr(1) - N(1)	69.7(2)
Zr(1) - N(3) - C(3)	126.4(3)	Zr(1) - N(3) - C(20)	121.5(3)
C(3) - N(3) - C(20)	112.0(4)	Zr(1) - N(2) - C(9)	126.2(3)
Zr(1) - N(2) - C(10)	122.7(4)	C(9) - N(2) - C(10)	111.0(4)

The structure can best be described as a distorted trigonal bipyramid with the amide nitrogens (N(2) and N(3)) occupying the axial positions. The zirconium atom lies 2.4° out of the plane of the three nitrogen atoms. The Zr-amide distances (2.105(5) and 2.101(4) Å) are comparable to other zirconium-amido complexes[8,84-88]. Each amide is sp^2-hybridized as evidenced by the sum of the angles about each nitrogen (N(2) = 359.9° and N(3) = 359.9°). The aryl rings lie perpendicular to the plane of the ligand with dihedral angles of 89.8° and 89.6°. The rigid coordination of the ligand and enforced location of the aryl ethyl groups necessarily protects the metal about the N_3-plane.

References on page 190

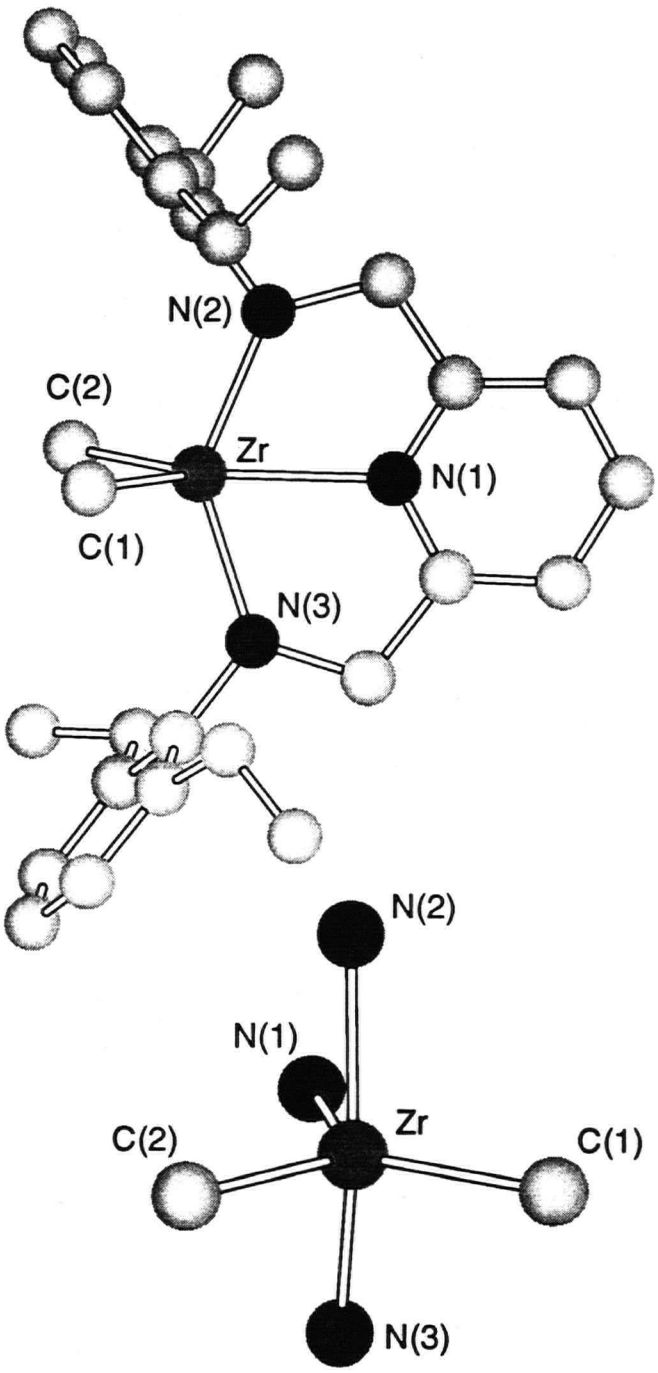

*Figure 2- 10. Molecular structure of complex **5b** deduced from X-ray crystallography*

References on page 190

2.1.1 MO calculation

The coordination sphere of compound **5b** resembles that of Cp_2ZrMe_2[89] (Figure 2- 11).

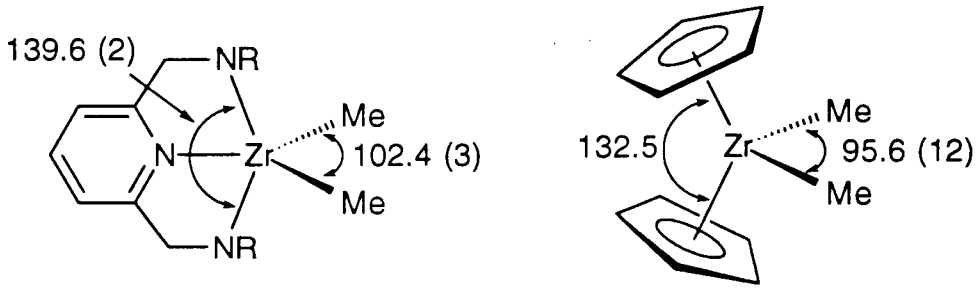

*Figure 2- 11. Geometry of complex **5b** versus that of Cp_2ZrMe_2*

The amide–Zr–amide and Me–Zr–Me angles in **5b** are about 7° larger than the Cent–Zr–Cent (Cent = Cp centroid) and Me–Zr–Me angles in Cp_2ZrMe_2, as expected for a distorted trigonal bipyramid versus a distorted tetrahedron. Moreover, the Zr–Me bond and the L–Zr (L = amide, Cent) of complex **5b** and Cp_2ZrMe_2 are comparable and hence the frontier orbitals of each fragment (less the Zr–*Me* groups) should be similar.

Extended Hückel molecular orbital calculations[78] were performed on a model (**5'**) derived from the molecular structure of complex **5b** and compared to the frontier orbitals of Cp_2Zr[90] (Figure 2- 12). The complete MO calculations data can be found in the Appendix. The b_2 orbital of Cp_2Zr and the $5b_2$ (d_{xz}) orbital of **5'** have very similar energies as a consequence of limited π-donation from the pyridine-nitrogen to the zirconium (contribution: Zr ≈ 90.6 %; $N_{pyridine}$ ≈ 1.3 %). In contrast, the $13a_1$ ($d_{x^2-y^2}$) orbital of **5'** is raised in energy relative to the $2a_1$ orbital of Cp_2Zr due to significant σ-donation from the pyridine (contribution: $N_{pyridine}$ ≈ 11.1 %). This also raises the energy of the $12a_1$ (d_{z^2}) orbital of **5'**, although to a much lesser extent (contribution: Zr ≈ 99.3 %; $N_{pyridine}$ ≈ 0.5 %).

References on page 190

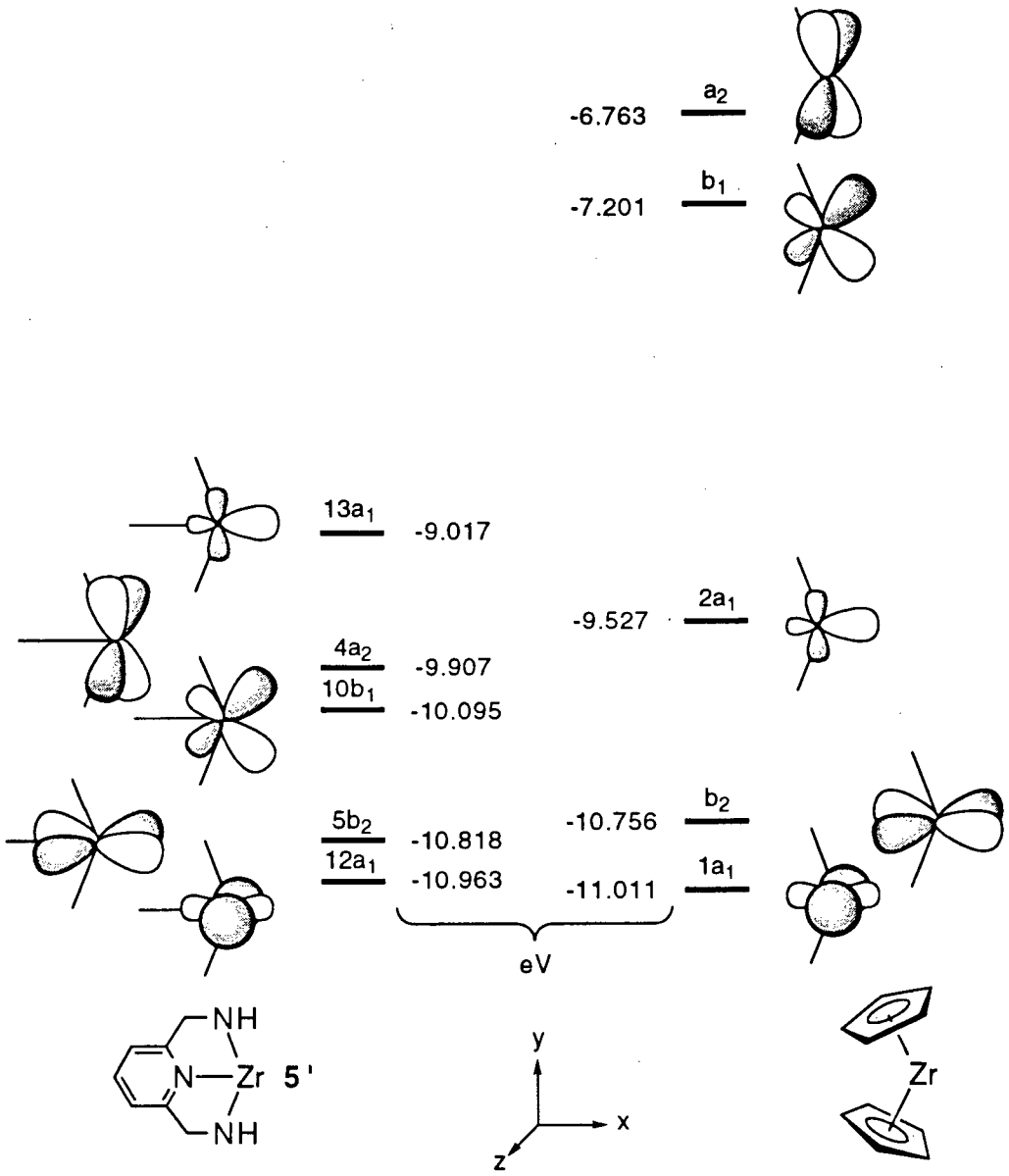

Figure 2- 12. Molecular orbital diagram, $(PyN_2)M$ Vs Cp_2M

It was noted that the reaction of the mixed amide complex **2a** $(BDPP)Zr(NMe_2)_2$ with $[Me_2NH_2]Cl$ resulted in the protonolysis of the more basic amides of the pyridine-diamide ligand. This is consistent with the observation of a ligand centered non-bonding pair of electrons on the amides (Figure 2- 13, $4b_2$, contribution: Zr ≈ 4.2 %; N_{amide} ≈ 75.8 %). The $2a_2$ orbital of **5'** represents the amide–zirconium π-bonding combination while the $4a_2$ orbital constitutes the π-anti-bonding combination. Consequently, the pyridine-diamide ligand is formally an 8-electron

References on page 190

donor, four electrons less than the combination of two cyclopentadienyl ligands. As a result, the zirconium atom in complexes bearing the pyridine-diamide ligand should be more electrophilic than a metallocene-based complex.

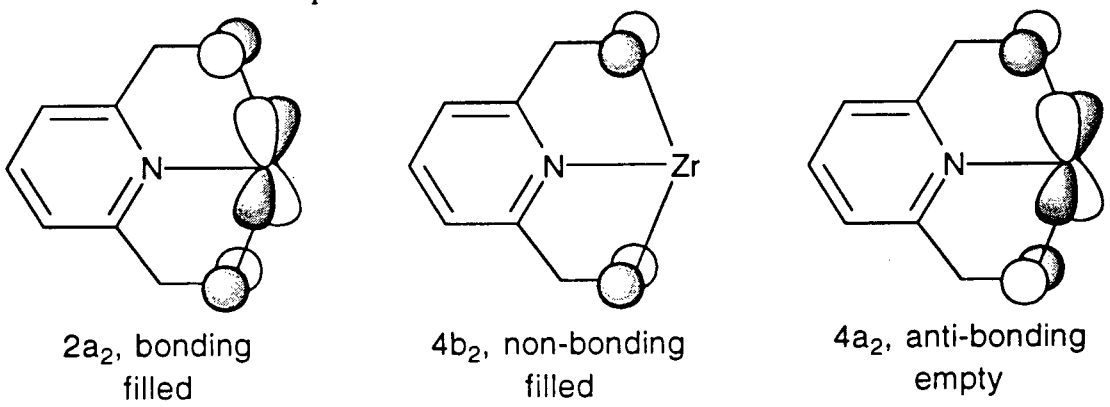

Figure 2- 13. Orbital interactions between the amide ligands and the metal

2.1.2 Reactivity of complex 5a

Complex **5a** reacts cleanly with one equivalent of ^{t}BuNH$_2$ at room temperature in hexanes to give the mixed amide-alkyl complex **24a** and one equivalent of methane (eq. 6).

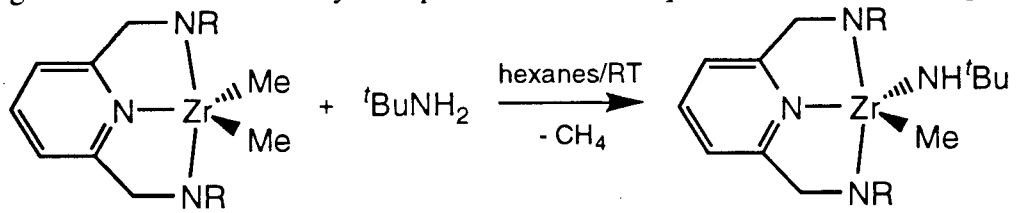

5a, R = 2,6-^{i}Pr$_2$C$_6$H$_3$ **24a** (6)

The AB quartet observed for the ligand methylene (NCH_2) protons in the ^{1}H NMR spectrum of complex **24a** is consistent with asymmetry about the ZrN_3 plane and a complex with C_s geometry. The amine proton (NH^{t}Bu) appears as a broad singlet at δ 3.98 ppm.

Compound **24a** appears to be ideally suited for an alkane elimination between the amide and methyl groups to give an imido complex. Moreover, the $13a_1$, $5b_2$ and $10b_1$ orbitals of the metal are of appropriate symmetry for the formation of pseudo M≡N triple bond[91] (Figure 2- 14).

References on page 190

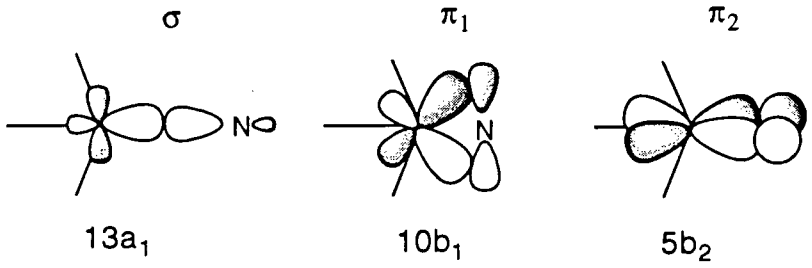

Figure 2- 14. Metal-imido pseudo triple bond

The thermolysis of compound **24a** results in the activation of one of the ligand isopropyl methyl groups (eq. 7). One equivalent of methane is released during the reaction and was detected by ^{1}H NMR spectroscopy.

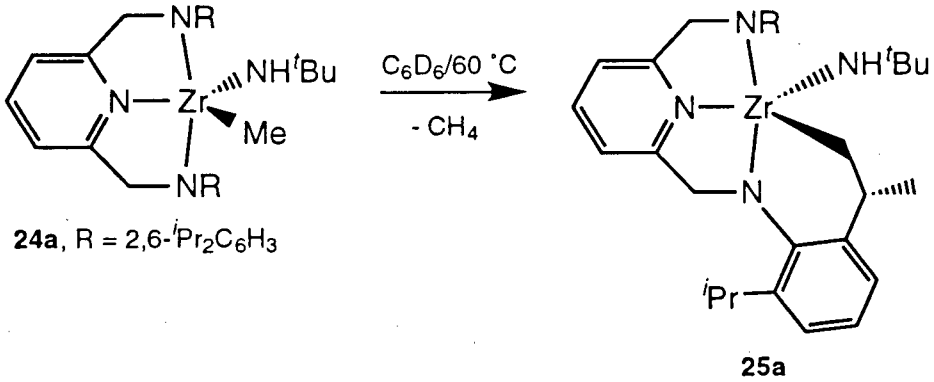

24a, R = 2,6-^{i}Pr$_2$C$_6$H$_3$ (7)

25a

The ^{1}H NMR spectrum of complex **25a** displays two AB quartets for the ligand methylene protons (NCH_2), seven doublets for the isopropyl methyls, three septets for the isopropyl methines and one multiplet for the activated isopropyl group consistent with C_1-symmtery. The amine proton (NH_tBu) appears as a broad singlet at δ 4.02 ppm.

The solid state structure of complex **25a** was determined by X-ray crystallography. The molecular structure of complex **25a** is shown in Figure 2- 15 and selected bond distances and angles can be found in Table 2- 2. The complete crystallographic data can be found in the appendix.

References on page 190

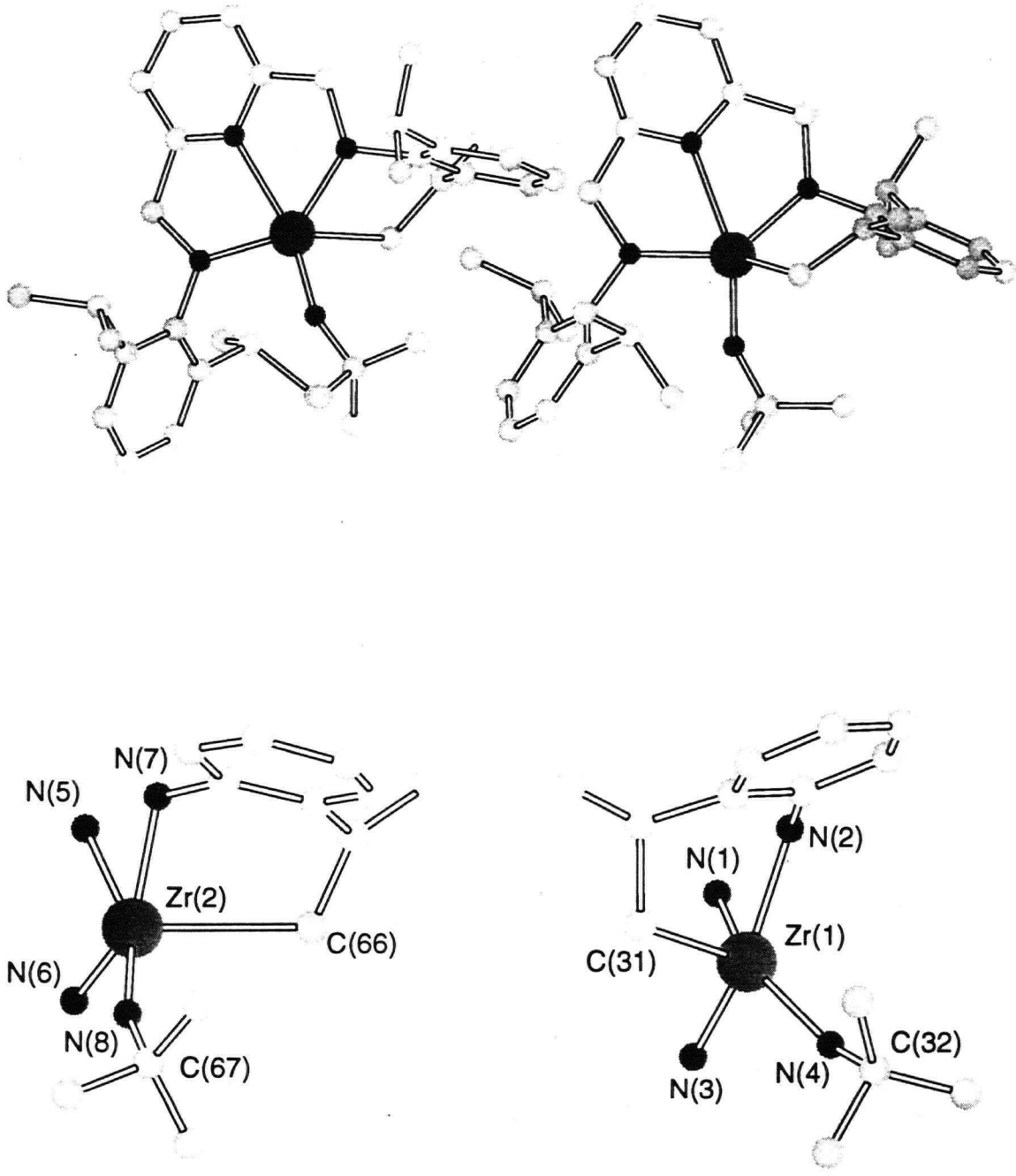

Figure 2- 15. Molecular structure of complex ***25a*** *from X-ray crystallographic analysis*

References on page 190

*Table 2- 2. Selected Bond Distances (Å) and Angles (°) for Complex **25a**[a]*

Bond Distances			
Zr(1)-N(1)	2.352 (8) {2.313 (9)}	Zr(1)-N(4)	2.036(9) {1.893 (12)}
Zr(1)-N(2)	2.106 (7) {2.061 (9)}	Zr(1)-C(31)	2.268 (12) {2.65 (2)}
Zr(1)-N(3)	2.093 (8) {2.090 (8)}	N(4)-C(32)	1.401 (14) {1.44 (2)}
Bond Angles			
N(2)-Zr(1)-N(3)	139.6 (3) {140.6 (4)}	N(4)-Zr(1)-C(31)	103.1 (4) {97.3 (9)}
N(1)-Zr(1)-N(4)	145.8 (4) {160.4 (7)}	N(2)-Zr(1)-C(31)	109.1 (4) {108.3 (7)}
Zr(1)-N(4)-C(32)	152.1 (9) {162 (2)}	N(3)-Zr(1)-C(31)	88.7 (4) {81.8 (6)}
N(1)-Zr(1)-C(31)	111.1 (4) {102.2 (6)}		

a: numbers in brackets for second asymmetric molecule

Two asymmetric molecules were located in the unit cell. The four nitrogen atoms are located in the basal plane of a square-based pyramid and the activated isopropyl carbon occupies the apical position. The high Zr–N–C bond angle (152° and 161.5°) is too large for a simple amide ligand and suggests the presence of significant α-hydrogen agostic interaction. The proposed agostic interaction is consistent with the abscence of an N–H stretch in the IR spectrum of complex **25a**. The geometry about the nitrogen of the ^{tert}Bu-amide group suggests that the proton is located trans to the activated carbon. A similar agostic interaction is proposed for complex **24a**.

Although the necessary labelling studies have not bee performed, a possible mechanism for the formation of complex **25a** may involve a highly reactive imido compound (Scheme 2- 1, **I**). The newly formed imido complex activates one of the ligand isopropyl methyl C–H bonds.

References on page 190

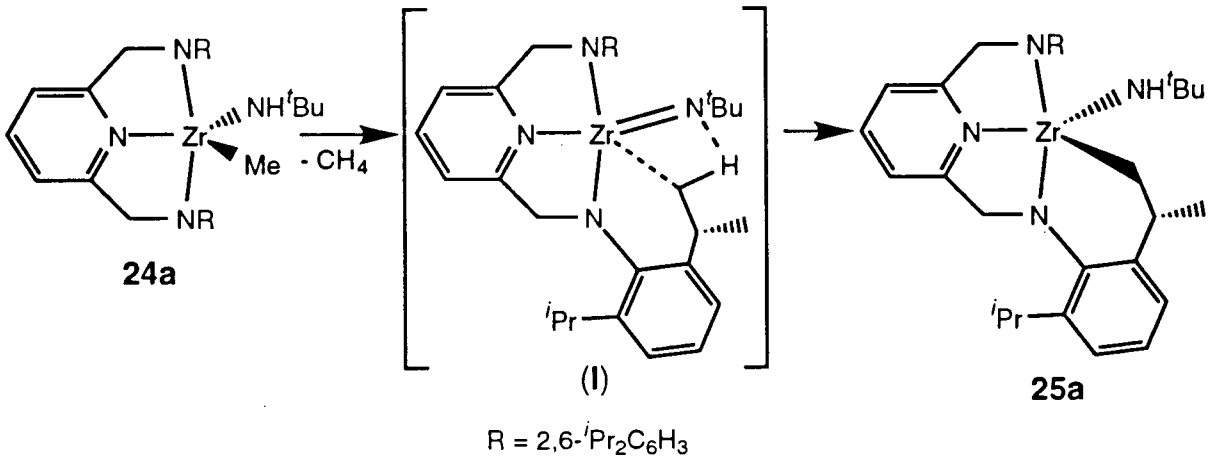

Scheme 2- 1. Proposed mechanism for ligand CH activation

Other imidozirconium complexes bearing amide ancillary ligands undergo C–H activation of alkanes and arenes[92-94]. For example, the transient bis(amido)imido complex (^{t}Bu$_3$SiNH)$_2$Zr=NSi^{t}Bu$_3$ has been shown to add the C–H bond of benzene and methane across the Zr=N linkage[92].

2.1.3 Other alkyl complexes

Complexes **3a-c** can be alkylated using various alkylating reagents (Scheme 2- 2).

The addition of 2.2 equivalents of PhCH$_2$MgBr to ether suspensions of **3a-c** at -78 °C affords the bright yellow dibenzyl derivatives **6a-c** in good yield. Alternatively, complexes **6a-c** can be synthesized from Zr(CH$_2$Ph)$_4$[95] and the diamines **1a-c** in toluene at room temperature.

References on page 190

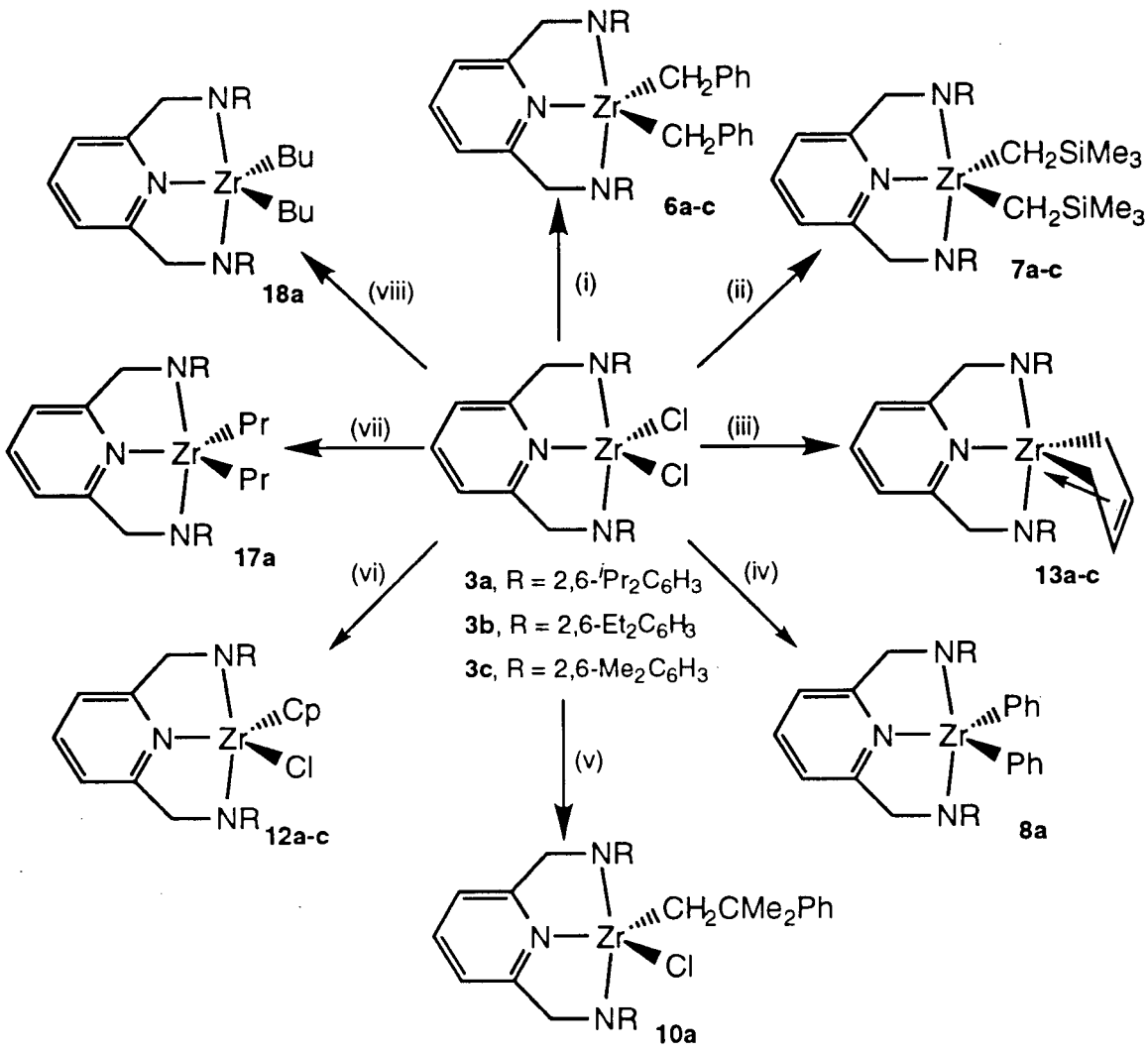

Scheme 2- 2. Alkylation of complexes ***3a-b***[¥]

[¥] Reagents and conditions. (i) 2 equivalents $PhCH_2MgBr$, Et_2O, 23 °C; (ii) 2.2 equivalents $LiCH_2SiMe_3$, Et_2O, -20 °C; (iii) 1.3 equivalents $(C_4H_6)Mg•2THF$, Et_2O, -20 °C; (iv) 2.2 equivalents PhMgCl, Et_2O, -30 °C; (v) 1.2 equivalents $PhMe_2CCH_2MgCl$, Et_2O, -20 °C; (vi) 1.2 equivalents NaCp•DME, Et_2O, -20 °Cl (vii) 2.5 equivalents PrMgCl, hexanes, -30 °C; (viii) 2.5 equivalents BuMgCl, hexanes, -30 °C.

References on page 190

The room temperature ^{1}H NMR spectrum of complex **6a** displays broad resonances for all the signals but those corresponding to the *meta* and *para* protons of the pyridine ring. This suggests facile exchange of differing groups on either face of the plane defined by the pyridine ring. The ^{1}H NMR spectrum of this complex is well resolved at -40°C as shown in Figure 2- 17. At this temperature, two septets (①) and an AB quartet (②) are observed for the C*H*$(CH_3)_2$ and the NC*H*$_2$ protons, respectively. These observations combined with the two distinct C*H*$_2$Ph signals (2.10 and 1.64 ppm, not shown) and the high-field ortho-H resonance (5.90 ppm, ③) of one ot the CH_2Ph groups suggest two different benzyl environments. Although NMR spectroscopy is insufficient to unequivocally establish the coordination mode, these resonances are characteristic of a η^2-$PhCH_2$ group (Figure 2- 16)[96-98].

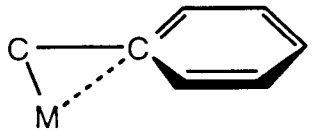

Figure 2- 16. η^2-CH_2Ph group

The high temperature limiting spectrum displays a singlet for the ligand methylene protons (NC*H*$_2$) and a single sharp resonance attributable to the C*H*$_2$Ph protons. These resonances are characteristic for a complex with C_{2v} symmetry. The resonances coalesce at 10 °C yielding a barrier to 'benzyl flipping' (eq. 8) of $\Delta G^{\ddagger}$ = 13.5 (5) kcal mol^{-1}. In contrast to complex **6a**, the room temperature ^{1}H NMR spectra of compounds **6b** and **6c** display sharp resonances for species with C_{2v} symmetry. However, upon cooling both compounds show resonances consistent with both η^1- and η^2-benzyl ligands (Table 2- 3).

Table 2- 3. Fluxional η^1-η^2-CH_2Ph

Complex	Coalescence temperature (°C)	$\Delta G^{\ddagger}$ (kcal/mol)
6a	10	13.5 (5)
6b	-20	11.5 (5)
6c	-30	11.2 (5)

References on page 190

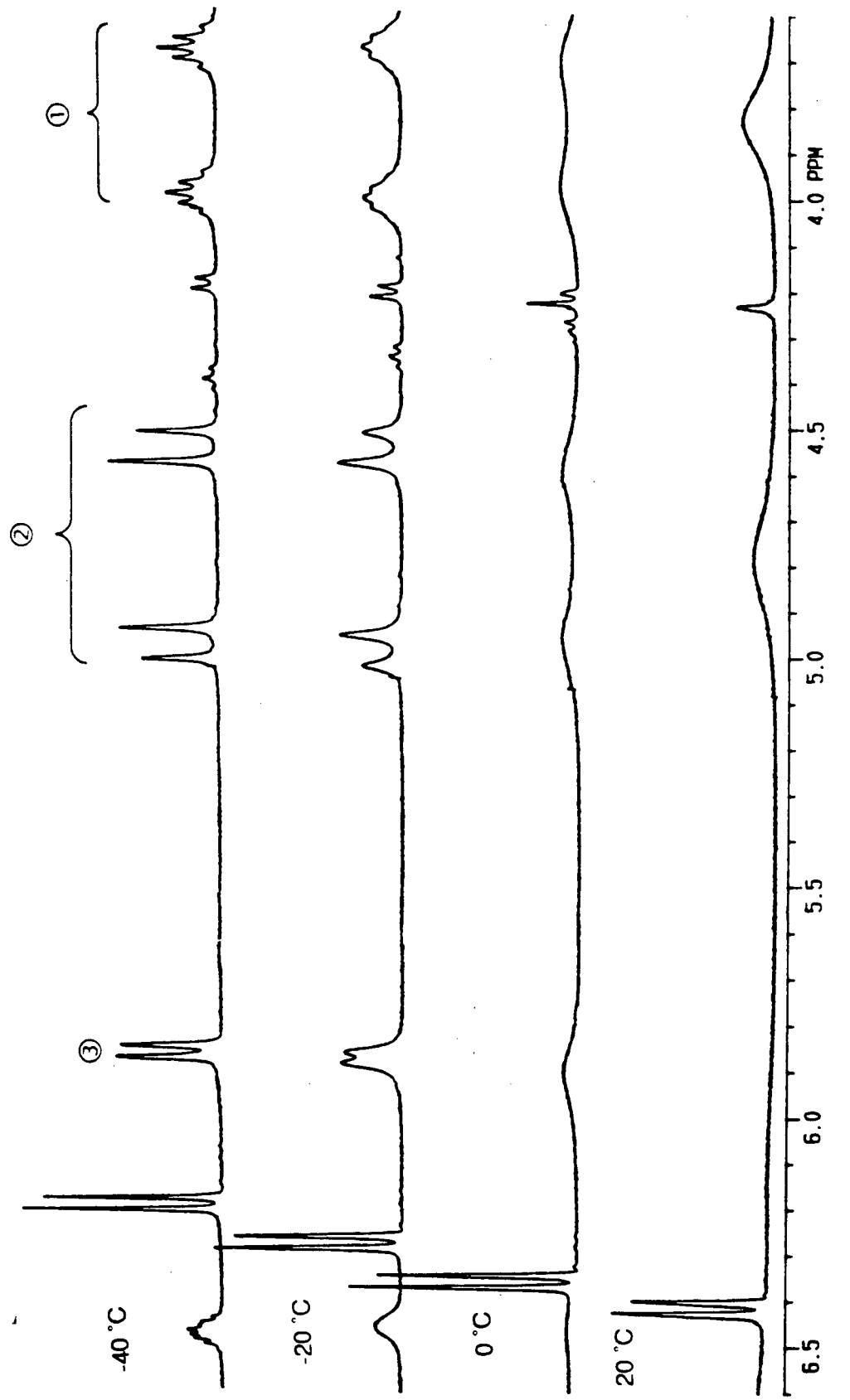

*Figure 2- 17. Variable-temperature ^{1}H NMR spectra of couplex **6a** (300MHz, $CD_3C_6D_5$)*

References on page 190

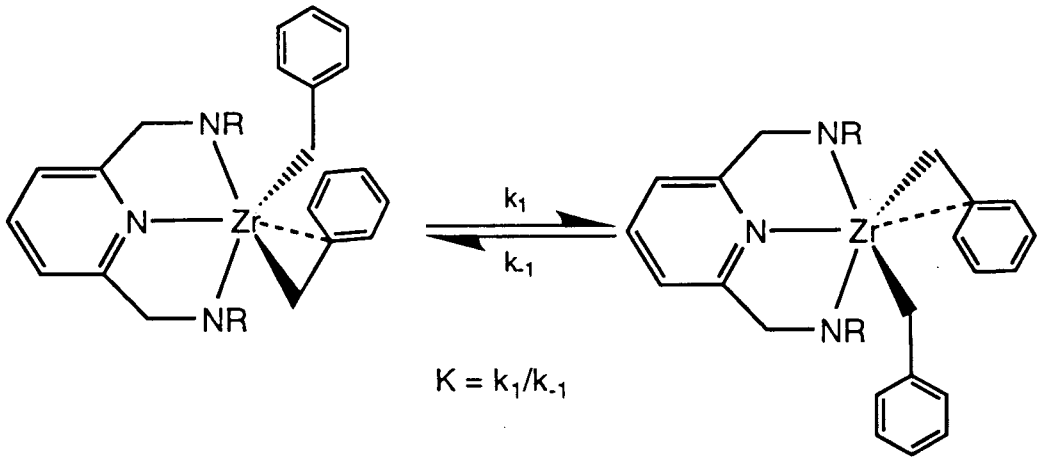

(8)

Interestingly, the low temperature (-80 °C) limiting spectrum of compound **6c** displays two distinct resonances for the inequivalent aryl methyl groups consistent with restricted rotation about the N-C_{ipso} bond at this temperature. The room temperature ^{1}H NMR spectrum[99] of the metallocene bis(benzyl) derivative $Cp_2Zr(CH_2Ph)_2$ shows no evidence of η^2-benzyl ligands. This is likely a result of the reduced electrophilicity of the metal in a metallocene fragment compared to a bis(amide) complex. As further evidence, the structurally characterized cationic benzyl derivative $[Cp_2Zr(\eta^2\text{-}CH_2Ph)(N{\equiv}CMe)]^+(BPh_4)^-$ and the spectroscopically identified base-free complex $[(\eta^5\text{-}C_5H_4Me)_2Zr(\eta^2\text{-}CH_2Ph)]^+(BPh_4)^-$[96], clearly show the presence of an η^2-benzyl moiety.

Yellow single crystals of (BDPP)Zr(η^2-CH_2Ph)(CH_2Ph) (**6a**) suitable for an X-ray analysis were grown by diffusion of cyclohexane into a saturated CH_2Cl_2 solution of complex **6a**. The poor quality of the crystallographic data limited the refinement of the final structure and only connectivity could be established. Attempts to grow better quality crystals from different solvent mixtures were unsuccessful. The molecular structure of complex **6a** (Figure 2- 18) clearly shows that one of the two benzyl groups is coordinated as an η^1 ligand with no significant Zr–C_{ipso} interaction {Zr-C(4): ca. 3.2 Å; Zr-C(1)-C(4): ca. 110°). The second benzyl group is bound in an η^2 fashion. The acute Zr-C(2)-C(3) angle (ca. 80°) results in the close proximity of the phenyl ring. The C_{ipso} is particularly close to the metal with a Zr-C(3) bond distance of approximately 2.6 Å (typical Zr-C_{ipso} bond distances for similar complexes range from 2.59 Å to 2.64 Å)[96-98].

References on page 190

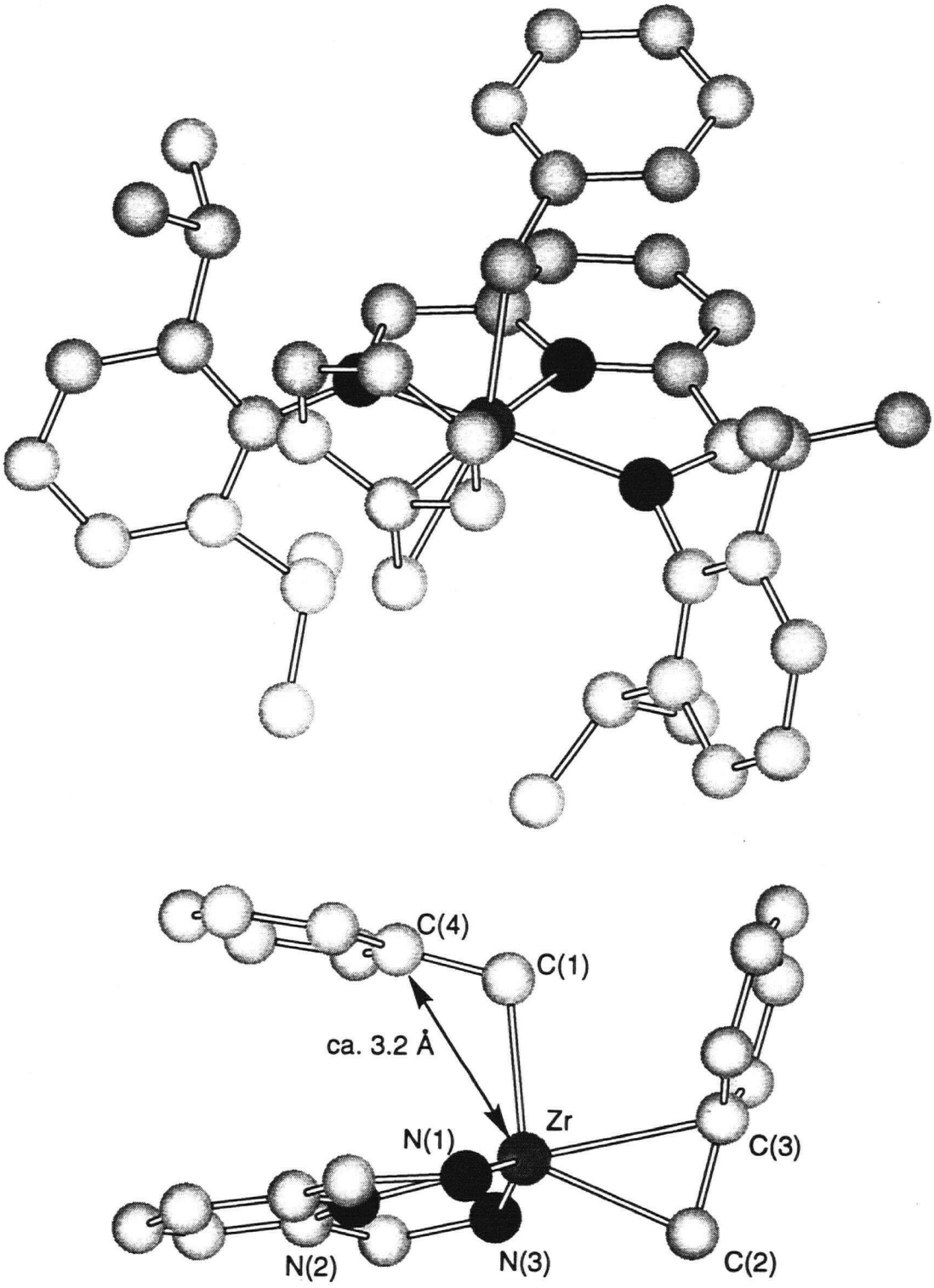

Figure 2- 18. Molecular structure of complex ***6a***

References on page 190

The geometry about the zirconium is best described as a square-based pyramid with the benzylic carbon of the η^1-CH_2Ph in the apical position. The three nitrogen atoms and the benzylic carbon of the η^2-CH_2Ph are located in the remaining four sites.

Complex **6a** was reacted with one equivalent of $B(C_6F_5)_3$[100] in C_6D_6 and the solution behavior of the product was studied by ^1H NMR spectroscopy (eq. 9).

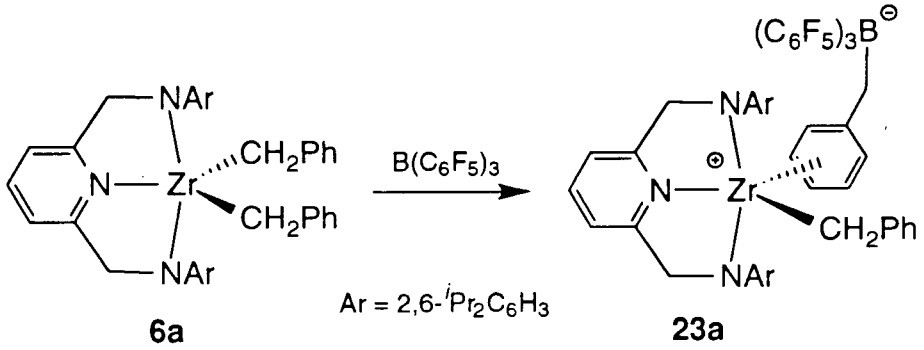

6a **23a** **(9)**

The ^1H NMR spectrum of complex **23a** shows two sets of benzyl resonances. One set of resonances appear at 6.75 (t), 6.58 (t), 6.38 (d) and 2.40 (s) ppm which is typical for η^1-benzyl group bound to zirconium[96,98,101,102]. A doublet at 6.25 ppm, triplet at 6.27 and triplet at 6.04 ppm are observed for the benzyl group bound to the boron. Although it is not possible to establish with certainty the cation-anion interaction, these resonances combined with the broad signal at 3.57 ppm ($PhCH_2B$) are indicative of a η^6-$PhCH_2$ group of a $\{(\eta^6\text{-}PhCH_2)B(C_6F_5)_3\}$ moiety[103-105]. No "free" $\{(PhCH_2)B(C_6F_5)_3\}$ anion was observed by ^1H NMR spectroscopy[104]. The implications of this reaction on the catalytic activity of complex **6a** in the polymerization of ethylene are discussed in the following sections.

Compounds **3a-c** react cleanly with NaCp•DME in Et_2O at -20 °C to give the mono(cyclopentadienyl) derivatives **12a-c** in good yield (Scheme 2- 2). The ^1H NMR spectra of complexes **12a-c** are consistent with η^5-coordination of the cyclopentadienyl ligand. It is noteworthy that the geometry about the zirconium in the η^5-Cp complexes (**12a-c**) is closely related to that of the proposed η^6-$PhCH_2$ complex **23a** (Figure 2- 19). It has been proposed[106] that the tris(methylcyclopentadienyl) derivative $(C_5H_4Me)_3ZrCl$ contains two η^5-coordinated

References on page 190

MeCp rings and one η^1-coordinated ring. There is no evidence of an η^1-Cp ligand in the low temperature ^{1}H NMR spectrum of complex **12a.**

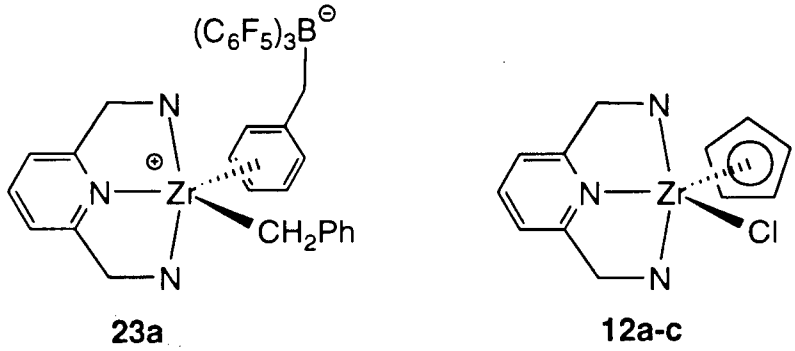

Figure 2- 19. η^5-Cp vs η^6-$PhCH_2$ structures

The addition of 2.2 equivalents of $LiCH_2SiMe_3$ to a diethyl ether solution of complexes **3a-c** yields the bis(trimethylsilylmethyl) derivatives **7a-c** (Scheme 2- 2) in high yield. The room temperature ^{1}H NMR spectra of compounds **7b** and **7c** are consistent with complexes with C_{2v} symmetry. For example, the ^{1}H NMR spectrum of complex **7c** displays a singlet for the ligand methylene protons and resonances attributable to two equivalent CH_2SiMe_3 ligands. In both cases, the spectrum remains unchanged from -80 °C to +80 °C. In contrast, the room temperature ^{1}H NMR spectrum of complex **7a**, which bears the bulky 2,6-diisopropylphenyl substituents, is broad and featureless. The high temperature (+70 °C) limiting spectrum shows resonances for the expected C_{2v}-symmetric product. The low temperature limiting spectrum displays sharp resonances consistent with asymmetry about the N_3M plane and a complex with C_s-symmetry. For example, an AB quartet is observed for the ligand methylene protons (CH_2N). The absence of fluxionality in complex **7b** and **7c** suggests that the origin of this behavior in compound **7a** is steric and not electronic. Steric interactions between the isopropyl substituents and the trimethylsilyl groups in compound **7a** may prevent the two alkyl groups from being simultaneously directed outward (Figure 2- 20, **I**).

References on page 190

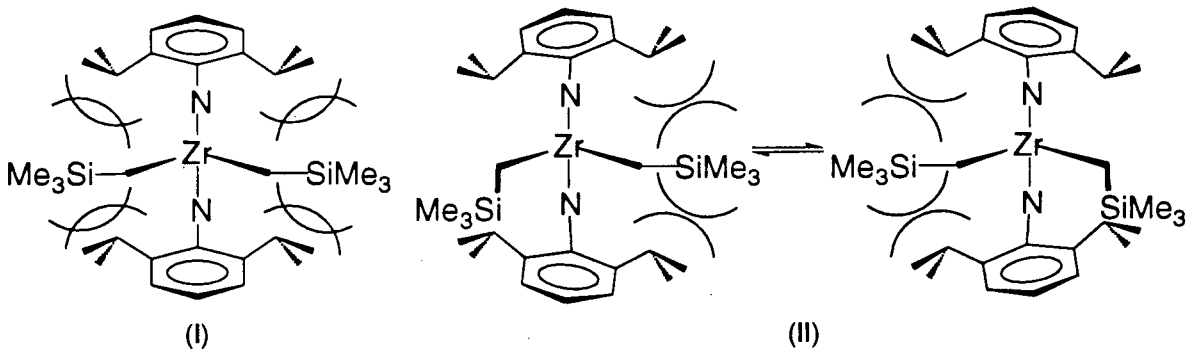

*Figure 2- 20. Fluxional behavior of complex **7a***

The resonances coalesce at 20 °C yielding a barrier to 'trimethylsilylmethyl flipping' of $\Delta G^{\ddagger}$ = 13.4 (5) kcal mol^{-1}. Interestingly, both trimethylsilyl groups are arranged in the least sterically hindered position (both directed outward) in the molecular structure of $Cp_2Zr(CH_2SiMe_3)_2$[107].

Complex **3a** reacts with PhMgCl in Et_2O at -30 °C to give the diphenyl complex **8a** (Scheme 2- 2). The ^1H NMR spectrum for complex **8a** displays a single sharp resonance for the ligand methylene protons (CH_2N) and two doublets for the ligand isopropyl methyl groups as expected for a complex with C_{2v}-symmetry. The $^{13}C\{^1H\}$ NMR spectrum displays a low-field resonance (δ 190.41 ppm) for the phenyl ipso-carbon similar to other reported values[108]. The thermolysis of Cp_2ZrPh_2[109,110] in toluene or benzene at 70 °C affords a complicated mixture including benzene. It is believed that the decomposition involves a benzyne-zirconium intermediate (Figure 2- 21) which then reacts with the aromatic solvent to give $Cp_2ZrArPh$[111]. Complex **3a** does not react when heated to 110 °C for 7 days in toluene.

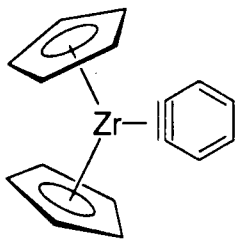

Figure 2- 21. Cp_2Zr(benzyne)

References on page 190

The addition of excess $PhMe_2CCH_2MgCl$ to complex **3a** in Et_2O at -20 °C affords the mono(neophyl) derivative **10a** (Scheme 2- 2). The ^1H NMR spectrum of complex **10a** displays an AB quartet for the ligand methylene protons (CH_2N) as well as two isopropyl methines and four isopropyl methyl resonances as expected for a complex with asymmetry about the N_3M plane and restricted rotation about the N-C_{ipso} bond. A similar reaction using complex **3b** affords what appears (by ^1H NMR spectroscopy) to be the bis(neophyl) derivative $(BDEP)Zr(CH_2CMe_2Ph)_2$. The complex is, however, unstable and decomposes within days at room temperature.

The dichloride complexes **3a-c** react with $Mg(C_4H_6)\cdot 2THF$ in ether at -20 °C to give the zirconium diene derivatives **13a-c** (Scheme 2- 2). The proton NMR spectrum of complex **13a** (Figure 2- 22) displays two ligand methylene (CH_2N) singlets. This is characteristic of a complex with C_s-symmetry where the mirror symmetry is perpendicular to the plane of the meridionally coordinated pyridine diamide ligand. Similar resonances for the ligand methylene protons (CH_2N) are observed in the proton NMR spectra of complexes **13b,c**. The presence of two isopropyl methine and four isopropyl methyl resonances in the ^1H NMR spectrum of complex **13a** is also consistent with this symmetry and indicates restricted rotation about the N-C*ipso* bond.

The diene fragment resonances observed in the ^1H NMR spectra of complexes **13a-c** (Table 2- 4) suggest an *s-cis* bent metallacyclo-3-pentene structure[112,113] with significant π-donation from the metallacyclopentene double bond (Figure 2- 23).

*Table 2- 4. Butadiene ^1H NMR resonances of complex **13a-c***

Complex	δ, ppm		
	Hm	**Hs**	**Ha**
13a	4.72	3.56	0.28
13b	4.92	3.41	0.16
13c	4.98	3.42	0.17

References on page 190

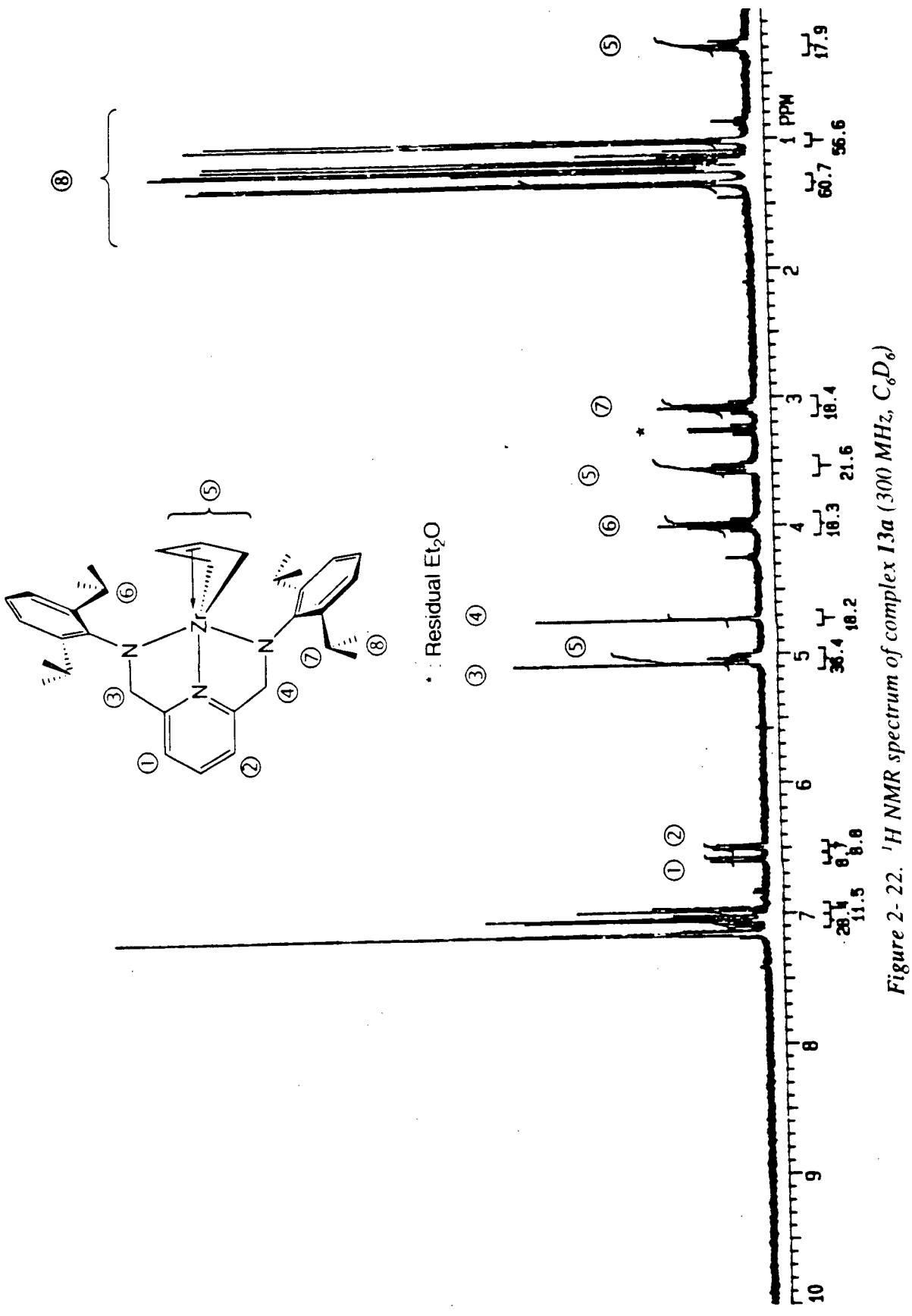

Figure 2- 22. ^1H NMR spectrum of complex 13a (300 MHz, C_6D_6)

References on page 190

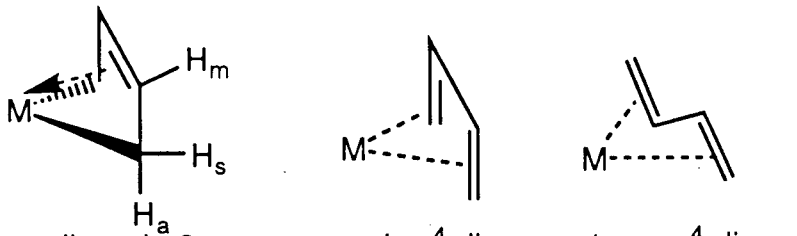

s-cis-metallacyclo-3-pentene *s-cis*-η^4-diene *s-trans*-η^4-diene

Figure 2- 23. Coordination modes of butadiene

The metallocene-based diene complexes Cp_2Zr(diene) and Cp_2Hf(diene) often show fluxional behavior where the topomerization occurs through a planar 16-electron metallacyclopentene transition state (Scheme 2- 3, **I**)[114-117]. The activation barriers vary between 6.5 and 12.4 kcal mol^{-1},[115,116,118] depending upon the steric bulk of the diene ligands.

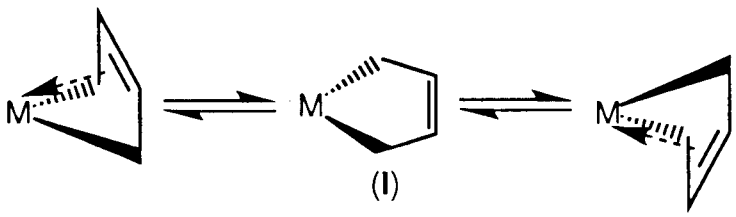

Scheme 2- 3. Topomerization of s-cis-metallacyclopentene

Moreover, the zirconocene derivative $Cp_2Zr(\eta^4\text{-}C_4H_6)$ exists in two isomeric forms having the butadiene coordinated in either the *s-cis* or *s-trans* configuration[112]. The mode of coordination of the conjugated diene is controlled not only kinetically but also thermodynamically. In general, dienes bearing alkyl or aryl substitution at the C_1 and/or C_4 atoms kinetically favor the coordination in the *s-trans* form. On the other hand substitution at the C_2 and/or C_3 carbons always brings about the predominance of *s-cis* coordination (Table 2- 5)[114,117,119,120]. However, the *s-trans* isomer in some cases isomerizes to the more thermodynamically stable *s-cis* isomer upon heating. The activation barrier ($\Delta G^{\ddagger}$) for the interconversion of Cp_2Zr(butadiene) is

References on page 190

calculated to be 23 kcal mol^{-1} and that for Cp_2^*Zr(butadiene) is estimated to be >30 kcal mol^{-1}[119,120].

Table 2- 5. s-Cis / s-Trans ratio (%) for $Cp_2(R^1CH=CR^2CR^3=CHR^4)$ in C_6D_6

R^1	R^2	R^3	R^4	*s-cis/s-trans*
Ph	H	H	H	2/98
H	H	H	H	10/90 - 60/40[a]
H	CH_3	H	H	100/0

[a] Varied depending on the temperature

In contrast, no evidence of η^4-diene coordination is observed for complexes **13a-c**. Furthermore, the C_S-symmetry of compound **13a** is retained to +80 °C and no evidence of syn/anti proton exchange is observed; consistent with rigid coordination of the diene fragment to the highly electrophilic zirconium center and a significantly stronger π-interaction with zirconium.

The solid state structure of complex **13a** was determined by X-ray crystallography. The complete data set can be found in the Appendix. The molecular structure of complex **13a** can be found in Figure 2- 24 and relevant bond distances and angles in Table 2- 6.

The molecular structure of complex **13a** is best described as a distorted trigonal bipyramid with the two amides located in the axial positions and the pyridine-nitrogen and the α-carbon of the diene fragment occupy the equatorial positions. The amide- and pyridine-zirconium bond distances are statistically the same as those found in complex **5b** (Table 2- 1 and Figure 2- 10). The long-short-long bond alternation in the diene fragment coupled with the short Zr–C(17) and long Zr–C(18) bonds, confirm the *s-cis* bent metallacyclo-3-pentene formulation.

References on page 190

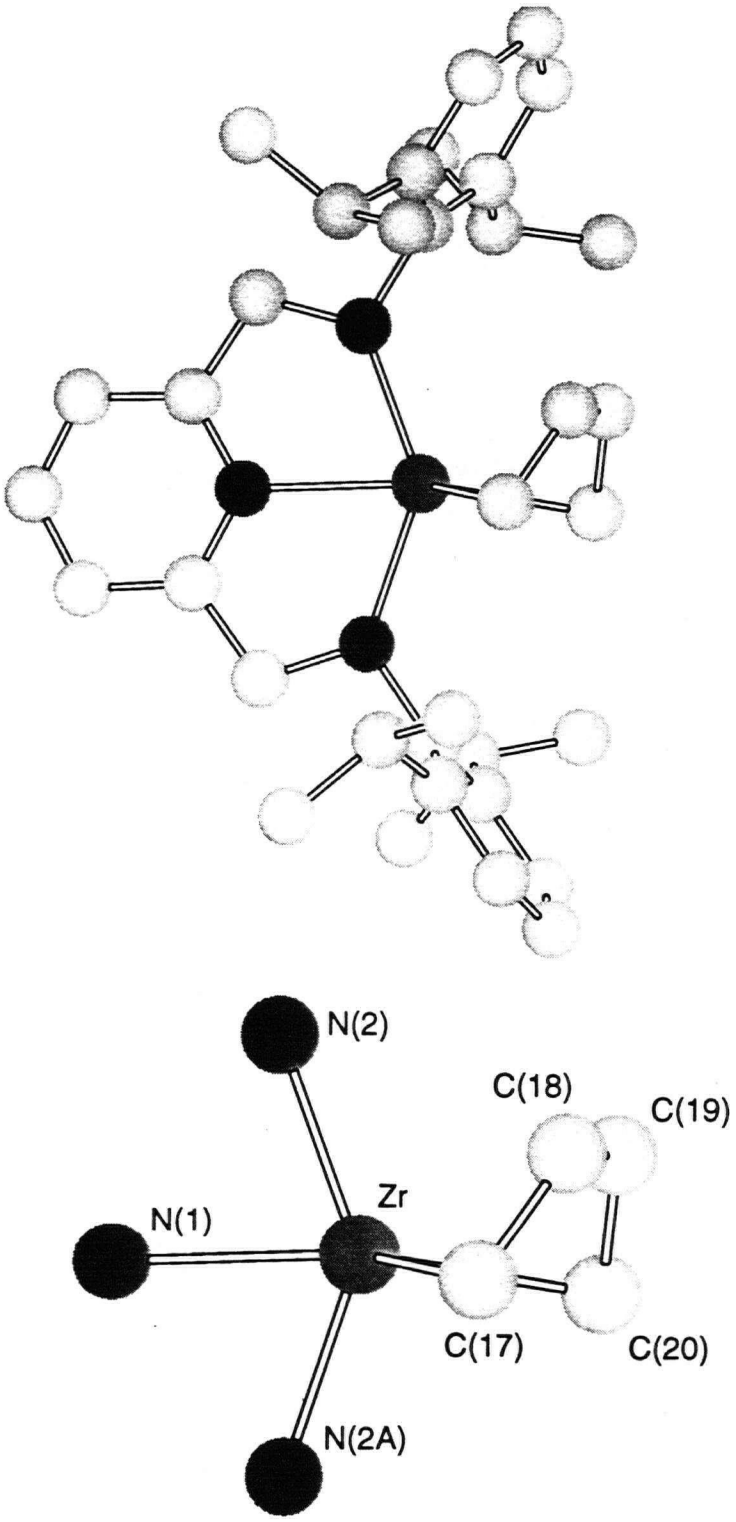

Figure 2- 24. Molecular structure of complex ***13a*** *from X-ray crystallography*

References on page 190

*Table 2- 6. Selected Bond Distances (Å) and Angles (°) for complex **13a***

Bond Distances			
Zr–N(1)	2.307 (13)	Zr-C(18)	2.47 (2)
Zr–N(2)	2.111 (8)	Zr-C(19)	2.47 (2)
Zr–N(2A)	2.111 (8)	C(17)–C(18)	1.56 (3)
Zr–C(17)	2.36 (2)	C(18)–C(19)	1.36 (3)
Zr–C(20)	2.33 (2)	C(19)–C(20)	1.55 (3)
Bond Angles			
N(2)–Zr–N(2A)	140.0 (4)	Zr–C(20)–C(19)	37.5 (7)
N(1)–Zr–C(17)	133.3 (6)	C(17)–C(18)–C(19)	126 (2)
N(1)–Zr–C(20)	141.4 (7)	C(20)–C(19)–C(18)	121 (2)
Zr–C(17)–C(18)	37.7 (7)		

The qualitative molecular orbital diagram describing the bonding of a diene ligand with the pyridine-diamide-zirconium fragment is shown in Figure 2- 25. Overlap of the $5b_2$ and $13a_1$ frontier orbitals of the $(PyN_2)Zr$ fragment with the filled σ_1 and σ_2 orbitals of the diene {carbons C(17) and C(20)} account for the σ-bonds between Zr and these carbons. Mixing between the π_1 {C(18) and C(19)} and the $10b_1$ orbital of the metal fragment results in the formation a filled π-type molecular orbital.

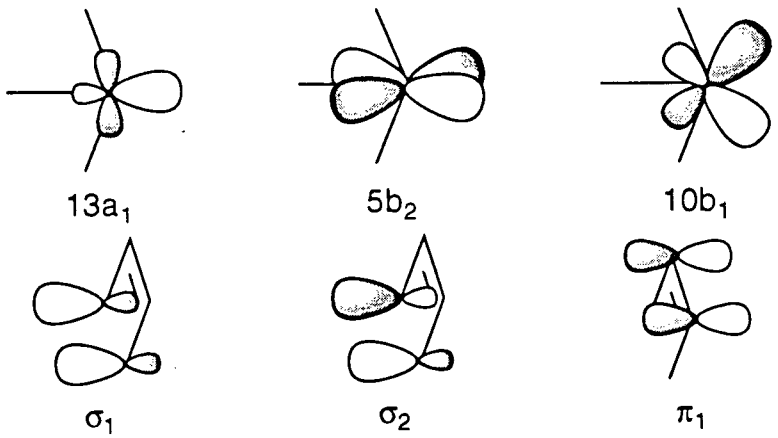

*Figure 2- 25. Bonding interactions for complexes **13a-c**.*

References on page 190

This is consistent with a 2σ-1π bonding mode of the diene and the *s-cis*-bent metallacyclo-3-pentene molecular structure.

The diene complex **13a** does not react with unsaturated substrates over several days at 23 °C. However, products derived from insertion into the Zr–C σ-bond are observed upon heating to 90 °C in benzene (Scheme 2- 4).

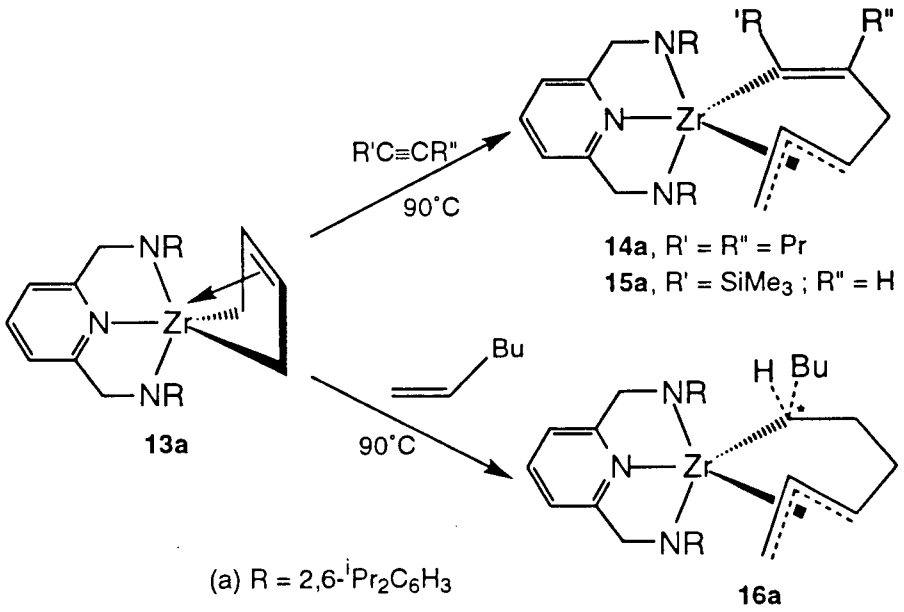

*Scheme 2- 4. Reaction of complex **13a** with unsaturated substrates*

The ^{1}H and $^{13}C\{^{1}H\}$ NMR spectra of complexes **14a, 15a** and **16a** show resonances characteristic for the Zr-allyl functional group and one σ-vinyl group[121-125]. The ^{1}H NMR spectrum of complex **14a** displays two AB quartets for the ligand methylene (NCH_2) protons indicative of a complex with C_1 symmetry. There is no evidence for syn/anti proton exchange in the allyl group to 80 °C, suggesting that this moiety is firmly coordinated to the electrophilic zirconium center. The metallocene-based complex $Cp_2Zr(\eta^4$-isoprene) reacts with 2-butyne to give a similar σ,π-allyl derivative which has been structurally characterized[123].

References on page 190

The reaction of compound **13a** with excess $HC{\equiv}CSiMe_3$ affords a single isomer derived from 2,1-insertion of the acetylenic unit into the zirconium-carbon bond. The substitution pattern of the complex is established on the basis of ^1H NMR spectroscopy, ^1H COSY and NOE experiments. For example, irradiation of the low-field signal (δ 8.02 ppm) results in an enhancement of the metallacycle C=C-CH_2 protons (Figure 2- 26). The irradiation of other groups is also consistent with 2,1-insertion.

The reaction of complex **13a** with excess 1-hexene affords a single isomer derived from 2,1-insertion of the α-olefin into the Zr–C bond. The presence of two AB quartets for the ligand methylene protons (NCH_2) is consistent with a complex with C_1 symmetry. The 2,1-insertion of the olefin was confirmed by ^{13}C-APT spectroscopy. An inverted peak is observed for the carbon attached to the zirconium characteristic of a tertiary carbon. In a similar way, most 1-alkenes (1-butene, 1-octene, etc.) react with Cp_2Zr(diene) in a 1,2 fashion to give complexes with one σ- and η^3-allyl M–C bonds[121-123]. The reaction is believed to result from a [2+2]-type oxidative coupling of the alkene and the diene (Scheme 2- 5)[113].

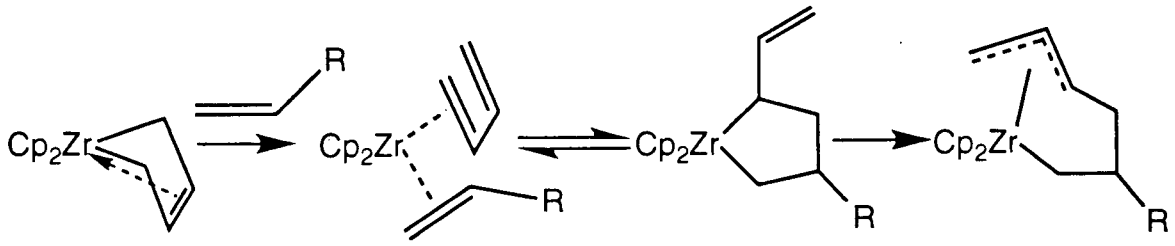

Scheme 2- 5. Reaction of Cp_2Zr(diene) with α-olefins

The reaction of complex **3a** with 2.2 equivalents of PrMgCl or BuMgBr affords the di(alkyl) derivatives **17a** and **18a**, respectively (Scheme 2- 2). The ^1H NMR spectra of complexes **17a** and **18a** display the resonances expected for complexes with C_{2v} symmetry.

The reaction of complex **3a** and 2.2 equivalents of EtMgCl does not afford the expected diethyl derivative (BDPP)$ZrEt_2$. The ^1H NMR spectrum of the crude reaction mixture is

References on page 190

consistent with activation of one of the isopropylmethyls of the ligand. Attempts to isolate the ligand activated complex were unsuccessful as a result of the high solubility of the compound.

Related complexes (**21a** and **22a**) were obtained by the thermolysis of complexes **17a** and **18a** (80°C, C_6D_6, 12 hours), respectively (eq. 10). The ^{1}H NMR spectrum of complex **21a** (Figure 2- 27) displays two AB patterns (③/❸) for the ligand methylene (NCH_2) protons and three isopropyl methine resonances (④). These resonances are consistent with C_1-symmetry and activation of one of the ligand isopropylmethyl groups.

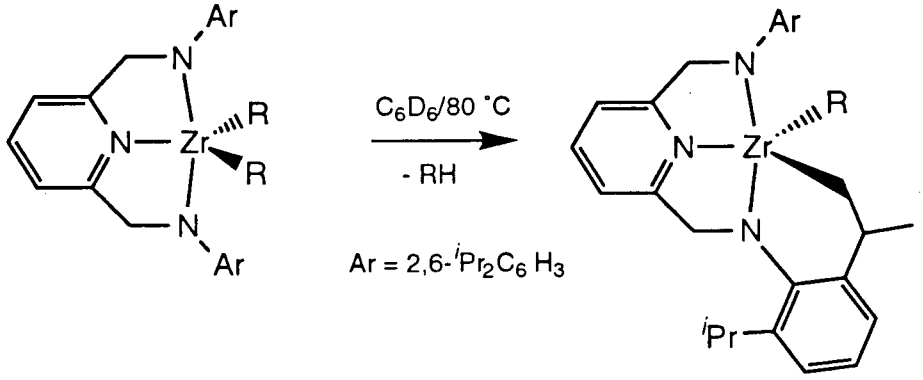

(10)

17a, R = Pr
18a, R = Bu

21a, R = Pr
22a, R = Bu

Charaterization of the gas formed by the reaction of complex **3a** and two equivalents of D_5-EtMgCl showed that CD_3CD_3 is formed. Moreover, no butene was detected from the thermolysis of complex **18a** (within the detection limits of ^{1}H NMR spectroccopy). Based on these observations, two mechanisms can be proposed for these reactions. The first pathway (Scheme 2- 6, **I**) involves β-hydride elimination, followed by alkane reductive elimination to give a Zr^{II}-olefin complex. A similar reaction has been observed with dialkylzirconocene complexes[126]. The activation of the isopropyl methyl C–H bond results in the formation of a mono(hydride) alkene complex. Insertion of the olefin into the M–H bond affords the final product. A similar pathway, which involves a metal centre with a d^2-electronic configuration, has been proposed for ligand activation of titanium pyridine diamide complexes (chapter one). This

References on page 190

route is not likely given that no olefins was oberved in a sealed tube experiment which requires *quantitative* reinsertion of the olefin in the metal-hydride bond.

The second route (Scheme 2- 6, **II**) involves the formation of an alkylidene intermediate via α-elimination of alkane. The proposed alkylidene intermediate is very similar to the imido species proposed earlier for ligand activation of an alkyl-amido complex (Scheme 2- 1). Moreover, α-elimination in the presence of β-hydrogens has been reported for tungsten amide complexes[127] and alkylidene complexes of zirconium are known[128-130].

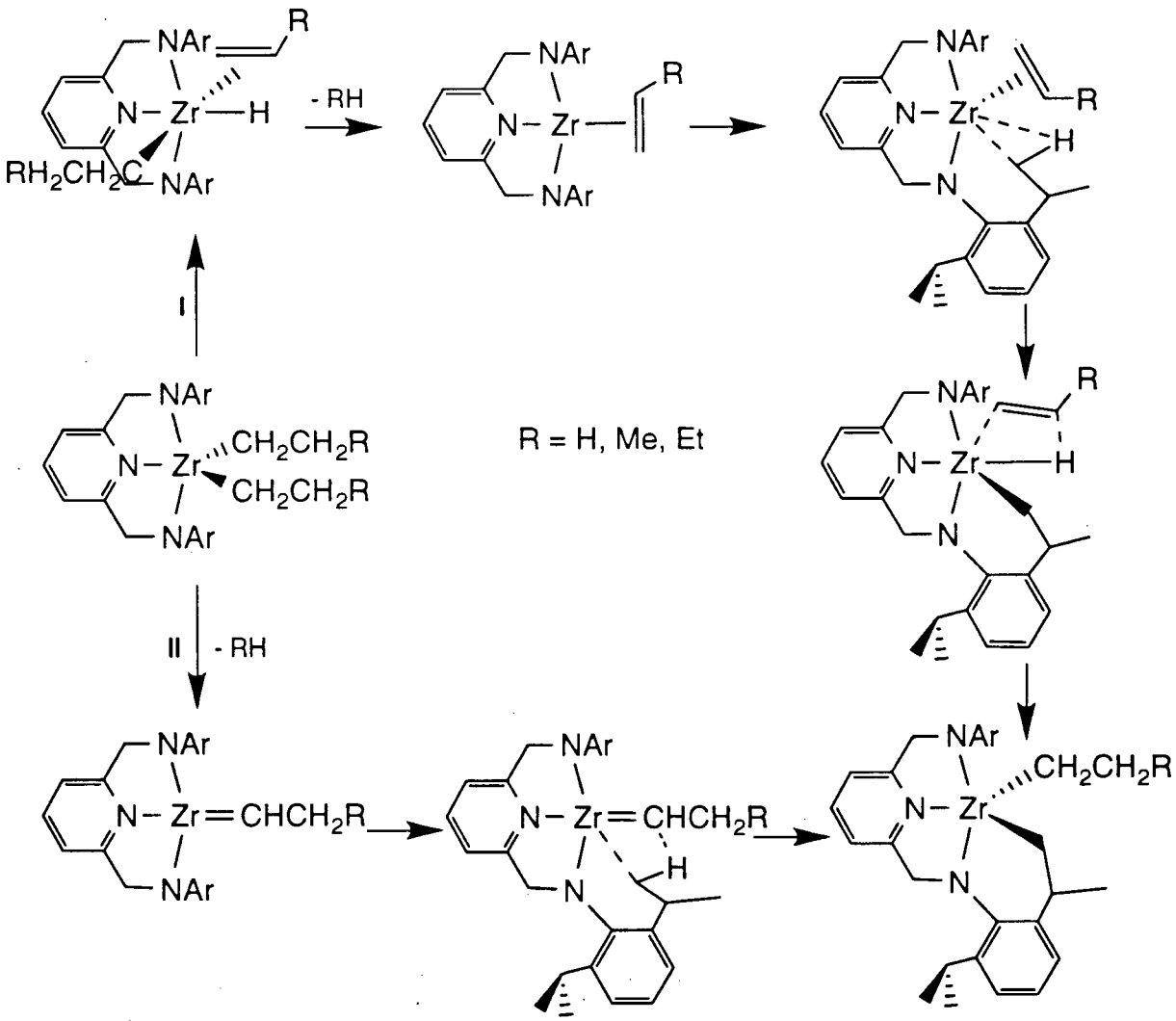

Scheme 2- 6. Mechanism of ligand C-H activation

References on page 190

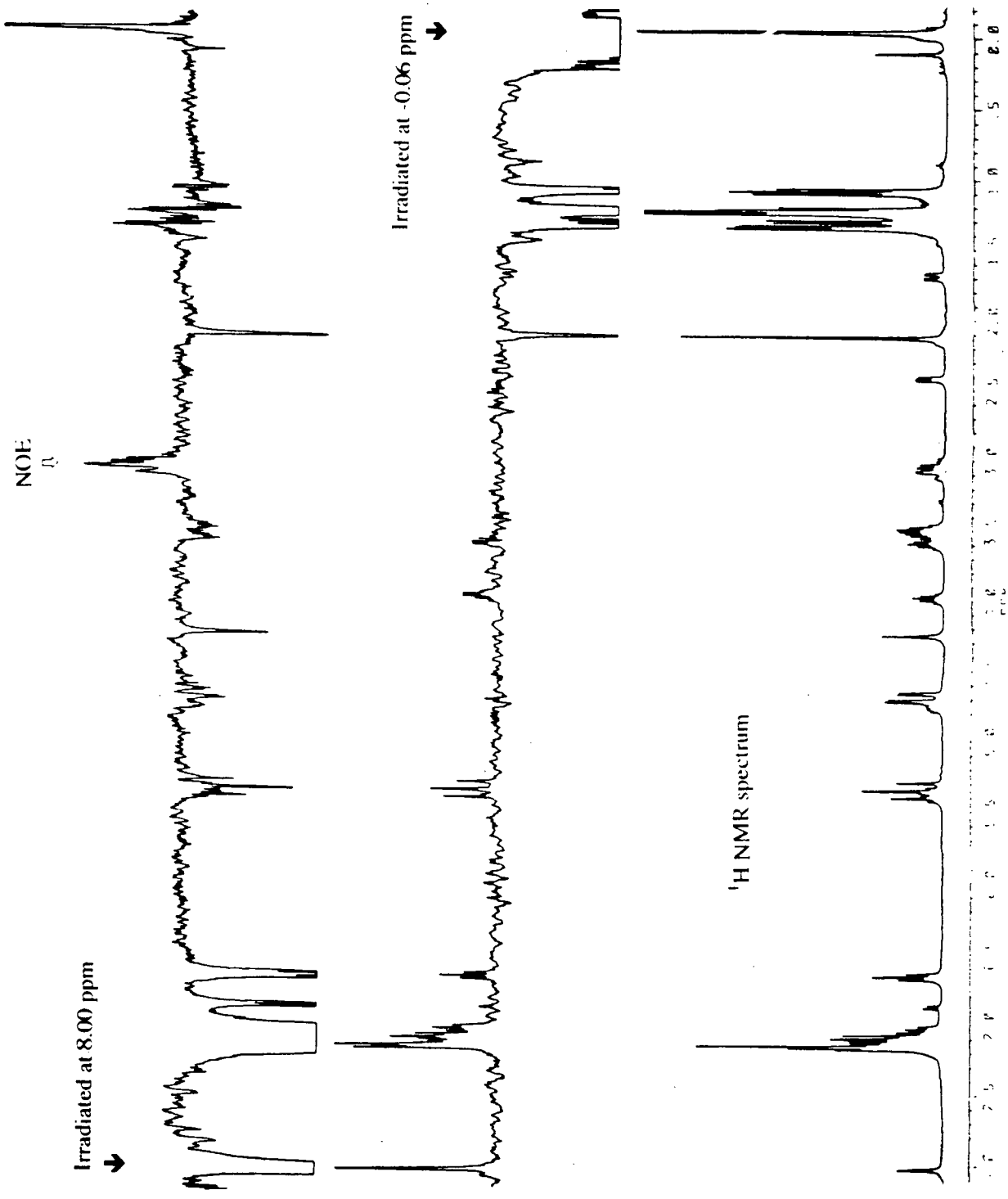

Figure 2- 26. ^{1}H NOE spectra of complex 13a (400 MHz, C_6D_6)

References on page 190

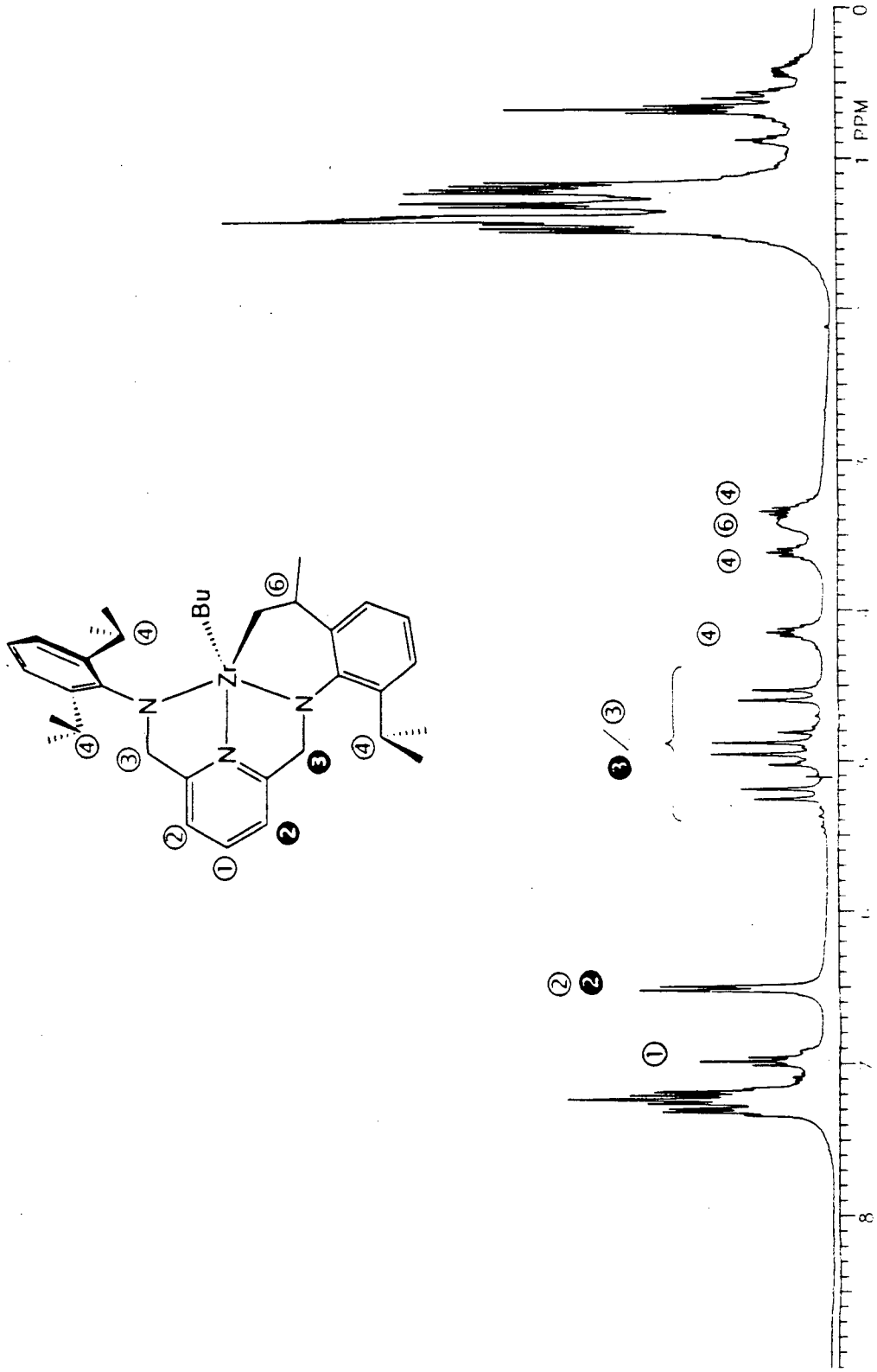

*Figure 2- 27. ^1H NMR spectrum of complex **21a** (300 MHz, C_6D_6)*

References on page 190

2.2 Ortho-substituted aryl diamido complexes

As previously noted, bis(2-phenyl-indenyl)zirconiumdichloride acts as a catalyst precursor for the polymerization of propylene in a stereoblock fasion. The indenyl ligands rotate about the metal-ligand bond and cause the catalyst to isomerize between chiral-like and achiral-like structures. The chiral-like C_2-geometry leads to isotactic polypropylene while the achiral-like C_s-geometry generates atactic polypropylene, resulting in a stereo block copolymer (Figure 2- 6).

With this oscillating catalyst system in mind, several ortho-substituted aryl diamido complexes of zirconium were prepared. Restricted rotation about the N-C_{ipso} bond has been observed for pyridine diamide complexes bearing 2,6-disubstituted phenyl groups. A small enough ortho-substituent might allow some rotation about the N-C_{ipso} bond. The resulting complex would alternate between chiral-like and achiral-like geometries in a way similar to the bis(2-phenyl-indenyl)zirconiumdichloride complex (Figure 2- 28).

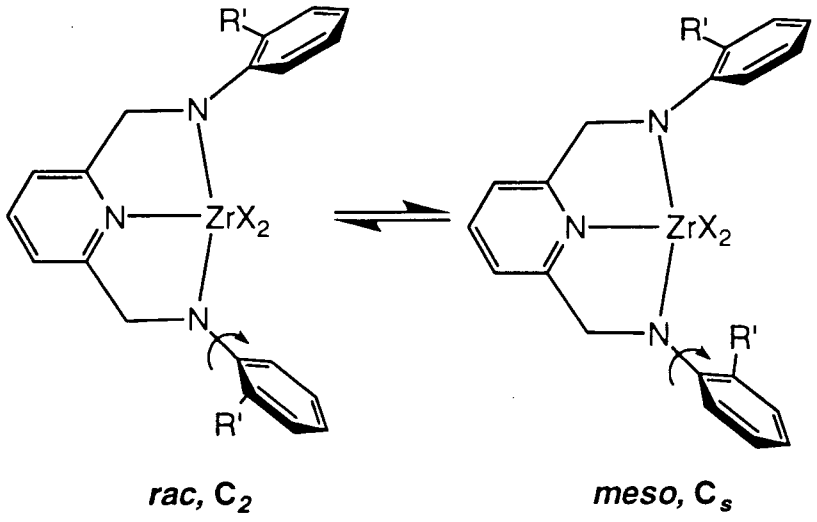

Figure 2- 28. Asymmetric ligand

The reaction of two equivalents of LiNHR (R = 2-phenylphenyl, 2-isopropylphenyl, 2-'butylphenyl, 2-isopropyl-6-methylphenyl) with 2,6-bis(bromomethyl)pyridine[77] yields the diamine $(BPhP)H_2$ (**1f**), $(BMPP)H_2$ (**1g**), $(BMBP)H_2$ (**1h**) and $(MPPP)H_2$ (**1i**) (eq. 11). Compounds **1g,h,i** can be isolated as white crystalline solids while the diamine **1f** is a viscous

References on page 190

oil. All four compounds can be prepared in nearly quantitative yield (by ^{1}H NMR spectroscopy) on a scale of 5-10 g.

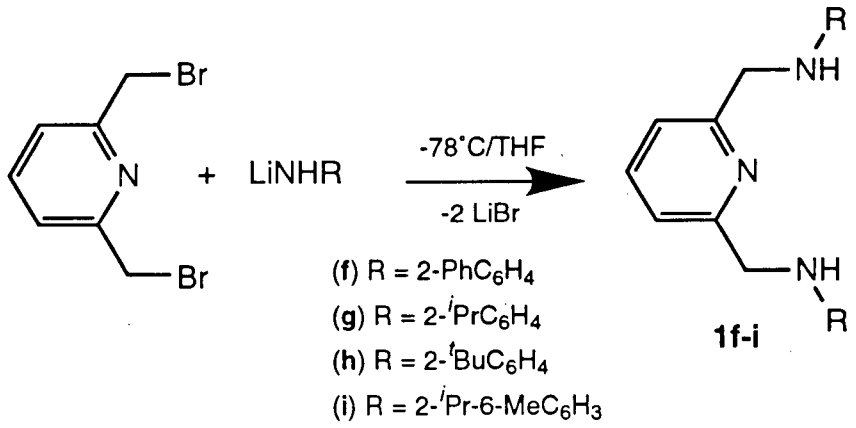

(11)

The diamines **1f-i** react cleanly with $Zr(NMe_2)_4$[1] at 23 °C to give two equivalents of $HNMe_2$ and the yellow crystalline mixed amide complexes **2f-i** (eq. 12). The amide complexes **2f-h** are isolated from hexanes in >90 % yield, however, the high solubility of compound **2i** in hexanes limits its isolation. These aminolysis reactions are unaffected by the presence of excess dimethylamine[53], hence only the kinetic products are observed.

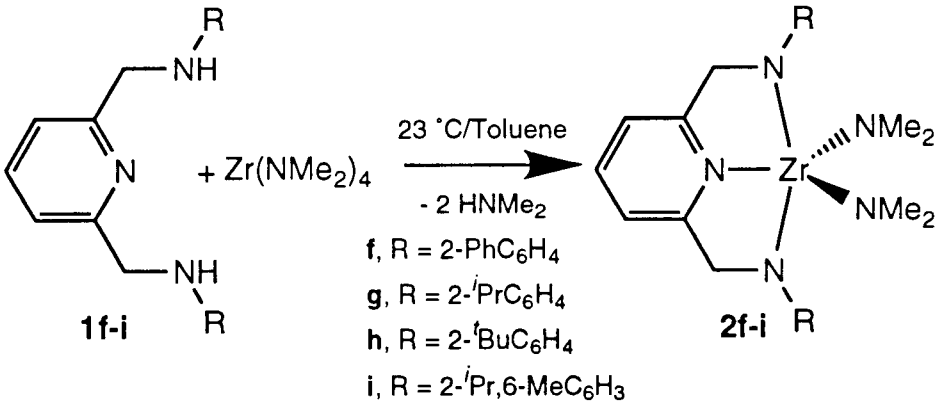

(12)

The room temperature ^{1}H NMR spectrum for complex **2f** exhibits a single sharp resonance for the methylene protons of the ligand (NCH_2) and a singlet for the dimethylamido groups. These observations are consistent with C_{2v}-symmetry resulting from free rotation about the N–C_{ipso} bond. The spectrum remains unchanged to -80 °C. Modeling studies[78] on compound **2f**, using the X-ray coordinates of complex **5b** as a starting point, predict a large

References on page 190

barrier to rotation about the N–C_{ipso} bond when the *o*–phenyl groups pass by the dimethylamido groups (Figure 2- 29).

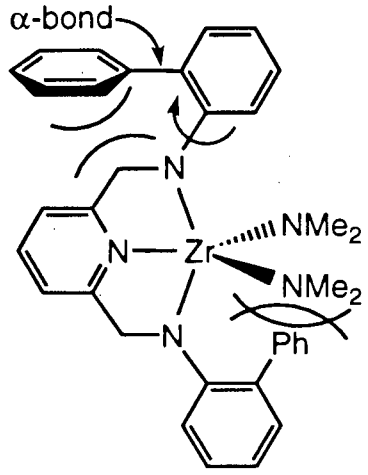

Figure 2- 29. Steric interactions in complex 2f

Rotation about the Ph-Ar α-bond allows the *o*–phenyl groups to pass by the methylene protons of the ligand backbone without significant steric interactions. Furthermore, these calculations suggest that the ease of rotation decreases in the following way: *o*–Ph > *o*–^{i}Pr > *o*–^{t}Bu (*vide infra*).

The room temperature ^{1}H NMR spectrum of complex **2g** also exhibits a single sharp resonance (Figure 2- 30, ①) for the ligand methylene protons (NCH_2), one septet (②) for the isopropyl methines and one doublet (③) for the isopropyl methyl groups. Again, this is consistent with free rotation about the N–C_{ipso} bond resulting in the spectroscopically observed C_{2v}-symmetry. Unlike complex **2f**, resonances attributable to two isomeric compounds are observed upon cooling complex **2g** (Figure 2- 30). The low temperature (-80 °C) limiting ^{1}H NMR spectrum of compound **2g** in d_8-toluene shows three dimethylamido (NMe_2) resonances (④) in a ratio of 1:1:1.2. Moreover, overlapping ligand resonances are observed for the two complexes. For example, two AB quartets are observed for the ligand methylene protons (⑤).

References on page 190

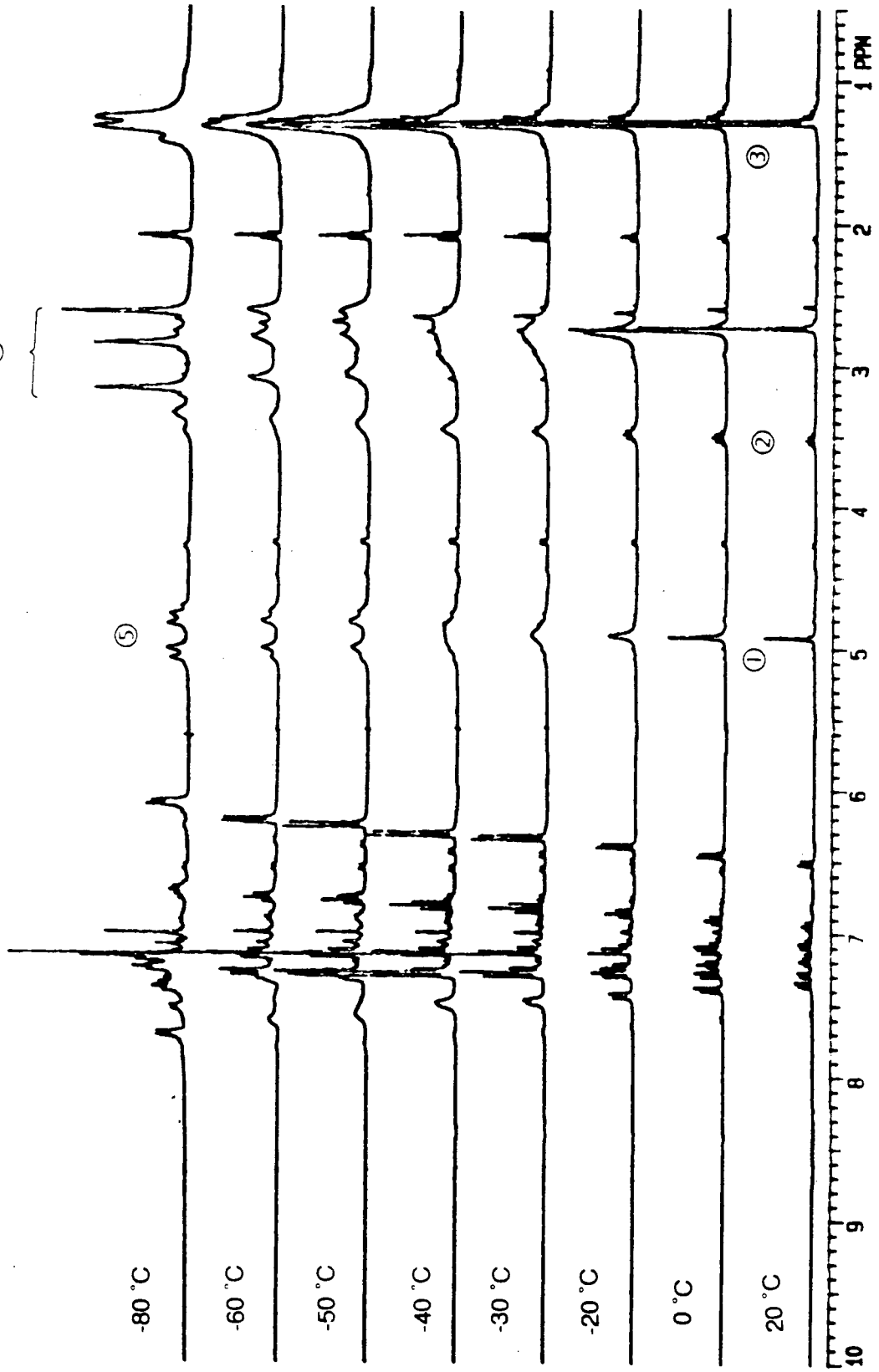

Figure 2- 30. Variable-temperature ^{1}H NMR spectra of couplex **2g** *(300MHz, $CD_3C_6D_5$)*

References on page 190

These resonances are in agreement with an approximately 1.67:1 mixture of the C_s-symmetric *meso* and C_2-symmetric *rac* rotameric isomers in solution at -80 °C (Figure 2- 31). The C_s-symmetric *meso* rotamer has a mirror of symmetry that runs perpendicular to the ZrN_3 plane. Therefore, the two isopropylphenyl methine groups are chemically and magnetically equivalent. Moreover, the isopropyl methyl groups appear as two doublets as a result of the rigid aryl orientation. The two dimethylamido ligands are not related by this mirror plane and appear as two singlets of equal intensity. On the other hand, the C_2-symmetric *rac* rotamer has a C_2 access of rotation coincidental with the pyridine–zirconium bond. Consequently, the two dimethylamido groups are related by symmetry and are equivalent. Similarly, the two isopropylphenyl substituents are also equivalent resulting in one isopropyl methine and two isopropyl methyl resonances. In both rotamers, the ligand methylene protons are inequivalent giving rise to two AB quartets (NCH_AH_B).

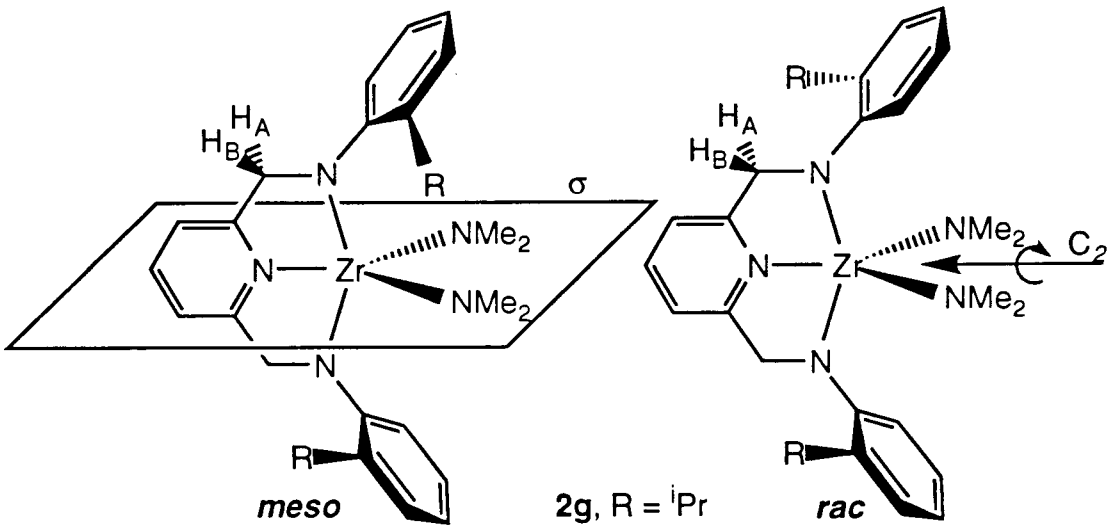

Figure 2- 31. Meso and rac rotameric isomers of complex ***2g***

The resonances coalesce at -40 °C yielding a barrier to rotation of the aryl groups of $\Delta G^{\ddagger}$ = 11.2 (5) kcal mol^{-1} [131].

References on page 190

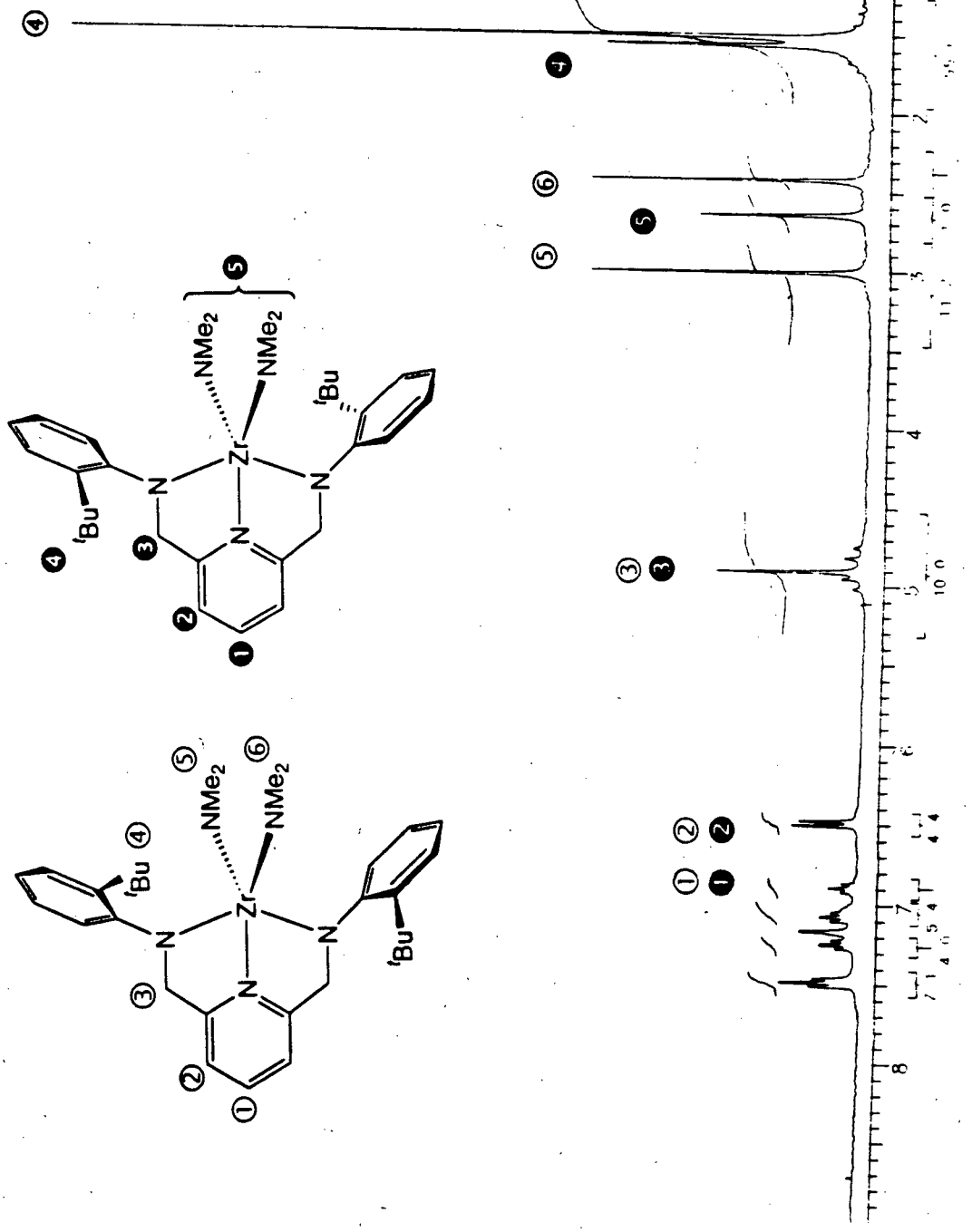

*Figure 2- 32. Room temperature ^{1}H NMR spectrum of couplex **2h** (300MHz, $CD_3C_6D_5$)*

References on page 190

In contrast to compounds **2f** and **2g**, the room temperature ^{1}H NMR spectrum for complex **2h** displays resonances for two distinct species (Figure 2- 32). The ^{1}H NMR spectrum of complex **2h** displays three dimethylamido resonances consistent with the presence of both *meso* (⑤ and ⑥) and *rac* (❺) rotameric isomers in a 2.6:1 ratio. Moreover, an AB quartet (❸) for the ligand methylene protons (NCH_AH_B) and a singlet (❹) for the equivalent ^{t}Bu groups are observed for the *rac* isomer. In addition to these resonances, the *meso* isomer displays a singlet (③) for the *tert*-butyl substituents and an apparent singlet (④) is observed for the ligand methylene protons instead of the expected AB pattern. This is characteristic for a system where the chemical shift difference between H_A and H_B is small ($\Delta\upsilon \leq 0.4$ Hz)[132]. The ^{13}C{^{1}H} NMR spectrum of complex **2h** is also consistent with the presence of both rotamers.

As noted above, the *rac/meso* ratio is unaffected by added dimethylamine. Thus, only the kinetic products are obtained. In contrast, the reaction of (EBI)H_2 (EBI = 1,2-bis(1-indenyl)ethane) with $Zr(NMe_2)_4$ initially yields (EBI)$Zr(NMe_2)_2$ in a *rac/meso* ratio of 2:1 but the ratio increases to 13:1 with time (100 °C, 17h)[53] . This suggests that the amine elimination is reversible and that the *meso* and *rac*-complexes are formed at comparable rates but the *rac* isomer is the thermodynamically preferred product. Moreover, it was demonstrated that the epimerization of *meso* to *rac* is catalyzed by Me_2NH and is inhibited when the amine is removed from the reaction mixture.

Interestingly, the reaction of $Me_2Si(C_5H_4$-3-^{t}Bu$)_2$ and $Zr(NMe_2)_4$ yields [$Me_2Si(C_5H_3$-3-^{t}Bu$)_2$]$Zr(NMe_2)_2$ in a *rac/meso* ration of 1:2[133]. In this case, the higher *meso* preference is interpreted as a result of a lateral deformation of the *ansa* ligand system to reduce steric interactions. A similar 'deformation' whereby the metal adopts a square-based pyramidal (sbp) geometry instead of a trigonal bipyramidal (tbp) conformation is proposed to account for the preferred *meso* rotamer of compound **2h**(Figure 2- 33). As a result of this deformation, some of the steric strain associated with the *meso* isomer is relieved relative to the *rac* isomer. It is not

References on page 190

possible to distinguish spectroscopically between the proposed sbp and tbp complexes since both compounds possess C_s–symmtery.

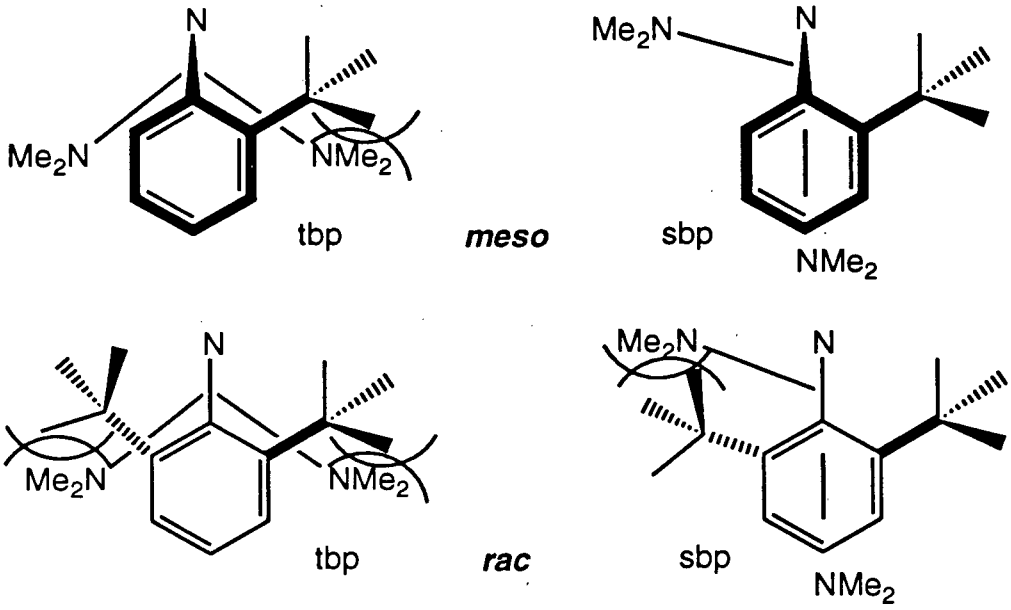

Figure 2- 33. Structural deformation

The energy difference between sbp and tbp geometries is expected to be quite small given the d^0 electronic configuration of zirconium. A similar change in hybridization has been observed in other d^0 group 4 complexes bearing the pyridine diamide ligand. The mono(neophyl) derivative $[2,6\text{-}(RNCH_2)_2NC_5H_3]TiBr(CH_2CMe_2Ph)$ (R = 2,6-$Me_2C_6H_3$) (see chapter one) displays a sbp geometry in the solid state with the largest group occupying the apical position. This geometry minimizes the interaction between the orthomethyl groups of the aryl and the bulky neophyl ligand. In a similar way, the di(benzyl) complex (**6a**), exhibits a sbp geometry in the solid state.

The room temperature ^1H NMR spectrum for complex **2j** displays resonances for two rotameric isomers. These species do not interconvert bwtween -80 °C and +80 °C. Restricted rotation about the N–C_{ipso} bond is expected for complexes bearing 2,6-disubstitued aryl groups. The *rac/meso* ratio of 1.3:1 (from ^1H NMR spectroscopy) suggests that during the aminolysis

References on page 190

reaction the aryl groups have minimal influence on one another; in other words, a near statistical distribution of isomers is produced.

The mixed amide complexes **2f-i** react with excess $ClSiMe_3$ to afford the dichloride derivatives **3f-i** in 80-90% isolated yield (eq. 13). Upon addition of $ClSiMe_3$ the solutions turn black which is attributed to minor impurities given the high isolated yields.

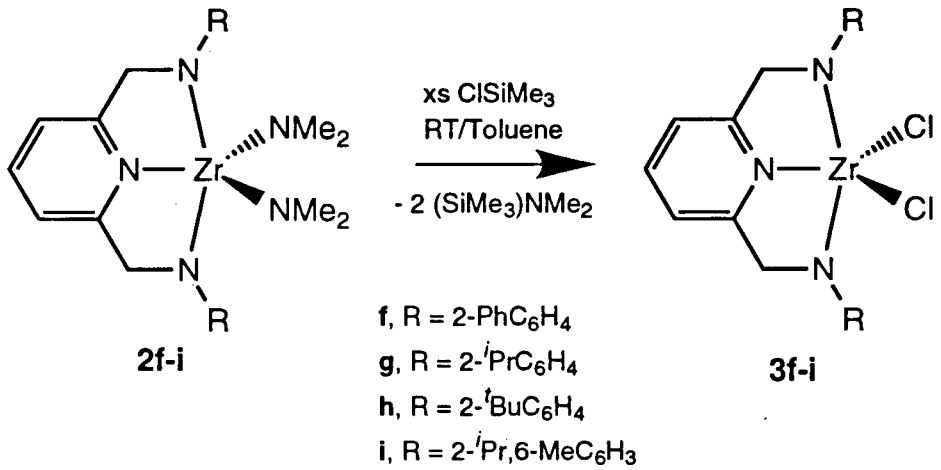

2f-i

f, R = 2-PhC_6H_4
g, R = 2-$^{i}PrC_6H_4$
h, R = 2-$^{t}BuC_6H_4$
i, R = 2-^{i}Pr,6-MeC_6H_3

3f-i

(13)

Similarly to the mixed amide derivative **2f**, the ^1H NMR spectrum of complex **3f** displays a sharp singlet for the ligand methylene protons (NCH_2), consistent with rapid rotation about the $N–C_{ipso}$ bond. The room temperature ^1H NMR spectrum of complex **3g** displays broad featureless resonances for the methylene (NCH_2), the isopropyl methine, and the isopropyl methyl protons of the ligand. The high temperature ^1H NMR limiting spectrum (+60 °C) is consistent with rapid rotation about the $N–C_{ipso}$ bond. The low temperature limiting spectrum (-60 °C) displays resonances for the two rotamers in a ratio of about 2:3. It is not possible to distinguish between C_s- and C_2-symmetric compounds in the absence of NMR active groups in the equatorial plane of an idealized tbp geometry. As a result, it is not possible to discern which isomer predominates in solution. The resonances coalesce at +10 °C and the barrier to rotation is $\Delta G^{\ddagger}$ = 13.8 (5) kcal mol^{-1}.

The *rac*/*meso* ratio in the mixed amide complex **2h** is 1:2.6. Interestingly, a single isomer of the dichloride complex **3h** is formed upon reaction with excess $ClSiMe_3$. Again, it is not

References on page 190

possible to distinguish between the *rac* and *meso* isomer in the absence of NMR active group in the equatorial plane of the tbp. However, the following results suggest that the *meso* rotamer is formed preferentially.

The reaction of **3h** with two equivalents of $PhCH_2MgCl$ or $PhCMe_2CH_2MgCl$ yields the *meso* dibenzyl (**6h**) and dineophyl (**9h**) derivatives, respectively (eq. 14). Alternatively, the dibenzyl complex **6h** can be prepared from $Zr(CH_2Ph)_4$[95] and the diamine **1h**.

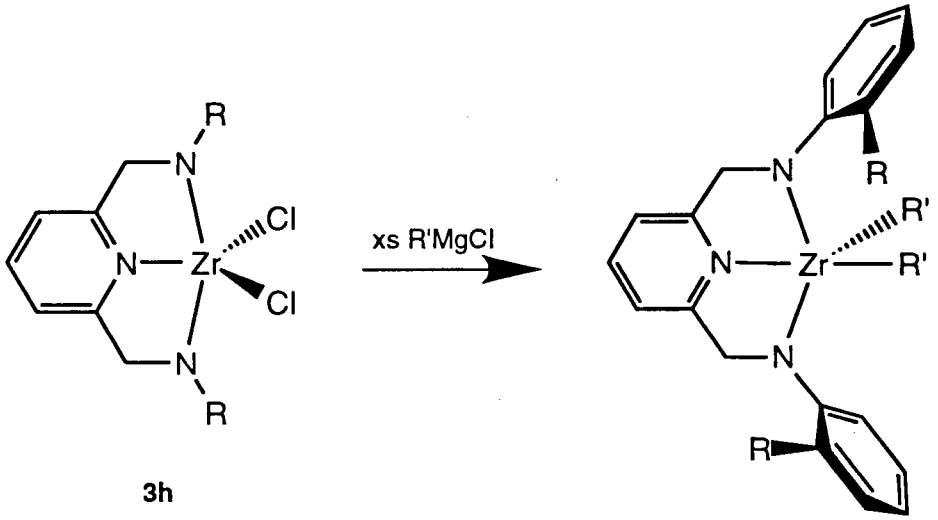

3h

***meso*-6h**, R = *tert*-Bu; R' = CH_2Ph
***meso*-9h**, R = *tert*-Bu; R' = CH_2CMe_2Ph

(14)

The ^1H NMR spectra of complexes **6h** and **9h** display a single AB quartet for the ligand methylene protons (NCH_AH_B) and one *tert*-butyl resonance in accordance with the presence of a single isomer. Moreover, two distinct benzyl resonances ($ZrCH_2Ph$) are observed for compound **6h** consistent with a C_s-symmetric *meso* rotamer. Similarly, the ^1H NMR of complex **9h** displays two singlets for the neophyl methylene (CH_2CMe_2Ph) resonances and two singlets for the neophyl methyl (CH_2CMe_2Ph) groups.

The mono(alkyl) derivatives $[2,6\text{-}(RNCH_2)_2NC_5H_3]ZrClR'$ **10h** (R' = CH_2CMe_2Ph) and **11h** {R' = $Si(SiMe_3)_2$} can be prepared from compound **3h** and the corresponding alkylating reagent (eq. 15).

References on page 190

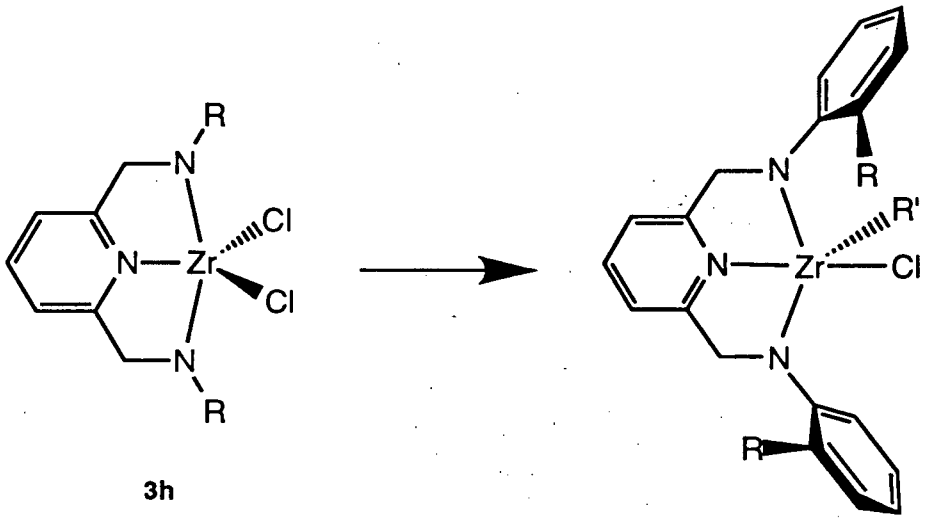

3h

***meso*-10h**, R = *tert*-Bu; R' = CH_2CMe_2Ph
***meso*-11h**, R = *tert*-Bu; R' = $Si(SiMe_3)_3$

(15)

Reaction conditions: **10h**, $PhCMe_2CH_2MgCl$, CH_2Cl_2, -78 °C; **11h**, $(Me_3Si)_3SiLi \cdot 3thf$[134], hexanes, -78 °C.

The ^1H NMR spectrum of complex **10h** displays one AB quartet for the ligand methylene protons (NCH_AH_B), a singlet for the ligand *tert*-butyl groups, and two singlets (CH_2CMe_2Ph and CH_2CMe_2Ph) for the neophyl fragment. These resonances are consistent with the C_s-symmetric *meso* isomer being the only species present in solution. The *rac* isomer can be ruled out since asymmetry about the ZrN_3 plane removes the C_2 rotational axis (Figure 2- 31). Thus, a complex with C_1 symmetry would be obtained. Similarly, the ^1H NMR spectrum of complex **11h** displays resonances characteristic for the *meso* isomer.

As expected, the ^1H NMR spectrum of compound **3i** displays resonances for two rotamers in a ratio of about 1.15:1. It would appear that no change in the isomeric ratio, within limits of detection, takes place during the metathesis reaction with $ClSiMe_3$. The ^1H NMR spectrum remains unchanged at 80 °C.

The dichloride complexes **3f-i** react with 2 equivalents of MeMgX (X = Cl, Br) to afford the dimethyl derivatives (**5f-i**) in 67-85 % yield as white crystalline solids (eq. 16). The ^1H and

References on page 190

$^{13}C\{^1H\}$ NMR spectra of complexes **5f-i** displays Zr-Me resonances similar to what has been obtained for complexes **5a-e** and other related compounds[23,80-83].

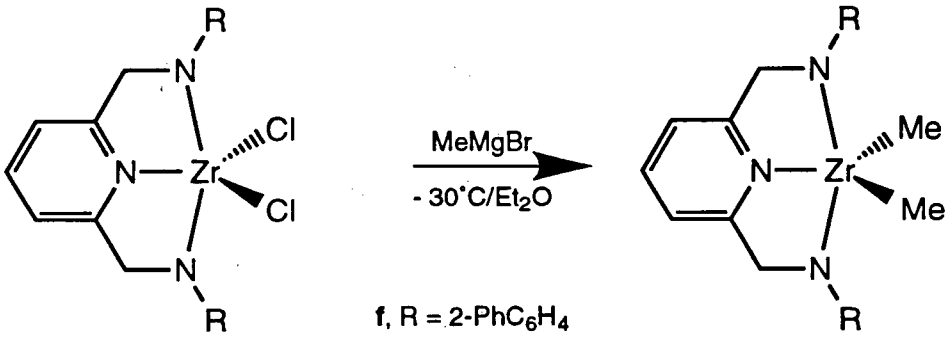

3f-i **5f-i** (16)

f, R = 2-PhC_6H_4
g, R = 2-^{i}PrC_6H_4
h, R = 2-^{t}BuC_6H_4
i, R = 2-^{i}Pr,6-MeC_6H_3

The ^1H NMR spectrum of the 2-phenylaryl substituted complex **5f** displays a single resonance for the Zr-*Me* groups down to -80 °C, consistent with free rotation about the N-C_{ipso} bond and a C_{2v}-symmetric complex

The room temperature ^1H NMR spectrum of complex **5g** (Figure 2- 34) displays a singlet for the ligand methylene protons (NCH_2), a septet for the isopropyl methine, a doublet for the chemically equivalent methyl groups, and a singlet for the Zr-Me_2 groups.

These resonances are consistent with free rotation about the N–C_{ipso} bond and a C_{2v}-symmetric complex. The low temperature (-60 °C) limiting spectrum shows overlapping resonances for the ligand methylene protons (NCH_2), the isopropyl methines and the isopropyl methyl groups. Furthermore, three broad zirconium methyl resonances in a ratio of 1:1.3:1 are observed. These resonances are attributable to a *rac/meso* ratio of 1:1.5. The above resonances coalesce at -20 °C yielding a barrier to rotation of the aryl groups of $\Delta G^{\ddagger} = 12.0$ (5) kcal mol^{-1}.

References on page 190

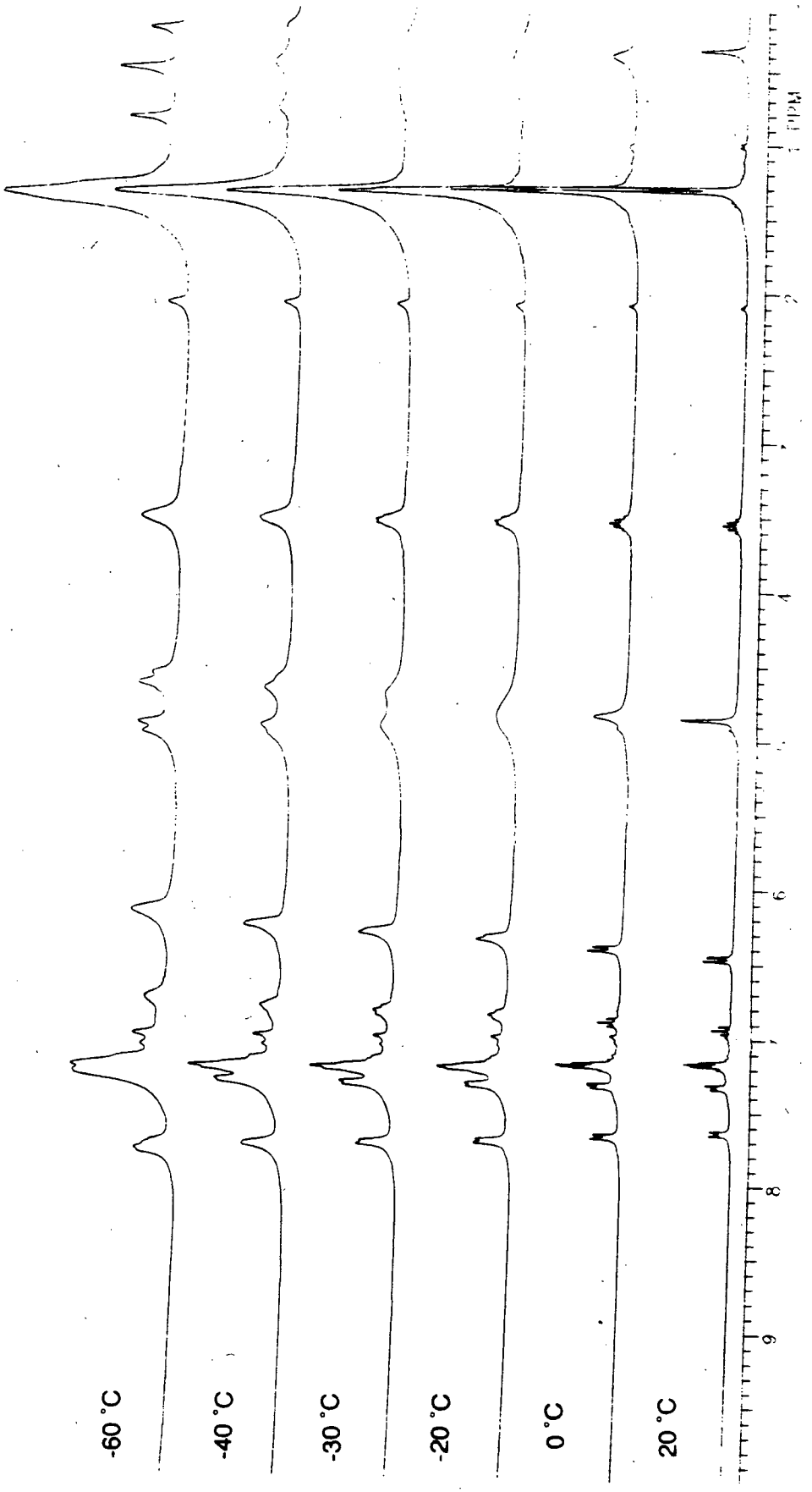

Figure 2- 34. Variable-temperature ^{1}H NMR spectra of couplex **5g** *(300MHz, $CD_3C_6D_5$)*

References on page 190

As mentioned above, the reaction of the dichloride derivative **3h** with bulky alkylating reagents affords exclusively C_s-symmetric complexes. Interestingly, the reaction of complex **3h** with two equivalents of MeMgBr yields a mixture of rotameric isomers of the dimethyl complex (**5h**) in a ratio of about 1:3 (*rac/meso*). The ^{1}H NMR spectrum of complex **5h** remains unchanged from -80 °C to +80 °C as observed with other derivatives bearing a *tert*-butyl group in the 2-position of the aryl ring (**3h** and **4h**).

The isomerization to yield a mixture of rotamers can be rationalized in the following way. The metathesis reaction involves an octahedral four-centred transition state as shown in Figure 2-35, (**II**). The two ^{t}Bu groups in complex **3h** direct the alkylating agent trans to the pyridine. Modeling studies[78] on this transition state show that the barrier to rotation of the aryl group in the octahedral transition state is much less (ca. 19 kcal mol^{-1}) than for the five coordinate complex (Figure 2- 35, **I**). When the incoming alkylating reagent is small (i.e., CH_3MgBr), free rotation about the N–C_{ipso} bond result in the isomerization of the complex and a mixture of rotamers is obtained (*meso/rac*, 3:1). Further isomerization is necessary to obtain a complex with the alkyl group located in the apical position. The non-statistical distribution of the two rotamers is interpreted as a result of some kinetic control inferred by the two *tert*–butyl groups on one another.

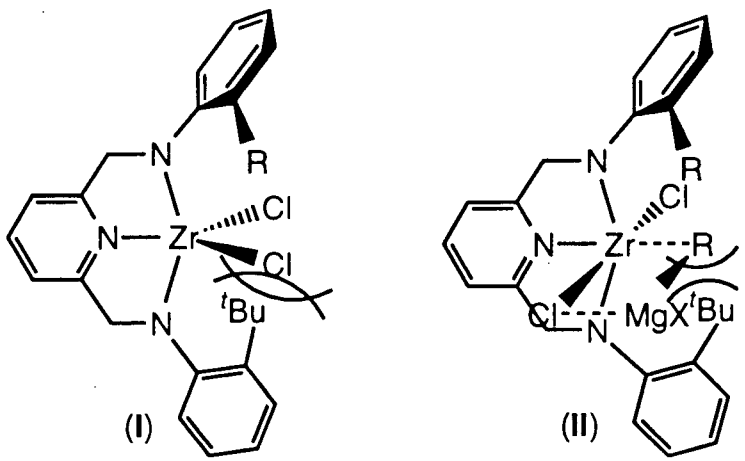

Figure 2- 35. Proposed steric interactions during alkylation

References on page 190

A similar ratio was obtained in the synthesis of the dimethylamido complex **2h** (2.6:1). However, when the incoming group is large (i.e., $PhCH_2MgCl$, $PhCMe_2CH_2MgCl$ or $\{Me_3Si\}_3SiLi\bullet 3thf$), rotation about the $N–C_{ipso}$ bond is inhibited and the original *meso* configuration is retained.

A similar mechanism is proposed to account for the formation of the *meso* rotamer as the only product from the reaction of complex **3h** with excess Me_3SiCl. Again, the isomerization is believed to take place from an octahedral transition state. In this case, rotation about the $N–C_{ipso}$ bond to give the *meso* rotamer takes place to relieve strain due to strong steric interactions between one of the *tert*-butyl groups in the *rac* rotamer and the incoming Me_3Si fragment (Figure 2- 36, **I**).

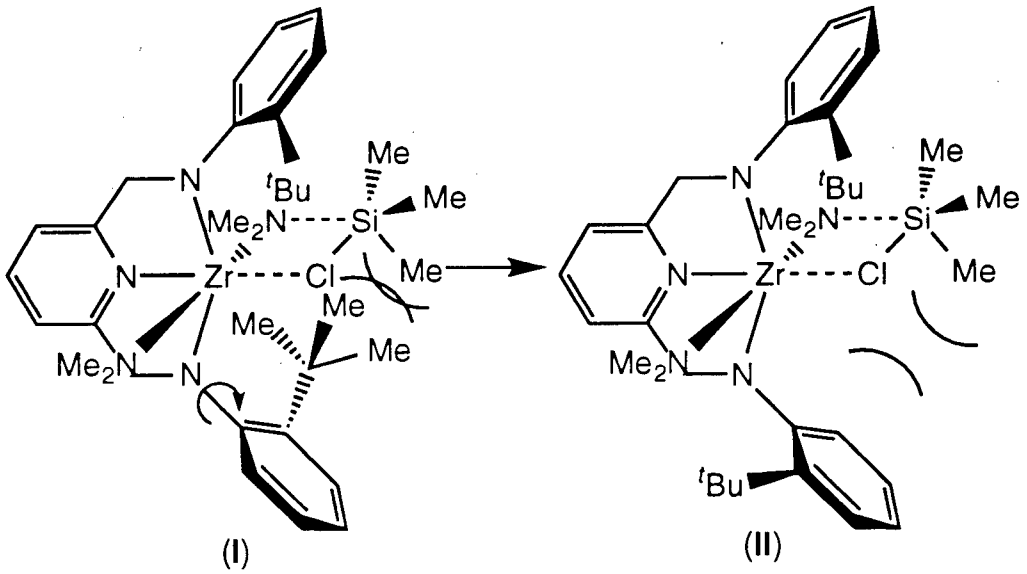

Figure 2- 36. Proposed steric interactions in the transition state

2.3 Alkyl diamido complexes

As described in chapter one, the addition of solid 2,6-bis(bromomethyl)pyridine to a large excess of H_2NR (R = Cy, ^{i}Pr, CH^iPr_2, ^{t}Bu, $CH_2CH_2NMe_2$) in hexanes at room temperature affords the oily diamines 2,6-$(HRNCH_2)_2NC_5H_3$ {(iPAP)H_2 (**1j**) R = ^{i}Pr; (CyAP)H_2 (**1k**) R = Cy; (LiAP)H_2 (**1l**) R =CH^iPr_2; (tBAP)H_2 (**1m**) R= ^{t}Bu; (DMEAP)H_2 (**1n**) R = $CH_2CH_2NMe_2$}

References on page 190

in quantitative yield(eq. 17). Compounds **1j-n** can be prepared on a scale of 10-15 g as colorless oils.

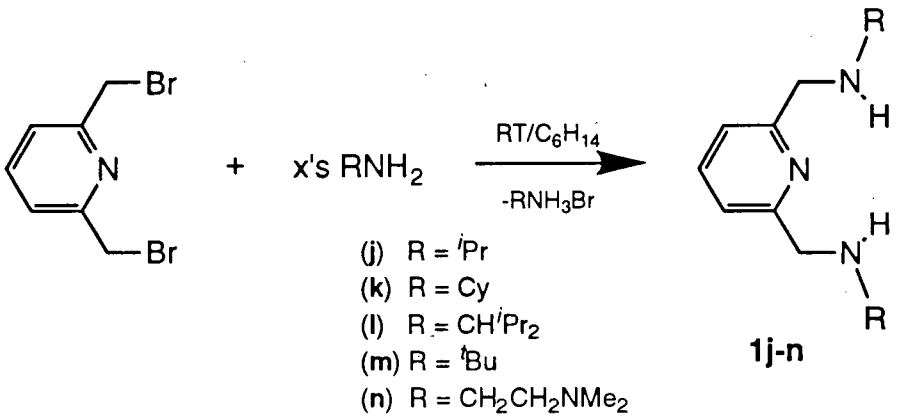

(17)

The diamines **1j-n** react rapidly with $Zr(NMe_2)_4$ at room temperature to give the mixed amide complexes **2j-n** (eq. 18). Compounds **2j-l** can be isolated in nearly quantitative yield as bright yellow crystalline solids. The bis(dimethylamido) complexes **2m-n** are too soluble to be isolated and were used without further purification.

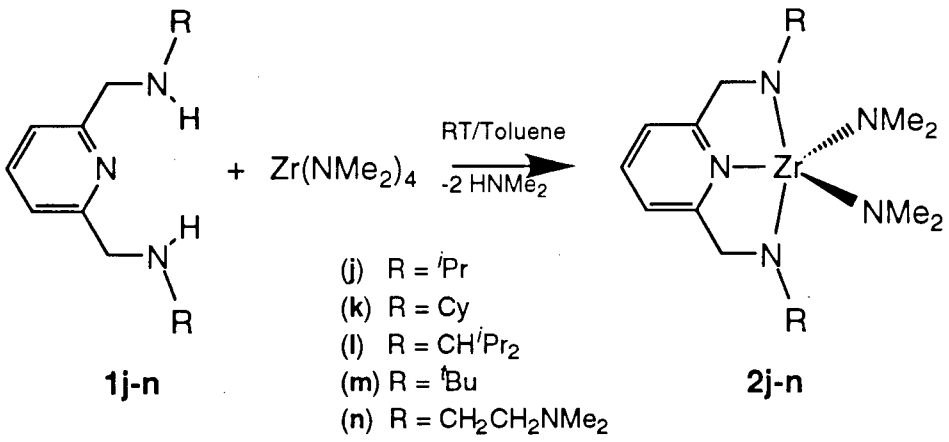

(18)

The ^1H NMR spectra of complexes **2j-n** display a single sharp resonance for the ligand methylene protons and a singlet for the dimethylamido fragments consistent with C_{2v}-symmetry. Interestingly, the methine protons (NC*H*) in complex **2j** appear as a septet at an unusually high chemical shift (4.45 ppm). In a similar way, the methine protons in complex **2k** (δ 3.87) and **2l** (δ 3.25) also appear at low field (*vide infra*). The ^1H NMR spectrum of complex **2n** displays a singlet for the ligand $CH_2CH_2N\mathit{Me}_2$ groups at 2.23 ppm; for comparison, these same protons

References on page 190

appear at 2.02 ppm for the diamine **1n**. Moreover, the ^{1}H NMR spectrum for complex **2n** remains unchanged from -80 °C to +80 °C suggesting that the amine functionalities are not interacting with the zirconium atom.

The dichloride complexes **3j-n** are formed in good yield from the reaction of complexes **2j-n** and excess Me_3SiCl at room temperature (eq. 19).

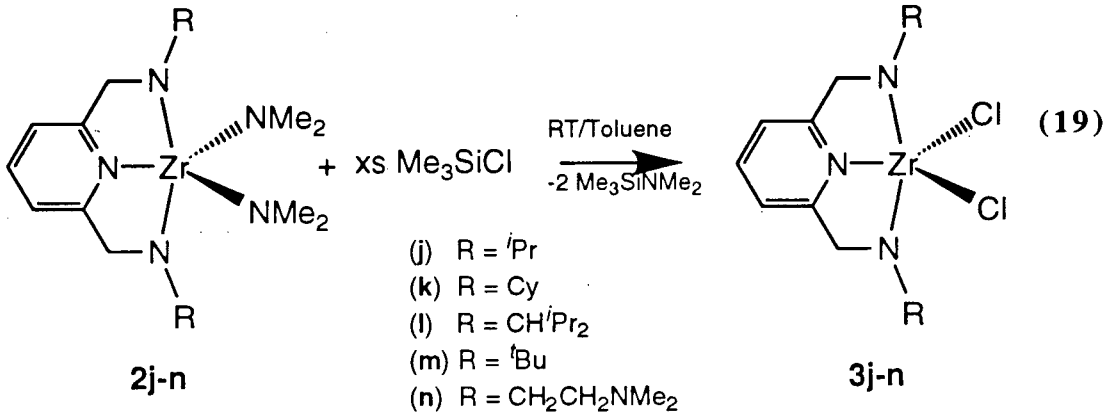

(19)

Complexes **3j-m** can be crystallized from CH_2Cl_2 as white crystalline solids. The high solubility of complex **3n** limited its purification. Again, spectral data for complexes **3j-n** are consistent with meridional coordination of the pyridine-diamide ligand.

The addition of 2.5 equivalents of MeMgBr to the dichloride complexes **3j-n** affords the dimethyl derivatives **5j-m** in good yield (eq. 20) as bright yellow solids.

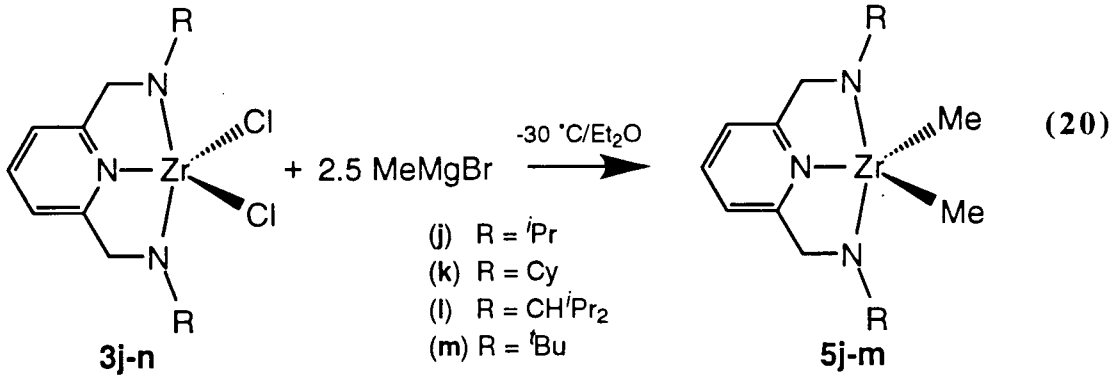

(20)

The C_{2v}-symmetry of complexes **5j-m** is evidenced by a single sharp resonance (^{1}H NMR) for the ligand methylene protons (NCH_2). The ^{1}H and $^{13}C\{^1H\}$ NMR spectra of complex

References on page 190

5j display a Zr–CH_3 resonance at δ 0.34 ppm and a Zr–CH_3 at δ 31.26 ppm. Similar resonances are observed for complexes **5k-m** and other related complexes[23,80-83].

The ligand isopropyl methine protons ($CHMe_2$) appear at an unusually high chemical shift (septet at δ 4.97 ppm) in ^{1}H NMR spectrum of complex **5j**. In comparison, a chemical shift of 5.04 ppm is obtained with the electronegative chloride substituents while the π-donating dimethylamido substituents result in a chemical shift of 4.45 ppm. A similar behavior is observed for complexes **5k** and **5l**.

As a result of the meridional coordination of the ligand, the ligand methine protons are directed in between the substituents in the equatorial plane of a trigonal bipyramidal structure. It would appear that the equatorial substituents strongly influence the chemical environment of the methine protons.

The possibility of a β-hydrogen agostic interaction with the $10b_1$ orbital (d_{xy}) is dismissed based on the observed $^1J_{CH}$ coupling constant of 129 Hz. In comparison, a $^1J_{CH}$ coupling constant of 131 Hz was observed for the diamine **1k**.

The solid state structure of complex **5k** was determined by X-ray crystallography. The complete crystallographic data set can be found in the Appendix. The molecular structure of complex **5k** can be found in Figure 2- 37 and relevant bond distances and angles in Table 2- 7.

*Table 2- 7. Selected Bond Distances (Å) and Angles (°) for Complex **5k***

Bond Distances			
Zr–N(1)	2.076 (3)	Zr–C(20)	2.272 (4)
Zr–N(2)	2.332 (3)	Zr–C(21)	2.272 (4)
Zr–N(3)	2.073 (3)		
Bond Angles			
N(3)–Zr–N(1)	138.36 (11)	N(2)–Zr–C(21)	124.99 (13)
N(2)–Zr–C(20)	130.92 (13)	C(20)–Zr–C(21)	104.1 (2)

References on page 190

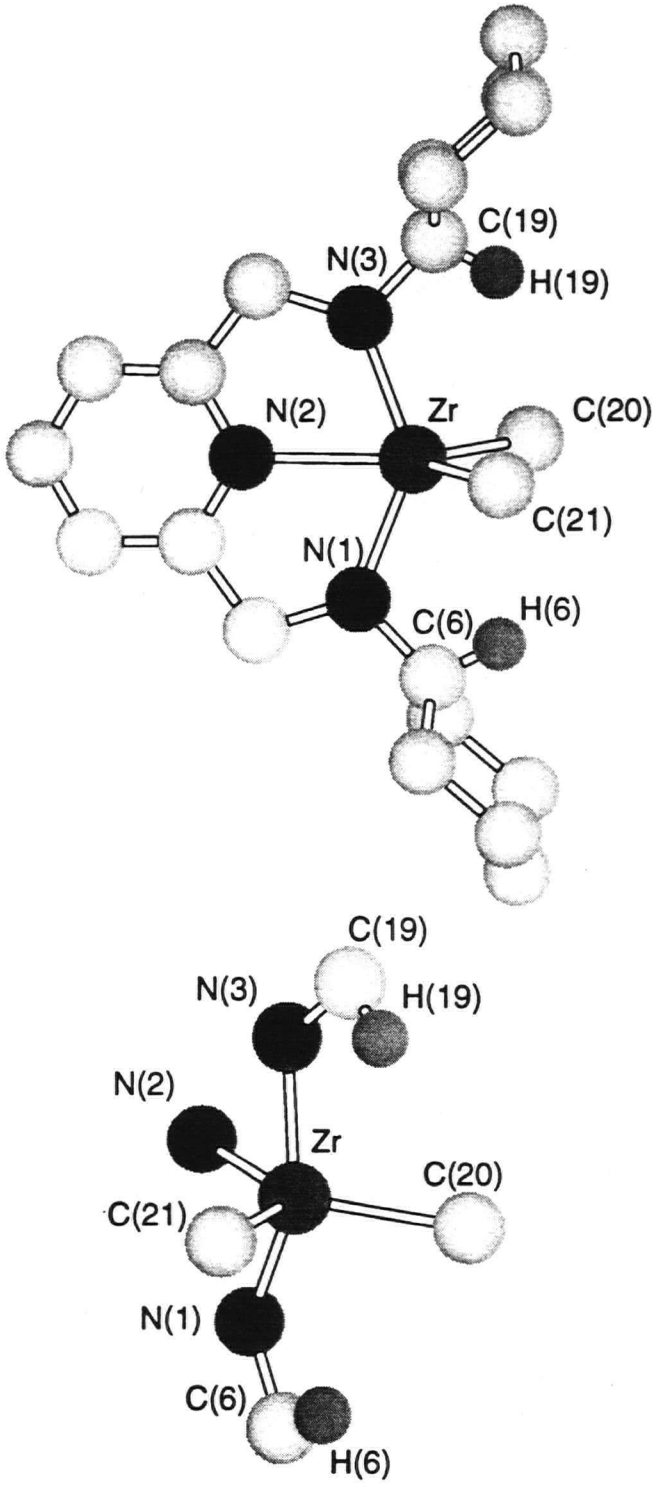

Figure 2- 37. Molecular structure of complex ***5k*** *from X-ray analysis*

References on page 190

The molecular structure of complex **5k** is very similar to that of complex **5b**. It can best be described as a distorted trigonal bipyramid with the amide nitrogen atoms {N(1) and N(3)} occupying the axial positions (Figure 2- 37). The Zr–amide and Zr–Me distances are comparable to those observed in complex **5b** and other zirconium-amido complexes[8,84-88]. The methine carbons are sp^3-hybridized as evidenced by the C–H bond distances (0.963 Å and 1.021 Å) and N–C–H bond angles (105.9° and 105.3°).

The solid state structure of complex **5m** was determined by X-ray crystallography. The complete crystallographic data can be found in the Appendix. The molecular structure of complex **5m** can be found in Figure 2- 38 and relevant bond distances and angles in Table 2- 8.

*Table 2- 8. Selected Bond Distances (Å) and Angles (°) for Complex **5m**[a]*

Bond Distances			
Zr(1)–N(1)	2.118 (2) {2.106 (2)}	Zr(1)–C(16)	2.290 (3) {2.281 (3)}
Zr(1)–N(2)	2.290 (2) {2.297 (3)}	Zr(1)–C(17)	2.247 (3) {2.281 (3)}
Zr(1)–N(3)	2.115 (2) {2.106 (2)}		
Bond Angles			
N(1)–Zr(1)–N(3)	141.29 (8) {141.01 (13)}	C(16)–Zr(1)–C(17)	119.13 (12) {115.5 (2)}
N(2)–Zr–C(16)	121.08 (10) {122.24 (8)}	Zr(1)–N(1)–C(4)	123.5 (2) {123.9 (2)}
N(2)–Zr–C(17)	119.79 (9) {122.24 (8)}	Zr(1)–N(3)–C(12)	123.6 (2) {123.9 (2)}

a, numbers in brackets for second asymmetric molecule

References on page 190

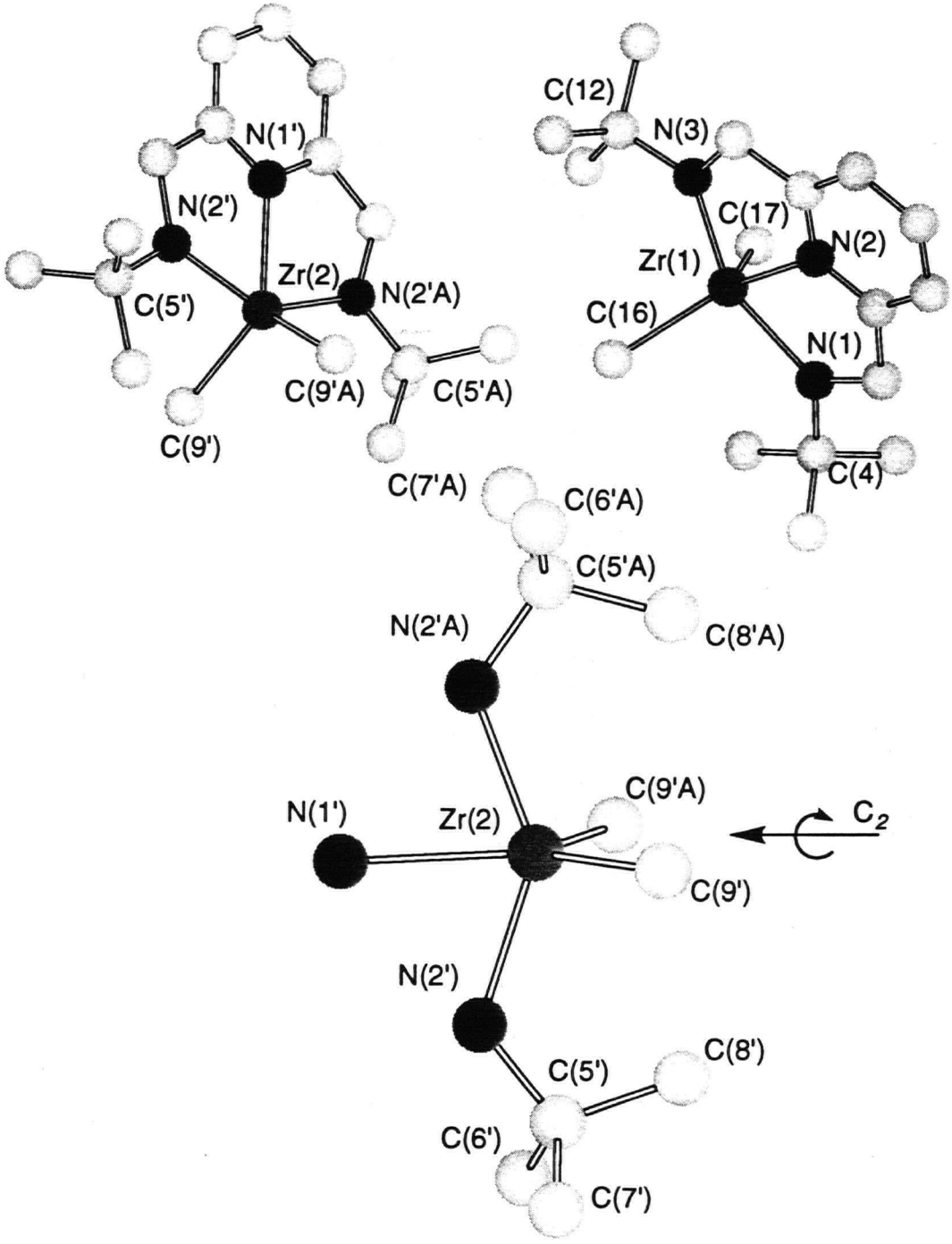

Figure 2- 38. Top, Molecular structure of complex ***5m****. Two asymmetric molecules were located in the unit cell; Bottom, core of the* C_{2v}*-symmetric molecule*

References on page 190

Two asymmetric molecules were located in the unit cell. The Zr–amide and Zr–Me bond distances in both molecules are comparable to those observed in other dimethyl derivatives bearing the pyridine-diamide ligand (**5b** and **5j**). The Zr–N–C angle is about 7.5° larger than the one observed for complex **5j**, consistent with the larger *tert*-butyl group (Figure 2- 39). Interestingly, one of the asymmetric molecules has C_2-symmetry as evidenced by the C_2 axis of rotation along the $Zr–N_{pyridine}$ bond and the absence of any mirror plane.

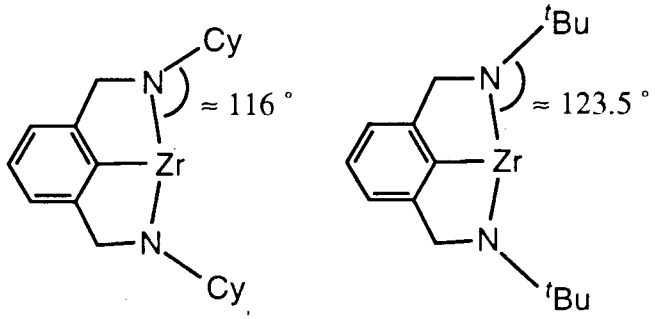

Figure 2- 39. Variation of the Zr–N–C angle

X-ray analysis using a different crystal of the dimethyl derivative showed Cl/CH_3 (1:2) disorder at one of the equatorial positions (**5m'**). The remaining atoms did not show any disorder. This was interpreted as a result of cocrystallization of the dimethyl and methylchloride derivatives with 66.6 % and 33.4 % respective occupancies. The disordered structure (**5m'**) is shown in Figure 2- 40 and relevant bond distances and angles in Table 2- 9.

*Table 2- 9. Selected Bond Distances (Å) and Angles (°) for **5m'***

Bond Distances					
Zr-N(1)	2.099 (3)	Zr-N(3)	2.105 (3)	Zr-C	2.225 (9)
Zr-N(2)	2.277 (2)	Zr-C(1)	2.305 (4)	Zr-Cl	2.549 (4)
Bond Angles					
N(1)-Zr-N(3)	141.56 (10)	N(2)-Zr-C	127.2 (3)	C(1)-Zr-C	115.2 (3)
N(2)-Zr-C(1)	117.55 (12)	N(2)-Zr-Cl	121.64 (13)	C(1)-Zr-Cl	120.8 (2)

References on page 190

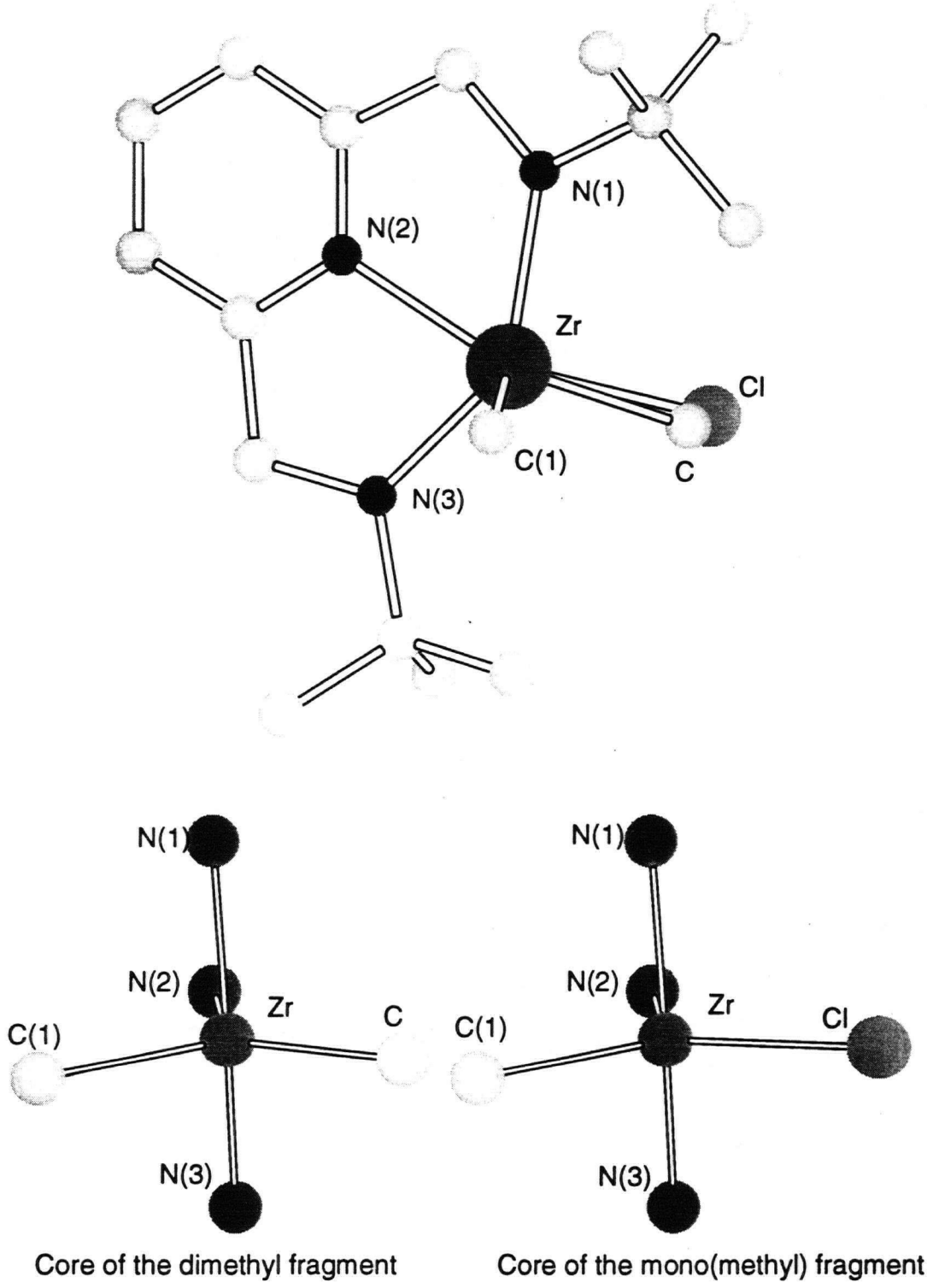

Figure 2- 40. Molecular structure of complex ***5m'*** *from X-ray crystallography*

References on page 190

(tBAP)ZrMe$_2$ structure from 5m

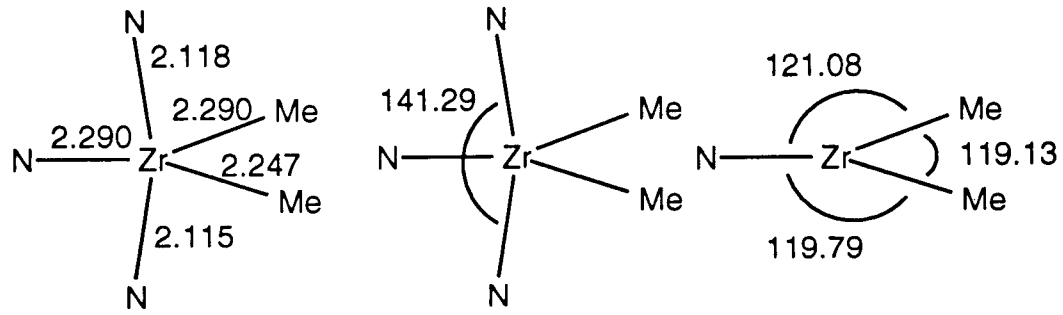

(tBAP)ZrMe$_2$ structure from 5m'

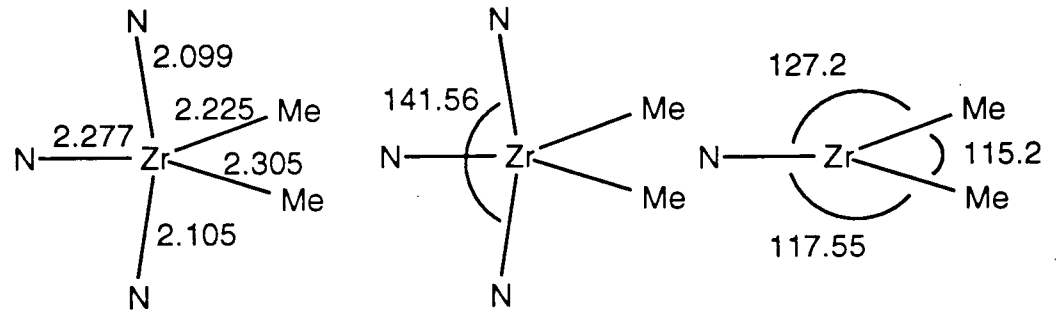

Figure 2- 41. Comparison between the structure of ***5m*** *and* ***5m'***

The bond distances in the molecular structure of the dimethyl derivative portion of the analysis are comparable (Figure 2- 41) to those obtained from the structure previously described (Figure 2- 38 and Table 2- 8).

Attempts to synthesis the mono(methyl) derivative were unsuccessful. The reaction of the dichloride precursor **3m** with 1 equivalent of methyl Grignard affords a 50 % yield of the dimethyl derivative **5m**.

2.3.1 Other alkyl complexes

The reaction of the dichloride complex **3m** with 2 equivalents of $PhCH_2MgCl$ affords the dibenzyl derivative (tBAP)Zr$(CH_2Ph)_2$ **6m** in good yield (eq. 21).

References on page 190

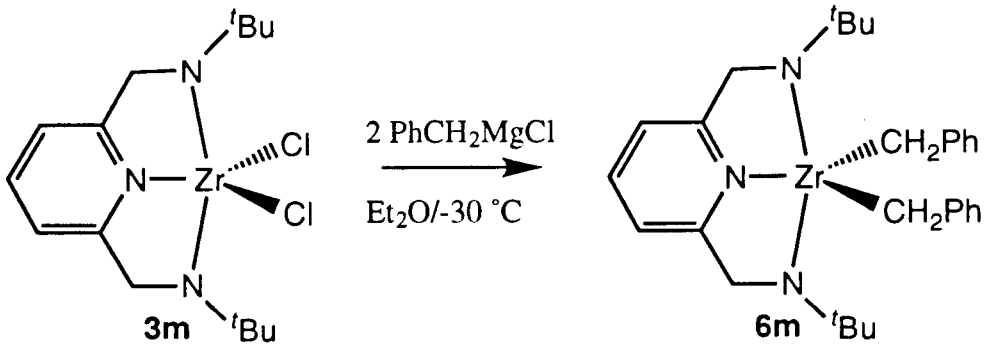

(21)

The temperature independent (-80 °C to +80 °C) ^{1}H NMR spectrum of complex **6m** displays a single sharp resonance for the ligand methylene protons (NCH_2) and one benzyl CH_2Ph signal. This is consistent with a complex with C_{2v}-symmetry and two equivalent benzyl groups. It is not possible to determine if rapid η^1-η^2 exchange of the benzyl groups is taking place.

The addition of 2 equivalents of EtMgCl to the dichloride complex **3j** affords the diethyl derivative **19j** in good yield (eq. 22). Again, spectroscopic data are consistent with a complex with C_{2v}-symmetry. Complex **19j** decomposes slowly at 80 °C in C_6D_6 (48 hours) yielding a mixture of intractable compounds {no ethylene or free diamine (**1j**) were detected by ^{1}H NMR spectroscopy}. This differs significantly from what has been observed with the dibutyl and dipropyl complexes bearing the 2,6-diisopropylphenyl substituents on the amides. The protons of the isopropyl groups of the ligand cannot get close enough to the metal center for C–H bond activation. Assuming that the first step in the thermolysis of both systems is similar (Scheme 2-6), the proposed alkylidene species or Zr^{II}-olefin transition state is not stabilized and decomposes.

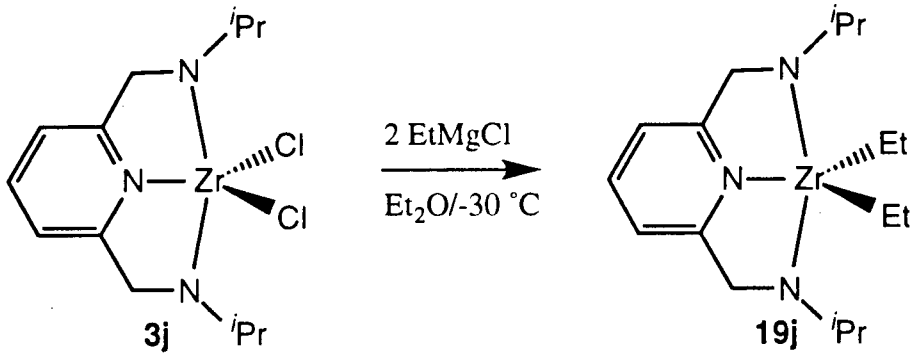

(22)

References on page 190

The reaction of 1 equiv of ^{i}PrMgCl with complex **3j** affords the mono(isopropyl) derivative **20j** (eq. 23).

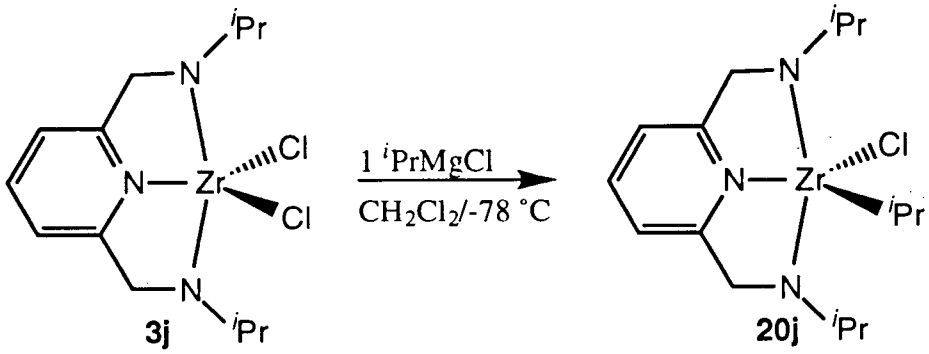

(23)

The ^{1}H NMR spectrum for complex **20j** displays the expected AB quartet for the ligand methylene protons (NCH_AH_B) and two doublets for the ligand isopropyl methyl groups consistent with C_s-symmetry.

The solid state structure of complex **20j** was determined by X-ray analysis. The complete crystallographic data can be found in the Appendix. The molecular structure of complex **20j** can be found in Figure 2- 42 and relevant bond distances and angles in Table 2- 10.

The two amide nitrogens occupying the axial positions of a distorted trigonal bipyramid. The zirconium atom is located 0.028 Å above the plane formed by the three nitrogen atoms. The distortion may take place in order to minimize steric interactions between the isopropyl groups of the ligand and the isopropyl group attached to the metal. The Zr–amide bond distances are similar to those already observed for related complexes (**5b**, **5k**, **5m** and **5m'**).

The short Zr•••C(15) contact of 3.06 Å and the Zr-C(14)-C(15) angle of 106.7 (2)° may be a result of agostic interaction. Moreover, C(14) significantly deviates from tetrahedral geometry as indicated by the large Zr-C(14)-C(16) angle of 116.9 (2)°.

References on page 190

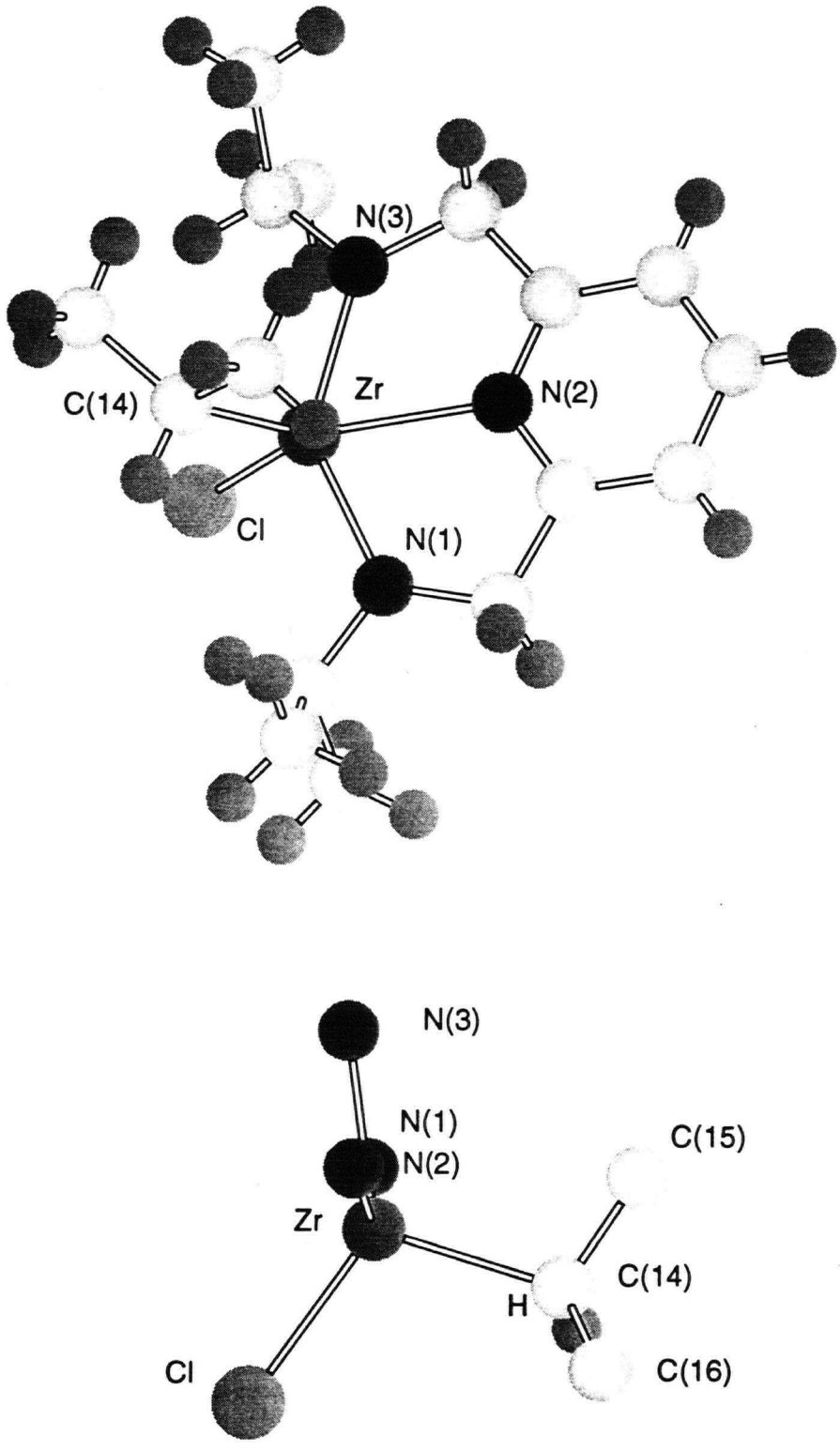

*Figure 2- 42. Molecular structure of complex **20j** from X-ray crystallography*

References on page 190

*Table 2- 10. Selected Bond Distances (Å) and Angles (°) for complex **20j***

Bond Distances			
Zr–N(1)	2.053 (2)	Zr–C(14)	2.255 (3)
Zr–N(2)	2.304 (2)	C(14)–C(15)	1.523 (4)
Zr–N(3)	2.059 (2)	C(14)–C(16)	1.523 (4)
Zr–Cl	2.445 (7)	Zr•••C(15)	3.06
Bond Angles			
N(3)–Zr–N(1)	139.10 (8)	Zr–C(14)–C(15)	106.7 (2)
N(2)–Zr–Cl	137.00 (5)	Zr–C(14)–C(16)	116.9 (2)
N(2)–Zr–C(14)	114.48 (8)	C(15)–C(14)–C(16)	111.5 (3)
C(14)–Zr–(Cl)	108.48 (7)		

As noted for complex **19j**, the thermolysis of complex **20j** (C_6H_6, 80 °C, 48 hours) also yields a mixture of intractable complexes. No propylene was detected by ^1H NMR spectroscopy. Complex **20j** does not decompose when heated (110 °C, 12 hours) in the presence of excess PMe_3.

2.4 Polymerization

The polymerization of ethylene by selected pyridine diamide complexes was studied and the results are summarized in Table 2- 11. The polymerization reactions were initiated at approximately 60 °C resulting in a rapid 10-25 °C exotherm. After the desired time, a HCl – MeOH mixture was added to terminate the polymerization reaction.

Catalysts **3a**, **5a** and **6a** yield polyethylene with a number averaged molecular weight around 1000 g/mol (this correspond to approximately 35 repeating units)[135]. Assuming that all the catalyst is active, each metal centre initiates about 800 polymer chains. As a result, most of the polymer chains are formed by a cationic hydride species generated by chain termination via β-hydrogen elimination. This indicates that the active catalytic centres are similar for all three

References on page 190

complexthat chain-end effects are negligible. Thus, the difference in activities likely arise from the difference in cation-anion interactions.

Table 2- 11. Ethylene polymerization results¥

#	Catalyst Precursor	Cat. ($x10^3$mmol)	T (°C)	time (sec)	Yield P.E. (g)	Activity[b] ($x\ 10^{-3}$)	N[c]
1	Cp_2ZrCl_2	8.21	58	180	30.70	74.8 (5)	1.00 (1)
2	(BDPP)Zr($CH_2Ph)_2$ (**6a**)	13.71	57	150	11.13	19.5 (5)	0.26 (1)
3	(BDPP)Zr($CH_2Ph)_2$ (**6a**)	13.71	60	120	9.85	21.6 (5)	0.29 (1)
4	(BMBP)Zr($CH_2Ph)_2$ (**6h**)	11.89	60	90	7.85	26.4 (5)	0.35 (1)
5	(BMBP)Zr($CH_2Ph)_2$ (**6h**)	19.31	60	120	16.71	26.0 (5)	0.35 (1)
6	(tBAP)Zr($CH_2Ph)_2$ (**6m**)	15.36	60	120	0	0	0
7	(BDPP)ZrMe_2 (**5a**)	12.13	60	105	5.91	16.7 (5)	0.22 (1)
8	(BDPP)ZrMe_2 (**5a**)	20.80	60	120	11.88	17.1 (5)	0.23 (1)
9	(BDPP)ZrCl_2 (**3a**)	12.95	60	120	6.40	14.8 (5)	0.20 (1)
10	(BDPP)ZrCl_2 (**3a**)	9.71	60	120	5.07	15.7 (5)	0.21 (1)
11	(BDPP)Zr($CH_2Ph)_2$ (**6a**)[a]	6.86	60	90	6.30	36.8 (5)	0.49 (1)
12	(BDPP)Zr($CH_2Ph)_2$ (**6a**)[a]	9.60	60	120	11.90	37.2 (5)	0.50 (1)
14	(BDPP)Zr($CH_2Ph)_2$ (**6a**)[d]	8.23	60	120	3.45	12.6 (5)	0.17 (1)

Reaction conditions: solvent = heptane (200 mL); Cocatalyst = MAO, 5000 equivalents; P = 100 Psi of ethylene; **a**, polymerization done in the presence of 30 g of 1-hexene; **b**, g polyethylene mmol cat.$^{-1}$ h^{-1}; **c**, activity vs Cp_2ZrCl_2; **d**, solvent = toluene (200 mL). ¥: selected molecular weights less than 1000 g/mol

2.4.1 Counterion effect

When toluene solutions of Cp_2ZrCl_2 are treated with MAO, a fast, initial ligand exchange reaction generates primarily the monomethyl complex $Cp_2ZrMeCl$; with time, the dimethyl

References on page 190

complex Cp_2ZrMe_2 is formed[136,137]. A methyl or chloride fragment is then abstracted by an Al centre to generate a cationic zirconium species stabilized by the weakly coordinating CH_3/Cl–MAO$^-$ anion. The low coordinating capability of the anion in this ion pair is crucial for catalytic activity[138]. The interaction must be weak enough to allow an olefin to displace the anion from the coordination sphere of the zirconium. Interestingly, the addition of $AlMe_3$ and $AlEt_3$ has been shown to stabilize cationic catalysts by formation of AlR_3 adducts[54,139].

The activity of the dichloride complex (**3a**) is slightly less than that of the dimethyl derivative (**5a**) (Table 2- 12). Higher coordinating ability of the aluminate anion bearing a chloride group instead of a methyl group may explain the difference in activity. The activity of the dibenzyl complex (**6a**) is much higher than that of the dimethyl or dichloride complexes. It was noted earlier that the reaction of complex **6a** with $B(C_6F_5)_3$ affords a cationic benzyl derivative with what appears to be η^6-coordination of the benzylborate anion (**23a**, eq. 9). A similar interaction between the $PhCH_2$–MAO$^-$ anion and the cationic zirconium complex is proposed. The weakly coordinating anion stabilizes the catalytic centre and is displaced easily by the ethylene monomer.

However, it is important to keep in mind that the activation of the dichloride complex requires extra steps to obtain the active species (Scheme 2- 7). As a result, complex **3a** may take longer to form the cationic complex and appear to ba a less active catalysts. On the other hand, the activity of the dibenzyl derivative **6a** is much greated than that of complex **5a**. The bulky benzyl groups should slow down the activation of complex **6a** relative to that of complex **5a**. Again, this is consistent with cation-anion interactions being the key factor determining the activity of this class of catalysts.

References on page 190

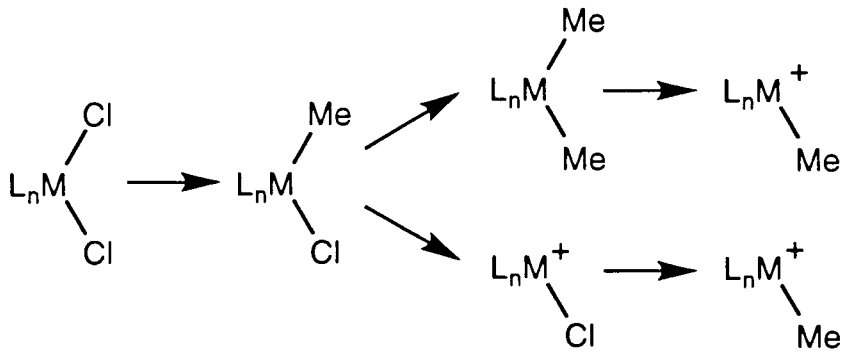

Scheme 2- 7. Reaction of MAO with dichloride complex

Table 2- 12. Counter-ion effect

Catalyst	Solvent	Activity (g mmol cat^{-1} h^{-1})[a]
$(BDPP)ZrCl_2$ (**3a**)	Heptane	15.2×10^3
$(BDPP)ZrMe_2$ (**5a**)	Heptane	16.9×10^3
$(BDPP)Zr(CH_2Ph)_2$ (**6a**)	Heptane	20.5×10^3
$(BDPP)Zr(CH_2Ph)_2$ (**6a**)	Toluene	12.6×10^3
Cp_2ZrCl_2	Toluene	74.8×10^3

a : average of two experiments

It is noteworthy that a large excess of toluene inhibits the polymerization and a lower activity is obtained. In this case, the toluene may compete with ethylene for the available coordination site. However, the lower activity may also be a result of better charge separation between the cation and anion when toluene is used as the solvent[140-142].

2.4.2 Ligand effect

The activity of the *meso*-$(BMBP)Zr(CH_2Ph)_2$ (**6h**) is about 25% higher than that of complex **6a** (Table 2- 13). The 2,6-diisopropylphenyl substituents in complex **6a** protects the metal on both sides of the N_3Zr plane (Figure 2- 43, **I**). On the other hand, the *tert*-butyl substituents in complex **6h** are both located on the same side of the N_3Zr plane in a *meso* structure (Figure 2- 43, **II**). Assuming that the *meso* structure persists throughout the

References on page 190

polymerization, the metal centre is well protected on one side and the other face is left open. Consequently, olefin coordination is facilitated and a higher activity is observed. The *rac* isomer is also more open than complex **6a** (Figure 2- 43, **III**) and it is not possible to confirm that the *meso* structure is retained under polymerization conditions. Interestingly, complex **6m** does not catalyze the polymerization of ethylene (Table 2- 13). It would appear that this alkyl ligand does not efficiently stabilize the metal centre and decomposition of the active complex occurs.

Table 2- 13. Ligand effect

Catalyst	Activity (g mmol cat^{-1} h^{-1})[a]
$(BMBP)Zr(CH_2Ph)_2$ (**6h**)	26.2×10^3
$(BDPP)Zr(CH_2Ph)_2$ (**6a**)	20.5×10^3
$(tBAP)Zr(CH_2Ph)_2$ (**6m**)	0

a : average of two experiments

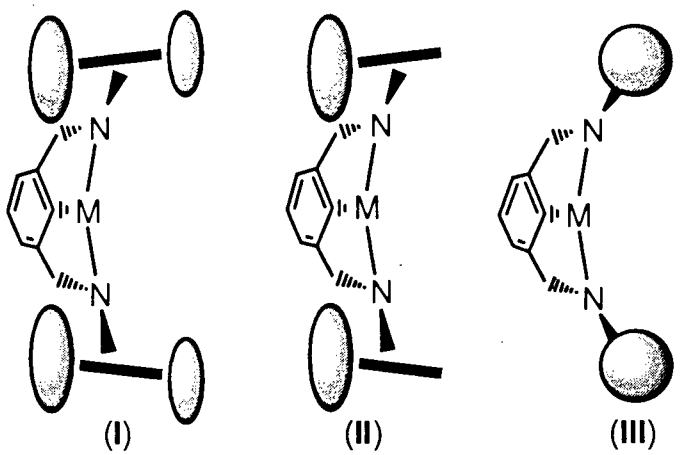

Figure 2- 43. Steric protection

2.4.3 Co-polymerization

The polyethylene obtained with complex **6a** contains a small number of butyl chain (Table 2- 14). This branching is a result of insertion of α-olefin formed by β-hydrogen elimination of the growing polymer chain. Interestingly, no increase in the branching is observed when the

References on page 190

polymerization is carried out in the presence of 1-hexene. This indicates that 1-hexene is not incorporated in the polymer chain. However, the activity nearly doubles. This is interpreted as a result of stabilization of the active catalytic species by coordinated 1-hexene.

The dibenzyl derivative does not efficiently polymerize neat 1-hexene and a mixture of oligomers (n = 3 to 5) is obtained after 24 hours at 60 °C.

Table 2- 14. Ethylene/1-hexene co-polymerization

Catalyst	Monomers	Activity (g mmol cat^{-1} h^{-1})[a]	Branching (/1000 CH_2)
(BDPP)Zr(CH_2Ph)$_2$ (**6a**)	Ethylene	20.5 x 10^3	21
(BDPP)Zr(CH_2Ph)$_2$ (**6a**)	Ethylene/1-hexene[b]	37.0 x 10^3	22
(BDPP)Zr(CH_2Ph)$_2$ (**6a**)	1-hexene	0	n.a.

a : average of two experiments; b : 30 g of 1-hexene were added to the reaction mixture

References on page 190

3 Conclusions

A high yield route to pyridine-diamide complexes of zirconium has been demonstrated. The availability of substituted anilines and alkylamines provides an opportunity to vary the sterics with little change to the electronic environment about the metal. The coordination geometry of the pyridine-diamide ligand system is very similar to a metallocene (Cp_2ZrX_2). The frontier orbitals of this fragment resemble those of a metallocene ($1a_1$, b_2 and $2a_1$). A ligand centered non-bonding pair of electrons gives rise to an unusually low electron count at zirconium. As a result, pyridine-diamide complexes of zirconium are expected to be more electrophilic than metallocene complexes.

A series of ortho-substituted aryl diamide complexes of zirconium have been prepared in high yield. Depending on the size of the ortho substituent on the aryl group, rotameric isomers, derived from restricted rotation about the N-C_{ipso} bond, can be observed spectroscopically and the barriers to isomerization measured. In the case of the 2-phenylaryl moiety, rapid isomerization is observed at all temperatures regardless of the substituents bound to zirconium in the equatorial plane. The 2-isopropylaryl substituted complexes exhibit fluxional behavior with the low temperature limiting ^{1}H NMR spectra showing resonances for species consistent with *meso* and *rac* rotamers. In contrast, the 2-*tert*-butylaryl derivatives are 'locked' as five coordinate species but can isomerize during metathesis reactions at the metal center. The 2-isopropyl-6-methyl complexes are also locked, however, the rotameric ratios remain the same in all derivatives of this ligand system.

Pyridine-diamide complexes of zirconium bearing the 2,6-diisopropyl substituents are active catalysts for the polymerization of ethylene. The dibenzyl derivative is the most active species. This is interpreted to be a result of η^6-coordination of the benzyl-MAO$^-$ anion which stabilizes the catalytic complex or prevents β-hydride elimination which leads to catalyst deactivation. The more open coordination sphere with complexes bearing the ortho-^{tert}butyl substituents results in a higher activity.

References on page 190

4 Experimental Details

General Details. See chapter one for general details. $(BDPP)H_2$ (**1a**), $(BDMP)H_2$ (**1c**), $(iPAP)H_2$ (**1j**), $(CyAP)H_2$ (**1k**) and $(tBAP)H_2$ (**1m**) were prepared as described in chapter one. The zirconium(IV) chloride was purchased from Alfa and used as received. The 2-isopropyl-6-methylaniline, 2-*tert*-butylaniline, 2-phenylaniline, 2-isopropylaniline, 2,4,6-trichloroaniline, 2,4,6-tribromoaniline were purchased from Aldrich and distilled under reduced pressure before use. The 2,4-dimethyl-3-aminopentane, 2-dimethylamino-ethylamine, ethylmagnesium bromide, propylmagnesium chloride, isopropylmagnesium chloride and butylmagnesium chloride were purchased from Aldrich and used as received. The $(SiMe_3)_3SiLi(thf)_3$[134], $ZrCl_2[N(SiMe_3)_2]_2$[80] and $Zr(NMe_2)_4$[1-4] were synthesised using previously reported syntheses.

2,6-$(RHNCH_2)_2$-NC_5H_3, (R = 2,6-diethylphenyl), $(BDEP)H_2$ (1b). A THF (150 mL) solution of LiNHR (10.40 g, 67.02 mmol) was added slowly to a stirring THF (100 mL) solution of 2,6-bis(bromomethyl)pyridine (8.876 g, 33.50 mmol) at -78°C. The mixture was warmed to room temperature and stirred for 12 h. The solution was quenched with a saturated $NaHCO_3$ solution (100mL) and extracted with dichloromethane. The solvent was removed in *vacuo* to give a yellow oil (**1b**) which was used as isolated (9.753 g, 24.29 mmol, 73 %). ^1H NMR δ 7.10-6.90 (m, 6H, Ar and py), 6.80 (d, 2H, py), 4.35 (br s, 2H, N*H*), 4.19 (s, 4H, NCH_2), 2.72 (q, 8H, CH_2CH_3), 1.21 (t, 12H, CH_2CH_3). $^{13}C\{^1H\}$ NMR δ 148.93, 145.77, 136.86, 136.36, 127.17, 123.20, 120.27, 56.44, 25.10, 15.17. MS (EI) *m/z* 401.284 (M^+). Calcd for $C_{27}H_{35}N_3$: 401.283.

2,6-$(RHNCH_2)_2NC_5H_3$, (R = 2,4,6-trichlorophenyl), $(TCPP)H_2$ (1d). The preparation of compound **1d** is identical to that of **1b**. LiNHR (1.030 g, 5.089 mmol) and 2,6-bis(bromomethyl)pyridine (0.674 g, 2.544 mmol) gave white crystalline **1d** (0.580 g, 1.169 mmol, 46 %). ^1H NMR δ 6.95 (s, 4H, Ar), 6.93 (t, 1H, py), 6.57 (d, 2H, py), 5.53 (br t, 2H,

References on page 190

N*H*), 4.42 (d, 4H, NCH_2). $^{13}C\{^1H\}$ NMR δ 153.38, 142.18, 136.87, 128.69, 125.72, 125.11, 120.21, 52.00. MS (EI) *m/z* 498.915 (M^+). Calcd for $C_{19}H_{13}N_3{}^{35}Cl_3{}^{37}Cl_3$: 498.915.

2,6-$(RHNCH_2)_2NC_5H_3$, (R = 2,4,6-tribromophenyl), $(TBPP)H_2$ (1e). The preparation of compound **1e** is identical to that of **1b**. LiNHR (2.540 g, 7.565 mmol) and 2,6-bis(bromomethyl)pyridine (1.004 g, 3.789 mmol) gave white crystalline **1e** (1.875 g, 2.458 mmol, 65 %). Compound **1e** is thermally unstable and decompose to a dark brown oil within days at room temperature. ^1H NMR δ 7.34 (s, 4H, Ar), 6.95 (t, 1H, py), 6.65 (d, 2H, py), 5.44 (br t, 2H, N*H*), 4.41 (d, 4H, NCH_2). $^{13}C\{^1H\}$ NMR δ 165.25, 144.86, 136.87, 135.14, 120.32, 116.50, 113.41, 52.65. MS (EI) *m/z* 762.614 (M^+). Calcd for $C_{19}H_{13}N_3{}^{79}Br_3{}^{81}Br_3$: 762.615.

2,6-$(RHNCH_2)_2NC_5H_3$, (R = 2-phenylphenyl), $(BPhP)H_2$ (1f). The preparation of compound **1f** is identical to that of **1b**. LiNHR (5.144 g, 29.4 mmol) and 2,6-bis(bromomethyl)pyridine (3.890 g, 14.7 mmol) gave a yellow oily liquid **1b** (6.000 g, 13.6 mmol, 93 %). ^1H NMR δ 7.50 (d, 4H, m Ar/Ph), 7.40-7.09 (m, 10H, Ar/Ph), 6.97 (t, 1H, py), 6.80 (t, 2H, Ar/Ph), 6.73 (d, 2H, Ar/Ph), 6.60 (d, 2H, Ar), 5.15 (t, 2H, N*H*), 4.08 (d, 4H, NCH_2). $^{13}C\{^1H\}$ NMR δ 158.28, 145.17, 140.31, 136.79, 130.61, 129.84, 129.16, 128.17, 127.39, 119.27, 117.64, 111.26, 49.25. MS (EI) *m/z* 441.220 (M^+). Calcd. for $C_{31}H_{27}N_3$: 441.220.

2,6-$(RHNCH_2)_2NC_5H_3$, (R = 2-isopropylphenyl), $(BMPP)H_2$ (1g). The preparation of compound **1g** is identical to **1b** except for the work up. LiNHR (5.335 g, 37.4 mmol)) and 2,6-bis(bromomethyl)pyridine (5.000 g, 18.9 mmol) yield a white solid. The solid was dissolved in a minimal amount of ether, hexanes added until the solution was cloudy, and cooled to -30 °C. A white crystalline solid (**1g**) was isolated by filtration and dried under vacuum (4.500 g, 12.0 mmol, 63 %). ^1H NMR δ 7.18 (dd, 2H, Ar), 7.11 (dd, 2H, Ar), 6.97 (m, 1H, py), 6.84 (td, 2H, Ar), 6.77 (d, 2H, py), 6.62 (dd, 2H, Ar), 4.77 (br s, 2H, N*H*), 4.29 (s, 4H, NCH_2), 2.87 (sept, 4H, C*H*Me_2), 1.23 (d, 12H, CHMe_2). $^{13}C\{^1H\}$ NMR δ 158.68, 144.98,

References on page 190

136.94, 132.43, 127.21, 125.31, 119.77, 118.09, 111.33, 49.61, 27.70, 22.49. MS (EI) *m/z* 373.252 (M^+). Calcd. for $C_{25}H_{31}N_3$: 373.252.

2,6-$(RHNCH_2)_2NC_5H_3$, (R = 2-*t*-butylphenyl), $(BMBP)H_2$ (1h). The preparation of compound **1h** is identical to that of **1g**. LiNHR (5.865 g, 37.8 mmol) and 2,6-bis(bromomethyl)pyridine (5.000 g, 18.9 mmol) gave a white crystalline solid **1h** (5.820 g, 14.4 mmol, 76 %). ^{1}H NMR δ 7.35 (d, 2H, Ar), 7.16 (dd, 2H, Ar), 7.02 (td, 1H, py), 6.84 (d 2H, Ar), 6.82 (t, 2H, py), 6.628 (d, 2H, Ar), 4.24 (br s, 2H, NH), 4.32 (s, 4H, NCH_2), 1.49 (s, 18H, *t*-Bu). $^{13}C\{^1H\}$ NMR δ 158.39, 146.24, 137.04, 133.55, 54.52, 55.33, 54.48, 56.22, 49.82, 34.41, 30.08. MS (EI) *m/z* 401.283 (M^+). Calcd. for $C_{27}H_{35}N_3$: 401.283.

2,6-$(RHNCH_2)_2NC_5H_3$, (R = 2-methyl-6-isopropylphenyl), $(MPPP)H_2$ (1i). The preparation of compound **1i** is identical to that of **1g**. LiNHR (7.750 g, 49.9 mmol) and 2,6-bis(bromomethyl)pyridine (5.000 g, 18.9 mmol) gave a white crystalline solid **1i** (4.910 g, 12.2 mmol, 65 %). ^{1}H NMR δ 7.13 (d, 2H, Ar), 7.03-7.00 (m, 5H, py/Ar), 6.75 (d, 2H, py), 4.34 (s, 2H, N*H*), 4.18 (s, 4H, NCH_2), 3.45 (sept, 2H, $CHMe_2$), 2.31 (s, 6H, Me), 1.21 (d, 12H, $CHMe_2$). $^{13}C\{^1H\}$ NMR δ 159.01, 145.46, 141.45, 136.75, 131.21, 128.88, 124.13, 123.39, 120.29, 55.33, 27.99, 24.16, 19.03. MS (EI) *m/z* 401.283 (M^+). Calcd. for $C_{27}H_{35}N_3$: 401.283.

2,6-$(RHNCH_2)_2NC_5H_3$, (R = diisopropylmethyl), $(LiAP)H_2$ (1l). Solid 2,6-bis(bromomethyl)pyridine (1.000 g, 3.774 mmol) was added to a solution 2,4-dimethyl-3-aminopentane (4.350 g, 37.75 mmol) in hexanes (50mL). The solution got warm and a white solid started to form within minutes. The solution was allowed to stir for 12 hours at 23 °C and was quenched with 100mL of a saturated aqueous $NaHCO_3$ solution and extracted with CH_2Cl_2. The solvent was removed in *vacuo* to yield a light yellow liquid **1l** (1.220 g, 3.657 mmol, 97 %). ^{1}H NMR δ 7.16 (t, 1H, py), 6.99 (d, 2H, py), 3.97 (s, 4H, NCH_2), 1.99 (t, 2H, NCH^iPr_2), 1.74 (d of sept, 4H, $CHMe_2$), 0.98 (d, 12H, $CHMe_2$), 0.95 (d, 12H, $CHMe_2$). $^{13}C\{^1H\}$ NMR δ

References on page 190

160.21, 136.45, 120.24, 69.52, 57.58, 31.26, 21.15, 18.43. MS (EI) *m/z* 332.307 (M^+). Calcd for $C_{21}H_{38}N_3$: 332.307.

2,6-$(RHNCH_2)_2NC_5H_3$, (R = 2-dimethylaminoethyl), $(DMEAP)H_2$ (1n). The preparation of compound **1n** is identical to that of **1l**. 2,6-bis(bromomethyl)pyridine (2.500 g, 9.436 mmol) and 2-dimethylamino-ethylamine (16.64 g, 188.8 mmol) gave a light yellow liquid **1n** (2.192 g, 7.844 mmol, 83 %). ^{1}H NMR δ 7.06 (t, 1H, py), 7.03 (d, 2H, py), 3.89 (s, 4H, NCH_2), 2.85 (br s, 2H, NH), 2.61 (t, 4H, CH_2), 2.31 (t, 4H, CH_2), 2.02 (s, 6H, NMe_2). ^{13}C{^{1}H} NMR δ 160.46, 136.58, 120.09, 59.48, 55.72, 47.28, 45.46. MS (EI) *m/z* 279.243 (M^+). Calcd for $C_{15}H_{29}N_5$: 279.242.

(BDPP)Zr$(NMe_2)_2$ (2a). A toluene solution of $Zr(NMe_2)_4$ (1.748 g, 6.534 mmol) was added to a toluene solution (50 mL) of **1a** (2.990 g, 6.532 mmol) at 23 °C. The solution was refluxed for 12 hours. The solvent was removed in *vacuo* and the resulting solid extracted with hexanes (3 × 50 mL) and filtered through Celite. The volume of the filtrate was reduced to 50 mL and cooled to -30 °C for 12 h. Yellow crystalline **2a** was isolated by filtration and dried under vacuum (3.742 g, 5.892 mmol, 90 %). ^{1}H NMR δ 7.20-7.05 (m, 6H, Ar), 6.87 (t, 1H, py), 6.47 (d, 2H, py), 4.81 (s, 4H, NCH_2), 3.69 (sept, 4H, CHMe$_2$), 2.53 (s, 12H, N(CH_3)$_2$), 1.31 (d, 12H, CHMe_2), 1.29 (d, 12H, CHMe_2). ^{13}C{^{1}H} NMR δ 163.26, 150.89, 146.28, 137.56, 124.59, 123.73, 117.18, 60.62, 41.51, 28.06, 26.44, 24.69. Calcd for $C_{35}H_{53}N_5Zr$: C, 66.20; H, 8.41; N, 11.03. Found: C, 66.69; H, 8.39; N, 10.77.

(BDEP)Zr$(NMe_2)_2$ (2b). The preparation of compound **2b** is identical to that of **2a**. $Zr(NMe_2)_4$ (1.000 g, 3.738 mmol) and compound **1b** (1.500 g, 3.735 mmol) gave yellow crystalline **2b** (1.950 g, 3.368 mmol, 90 %). ^{1}H NMR δ 7.21 (d, 6H, Ar), 7.05 (m, 2H, Ar), 6.88 (t, 1H, py), 6.47 (d, 2H, py), 4.69 (s, 4H, NCH_2), 2.86 (m, 8H, CH_2CH$_3$), 2.58 (s, 12H, N(CH_3)$_2$), 1.29 (t, 12H, CH$_2$CH_3). ^{13}C{^{1}H} NMR δ 164.07, 152.54, 141.22, 138.63, 126.03, 123.83, 117.30, 62.27, 41.44, 24.39, 15.85.

References on page 190

(BDMP)Zr(NMe$_2$)$_2$ (2c). The preparation of compound **2c** is identical to that of **2a**. Zr(NMe$_2$)$_4$ (1.000 g, 3.738 mmol) and compound **1c** (1.300 g, 3.763 mmol) gave yellow crystalline **2c** (1.791 g, 3.425 mmol, 92 %). ^{1}H NMR δ 7.16 (d, 4H, Ar), 6.97 (m, 2H, Ar), 6.90 (t, 1H, py), 6.46 (d, 2H, py), 4.63 (s, 4H, NCH_2), 2.58 (s, 12H, N(CH_3)$_2$), 2.37 (s, 12H, Me). ^{13}C{^{1}H} NMR δ 164.45, 153.25, 137.54, 135.67, 128.58, 123.34, 117.34, 63.70, 41.32, 18.86.

(TCPP)Zr(NMe$_2$)$_2$ (2d). The preparation of compound **2d** is identical to that of **2a**. Zr(NMe$_2$)$_4$ (1.500 g, 5.607 mmol) and compound **1d** (2.780 g, 5.544 mmol) gave yellow crystalline **2d** (3.020 g, 4.485 mmol, 81 %). ^{1}H NMR δ 7.19 (s, 4H, Ar), 6.88 (t, 1H, py), 6.42 (d, 2H, py), 4.62 (s, 4H, NCH_2), 2.76 (s, 12H, NMe_2). ^{13}C{^{1}H} NMR δ 163.58, 151.03, 138.38, 134.44, 128.15, 126.69, 117.47, 62.05, 41.82.

(TBPP)Zr(NMe$_2$)$_2$ (2e). The preparation of compound **2e** is identical to that of **2a**. Zr(NMe$_2$)$_4$ (0.585 g, 2.187 mmol) and compound **1e** (1.668 g, 2.187 mmol) gave yellow crystalline **2e** (1.568 g, 1.668 mmol, 76 %). ^{1}H NMR δ 7.59 (s, 4H, Ar), 6.90 (t, 1H, py), 6.44 (d, 2H, py), 4.61 (s, 4H, NCH_2), 2.73 (s, 12H, NMe_2). ^{13}C{^{1}H} NMR δ 163.28, 153.64, 138.29, 124.40, 125.77, 117.45, 114.59, 62.02, 42.01.

(BPhP)Zr(NMe$_2$)$_2$ (2f). The preparation of compound **22f** is identical to that of **2a**. Zr(NMe$_2$)$_4$ (3.635 g, 13.6 mmol) and compound **1f** (6.000 g, 13.6 mmol) gave yellow crystalline **2f** (7.715 g, 12.5 mmol, 92%). ^{1}H NMR δ 7.74 (d, 2H, Ar/Ph), 7.71 (d, 2H, Ar/Ph), 7.36-7.32 (m, 4H, Ar/Ph), 7.11-6.98 (m, 8H, Ar/Ph), 6.56 (t, 1H, py), 6.00 (d, 2H, py), 4.66 (s, 4H, NCH_2), 2.94 (s, 12H, NMe_2). ^{13}C{^{1}H} δ 164.67, 153.33, 143.59, 137.46, 135.30, 131.95, 128.45, 128.32, 128.196, 127.76, 126.34, 122.55, 116.93, 63.29, 41.92.

(BMPP)Zr(NMe$_2$)$_2$ (2g). The preparation of compound **2g** is identical to **2a**. Zr(NMe$_2$)$_4$ (2.150 g, 8.03 mmol) and **1g** (3.000 g, 8.03 mmol) gave **2g** as a yellow crystalline solid (4.100 g, 7.44 mmol, 93%). ^{1}H NMR δ 7.41 (dd, 2H, Ar), 7.32 (dd, 2H, Ar), 7.21 (td, 2H, Ar), 1.11 (td, 2H, Ar), 8.87 (t, 1H, py), 6.42 (d, 2H, py), 4.93 (s, 4H, NCH_2), 3.53 (sept,

References on page 190

4H, C*H*Me_2), 2.76 (s, 12H, NMe_2), 1.29 (d, 12H, CH*Me*$_2$). $^{13}C\{^1H\}$ δ 164.64, 152.91, 145.71, 137.59, 129.27, 126.32, 126.14, 124.04, 117.34, 67.26, 42.03, 27.29, 25.23.

(BMBP)Zr(NMe$_2$)$_2$ (2h). The preparation of compound **2h** is identical to **2a**. $Zr(NMe_2)_4$ (2.150 g, 8.04 mmol) and **1h** (3.000 g, 8.03 mmol) gave **2h** a yellow crystalline solid (3.987 g, 7.24 mmol, 90%). The following data is for both rotamers (*meso*/*rac*, 2.6:1). ^1H NMR δ 7.48 (t, Ar), 7.24 (t, Ar), 7,07 (t, Ar), 6.90 (t, py), 6.49 (d, py), 4.91 (s, *meso* NC*H*$_2$), 4.90 (AB quartet, $^2J_{HH}$ = 20.0 Hz, *rac* NC*H*$_2$), 3.01 (s, *meso* N*Me*$_2$), 2.65 (s, *rac* N*Me*$_2$), 2.42 (s, *meso* N*Me*$_2$), 1.57 (s, *rac* C*Me*$_3$), 1.51 (s, *meso* C*Me*$_3$). $^{13}C\{^1H\}$ δ 163.88, 163.14, 156.07, 154.46, 146.67, 137.73, 132.32, 132.12, 128.90, 127.94, 126.95, 126.76, 124.30, 123.73, 117.25, 68.40, 43.25, 42.15, 41.05, 36.56, 32.64, 32.41.

(MPPP)Zr(NMe$_2$)$_2$ (2i). The preparation of compound **2i** is identical to **2a**. $Zr(NMe_2)_4$ (2.671 g, 10.0 mmol) and **1i** (4.010 g, 10.0 mmol) gave **2i** as a yellow crystalline solid (3.090 g, 5.34 mmol, 54%). The following data is for both rotamers (*meso*/*rac*, 1:1.13). ^1H NMR δ 7.27-7.23 (m, Ar/Ph), 7.16-7.05 (m, Ar/Ph), 6.93 (t, py), 6.48 (d, py), 4.68 (AB quartet, $^2J_{HH}$ = 20.3 Hz, *rac* NC*H*$_2$), 4.65 (AB quartet, $^2J_{HH}$ = 20.3 Hz, *meso* NC*H*$_2$), 4.00 (sept, *meso* C*H*Me_2), 3.82 (sept, *rac* C*H*Me_2), 2.88 (s, *meso* N*Me*$_2$), 2.57 (s, *rac* N*Me*$_2$), 2.32 (s, *rac* Me), 2.30 (s, *meso* N*Me*$_2$), 2.19 (s, *meso* Me), 1.39 and 1.38 (d, *meso* CH*Me*$_2$), 1.32 and 1.29 (d, *rac* CH*Me*$_2$). $^{13}C\{^1H\}$ δ 164.12, 163.81, 152.39, 152.12, 146.41, 146.38, 137.60, 137.54, 135.37, 135.10, 123.86, 123.77, 117.25, 65.06, 64.92, 42.59, 41.33, 40.08, 27.64, 26.92, 26.76, 24.28, 24.04, 19.16, 19.07.

(iPAP)Zr(NMe$_2$)$_2$ (2j). The preparation of compound **2j** is identical to that of **2a**. Compound **1j** (0.500 g, 2.259 mmol) and $Zr(NMe_2)_4$ (0.604 g, 2.258 mmol) yielded yellow crystalline **2j** (0.829 g, 2.079 mmol, 92 %). ^1H NMR δ 6.91 (t, 1H, py), 6.54 (d, 2H, py), 4.52 (s, 4H, NC*H*$_2$), 4.45 (sept, 2H, NC*H*Me_2), 3.22 (s, 12H, N*Me*$_2$), 4.34 (d, 12H, NCH*Me*$_2$). $^{13}C\{^1H\}$ NMR δ 165.89, 136.39, 117.20, 56.32, 50.10 ($^1J_{CH}$ = 130 Hz), 44.11, 23.58.

References on page 190

(CyAP)Zr(NMe$_2$)$_2$ (2k). The preparation of compound **2k** is identical to that of **2a**. Compound **1k** (1.000 g, 3.317 mmol) and Zr(NMe$_2$)$_4$ (0.887 g, 3.316 mmol) yielded yellow crystalline **2k** (1.428 g, 2.982 mmol, 90 %). ^{1}H NMR δ 6.90 (t, 1H, py), 6.55 (d, 2H, py), 4.57 (s, 4H, NC*H*$_2$), 3.87 (tt, 2H, NC*H*), 3.22 (s, 12H, N*Me*$_2$), 1.94 (m, 8H, Cy), 1.66 (m, 10H, Cy), 1.18 (m, 2H, Cy). ^{13}C{^{1}H} NMR δ 166.01, 136.35, 117.11, 59.71 ($^1J_{CH}$ = 131 Hz), 57.94, 44.30, 34.86, 27.24, 26.94.

(LiAP)Zr(NMe$_2$)$_2$ (2l). The preparation of compound **2l** is identical to that of **2a**. Compound **1l** (1.000 g, 2.998 mmol) and Zr(NMe$_2$)$_4$ (0.957 g, 3.577 mmol) yielded yellow crystalline **2l** (1.390 g, 2.721 mmol, 91 %). ^{1}H NMR δ 6.94 (t, 1H, py), 6.56 (d, 2H, py), 4.56 (s, 4H, NC*H*$_2$), 3.25 (t, 2H, C*H*^{i}Pr$_2$), 3.02 (s, 12H, N*Me*$_2$), 2.14 (d of sept, 4H, CH(C*H*Me$_2$)$_2$), 1.18 (d, 12H, CH*Me*$_2$), 1.01 (d, 12H, CH*Me*$_2$). ^{13}C{^{1}H} NMR δ 165.62, 136.52, 116.94, 70.81, 58.04, 43.56, 43.45, 30.72, 22.07, 21.49.

(tBAP)Zr(NMe$_2$)$_2$ (2m). The preparation of compound **2m** is identical to that of **2a**. Compound **1m** (3.500 g, 14.04 mmol) and Zr(NMe$_2$)$_4$ (3.750 g, 14.02 mmol) yielded dark brown liquid **2m** (5.925 g, 13.88 mmol, 99 %). Because of its high solubiliy, compound **2m** was not isolated and was used *in situ*. ^{1}H NMR δ 6.81 (t, 1H, py), 6.55 (d, 2H, py), 4.70 (s, 4H, NC*H*$_2$), 2.89 (s, 12H, N*Me*$_2$), 1.47 (s, 18H, C*Me*$_3$). ^{13}C{^{1}H} NMR δ 166.43, 136.45, 116.91, 59.72, 56.07, 42.53, 31.22.

(DMEAP)Zr(NMe$_2$)$_2$ (2n). The preparation of compound **2n** is identical to that of **2a**. Compound **1n** (0.600 g, 2.147 mmol) and Zr(NMe$_2$)$_4$ (0.575 g, 2.149 mmol) yielded dark brown liquid **2n** (0.887 g, 1.942 mmol, 90 %). Because of its high solubiliy, compound **2n** was not isolated and was used *in situ*. ^{1}H NMR δ 6.92 (t, 1H, py), 6.56 (t, 2H, py), 4.56 (s, 4H, NC*H*$_2$), 3.75 (t, 4H, CH$_2$), 3.19 (s, 12H, N*Me*$_2$), 2.55 (t, 4H, CH$_2$), 2.23 (s, 12H, N*Me*$_2$). ^{13}C{^{1}H} NMR δ 165.54, 138.68, 117.09, 64.44, 62.59, 52.33, 46.48, 43.97.

References on page 190

(BDPP)$ZrCl_2$ (3a). Neat Me_3SiCl (5.200 g, 47.86 mmol) was added to a toluene solution (50 mL) of **2a** (3.000 g, 4.724 mmol) at 23 °C. The solution was stirred for 12 hours allowing the precipitation of a white solid. The solution was cooled to -30 °C. White crystalline **3a** was isolated by filtration and dried under vacuum (2.862 g, 4.632 mmol, 98 %). ^{1}H NMR δ 7.20-7.10 (m, 6H, Ar), 6.76 (t, 1H, py), 6.27 (d, 2H, py), 4.81 (s, 4H, NCH_2), 3.74 (sept, 4H, CHMe$_2$), 1.54 (d, 12H, CHMe_2), 1.20 (d, 12H, CHMe_2). ^{13}C{^{1}H} NMR δ 162.94, 146.03, 138.86, 127.40, 124.72, 117.74, 68.19. 28.59. 27.03. 24.78.

(BDEP)$ZrCl_2$ (3b). The preparation of compound **3b** is identical to that of **3a**. Neat Me_3SiCl (2.705 g, 24.90 mmol) and compound **2b** (1.434 g, 2.477 mmol) gave white crystalline **3b** (1.378 g, 2.453 mmol, 99 %). ^{1}H NMR δ 7.20-7.10 (m, 6H, Ar), 6.86 (t, 1H, py), 6.37 (d, 2H, py), 4.63 (s, 4H, NCH_2), 2.98 (m, 8H, CH_2CH$_3$), 1.29 (t, 12H, CH$_2$CH_3). ^{13}C{^{1}H} NMR δ 163.93, 154.80, 141.74, 138.68, 127.12, 126.72, 117.81, 67.20, 24.60, 15.58.

(BDMP)$ZrCl_2$ (3c). The preparation of compound **3c** is identical to that of **3a**. Neat Me_3SiCl (9.430 g, 86.80 mmol) and compound **2c** (4.538 g, 8.679 mmol) gave white crystalline **3c** (4.021 g, 7.953 mmol, 92 %). ^{1}H NMR δ 7.09 (m, 4H, Ar), 7.03 (m, 2H, Ar), 6.84 (t, 1H, py), 6.36 (d, 2H, py), 4.44 (s, 4H, NCH_2), 2.46 (s, 12H, Me). ^{13}C{^{1}H} NMR δ 163.01, 153.03, 138.46, 136.24, 129.31, 127.37, 117.70, 65.60, 19.30.

(TCPP)$ZrCl_2$ (3d). The preparation of compound **3d** is identical to that of **3a**. Neat Me_3SiCl (5.000 g, 46.02 mmol) and compound **2d** (3.025 g, 4.492 mmol) gave white crystalline **3d** (2.628 g, 4.005 mmol, 89 %). ^{1}H NMR δ 7.12 (s, 4H, Ar), 6.88 (t, 1H, py), 6.42 (d, 2H, py), 4.75 (s, 4H, NCH_2). ^{13}C{^{1}H} NMR δ 163.05, 148.76, 138.71, 134.59, 129.45, 117.48, 72.40.

(TBPP)$ZrCl_2$ (3e). The preparation of compound **3e** is identical to that of **3a**. Neat Me_3SiCl (0.867 g, 7.980 mmol) and compound **2i** (0.750 g, 0.798 mmol) gave white crystalline **3e** (0.657 g, 0.712 mmol, 89 %). ^{1}H NMR δ 7.48 (s, 4H, Ar), 6.74 (t, 1H, py), 6.25 (d, 2H,

References on page 190

py), 4.58 (s, 4H, NCH_2). Compound **3e** is poorly soluble in organic solvents which precludes its convenient characterization by $^{13}C\{^1H\}$ NMR spectroscopy.

(BPhP)ZrCl$_2$ (3f). The preparation of compound **3f** is identical to that of **3a**. Neat Me_3SiCl (4.000 g, 36.82 mmol) and compound **2f** (2.315 g, 3.74 mmol) gave white crystalline **3f** (2.152 g, 3.57 mmol, 96 %). ^1H NMR δ 8.44 (d, 2H, Ph), 7.90-7.80 (m, 4H, Ph), 7.40-6.90 (m, 12H, Ar/Ph), 6.39 (t, 1H, py), 5.84 (d, 2H, py), 4.54 (s, 4H, NCH_2). Compound **3a** is poorly soluble in organic solvents which precludes its convenient characterization by $^{13}C\{^1H\}$ NMR spectroscopy.

(BMPP)ZrCl$_2$ (3g). The preparation of compound **3g** is identical to **3a**. Excess Me_3SiCl (3.000 g, 27.61 mmol) and **2g** (1.500 g, 2.72 mmol) affords **3g** as a beige solid (1.190 g, 2.23 mmol, 82 %). ^1H NMR δ 7.98 (br d, 2H, Ar), 7.29 (m, 2H, Ar), 7.15 (m, 4H, Ar), 6.89 (t, 1H, py), 6.34 (d, 2H, py), 4.73 (br s, 4H, NCH_2), 3.48 (br sept, 4H, CHMe$_2$), 1.33 (br s, 12H, CHMe_2). $^{13}C\{^1H\}$ (d_8-toluene, 80 °C) δ 164.31, 147.20, 146.33, 138.63, 130.34, 127.41, 127.33, 126.74, 117.71, 69.32, 27.60, 25.01.

(BMBP)ZrCl$_2$ (3h). The preparation of compound **3h** is identical to **3a**. Excess Me_3SiCl (1.500 g, 13.81 mmol) and **2h** (1.000 g, 1.73 mmol) affords **3h** as a beige solid (0.860 g,1.54 mmol, 89 %). ^1H NMR δ 7.95 (d, 2H, Ar), 7.47 (d, 2H, Ar), 7.18 (m, 4H, Ar), 6.81 (t, 1H, py), 6.34 (d, 2H, py), 4.78 (AB quartet, $^2J_{HH}$ = 20.1 Hz, 4H, NCH_2), 1.47 (s, 18H, *t*-Bu). $^{13}C\{^1H\}$ δ 162.66, 147.23, 146.05, 138.79, 131.46, 131.01, 127.46, 127.16, 117.76, 70.21, 37.09, 33.31.

(MPPP)ZrCl$_2$ (3i). The preparation of compound **3i** is identical to **3a**. Excess Me_3SiCl (3.000 g, 27.61 mmol) and **2i** (1.700 g, 2.94 mmol) affords **3i** as a beige solid (1.327 g, 2.36 mmol, 80 %). The following data is for both rotamers (*meso*/*rac*, 1:1.15). ^1H NMR (CD_2Cl_2) δ 8.04 (t, py), 7.52 (d, py), 7.25-7.09 (m, Ar), 5.06 (AB quartet $^2J_{HH}$ = 21.3 Hz, NCH_2), 5.05 (AB quartet $^2J_{HH}$ = 21.3 Hz, NCH_2), 3.56 (sept, CHMe$_2$), 3.48 (sept, CHMe$_2$), 2.35 (s, Me), 2.31 (s, Me), 1.35 (d, CHMe_2), 1.32 (d, CHMe_2), 1.18 (d, CHMe_2), 1.16 (d,

References on page 190

CHMe_2). $^{13}C\{^1H\}$ NMR ($CDCl_2$) δ 164.16, 164.12, 147.52, 147.38, 145.22, 145.19, 141.53, 139.92, 136.18, 136.05, 129.33, 128.74, 128.70, 128.51, 127.41, 126.87, 125.59, 125.21, 124.77, 118.74, 67.20, 67.16, 28.03, 27.91, 27.73, 27.54, 23.81, 23.42, 19.50, 19.46.

(iPAP)$ZrCl_2$ (3j). The preparation of complex **3j** is identical to that of **3a**. Compound **2j** (0.750 g, 1.881 mmol) and Me_3SiCl (1.000 g, 9.204 mmol) yielded white crystalline **3j** (0.558 g, 1.463 mmol, 78 %). ^1H NMR δ 6.90 (t, 1H, py), 6.46 (d, 2H, py), 5.04 (sept, 2H, C*H*Me_2), 4.22 (s, 4H, NCH_2), 1.26 (d, 12H, CHMe_2). $^{13}C\{^1H\}$ NMR δ 164.76, 137.31, 117.54, 56.55, 47.49, 20.60.

(CyAP)$ZrCl_2$ (3k). The preparation of complex **3k** is identical to that of **3a**. Compound **2k** (1.100 g, 2.297 mmol) and Me_3SiCl (2.500 g, 10.44 mmol) yielded white crystalline **2k** (0.986 g, 2.136 mmol, 93 %). ^1H NMR δ 6.89 (t, 1H, py), 6.45 (d, 2H, py), 4.47 (br t, 2H, NC*H*), 4.25 (s, 4H, NCH_2), 2.18 (m, 4H, Cy), 1.83 (m, 4H, Cy), 1.40 (m, 10H, Cy), 1.05 (m, 2H, Cy). $^{13}C\{^1H\}$ NMR δ 165.02, 137.34, 117.50, 58.16, 56.24, 31.66, 26.83, 26.36.

(LiAP)$ZrCl_2$ (3l). The preparation of complex **3l** is identical to that of **3a**. Compound **2l** (1.390 g, 2.721 mmol) and Me_3SiCl (5.000 g, 46.02 mmol) yielded grey crystalline **3l** (1.166 g, 2.282 mmol, 84 %). ^1H NMR δ 6.88 (t, 1H, py), 6.42 (d, 2H, py), 4.23 (s, 4H, NCH_2), 4.21 (t, 2H, C*H*^{i}Pr_2), 2.08 (d of sept, 4H, C*H*Me_2), 1.22 (d, 12H, CHMe_2), 1.11 (d, 12H, CHMe_2). ^1H NMR ($CDCl_3$) δ 7.89 (t, 1H, py), 7.42 (d, 2H, py), 4.86 (s, 4H, NCH_2), 3.91 (t, 2H, C*H*^{i}Pr_2), 2.11 (d of sept, 4H, C*H*Me_2), 1.13 (d, 12H, CHMe_2), 1.08 (d, 12H, CHMe_2). $^{13}C\{^1H\}$ NMR ($CDCl_3$) δ 165.15, 138.34, 117.88, 66.00, 59.16, 32.29, 22.9, 21.17.

(tBAP)$ZrCl_2$ (3m). The preparation of complex **3m** is identical to that of **3a**. Compound **2m** (5.925 g, 13.88 mmol) and Me_3SiCl (10.00 g, 41.75 mmol) yielded grey crystalline **3m** (5.120 g, 12.50 mmol, 90 %). ^1H NMR δ 6.80 (t, 1H, py), 6.32 (7, 2H, py),

References on page 190

4.40 (s, 4H, NCH_2), 1.68 (s, 18H, CMe_3). $^{13}C\{^1H\}$ NMR δ 166.43, 136.45, 116.91, 59.72, 56.07, 42.53, 31.22.

(DMEAP)$ZrCl_2$ (3n). The preparation of complex **3n** is identical to that of **3a**. Compound **2n** (0.887 g, 1.842 mmol) and Me_3SiCl (2.500 g, 23.01 mmol) yielded dark brown solid **3n** (0.756 g, 1.720 mmol, 94 %). ^1H NMR δ 6.90 (t, 1H, py), 6.49 (d, 2H, py), 4.51 (s, 4H, NCH_2), 3.31 (t, 4H, CH_2), 2.93 (br s, 4H, CH_2), 2.49 (s, 12H, NMe_2). $^{13}C\{^1H\}$ NMR δ 164.10, 136.82, 116.36, 67.95, 64.32, 54.82, 49.42.

(BDPP)$ZrCl_2${$HN(SiMe_3)_2$} (4a). To a toluene solution of $ZrCl_2\{N(SiMe_3)_2\}_2$ (0.100 g, 0.207 mmol) was added a toluene solution (50 mL) of **1a** (0.096 g, 0.210 mmol) at 23 °C. The solution was refluxed for 12 hours. The solvent was removed in *vacuo* to give a yellow oily solid **4a** (0.106 g, 0.136 mmol, 66 %). ^1H NMR δ 7.30-7.10 (m, 6H, Ar), 6.98 (t, 1H, py), 6.48 (d, 2H, py), 5.20 (AB quartet, $^2J_{HH}$ = 20.0 Hz, 4H, NCH_2), 4.06 (sept, 2H, CHMe$_2$), 3.16 (sept, 2H, CHMe$_2$), 1.57 (d, 6H, CHMe_2), 1.46 (d, 6H, CHMe_2), 1.38 (d, 6H, CHMe_2), 1.07 (d, 6H, CHMe_2), 0.27 and 0.16 {s, 18H each, ZrNH(SiMe_3)$_2$ and free HN(SiMe_3)$_2$}.

(BDPP)$ZrMe_2$ (5a). To a diethylether (25 mL) suspension of compound **3a** (0.250 g, 0.405 mmol) was added 2.2 equiv of MeMgBr (0.49 mL, 1.80 M, 0.88 mmol) at 23 °C. The suspension was stirred for 12h. The solvent was remover in *vacuo*. The resulting solid was extractred with toluene (3 x 10 mL) and filtered through Celite to give a light-yellow solution. The solvent was removed in *vacuo*, the solid dissolved in a minimum amount of diethylether and cooled to -30 °C for 12 h. White crystalline **5a** was isolated by filtration and dried under vaccum (0.207 g, 0.359 mmol, 89 %). ^1H NMR δ 7.30-7.20 (m, 6H, Ar), 6.88 (t, 1H, py), 6.40 (d, 2H, py), 4.95 (s, 4H, NCH_2), 3.84 (sept, 4H, CHMe$_2$), 1.41 (d, 12H, CHMe_2), 1.21 (d, 12H, CHMe_2), 0.45 (s, 6H, ZrCH_3). $^{13}C\{^1H\}$ NMR δ 163.94, 147.12, 137.98, 126.38, 124.44, 117.36, 67.48, 44.71, 28.32, 28.17, 24.18. Anal. Calcd for $C_{33}H_{47}N_3Zr$: C, 68.70; H, 8.21; N, 7.28. Found: C, 69.50; H, 8.57; N, 7.49.

References on page 190

(BDEP)ZrMe$_2$ (5b). The preparation of compound **5b** is identical to that of **5a**. Compound **3b** (0.400 g, 0.712 mmol) and MeMgBr (0.87 mL, 1.80 M, 1.57 mmol) gave white crystalline **5b** (0.307 g, 0.589 mmol, 83 %). ^{1}H NMR δ 7.30-7.20 (m, 6H, Ar), 6.87 (t, 1H, py), 6.45 (d, 2H, py), 4.77 (s, 4H, NCH_2), 2.94 (q, 8H, CH_2CH$_3$), 1.27 (t, 12H, CH$_2$CH_3), 0.29 (s, 6H, ZrCH_3). ^{13}C{^{1}H} NMR δ 164.34, 146.73, 142.63, 137.83, 126.60, 126.08, 117.60, 66.41, 42.83, 24.14, 16.17. Anal. Calcd for $C_{29}H_{39}N_3Zr$: C, 66.87; H, 7.55; N, 8.07. Found: C, 66.37; H, 7.71; N, 7.83.

(BDMP)ZrMe$_2$ (5c). The preparation of compound **5c** is identical to that of **5a**. Compound **3c** (0.100 g, 0.198 mmol) and MeMgBr (0.24 mL, 1.80 M, 0.432 mmol) gave white crystalline **5c** (0.074 g, 0.159 mmol, 80 %). ^{1}H NMR δ 7.16 (m, 4H, Ar), 7.06 (m, 2H, Ar), 6.88 (t, 1H, py), 6.44 (d, 2H, py), 4.58 (s, 4H, NCH_2), 2.40 (s, 12H, Me), 0.34 (s, 6H, ZrCH_3). ^{13}C{^{1}H} NMR δ 164.34. 142.83. 137.56. 136.81. 128.87. 125.47, 117.42, 64.60, 47.88, 18.54.

(TCPP)ZrMe$_2$ (5d). The preparation of compound **5f** is identical to that of **5a**. Compound **3d** (0.700 g, 1.067 mmol) and MeMgBr (1.99 mL, 1.34 M, 2.67 mmol) gave white crystalline **5d** (0.377 g, 0.613 mmol, 57 %). ^{1}H NMR δ 7.21 (s, 4H, Ar), 6.79 (t, 1H, py), 6.34 (d, 2H, py), 4.62 (s, 4H, NCH_2), 0.68 (s, 6H, ZrMe_2). ^{13}C{^{1}H} NMR δ 163.48, 144.86, 138.30, 137.10, 131.11, 117.82, 62.91, 47.38.

(TBPP)ZrMe$_2$ (5e). The preparation of compound **5e** is identical to that of **5a**. Compound **3e** (0.150 g, 0.163 mmol) and MeMgBr (0.30 mL, 1.34 M, 0.40 mmol) gave white crystalline **5e** (0.112 g, 0.127 mmol, 69 %). ^{1}H NMR δ 7.60 (s, 4H, Ar), 6.81 (t, 1H, py), 6.34 (d, 2H, py), 4.68 (s, 4H, NCH_2), 0.77 (s, 6H, ZrMe). ^{13}C{^{1}H} NMR δ 163.36, 147.68, 138.41, 135.25, 119.10, 117.86, 62.86, 49.68.

(BPhP)ZrMe$_2$ (5f). The preparation of compound **5f** is identical to that of **5a**. Compound **3f** (1.000 g, 1.66 mmol) and MeMgBr (3.70 mL, 0.99 M, 3.67 mmol) gave white

References on page 190

crystalline **5f** (0.625 g, 1.11 mmol, 67 %). ^{1}H NMR δ 8.10 (d, 2H, Ph), 7.73 (d, 4H, Ph), 7.38 (d, 2H, Ar/Ph), 7.31-7.28 (m, 2H, Ar/Ph), 7.15-7.08 (m, 6H, Ar/Ph), 6.99 (m, 2H, Ar/Ph), 6.49 (t, 1H, py), 5.93 (d, 2H, py), 4.62 (s, 4H, NCH_2), 0.73 (s, 6H, Zr-*Me*). ^{13}C{^{1}H} NMR δ 164.02, 148.94, 142.66, 137.59, 136.82, 133.01, 129.06, 128.68, 128.49, 128.17, 126.84, 125.21, 116.97, 64.51, 42.38. Anal. Calcd. for $C_{33}H_{31}N_3Zr$: C, 70.67; H, 5.57; N, 7.49. Found: C, 70.60; H, 5.55; N.7.19.

(BMPP)ZrMe$_2$ (5g). The preparation of compound **5g** is identical to that of **5a**. Compound **3g** (0.500 g, 0.94 mmol) and MeMgBr (0.78 mL, 3.0 M, 2.34 mmol) gave white crystalline **5g** (0.445 g, 0.90 mmol, 85 %). ^{1}H NMR δ 7.69 (m, 2H, Ar), 7.36 (m, 2H, Ar), 7.20 (m, 4H, Ar), 6.87 (t, 1H, py), 6.38 (d, 2H, py), 4.84 (s, 4H, NCH$_2$), 3.57 (sept, 4H, C*H*Me$_2$), 1.31, (d, 12H, CH*Me*$_2$), 0.46 (br s, 6H, Zr-*Me*). ^{13}C{^{1}H} NMR δ 164.02, 148.50, 147.54, 131.08, 129.27, 127.21, 126.67, 126.29, 117.35, 58.31, 41.23 (Zr-CH_3), 27.25, 25.39. Anal. Calcd. for $C_{27}H_{35}N_3Zr$: C, 65.81; H, 7.16; N, 8.53. Found: C, 66.03; H, 7.18; N, 8.68.

(BMBP)ZrMe$_2$ (5h). The preparation of compound **5h** is identical to **5a**. MeMgCl (0.52 mL, 3.0 M, 1.55 mmol) and **3h** (0.350 g, 0.62 mmol) gave **5h** as a white crystalline solid (0.234 g, 0.45 mmol, 73%). The following data is for both rotamers (*meso*/*rac*, 3:1). ^{1}H NMR δ 7.78 (d, Ar), 7.54 (d, Ar), 7.20 (m, Ar), 6.87 (t, py), 6.43 (d, py), 4.91 (AB quartet, $^2J_{HH}$ = 20.7 Hz, *meso* NCH_2), 4.83 (AB quartet, $^2J_{HH}$ = 20.7 Hz, *rac* NCH_2), 1.55 (s, *rac* *t*-Bu), 1.49 (s, *meso* *t*-Bu), 0.82 (s, *meso* Zr-Me), 0.62 (s, *rac* Zr-Me), 0.26 (s, *meso* Zr-Me). ^{13}C{^{1}H} NMR δ 163.66, 163.21, 149.43, 147.18, 137.90, 133.98, 132.75, 130.93, 127.06, 126.92, 126.02, 125.88, 117.47, 70.03, 69.71, 45.71 (Zr-CH_3), 44.73 (Zr-CH_3), 39.57, 37.18, 33.34. Anal. Calcd. for $C_{29}H_{39}N_3Zr$: C, 66.87; H, 7.55; N, 8.07. Found: C, 66.64; H, 7.77; N, 7.91.

(MPPP)ZrMe$_2$ (5i). The preparation of compound **5i** is identical to **5a**. MeMgCl (0.75 mL, 3.0 M, 2.23 mmol) and **3i** (0.500 g, 0.89 mmol) gave **5i** as a white crystalline solid (0.316 g, 0.61 mmol, 69%). The following data is for both rotamers (*meso*/*rac*, 1:1.14). ^{1}H

References on page 190

NMR δ 7.23-7.00 (m, Ar), 6.91 (t, py), 6.45 (d, py), 4.75 (AB quartets $^2J_{HH}$ = 20.8 Hz, NC*H*$_2$), 4.74 (AB quartets $^2J_{HH}$ = 20.8 Hz, NC*H*$_2$), 3.90 (sept, C*H*Me$_2$), 2.38 (s, Me), 2.11 (s, Me), 1.45 (d, CH*Me*$_2$), 1.43 (d, CH*Me*$_2$), 1.25 (d, CH*Me*$_2$), 1.23 (d, CH*Me*$_2$), 0.45 (s, *meso* Zr-*Me*), 0.39 (s, *rac* Zr-*Me*), 0.32 (s, *meso* Zr-*Me*). $^{13}C\{^1H\}$ NMR δ 164.23, 164.17, 147.78, 147.75, 147.28, 137.79, 136.43, 129.28, 128.67, 128.51, 125.97, 125.64, 124.54, 117.42, 65.96, 44.35, 43.71, 42.67, 28.63, 28.51, 27.71, 23.75, 23.63, 21.40, 19.09. Anal. Calcd. for $C_{29}H_{39}N_3Zr$: C, 66.87; H, 7.55; N, 8.07. Found: C, 66.79; H, 7.51; N, 8.24.

(iPAP)ZrMe$_2$ (5j). The preparation of complex **5j** is identical to that of **5a**. Compound **3j** (0.500 g, 1.311 mmol) and MeMgBr (1.09 mL, 3.00 M, 3.27 mmol) gave white crystalline **5j** (0.358 g, 1.051 mmol, 80 %). ^1H NMR δ 6.90 (t, 1H, py), 6.50 (d, 2H, py), 4.97 (sept, 2H, C*H*Me$_2$), 4.43 (s, 4H, NC*H*$_2$), 1.40 (d, 12H, CH*Me*$_2$), 0.34 (s, 6H, Zr*Me*). $^{13}C\{^1H\}$ NMR δ 165.00, 136.56, 117.25, 56.14, 46.34 ($^1J_{CH}$ = 129 Hz), 31.26, 21.99. Anal. calcd. for $C_{15}H_{27}N_3Zr$: C, 52.89; H, 7.99; N, 12.34. Found: C, 52.66; H, 7.82; N, 12.55.

(CyAP)ZrMe$_2$ (5k). The preparation of complex **5k** is identical to that of **5a**. Compound **3k** (0.500 g, 1.083 mmol) and MeMgBr (2.02 mL, 1.34 M, 2.71 mmol) gave white crystalline **5k** (0.395 g, 0.939 mmol, 87 %). ^1H NMR δ 6.91 (t, 1H, py), 6.51 (t, 2H, py), 4.50 (s, 4H, NC*H*$_2$), 4.45 (buried, 2H, NC*H*), 2.11 (m, 4H, Cy), 1.90 (m, 4H, Cy), 1.60 (m, 10H, Cy), 1.15 (m, 2H, Cy), 0.39 (s, 6H, Zr*Me*). $^{13}C\{^1H\}$ NMR δ 165.21, 136.52, 117.15, 57.71, 55.61, 33.31, 31.05, 27.35, 26.66. Anal. calcd. for $C_{21}H_{35}N_3Zr$: C, 59.95; H, 8.38; N, 9.99. Found: C, 59.99; H, 8.46; N, 9.87.

(LiAP)ZrMe$_2$ (5l). The preparation of complex **5l** is identical to that of **5a**. Compound **3l** (0.700 g, 1.148 mmol) and MeMgBr (1.33 mL, 3.00 M, 3.99 mmol) gave white crystalline **5l** (0.468 g, 1.033 mmol, 90 %). ^1H NMR δ 6.92 (t, 1H, py), 6.50 (d, 2H, py), 4.55 (s, 4H, NC*H*$_2$), 4.19 (t, 2H, C*H*^{i}Pr$_2$), 2.20 (d of sept, 4H, C*H*Me$_2$), 1.21 (d, 12H, CH*Me*$_2$), 1.16 (d, 12H, CH*Me*$_2$), 0.57 (s, 6H, Zr*Me*). $^{13}C\{^1H\}$ NMR δ 165.16, 136.72,

References on page 190

129.28, 125.50, 117.06, 65.74, 58.54, 37.68, 32.60, 22.80, 21.91. Anal. calcd. for $C_{23}H_{43}N_3Zr$: C, 61.01; H, 9.57; N, 9.28. Found: C, 60.86; H, 9.48; N, 9.35.

(tBAP)ZrMe$_2$ (5m). The preparation of complex **5m** is identical to that of **5a**. Compound **3m** (0.500 g, 1.221 mmol) and MeMgBr (4.10 mL, 1.34 M, 5.49 mmol) gave white crystalline **5m** (0.328 g, 0.890 mmol, 73 %). ^{1}H NMR δ 6.88 (t, 1H, py), 6.46 (t, 2H, py), 4.56 (s, 4H, NCH_2), 1.66 (s, 18H, CMe_3), 0.42 (s, 6H, ZrMe). ^{13}C{^{1}H} NMR δ 165.03, 136.60, 116.83, 59.19, 55.00, 35.33, 29.25. Anal. calcd. for $C_{17}H_{31}N_3Zr$: C, 55.38; H, 8.47; N, 11.40. Found: C, 55.70; H, 8.35; N, 11.34.

(BDPP)Zr(CH$_2$Ph)$_2$ (6a). To a diethylether (25 mL) suspension of compound **3a** (0.100 g, 0.162 mmol) was added 2.2 equiv of PhCH$_2$MgBr (0.32 mL, 1.13 M, 0.36 mmol) at 23 °C. The suspension was stirred for 12h. The solvent was removed in *vacuo*. The resulting solid was extracted with toluene (3 x 10 mL) and filtered through Celite to give a bright-yellow solution. The solvent was removed in *vacuo*, the solid dissolved in a minimum amount of dichloromethane and cooled to -30 °C for 12 h. Yellow crystalline **6a** was isolated by filtration and dried under vacuum (0.093 g, 0.128 mmol, 79 %). ^{1}H NMR (d$_8$-toluene, 23 °C) δ 7.30-6.90 (m, Ar and CH$_2$Ph), 6.82 (t, 1H, py), 6.35 (d, 2H, py), 4.82 (br s, 4H, NCH_2), 3.85 (br s, 4H, CHMe$_2$), 1.92 (br s, 4H, CH_2Ph), 1.45 (br s, 12H, CHMe_2), 1.21 (d, 12H, CHMe_2). ^{1}H NMR (d$_8$-toluene, -40 °C) δ 7.30-6.90 (m, 6H, Ar and CH$_2$Ph), 6.82 (m, 4H, *m* -Ph), 6.75 (t, 1H, py), 6.51 (m, 2H, *p* -Ph), 6.23 (d, 2H, py), 5.90 (d, 4H, *o* -Ph), 4.81 (AB quartet, $^2J_{HH}$ = 20.2 Hz, 4H, NCH_2), 4.03 (sept, 2H, CHMe$_2$), 3.71 (sept, 2H, CHMe$_2$), 2.10 (s, 2H, CH_2Ph), 1.64 (s, 2H, CH_2Ph), 1.51 (d, 6H, CHMe_2), 1.40 (d, 6H, CHMe_2), 1.38 (d, 6H, CHMe_2),1.08 (d, 6H, CHMe_2). Partial ^{13}C{^{1}H} NMR (d$_8$-toluene, 23 °C) δ 68.87 (NCH_2). Anal. Calcd for $C_{45}H_{55}N_3Zr \cdot 1/4\ CH_2Cl_2$: C, 72.43; H, 7.45; N, 5.60. Found: C, 72.65; H, 7.62; N, 5.59.

(BDEP)Zr(CH$_2$Ph)$_2$ (6b). The preparation of compound **6b** is identical to that of **6a**. Compound **3b** (0.300 g, 0.534 mmol) and PhCH$_2$MgBr (1.42 mL, 1.13 M, 1.60 mmol) gave a yellow oily solid **6b**. The high solubility of the product made its isolation from the crude oil

References on page 190

impossible. ^{1}H NMR δ 7.40-6.50 (m, 15H, py, Ar and Ph), 6.35 (d, 4H, Ph), 4.55 (s, 4H, NCH_2), 2.89 (q, 8H, CH_2Me), 1.61 (s, 4H, ZrCH_2Ph), 1.26 (t, 12H, CH$_2$*Me*). ^{13}C{^{1}H} NMR δ 162.74, 149.81, 141.59, 137.76, 129.59, 126.83, 126.18, 125.79, 122.01, 117.17, 65.69, 60.95, 24.66, 15.15.

(BDMP)Zr(CH$_2$Ph)$_2$ (6c). The preparation of compound **6c** is identical to that of **6a**. Compound **3c** (0.075 g, 0.148 mmol) and PhCH$_2$MgBr (0.29 mL, 1.13 M, 0.33 mmol) gave a yellow solid **6c** (0.089 g, 0.144 mmol, 97 %). ^{1}H NMR δ 7.08 (m, 4H, Ar), 6.98 (m, 2H, Ar), 6.87 (m, 4H, Ph), 6.84 (t, 1H, py), 6.67 (m, 2H, Ph), 6.36 (m, 4H, Ph), 6.34 (d, 2H, py), 4.42 (s, 4H, NCH_2), 2.37 (s, 12H, Me), 1.663 (s, 4H, ZrCH_2Ph). ^{13}C{^{1}H} NMR δ 162.85, 150.76, 137.59, 136.25, 129.64, 126.69, 125.40, 121.94, 117.13, 64.12, 60.62, 60.57, 19.62. Anal. Calcd for $C_{37}H_{39}N_3Zr$: C, 72.03; H, 6.37; N, 6.81. Found: C, 71.89; H, 6.65; N, 6.82.

(BMPP)Zr(CH$_2$Ph)$_2$ (6g). The preparation of compound **6g** is identical to that of **6a**. Compound **3g** (0.500 g, 0.937 mmol) and PhCH$_2$MgBr (2.63 mL, 0.89 M, 2.34 mmol) gave a yellow solid **6g** (0.512 g, 0.794 mmol, 85 %). ^{1}H NMR δ 7.55 (br m, 2H, Ar/Ph), 7.30 (m, 2H, Ar/Ph), 7.15 (m, 4H, Ar/Ph), 6.80 (br s, 6H, Ar/Ph), 6.48 (t, 1H, py), 6.48 (br s, 2H, Ar/Ph), 6.29 (d, 2H, py), 5.68 (br s, 2H, Ph), 4.65 (br s, 4H, NCH_2), 3.50 (br s, 2H, C*H*Me$_2$), 2.15 (br s, 4H, CH_2Ph), 1.18 (br s, 12H, CH*Me*$_2$). ^{13}C{^{1}H} NMR δ 162.91, 148.83, 147.10, 137.40, 130.47, 130.07, 126.56, 126.41, 117.07, 67.94, 26.92, 22.51.

(BMBP)Zr(CH$_2$Ph)$_2$ (6h). The preparation of compound **6h** is identical to that of **6a**. Compound **3h** (0.500 g, 0.890 mmol) and PhCH$_2$MgBr (2.50 mL, 0.89 M, 2.22 mmol) gave a yellow solid **6h** (0.438 g, 0.651 mmol, 73 %). ^{1}H NMR δ 7.50 (m, 1H, Ar), 7.42 (m, 1H, Ar), 7.18 (m, 4H, Ar and Ph), 7.04 (m, 2H, Ar and Ph), 6.81 (t, 2H, Ar and Ph), 6.73 (t, 1H, py), 6.35 (d, 2H, py), 5.71 (m, 2H, Ph), 4.66 (AB quartet, $^2J_{HH}$ = 20.5 Hz, 4H, NCH_2), 2.34 (s, 2H, CH_2Ph), 1.80 (s, 2H, CH_2Ph), 1.46 (s, 18H, C*Me*$_3$). ^{13}C{^{1}H} δ 161.91, 149.65, 148.98, 146.61, 137.36, 137.07, 132.96, 131.10, 130.31, 130.12, 127.36, 126.56, 126.32, 124.95,

References on page 190

124.14, 119.58, 117.07, 69.41, 65.16, 56.69, 37.17, 33.47. Anal. Calcd. for $C_{41}H_{47}N_3Zr$: C, 73.17; H, 7.04; N, 6.24. Found: C, 73.10; H, 7.15; N, 6.39.

(tBAP)Zr(CH_2Ph)$_2$ (6m). The preparation of compound **6m** is identical to that of **6a**. Compound **3m** (0.500 g, 1.221 mmol) and $PhCH_2MgBr$ (2.75 mL, 0.89 M, 2.45 mmol) gave a yellow solid **6m** (0.497 g, 0.954 mmol, 78 %). ^{1}H NMR δ 6.86 (m, 6H, Ph), 6.72 (m, 4H, Ph), 6.60 (t, 1H, py), 6.41 (d, 2H, py), 4.24 (s, 4H, NCH_2), 2.50 (s, 4H, CH_2Ph), 1.48 (s, 18H, CMe_3). ^{13}C{^{1}H} NMR δ 164.37, 148.09, 136.64, 127.81, 127.63, 127.59, 120.43, 116.70, 61.69, 58.58, 55.48, 28.33. Anal. calcd. for $C_{29}H_{39}N_3Zr$: C, 66.87; H, 7.55; N, 8.07. Found: C, 67.05; H, 7.57; N, 7.78.

(BDPP)Zr(CH_2SiMe_3)$_2$ (7a). To a diethylether (25 mL) suspension of compound **3a** (0.100 g, 0.178 mmol) was added 2.2 equiv of Me_3SiCH_2Li (0.037 g, 0.393 mmol) at -20 °C. The suspension was stirred for 12h. The solvent was removed in *vacuo*. The resulting solid was extracted with toluene (3 x 10 mL) and filtered through Celite to give a bright-yellow solution. The solvent was removed in *vacuo*, the solid dissolved in a minimum amount of hexanes and cooled to -30 °C for 12 h. Yellow crystalline **7a** was isolated by filtration and dried under vacuum (0.109 g, 0.156 mmol, 88 %). ^{1}H NMR δ 7.24 (b, 6H, Ar), 6.86 (t, 1H, py), 6.40 (d, 2H, py), 5.0 (br s, 4H, NCH_2), 1.52 and 1.28 (br s, 12H each, CHMe_2), -0.13 (br s, 18H, SiMe_3). ^{1}H NMR (d_8-toluene, T = 70 °C) δ 7.20-7.25 (m, 6H, Ar), 6.98 (t, 1H, py), 6.54 (d, 2H, py), 4.96 (s, 4H, NCH_2), 3.91 (br s, 4H, CHMe$_2$), 1.49 and 1.26 (d, 12H each, CHMe_2), 0.65 (s, 4H, ZrCH_2Si), -0.18 (s, 18H, SiMe_3). ^{13}C{^{1}H} NMR δ 146.13, 127.38, 124.68, 117.32, 67.78, 28.18, 27.46, 24.25, 2.82. Anal. Calcd for $C_{39}H_{63}N_3Si_2Zr$: C, 64.94; H, 8.80; N, 5.83. Found: C, 64.94; H, 8.77; N, 5.95.

(BDEP)Zr(CH_2SiMe_3)$_2$ (7b). The preparation of compound **7b** is identical to that of **7a**. Compound **3b** (0.100 g, 0.178 mmol) and Me_3SiCH_2Li (0.037 g, 0.393 mmol) gave yellow crystalline **7b** (0.109 g, 0.156 mmol, 88 %). ^{1}H NMR δ 7.25-7.15 (m, 6H, Ar), 6.88 (t, 1H, py), 6.43 (d, 2H, py), 4.77 (s, 4H, NCH_2), 3.05 (m, 8H, CH_2Me), 1.33 (t, 12H, CH$_2$$Me$), 0.54

References on page 190

(s, 4H, ZrCH_2Si), -0.13 (s, 18H, SiMe_3). $^{13}C\{^1H\}$ NMR δ 163.33, 149.42, 141.39, 138.43, 126.75, 125.84, 117.58, 66.60, 58.79, 24.57, 15.75, 2.99.

(BDMP)Zr(CH_2SiMe_3)$_2$ (7c). The preparation of compound **7c** is identical to that of **7a**. Compound **3c** (0.100 g, 0.198 mmol) and Me_3SiCH_2Li (0.041 g, 0.435 mmol) gave yellow crystalline **7c** (0.103 g, 0.169 mmol, 85 %). ^1H NMR δ 7.15 (d, 4H, Ar), 7.03 (m, 2H, Ar), 6.91 (t, 1H, py), 6.47 (d, 2H, py), 4.64 (s, 4H, NCH_2), 2.48 (s, 12H, Me), 0.61 (s, 4H, ZrCH_2Si), -0.13 (s, 18H, SiMe_3). $^{13}C\{^1H\}$ NMR δ 163.49, 150.53, 138.32, 135.85, 129.34, 125.39, 117.53, 64.94, 58.43, 19.54, 3.00.

(BDPP)ZrPh_2 (8a). To a diethylether suspension (10 mL) of complex **3a** (0.250 g, 0.405 mmol) was added 2.2 equiv of PhMgBr (0.80 mL, 1.12 M, 0.90 mmol) at -30 °C. The solution was stired at roomt temperature for 12 hours. The solvent was removed in *vacuo*. The solid was extracted with toluene. The solvent was removed under vaccum. The solid dissolved in a minimum amount of a 50:50 toluene:hexanes mixture and the solution was cooled to -30 °C. White crystalline **8a** was isolated by filtration and dried under vaccum (0.197 g, 0.281 mmol, 69 %). ^1H NMR δ 7.30-7.10 (m, 12H, Ar and Ph), 7.05 (m, 4H, Ar and Ph), 6.92 (t, 1H, py), 6.45 (d, 2H, py), 4.94 (s, 4H, NCH_2), 3.54 (sept, 4H, CHMe$_2$), 1.14 (d, 12H, CHMe_2), 0.91 (d, 12H, CHMe_2). $^{13}C\{^1H\}$ NMR δ 190.41, 163.10, 149.06, 145.97, 138.40, 133.84, 126.71, 125.95, 124.29, 117.61, 68.21, 28.38, 26.41, 23.97.

(BMBP)Zr(CH_2CMe_2Ph)$_2$ (9h). To a diethylether (25 mL) suspension of compound **3h** (0.100 g, 0.178 mmol) was added 2.2 equiv of $PhCMe_2CH_2MgCl$ (0.56 mL, 0.69 M, 0.39 mmol) at -20 °C. The suspension was stirred for 12h. The solvent was removed in *vacuo*. The resulting solid was extracted with toluene (3 x 10 mL) and filtered through Celite to give a colorless solution. The solvent was removed in *vacuo*, the solid dissolved in a minimum amount of diethylether and cooled to -30 °C for 12h. White crystalline **9h** was isolated by filtration and dried under vacuum (0.107 g, 0.162 mmol, 94 %). ^1H NMR δ 7.66 (d, 2H, Ar), 7.55 (d, 2H, Ar), 7.30-6.95 (m, 14H, Ar/Ph), 6.89 (t, 1H, py), 6.43 (d, 2H, py), 4.75 (AB quartet, $^2J_{HH}$ =

References on page 190

20.8 Hz, 4H, NCH_2), 1.61 (s, 2H, CH_2CMe$_2$Ph), 1.39 (s, 18H, CMe_3), 1.36 (s, 6H, CH$_2$CMe_2Ph), 1.04 (s, 2H, CH_2CMe$_2$Ph), 1.01 (s, 6H, CH$_2$CMe_2Ph). ^{13}C{^{1}H} NMR δ 162.54, 155.94, 154.22, 150.42, 146.25, 137.90, 132.23, 131.66, 127.45, 127.30, 126.88, 126.04, 125.41, 125.30, 125.03, 124.43, 117.47, 86.50, 82.53, 69.54, 43.81, 40.58, 37.11, 34.51, 33.44, 32.63.

(BDPP)Zr(CH$_2$CMe$_2$Ph)Cl (10a). To a diethylether (25 mL) suspension of compound **3a** (0.100 g, 0.162 mmol) was added 1.2 equiv of PhCMe$_2$CH$_2$MgCl (0.22 mL, 0.88 M, 0.19 mmol) at -20 °C. The suspension was stirred for 12h. The solvent was removed in *vacuo*. The resulting solid was extracted with toluene (3 x 10 mL) and filtered through Celite to give a colorless solution. The solvent was removed in *vacuo*, the solid dissolved in a minimum amount of diethylether and cooled to -30 °C for 12h. White crystalline **10a** was isolated by filtration and dried under vacuum (0.109 g, 0.152 mmol, 94 %). ^{1}H NMR δ 7.25-7.00 (m, 11H, Ar and Ph), 6.86 (t, 1H, py), 6.38 (d, 2H, py), 4.76 (AB quartet, $^2J_{HH}$ = 20.9 Hz, 4H, NCH_2), 4.31 and 3.27 (sept, 2H each, CHMe$_2$), 2.05 (s, 2H, CH_2CMe$_2$Ph), 1.44, 1.37 and 1.35 (d, 6H each, CHMe_2), 1.29 (s, 6H, CH$_2$CMe_2Ph), 1.12 (d, 6H, CHMe_2). ^{13}C{^{1}H} NMR δ 163.38, 154.39, 148.81, 145.81, 144.84, 138.81, 126.51, 125.26, 125.12, 124.75, 124.58, 117.82, 80.17, 68.06, 44.04, 33.37, 29.14, 27.60, 26.51, 26.41, 25.24, 25.08. Anal. Calcd for $C_{41}H_{54}ClN_3Zr$: C, 68.82; H, 7.61; N, 5.87. Found: C, 69.16; H, 7.72; N, 5.84.

(BMBP)Zr(CH$_2$CMe$_2$Ph)Cl (10h). To a dichloromethane (50 mL) solution of compound **3h** (0.500 g, 0.890 mmol) was added 1 equiv of PhCMe$_2$CH$_2$MgCl (1.01 mL, 0.88 M, 0.89 mmol) at -78 °C. The solution was allowed to warm up to room temperature slowly and stirre for 12 hours. The solvent was removed in *vacuo*. The resulting solid was extracted with toluene (3 x 10 mL) and filtered through Celite to give a colorless solution. The solvent was removed in *vacuo*, the solid dissolved in a minimum amount of diethylether and cooled to -30 °C for 12h. White crystalline **10h** was isolated by filtration and dried under vacuum (0.357 g, 0.541 mmol, 61 %). ^{1}H NMR δ 7.55 (d, 2H, Ar), 7.52 (d, 2H, Ar), 7.25-7.00 (m, 9H, Ar/Ph), 6.93

References on page 190

(t, 1H, py), 6.47 (d, 2H, py), 4.71 (AB quartet, $^2J_{HH}$ = 20.8 Hz, 4H, NCH_2), 2.14 (s, 2H, CH_2CMe$_2$Ph), 1.46 (s, 18H, CMe_3), 1.38 (s, CH$_2$CMe_2Ph). $^{13}C\{^1H\}$ NMR δ 163.09, 153.77, 149.71, 145.88, 138.48, 131.59, 130.90, 129.32, 126.94, 126.35, 125.46, 125.19, 117.76, 82.08, 69.82, 43.70, 37.10, 34.38, 33.59.

(BMBP)Zr(Si(SiMe$_3$)$_3$)Cl (11h). To an hexanes (15 mL) solution of compound **3h** (0.500 g, 0.890 mmol) was added 1 equiv of (Me$_3$Si)$_3$SiLi•3THF (0.460 g, 0.977 mmol) at -78 °C. The solution was allowed to warm up to room temperature slowly and stirre for 12 hours. The solvent was removed in *vacuo*. The resulting solid was extracted with hexanes (3 x 10 mL) and filtered through Celite to give a colorless solution. The solvent was removed in *vacuo* to give white solid **11h** (0.650 g, 0.840 mmol, 94 %). ^1H NMR δ 8.12 (d, 2H, Ar), 7.47 (d, 2H, Ar), 7.34 (t, 2H, Ar), 7.16 (t, 2H, Ar), 6.91 (t, 1H, py), 6.41 (t, 2H, py), 5.12 (AB quartet, $^2J_{HH}$ = 21.4 Hz, 4H, NCH_2), 1.35 (s, 18H, CMe_3), 0.45 (s, 27H, SiMe_3). $^{13}C\{^1H\}$ NMR δ 161.99, 149.10, 143.57, 139.11, 132.79, 131.11, 127.09, 126.81, 117.88, 69.49, 36.87, 33.32, 33.14, 6.16.

(BDPP)ZrCpCl (12a). To a diethylether (25 mL) suspension of compound **3a** (0.100 g, 0.162 mmol) was added 1.3 equiv of NaCp•DME (0.038 g, 0.213 mmol) at -20 °C. The suspension was stirred for 12h. The solvent was removed in *vacuo*. The resulting solid was extracted with toluene (3 x 10 mL) and filtered through Celite to give a colorless solution. The solvent was removed in *vacuo*, the solid dissolved in a minimum amount of diethylether and cooled to -30 °C for 12 h. White crystalline **12a** was isolated by filtration and dried under vacuum (0.093 g, 0.144 mmol, 89 %). ^1H NMR δ 7.25-7.10 (m, 6H, Ar), 6.75 (t, 1H, py), 6.33 (d, 2H, py), 6.04 (s, 5H, Cp), 4.78 (AB quartet, $^2J_{HH}$ = 20.2 Hz, 4H, NCH_2), 3.90 and 3.23 (sept, 2H each, CHMe$_2$), 1.53, 1.35, 1.32 and 0.92 (d, 6H each, CHMe_2). $^{13}C\{^1H\}$ NMR δ 161.50, 157.38, 145.12, 142.52, 137.61, 125.24, 124.77, 123.81, 116.56, 116.26 (Cp), 68.30, 28.70, 27.82, 27.67, 26.68, 24.04, 23.54. Anal. Calcd for $C_{36}H_{46}ClN_3Zr$: C, 66.78; H, 7.16; N, 6.49. Found: C, 66.98; H, 7.24; N, 6.35.

References on page 190

(BDEP)ZrCpCl (12b). The preparation of compound **12b** is identical to that of **12a**. Compound **3b** (0.100 g, 0.178 mmol) and NaCp•DME (0.040 g, 0.224 mmol) gave white crystalline **12b** (0.091 g, 0.154 mmol, 87 %). ^{1}H NMR δ 7.25-7.00 (m, 6H, Ar), 6.79 (t, 1H, py), 6.37 (d, 2H, py), 5.89 (s, 5H, Cp), 4.51 (AB quartet, $^{2}J_{HH}$ = 20.6 Hz, 4H, NCH_2), 3.05 and 2.49 (m, 4H each, CH_2Me), 1.39 and 1.08 (t, 6H each, CH_2*Me*). ^{13}C{^{1}H} NMR δ 161.48, 159.444, 140.21, 137.62, 137.50, 126.88, 126.11, 124.74, 116.85, 116.38 (Cp), 67.14, 24.59, 24.05, 15.88, 14.84.

(BDMP)ZrCpCl (12c). The preparation of compound **12c** is identical to that of **12a**. Compound **3c** (0.100 g, 0.198 mmol) and NaCp•DME (0.045 g, 0.253 mmol) gave white crystalline **12c** (0.093 g, 0.174 mmol, 88 %). ^{1}H NMR δ 7.15-6.98 (m, 6H, Ar), 6.83 (t, 1H, py), 6.38 (d, 2H, py), 5.88 (s, 5H, Cp), 4.45 (AB quartet, $^{2}J_{HH}$ = 20.9 Hz, 4H, NCH_2), 2.55 and 1.98 (s, 6H each, Me). ^{13}C{^{1}H} NMR δ 161.75, 159.36, 137.38, 134.89, 132.19, 129.33, 128.76, 124.35, 116.90, 116.43 (Cp), 65.39, 19.00, 18.75.

(BDPP)Zr(C_4H_6) (13a). To a diethylether (25 mL) suspension of compound **3a** (0.100 g, 0.162 mmol) was added 1.3 equiv of C_4H_6Mg•2THF (0.044 g, 0.198 mmol) at -20 °C. The suspension was stirred for 12h. The solvent was removed in *vacuo*. The resulting solid was extracted with toluene (3 x 10 mL) and filtered through Celite to give a bright-yellow solution. The solvent was removed in *vacuo*, the solid dissolved in a minimum amount of diethylether and cooled to -30 °C for 12 h. Yellow crystalline **13a** was isolated by filtration and dried under vacuum (0.093 g, 0.155 mmol, 96 %). ^{1}H NMR δ 7.15-7.00 (m, 2H, Ar), 6.98 (t, 1H, py), 6.57 (d, 1H, py), 6.49 (d, 1H, py), 5.07 (s, 2H, NCH_2), 5.03 (m, 2H, ZrCHCH_2), 4.72 (s, 2H, NCH_2), 4.00 (sept, 2H, C*H*Me$_2$), 3.56 (m, 2H, ZrCHCH_2), 3.08 (sept, 2H, C*H*Me$_2$), 2.38 (sept, 6H each, C*H*Me$_2$), 1.33, 1.23, 1.16 and 1.01 (d, 6H each, CH*Me*$_2$), 0.28 (m, 2H, ZrC*H*CH$_2$). ^{13}C{^{1}H} NMR δ 165.52, 164.58, 150.75, 149.92, 146.10, 143.78, 137.69, 125.21, 124.89, 124.31, 123.46, 119.35, 117.65, 117.20, 67.99, 67.73, 58.20, 28.48, 27.98, 27.78, 27.48, 24.33, 23.27.

References on page 190

(BDEP)Zr(C_4H_6) (13b). The preparation of compound **13b** is identical to that of **13a**. Compound **3b** (0.100 g, 0.178 mmol) and C_4H_6Mg•2THF (0.044 g, 0.198 mmol) gave yellow crystalline **13b** (0.083 g, 0.152 mmol, 85 %). ^{1}H NMR δ 7.15-7.00 (m, 2H, Ar), 6.97 (t, 1H, py), 6.59 (d, 1H, py), 6.51 (d, 1H, py), 4.92 (m, 2H, ZrCHCH_2), 4.83 (s, 2H, NCH_2), 4.47 (s, 2H, NCH_2), 3.41 (m, 2H, ZrCHCH_2), 2.97 (m, 4H, CH_2Me), 2.38 (m, 4H, CH_2Me), 1.24 and 1.11 (t, 6H each, CH_2Me), 0.16 (m, 2H, ZrCHCH_2). ^{13}C{^{1}H} NMR δ 165.64, 164.75, 140.95, 138.82, 137.58, 129.35, 126.39, 125.46, 124.72, 124.36, 119.64, 117.79, 117.34, 67.06, 66.57, 58.50, 23.66, 23.36, 15.73, 15.29.

(BDMP)Zr(C_4H_6) (13c). The preparation of compound **13c** is identical to that of **13a**. Compound **3c** (0.100 g, 0.198 mmol) and C_4H_6Mg•2THF (0.049 g, 0.249 mmol) gave yellow crystalline **13c** (0.093 g, 0.190 mmol, 96 %). ^{1}H NMR δ 7.15-6.80 (m, 2H, Ar), 6.91 (t, 1H, py), 6.62 (d, 1H, py), 6.52 (d, 1H, py), 4.98 (m, 2H, ZrCHCH_2), 4.47 (s, 2H, NCH_2), 4.36 (s, 2H, NCH_2), 3.42 (m, 2H, ZrCHCH_2), 2.39 and 1.95 (s, 6H each, Me), 0.17 (m, 2H, ZrCHCH_2). ^{13}C{^{1}H} NMR δ 165.69, 164.80, 153.40, 151.57, 137.47, 135.49, 133.38, 129.23, 128.24, 124.28, 123.94, 119.59, 117.76, 117.31, 65.31, 64.73, 58.54, 18.36.

(BDPP)Zr($C_6H_6Pr_2$) (14a). A benzene (10 mL) solution of compound **13a** (0.100 g, 0.17 mmol) and an excess of 4-octyne (0.050 g, 0.45 mmol) was heated to 90 °C for 12 hours. The solution changed from yellow to orange. The solvent was removed *in vacuo* and the resulting solid was recrystalize at -30 °C from a toluene/pentane mixture (10/50). White crystalline **14a** was isolated by filtration and dried under vaccum (0.098 g, 0.014 mmol, 84 %). ^{1}H NMR δ 7.25-7.10 (m, 6H, Ar), 7.00 (t, 1H, py), 6.55 (d, 2H, py), 5.35 (m, 1H, $ZrCH_2CH$=$CHCH_2$), 5.01 (AB quartet, $^2J_{HH}$ = 20.6 Hz, 2H NCH_2), 4.94 (AB quartet, $^2J_{HH}$ = 20.6 Hz, 2H, NCH_2), 4.42 (m, 1H, $ZrCH_2CH$=CHCH_2), 4.05 (sept, 1H, CHMe$_2$), 3.66 (m, 3H, CHMe$_2$), 3.12 (d, 2H, ZrCH$_2$CH=CHCH_2), 2.45 (dd, 1H, ZrCH_2CH=CHCH$_2$), 2.25 (m, 2H, CH_2CH$_2$CH$_3$), 2.1 (m, 2H, CH_2CH$_2$CH$_3$), 1.60 (m, 1H, ZrCH_2CH=CHCH$_2$), 1.60 (m, 2H, CH$_2$CH_2CH$_3$), 1.10-1.50 (8 doublets, 3H each, CHMe_2), 1.10-1.50 (buried, 2H, CH$_2$CH_2CH$_3$), 0.88 (t, 3H,

References on page 190

$CH_2CH_2CH_3$), 0.60 (t, 3H, $CH_2CH_2CH_3$). $^{13}C\{^1H\}$ NMR δ 187.97, 168.97, 163.87, 163.51, 148.38, 147.04, 146.43, 145.84, 145.72, 138.82, 137.91, 129.29, 126.28, 125.45, 124.62, 124.52, 124.38, 123.27, 119.23, 117.38, 117.31, 68.06, 67.66, 67.27, 42.23, 38.91, 34.83, 28.52, 28.44, 28.27, 28.20, 28.07, 27.87, 27.64, 27.35, 24.92, 24.27, 24.07, 23.96, 23.45, 23.25, 15.52, 15.40.

(BDPP)Zr($C_6H_7SiMe_3$) (15a). The preparation of compound **15a** is identical to that of complex **14a**. Compound **13a** (0.050 g, 0.09 mmol) and trimethylsilylacetylene (0.020 g, 0.20 mmol) gave white crystalline **15a** (0.046 g, 0.07 mmol, 79 %). ^1H NMR δ 8.02 (t, 1H, $C(SiMe_3)=CH$), 7.25-7.10 (m, 6H, Ar), 6.98 (d, 1H, py), 6.58 (d, 1H, py), 6.55 (d, 1H, py), 5.38 (m, 1H, $ZrCH_2CH=CHCH_2$), 5.03 (AB quartet, $^2J_{HH}$ = 20.6 Hz, 2H, NCH_2), 4.99 (AB quartet, $^2J_{HH}$ = 20.3 Hz, 2H, NCH_2), 4.78 (m, 1H, $ZrCH_2CH=CHCH_2$), 3.98 (sept, 1H, $CHMe_2$), 3.59 (sept, 1H, $CHMe_2$), 3.48 (m, 2H, $CHMe_2$), 3.02 (m, 2H, $ZrCH_2CH=CHCH_2$), 2.43 (dd, 1H, $ZrCH_2CH=CHCH_2$), 1.70 (dd, 1H, $ZrCH_2CH=CHCH_2$), 1.20-1.40 (6 doublets, 18H, $CHMe_2$), 1.09 (d, 3H, $CHMe_2$), 1.07 (d, 3H, $CHMe_2$), -0.03 (s, 9H, $SiMe_3$). $^{13}C\{^1H\}$ NMR δ 193.83, 172.22, 164.53, 164.04, 147.97, 147.35, 147.06, 146.67, 145.75, 145.55, 141.35, 138.22, 126.52, 125.73, 124.72, 124.58, 124.48, 123.94, 123.34, 117.61, 68.11, 67.52, 67.27, 42.84, 28.74, 28.61, 28.31, 28.25, 28.07, 27.22, 27.09, 23.88, 23.80, 23.21, 22.73, 1.42.

(BDPP)Zr(C_6H_9β-Bu) (16a). The preparation of compound **16a** is identical to that of complex **14a**. Compound **13a** (0.250 g, 0.43 mmol) and 1-hexene (0.100 g, 1.19 mmol) gave white crystalline **16a** (0.213 g, 0.31 mmol, 73 %). ^1H NMR δ 7.20-7.05 (m, 6H, Ar), 6.87 (t, 1H, py), 6.45 (d, 1H, py), 6.44 (d, 1H, py), 5.41 (m, 1H, $ZrCH_2CH=CHCH_2$), 4.80 (AB quartet, $^2J_{HH}$ = 19.8 Hz, 2H, NCH_2), 4.69 (AB quartet, $^2J_{HH}$ = 19.8 Hz, 2H, NCH_2), 3.80 (m, 3H, $CHMe_2$), 3.80 (m, 1H, $ZrCH_2CH=CHCH_2$), 3.38 (sept, 1H, $CHMe_2$), 3.17 (m, 1H, $ZrCH_2CHBu$), 2.93 (br d, 1H, $ZrCH_2CH=CHCH_2$), 2.51 (dd, 1H, $ZrCH_2CH=CHCH_2$) 2.17 (m, 1H, $ZrCH_2CH=CHCH_2$), 1.72 (m, 1H, $ZrCH_2CHBu$), 1.46 (m, 1H, $ZrCH_2CH=CHCH_2$),

References on page 190

1.28-1.43 (5 doublets, 15H, CH*Me*$_2$), 1.28-1.43 (buried, 6H, C*H*$_2$C*H*$_2$C*H*$_2$), 1.22 (d, 3H, CH*Me*$_2$), 1.08 (d, 3H, CH*Me*$_2$), 1.05 (d, 3H, CH*Me*$_2$), 0.92 (t, 3H, CH$_2$C*H*$_3$), 0.12 (t, 1H, ZrC*H*$_2$CHBu). ^{13}C{^{1}H} NMR δ 163.03, 162.82, 149.55, 148.22, 146.27, 145.90, 145.51, 137.76, 135.93, 125.79, 125.08, 124.45, 124.23, 123.86, 123.63, 120.48, 117.18, 67.19, 67.01, 66.51, 56.95, 54.10, 42.49, 41.37, 31.11, 29.50, 29.39, 28.03, 27.67, 27.54, 27.46, 26.96, 26.53, 24.80, 24.47, 24.04, 23.47, 14.51. Anal. Calcd for $C_{41}H_{59}N_3Zr$: C, 71.87; H, 8.68; N, 6.13. Found: C, 72.00; H, 8.80; N, 6.12.

(BDPP)ZrPr$_2$ (17a). To an hexanes (15 mL) suspension of complex **3a** (0.500 g, 0.809 mmol) was added 2.5 equiv of PrMgCl (1.01 mL, 2.00 M, 2.02 mmol) at -30 °C. The reaction was stired at room temperature for 12 hours. The solvent was removed under vaccum and the solid extracted with hexanes. The volume of the solution was reduce to 5 mL. The solution was cooled to -30 °C for 12 hours. White crystalline **17a** was isolated by filtration and dried under vaccum (0.369 g, 0.445 mmol, 55 %). ^{1}H NMR δ 7.25-7.10 (m, 6H, Ar), 6.87 (t, 1H, py), 6.41 (d, 2H, py), 4.95 (s, 4H, NC*H*$_2$), 3.90 (sept, 4H, C*H*Me$_2$), 1.46 (d, 12H, CH*Me*$_2$), 1.40 (m, 8H, C*H*$_2$C*H*$_2$Me), 1.28 (d, 12H, CH*Me*$_2$), 0.82 (t, 6H, CH$_2$CH$_2$*Me*). ^{13}C{^{1}H} NMR δ 163.09, 148.17, 146.50, 138.05, 129.29, 125.87, 124.19, 117.40, 67.43, 64.02, 28.13, 27.82, 27.43, 24.57, 20.26, 19.86. Anal. Calcd for $C_{37}H_{55}N_3Zr$: C, 70.20; H, 8.76; N, 6.64. Found: C, 70.46; H, 8.55; N, 6.47.

(BDPP)ZrBu$_2$ (18a). The preparation of complex **18a** is identical to that of **17a**. Complex **3a** (0.500 g, 0.809 mmol) and BuMgCl (1.01 mL, 2.00 M, 2.02 mmol) gave white crystalline **18a** (0.434 g, 0.656 mmol, 81 %). ^{1}H NMR δ 7.25-7.10 (m, 6H, Ar), 6.82(t, 1H, py), 6.36 (d, 2H, py), 4.90 (s, 4H, NC*H*$_2$), 3.83 (sept, 4H, C*H*Me$_2$), 1.40 (d, 12H, CH*Me*$_2$), 1.36 (buried, 4H, Bu), 1.22 (d, 12H, CH*Me*$_2$), 1.09 (m, 4H, Bu), 0.81 (m, 4H, Bu), 0.70 (t, 6H, Bu). ^{13}C{^{1}H} NMR δ 163.11, 148.29, 146.52, 138.11, 125.83, 124.20, 117.44, 67.42, 60.38, 28.61, 28.15, 27.48, 24.60, 14.14.

References on page 190

(iPAP)ZrEt$_2$ (19j). The preparation of complex **19j** is identical to that of **17a**. Complex **3j** (0.500 g, 1.670 mmol) and EtMgCl (1.69 mL, 2.00 M, 3.38 mmol) gave white crystalline **19j** (0.418 g, 1.134 mmol, 68 %). ^{1}H NMR δ 6.92 (t, 1H, py), 6.54 (d, 2H, py), 4.94 (sept, 2H, NC*H*Me$_2$), 4.47 (s, 4H, NC*H*$_2$), 1.61 (t, 4H, C*H*$_2$Me), 1.40 (d, 12H, NCH*Me*$_2$), 0.82 (q, 6H, CH$_2$*Me*). ^{13}C{^{1}H} NMR δ 165.11, 136.57, 117.28, 55.90, 46.89, 44.59, 22.26, 12.13.

(iPAP)ZrCl(^{i}Pr) (20j). To a dichloromethane solution of complex **3j** (1.000 g, 2.622 mmol) was added 1 equiv of ^{i}PrMgCl (1.31 mL, 2.00 M, 2.62 mmol) at -78 °C. The solution was allowed to warm up to room temperature and stired for 12 hours. The solvent was removed in *vacuo* . The resulting brown solid was extracted with toluene (3 x 15 mL) and filtered through Celite. The solvent was removed in *vacuo*. The solid was dissolved in a minimum ammount of diethylether and cooled to -30 °C for 12 hours. White crystalline **20j** was isolated by filtration and dried under vaccum (0.813 g, 1.670 mmol, 64 %). ^{1}H NMR δ 6.93 (t, 1H, py), 6.48 (d, 2H, py), 5.07 (sept, 2H, NC*H*Me$_2$), 4.32 (AB quartet, $^2J_{HH}$ = 20.4 Hz, 4H, NC*H*$_2$), 1.44(m, 6H, CH*Me*$_2$), 1.44 (m, 1H, C*H*Me$_2$), 1.35 (d, 6H, NCH*Me*$_2$), 1.27 (d, 6H, NCH*Me*$_2$). ^{13}C{^{1}H} NMR δ 165.01, 136.89, 117.40, 55.97, 55.64, 47.41, 21.83, 21.74, 21.29. Anal. Calcd for $C_{16}H_{28}N_3ZrCl$: C, 49.39; H, 7.25; N, 10.80. Found: C, 48.99; H, 7.35; N, 10.74.

(BDPP')ZrPr (21a). A benzene solution (15 mL) of complex **17a** (0.500 g, 0.790 mmol) was heated to 65 °C for 12 hours. The solvent was removed in *vacuo*. The resulting light yellow solid was extracted with pentane (3 x 50 mL) and filtered through Celite. The solvent was removed in *vacuo*. The solid was dissolved in a minium ammount of a 50:50 hexanes:diethylether solution and cooled to -30 °C for 24 hours. White crystalline **21a** was isolated by filtration and dried under vaccum (0.352 g, 0.598 mmol, 76 %). ^{1}H NMR δ 7.45-7.15 (m, 6H, Ar), 7.00 (t, 1H, py), 6.52 (d, 2H, py), 4.92 (AB quartet, $^2J_{HH}$ = 20.5 Hz, 2H, NC*H*$_2$), 4.90 (AB quartet, $^2J_{HH}$ = 20.6 Hz, 2H, NC*H*$_2$), 4.15 (sept, 1H, C*H*Me$_2$), 3.62 (sept, 1H, C*H*Me$_2$), 3.43 (br m, 1H, C*H*(Me)CH$_2$), 3.34 (sept, 1H, C*H*Me$_2$), 1.47 (d, 3H, CH*Me*$_2$), 1.35-1.45 (m, 11H, CH*Me*$_2$

References on page 190

and CH(*Me*)CH_2), 1.30 (d, 3H, CH*Me*$_2$), 1.20 (d, 3H, CH*Me*$_2$), 1.17 (d, 3H, CH*Me*$_2$), 0.89 (m, 2H, CH_2 Pr), 0.68 (t, 3H, CH_2CH_2*Me*), 0.44 (m, 2H, CH_2 Pr). $^{13}C\{^1H\}$ NMR δ 165.40, 164.15, 148.97, 148.08, 147.08, 146.12, 145.28, 138.01, 126.11, 125.84, 124.54, 124.17, 123.05, 117.77, 117.41, 67.70, 65.23, 63.88, 59.87, 37.90, 28.05, 27.88, 26.60, 26.42, 25.07, 24.30, 23.96, 20.03, 18.21. Anal. Calcd for $C_{34}H_{47}N_3Zr$: C, 69.34; H, 8.04; N, 7.13. Found: C, 69.52; H, 8.19; N, 6.99.

(BDPP')ZrBu (22a). The preparation of complex **22a** is identical to that of **21a**. Compound **18a** (0.500 g, 0.756 mmol) gave white crystalline **22a** (0.328 g, 0.544 mmol, 72 %). ^1H NMR δ 7.45-7.15 (m, 6H, Ar), 6.92 (t, 1H, py), 6.47 (d, 2H, py), 4.91 (AB quartet, $^2J_{HH}$ = 20.7 Hz, 2H, NC*H*$_2$), 4.89 (AB quartet, $^2J_{HH}$ = 20.6 Hz, 2H, NC*H*$_2$), 4.17 (sept, 1H, C*H*Me$_2$), 3.63 (sept, 1H, C*H*Me$_2$), 3.41 (br m, 1H, C*H*(Me)CH$_2$), 3.33 (sept, 1H, C*H*Me$_2$), 1.50 (d, 3H, CH*Me*$_2$), 1.43 (d, 3H, CH*Me*$_2$), 1.41 (d, 3H, CH*Me*$_2$), 1.39 (d, 3H, CH*Me*$_2$), 1.32 (d, 3H, CH*Me*$_2$), 1.21 (d, 3H, CH*Me*$_2$), 1.16 (d, 3H, CH*Me*$_2$), 1.00 (m, 2H, CH(Me)CH_2), 1.00 (m, 2H, CH_2 Bu), 0.66 (m, 2H, CH_2 Bu), 0.66 (t, 3H, $CH_2CH_2CH_2$*Me*), 0.38 (m, 2H, CH_2 Bu). $^{13}C\{^1H\}$ δ 165.50, 164.21, 149.13, 148.07, 147.06, 146.31, 145.27, 137.91, 126.06, 125.85, 124.52, 124.15, 123.03, 117.74, 117.37, 67.69, 65.22, 62.92, 56.14, 38.00, 28.34, 28.05, 27.92, 27.88, 27.81, 26.62, 26.54, 26.43, 25.00, 24.26, 23.91, 14.32.

[(BDPP)Zr(CH_2Ph)]$^+$[PhCH_2B(C_6F_5)$_3$]$^-$ (23a). A C_6D_6 solution of complex **6a** (0.050 g, 0.069 mmol) was added to solid B(C_6F_5)$_3$ (0.035 g, 0.068 mmol) at 23 °C. The solution was allowed to react for 30 minutes. ^1H NMR δ 7.20-6.90 (m, 6H, ph), 6.75 (t, 2H, meta ZrCH$_2$*Ph*), 6.70 (t, 1H, py), 6.25 (d, 2H, ortho BCH$_2$*Ph*), 6.58 (t, 1H, para ZrCH$_2$*Ph*), 6.38 (d, 2H, ortho ZrCH$_2$*Ph*), 6.27 (t, 1H, para BCH$_2$*Ph*), 6.13 (d, 2H, py), 6.04 (t, 2H, meta BCH$_2$*Ph*), 4.33 (AB quartet, 4H, NC*H*$_2$), 3.57 (br m, 2H, BC*H*$_2$Ph), 3.20 (sept, 2H, C*H*Me$_2$), 2.59 (sept, 2H, C*H*Me$_2$), 2.40 (s, 2H, ZrC*H*$_2$Ph), 1.43 (d, 6H, CH*Me*$_2$), 1.14 (d, 6H, CH*Me*$_2$), 1.04 (d, 6H, CH*Me*$_2$), 0.61 (d, 6H, CH*Me*$_2$).

References on page 190

(BDPP)Zr(HN*t*-Bu)Me (24a). An hexane solution of *t*-BuNH$_2$ (1.73 mL, 1.00 M, 1.73 mmol) was added to an hexanes suspension (10 mL) of complex **5a** (1.000 g, 1.733 mmol). The reaction mixture was stired at room temperature for 12 hours. The solution was filtered to remove any insoluble impurities. The solvent was removed under vaccum to afford white crystalline **24a** (0.987 g, 1.557 mmol, 90 %). ^{1}H NMR δ 7.25-7.10 (m, 6H, Ar), 6.85 (t, 1H, py), 6.42 (d, 2H, py), 4.92 (AB quartet, $^2J_{HH}$ = 20.4 Hz, 4H, NC*H*$_2$), 4.21 (sept, 2H, C*H*Me$_2$), 3.98 (br s, 2H, N*H*), 3.48 (sept, 2H, C*H*Me$_2$), 1.57 (d, 6H, CH*Me*$_2$), 1.42 (d, 6H, CH*Me*$_2$), 1.37 (d, 6H, CH*Me*$_2$), 1.13 (d, 6H, CH*Me*$_2$), 0.77 (s, 9H, C*Me*$_3$), 0.63 (s, 3H, Zr*Me*). ^{13}C{^{1}H} NMR δ 163.02, 150.26, 146.93, 144.78, 125.45, 124.24, 124.20, 117.37, 66.92, 54.45, 28.50, 27.70, 27.37, 26.91, 24.70, 24.60, 14.60. Anal. Calcd for $C_{36}H_{54}N_4Zr \cdot C_6H_{14}$: C, 70.04; H, 9.52; N, 7.78. Found: C, 69.73; H, 9.04; N, 7.63.

(BDPP')Zr(HN*t*-Bu) (25a). A benzene solution (25 mL) of complex **24a** (0.500 g, 0.789 mmol) was heated to 80 °C in a glass bomb for 12 hours. The solvent was removed *in vacuo*. The resulting white solid was dissolved in a minimum ammount of pentane and cooled to -30 °C for 24 hours. White crystalline **25a** was isolated by filtration and dried under vaccum (0.315 g, 0.510 mmol, 65 %) (quantitative by ^{1}H NMR spectrsocopy). ^{1}H NMR δ 7.40-7.10 (m, 6H, Ar), 6.92 (t, 1H, py), 6.47 (d, 1H, py), 6.43 (d, 1H, py), 4.92 (AB quartet, $^2J_{HH}$ = 20.5 Hz, 2H, NC*H*$_2$), 4.79 (AB quartet, $^2J_{HH}$ = 20.5 Hz, 2H, NC*H*$_2$), 4.15 (sept, 1H, C*H*Me$_2$), 4.02 (s, 1H, N*H*), 3.57 (sept, 1H, C*H*Me$_2$), 3.42 (m, 1H, C*H*(Me)CH$_2$), 3.17 (sept, 1H, C*H*Me$_2$), 1.52 (d, 3H, CH*Me*$_2$), 1.47 (d, 3H, CH*Me*$_2$), 1.40 (buried, 2H, CH(Me)C*H*$_2$), 1.37 (d, 3H, CH*Me*$_2$), 1.34 (d, 3H, CH*Me*$_2$), 1.26 (d, 3H, CH*Me*$_2$), 1.24 (d, 3H, CH*Me*$_2$), 1.16 (d, 3H, CH*Me*$_2$), 0.81 (s, 9H, N'*Bu*). ^{13}C{^{1}H} NMR δ 165.89, 163.82, 149.73, 148.83, 147.61, 146.83, 146.41, 144.56, 137.81, 125.60, 124.79, 124.33, 124.06, 12.56, 117.52, 117.23, 67.96, 65.40, 57.55, 54.21, 38.18, 33.99, 27.95, 27.86, 27.57, 27.09, 26.87, 26.75, 26.57, 25.02, 24.75, 24.42, 24.12. Anal. Calcd for $C_{36}H_{54}N_4Zr \cdot C_5H_{12}$: C, 69.61; H, 9.05; N, 8.12. Found: C, 69.39; H, 8.89; N, 7.66.

References on page 190

Molecular Orbital Calculations. All molecular orbital calculations were performed on a CAChe Worksystem, a product developed by Tektronix. The parameters used for the Extended Hückel calculations of the pyridine diamide model (restricted to C_{2v} symmetry) were taken from the literature[143]and are listed in the Appendix. The bond lengths and angles were taken from the X-ray crystal structure analysis of (BDEP)$ZrMe_2$ (**5b**) (*vide infra*). The Cartesian coordinates, a full list of the eigenvalues and symmetry labels for the model can be found in the Appendix.

Ethylene polymerization. The solvents (heptane, toluene) and 1-hexene were freshly distilled from Na/K before use. In a glovebox, a 500 mL stirred reactor was charged with the desired amounts of solvent, cocatalyst and comonomer. The metal complex was suspended in heptane (0.5 mL). The suspension was then transferred to a catalyst addition device and the reactor sealed. The reactor was purged with ethylene and heated to 60 °C. The catalyst was injected and the reactor pressurized to 100 psi with ethylene. The polymerization was allowed to proceed for the desired time and the solution was quenched with 15 mL of a 1.0 M HCl/MeOH solution. The polymer was filtered off, washed with water and acetone, and dried to constant weight at 100 °C.

X-ray Crystallographic Analysis of complex 5b. A suitable crystal of **5b** was grown from a saturated ether solution at -30 °C. Crystal data may be found in the appendix. Data were collected on a Siemens P4 diffractometer with the XSCANS software package[144]. The Laue symmetry 2/m was determined by merging symmetry equivalent positions. A total of 5706 data were collected in the range of θ = 1.77-25.0° ($-1 \le h \le 14$, $-1 \le k \le 18$, $-18 \le l \le 17$). Three standard reflections monitored at the end of every 297 reflection collected showed no decay of the crystal. The data processing, solution and refinement were done using *SHELXTL-PC* programs[145]. The faces of the crystal were indexed and the distance between them measured for a Gaussian absorption correction on the data. During the least-squares cycles, the isotropic temperature factor for methyl groups C(19) and C(29) were relatively high, 0.15 and 0.13,

References on page 190

respectively. Attempts to model the disorder did not yield satisfactory results. Anisotropic thermal parameters were refined for all non-hydrogen atoms except the carbons in the two phenyl rings. The phenyl and pyridine were restrained to have two-fold symmetry. The C-Me distances were restrained to be equal using the option SADI. Some hydrogen atoms were observed in the least-squares cycles, however, no attempt was made to locate them. All hydrogen atoms were placed in calculated positions. In the final difference Fourier synthesis the electron density fluctuates in the range 0.891 to -0.421 e $Å^3$.

X-ray Crystallographic Analysis of complex 5k. Unit-cell parameters were calculated from reflections obtained from 60 data frames collected at different sections of the Ewald sphere. The systematic absences in the diffraction data and the determined unit-cell parameters were uniquely consistent for the reported space group. Semi-empirical absorption correction, based on redundant data at varying effective azimuthal angles, was applied to the data.

All non-hydrogen atoms were refined with anisotropic displacement coefficients. All hydrogen atoms were treated as idealized contributions.

The structure was solved by direct methods, completed by subsequent Fourier syntheses and refined with full-matrix least-squares methods. All scattering factors and anomalous dispersion coefficients are contained in the SHELCTL 5.03 program library[146].

X-ray Crystallographic Analysis of complex 6a. Air-sensitive, yellow needle-like crystals were grown from a mixture of dichloromethane an cyclohexane. A preliminary examination of several crystals indicated that they were poorly diffracting and twinned. A cut-crystal with the dimension 0.35 x 0.30 x 0.15 mm, mounted inside a Lindemann capillary tube and flame sealed, was found suitable and used for the data collection. The X-ray diffraction experiments were carried out on a Siemens P4 diffractometer with XSCANS software package[144] using graphite monochromated Mo Kα radiation at 25 °C. The cell constants were obtained by centering 21 reflections ($9.2 \leq 2\theta \leq 24.9°$). The Laue symmetry 2/m was determined

References on page 190

by merging symmetry equivalent reflections. A total of 3654 data ware collected in the δ range 1.880 - 21.0 ° (-12≤h≤0, 0≤k≤20, -13≤l≤14) in ω scab mode at variable scan speed (2-30 deg.min). Background measurements were made at the ends of the scan range each for 0.5% of total scan time. Three standard reflections monitored at the end of every 297 reflection collection indicated that the crystal was decaying. At the end of 2δ = 42°, the crystal decay was 26.3 % and therefore data collection was stopped. The data processing, solution and refinements were done using SHELXTL PC programs[145]. No absorption was applied to the data (μ = 0.311 mm^{-1}). Due to low data-to-parameter ration (6.3:1), only Zr(1) was refined anisotropically. Individual isotropic thermal parameters were refined for the rest of the non-hydrogen atoms. The four phenyl groups were treated as regular hexagons and ideal geometry was imposed on all the 2-propyl groups using DFIX (C–C = 1.542 Å and C...C = 1.633 x d(C–C)). No attempt was made to locate the hydrogen atoms. However all the hydrogen atoms were placed in the calculated position. In the final least-squares refinement cycle on F, the model converged to R= 0.0972, wR = 0.1077 and Goof = 1.62 for 989 observations with Fo≥4σ (Fo) and 156 parameters. In the final difference Fourier synthesis the electron density fluctuates in the range 0.46 to -0.48 e $Å^3$. There were no shifts in the final cycles.

X-ray Crystallographic Analysis of complex 13a. Unit-cell parameters were calculated from reflections obtained from 60 data frames collected at different sections of the Ewald sphere. The systematic absences in the diffraction data and the determined unit-cell parameters are consistent for space groups I42d and $I4_1md$. Although both space groups were explored, only the solution in I42d yielded chemically reasonable and computationally stable results. No absorption corrections were required (μ = 3.36 cm^{-1}).

The compound molecule is located on a two-fold axis with the conjugated diene disordered with a 50/50 site occupation distribution. The diene ligand was refined as a flat, rigid body with chemically equivalent bonds restrained to be equal. A cocrystallized, partially occupied, ether solvent molecule was located severely disordered at a four-fold rotoinversion axis with a net

References on page 190

compound to solvent occupancy ratio of 1:0.35. The flack parameter refined to 0.0(2) indicating that the true hand of the data was correctly determined. The distorted conjugated diene and solvent molecule were refined isotropically without hydrogen atoms. All non-hydrogen undistorted atoms were refined with anisotropic displacement coefficients. All hydrogen groups were treated as idealized contributions except those on the disordered groups which were ignored. The largest remaining features in the final electron density map are located 0.8 Å near the zirconium atom and were considered as artifacts arising from less than ideal absorption corrections.

The structure was solved by direct methods, completed by subsequent Fourier syntheses and refined with full-matrix least-squares methods. All scattering factors and anomalous dispersion coefficients are contained in the SHELXTL 5.03 program library[146].

References on page 190

5 References

(1) Bradley, D. C.; Thomas, I. M. *Chemical Society London. Proceedings* **1959**, 225.

(2) Bradley, D. C.; Thomas, I. M. *J. Chem. Soc.* **1960**, 3857.

(3) Bradley, D. C.; Gitlitz, M. H. *J. Chem. Soc. (A)* **1969**, 980.

(4) Gibbins, S. G.; Lappert, M. F.; Pedley, J. B.; Sharp, G. J. *J. Chem. Soc., Dalton Trans.* **1975**, 72.

(5) Airoldi, C.; Bradley, D. C. *Inorg. Nucl. Chem. Letters* **1975**, *11*, 155.

(6) Chandra, G.; Lappert, M. F. *J. Chem. Soc. (A)* **1968**, 1940.

(7) Chandra, G.; George, T. A.; Lappert, M. F. *J. Chem. Soc., Chem. Commun.* **1967**, 687.

(8) Airoldi, C.; Bradley, D. C.; Chudzynska, H.; Hursthouse, M. B.; Malik, K. M. A.; Raithby, P. R. *J. Chem. Soc., Dalton Trans.* **1980**, 2010.

(9) Andersen, R. A. *Inorg. Chem.* **1979**, *18*, 1724.

(10) Bürger, H.; Wiegel, K. *Z. Anorg. Allg. Chem.* **1976**, *426*, 301.

(11) Bürger, H.; Schlingmann, M.; Pawelke, V. *Z. Anorg. Chem.* **1976**, *419*, 116, 121.

(12) Ziegler, K.; Holzkamp, E.; Breil, H.; Martin, H. *Angew. Chem.* **1955**, *67*, 541.

(13) Ziegler, K. *Angew. Chem.* **1964**, *76*, 545.

(14) Natta, G.; Corradini, P. *Atti Accad. naz. Lincei Mem. Cl. Sci. Fis. Mat. Nat. Sez. II* **1955**, *5*, 73.

(15) Natta, G. *Angew. Chem.* **1956**, *68*, 393.

(16) Natta, G. *Angew. Chem.* **1964**, *76*, 553.

(17) Natta, G.; Pino, P.; Massanti, G.; Giannini, U. *J. Am. Chem. Soc.* **1957**, *79*, 2975.

(18) Natta, G.; Pino, P.; Mazzanti, G.; Giannini, U.; Mantica, E.; Peraldo, M. *Chim. Ind. (Paris)* **1957**, *39*, 19.

(19) Breslow, D. S.; Newburg, N. R. *J. Am. Chem. Soc.* **1957**, *79*, 5072.

(20) Breslow, D. S. *US Pat. Appl. 537039*; Breslow, D. S., Ed., 1955.

(21) Jordan, R. F. *Advances in Organometallic Chemistry* **1991**, *32*, 325.

References on page 190

(22) Jordan, R. F. *J. Chem. Educ.* **1988**, *65*, 285.

(23) Jordan, R. F.; Dasher, W. E.; Echols, S. F. *J. Am. Chem. Soc.* **1986**, *108*, 1718.

(24) Jordan, R. F.; Bajgur, C. S.; Willet, R.; Scott, B. *J. Am. Chem. Soc.* **1986**, *107*, 7410.

(25) Jordan, R. F.; Lapointe, R. E.; Bajgur, C. S.; Echols, S. F.; Willet, R. *J. Am. Chem. Soc.* **1987**, *109*, 4111.

(26) Jordan, R. F.; Bajgur, C. S.; Dasher, W. E.; Rheingold, A. L. *Organometallics* **1987**, *6*, 1041.

(27) Jordan, R. F.; Lapointe, R. E.; Bradley, P. K.; Baenziger, N. *Organometallics* **1989**, *8*, 2892.

(28) Jordan, R. F.; Bradley, P. K.; Lapointe, R. E.; Taylor, D. F. *New J. Chem.* **1990**, *14*, 505.

(29) Jordan, R. F.; Bradley, P. K.; Baensiger, N. C.; Lapointe, R. E. *J. Am. Chem. Soc.* **1990**, *112*, 1289.

(30) Jordan, R. F.; Lapointe, R. E.; Baenziger, N.; Hinch, G. D. *Organometallics* **1990**, *9*, 1539.

(31) Crowther, D. J.; Borkowsky, S. L.; Swenson, D.; Meyer, T. Y.; Jordan, R. F. *Organometallics* **1993**, *12*, 2897.

(32) Bochmann, M.; WIlson, L. M.; Hursthouse, M. B.; Short, R. L. *J. Chem. Soc., Chem. Commun.* **1986**, 1610.

(33) Bochmann, M.; Wilson, L. M.; Hursthouse, M. B.; Short, R. L. *Organometallics* **1987**, *6*, 2556.

(34) Bochmann, M.; Wilson, L. M.; Hursthouse, M. B.; Motevalli, M. *Organometallics* **1988**, *7*, 1148.

(35) Bochmann, M.; Jaggar, A. J.; Nicholls, J. C. *Angew. Chem.* **1990**, *102*, 830.

(36) Bochmann, M.; Jaggar, A. J.; Nicholls, J. C. *Angew. Chem., Int. Ed. Engl.* **1990**, *29*, 780.

References on page 190

(37) Bochmann, M.; Jaggar, A. J. *J. Organomet. Chem.* **1992**, *424*, C5.

(38) Bochmann, M.; Lancaster, S. J. *J. Organomet. Chem.* **1992**, *434*, C1.

(39) Eshuis, J. J. W.; Tan, Y. Y.; Teuben, J. H. *J. Mol. Catal.* **1990**, *62*, 277.

(40) Eshuis, J. J. W.; Tan, Y. Y.; Meetsma, A.; Teuben, J. H.; Renkema, J.; Evens, G. G. *Organometallics* **1992**, *11*, 362.

(41) Taube, R.; Krukowka, L. *J. Organomet. Chem.* **1988**, *347*, C9.

(42) Hlatky, G. G.; Turner, H. W.; eckman, R. R. *J. Am. Chem. Soc.* **1989**, *111*, 2728.

(43) Hlatky, G. G.; eckman, R. R.; Turner, H. W. *Organometallics* **1992**, *11*, 1413.

(44) Patat, F.; Sinn, H. *Angew. Chem.* **1958**, *70*, 496.

(45) Collins, S.; Kuntz, B. A.; Taylor, N. J.; Ward, D. G. *J. Organomet. Chem.* **1988**, *342*, 21.

(46) Ewen, J. A. *J. Am. Chem. Soc.* **1984**, *106*, 6355.

(47) Wild, F. R. W. P.; Zsolnai, L.; Huttner, G.; Brintzinger, H. H. *J. Organomet. Chem.* **1982**, *232*, 233.

(48) Wild, F. R. W. P.; Wasiucionek, M.; Huttner, G.; Brintzinger, H. H. *J. Organomet. Chem.* **1985**, *288*, 63.

(49) Waymouth, R. M.; Bangerter, F.; Pino, P. *Inorg. Chem.* **1988**, *27*, 758.

(50) Collins, S.; Gauthier, W. J.; Holden, D. A.; kuntz, B. A.; Taylor, N. J.; Ward, D. G. *Organometallics* **1991**, *10*, 2061.

(51) Grossman, R. B.; Doyle, R. A.; Buchwald, S. L. *Organometallics* **1991**, *10*, 1501.

(52) Piemontesi, F.; Camurati, I.; Resconi, L.; Balboni, D.; Sironi, A.; Moret, M.; Zeigle, R.; Piccolrovazzi, N. *Organometallics* **1995**, *14*, 1256.

(53) Diamond, G. M.; Rodewald, S.; Jordan, R. F. *Organometallics* **1995**, *14*, 5.

(54) Bochmann, A.; Lancaster, S. J. *Angew. Chem., Int. Ed. Engl.* **1994**, *33*, 1634.

(55) Mengele, W.; Diebold, J.; Troll, C.; Röll, W.; Brintzinger, H.-H. *Organometallics* **1993**, *12*, 1931-1935.

References on page 190

(56) Brintzinger, H. H.; Fischer, D.; Mülhaupt, R.; Rieger, B.; Waymouth, R. M. *Angew. Chem., Int. Ed. Engl.* **1995**, *34*, 1143.

(57) Kaminsky, W.; Külper, K.; Brintzinger, H. H.; Wild, F. R. W. P. *Angew. Chem.* **1985**, *95*, 507.

(58) Kaminsky, W.; Kulper, K.; Brintzinger, H. H.; Wild, F. R. W. P. *Angew. Chem., Int. Ed. Engl.* **1985**, *24*, 507.

(59) Razavi, A.; Atwood, J. L. *J. Am. Chem. Soc.* **1993**, *115*, 7529.

(60) Razavi, A.; Thewalt, U. *J. Organomet. Chem.* **1993**, *445*, 111.

(61) Razavi, A.; Ferrara, J. *jomv* **1992**, *435*, 299.

(62) Waymouth, R. M.; Coates, G. R. *Science* **1995**, *267*, 222.

(63) Ewen, J. A.; Elder, M. J.; jones, R. L.; Haspeslagh, L.; Atwood, J. L.; Bott, S. G.; Robinson, K. *Makromol. Chem. Macromol. Symp.* **1991**, *48/49*, 253.

(64) Ewen, J. A.; Elder, M. J.; Jones, R. L.; Curtis, S.; CHeng, H. N. *Stud. Surf. Sci. Catal.* **1990**, *56*, 439.

(65) Ewen, J. A.; Jones, R. L.; Razavi, A. *J. Am. Chem. Soc.* **1988**, *110*, 6255.

(66) Mislow, K.; Raban, M. *Stereoisomeric Relationships of Groups in Molecultes*; Mislow, K.; Raban, M., Ed., 1967, pp 1-38.

(67) Ewen, J. A.; Elder, M. J.; Jones, R. L.; Haspeslagh, L.; Atwood, J. L.; Bott, S. G.; Robinson, K. *Makromol. Chem. Macromol. Symp.* **1991**, *48/49*, 253.

(68) Ewen, J. A.; Elder, M. J. *Eur. Pat. Apppl. EP-A - 537130*; Ewen, J. A.; Elder, M. J., Ed., 1993.

(69) Zambelli, A.; Grassi, A.; Galimberti, M.; Mazzocchi, R.; Piemontesi, F. *Makromol. Chem. Rapid. Commun.* **1991**, *12*, 253.

(70) Busico, V.; Mevo, L.; Palumbo, G.; Zambelli, A. *Makromol. Chem.* **1983**, *184*, 2193.

(71) Canich, J. A. ; Canich, J. A., Ed., European Patent Application EP-420-436-A1; Vol. April 4, 1991.

References on page 190

(72) Canich, J. A.; Turner, H. W. ; Canich, J. A.; Turner, H. W., Ed., W. PCT Int. Appl. WO 92/12162; Vol. filing date December 26, 1991.

(73) Stevens, J. C.; Timmers, F. J.; Wilson, D. R.; Schmidt, G. F.; Nickias, P. N.; Rosen, R. K.; Knight, G. W.; Lai, S. Y. *Constrained Geometry Addition Polymerization Catalysts*; Stevens, J. C.; Timmers, F. J.; Wilson, D. R.; Schmidt, G. F.; Nickias, P. N.; Rosen, R. K.; Knight, G. W.; Lai, S. Y., Ed.; (Dow) European Patent Application EP-416-815-A2, March 13,1991.

(74) Shapiro, P. J.; Bunel, E.; Schaefer, W. P.; Bercaw, J. E. *Organometallics* **1990**, *9*, 867.

(75) Okuda, J.; Schattenmann, F. J.; Wocadlo, S.; Massa, W. *Organometallics* **1995**, *14*, 789.

(76) van der Linden, A.; Schaverien, C. J.; Meijboom, N.; Ganter, C.; Orpen, A. G. *J. Am. Chem. Soc.* **1995**, *117*, 3008.

(77) Haeg, M. E.; Whitlock, B. J.; Whitlock Jr., H. W. *J. Am. Chem. Soc.* **1989**, *111*, 692.

(78) Calculations were performed using CAChe Scientific software by Tektronix.

(79) Mu, Y.; Piers, W. E.; MacGillivray, L. R.; Zaworotko, M. J. *Polyhedron* **1995**, *14*, 1.

(80) Andersen, R. A. *Inorganic Chemistry* **1979**, *18*, 2928.

(81) Warren, T. H.; Schrock, R. R.; Davis, W. M. *Organometallics* **1996**, *15*, 562.

(82) Anderson, H. H. *J. Am. Chem. Soc.* **1953**, *75*, 1576.

(83) Cummins, C. C.; Baxter, S. M.; Wolczanski, P. T. *J. Am. Chem. Soc.* **1988**, *110*, 8731.

(84) Hughes, A. K.; Meetsma, A.; Teuben, J. A. *Organometallics* **1993**, *12*, 1936.

(85) Alcock, N. M.; Pierce-Butler, M.; Willey, G. R. *J. Chem. Soc., Chem. Commun.* **1974**, 627.

(86) Bai, Y.; Roesky, H. W.; Noltemeyer, M.; Witt, M. *Chem. Ber.* **1992**, *125*, 825.

(87) Cummins, C. C.; Duyne, G. D. V.; Schaller, C. P.; Wolczanski, P. T. *Organometallics* **1991**, *10*, 164.

(88) Planalp, R. P.; Andersen, R. A.; Zalkin, A. *Organometallics* **1983**, *2*, 16.

References on page 190

(89) Hunter, W. E.; Hrncir, D. C.; Bynum, V.; Penttila, R. A.; Atwood, J. L. *Organometallics* **1983**, *2*, 750.

(90) Lauher, J. W.; Hoffmann, R. *J. Am. Chem. Soc.* **1976**, *98*, 1729.

(91) Nugent, W. A.; Haymore, B. L. *Coord. Chem. Rev.* **1980**, *31*, 123.

(92) Cummins, C. C.; Baxter, S. M.; Wolczanski, P. T. *J. Am. Chem. Soc.* **1988**, *110*, 8733.

(93) Rocklage, S. M.; Schrock, R. R.; Churchill, M. R.; Wasserman, J. H. *Organometallics* **1982**, *1*, 1332.

(94) Edwards, D. S.; Schrock, R. R. *J. Am. Chem. Soc.* **1982**, *104*, 6806.

(95) Scholz, J. *Chem. Ber.* **1987**, *120*, 1369.

(96) Jordan, R. F.; LaPointe, R. E.; Bajgur, C. S.; Echols, S. F.; Willett, R. *J. Am. Chem. Soc.* **1987**, *109*, 4111.

(97) Bochmann, M.; Lancaster, S. J. *Organometallics* **1993**, *12*, 633.

(98) Latesky, S. L.; McMullen, A. K.; Niccolai, G. P.; Rothwell, I. P.; Huffman, J. C. *Organometallics* **1985**, *4*, 902.

(99) Fachinetti, G.; Floriani, C. *jsccc* **1972**, 654.

(100) Massey, A. G.; Park, A. J. *J. Organomet. Chem.* **1964**, *2*, 245.

(101) Scholz, J.; Rehbaum, F.; Thiele, K. H.; Goddard, R.; Betz, P.; Kruger, C. J. *J. Organomet. Chem.* **1993**, *443*, 93.

(102) Jordan, R. F.; Lapointe, R. E.; Baenziger, N.; Hinch, G. D. *Organometallics* **1990**, *9*, 1539.

(103) Bochmann, M.; Karger, G.; Jagger, A. J. *J. Chem. Soc., Chem. Commun.* **1990**, 1038.

(104) Pellecchia, C.; Immirzi, A.; Grassi, A.; Zambelli, A. *Organometallics* **1993**, *12*, 4473.

(105) Pellecchia, C.; Grassi, A.; Immirzi, A. *J. Am. Chem. Soc.* **1993**, *15*, 1160.

(106) Etievant, P.; Gautheron, B.; Tainturier, G. *Bull. Soc., Chim. Fr.* **1978**, *II*, 292.

(107) Jeffery, J.; Lappert, M. F.; Luong-Thi, N. T.; Webb, M.; Atwood, J. L.; Hunter, W. E. *J. Chem. Soc., Dalton Trans.* **1981**, 1593.

References on page 190

(108) Schock, L. E.; Brock, C. P.; Marks, T. J. *Organometallics* **1987**, *6*, 232.

(109) Samuel, E.; Rausch, M. D. *J. Am. Chem. Soc.* **1973**, *95*, 6263.

(110) Chaudari, M.; Stone, F. G. A. *J. Chem. Soc. (A)* **1966**, 838.

(111) Erker, G. *J. Organomet. Chem.* **1977**, *134*, 189.

(112) Erker, G.; Krüger, C.; Müller, G. *Adv. Organomet. Chem.* **1985**, *24*, 1.

(113) Yasuda, H.; Tatsumi, K.; Nakamura, A. *Acc. Chem. Res.* **1985**, *18*, 120.

(114) Yasuda, H.; Kajihara, Y.; Mashima, K.; Lee, K.; Nakamura, A. *Chem. Lett.* **1981**, 519.

(115) Erker, G.; Engel, K.; Krüger, C.; Chiang, A.-P. *Chem. Ber.* **1982**, *115*, 3311.

(116) Lubke, B.; Edelmann, F.; Behrens, U. *Chem. Ber.* **1983**, *116*.

(117) Yasuda, H.; Kajihara, Y.; Mashima, K.; Nagasuma, K.; Lee, Y.; Nakamura, A. *Organometallics* **1982**, *1*, 388.

(118) Krüger, C.; Müller, G.; Erker, G. *Organometallics* **1985**, *4*, 215.

(119) Dorf, U.; Engel, K.; Erker, G. *Organometallics* **1982**, *2*, 462.

(120) Kai, Y.; Kanehisa, N.; Miki, K.; Kasai, N.; Akita, M.; Yasuda, H.; Nakamura, A. *Bull. Chem. Soc. Jpn.* **1983**, *56*, 3735.

(121) Yasuda, H.; Kajihara, Y.; Nagasuna, K.; Mashima, K.; Nakamura, A. *Chem. Lett.* **1980**, 719.

(122) Erker, G.; Engle, K.; Dorf, U.; Atwood, J. L.; Hunter, W. E. *Angew. Chem., Int. Ed. Engl.* **1982**, *21*, 914.

(123) Kai, Y.; Kanehiso, N.; Miki, K.; Kasai, N.; Mashima, K.; Nagasuma, K.; Yasuda, H.; Nakamura, A. *Chem. Lett.* **1982**, 1979.

(124) Erker, G.; Berg, K.; Krüger, C.; Müler, G.; Angermund, K.; Benn, R.; Schroth, G. *Angew. Chem., Int. Ed. Engl.* **1984**, *23*, 455.

(125) Temme, B.; Karl, J.; Erker, G. *Chem. Eur. J.* **1996**, *2*, 919.

(126) Dioumaev, V. K.; Harrod, J. F. *Organometallics* **1997**, *16*, 1452.

References on page 190

(127) Schrock, R. R.; Shih, K. Y.; Dobbs, D. A.; Davis, W. M. *J. Am. Chem. Soc.* **1995**, *117*, 6609.

(128) Wengrovius, J. H.; Schrock, R. R. *J. Organomet. Chem.* **1981**, *205*, 319.

(129) Hartner, F. W. J.; Schwartz, J.; Clift, S. M. *J. Am. Chem. Soc.* **1983**, *105*, 640.

(130) Fryzuk, M.; Mao, S. S. H.; Zaworotko, M. J.; MacGillivray, L. R. *J. Am. Chem. Soc.* **1993**, *115*, 5336.

(131) McClure *NMR Spectroscopy Techniques*; 2nd ed.; Marcel Dekker In.: New York, 1996; Vol. 21.

(132) Lambert, J. B.; Shurvell, H. F.; Lightner, D.; Cooks, R. G. *Introduction to Organic Spectroscopy*; Macmillan Publishing Company: New York, 1987.

(133) Diamond, G. M.; Jordan, R. F.; Petersen, J. L. *Organometallics* **1996**, *15*, 4045.

(134) Gutekunst, G.; Brook, A. G. *J. Organomet. Chem.* **1982**, *225*, 1.

(135) *Unpublished results.*

(136) Kaminsky, W.; Bark, A.; Steiger, R. *J. Mol. Catal.* **1992**, *74*, 109.

(137) Kaminsky, W.; Steiger, R. *Polyhedron* **1988**, *7*, 2375.

(138) Siedle, A. R.; Hanggi, B.; Newmark, R. A.; Mann, K. R.; Wilson, T. *Synthetic, Structural and Industrial Aspects of Stereospecific Polymerization*; Siedle, A. R.; Hanggi, B.; Newmark, R. A.; Mann, K. R.; Wilson, T., Ed., 1995, pp 89.

(139) Ewen, J. A.; Elder, M. J. *Stabilisation of cationic alkyl using AlR3*; Ewen, J. A.; Elder, M. J., Ed.; Eur. Pat. Appl. 426637, 426638, 1991.

(140) Vizzini, J. C.; Chien, J. C. W.; Babu, G. N.; Newmark, R. A. *J. Polym. Sci. A, Polym. Chem.* **1994**, *32*, 2049.

(141) Herfert, N.; Fink, G. *Makromol. Chem.* **1992**, *193*, 773.

(142) Longo, P.; Olivia, L.; Grassi, A.; Pellechia, C. *Makromol. Chem.* **1989**, *190*, 2357.

(143) Hoffmann, R. *J. Chem. Phys.* **1963**, *39*, 1397.

(144) *XSCANS*; Siemens Analytical X-Ray Instruments Inc.: Madison, 1990.

References on page 190

(145) Sheldrick, G. M. *SHELXTL-PC*; V4.1 ed.; Sheldrick, G. M., Ed.; Siemens Analytical X-Ray Instruments Inc.: Madison, WI, U.S.A., 1990.

(146) Sheldrick, G. M. *SHELXL-93*; Sheldrick, G. M., Ed.; Institute fuer Anorg. Chemie: Goettingen, Germany, 1993.

References on page 190

"What differentiates man from other animals is perhaps feeling rather than reason. I have seen a cat reason more often than laugh or weep. Perhaps it laughs or weeps within itself - but then perhaps within itself a crab solves equations of the second degree."

Miguel De Unamuno

Chapter Three. Tantalum Complexes

1 Introduction

1.1 Generalities

There are many homoleptic Ta^{V} amide complexes known {$Ta(NR_2)_5$; R = Me[1-3], Et[4], Pr[2], Bu[2]; $Ta(NMeBu)_5$[2]}. On the other hand, very few tetra-amide complexes of tantalum have been reported[5] {e.g., $Ta(NMeBu)_4$[2]}. This is in contrast to the behavior of niobium(V) which upon addition of $LiNR_2$ gives products which contain increasing proportions of Nb^{IV} as the size of the dialkylamido group is increased. The dearth of Ta^{IV} derivatives may be due to the relative instability of the +4 oxidation state for Ta. Thus $Ta(NMe_2)_5$ is readily obtained from $TaCl_5$ and $LiNMe_2$ but the sterically demanding Ta^{V} amide complexes, $Ta(NR_2)_5$ (R = Et, Pr, Bu), decompose rapidly to the Ta^{V} imide complexes $Ta(NR_2)_3(=NR)$ upon heating[2,6]. It is believed that the first step in the decomposition of $M(NR_2)_5$ (M = Nb, Ta) derivatives is the same in both cases; reductive elimination of a dialkylamino radical and formation of a Nb^{IV} or Ta^{IV} species. In the case of niobium a relatively stable tetrakis(dialkylamido)niobium(IV) complex is produced. However, in the case of tantalum, the tetravalent $Ta(NR_2)_4$ is unstable and reacts with the R_2N radical to produce $RN{=}Ta(NR_2)_3$, R_2NH and olefin (Scheme 3- 1).

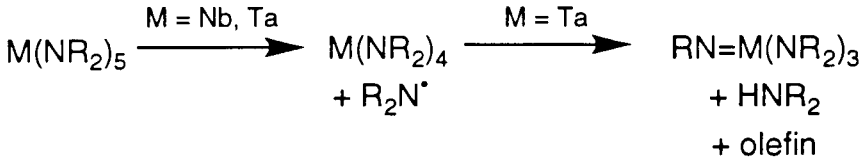

Scheme 3- 1. Nb(IV) vs Ta(IV) amide complexes

Heteroleptic amide complexes of tantalum are also known. Base-free pentacoordinated complexes such as $F_4Ta(NEt_2)$ or $F_3Ta(NR_2)_2$ or the hexacoordinated solvate complexes $F_4Ta(NEt_2)$•py or $F_3Ta(NEt_2)_2$•py have been synthesized[7].

References start on page 238

1.2 Alkyne polymerization

Certain group 5[8-11] metal complexes are active catalysts for the polymerization and cyclization of alkynes. Two mechanisms have been proposed for the polymerization of alkynes. The first one appears to proceed by way of insertion, similar to ethylene polymerization[12] (Scheme 3- 2), to give an alkenyl propagating species.

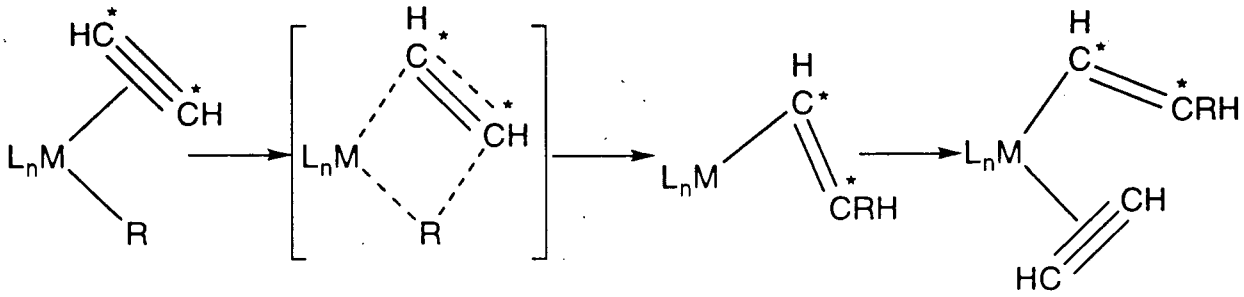

Scheme 3- 2. Polymerization of alkynes, insertion mechanism

The second mechanism proceeds via an alkylidene complex (Scheme 3- 3).

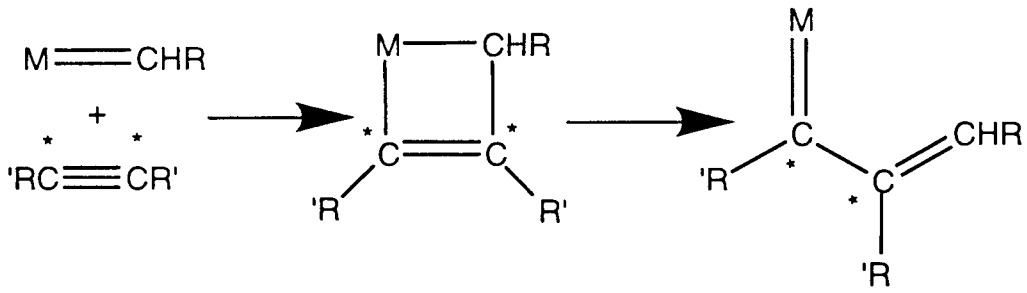

Scheme 3- 3. Polymerization of alkynes, alkylidene mechanism

A clear distinction can be drawn between these two mechanisms. Scheme 3- 2 predicts that the two carbons of a given monomer (C*) unit will end up doubly bonded to one another in the resulting polymer. According to the mechanism in Scheme 3- 3 these same carbons will be connected by a single bond. Through the use of ^{13}C NMR spectroscopy, it was confirmed that the polymer formed with the $MoCl_5/Ph_4Sn$ system contains labeled carbons joined by C–C single

References start on page 238

bonds consistent with the alkylidene mechanism. In contrast, the titanium-based catalyst $Ti(OBu)_4/Et_3Al$ gives a polymer in which labeled carbons are separated by C=C double bonds as expected for an insertion-type mechanism[13-15].

Metal alkyl complexes with a formal d^2 configuration are known to insert alkynes, however, the alkenyl complexes are typically reluctant to engage in further insertions. For example, the d^2 η^2-alkyne complex $Tp^*NbCl(CH_2CH_3)(\eta^2\text{-}PhC{\equiv}CCH_2CH_3)$ (Tp^* = hydrotris(3,5-dimethyl-pyrazolyl)borate) readily inserts the coordinated alkyne $PhC{\equiv}CCH_2CH_3$, but stops short of inserting additional alkyne.[16] Precursor complexes of the type $L_nTa(\eta^2\text{-}RC{\equiv}CR)X$ (**A**, X = alkyl, hydride, or halide),[17] where the metal is formally in the +3 oxidation state, are ideally suited for studying the insertion mechanism. The formation of metallacyclopentadiene complexes resulting from the coupling of alkynes impedes the coordination insertion process making the choice of ancillary ligand system (L_n) for complexes of type **A** critical. For instance, η^2-alkyne complexes are obtained with bis(cyclopentadienyl) templates (e.g., $Cp_2Ta(\eta^2\text{-}RC{\equiv}CR)X$)[18-26] and mono(pentamethylcyclopentadienyl) ligation (e.g., $Cp^*Ta(\eta^2\text{-}RC{\equiv}CR)X_2$)[27-29], while less coordinatively saturating alkoxide ligands yield metallacycles (e.g., $(DIPP)_3Ta(C_4Et_4)$, DIPP = 2,6-diisopropylphenoxide)[30,31]. Interestingly, the reduction of $(DIPP)_2TaCl_3$ in the presence of bis(trimethylsilyl)acetylene affords the η^2-alkyne complex $(DIPP)_2ClTa(\eta^2\text{-}Me_3SiC{\equiv}CSiMe_3)$[32].

References start on page 238

2 Results and Discussion

2.1 Pyridine diamide complexes of tantalum

The silylated diamines **1a-e** react with $TaCl_5$ to form the corresponding trichloride complexes (**2a-e**) (eq. 1). The elimination of $ClSiMe_3$ provides the necessary driving force for the reaction and was detected by ^1H NMR spectroscopy.

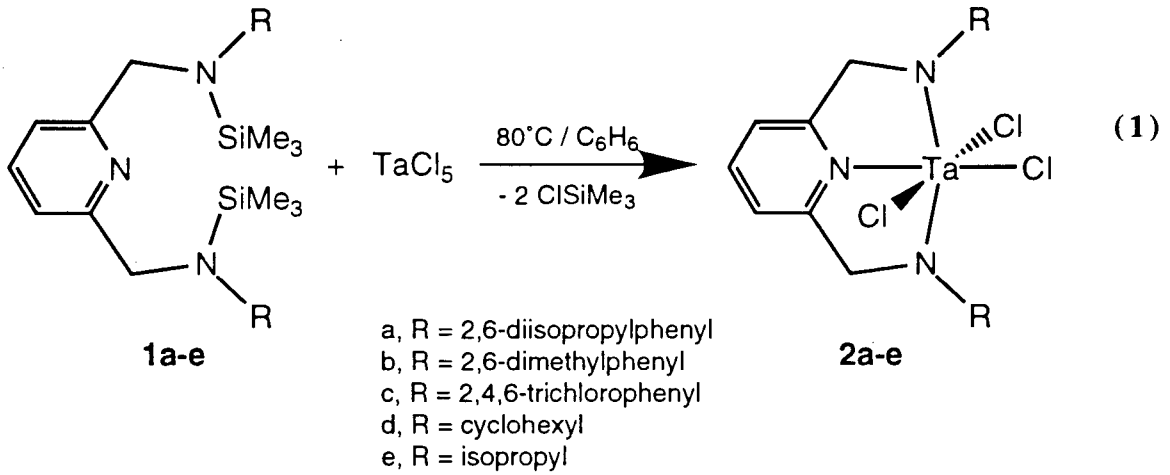

1a-e

a, R = 2,6-diisopropylphenyl
b, R = 2,6-dimethylphenyl
c, R = 2,4,6-trichlorophenyl
d, R = cyclohexyl
e, R = isopropyl

2a-e

(1)

The ^1H NMR spectrum of complex **2a** displays a singlet at 5.84 ppm for the methylene (CH_2N) protons of the ligand, consistent with the C_{2v} symmetry and meridional conformation of the ligand. A facial coordination of the ligand would yield a complex with C_s symmetry and the methylene (CH_2N) protons would appear as an AB pattern. Compound **2a** also displays diastereotopic isopropyl methyl groups. This inequivalence has been interpreted as a consequence of restricted rotation around the N-aryl C_{ipso} bond. The proton NMR spectrum of compound **2a** remains unchanged at 80°C. Similarly, the ^1H NMR spectra of complexes **2b-e** display a singlet for the ligand methylene protons (CH_2N) at approximately 5.8 ppm.

Compounds **2a-c** can be alkylated with 3 equivalents of MeMgBr or MeLi to give the trimethyl derivatives **3a-c** (eq. 2).

References start on page 238

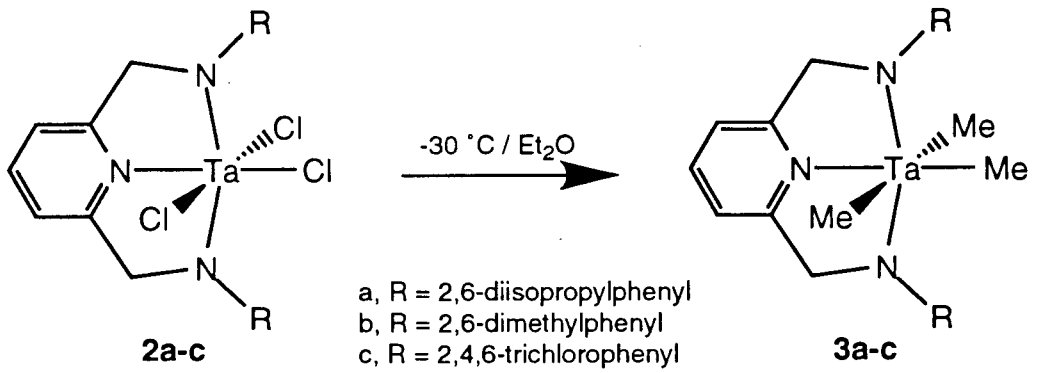

(2)

The ^{1}H NMR spectra of complexes **3a-c** show two different Ta-Me groups, one trans to the pyridine ring of the ligand and two cis. The C_{2v} symmetry and the restricted rotation of the N-aryl C_{ipso} bond observed with complex **2a** are retained upon alkylation.

Other metathetical reactions involving larger alkylating reagents (i.e., $PhCH_2MgCl$ and Me_3SiCH_2Li) yield intractable materials. Certain Ta(V) or Nb(V) complexes which contain at least two neopentyl groups are known to eliminate neopentane, affording neopentylidene complexes, by a process called α-hydrogen abstraction[33-37]. In a similar way, Ta(V) and Nb(V) complexes that contain two or more Me_3SiCH_2[38,39] and $PhCH_2$[36,37,40-42] groups also yield alkylidene complexes. However, unlike neopentylidene complexes, benzylidene and trimethylsilylmethylidene compounds are often unstable and decompose under the reaction conditions. The monocyclopentadienyl complex $Ta(\eta^5\text{-}C_5H_5)(CHCMe_3)Cl_2$[34,37] and the dicyclopentadienyl derivative $Ta(\eta^5\text{-}C_5H_5)_2(CHCMe_3)Cl$[37] are amongst the best studied examples. A similar type of reaction is proposed to account for the difficulties associated with the synthesis of the tris(benzyl) and tris(trimethylsilylmethyl) complexes (Scheme 3- 4). The α-hydrogen transfer can take place between two adjacent alkyl groups to give the alkylidene alkyl complex (Scheme 3- 4, i). Another possible pathway involves α-hydrogen transfer to one of the amide groups to give an alkylidene dialkyl complex with a partly protonated ligand moiety (Scheme 3- 4, ii). The same reaction can then take place a second time to completely protonate the ligand and to give a potentially unstable dialkylidene alkyl complex.

References start on page 238

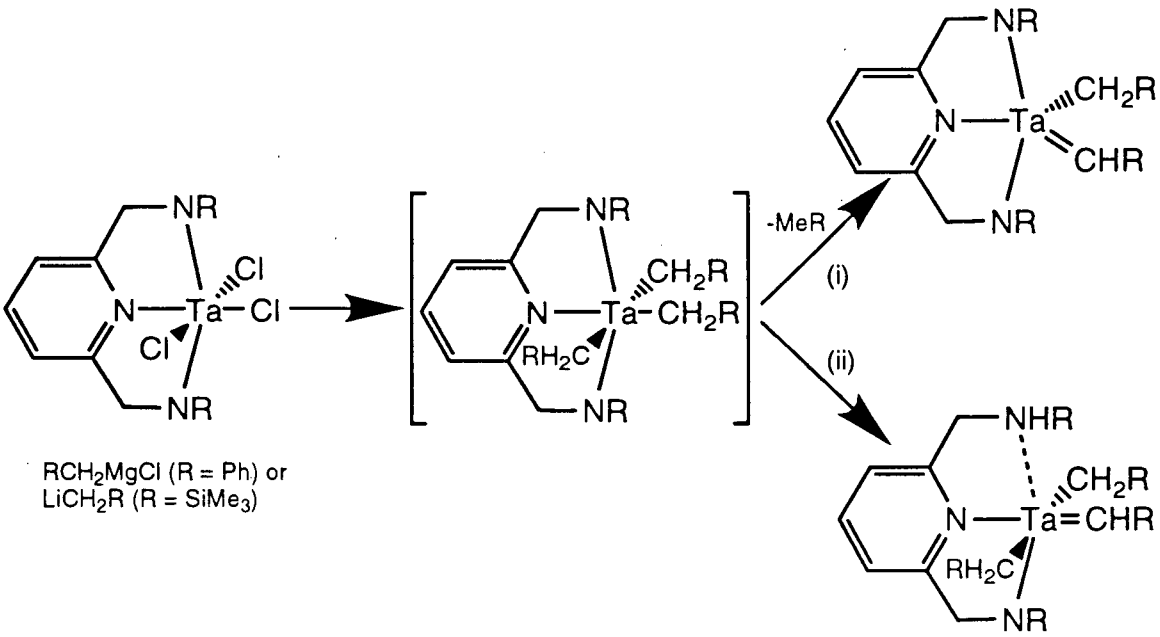

Scheme 3- 4. Alkylidene formation

2.2 Reduction chemistry of pyridine diamide complexes of tantalum

The two-electron reduction of the trichloride complexes **2a,b,d,e** with excess Na/Hg (1% or 2%) in the presence of alkynes affords the pseudo 5-coordinate Ta(III) derivatives (Scheme 3-5).

A single low-field (δ ca. 238 ppm) acetylenic carbon resonance is observed in the $^{13}C\{^{1}H\}$ NMR spectra of complexes **4a,b, 7a,b** and **8a**, suggesting that the alkyne is acting as 4-electron donor[43-45]. The three main orbital interactions involved in the overall bonding are described in Figure 3- 1.

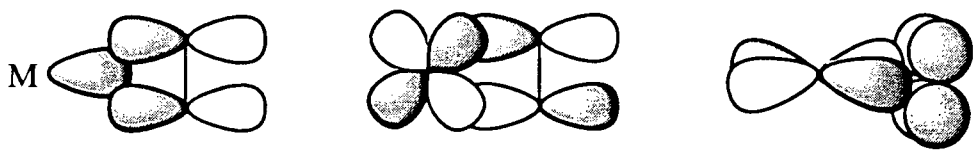

Figure 3- 1. 4 e⁻ interaction of an alkyne with a metal

References start on page 238

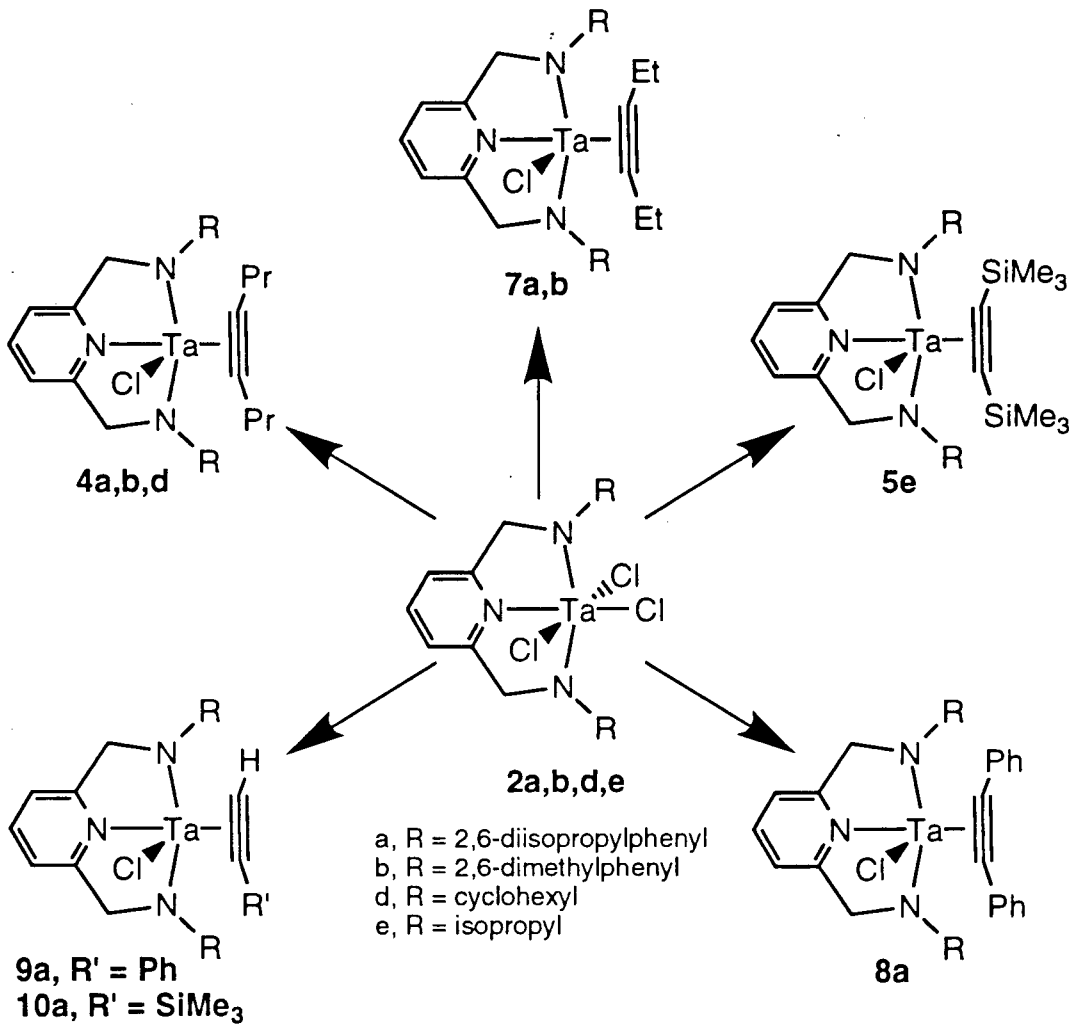

Scheme 3- 5. Reduction of the trichloride complexes 2a,b,d,e

The methylene protons of the ligand (CH_2N) appear as an AB quartet in the ^1H NMR spectra of the η^2-alkyne complexes. This indicates asymmetry about the N_3-plane of the ligand. As a result of the C_s symmetry and the restricted rotation around the N-aryl C_{ipso} bond two isopropyl methine and four isopropyl methyl resonances are observed in the proton and carbon NMR spectra of complexes **4a, 7a, 8a, 9a and 10a.**

Free rotation of the alkyne on the NMR timescale in complexes **4a,b, 7a,b** and **8a** is advanced since both ends of the coordinated alkynes are equivalent by ^1H and $^{13}C\{^1H\}$ NMR

References start on page 238

spectroscopy. This process equilibrates the diastereotopic ethyl methylene protons in (BDPP)TaCl(η^2-EtC≡CEt) and causes them to appear as a quartet in the proton NMR spectrum. It is not possible to determine by spectroscopic means if the alkyne is freely rotating in complexes **9a** and **10a.**

Interestingly, the presence of two acetylenic resonances in the $^{13}C\{^1H\}$ spectra of complexes **4d** and **5e** indicates that the rotation of the alkyne is inhibited. This is attributed to the different steric requirements of the alkyl ligands compared to the 2,6-disubstituted aryl ligands. The 2,6-substituted phenyl rings in the BDPP and BDMP ligands block both faces of the N_3 plane and create a protective "pocket" trans to the pyridine and rotation of the alkyne located trans to the pyridine is not restricted (Figure 3- 2, I). On the other hand, rotation of the alkyne in complexes **4d** and **5e** results in strong steric interactions with the alkyl groups of the ligand (Figure 3- 2, II). Consequently, rotation of the alkyne is restricted and two signals are observed for the acetylenic carbons in the $^{13}C\{^1H\}$ NMR spectra.

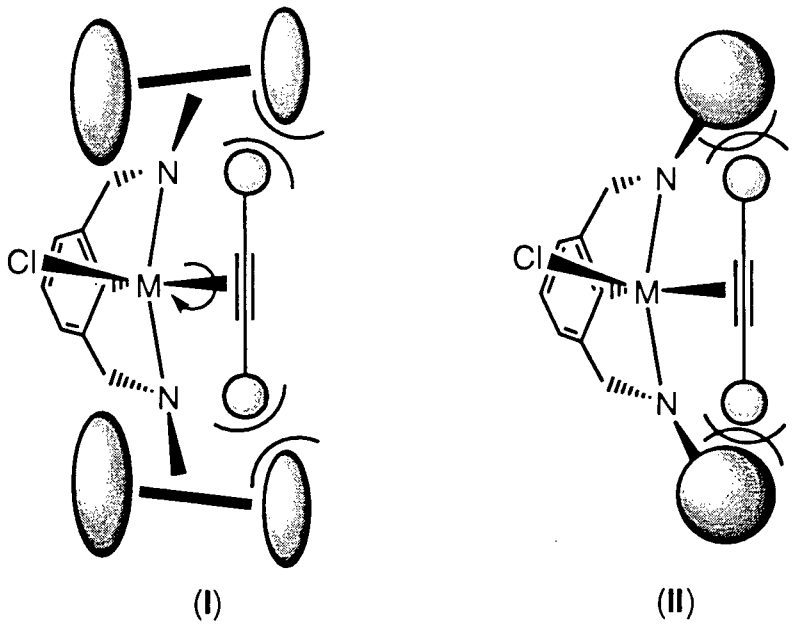

Figure 3- 2. Alkyl vs 2,6-substitutedphenyl ligands

References start on page 238

2.3 Metallocene vs pyridine diamide tantalum alkyne complexes

It is interesting to compare metallocene-based and pyridine diamide tantalum alkyne complexes. The similarities between the frontier orbitals of the Cp_2M fragment and the PyN_3M fragment have been discussed in detail in Chapter 2. Complexes of the type $Cp_2MX(\eta^2\text{-alkyne})$ (M = Nb, Ta; Cp = η^5-C_5H_5[21-26], η^5-C_5H_4Me[20], η^5-$C_5H_4{}^iPr$[18]; X = H, alkyl, halide) are known and display high-field η^2-alkyne carbon resonances (*C*≡*C*, 140 ppm) characteristic of an alkyne behaving as a two-electron donor[43-45]. In contrast, the η^2-alkyne (*C*≡*C*) carbons are observed at ca. 240 ppm in complexes **4a,b, 7a,b** and **8a**. The difference in electron donating ability of the two ancillary ligand systems may explain the marked difference in ^{13}C chemical shift. The pyridine diamide ligand can be viewed as an electron deficient cyclopentadienyl equivalent donating 8-electrons to the metal centre compare to 12-electrons for two Cp ligands. As a result, the formal electron count for the d^2-fragment PyN_3TaCl is 12 while the d^2-Cp_2TaCl is formally a 16-electron fragment. The more electrophilic metal bearing the pyridine diamide ligand can therefore accept more electron density from the alkyne, hence a higher chemical shift is observed for the η^2-alkyne carbons (*C*≡*C*). Comparatively, the low-field $^{13}C_{alkyne}$ resonance (ca. 220 ppm) observed for the mono(cyclopentadienyl) complexes $(\eta^5\text{-}C_5Me_5)MCl_2(RC{\equiv}CR)$[28,46] is consistent with the alkyne acting as a 4-electron ligand and the 12 electron count of the d^2-$CpTaCl_2$ fragment.

The steric requirements of the pyridine alkyl-amide ligands are comparable to those observed with the metallocene ancillary ligands. For example, the ^1H NMR spectrum of $Cp_2TaEt(MeC{\equiv}CH)$[26] suggests the structure indicated in Figure 3- 3 in which the alkyne C≡C bond lies in the same plane as the Ta atom and the ethyl group. Restricted rotation about the Ta–(η^2-C≡C) bond was confirmed by the presence two η^2-propyne methyl resonances (exo, 2.91 ppm; endo, 2.74). This is similar to the behavior observed with complexes **4d** and **5e** and two low-field acetylenic resonances are obtained in the ^{13}C NMR spectrum.

References start on page 238

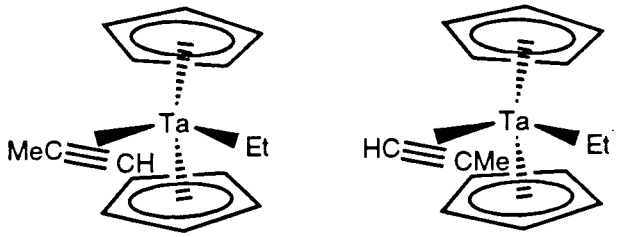

exo endo

Figure 3- 3. exo and endo conformation of $Cp_2TaEt(MeC{\equiv}CH)$

2.4 Crystal structure of (BDPP)Ta(η^2-PrC≡CPr)Cl

Yellow single crystals of (BDPP)Ta(η^2-PrC≡CPr)Cl (**4a**) suitable for an X-ray analysis were grown from a saturated ether solution at -30°C. The molecular structure of complex **4a** is shown in Figure 3- 4, and selected bond distances and angles are given in Table 3- 1. The complete crystallographic data can be found in the Appendix.

Table 3- 1. Selected Bond Distances (Å) and Angles (deg) for 4a

Bond Distances			
Ta(1) - N(1)	2.053 (6)	Ta(1) - C(32)	2.062 (7)
Ta(1) - N(3)	2.033 (6)	Ta(1) - C(36)	2.085 (7)
Ta(1) - N(2)	2.255 (6)	C(32) - C(36)	1.287 (11)
Ta(1) - Cl(1)	2.361 (2)	Acet* - Ta	1.97
Bond Angles			
N(3) - Ta(1) - N(1)	137.2 (2)	C(36) - C(32) - C(33)	132.6 (8)
N(2) - Ta(1) - Cl(1)	93.7 (2)	C(32) - C(36) - C(37)	137.2 (8)

Acet* = midpoint of C(32) - C(36)

The geometry around the Ta centre can be best described as a distorted square pyramid with the three nitrogen atoms of the ligand and the midpoint of the alkyne forming the base of the square pyramid and the chloride {Cl(1)} occupying the apical position.

References start on page 238

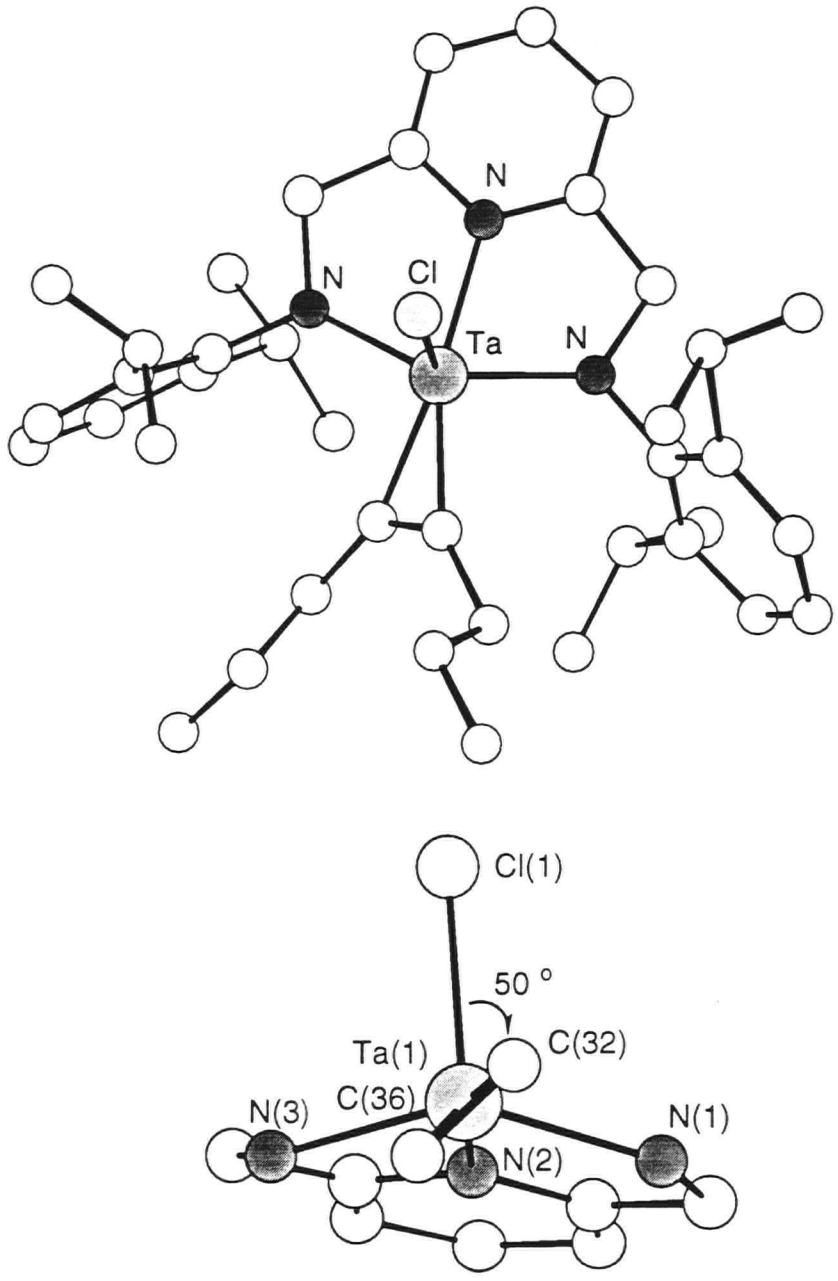

*Figure 3- 4. Molecular structure of (BDPP)Ta(Ta(η^2-PrC≡CPr)Cl (**4a**) deduced from single crystal X-ray analysis*

References start on page 238

The 4-octyne unit is located trans to the pyridine of the BDPP ligand and is rotated by 50° with respect to the Cl(1)-Ta(1)-N(2) plane (Figure 3- 4). The bond distances in the Ta-alkyne moiety are comparable to those reported for other mononuclear Ta(III) alkyne complexes[29,31,47]. Each amide nitrogen is sp^2-hybridized as evidenced by the sum of the angles about each nitrogen {N(1) = 359.5° and N(3) = 359.9°}.

The reduction of complex **2a** in the presence of the terminal alkynes PhC≡CH and $Me_3SiC{\equiv}CH$ affords the η^2-alkyne complexes **9a** and **10a**, respectively. Complexes **9a** and **10a** necessarily display two low-field acetylenic resonances in the $^{13}C\{^1H\}$ NMR spectra. The ^1H NMR spectra of complexes **9a** (Figure 3- 5) and **10a** display low-field resonances for the coordinated η^2–*H*C≡CR. The AB quartet observed for the ligand methylene protons (NCH_2) as well as the two isopropyl methine and for isopropyl methyl signals are consistent with C_s symmetry and restricted rotation about the 2,6-diisopropylphenyl–nitrogen bond. The ^1H NMR spectrum of the hydrolysis (D_2O) products of compound **9a** is consistent with a formal metallacyclopropene Ta^V species (eq. 3).

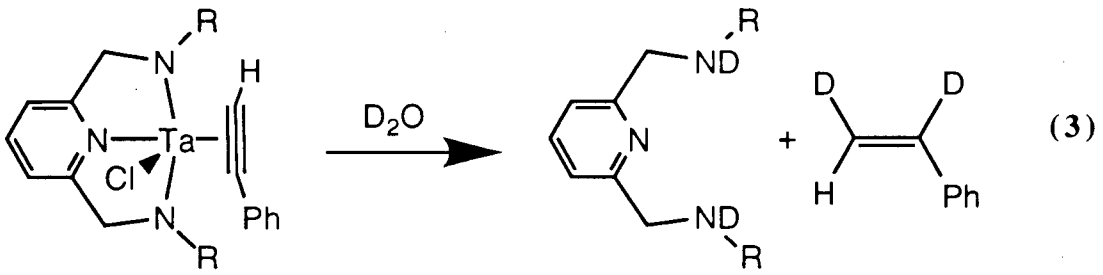

(3)

References start on page 238

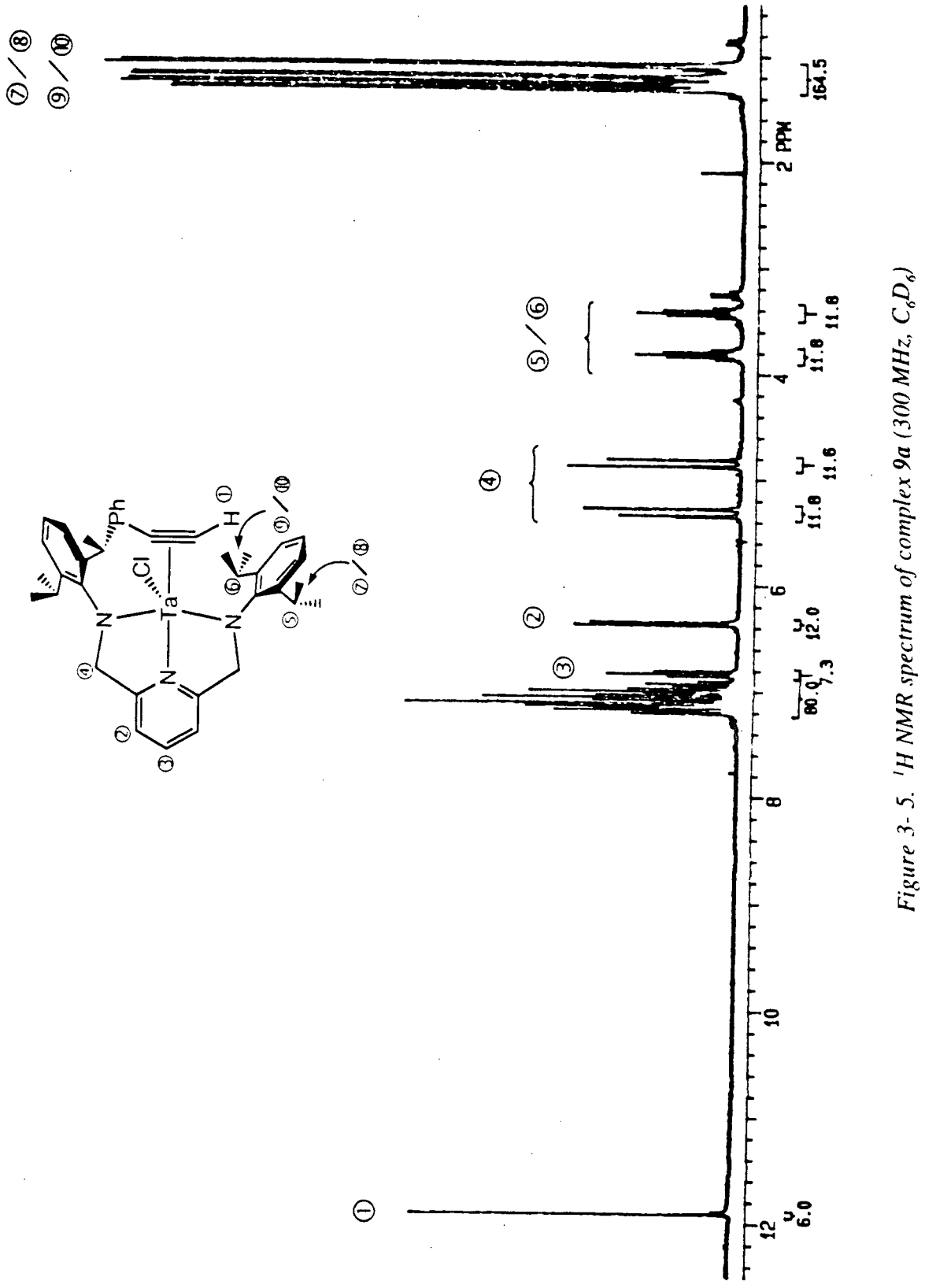

*Figure 3- 5. ^1H NMR spectrum of complex **9a** (300 MHz, C_6D_6)*

References start on page 238

Interestingly, the reduction of complex **2e** in the presence of an excess of the terminal acetylene $Me_3SiC{\equiv}CH$ affords the metallacyclopentadiene alkynyl complex (iPAP)Ta{$C_4\alpha$-α'$(Me_3Si)_2H_2$}($C{\equiv}CSiMe_3$) (**6e**) (eq. 4). The α,α' substitution pattern for the metallacycle is proposed based on the two low-field doublets (①/②) observed in the ^1H NMR spectrum of complex **6e** (Figure 3- 6). Moreover, the presence of three distinct $SiMe_3$ in the ^1H and $^{13}C\{^1H\}$ NMR spectra in consistent with the proposed structure. The alkynyl fragment is formed via the metathesis of one of the chloride with $NaC{\equiv}CSiMe_3$. It has already been reported that Na and other alkali metals react with acetylene to give $NaC{\equiv}CH$[48].

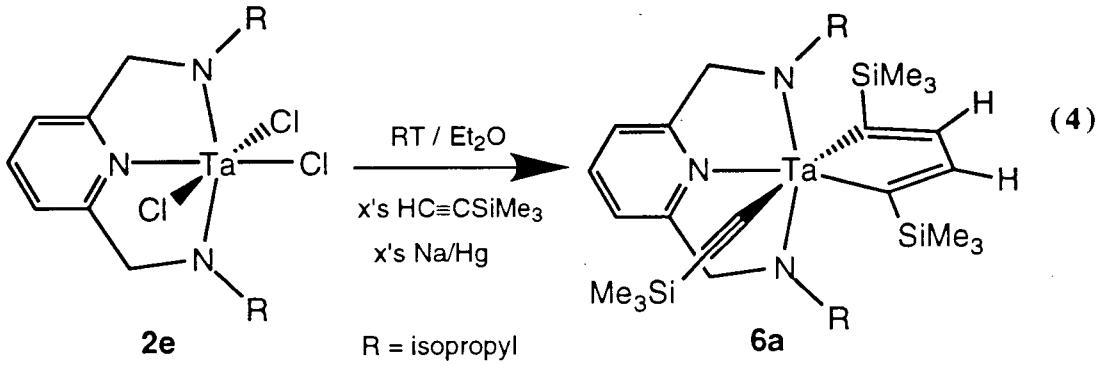

(4)

In contrast, compounds **4a,b,d, 7a,b, 8-10a** show no evidence of metallacycle formation even under forcing conditions (excess alkyne, 110 °C). Furthermore, the coordinated alkynes do not exchange with free alkyne. For example, no reaction occurs between compound **4a** and 50 equivalents of phenylacetylene at 80 °C.

References start on page 238

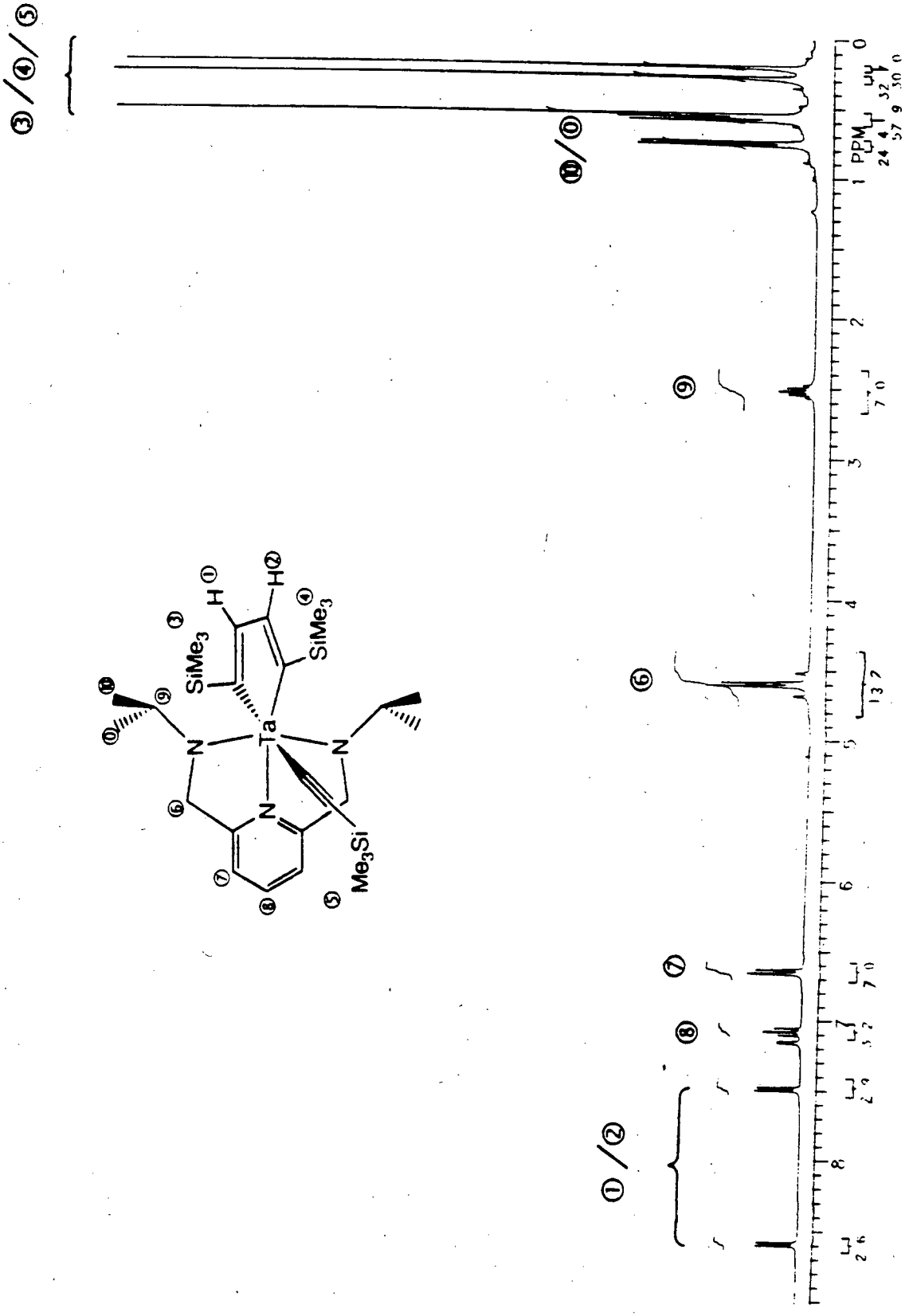

Figure 3- 6. ^1H NMR spectrum of complex 6e (300 MHz, C_6D_6)

References start on page 238

2.5 Reactivity of the η^2-alkyne complexes

Complex **4a** can be alkylated with 1 equivalent of MeMgBr to give (BDPP)Ta(η^2-PrC≡CPr)Me (**5**) (eq. 5).

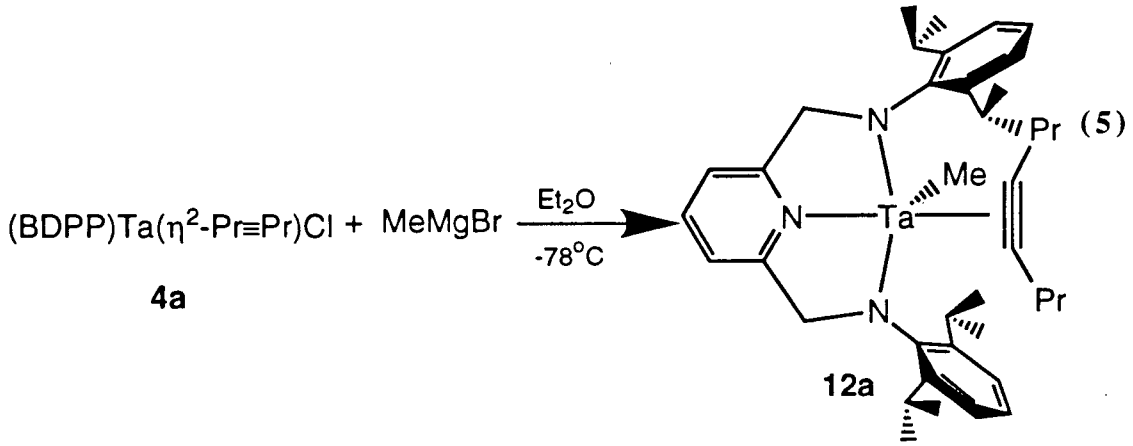

(5)

The ^1H and ^{13}C NMR spectra of compound **12a** are similar to those obtained for compound **4a** with additional resonances for the Ta–CH_3 group at 0.44 and 37.94 ppm, respectively. The asymmetry about the N_3-Ta plane as well as the restricted rotation around the N-aryl C_{ipso} bond are retained. The coordinated 4-octyne in complex **12a** does not insert into the Ta–Me bond at elevated temperatures (110 °C), even in the presence of PMe_3.

The methyl complex **12a** reacts with the Lewis acid $B(C_6F_5)_3$[49] in the presence of excess alkyne to afford the cationic tantalacyclopentadiene complex **13a** (eq. 6). Compound **13a** is only slightly soluble in benzene and decomposes within hours in dichloromethane.

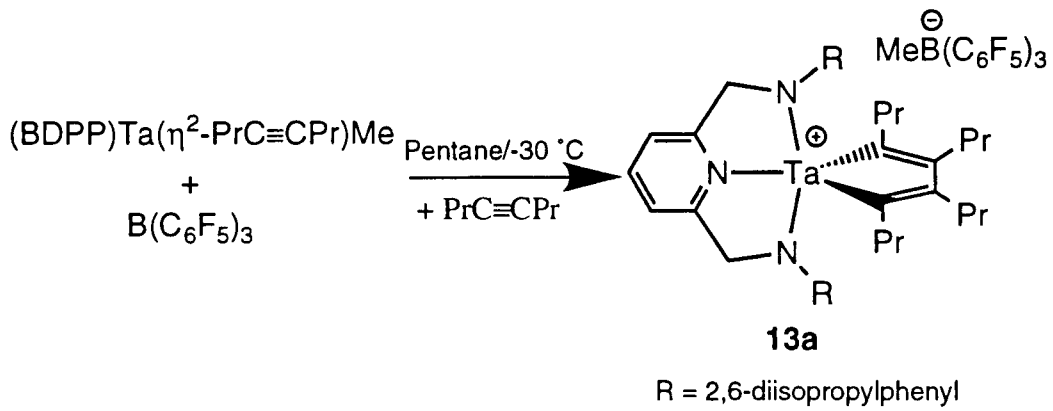

(6)

References start on page 238

The ^{1}H NMR spectrum of complex **13a** displays a singlet for the ligand methylene protons (NCH_2) as expected for a complex with C_{2v} symmetry. Restricted rotation of the phenyl rings is maintained as evidenced by the two isopropyl methyl resonances. Compound **13a** does not react further with excess 4-octyne (25 °C). Decomposition to free ligand and insoluble products occurs upon heating (60 °C) of a benzene solution containing **13a** and 50 equivalents of 4-octyne.

Complex **12a** reacts with excess phenylacetylene in toluene at 110 °C to give methane (confirmed by ^{1}H NMR spectroscopy) and the metallacycle **18a** in quantitative yield by ^{1}H NMR spectroscopy (eq. 7).

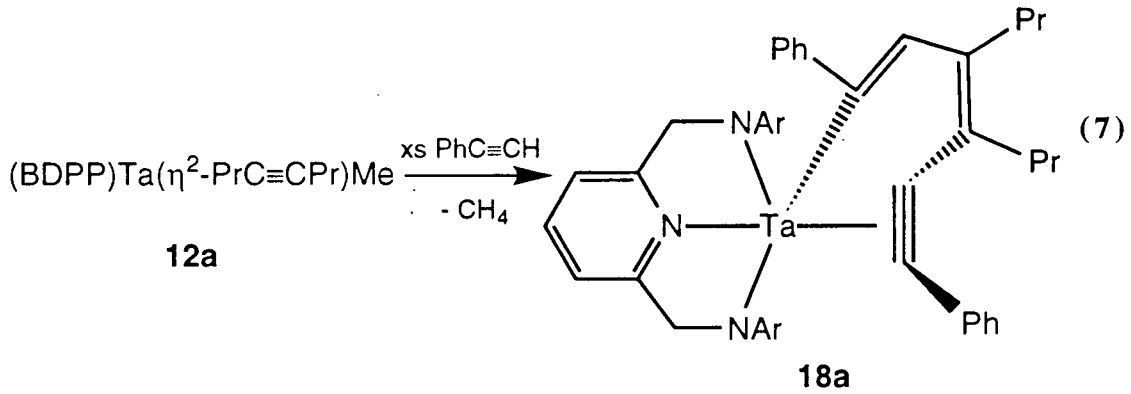

(7)

Two low-field acetylenic resonances (δ 220.26 and 189.90 ppm) are observed in the ^{13}C{^{1}H} NMR spectrum of complex **18a**. Moreover, the ^{1}H NMR spectrum displays resonances for two inequivalent propyl chains and two distinct phenyl groups. The ligand resonances in the proton and carbon NMR spectra of complex **18a** are consistent with C_s symmetry in solution.

The solid state structure of complex **18a** was determined by single crystal X-ray analysis. The molecular structure of complex **18a** can be found in Figure 3- 7 and relevant bond distances and angles in Table 3- 2. The complete crystallographic data can be found in the Appendix.

References start on page 238

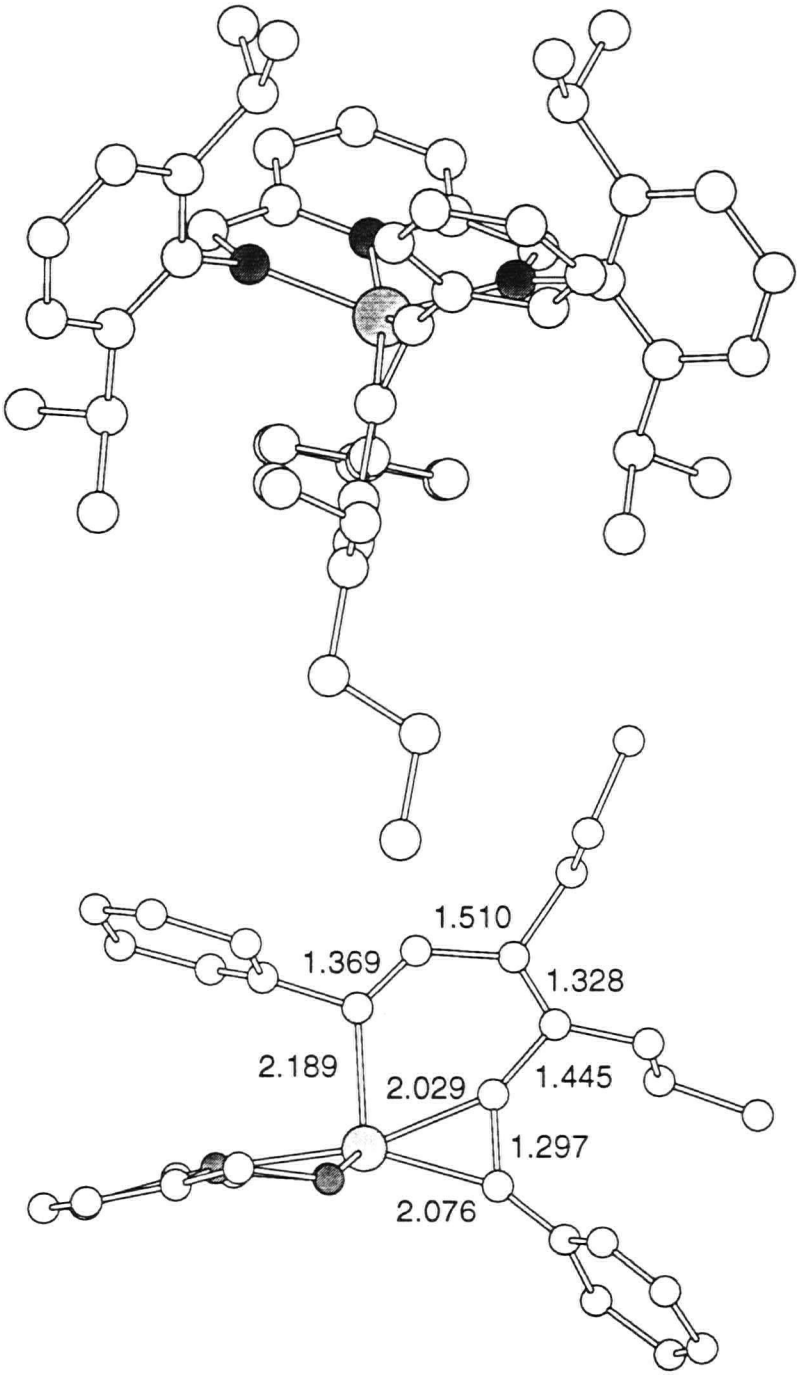

Figure 3- 7. (top) Molecular structure of complex 18a deduced from single crystal X-Ray analysis.

References start on page 238

Table 3- 2. Selected Bond Distances (Å) and Angles (deg) for 18a

Bond Distances			
Ta–N(1)	2.006(11)	Ta–N(2)	2.005(10)
Ta–N(16)	2.225(6)	Ta–C(1)	2.075(14)
Ta–C(2)	2.030(12)	Ta–C(6)	2.19(2)
C(1)–C(2)	1.30(2)	C(2)–C(3)	1.45(2)
C(3)–C(4)	1.33(2)	C(4)–C(5)	1.51(2)
C(5)–C(6)	1.37(2)		
Bond Angles			
N(1)–Ta–N(2)	137.9(2)	N(1)–Ta–N(16)	71.4(4)
N(2)–Ta–N(16)	72.6(4)	N(1)–Ta–C(6)	102.8(5)
N(2)–Ta–C(6)	100.2(5)	N(16)–Ta–C(6)	93.0(4)
Ta–C(6)–C(5)	127.2(10)	C(6)–C(5)–C(4)	129.9(13)
C(5)–C(4)–C(3)	122.1(13)	C(4)–C(3)–C(2)	116.4(12)
C(3)–C(2)–C(1)	140.0(13)		

The coordination geometry of tantalum in compound **18a** is very similar to that in complex **4a**. The acetylide group {C(1)-C(2)} resides in the basal plane of a distorted square pyramid (the octyne unit is in this position in compound **4a**), while the alkenyl carbon {C(6)} occupies the apical position {Cl(1) occupies the apical position in **4a**}. As a result of the metallacycle restraints, the acetylenic unit in compound **18a** is only rotated about 12° relative to the C(6)–Ta–N(16) plane. Comparatively, the 4-octyne in complex **4a** is rotated by 50° relative to the same plane. The alternating short and long bonds observed in the metallacyclic unit (Figure 3- 7, bottom) are consistent with the coupling of two alkyne molecules and an acetylide.

References start on page 238

Compound **18a** appears to result from the insertion of coordinated alkyne into a Ta–C≡CPh unit (**B**, Scheme 3- 6), followed by a 2,1-insertion of phenylacetylene into the newly formed alkenyl moiety (**C**, Scheme 3- 6).

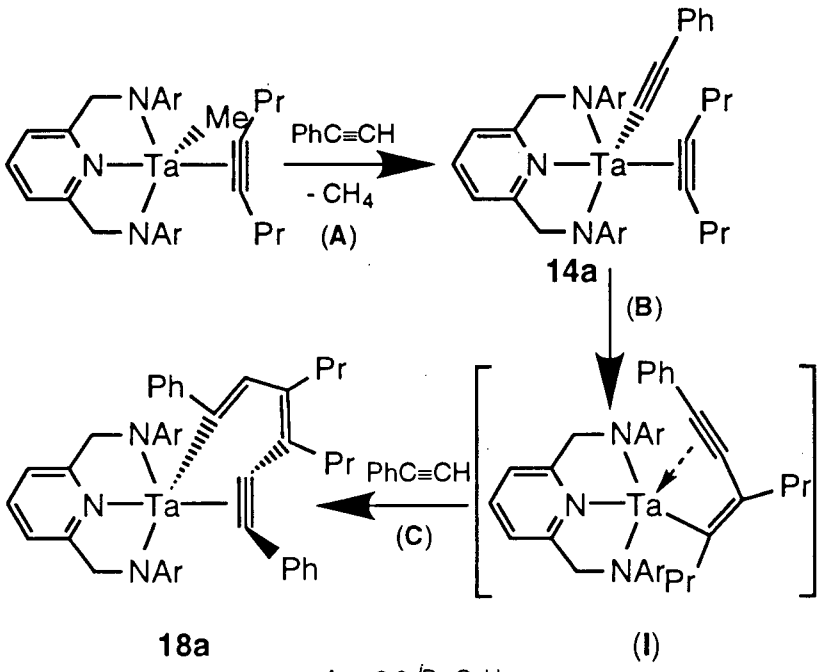

Scheme 3- 6. Coordination/insertion mechanism

The 2,1-insertion of phenylacetylene likely minimizes the interaction between the phenyl group and the propyl chains of the octyne. The Ta–C≡CPh unit is likely formed by the protonolysis of the methyl group in complex **12a** by PhC≡CH. A series of acetylide complexes were prepared in order to demonstrate that these compounds are intermediates in this reaction.

Compound **4a** reacts cleanly with LiC≡CR in ether at -30 °C to give the acetylide derivatives **14-17a** (eq. 8).

References start on page 238

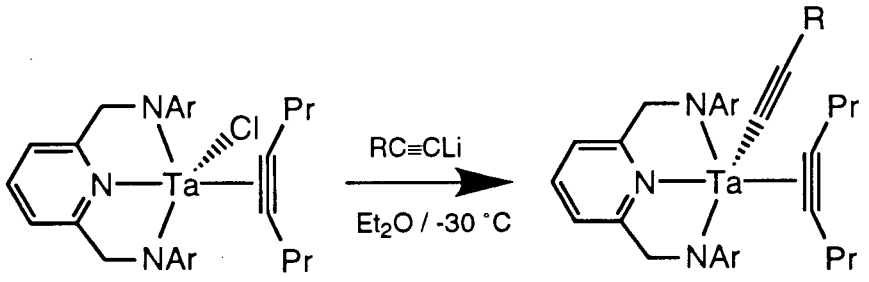

(8)

Ar = 2,6-$^{i}Pr_2C_6H_3$

14a, R = Ph
15a, R = *o*-$SiMe_3C_6H_4$
16a, R = Bu
17a, R = $SiMe_3$

The ^{1}H NMR spectra of compounds **14-17a** display an AB quartet at approximately 5.1 ppm for the ligand methylene protons (NCH_2), again indicating asymmetry about the Ta-N_3 plane of the ligand. The low-field acetylenic carbon resonances observed in the $^{13}C\{^{1}H\}$ NMR spectra of complexes **14-17a** are consistent with the octyne acting as a 4-electron donor[44].

The reaction of the phenylacetylide derivative **14a** with excess phenylacetylene in toluene (110°C) affords the metallacycle **18a** in quantitative yield by proton NMR spectroscopy. In a similar way, the acetylide complexes **16a** and **17a** react with 1-hexyne and trimethylsilylacetylene, respectively, to give the metallacyclic compounds **19a** and **21a** (eq. 9). However, compound **14a** does not react with internal alkynes (3-hexyne, 4-octyne) under similar conditions.

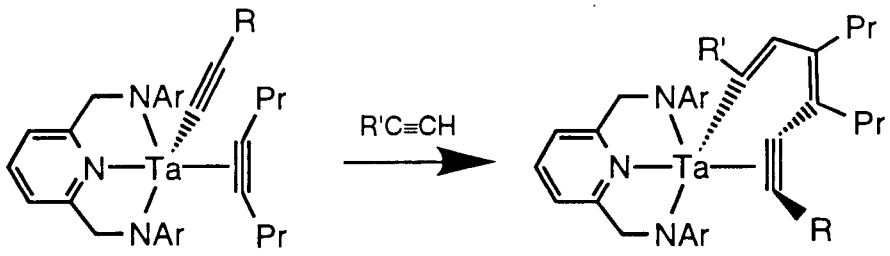

(9)

Ar = 2,6-$^{i}Pr_2C_6H_3$

18a, R = R' = Ph
19a, R = R' = Bu
20a, R = Bu, R' = Ph
21a, R = R' = $SiMe_3$
22a, R = $SiMe_3$, R' = Ph

References start on page 238

The ^{1}H NMR resonances attributable to the BDPP ligand in complex **19a** are very similar to those observed for complex **18a** which might indicate that the two complexes are isostructural. In contrast, the ^{1}H NMR spectrum of compound **21a** displays resonances characteristic for a complex with C_1 symmetry (C_s symmetry is observed in solution for complexes **18a** and **19a**). The observed C_1 symmetry may be explained by the steric demand of the acetylene-trimethylsilyl group. This causes the adjacent ligand aryl groups to twist about the N-C_{ipso} bond to avoid steric interactions. The formation of only one of the two possible regioisomers of the metallacycle (1,2- and 2,1-insertion) is indicated by the presence of only two trimethylsilyl in the ^{1}H and ^{13}C{^{1}H} NMR spectra of compound **21a**.

Compounds **16a** and **17a** react with excess phenylacetylene to give the corresponding mixed metallacycle complexes **20a** and **22a**, respectively. There is no evidence for the formation of complex **18a** which suggests that the starting acetylide unit is not protonated by the incoming PhC≡CH and is retained in the final product. Similarly to complex **21a**, complex **22a** which bears the bulky trimethylsilyl group on the η^2-alkyne displays C_1 symmetry in solution. In both cases, the ^{1}H NMR spectrum remains unchanged at 80 °C.

Surprisingly, compound **15a** which bears the bulky C≡C(*o*-$SiMe_3$)Ph group does not react with HC≡CPh, HC≡C$SiMe_3$ or HC≡CBu, even at elevated temperatures (110 °C). Modeling studies[50] suggest that rotation about the Ta–C≡C bond is inhibited by the Me_3Si group. Moreover, these studies also suggest that the endo isomer is more stable than the exo conformer. The exo conformation results in strong steric interactions between the Me_3Si group and the isopropyl groups of the ligand. On the other hand, the Me_3Si group in the endo conformer is directed toward the alkyne and may prevent approach of the two units.

References start on page 238

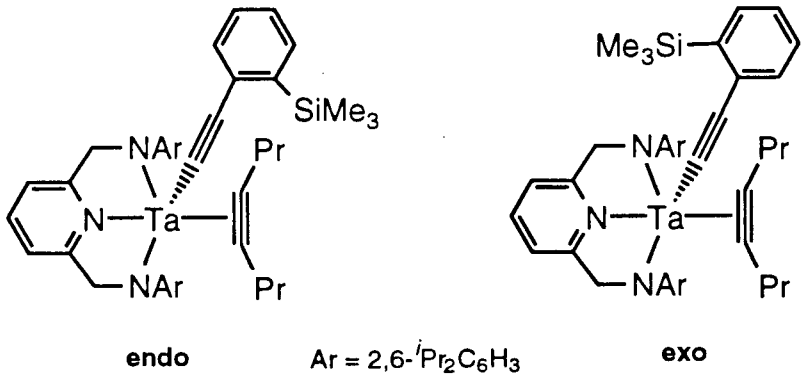

Figure 3- 8. endo and exo conformation

Attempts to trap the proposed intermediate alkenyl species (**I**, Scheme 3- 6) were unsuccessful. No reaction occurs between compound **14a** and a variety of Lewis bases (PMe_3, NEt_3, py) at 110 °C.

It appears that the relatively strong interaction between the alkyne unit of the metallacycle and tantalum prevents this system from undergoing multiple insertions of alkyne. Attempts to metathesize the chloride in complex **4a,b** with a phenyl, vinyl or –C≡N group were unsuccessful.

Another possible mechanism for the formation of complexes **18-22a** involves a metallacyclopentadiene acetylide intermediate (Scheme 3- 7) as observed with the smaller (iPAP) ligand (compound 6e, *vide supra*). We see no evidence of metallacyclopentadiene formation between compounds **4a,b** and HC≡CPh at elevated temperatures (110 °C).

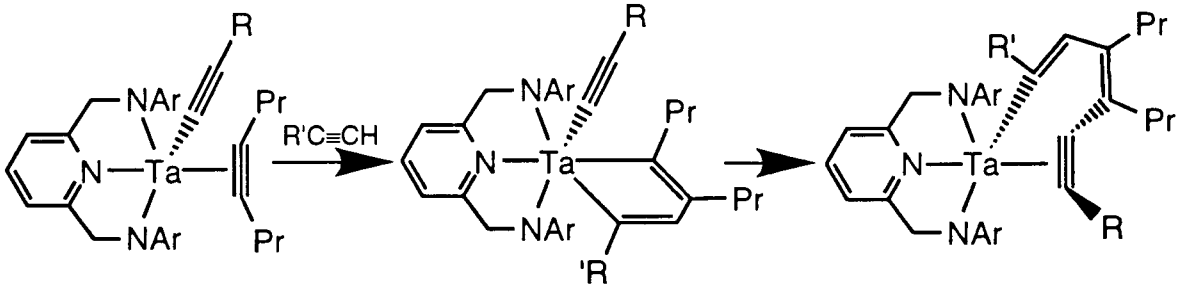

Scheme 3- 7. Metallacyclopentadiene acetylide mechanism

Although there are numerous reports of alkyne insertions into transition metal-hydrogen bonds[23-26], the are few examples of alkyne insertion into a transition metal-alkyl bond. Neutral

References start on page 238

scandocene[51], cationic titanocene[52], and cationic zirconocene[53,54] d^0 alkyl complexes readily insert alkyne to give η^1-vinyl species. However, the intermediate alkyl alkyne complexes are not detected. It has recently been reported that Tp*Nb(Cl)(CH_2R)(PhC≡CR') (eq. 10, **I**) (Tp* = hydrotris(3,5-dimethylpyrazolyl)borate) reacts with excess alkyne to yield the η^1-alkenyl complex (eq. 10, **II**)[16].

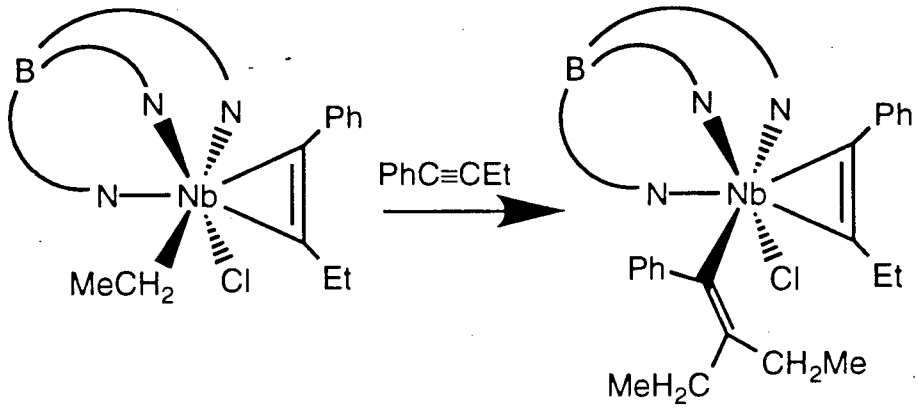

(10)

(I) **(II)**

The pyridine diamide system goes one step further and inserts two equivalents of alkyne into a metal-carbon bond.

References start on page 238

3 Conclusions

The elimination of Me_3SiCl provides a suitable driving force for the synthesis of pyridine diamide complexes of Ta^V (**2a-e**). The reduction of the trichloride complexes **2a,b** in the presence of excess alkyne affords the corresponding η^2-alkyne complexes. X-ray analysis of the η^2-octyne complex **4a** revealed a square pyramid geometry with the alkyne located in the basal plane.

The reduction of the pyridine (alkyl)amide complexes **2c,d** in the presence of the bulky alkynes $Me_3SiC{\equiv}CSiMe_3$ and $PrC{\equiv}CPr$ affords the expected η^2-alkyne tantalum complexes. Interestingly, the reduction of complex **2c** in the presence of excess $Me_3SiC{\equiv}CH$ affords the α,α'-tantalacyclopentadiene(acetylide) complex **6e**.

The high temperature reaction of complex **4a** with excess $PhC{\equiv}CH$ affords the doubly inserted products **18a**. The structure of complex **18a** was determined by X-ray analysis and is very similar to the structure of complex **4a**. The reaction appears to proceed via insertion of coordinated alkyne into a Ta-C≡CR bond. In a similar way, the acetylide complexes **14-17a** also insert various terminal alkynes to give the doubly inserted complexes **18-22a**. Attempts to induce further alkyne insertion were unsuccessful.

References start on page 238

4 Experimental Details

General Details. See chapter one for general details. $(BDPP)(SiMe_3)_2$ (**1a**), $(BDMP)(SiMe_3)_2$ (**1b**), $(CyAP)(SiMe_3)_2$ (**1d**) and $(iPAP)(SiMe_3)_2$ (**1e**) were prepared as described in chapter one. Tantalum(V) chloride was purchased from Alfa and used as received. Diphenylacetylene, phenylacetylene, 3-hexyne, 4-octyne and methylmagnesium bromide were purchased from Aldrich and used as received. The ortho-trimethylsilylphenylacetylene was prepared using a previously reported synthesis[55]. The lithium actetylides were prepared from the corresponding acetylene and *n*-BuLi in hexanes.

2,6-$[R(Me_3Si)NCH_2]_2$-NC_5H_3, (R = 2,4,6-trichlorophenyl) $(TCPP)(SiMe_3)_2$ (1c). A THF (150 mL) solution of $Li(Me_3Si)NR$ (10.20 g, 37.15 mmol) was added slowly to a THF (100 mL) solution of 2,6-bis(bromomethyl)pyridine (4.650 g, 17.55 mmol) at -78 °C. The mixture was allowed to warm to room temperature and stirred for 12 h. The solution was quenched with a saturated $NaHCO_3$ solution (100 ml) and extracted with ether (3 x 150 mL). The solvent was removed in *vacuo* to yield a yellow-brown viscous liquid. The oil was then dissolved in hot hexanes and cool to -30 °C. White crystalline **1c** was isolated by filtration and dried under vaccum (8.650 g, 13.51 mmol, 77 %). ^1H NMR δ 7.01 (s, 4H, Ar), 7.01 (t, 1H, py), 6.76 (d, 2H, py), 4.24 (s, 4H, NCH_2), 0.16 (s, 18H, $SiMe_3$). $^{13}C\{^1H\}$ NMR δ 158.71, 143.35, 138.11, 136.09, 130.55, 128.59, 55.39, 0.25. MS (EI) *m/z* 639.000 (M^+). Calcd for $C_{24}H_{29}N_3Si_2{}^{35}Cl_5{}^{37}Cl$: 639.000.

***mer*-(BDPP)$TaCl_3$ (2a).** Solid $TaCl_5$ (2.670 g, 7.454 mmol) was added in small portions to a benzene (150 mL) solution of **1a** (4.087 g, 6.768 mmol) at 23°C. The turbid solution immediately turned bright yellow and was heated to 80°C for 12h. The volatile components were removed under vacuum and the resulting solid dissolved in THF (50 mL). The solution was filtered through Celite and the solvent removed in *vacuo*. The resulting solid was washed with hexanes (3 × 50 mL) to yield a bright yellow crystalline solid **2a** (4.204 g, 5.658

References start on page 238

mmol, 84%). ^{1}H NMR δ 7.14 (m, 6H, Ar), 6.84 (t, 1H, py), 6.38 (d, 2H, py), 5.84 (s, 4H, NCH_2), 3.80 (sept, 4H, CHMe$_2$), 1.52 (d, 12H, CHMe_2), 1.12 (d, 12H, CHMe_2). ^{13}C{^{1}H} NMR δ 161.64, 148.84, 146.56, 139.66, 125.35, 122.28, 117.51, 71.78, 28.89, 27.57, 23.64. Anal. Calcd for $C_{31}H_{41}N_3TaCl_3$: C, 50.11; H, 5.56; N, 5.66. Found: C, 50.25; H, 5.68; N, 5.11.

***mer*-(BDMP)TaCl$_3$ (2b).** The preparation of compound **2b** is identical to that of **2a**. Solid $TaCl_5$ (1.000 g, 2.792 mmol) and compound **1b** (1.370 g, 2.797 mmol) yielded a bright yellow powder (**2b**) (1.321 g, 2.094 mmol, 75%). ^{1}H NMR (CD_2Cl_2) δ 6.16 (t, 1H, py), 6.64 (d, 2H, py), 7.14 (m, 6H, Ar), 5.98 (s, 4H, NCH_2), 2.38 (sept, 4H, CH_3). ^{13}C{^{1}H} (CD_2Cl_2) NMR δ 158.31, 145.04, 138.10, 133.66, 126.74, 125.27, 116.14, 66.81, 17.15.

***mer*-(TCPP)TaCl$_3$ (2c).** The preparation of compound **2c** is identical to that of **2a**. Solid $TaCl_5$ (1.298 g, 3.624 mmol) and compound **1c** (2.300 g, 3.591 mmol) gave a bright yellow powder (**2c**) (2.750 g, 3.520 mmol, 98 %). The high insolubility of complex **2c** limited its characterisation by NMR spectroscopy. Anal. Calcd for $C_{13}H_{21}Cl_3N_3Ta$: C, 30.82; H, 3.18; N, 8.29. Found: C, 30.42; H, 4.20; N, 8.57.

***mer*-(CyAP)TaCl$_3$ (2d).** The preparation of compound **2d** is identical to that of **2a**. Solid $TaCl_5$ (0.602 g, 1.681 mmol) and compound **1d** (0.750 g, 1.682 mmol) gave a bright yellow powder (**2d**) (0.521 g, 0.888 mmol, 53 %). ^{1}H NMR δ 6.94 (t, 1H, py), 6.45 (d, 2H, py), 5.63 (tt, 2H, NCH), 5.29 (s, 4H, NCH_2), 2.44 (d, 4H, Cy), 1.75 (d, 4H, Cy), 1.45 (m, 6H, Cy), 1.00 (m, 6H, Cy). ^{13}C{^{1}H} NMR δ 162.06, 138.63, 117.73, 61.08, 60.55, 30.61, 26.71, 26.11.

***mer*-(iPAP)TaCl$_3$ (2e).** The preparation of compound **2e** is identical to that of **2a**. Solid $TaCl_5$ (1.077 g, 3.007 mmol) and compound **1e** (1.000 g, 2.734 mmol) gave a bright yellow powder (**2a**) (0.698 g, 1.378 mmol, 50 %). ^{1}H NMR δ 6.82 (t, 1H, py), 6.32 (d, 2H,

References start on page 238

py), 5.97 (sept, 2H, NC*H*Me$_2$), 5.14 (s, 4H, NC*H*$_2$), 1.17 (d, 12H, NCH*Me*$_2$). ^{13}C{^{1}H} NMR δ 166.23, 138.41, 117.65, 59.54, 51.84, 19.60

***mer*-(BDPP)TaMe$_3$ (3a).** To a diethylether (25 mL) solution of compound **2a** (0.401 g, 0.538 mmol) was added 3.3 equiv. of MeMgBr (0.54 mL, 3.0 M, 1.6 mmol) at -78 °C. The solution was stirred for 12 h. The solvent was removed in *vacuo*. The resulting solid was extracted with toluene (3 × 10 mL) and filtered through Celite to give a bright yellow solution. The solvent was removed in *vacuo*, the solid dissolved in a minimum amount of diethylether, and cooled to -30°C for 12 h. Yellow crystalline **3a** was isolated by filtration and dried under vacuum (0.310 g, 0.455 mmol, 83%). ^{1}H NMR δ 7.14 (m, 6H, Ar), 6.84 (t, 1H, py), 6.63 (d, 2H, py), 5.04 (s, 4H, NC*H*$_2$), 3.56 (sept, 4H, C*H*Me$_2$), 1.42 (d, 12H, CH*Me*$_2$), 1.39 (s, 3H, Ta*Me*), 1.16 (d, 12H, CH*Me*$_2$), 0.86 (s, 6H, Ta*Me*). ^{13}C{^{1}H} NMR δ 161.27, 151.30, 145.28, 138.38, 126.36, 124.49, 116.78, 71.14, 69.09 (Ta*C*H$_3$), 65.80 (Ta*C*H$_3$), 28.44, 27.46, 23.95. Anal. Calcd for $C_{34}H_{50}N_3Ta$: C, 59.90; H, 7.39; N, 6.16. Found: C, 59.43; H, 7.35; N, 5.73.

***mer*-(BDMP)TaMe$_3$ (3b).** The preparation of compound **3b** is identical to that of **3a**. Compound **2b** (0.100 g, 0.159 mmol) and MeMgBr (0.29 mL, 1.8 M, 0.522 mmol) yielded orange crystalline **3b** (0.074 g, 0.130 mmol, 82%). ^{1}H NMR (CD_2Cl_2) δ 7.98 (t, 1H, py), 7.45 (d, 2H, py), 7.04 (d, 4H, Ar), 6.96 (m, 2H, Ar), 5.15 (s, 4H, NC*H*$_2$), 2.24 (s, 12H, *Me*), 0.57 (s, 3H, Ta*Me*), 0.19 (s, 6H, Ta*Me*). ^{13}C{^{1}H} NMR (CD_2Cl_2) δ 162.03, 151.98, 139.47, 135.43, 128.98, 125.38, 118.10, 68.81, 66.54 (Ta*Me*), 61.78 (Ta*Me*), 18.94.

***mer*-(TCPP)TaMe$_3$ (3c).** The preparation of compound **3c** is identical to that of **3a**. Compound **2c** (0.300 g, 0.384 mmol) and MeMgBr (1.0 mL, 1.34 M, 1.3 mmol) gave orange crystalline **3c** (0.180 g, 0.250 mmol, 65 %), ^{1}H NMR δ 7.09 (s, 4H, Ar), 6.81 (t, 1H, py), 6.32 (d, 2H, py), 4.70 (s, 4H, NC*H*$_2$), 1.50 (s, 3H, Ta*Me*), 1.03 (s, 6H, Ta*Me*). ^{13}C{^{1}H} NMR δ 161.33, 149.34, 138.84, 135.12, 129.30, 128.85, 117.25, 74.30, 69.76, 66.84.

(BDPP)Ta(η^2-PrC≡CPr)Cl (4a). A toluene (30 mL) solution of compound **2a**

References start on page 238

(0.500 g, 0.673 mmol) and 4-octyne (0.297 g, 2.70 mmol) was added to an excess of Na/Hg amalgam (0.460 g Na, 20.0 mmol; 46.0 g Hg). The mixture was stirred for 12h. The solution was decanted from the amalgam and filtered through Celite. The solvent was removed in *vacuo* to yield an orange-brown solid. The solid was dissolved in a minimum amount of diethylether and cooled to -30°C for 12h. Yellow crystalline **4a** was isolated by filtration and dried under vacuum (0.401 g, 0.513 mmol, 75%). ^{1}H NMR δ 7.19 (t, 2H, Ar), 7.13 (d, 4H, Ar), 6.85 (t, 1H, py), 6.39 (d, 2H, py), 5.12 (AB quartet, $^2J_{HH}$ = 20.1 Hz, 4H, NCH_2), 3.79 (sept, 2H, C*H*Me$_2$), 3.15 (sept, 2H, C*H*Me$_2$), 2.51 (m, 4H, ≡CCH_2), 1.46 (d, 6H, CHMe_2), 1.34 (m, 4H, CH_2CH$_3$), 1.32 (d, 6H, CHMe_2), 1.24 (d, 6H, CHMe_2), 1.01 (d, 6H, CHMe_2), 0.84 (t, 6H, CH$_2$CH_3). ^{13}C{^{1}H} NMR δ 237.01 (*C*≡*C*), 160.77, 154.41, 145.19, 142.96, 138.41, 125.49, 124.32, 123.57, 116.99, 70.95, 40.02, 28.60, 27.95, 26.66, 25.76, 24.61, 23.80, 21.94, 15.45. Anal. Calcd for $C_{39}H_{55}N_3TaCl$: C, 59.88; H, 7.09; N, 5.37. Found: C, 59.62; H, 7.19; N, 5.16.

(BDMP)Ta(η^2-PrC≡CPr)Cl (4b). The preparation of compound **4b** is identical to that of **4a**. Compound **2b** (0.250 g, 0.396 mmol), 4-octyne (0.153g, 0.500 mmol) and excess Na/Hg amalgam (0.090 g Na, 3.960 mmol; 9.0 g Hg) gave yellow crystalline **4b** (0.190 g, 0.219 mmol, 55 %). ^{1}H NMR δ 7.03 (d, 4H, Ar), 6.91 (t, 1H, py), 6.90 (t, 2H, Ar), 6.42 (d, 2H, py), 4.76 (AB quartet, $^2J_{HH}$ = 20.1 Hz), 2.65 (t, 4H, CH_2CH$_2$Me), 2.58 (s, 6H, Me), 2.12 (s, 6H, Me), 1.48 (q, 4H, CH$_2$CH_2Me), 0.83 (t, 6H, CH$_2$CH$_2$*Me*). ^{13}C{^{1}H} NMR δ 237.60, 160.70, 155.395, 138.13, 135.03, 133.11, 128.67, 124.76, 117.25, 67.34, 39.43, 22.45, 19.57, 19.05, 15.19.

(CyAP)Ta(η^2-PrC≡CPr)Cl (4d). The preparation of compound **4d** is identical to that of **4a**. Compound **2d** (0.250 g, 0.426 mmol), 4-octyne (0.150 g, 0.490 mmol) and excess Na/Hg amalgam (0.098 g Na, 4.260 mmol; 9.80 g Hg) gave yellow crystalline **4d** (0.187 g, 0.228 mmol, 53 %). ^{1}H NMR δ 6.99 (t, 1H, py), 6.46 (d, 2H, py), 4.66 (AB quartet, $^2J_{HH}$ = 20.1 Hz, 4H, NCH_2), 3.50 (m, 2H, NC*H*), 3.48 (m, 2H, CH_2CH$_2$Me), 2.86 (t, 2H, CH_2CH$_2$Me), 2.19 (m, 2H, CH$_2$CH_2Me), 2.05 (d, 2H, Cy), 0.80-1.80 (m, 23H, Pr and Cy),

References start on page 238

0.68 (t, 3H, CH_2CH_2Me). $^{13}C\{^1H\}$ NMR δ 201.95, 195.10, 165.31, 137.34, 128.93, 116.75, 59.85, 52.93, 50.26, 37.80, 30.94. 30.12, 27.17, 26.83, 26.57, 24.60, 23.99, 15.46, 14.60.

(iPAP)Ta($Me_3SiC{\equiv}CSiMe_3$)Cl (5e). The preparation of complex **5e** is identical to that of **4a**. Complex **2e** (0.250 g, 0.493 mmol), $Me_3SiC{\equiv}CSiMe_3$ (0.222 g, 1.303 mmol) and excess Na/Hg amalgam (0.120 g Na, 5.22 mmol; 12.0 g Hg) gave red crystalline **5e** (0.197 g, 0.327 mmol, 66 %). ^1H NMR δ 6.96 (t, 1H, py), 6.44 (d, 2H, py), 4.49 (s, 4H, NCH_2), 3.86 (sept, 2H, $NCHMe_2$), 1.09 (d, 6H, $NCHMe_2$), 0.70 (s, 9H, $SiMe_3$), 0.66 (d, 6H, $NCHMe_2$), -0.096 (s, 9H, $SiMe_3$). $^{13}C\{^1H\}$ NMR δ 221.73, 215.06, 165.13, 137.53, 116.90, 58.28, 42.47, 19.64, 17.50, 1.69, 1.16.

(iPAP)Ta{C_4α-α'($SiMe_3$)$_2H_2$}(CC$SiMe_3$) (6e). To a diethylether solution (50 mL) of complex **2e** (0.250 g, 0.493 mmol) was added 3 equivalents of $HC{\equiv}CSiMe_3$ (0.150 g, 1.527 mmol) and an excess of Na/Hg amalgam (0.113 g Na, 4.93 mmol; 11.3 g Hg). The solution was stired for 12 hours. The black solution was filtered and the solvent removed in *vacuo*. The resulting solid was dissolved in a minimum amount of hexanes and cooled to -30° for 12 hours. Bright red crystalline **6e** was isolated by filtration and dried under vaccum (0.217 g, 0.325 mmol, 66 %). ^1H NMR δ 8.60 (d, 1H, β-C*H*), 7.49 (d, 1H, β-C*H*), 7.08 (t, 1H, py), 6.65 (d, 2H, py), 4.60 (AB quartet, $^2J_{HH}$ = 20.1 Hz, 4H, NCH_2), 2.52 (sept, 2H, $NCHMe_2$), 0.75 (d, 6H, $NCHMe_2$), 0.58 (d, 6H, $NCHMe_2$), 0.55 (s, 9H, $SiMe_3$), 0.28 (s, 9H, $SiMe_3$), 0.21 (s, 9H, $SiMe_3$). $^{13}C\{^1H\}$ NMR δ 218.49, 204.50, 199.63, 167.27, 148.87, 145.63, 137.39, 128.87, 116.98, 59.46, 44.89, 21.42, 19.38, 2.54, 1.13, -0.09.

(BDPP)Ta(η^2-EtC≡CEt)Cl (7a). The preparation of compound **7a** is identical to that for **4a**. Compound **2a** (0.500 g, 0.673 mmol), 3-hexyne (0.200 g, 2.43 mmol) and excess Na/Hg amalgam (0.186 g Na, 8.09 mmol; 18.6 g Hg) gave yellow crystalline **7a** (0.417 g, 0.553 mmol, 82%). ^1H NMR δ 7.19, (t, 2H, Ar), 7.11 (d, 4H, Ar), 6.84 (t, 1H, py), 6.39 (d, 2H, py), 5.11 (AB quartet, $^2J_{HH}$ = 20.1 Hz, 4H, NCH_2), 3.79 (sept, 2H, $CHMe_2$), 3.13 (sept, 2H, $CHMe_2$), 2.59 (q, 4H, $\equiv CCH_2$), 1.46 (d, 6H, $CHMe_2$), 1.32 (d, 6H, $CHMe_2$), 1.21 (d, 6H,

References start on page 238

CHMe_2), 1.02 (d, 6H, CHMe_2), 0.94 (t, 6H, CH_2CH_3). $^{13}C\{^1H\}$ NMR δ 237.81 (*C*≡*C*), 160.76, 154.34, 145.17, 142.88, 138.41, 125.57, 124.35, 123.59, 117.01, 70.94, 30.56, 28.53, 27.94, 26.69, 25.76, 24.61, 23.77, 13.03. Anal. Calcd for $C_{37}H_{51}N_3TaCl$: C, 58.92; H, 6.82; N, 5.57. Found: C, 58.97; H, 6.70; N, 5.38.

(BDMP)Ta(η²-EtC≡CEt)Cl (7b). The preparation of compound **7b** is identical to that of **4a**. Compound **2b** (0.250 g, .396 mmol), 3-hexyne (0.081 g, 0.991 mmol) and excess Na/Hg amalgam (0.137 g Na, 5.95 mmol; 13.7g Hg) gave yellow crystalline **7b** (0.187 g, .276 mmol, 70%). ^1H NMR δ 7.00 (d, 4H, Ar), 6.88 (t, 2H, Ar), 6.78 (t, 1H, py), 6.41 (d, 2H, py), 4.67 (AB quartet, $^2J_{HH}$ = 20.2, 4H, NCH_2), 2.70 (q, 4H, ≡CCH_2), 2.56 (s, 6H, CH_3), 2.11 (s, 6H, CH_3), 0.95 (t, 6H, CH_2CH_3). $^{13}C\{^1H\}$ NMR δ 238.20 (*C*≡*C*), 160.70, 155.86, 138.14, 135.03, 133.08, 128.64, 124.78, 117.28, 67.22, 30.79, 19.65, 18.97, 13.52.

(BDPP)Ta(η²-PhC≡CPh)Cl (8a). The preparation of compound **8a** is identical to that for **4a**. Compound **2a** (1.001 g, 1.346 mmol), diphenylacetylene (0.288 g, 1.62 mmol) and excess Na/Hg amalgam (0.619 g Na, 26.9 mmol; 61.9 g Hg) gave yellow crystalline **8a** (0.567 g, 0.667 mmol, 51%). ^1H NMR δ 7.15-6.95 (m, 17H, Ar and Ph), 6.48 (d, 2H, py), 5.14 (AB quartet, $^2J_{HH}$ = 19.5 Hz, 4H, NCH_2), 4.02 (sept, 2H, C*H*Me$_2$), 3.30 (sept, 2H, C*H*Me$_2$), 1.30 (d, 6H, CHMe_2), 1.08 (d, 12H, CHMe_2), 1.04 (d, 6H, CHMe_2). $^{13}C\{^1H\}$ NMR δ 228.20 (*C*≡*C*), 159.94, 152.52, 147.23, 145.25, 144.13, 138.67, 126.96, 126.17, 124.55, 124.03, 117.37, 70.90, 28.85, 28.59, 27.56, 25.93, 24.33, 23.95. Anal. Calcd for $C_{45}H_{51}N_3TaCl$: C, 63.56; H, 6.05; N, 4.94. Found: C, 63.21; H, 6.07; N, 4.42.

(BDPP)Ta(η²-PhC≡CH)Cl (9a). The preparation of compound **9a** is identical to that for **4a**. Compound **2a** (0.250 g, 0.336 mmol), phenylacetylene (0.103 g, 1.01 mmol) and excess Na/Hg amalgam (0.230 g Na, 10.0 mmol; 23.0 g Hg) gave ivory crystalline **9a** (0.207 g, 0.267 mmol, 79%). ^1H NMR δ 11.91 (s, 1H, C≡C*H*) 7.20-6.90 (m, Ar and Ph), 6.83 (t, 1H, py), 6.36 (d, 2H, py), 5.08 (AB quartet, $^2J_{HH}$ = 20.3 Hz, 4H, NCH_2), 3.82 (sept, 2H, C*H*Me$_2$), 3.43 (sept, 2H, C*H*Me$_2$), 1.31 (d, 6H, CHMe_2), 1.26 (d, 6H, CHMe_2), 1.20 (d, 6H, CHMe_2),

References start on page 238

1.08 (d, 6H, CH*Me*$_2$). ^{13}C{^{1}H} NMR δ 236.45 (Ph*C*≡C), 225.81(C≡*C*H), 160.65, 152.78, 146.77, 145.38, 142.25, 138.68, 126.86, 125.94, 124.35, 123.69, 117.30, 70.60, 28.54, 27.96, 26.47, 26.27, 24.70, 23.99.

(BDPP)Ta(η^2-SiMe$_3$C≡CH)Cl (10a). The preparation of compound **10a** is identical to that of **4a**. Compound **2a** (0.250 g, 0.336 mmol), phenylacetylene (0.103 g, 1.01 mmol) and excess Na/Hg amalgam (0.230 g Na, 10.0 mmol; 23.0 g Hg) gave yellow crystalline **10a** (0.207 g, 0.267 mmol, 79%). ^{1}H NMR δ 13.15 (s, 1H, *H*C≡C), 7.25-7.15 (m, 6H, Ar), 6.86 (t, 1H, py), 6.38 (d, 2H, py), 5.06 (AB quartet, $^2J_{HH}$ = 20.2 Hz, 4H, NC*H*$_2$), 3.74 (sept, 2H, C*H*Me$_2$), 3.33 (sept, 2H, C*H*Me$_2$), 1.51 (d, 6H, CH*Me*$_2$), 1.33 (d, 6H, CH*Me*$_2$), 1.26 (d, 6H, CH*Me*$_2$), 1.07 (d, 6H, CH*Me*$_2$), 0.09 (s, 9H, Si*Me*$_3$). ^{13}C{^{1}H} δ 245.60 (C≡*C*Ph), 242.27 (C≡*C*H), 52.80, 145.19, 138.59, 126.06, 124.41, 123.95, 117.17, 70.87, 28.46, 27.94, 26.26, 25.86, 25.17, 23.44, -0.02.

(BDPP)Ta(η^2-PrC≡CPr)Me (12a). To a diethylether (25 mL) solution of compound **4a** (0.600 g, 0.767 mmol) was added 1.2 equivalents of MeMgBr (0.38 mL, 2.4 M, 0.91 mmol) at -78°C. The yellow solution was warmed to 25°C and stirred for 12h. The solvent was removed in *vacuo*. The resulting solid was extracted with toluene (3 × 10 mL) and filtered through Celite to give a bright yellow solution. The solvent was removed in vacuo, the solid dissolved in a minimum amount of diethylether and cooled to -30°C for 12h. Yellow crystalline **12a** was isolated by filtration and dried under vacuum (0.531 g, 0.697 mmol, 91%). ^{1}H NMR δ 7.22-7.10 (m, 6H, Ar), 6.88 (t, 1H, py), 6.45 (d, 2H, py), 5.05 (AB quartet, $^2J_{HH}$ = 20.5 Hz, 4H, NC*H*$_2$), 3.60 (sept, 2H, C*H*Me$_2$), 3.15 (sept, 2H, C*H*Me$_2$), 2.46 (m, 4H, ≡CC*H*$_2$), 1.42 (d, 6H, CH*Me*$_2$), 1.34 (m, 4H, C*H*$_2$CH$_3$), 1.33 (d, 6H, CH*Me*$_2$), 1.21 (d, 6H, CH*Me*$_2$), 1.05 (d, 6H, CH*Me*$_2$), 0.86 (t, 6H, CH$_2$C*H*$_3$), 0.44 (s, 3H, Me). ^{13}C{^{1}H} NMR δ 237.45 (*C*≡*C*), 161.93, 155.12, 144.61, 143.12, 138.05, 124.84, 124.02, 123.61, 116.98, 70.69, 39.06 (Ta-*C*H$_3$), 37.94, 28.78, 27.75, 26.49, 25.80, 24.56, 23.84, 22.10, 16.63. Anal. Calcd for $C_{40}H_{58}N_3Ta$: C, 63.06; H, 7.67; N, 5.52. Found: C, 63.02; H, 7.79; N, 6.38.

References start on page 238

[(BDPP)Ta(C_4Pr_4)]$^+$[MeB(C_6F_5)$_3$]$^-$ (13a). To a toluene (5 mL) solution of compound **12a** (0.050 g, 0.066 mmol) was added 1 equivalent of B(C_6F_5)$_3$ (0.034 g, 0.066 mmol) and excess of 4-octyne (0.050 g, 0.580 mmol). The yellow solution was stirred for 12 hours during which a dark orange oil separated from the solution. The mother liquor was decanted off and the oil washed with 3x5 mL of cold pentane. Residual solvent was removed *in vacuo* to afford compound **13a** as a dark orange oily liquid (0.073 g, 0.053 mmol, 80 %). ^{1}H NMR (CD_2Cl_2) δ 8.25 (t, 1H, py), 7.62 (d, 2H, py), 7.40-7.30 (m, 6H, Ar), 5.74 (s, 4H, NCH_2), 3.11 (s, 4H, CHMe$_2$), 3.03 (m, 4H, ≡CH_2), 2.69 (m, 4H, ≡CH_2), 1.40 (d, 12H, CHMe_2), 1.30 (d, 12H, CHMe_2), 1.07 (br m, 8H, CH_2CH$_3$), 0.87 (t, 12H, CH$_2$CH_3), 0.58 (q, 3H, BCH_3).

(BDPP)Ta(η^2-PrC≡CPr)(C≡CPh) (14a). To a diethylether (25 mL) solution of compound **4a** (0.500 g, 0.634 mmol) was added 1.1 equivalents of PhC≡CLi (0.076 g, 0.703 mmol) at -78°C. The yellow solution was warmed to 25°C and stirred for 12h. The solvent was removed in *vacuo*. The resulting solid was extracted with toluene (3 × 10 mL) and filtered through Celite to give a bright yellow solution. The solvent was removed in vacuo, the solid dissolved in a minimum amount of pentane and cooled to -30°C for 12h. Yellow crystalline **14a** was isolated by filtration and dried under vacuum (0.406 g, 0.479 mmol, 76%). ^{1}H NMR δ 7.59 (m, 2H, Ph), 7.22-7.10 (m, 7H, Ar and Ph), 7.01 (m, 2H, Ph), 6.80 (t, 1H, py), 6.38 (d, 2H, py), 5.08 (AB quartet, $^2J_{HH}$ = 20.2 Hz, 4H, NCH_2), 4.10 (sept, 2H, CHMe$_2$), 3.39 (sept, 2H, CHMe$_2$), 2.81 (m, 4H, ≡CCH_2), 1.53 (d, 6H, CHMe_2), 1.39 (d, 6H, CHMe_2), 1.36 (d, 6H, CHMe_2), 1.22 (m, 4H, CH_2CH$_3$), 1.10 (d, 6H, CHMe_2), 0.87 (t, 6H, CH$_2$CH_3). ^{13}C{^{1}H} NMR δ 233.64 (PrC≡CPr), 161.41, 153.22, 149.40, 145.21, 143.08, 138.16, 130.97, 127.12, 126.48, 126.23, 125.33, 124.32, 123.35, 117.05, 70.99, 40.96, 28.86, 27.84, 27.09, 25.93, 24.94, 24.10, 21.95, 15.52.

(BDPP)Ta(η^2-PrC≡CPr)(C≡C-*o*-$Me_3SiC_6H_4$) (15a). The preparation of complex **15a** is identical to that of complex **14a**. Complex **4a** (0.100 g, 0.128 mmol) and LiC≡C-*o*-

References start on page 238

$Me_3SiC_6H_4$ (0.023 g, 0.128 mmol) yielded orange crystalline **15a** (0.087 g, 0.095 mmol, 74 %). ^1H NMR δ 7.83 (d, 1H, Ph), 7.40 (d, 1H, Ph), 7.20-6.90 (m, 9H, Ar, py and Ph), 6.54 (d, 2H, py), 5.12 (AB quartet, $^2J_{HH}$ = 20.4 Hz, 4H, NCH_2), 3.99 (sept, 2H, CHMe$_2$), 3.43 (sept, 2H, CHMe$_2$), 2.87 (m, 4H, CH_2CH$_2$Me), 1.43 (d, 6H, CHMe_2), 1.37 (d, 6H, CHMe_2), 1.35 (m, 4H, CH$_2$CH_2Me), 1.30 (d, 6H, CHMe_2), 1.10 (d, 6H, CHMe_2), 0.91 (t, 6H, CH$_2$CH$_2$$Me$), 0.21 (s, 9H, SiMe$_3$). ^{13}C {^1H} NMR δ 233.304 (PrC≡CPr), 161.67, 153.07, 152.80, 145.27, 142.98, 138.25, 133.99, 133.54, 132.40, 129.22, 128.88, 126.26, 125.30, 124.29, 123.29, 117.20, 70.89, 40.83, 28.85, 27.78, 26.95, 25.96, 24.77, 24.06, 21.95, 15.50, -1.00. Anal. Calcd for $C_{50}H_{68}N_3SiTa$: C, 65.27; H, 7.45; N, 4.57. Found: C, 65.48; H, 7.59; N, 4.80.

(BDPP)Ta(η²-PrC≡CPr)(C≡CBu) (16a). The preparation of compound **16a** is identical to that of complex **14a**. Complex **4a** (0.100 g, 0.128 mmol) and LiC≡CBu (0.012 g, 0.128 mmol) yielded orange crystalline **16a** (0.077 g, 0.093 mmol, 73 %). ^1H NMR δ 7.24 (t, 2H, Ar), 7.14 (d, 4H, Ar), 6.85 (t, 1H, py), 6.41 (d, 2H, py), 5.09 (AB quartet, $^2J_{HH}$ = 20.1 Hz, 4H, NCH_2), 4.05 (sept, 2H, CHMe$_2$), 3.32 (sept, 2H, CHMe$_2$), 2.67 (m, 4H, CH_2CH$_2$Me), 2.22 (t, 2H, TaC≡CCH_2), 1.52 (d, 6H, CHMe_2), 1.44 (d, 6H, CHMe_2), 1.40 (m, 8H, CH_2 of octyne and butylacetylide), 1.31 (d, 6H, CHMe_2), 1.08 (d, 6H, CHMe_2), 0.88 (t, 6H, CH$_2$CH$_2$$Me$), 0.87 (t, 3H, CH$_2CH_2CH_2$$Me$). $^{13}C\{^1H\}$ NMR δ 235.46 (PrC≡CPr), 161.46, 153.90, 145.11, 143.04, 139.10, 137.98, 125.50, 125.08, 124.16, 123.33, 116.88, 70.78, 40.50, 32.09, 28.70, 27.64, 27.02, 25.79, 24.88, 23.95, 22.19, 22.04, 21.36, 15.53, 13.91.

(BDPP)Ta(η²-PrC≡CPr)(C≡CSiMe$_3$) (17a). The preparation of compound **17a** is identical to that of **14a**. Complex **4a** (0.100 g, 0.128 mmol) and LiC≡CSiMe$_3$ (0.013 g, 0.128 mmol) yielded yellow crystalline **17a** (0.102 g, 0.121 mmol, 95 %). ^1H NMR δ 7.19 (t, 2H, Ar), 7.15 (d, 4H, Ar), 6.77 (t, 1H, py), 6.34 (d, 2H, py), 5.00 (AB quartet, $^2J_{HH}$ = 20.2 Hz, 4H, NCH_2), 4.01 (sept, 2H, CHMe$_2$), 3.35 (sept, 2H, CHMe$_2$), 2.77 (m, 4H, CH_2CH$_2$Me), 1.51 (d, 6H, CHMe_2), 1.43 (d, 6H, CHMe_2), 1.32 (d, 6H, CHMe_2), 1.19 (m, 4H, CH$_2$CH_2Me), 1.06 (d, 6H, CHMe_2), 0.85 (t, 6H, CH$_2$CH$_2$$Me$), 0.26 (s, 9H, SiMe$_3$). ^{13}C {^1H}

References start on page 238

NMR δ 232.68 (Pr*C*≡*C*Pr), 169.14, 161.22, 153.05, 145.02, 143.08, 138.15, 130.89, 125.32, 124.33, 123.31, 117.04, 70.91, 40.89, 28.85, 27.52, 27.10, 25.88, 25.07, 24.11, 21.86, 15.47, 1.21.

(BDPP)Ta{PhC=CHCPr=CPr(η²-C≡CPh)} (18a). To a toluene solution (5 mL) of compound **14a** (0.100 g, 0.118 mmol) in a glass pressure vessel was added 1.5 equivalents of phenylacetylene (0.018 g, 0.177 mmol) at 25°C. The yellow solution was stirred at 110°C for 12 hours. The solvent was removed *in vacuo*. The resulting orange solid was dissolved in a minimum amount of diethyl ether and cooled to -30°C for 12 hours. Orange crystalline **18a** was isolated by filtration and dried under vacuum (0.108 g, 0.114 mmol, 97%). ^{1}H NMR δ 7.19-7.10 (m, 6H, Ar), 7.05 (s, 1H, PhC=C*H*), 7.04-6.98 (m, 4H, Ph), 6.90 (t, 2H, Ph), 6.82 (tt, 1H, Ph), 6.76 (t, 1H, py), 6.74 (tt, 1H, Ph), 6.25 (d, 2H, py), 5.60 (dd, 2H, Ph), 4.87 (AB quartet, $^2J_{HH}$ = 20.1 Hz, 4H, NCH_2), 4.10 (sept, 2H, C*H*Me$_2$), 3.36 (sept, 2H, C*H*Me$_2$), 2.24 (m, 4H, ≡CH_2), 1.62 (m, 2H, ≡CH_2), 1.43 (d, 6H, CH*Me*$_2$), 1.35 (d, 6H, CH*Me*$_2$), 1.22 (m, 2H, CH_2CH$_3$), 1.08 (d, 6H, CH*Me*$_2$), 1.01 (d, 6H, CH*Me*$_2$), 0.93 (t, 3H, CH$_2$CH_3), 0.51 (t, 3H, CH$_2$CH_3). ^{13}C{^{1}H} NMR δ 220.26 (PhC≡*C*H), 189.90 (Ph*C*≡CH), 160.83, 158.63, 154.09, 151.86, 147.39, 145.14, 144.72, 142.08, 137.95, 128.89, 127.16, 126.73, 125.69, 125.47, 124.08, 123.98, 123.87, 123.34, 116.85, 71.21, 37.31, 34.30, 29.03, 27.95, 27.83, 25.92, 24.88, 24.58, 23.52, 23.30, 15.24, 14.68. Anal. Calcd for $C_{55}H_{66}N_3Ta$: C, 69.53; H, 7.00; N, 4.42; Found: C, 69.95; H, 7.41; N, 4.71.

(BDPP)Ta{BuC=CHCPr=CPr(η²-C≡CBu)} (19a). The preparation of compound **19a** is identical to that of compound **18a**. Complex **16a** (0.100 g, 0.098 mmol) and HC≡CBu (0.010 g, 0.122 mmol) yielded red crystalline **19a** (0.086 g, 0.078 mmol, 80 %). ^{1}H NMR δ 7.17-7.05 (m, 6H, Ar), 6.91 (t, 1H, py), 6.85 (s, 1H, BuC=C*H*), 6.46 (d, 2H, py), 4.98 (AB quartet, $^2J_{HH}$ = 21.0 Hz, NCH_2), 3.66 (sept, 2H, C*H*Me$_2$), 3.59 (sept, 2H, C*H*Me$_2$), 2.77 (m, 2H, CH_2CH$_2$Me), 2.48 (m, 2H, CH_2CH$_2$Me), 2.34 (t, 2H, CH_2CH$_2$CH$_2$Me), 2.23 (br m, 2H, CH_2CH$_2$CH$_2$Me), 1.63 (m, 4H, CH$_2$CH_2CH$_2$Me), 1.42 (d, 6H, CH*Me*$_2$), 1.33 (d, 6H,

References start on page 238

CHMe_2), 1.26 (d, 6H, CHMe_2), 1.12 (d, 6H, CHMe_2), 1.30 (buried, 8H, CH_2 Pr and Bu), 1.00, 0.86, 0.82 and 0.71 (t, 3H each, CH_2Me Pr and Bu). $^{13}C\{^1H\}$ NMR δ 237.52, 236.28, 195.53, 162.11, 153.35, 145.00, 144.20, 141.34, 140.95, 138.11, 137.01, 128.09, 124.27, 123.25, 116.19, 71.52, 43.49, 39.59, 37.17, 35.27, 34.96, 31.15, 28.84, 27.29, 26.99, 25.99, 25.33, 24.50, 24.42, 23.76, 23.65, 21.99, 15.23, 14.81, 14.58, 14.10.

(BDPP)Ta{PhC=CHCPr=CPr(η²-C≡CBu)} (20a). The synthesis of compound **20a** is identical to that of **18a**. Complex **16a** (0.100 g, 0.098 mmol) and HC≡CPh (0.015 g, 0.147 mmol) yielded red crystalline **20a** (0.076 g, 0.068 mmol, 69 %). ^1H NMR δ 7.30-7.10 and 6.90-6.70 (m, 12H, Ar, Ph and py), 6.14 (d, 2H, Ph), 5.38 (AB quartet, $^2J_{HH}$ = 19.9 Hz, 4H, NCH_2), 4.16 (sept, 2H, CHMe$_2$), 3.39 (m, 2H, CH_2CH$_2$CH$_2$Me), 3.11 (s, 1H, PhC=CH), 3.05 (sept, 2H, CHMe$_2$), 2.30 (m, 2H, CH_2CH$_2$Me), 1.65 (m, 4H, CH_2 Pr or Bu), 1.60 (m, 4H, CH_2 Pr or Bu), 1.49 (d, 6H, CHMe_2), 1.43 (d, 6H, CHMe_2), 1.35 (d, 6H, CHMe_2), 1.22 (m, 5H, CH_2 and CH_3, Pr or Bu), 1.02 (d, 6H, CHMe_2), 0.97 (t, 3H, CH_3 Pr or Bu), 0.81 (t, 3H, CH_3 Pr or Bu). $^{13}C\{^1H\}$ NMR δ 221.17, 204.45, 163.86, 162.56, 156.19, 149.68, 148.58, 148.10, 143.55, 138.81, 127.03, 126.20, 125.16, 123.46, 123.27, 117.30, 70.91, 48.59, 34.79, 28.77, 28.65, 28.25, 27.55, 24.31, 23.44, 23.13, 22.84, 15.88, 15.40.

(BDPP)Ta{Me$_3$SiC=CHCPr=CPr(η²-C≡SiMe$_3$)} (21a). The synthesis of compound **21a** is identical to that of **18a**. Complex **17a** (0.100 g, 0.096 mmol) and HC≡CSiMe$_3$ (0.015 g, 0.153 mmol) yielded red crystalline **21a** (0.113 g, 0.088 mmol, 92 %). ^1H NMR δ 7.10-6.90 (m, 7H, Ar and py), 6.54 (d, 1H, py), 6.49 (d, 1H, py), 5.17 (AB quartet, $^2J_{HH}$ = 19.4 Hz, 2H, NCH_2), 4.93 (AB quartet, $^2J_{HH}$ = 20.4 Hz, 2H, NCH_2), 4.08 (sept, 1H, CHMe$_2$), 3.58 (sept, 1H, CHMe$_2$), 3.08 (sept, 1H, CHMe$_2$), 2.96 (m, 1H, CH_2CH$_2$Me), 2.90 (s, 1H, CH≡CSiMe$_3$), 2.67 (m, 2H, CHMe$_2$ and CH_2CH$_2$Me), 2.36 (m, 1H, CH_2CH$_2$Me), 2.24 (m, 1H, CH_2CH$_2$Me), 1.84 (m, 1H, CH$_2$CH_2Me), 1.64 (m, 1H, CH$_2$CH_2Me), 1.57 (d, 3H, CHMe_2), 1.51 (d, 3H, CHMe_2), 1.27 (d, 3H, CHMe_2), 1.26 (d, 3H, CHMe_2), 1.20 (m, 2H, CH$_2$CH_2Me), 1.10 (d, 3H, CHMe_2), 1.08 (d, 3H, CHMe_2), 1.08 (buried, 3H,

References start on page 238

CH_2CH_2Me), 1.06 (d, 3H, $CHMe_2$), 0.92 (d, 3H, $CHMe_2$), 0.74 (t, 3H, CH_2CH_2Me), 0.28 (s, 9H, $SiMe_3$), -0.19 (s, 9H, $SiMe_3$). $^{13}C\{^1H\}$ NMR δ 233.53, 190.05, 169.56, 167.86, 163.49, 162.93, 155.43, 154.54, 145.76, 144.21, 143.31, 142.58, 138.57, 132.39, 124.51, 123.93, 123.84, 123.51, 123.37, 122.32, 117.11, 116.88, 68.81, 68.59, 55.34, 33.06, 29.98, 29.03, 27.48, 27.36, 27.28, 26.10, 25.84, 25.12, 24.86, 24.25, 24.17, 24.00, 22.57, 14.83, 14.69, 3.95, -0.51.

(BDPP)Ta{Me_3SiC=CHCPr=CPr(η^2-C≡$SiMe_3$)} (22a). The synthesis of compound **22a** is identical to that of **18a**. Complex **17a** (0.100 g, 0.096 mmol) and HC≡CPh (0.015 g, 0.147 mmol) yielded red crystalline **22a** (0.097 g, 0.076 mmol, 79 %). ^1H NMR δ 7.50-6.50 (m, 10H, Ar, Ph and py), 6.37 (d, 1H, py), 6.35 (d, 1H, py), 6.21 (d, 2H, Ph), 5.01 (AB quartet, $^2J_{HH}$ = 20.1 Hz, 2H, NCH_2), 4.97 (AB quartet, $^2J_{HH}$ = 20.1 Hz, 2H, NCH_2), 4.10 (sept, 1H, $CHMe_2$), 3.77 (br m, 4H, $CHMe_2$ and PhC=CH), 2.55 (m, 1H, CH_2CH_2Me), 2.41 (m, 3H, CH_2CH_2Me), 1.78 (m, 4H, CH_2CH_2Me), 1.60 (d, 3H, $CHMe_2$), 1.53 (d, 3H, $CHMe_2$), 1.38 (d, 3H, $CHMe_2$), 1.31 (d, 3H, $CHMe_2$), 1.24 (d, 3H, $CHMe_2$), 1.00-0.84 (m, 15H, CH_2CH_2Me and $CHMe_2$), -0.29 (s, 9H, $SiMe_3$). $^{13}C\{^1H\}$ NMR δ 240.72, 234.10, 192.94, 161.07, 160.43, 156.69, 156.16, 154.01, 153.35, 153.02, 146.04, 144.64, 144.21, 144.05, 143.59, 140.09, 139.37, 138.96, 138.00, 136.14, 131.14, 127.11, 126.80, 126.72, 126.14, 125.86, 125.43, 124.84, 124.46, 124.64, 124.11, 123.90, 123.88, 116.70, 116.65, 71.76, 71.44, 38.95, 31.13, 30.33, 29.93, 28.05, 27.20, 26.94, 26.45, 26.29, 25.77, 25.39, 24.60, 24.23, 24.14, 22.86, 22.78, 15.34, 15.10, 0.54.

X-ray Crystallographic Analysis (4a). A suitable crystal of **4a** (dimension 0.45 × 0.23 × 0.20 mm) was grown from a saturated ether solution at -30°C. Data were collected on a Siemens P4 diffractometer with the XSCANS software package[56]. The cell constants were obtained by centering 25 reflections (18.0 ≤ 2θ ≤24.7°). The Laue symmetry $\bar{1}$ was determined by merging symmetry equivalent positions. The data were collected in the range of θ = 1.9–23° (-1≤h≤10, -11≤k≤12, -19≤l≤19) in ω mode at variable scan speeds (2–20 deg/min). Four standard reflections monitored at the end of every 297 reflections collected showed no decay of the crystal.

References start on page 238

The data processing, solution and refinement were done using *SHELXTL-PC* programs[57]. The final refinements were performed using SHELXL-93 software programs[58]. An empirical absorption correction was applied to the data using the routine 'XEMP' on the basis of the ψ scans of 11 reflections with 2θ ranging from 8.5 to 25.9° (μ = 2.995 mm^{-1}). The methyl carbon atoms attached to C(29) were found to be disordered. Three orientation (0.33/0.33/0.33) of C(30) and C(31) were located in the final difference Fourier methods. Isotropic thermal parameters were refined for these disordered carbon atoms. Anisotropic thermal parameters were refined for all non-hydrogen atoms. No attempt was made to locate the hydrogen atoms, however, they were placed in calculated positions. The C–C distances in the isopropyl groups were restrained to be equal using the option SADI. In the final difference Fourier synthesis the electron density fluctuates in the range 0.788 to -0.677 e $Å^{-3}$.

X-ray Crystallographic Analysis (18a). A suitable crystal of **18a** (dimension 0.10 × 0.1 × 0.1 mm) was grown from a saturated ether solution at -30°C. Data were collected on a Siemens Smart system CCD diffractometer. The data were collected in the range of θ = 1.47–21° (-17≤h≤17, -11≤k≤23, -28≤l≤27). Unit-cell parameters were calculated from reflections obtained from 60 data frames collected at different sections of the Ewald sphere. The systematic absences in the diffraction data and the determined unit-cell parameters were uniquely consistent for the reported space group. A trial application of semi-empirical absorption correction based on redundant data at varying effective azimuthal angles yielded T_{max}/T_{min} at unity and was ignored. A molecule of cocrystallized n-hexane solvent was located at the inversion centre. All C–C distances in the solvent molecule were constrained to be equal. All non-hydrogen atoms were refined with anisotropic displacement coefficients. All hydrogen atoms were treated as idealized contributions. The structure was solved by direct methods, completed by subsequent Fourier syntheses and refined with full-matrix least-squares methods. All scattering factors and anomalous dispersion coefficients are contained in the SHELXTL 5.03 program library[59]. In the final difference Fourier synthesis the electron density fluctuates in the range 0.667 to -0.634 e $Å^{-3}$.

References start on page 238

5 References

(1) Bradley, D. C.; Gitlitz, M. H. *J. Chem. Soc. (A)* **1969**, 980.

(2) Bradley, D. C.; Thomas, I. M. *Can. J. Chem.* **1962**, *40*, 1355.

(3) Bradley, D. C.; Thomas, I. M. *Chemical Society London. Proceedings* **1959**, 225.

(4) Bürger, H. *Monatsh.* **1964**, *95*, 671.

(5) Suh, S.; Hoffman, D. M. *Inorg. Chem.* **1996**, *35*, 5015.

(6) Bradley, D. C.; Gitlitz, M. H. *J. Chem. Soc. (A)* **1969**, 1894.

(7) Fuggle, J. C.; Sharp, D. W. A.; Winfield, J. M. *J. Chem. Soc., Dalton Trans.* **1972**, 1766.

(8) Masuda, T.; Isobe, E.; Higashimura, T.; Takada, K. *J. Am. Chem. Soc.* **1983**, *105*, 7473.

(9) Masuda, T.; Niki, A.; Isobe, E.; Higashimura, T. *Macromolecules* **1985**, *18*, 2109.

(10) Cotton, F. A.; Hall, W. T.; Cann, K. J.; Karol, F. J. *Macromolecules* **1981**, *14*, 233.

(11) Bruck, M. A.; Copenhaver, A. S.; Wigley, D. E. *J. Am. Chem. Soc.* **1987**, *109*, 6525.

(12) Clarke, T. C. *J. Am. Chem. Soc.* **1983**, *105*, 7797.

(13) Clarke, T. C.; Yannoni, Y. S.; Katz, T. J. *J. Am. Chem. Soc.* **1983**, *105*, 7787.

(14) Katz, T. J.; Hacker, S. M.; Kendrick, R. D.; Yannoni, C. S. *J. Am. Chem. Soc.* **1985**, *107*, 2182.

(15) Katz, T. J.; Ho, T. H.; Shih, N.-Y.; Ying, Y.-C.; Stuart, V. I. W. *J. Am. Chem. Soc.* **1984**, *106*, 2659.

(16) Etienne, M.; Mathieu, R.; Donnadieu, B. *J. Am. Chem. Soc.* **1997**, *119*, 3218.

(17) Chao, Y.-W.; Wexler, P. A.; Wigley, D. E. *Inorg. Chem.* **1989**, *28*, 3860.

(18) Green, M. L. H.; Jousseaume, B. *J. Organomet. Chem.* **1980**, *193*, 339.

(19) Gibson, V. C.; Parkin, G.; Bercaw, J. *Organometallics* **1991**, *10*, 220.

(20) Labinger, J. A.; Schwartz, J.; Townsend, T. M. *J. Am. Chem. Soc.* **1974**, *96*, 4009.

(21) Antinolo, A.; Fajardo, M.; Otero, A.; Royo, P. *J. Organomet. Chem.* **1983**, *246*, 269.

(22) Herberich, G. E.; Savvopoulos, I. *J. Organomet. Chem.* **1989**, *365*, 345.

(23) Herberich, G. E.; Hessner, B.; Mayer, H. *J. Organomet. Chem.* **1986**, *314*, 123.

References start on page 238

(24) Herberich, G. E.; Hoeveler, U. E. M.; Savvopoulos, I. *J. Organomet. Chem.* **1990**, *399*, 35.

(25) Herberich, G. E.; Mayer, H. *Organometallics* **1990**, *9*, 2655.

(26) Yasuda, H.; Yamamoto, H.; Takashi, A.; Nakamura, A.; Chen, J.; Kai, Y.; Kasai, N. *Organometallics* **1991**, *10*, 4058.

(27) Hirpo, W.; Curtis, M. D. *Organometallics* **1994**, *13*, 2706.

(28) Smith, G.; Schrock, R. R.; Churchill, M. R.; Youngs, W. J. *Inorg. Chem.* **1981**, *20*, 387.

(29) Curtis, M. D.; Real, J.; Hirpo, W.; Butler, W. D. *Organometallics* **1990**, *9*, 66.

(30) Strickler, J. R.; Bruck, M. A.; Wigley, D. E. *J. Am. Chem. Soc.* **1990**, *112*, 2814.

(31) Strickler, J. R.; Wexler, P. A.; Wigley, D. E. *Organometallics* **1991**, *10*, 118.

(32) Strickler, J. R.; Wexler, P. A.; Wigley, D. E. *Organometallics* **1988**, 2067.

(33) Schrock, R. R. *Acc. Chem. Res.* **1979**, *12*, 98.

(34) Wood, C. D.; McLain, S. J.; Schrock, R. R. *J. Am. Chem. Soc.* **1979**, *101*, 3210.

(35) Rupprecht, G. A.; Messerle, L. W.; Fellmann, J. D.; Schrock, R. R. *J. Am. Chem. Soc.* **1980**, *102*, 6236.

(36) Messerle, L. W.; Jennische, P.; Schrock, R. R.; Stucky, G. *J. Am. Chem. Soc.* **1980**, *102*, 6744.

(37) Schrock, R. R.; Messerle, L. W.; Wood, C. D.; Guggenberger, J. L. *J. Am. Chem. Soc.* **1978**, *100*, 3793.

(38) Lockwood, M. A.; Clark, J. R.; Bernardeta, P. C.; Rothwell, I. P. *J. Chem. Soc., Chem. Commun.* **1996**, 1973.

(39) Mowat, W.; Wilkinson, G. *J. Chem. Soc., Dalton Trans.* **1972**, 1120.

(40) Malatesta, V.; Ingold, K. U.; Schrock, R. R. *J. Organomet. Chem.* **1978**, *152*, C53.

(41) Wallace, K. C.; Liu, A. H.; Dewan, J. C.; Schrock, R. R. *J. Am. Chem. Soc.* **1988**, *110*, 4964.

(42) Schrock, R. R.; Fellmann, J. D. *J. Am. Chem. Soc.* **1978**, *100*, 3359.

References start on page 238

(43) Bradley, D. C.; Ghotra, J. S.; Hart, H. A. *J. Chem. Soc., Chem. Commun.* **1972**, 349.

(44) Templeton, J. L.; Ward, B. C. *J. Am. Chem. Soc.* **1980**, *102*, 3288.

(45) Theopold, K. H.; Holmes, S. J.; Schrock, R. R. *Angew. Chem., Int. Ed. Engl.* **1983**, *22*, 1010.

(46) Belmonte, P. A.; Cloke, F. G. N.; Theopold, K. H.; Schrock, R. R. *Inorg. Chem.* **1984**, *23*, 2365.

(47) Cotton, F. A.; Hall, W. T. *Inorg. Chem.* **1980**, *19*, 2352.

(48) Morrison, R. T.; Boyd, R. N., *Organic Chemistry*; 5th ed.; Morrison, R. T.; Boyd, R. N., Ed.; Allyn & Bacon, Inc.: Boston, 1987, pp 427.

(49) Massey, A. G.; Park, A. J. *J. Organomet. Chem.* **1964**, *2*, 245.

(50) .

(51) Cotter, W. D.; Bercaw, J. E. *J. Organomet. Chem.* **1991**, *417*, C1.

(52) Eisch, J. J.; Piotrowski, A. M.; Brownstein, S. K.; Gabe, E. J.; Lee, F. L. *J. Am. Chem. Soc.* **1985**, *107*, 7219.

(53) Jordan, R. F.; Lapointe, R. E.; Bradley, P. K.; Baezinger, N. *Organometallics* **1989**, *8*, 2892.

(54) Horton, A. D.; Orpen, A. G. *Organometallics* **1991**, *10*, 3910.

(55) Masuda, T.; Hamano, T.; Tshuchihara, K.; Higashimura, T. *Macromolecules* **1990**, *23(5)*, 1374.

(56) *XSCANS*; Siemens Analytical X-Ray Instruments Inc.: Madison, 1990.

(57) Sheldrick, G. M. *SHELXTL-PC*; V4.1 ed.; Sheldrick, G. M., Ed.; Siemens Analytical X-Ray Instruments Inc.: Madison, WI, U.S.A., 1990.

(58) Sheldrick, G. M. *SHELXL-93*; Sheldrick, G. M., Ed.; Institute fuer Anorg. Chemie: Goettingen, Germany, 1993.

(59) , "SHELXTL Version 5", Siemans Analytical X-ray Instruments Inc., Madison WI, 1994.

References start on page 238

" Stupidity does not consist in being without ideas. Such stupidity would be the sweet, blissful stupidity of animals, mollusks and the gods. Human stupidity consists in having lots of ideas, but stupid ones. Stupid ideas, with banners, hymns, loudspeakers and even thanks and flame-throwers as their instruments of persuasion, constitute the refined and the only really terrifying form of stupidity."

Henry De Montherlant

Chapter Four. Group 3 Metal Complexes

1 Introduction

Ziegler was the first to report the polymerization of ethylene at ambient pressure using a $TiCl_4/AlEt_3$ catalyst system[1,2]. This system is, however, heterogeneous and the active species is believed to be a neutral Ti^{III} or a cationic Ti^{IV} complex. The proposed mechanism involves the insertion of a C_2H_4 molecule into a metal-alkyl bond and requires a vacant coordination site (Scheme 4- 1).

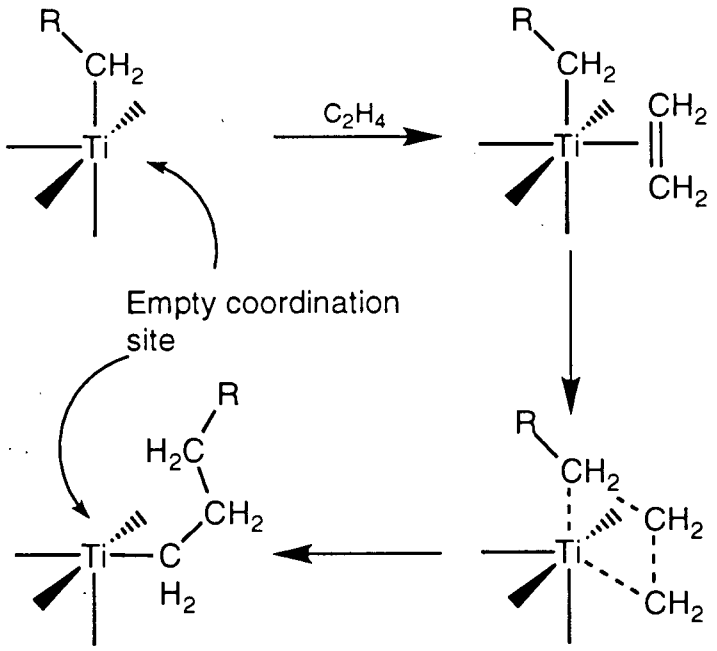

Scheme 4- 1. Cossee-Arlman Mechanism of Ziegler-Natta catalysis

Long after this discovery, other groups used cyclopentadienyl-based systems such as Cp_2TiPh_2, Cp_2ZrPh_2 or Cp_2ZrCl_2[3] as models for Ziegler-Natta catalysis. These systems are homogeneous and have comparable activities than the original heterogeneous catalysts. In homogeneous solutions, cations are postulated to be the catalytically active metal species. For

References start on page 253

example, the base-stabilized complex $Cp_2ZrMe(THF)^+$ has been isolated and used for the polymerization of ethylene (Figure 4- 1)[4-11].

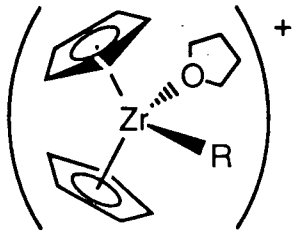

Figure 4- 1. Cationic Cp_2MR

In these polymerizations, an excess of an aluminum co-catalyst (500 to 10000 equiv), MAO (methylaluminoxane) is used. The co-catalyst is believed to play three roles. The first one is to act as an alkylating agent (Scheme 4- 2a). The second is to abstract one of the methyl groups to form *in situ* a cationic alkyl complex (Scheme 4- 2b). Finally, it is used to remove moisture from the system.

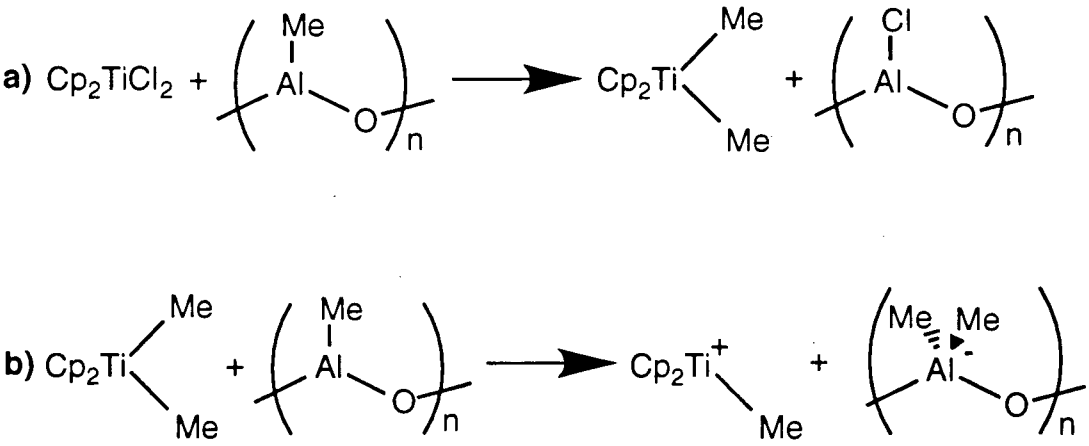

Scheme 4- 2. Roles of MAO

Other co-catalysts have since been developed. Boron-based co-catalysts such as $B(C_6F_5)_3$[12] or $(Ph_3C)[B(C_6F_5)_4]$[13] have been used in combination with transition metal complexes. These co-catalysts are however expensive to prepare.

References start on page 253

The synthesis of olefin polymerization catalysts that do not require a co-catalyst showed growing interest. Complexes based on an (alkyl)metallocene complex containing a Sc^{III}, Y^{III} or a trivalent lanthanide center of the type $Cp_2M^{III}R$ (Cp = η^5-C_5H_5, η^5-C_5Me_5; M = Sc[14-17], Y[15,18], La[19], Lu[20-25]; R = halide, alkyl, H) act as single component catalysts for the polymerization of ethylene. These complexes are generally more difficult to prepare and to handle than the isostructural cationic or neutral group 4 complexes. Moreover, these systems do not polymerize α-olefins very efficiently and short chain oligomers ($C_{\leq 24}$) are obtained for the few systems that effect propene oligomerization[19].

Complexes that contain a single Cp ligand where prepared in an attempt to generate a highly electrophilic and more open metal centre. With this in mind, the synthesis and catalytic activity of a scandium complex that contains a linked cyclopentadienyl-amide ligand (e.g., [(η^5-C_5Me_4)$SiMe_2$($NCMe_3$)]MCl, M = Sc[26]) (Figure 4- 2) was reported. This well-characterized, single-component organoscandium system is capable of catalyzing the regioselective polymerization of α-olefins with degrees of polymerization as high as 70.

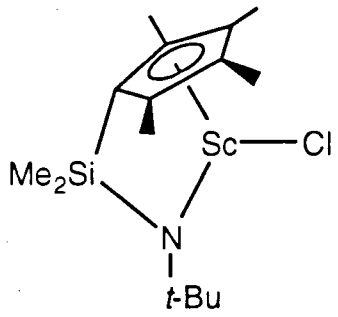

Figure 4- 2. Linked Cp-amide complex

There are very few homoleptic amide complexes known for scandium and yttrium. The use of sterically demanding di(alkyl) or di(silyl) amides has allowed the isolation of some tris(amido)metal(III) species [e.g., M{$N(SiMe_3)_2$}$_3$, M = Sc[27-30], Y[31,32]; $Y(N^iPr_2)_3$[33]]. These complexes are all monomeric in solution with a three coordinate metal environment. X-ray diffraction studies on the Sc{$N(SiMe_3)_2$}$_3$[30] confirm the three coordinate metal environment.

References start on page 253

However, the metal atom resides just above the N_3 plane. The deviation from planarity is attributed to rather ionic metal–nitrogen bonds, making the complex geometrically flexible. In contrast, the Ti^{III} complex $Ti\{N(SiMe_3)_2\}_3$[28,34] has a planar molecular geometry in the solid state (by X-ray analysis).

References start on page 253

2 Results and Discussion

The reaction between YCl_3 and compound **1a** {(BDPP)($SiMe_3$)$_2$} (160 °C) did not proceed and only starting materials were isolated from the reaction mixture. In a similar way, no reaction was observed between YCl_3•3THF and compound **1b** at 160 °C. The lack of reactivity of YCl_3 may in part be due to its polymeric structure which prevents coordination of the ligand. On the other hand, the coordinated solvent molecules in YCl_3•3THF are not labile and may also preclude coordination of the solvent.

The alkane elimination reaction between $Y(CH_2SiMe_3)_2$•2THF and the diamine **2a** {(BDPP)H_2} affords complex **3** in good yield (eq. 1).

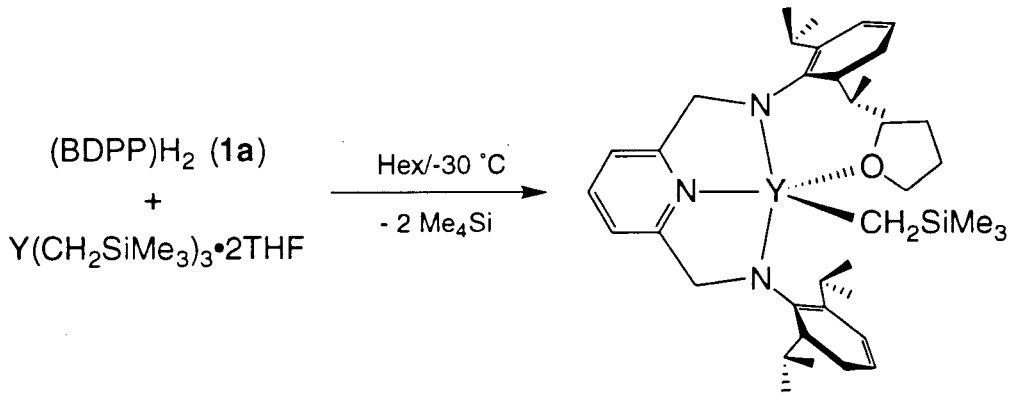

(1)

(3)

The compound is highly soluble in hexanes and is difficult to separate from unreacted free ligand and other impurities present in the reaction mixture. Moreover, complex **3** is extremely air and moisture sensitive and special care must be taken to ensure the absence of water or oxygen.

The room temperature ^{1}H NMR spectrum of complex **3** confirms the proposed solvent adduct structure shown above. Another interesting feature is the very broad resonances observed for the ligand fragment. The -60°C ^{1}H NMR spectrum displays a sharp AB quartet for the ligand methylene protons (NCH_2) and two isopropyl methine resonances. The coalescence temperature

References start on page 253

is approximately 15°C with an equilibrium constant K = 485 s^{-1}. This is attributed to the weak coordination of the tetrahydrofuran molecule (eq. 2).

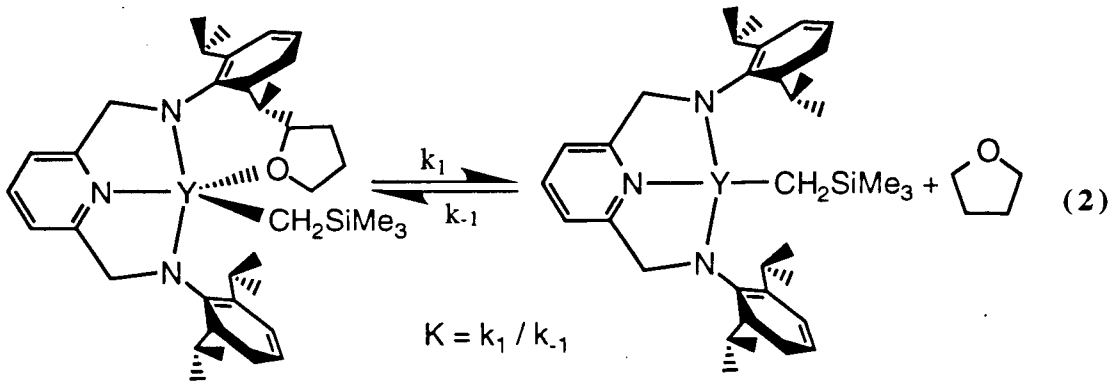

(2)

It is possible to exchange the THF molecule by recrystallization of complex **2** from diethyl ether. The room temperature ^{1}H NMR spectrum of the Et_2O complex **4** displays sharp resonances indicating that the Et_2O is strongly bounded to the yttrium centre. The AB quartet observed for the ligand methylene (NCH_2) protons and the two isopropyl methine resonances are consistent with a complex with C_s geometry.

The reaction between $Y(CH_2C_6H_4$-*o*-$NMe_2)_3$ and compound **1a** at room temperature does not result in the elimination of $CH_3C_6H_4$-*o*-NMe_2. Decomposition of the starting yttrium tri(alkyl) complexes is observed upon heating to 110 °C in Toluene-d_8. This might be a result of the saturated coordination sphere of the starting yttrium complex. Pre-coordination of the ligand is precluded by the presence of the pending amino donors of the alkyl groups. The alkane elimination seems to be limited to alkyl compounds derived from stable coordinatively unsaturated tris(alkyl)yttrium complexes. A more general pathway to the synthesis of yttrium alkyl complexes stabilized by the pyridine diamide ligand was sought.

A different approach to the synthesis of complex **3** involves pre-coordination of the ligand to the metal halide complex. The high temperature reaction (150 °C, 1,2-dichlorobenzene) between compound **1a** and YCl_3•3THF affords a white microcrystalline compound (**2**). Complex

References start on page 253

2 is insoluble in all common non-protic organic solvent and could not be characterized by spectroscopic means. The ^{1}H NMR spectrum of the hydrolysis product from compound **2** indicated the presence of one THF molecule for each ligand molecule. The stoichiometry YCl_3•THF•$(BDPP)H_2$ is advanced based on this result.

The reaction between complex **2** and 3.3 equiv of $ClMgCH_2SiMe_3$ in THF yields the previously characterized mono(alkyl) complex **3** in good yield. The addition of 3 equiv of $LiCH_2SiMe_3$ to a suspension of complex **2** in hexanes affords a dark purple solution and small amounts of compound **3**. The dark purple solution is similar to those obtained upon addition of *n*-BuLi to compound **1a** and result from abstraction of the CH_2N proton of the ligand. Similar results are obtained upon addition of $Li(CH_2C_6H_4$-*o*-$NMe_2)$ or NaCp•DME.

The addition of excess MeMgBr to a suspension of compound **2** in diethylether results in a rapid color change to light yellow. The reaction products are stable in coordinating solvents such as Et_2O or THF but gas evolution (likely methane) is observed upon addition of toluene or benzene. Attempts to synthesis the Ph or CH_2Ph derivatives from compound **3** and PhMgCl or $PhCH_2MgCl$ were unsuccessful.

It is clear from these results that the pyridine diamide ligand bearing the 2,6-diisopropylphenyl substituents does not efficiently stabilize yttrium complexes. This can be interpreted as a consequence of the large covalent radius of yttrium (1.78 Å)[35]. From single crystal X-ray analysis (see previous chapters), the average distance between the amide groups is approximately 2.48 Å {Figure 4- 3(I)}. A small metal such as titanium (cov. rad. 1.21 Å)[35] is located in between the amides and is sterically protected {Figure 4- 3(II)}. The slightly larger zirconium (cov. rad. 1.34 Å)[35] also fits between the two amides but is pulled out slightly resulting in a longer pyridine-nitrogen-metal bond (2.265 Å compared to 2.178 Å for Ti) {Figure 4- 3(III)}. For a large metal atom such as yttrium, the metal atom is too large to be located

References start on page 253

between the amide groups. In order to remain within bonding distance to the pyridine nitrogen, the metal atom must slip out of the protective pocket {Figure 4- 3(IV)}.

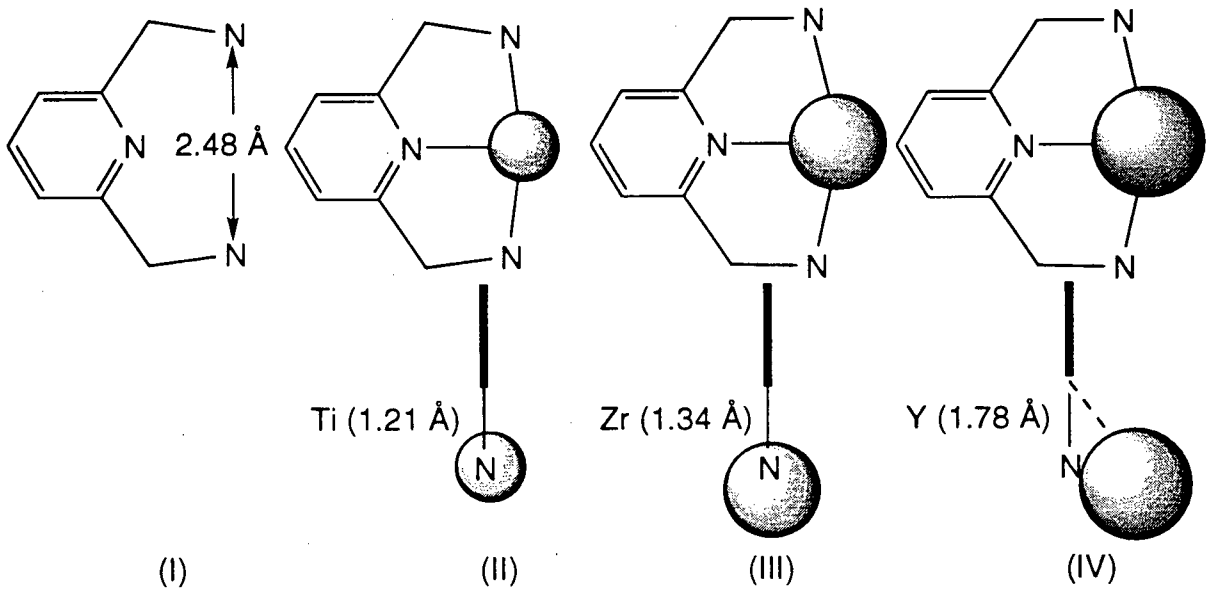

Figure 4- 3. Size of the metal vs coordination geometry

Attempts to synthesized the scandium complexes (BDPP)$ScCH_2SiMe_3$•L (L = THF, Et_2O) were unsuccessful partly due to the lack of a suitable starting material. For example, the tris(alkyl) complex $Sc(CH_2SiMe_3)_3$•2THF[36],which is stable at temperatures below 0 °C, does not react with the diamine **1a** at low temperature. Interestingly, the linked Cp-amine ligand {$Cp(H)(CH_2CH_2NMe_2)SiMe_2NR(H)$} reacts cleanly with $Sc(CH_2SiMe_3)_3$•2THF[37]. In this case, as a result of its lower pk_a (ca. 16[38]), the CpH reacts easily with the metal centre. In the pyridine diamine case, the high pk_a (ca. 38[38]) of the amine groups render the alkane elimination more difficult and the scandium starting material decomposes when the reaction mixture is allowed to warm to room temperature. Similar results were obtained upon stirring the reaction mixture at 0°C for a prolonged period of time (18 hours). Moreover, the coordinated solvent molecules in $ScCl_3$•3THF are not labile and the formation of ligand adducts as described earlier for yttrium was not possible.

References start on page 253

3 Conclusions

The reaction between $Y(CH_2SiMe_3)_3$•2THF and $(BDPP)(H_2)$ affords the base adduct complex **3**. Alternatively, complex **3** can be synthesized by pre-coordination of the ligand to form the ligand adduct **2** followed by alkylation using an excess of $ClMgCH_2SiMe_3$. The ^1H NMR spectrum of complex **3** suggests rapid coordination-decoordination of the THF molecule. The THF molecule in complex **3** can be exchanged by crystallization in diethylether to form complex **4**. In contrast to complex **3**, the diethylether molecule in complex **4** is firmly bound to the yttrium centre.

Attempts to generates other yttrium alkyl derivatives bearing the pyridine diamide ligand were unsuccessful. The large covalent radius of yttrium forces the metal centre to slip out of the protective pocket created by the substituted aryl groups of the ligand.

As a result of the lack of a convenient starting material, the scandium complex $(BDPP)ScCH_2SiMe_3$•L (L = THF, Et_2O) was not synthesized.

References start on page 253

4 Experimental Details

General details. See chapter one for general details. The ligands (BDPP)(H_2) (**1a**) and (BDPP)($SiMe_3$)$_2$ (**1b**) were prepared as described in chapter one. The YCl_3 was purchased from Alfa and used as received. The YCl_3•3THF[39], Y(CH_2SiMe_3)•2THF[36] and $ScCl_3$•3THF[39] were prepared using previously reported synthesis.

Y($CH_2C_6H_4$-*o*-NMe_2)$_3$. To a THF suspension of YCl_3•3THF (2.000 g, 4.859 mmol) was added 3.3 equiv of Li($CH_2C_6H_4$-*o*-NMe_2) (2.260 g, 16.01 mmol) at -30 °C. The solution was stired at room temperature for 12 hours. The solvent was removed under vaccum to give a light yellow solid. The solid was extracted with toluene (2*50mL) and filtered. The volume was reduced to 15 mL and the solution cooled to -30 °C for 12 hours. White crystalline Y($CH_2C_6H_4$-*o*-NMe_2)$_3$ was isolated by filtration and dried under vaccum (1.720 g, 3.512 mmol, 72 %). ^{1}H NMR δ 7.06 (dd, 1H, Ph), 6.97 (m, 1H, Ph), 6.82 (dd, 1H, Ph), 6.65 (m, 1H, Ph), 2.09 (s, 6H, N*Me*$_2$), 1.62 (s, 2H, C*H*$_2$).

YCl_3{(BDPP)H_2}•THF (2). To a 1,2-dichlorobenzene solution (25 mL) of ligand **1a** (0.500 g, 1.092 mmol) was added one equiv of solid YCl_3•3THF (0.410 g, 1.000 mmol). The suspension was then heated in a 150 °C oil bath for 12 hours. The solution was cooled to 23 °C then added to 150 mL of cold hexanes resulting in immediate precipitation of a white solid. The solid (**2**) was isolated by filtration and was dried under vaccum at 60 °C for 12 hours (0.675 g, 0.928 mmol, 93 %). The ^{1}H NMR spectrum of the hydrolysis product from this solid indicates that one THF molecule remains in the complex.

(BDPP)Y(CH_2SiMe_3)•THF (3). Method A To an hexanes solution (15 mL) containing Y(CH_2SiMe_3)•2THF (0.100 g, 0.202 mmol) was added one equiv of the ligand **1a** (0.092 g, 0.202 mmol) at room temperature. The solution changed from colorless to orange and was stirred for 12 hours. The solution was filtered and the solvent removed under vaccum. The solid was dissolved in a minimum ammount of hexanes and 2 drops of THF were added to the

References start on page 253

solution. The solution was cooled to -30 °C for 12 hours. A white solid (**3**) was isolated by filtration and dried under vaccum (0.115 g, 0.163 mmol, 81 %).

Method B To a THF solution (25 mL) of compound **2** (0.500 g, 0.690 mmol) was added 3.3 equiv of a diethylether solution of Me_3SiCH_2MgCl (1.93 mL, 1.18 M, 2.28 mmol) at -30 °C. The solution was stirred at room temperature for 12 hours. The solvent was removed under vaccum. The solid was extracted with hexanes (3*25mL) and filtered. The solvent was reduced to 15 mL and 2 drops of THF were added to the solution. The solution was cool to -30 °C for 12 hours. A white solid (**3**) was isolated by filtration and dried under vaccum (.398 g, 0.566 mmol, 82 %). ^{1}H NMR δ 7.25-7.10 (m, 6H, Ar), 6.68 (t, 1H, py), 6.65 (d, 1H, py), 5.01 (br s, 4H, NCH_2), 4.02 (br s, 4H, CHMe$_2$), 3.22 (br s, 4H, THF), 1.35 (d s, 12H, CHMe_2), 1.28 (d, 12H, CHMe_2), 1.15 (br s, 4H, THF), 0.19 (s, 9H, CH_2SiMe_3), -0.38 (d, $^2J_{YH}$ = 3.6 Hz, 2H, CH_2SiMe$_3$).

(BDPP)Y(CH_2SiMe_3)•Et_2O (4). Complex **4** is obtained by recrystallisation of complex **3** from Et_2O. ^{1}H NMR δ 7.25-7.10 (m, 6H, Ar), 6.93 (t, 1H, py), (6.62 (d, 2H, py), 5.01 (AB quartet, $^2J_{HH}$ = 20.0 Hz, 4H, NCH_2), 4.58 (sept, 2H, CHMe$_2$), 3.53 (sept, 2H, CHMe$_2$), 2.80 (q, 4H, MeCH_2O), 1.53 (d, 6H, CHMe_2), 1.480 (d, 6H, CHMe_2), 1.17 (d, 6H, CHMe_2), 1.11 (d, 6H, CHMe_2), 0.23 (t, 6H, MeCH$_2$O), 0.21 (s, 9H, CH_2SiMe_3), -0.33 (d, $^2J_{YH}$ = 3.6 Hz, 2H, CH_2SiMe$_3$).

References start on page 253

5 References

(1) Ziegler, K. *Angew. Chem.* **1964**, *76*, 545.

(2) Ziegler, K.; Holzkamp, E.; Breil, H.; Martin, H. *Angew. Chem.* **1955**, *67*, 541.

(3) Ewen, J. A. *J. Am. Chem. Soc.* **1984**, *106*, 6355.

(4) Jordan, R. F.; Bajgur, C. S.; Willet, R.; Scott, B. *J. Am. Chem. Soc.* **1986**, *107*, 7410.

(5) Jordan, R. F.; Lapointe, R. E.; Bajgur, C. S.; Echols, S. F.; Willet, R. *J. Am. Chem. Soc.* **1987**, *109*, 4111.

(6) Jordan, R. F.; Bajgur, C. S.; Dasher, W. E.; Rheingold, A. L. *Organometallics* **1987**, *6*, 1041.

(7) Jordan, R. F.; Lapointe, R. E.; Bradley, P. K.; Baenziger, N. *Organometallics* **1989**, *8*, 2892.

(8) Jordan, R. F.; Bradley, P. K.; Lapointe, R. E.; Taylor, D. F. *New J. Chem.* **1990**, *14*, 505.

(9) Jordan, R. F.; Bradley, P. K.; Baensiger, N. C.; Lapointe, R. E. *J. Am. Chem. Soc.* **1990**, *112*, 1289.

(10) Jordan, R. F.; Lapointe, R. E.; Baenziger, N.; Hinch, G. D. *Organometallics* **1990**, *9*, 1539.

(11) Crowther, D. J.; Borkowsky, S. L.; Swenson, D.; Meyer, T. Y.; Jordan, R. F. *Organometallics* **1993**, *12*, 2897.

(12) Massey, A. G.; Park, A. J. *J. Organomet. Chem.* **1964**, *2*, 245.

(13) Chien, J. C. W.; Tsai, W.-M.; Rausch, M. D. *J. Am. Chem. Soc.* **1991**, *113*, 8570.

(14) Coutts, R. S. P.; Wailes, P. C. *J. Organomet. Chem.* **1970**, *25*, 117.

(15) Holton, J.; Lappert, M. F.; Ballard, D. G. H.; Pearce, R.; Atwood, J. L.; Hunter, W. E. *J. Chem. Soc., Dalton Trans.* **1979**, 54.

(16) Thompson, M. E.; Baxter, S. M.; Bulls, A. R.; Burger, B. J.; Nolan, M. C.; Santarsiero, B. D.; Schaefer, W. P.; Bercaw, J. E. *J. Am. Chem. Soc.* **1987**, *109*, 203.

References start on page 253

(17) Burger, B. J.; Thompson, M. E.; Cotter, W. D.; Bercaw, J. E. *J. Am. Chem. Soc.* **1990**, *112*, 1566.

(18) Evans, W. J.; Peterson, T. T.; Rausch, M. D.; Hunter, W. E.; Zhang, H.; Atwood, J. L. *Organometallics* **1985**, *4*, 554.

(19) Jeske, G.; Lauke, H.; Mauermann, H.; Swepston, P. N.; Schumann, H.; Marks, T. J. *J. Am. Chem. Soc.* **1985**, *107*, 8091.

(20) Watson, P. L.; Parshall, G. W. *Acc. Chem. Res.* **1985**, *18*, 51.

(21) Watson, P. L. *J. Am. Chem. Soc.* **1982**, *104*, 337.

(22) Schumann, H.; Rosenthal, E. C. E.; Kociok-Köhn, G.; Molander, G. A. *J. Organomet. Chem.* **1995**, *496*, 233.

(23) Schumann, H.; Messe-Marktscheffel, J. A.; Hahn, F. E. *J. Organomet. Chem.* **1990**, *390*, 301.

(24) Schumann, H.; Genthe, W.; Bruncks, N.; Pickardt, J. *Organometallics* **1982**, *1*, 1194.

(25) Evans, W. J.; Dominguez, R.; Hanusa, T. P. *Organometallics* **1986**, *5*, 263.

(26) Shapiro, P. J.; Bunel, E.; Schaefer, W. P.; Bercaw, J. E. *Organometallics* **1990**, *9*, 867.

(27) Bradley, D. C.; Copperthwaite, R. G.; Cotton, S. A.; Gibson, J. F.; Sales, K. D. *J. Chem. Soc., Dalton Trans.* **1973**, 191.

(28) Alyea, E. C.; Bradley, D. C.; Copperthwaite, R. G. *J. Chem. Soc., Dalton Trans.* **1973**, 185.

(29) Alyea, E. C.; Bradley, D. C.; Copperthwaite, R. G. *J. Chem. Soc., Dalton Trans.* **1972**, 1580.

(30) Ghotra, J. S.; Hursthouse, M. B.; Welch, W. J. *J. Chem. Soc., Chem. Commun.* **1973**, 669.

(31) Bradley, D. C.; Ghotra, J. S.; Hart, F. A. *J. Chem. Soc., Dalton Trans.* **1973**, 1021.

(32) Bradley, D. C.; Ghotra, J. S.; Hart, H. A. *J. Chem. Soc., Chem. Commun.* **1972**, 349.

References start on page 253

(33) Lappert, M. F.; Power, P. P.; Sanger, A. R.; Srivastava, R. C. *Metal and Metalloid amides: Synthesis, Structures and Physical and Chemical Properties*; John Wiley & Sons: Chichester, 1980.

(34) Bradley, D. C.; Copperthwaite, R. G. *J. Chem. Soc., Chem. Commun.* **1971**, 764.

(35) Cotton, F. A.; Wilkinson, G.; Gauss, P. L. *Basic Inorganic Chemistry*; 2nd ed.; Interscience: New York, 1387.

(36) Lappert, M. F.; Pearce, R. *J. Chem. Soc., Dalton Trans.* **1973**, 126.

(37) Mu, Y.; Piers, W. E.; MacQuarrie, D. C.; Zaworotko, M. J.; Jr., V. G. Y. *Organometallics* **1996**, *15*, 2720.

(38) March, J. *Advanced Organic Chemistry; Reactions, Mechanisms and Structure*; 3rd ed.; Jon Wiley & Sons: New York, 1985.

(39) Manzer, L. E. *Inorg. Synth.* **1982**, *21*, 135.

References start on page 253

Appendix

1 MO calculation results:

Input Control Parameters

EHT option : Normal EHT

Basis Contraction : ST0-3G

Parameter K : 1.7500

Request MOs : HOMO -9999 to LUMO +3

Calculate dipole moment

Net molecular charge = 0.0000 a.u.

Standard parameters are from file: Alvarez Collected Parameters.

Calculated Number of valence electrons = 56

Table 1. Character table for C_{2v}-symmetry

C_{2v}	E	C_2	$\sigma_v(xz)$	$\sigma_v'(yz)$		
A_1	1	1	1	1	z	x^2, y^2, z^2
A_2	1	1	-1	-1	R_z	xy
B_1	1	-1	1	-1	x, R_y	xz
B_2	1	-1	-1	1	y, R_x	yz

Table 2. Alavarez parameters

Element	Orbital	IP Ev	Coeff	exponent	Coeff	Exponent
H	1s	13.600		1.300		
C	2p	11.400		1.625		
	2s	21.400		1.625		
N	2p	13.400		1.950		
	2s	26.000		1.950		
Zr	4d	11.180	0.621	3.835	0.577	1.505
	5p	6.760		1.776		
	5s	9.870		1.817		

Table 3. Orbital energies and labels

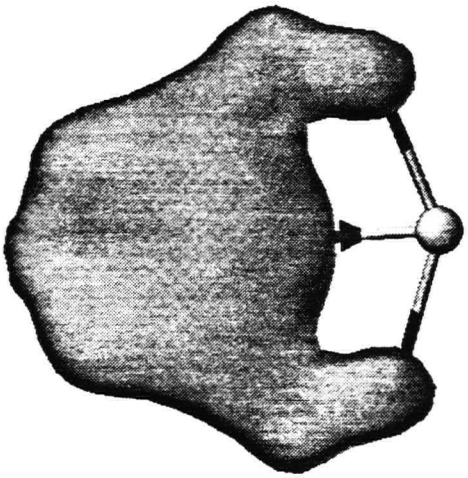

1, $1a_1$, -31.584 eV

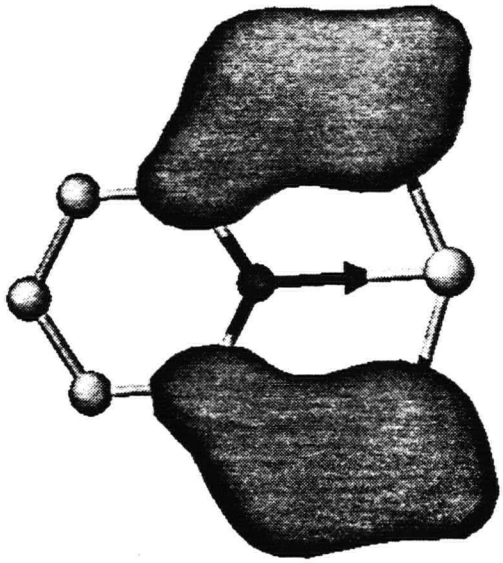

2, $1b_1$, -29.342 eV

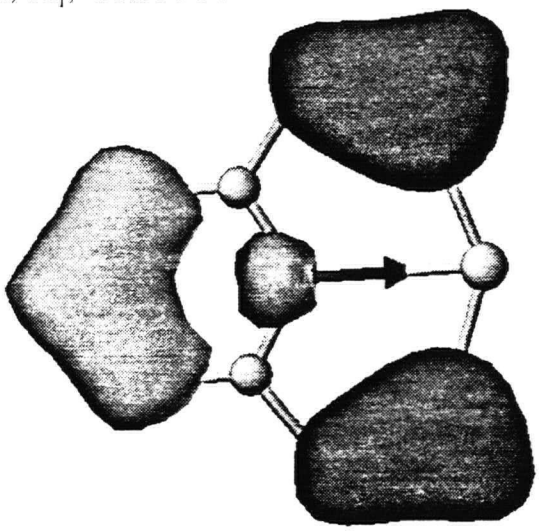

3, $2a_1$, -28.493 eV

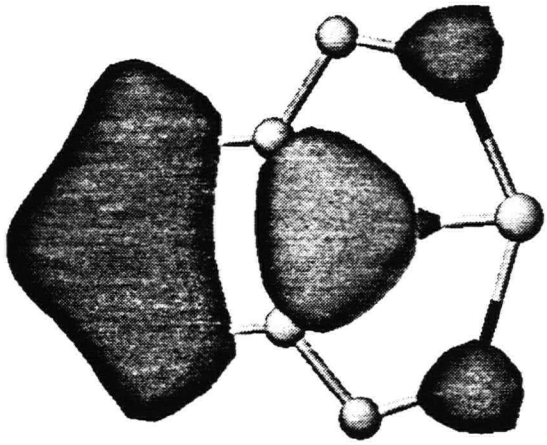

4, $3a_1$, -27.001 eV

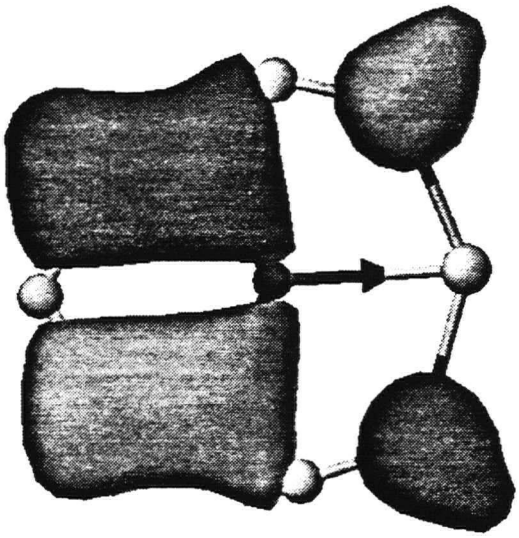

5, $2b_1$, -25.650 eV

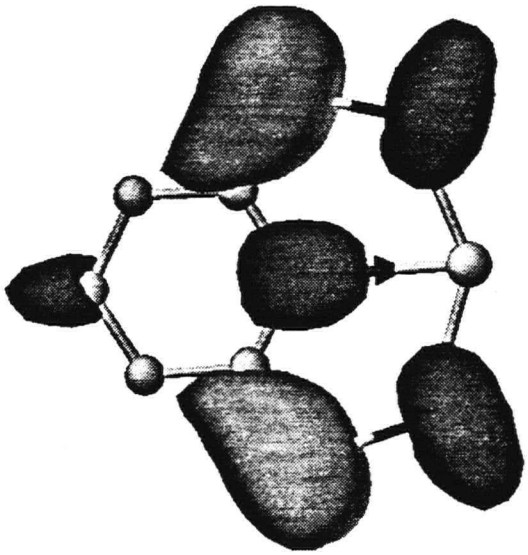

6, $4a_1$, -22.554eV

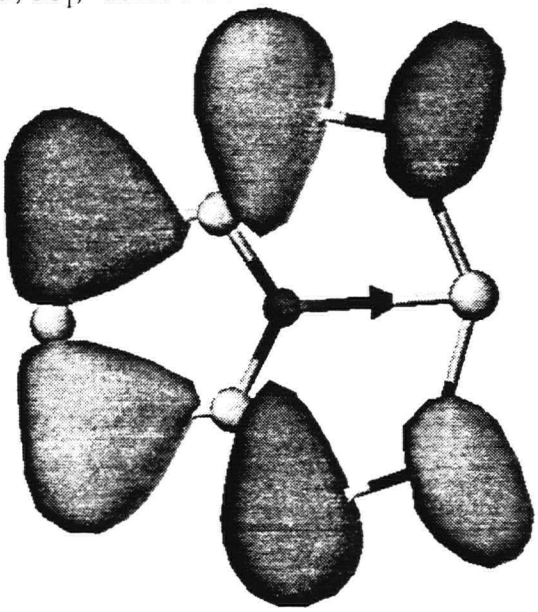

7, $3b_1$, -21.996 eV

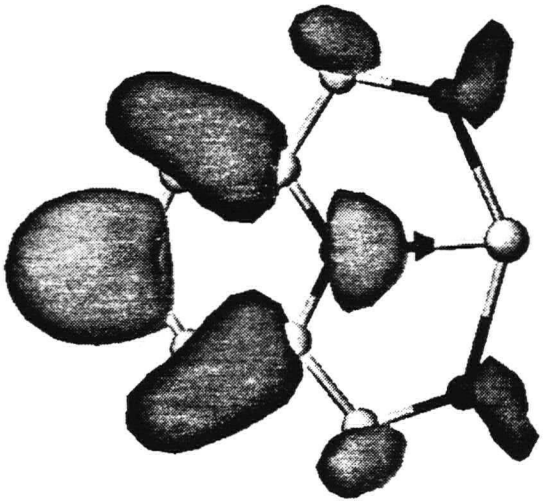

8, $5a_1$, -19.718 eV

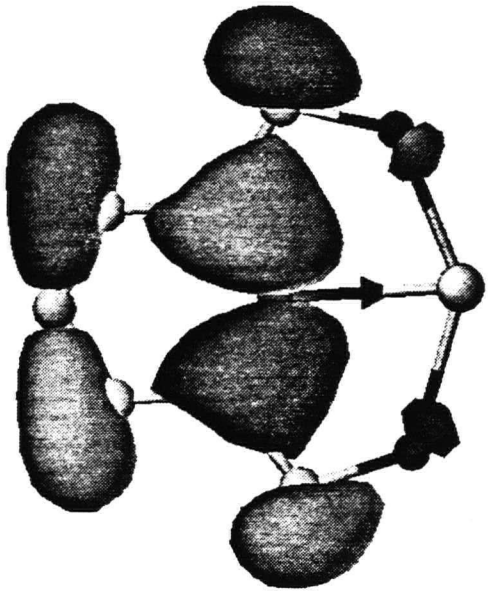

9, $4b_1$, -18.850 eV

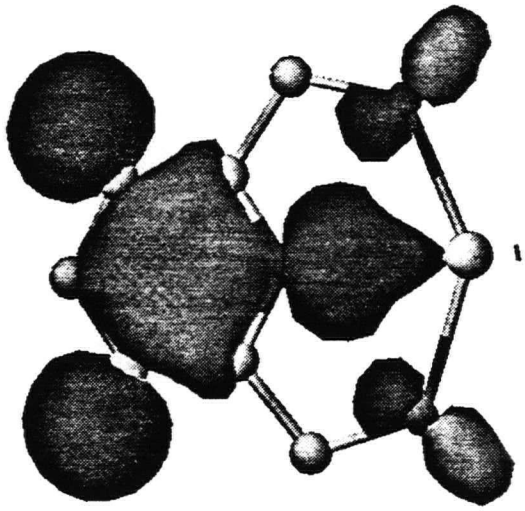

10, $6a_1$, -16.753 eV

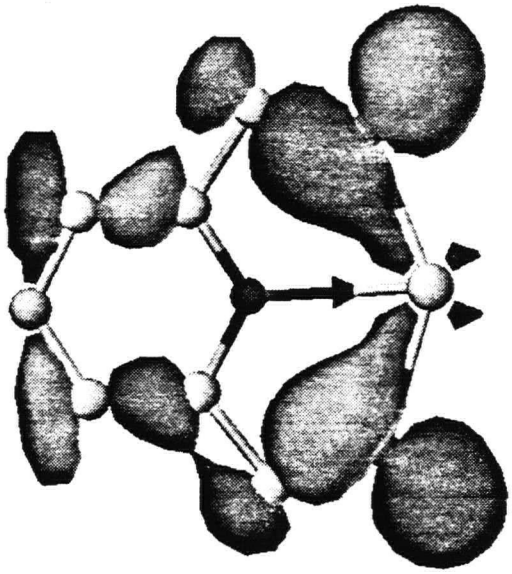

11, $5b_1$, -16.260 eV

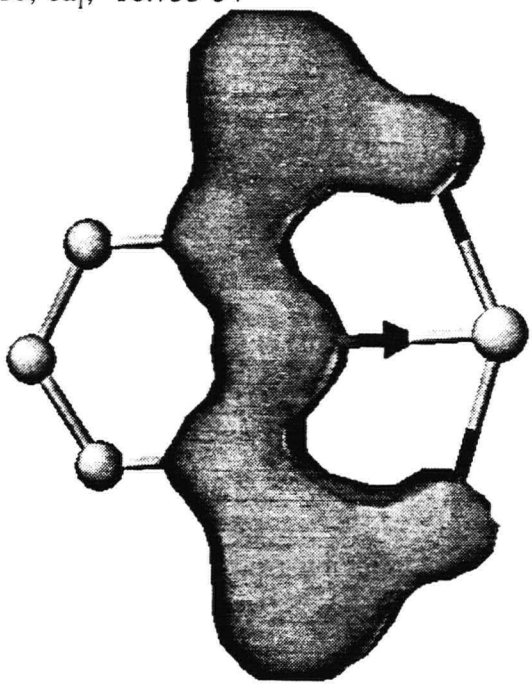

12, $1b_2$, -16.091 eV

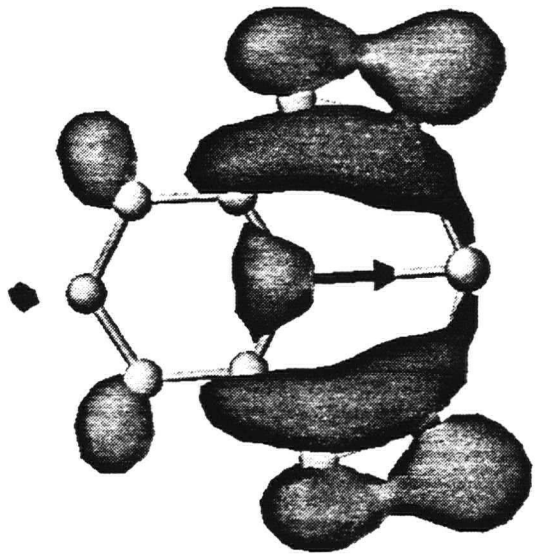

13, $7a_1$, -16.070 eV

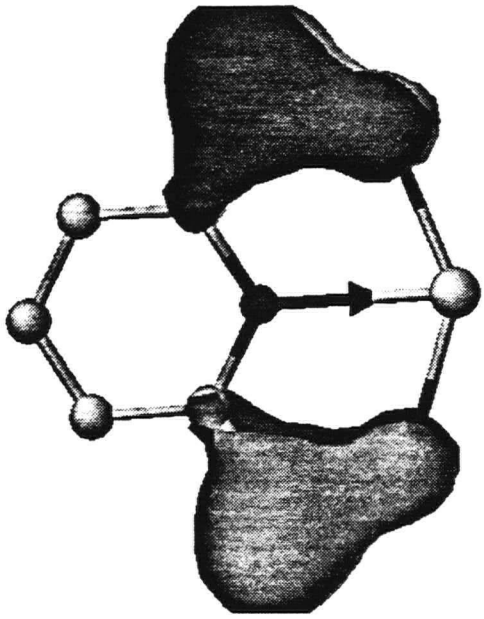

14, $1a_2$, -15.985 eV

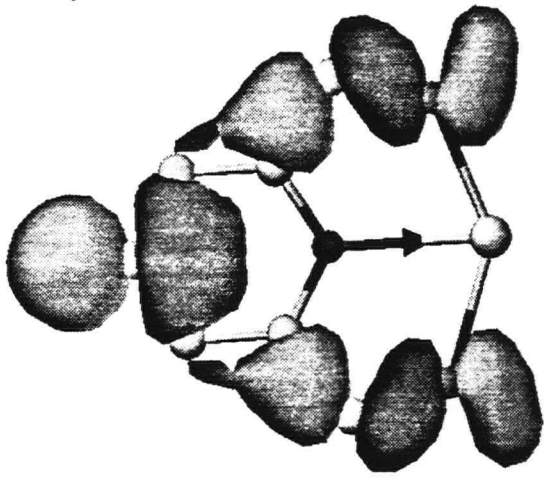

15, $8a_1$, -15.667 eV

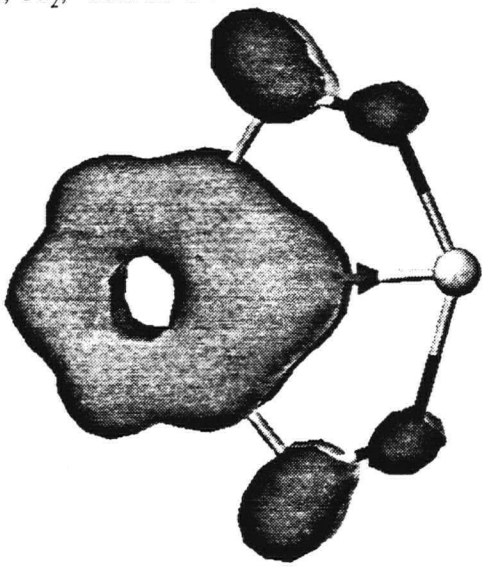

16, $2b_2$, -14.807 eV

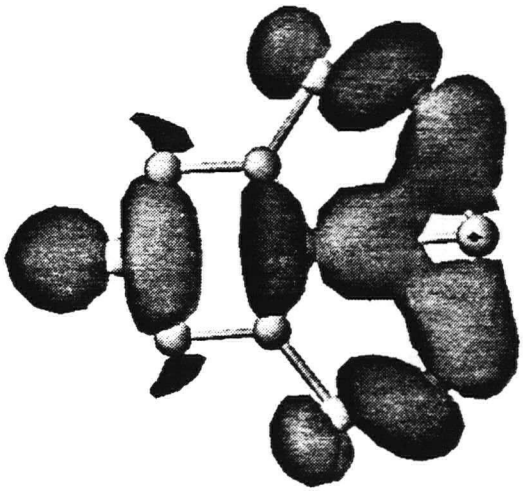

17, $9a_1$, -14.788 eV

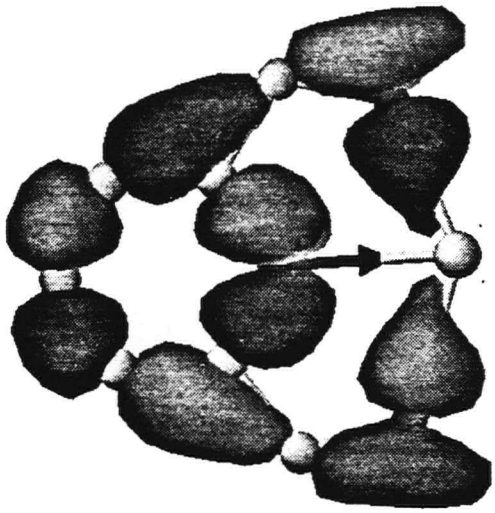

18, $5b_1$, -14.698 eV

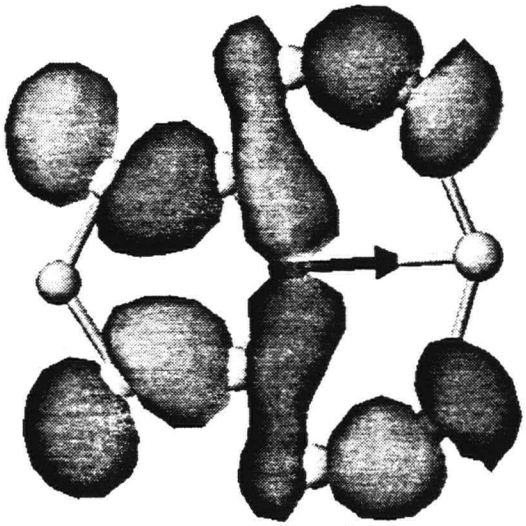

19, $6b_1$, -14.358 eV

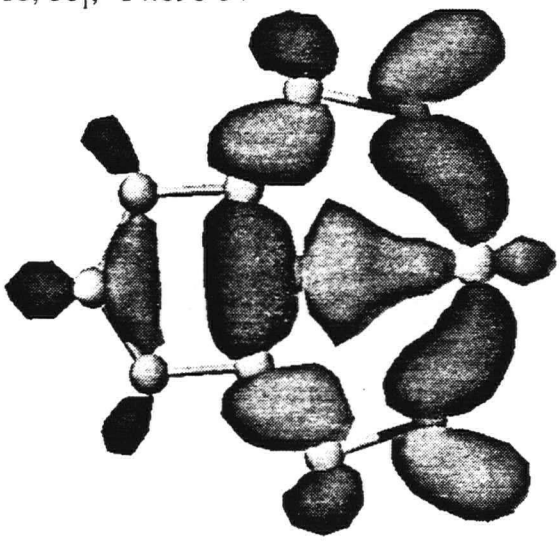

20, $10a_1$, -14.160 eV

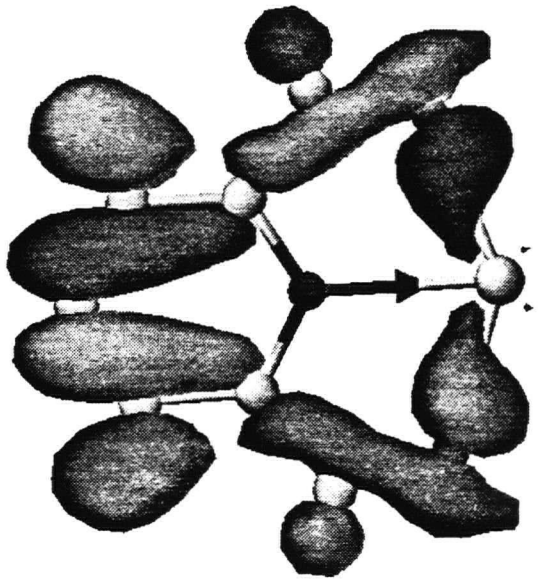

21, $8b_1$, -14.013 eV

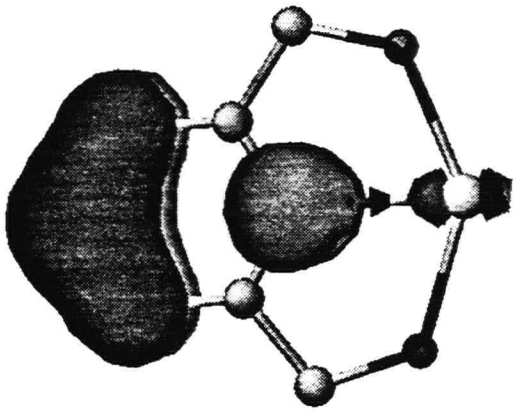

22, $3b_2$, -13.615 eV

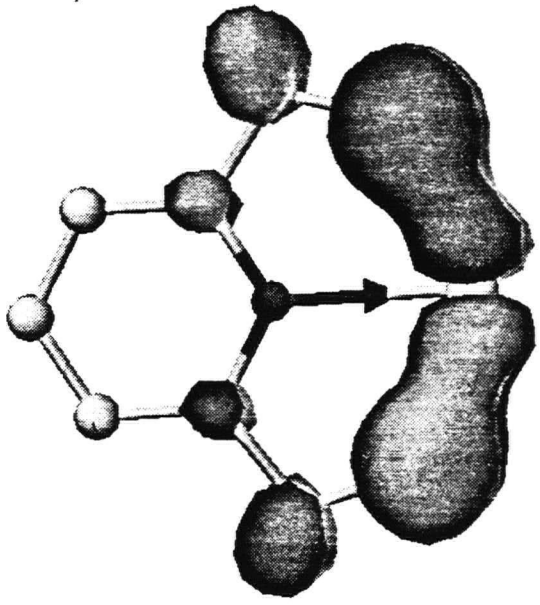

23, $2a_2$, -13.572 eV

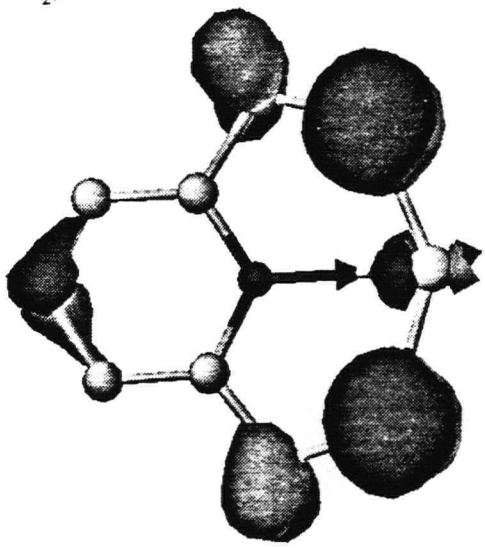

24, $4b_2$, -13.028 eV

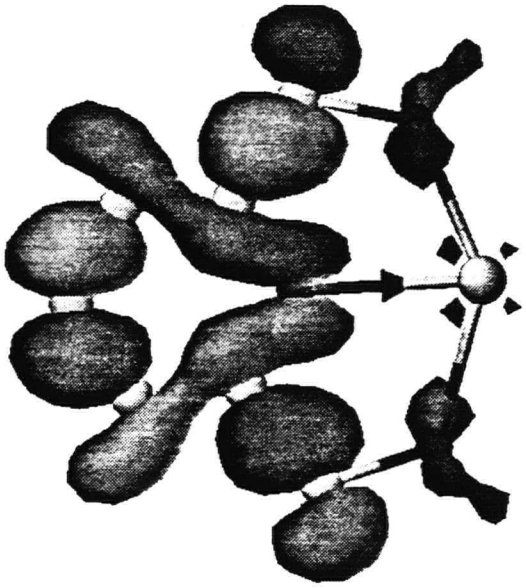

25, $9b_1$, -12.919 eV

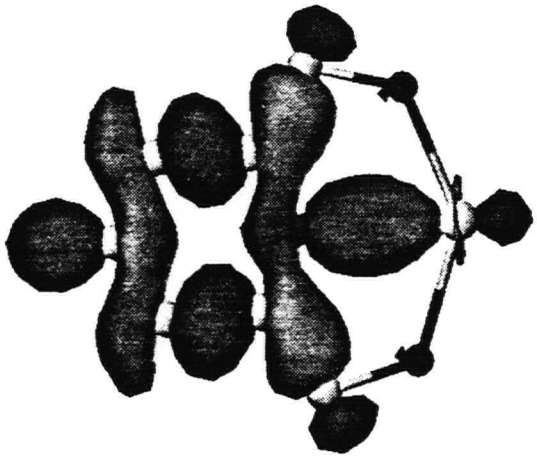

26, $11a_1$, -12.728 eV

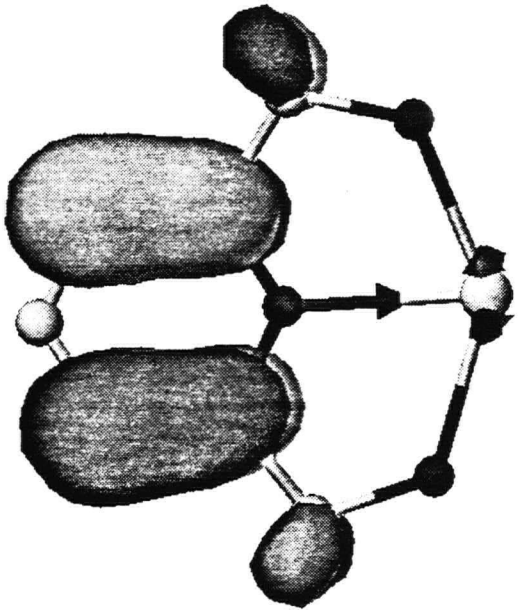

27, $3a_2$, -12.429 eV

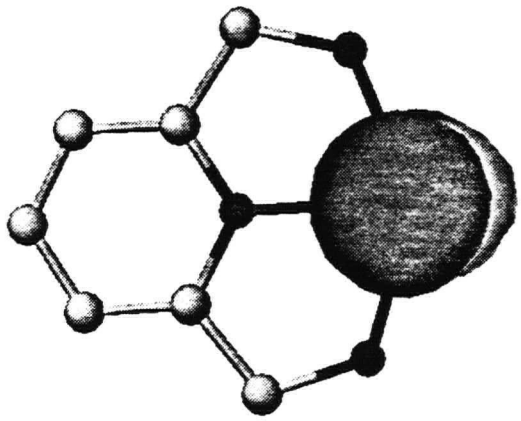

28, $12a_1$, -10.963 eV

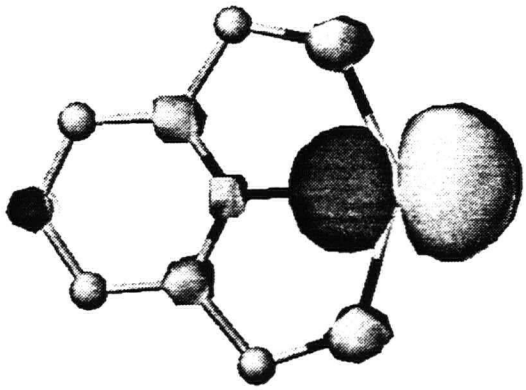

29, $5b_2$, -10.818 eV

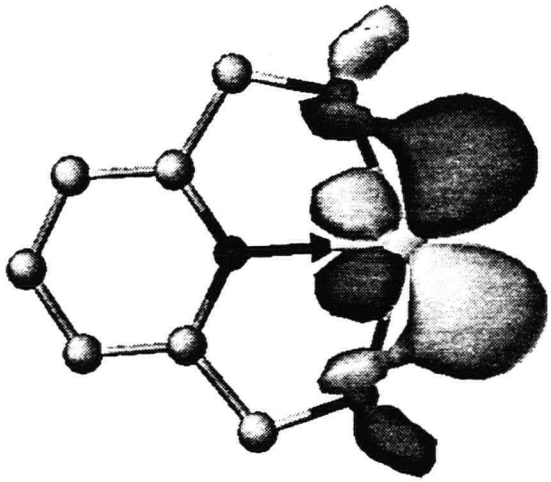

30, $10b_1$, -10.095 eV

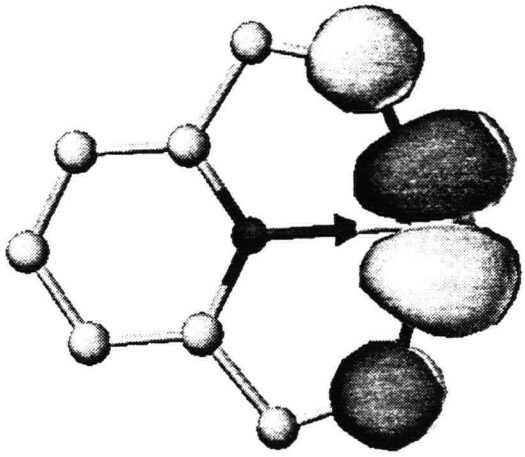

31, $4a_2$, -9.907 eV

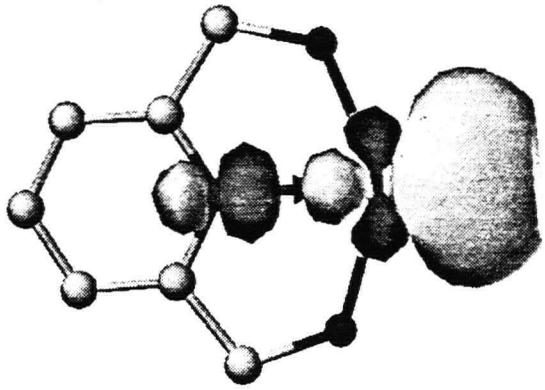

32, $13a_1$, -9.017 eV

2 Crystallographic data for (BDMP)TiBr(CH_2CMe_2Ph).

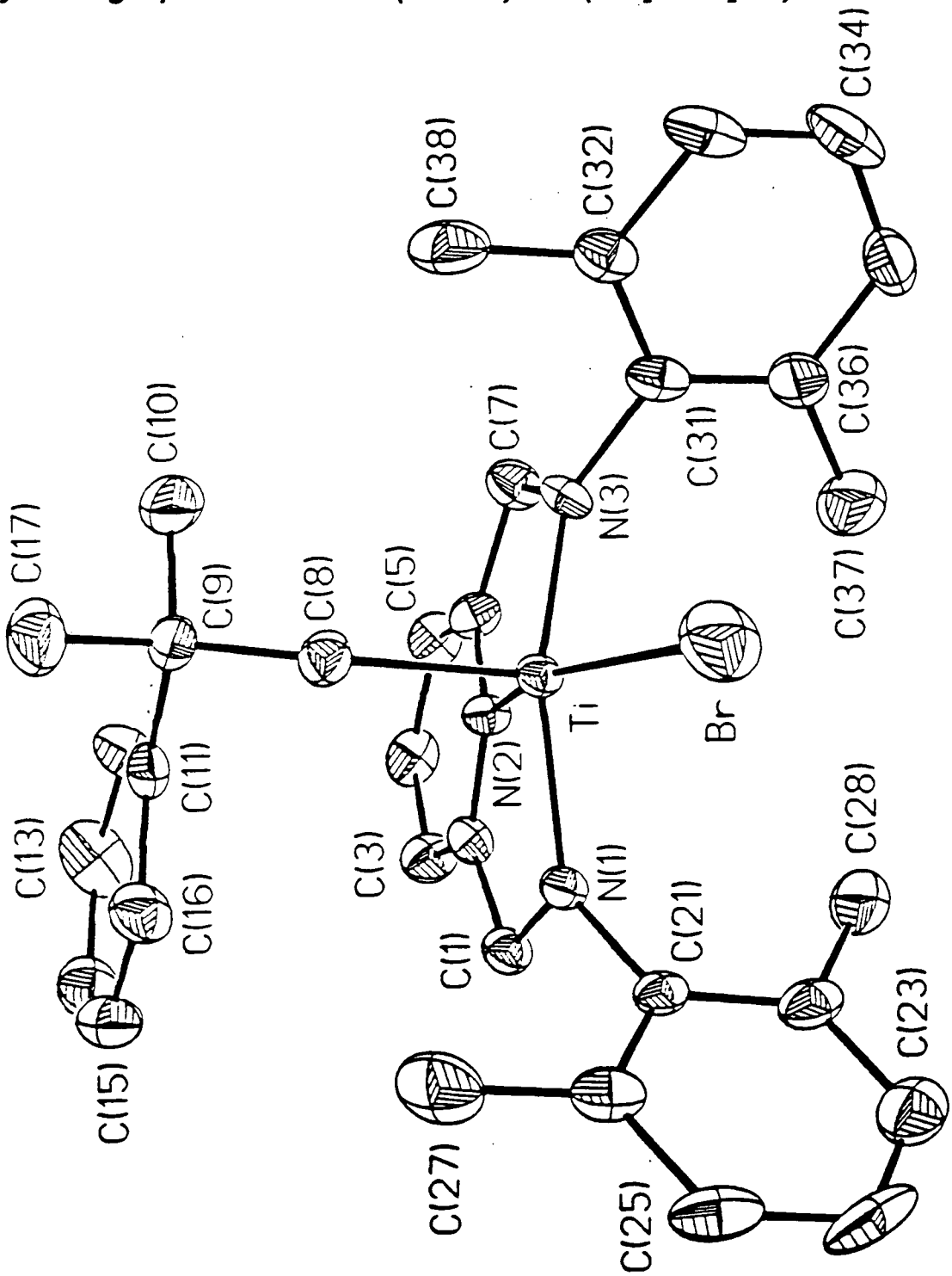

Table . Crystal data and structure refinement details.

Empirical formula	C_{39} H_{44} Br N_3 Ti
Formula weight	682.58
Temperature	298(2) K
Wavelength	0.71073 Å
Crystal system	monoclinic
Space group	$P2_1/n$
Unit cell dimensions	a = 14.892(2)Å b = 14.741(3)Å
	c = 16.080(3)Å β = 98.66(2)°
Volume	3489.8(12) $Å^3$
Z	4
Density (calculated)	1.299 Mg m^{-3}
Absorption coefficient	1.421 mm^{-1}
F(000)	1424
Crystal size	0.29 x 0.24 x 0.15 mm
θ range for data collection	1.74 to 24.97°
Index ranges	-1<=h<=17, -1<=k<=17, -19<=ℓ<=18
Reflections collected	7094
Independent reflections	6115 [R(int) = 0.0323]
Refinement method	Full-matrix least-squares on F^2
Data / restraints / parameters	6115 / 0 / 403
Goodness-of-fit on F^2	1.059
Final R indices [$I>2\sigma(I)$]	R_1 = 0.0706, wR_2 = 0.1869
R indices (all data)	R_1 = 0.1769, wR_2 = 0.2404
Largest diff. peak and hole	0.585 and -1.037 e $Å^{-3}$

Table . Atomic coordinates (x 10^4) and equivalent isotropic displacement parameters ($Å^2$ x 10^3).

Atom	x	y	z	U(eq)
Ti	5764(1)	-97(1)	2181(1)	23(1)
Br	5857(1)	1288(1)	1415(1)	62(1)
N(1)	5250(4)	411(4)	3147(3)	24(1)
N(2)	6130(4)	-1032(4)	3181(3)	27(1)
N(3)	6838(4)	-744(4)	1892(4)	31(2)
C(1)	5190(5)	-129(5)	3897(4)	30(2)
C(2)	5744(5)	-962(5)	3883(4)	27(2)
C(3)	5913(6)	-1620(6)	4507(5)	39(2)
C(4)	6500(6)	-2308(5)	4417(5)	40(2)
C(5)	6934(6)	-2335(5)	3713(5)	39(2)
C(6)	6748(5)	-1682(5)	3107(4)	32(2)
C(7)	7188(5)	-1573(5)	2339(5)	37(2)
C(8)	4631(5)	-758(5)	1480(4)	32(2)
C(9)	4274(5)	-1749(5)	1518(5)	32(2)
C(10)	4948(6)	-2394(6)	1253(6)	54(3)
C(17)	3408(6)	-1837(7)	865(5)	56(3)
C(11)	4011(5)	-1963(5)	2377(4)	31(2)
C(12)	4363(6)	-2694(6)	2851(5)	47(2)
C(13)	4062(7)	-2925(7)	3604(6)	62(3)
C(14)	3435(7)	-2411(7)	3906(6)	54(3)
C(15)	3081(6)	-1669(7)	3454(6)	53(2)
C(16)	3371(6)	-1447(6)	2699(5)	43(2)
C(21)	5045(5)	1344(5)	3284(4)	26(2)
C(22)	5727(6)	1916(5)	3662(5)	37(2)
C(23)	5533(7)	2799(6)	3826(5)	51(2)
C(24)	4670(8)	3119(6)	3618(6)	61(3)
C(25)	3991(7)	2579(6)	3241(5)	49(2)
C(26)	4158(6)	1682(6)	3064(5)	39(2)
C(27)	3399(6)	1087(7)	2662(6)	59(3)
C(28)	6689(6)	1579(7)	3882(6)	53(2)

Atom	x	y	z	U(eq)
C(31)	7450(5)	-424(5)	1347(4)	31(2)
C(32)	7304(5)	-635(5)	486(5)	36(2)
C(33)	7947(6)	-332(6)	-3(5)	45(2)
C(34)	8691(7)	140(6)	323(7)	58(3)
C(35)	8829(6)	351(6)	1163(7)	54(3)
C(36)	8211(5)	75(6)	1689(5)	43(2)
C(37)	8377(6)	337(7)	2599(6)	64(3)
C(38)	6500(6)	-1183(7)	101(5)	53(3)
C(41)	3504(14)	4998(17)	208(15)	135(7)
C(42)	3512(15)	5312(11)	1002(19)	138(8)
C(43)	4001(16)	4831(18)	1641(13)	143(10)
C(44)	4418(11)	4072(16)	1437(12)	125(6)
C(45)	4401(11)	3820(12)	661(12)	111(5)
C(46)	3955(13)	4269(16)	85(10)	122(6)

U(eq) is defined as one third of the trace of the orthogonalized U_{ij} tensor.

Table . Anisotropic displacement parameters ($Å^2 \times 10^3$).

Atom	U_{11}	U_{22}	U_{33}	U_{23}	U_{13}	U_{12}
Ti	26(1)	24(1)	22(1)	3(1)	7(1)	1(1)
Br	70(1)	57(1)	63(1)	12(1)	20(1)	-3(1)
N(1)	25(3)	25(3)	25(3)	1(3)	9(3)	2(3)
N(2)	31(3)	25(3)	26(3)	1(3)	8(3)	5(3)
N(3)	25(3)	40(4)	32(3)	2(3)	14(3)	-1(3)
C(1)	33(4)	32(4)	28(4)	3(3)	11(3)	0(4)
C(2)	28(4)	30(4)	24(4)	7(3)	5(3)	0(3)
C(3)	52(5)	44(5)	23(4)	4(4)	10(4)	1(4)
C(4)	54(5)	29(5)	38(5)	10(4)	2(4)	2(4)
C(5)	42(5)	26(4)	49(5)	9(4)	6(4)	10(4)
C(6)	35(4)	30(4)	30(4)	-1(3)	3(3)	7(4)
C(7)	34(5)	35(5)	44(5)	6(4)	12(4)	8(4)
C(8)	35(4)	34(5)	27(4)	-3(3)	3(3)	-5(4)
C(9)	34(4)	30(4)	32(4)	-4(3)	4(4)	-5(4)
C(10)	74(7)	39(5)	56(6)	-10(4)	30(5)	-15(5)
C(17)	55(6)	76(7)	36(5)	-5(5)	4(4)	-29(5)
C(11)	24(4)	32(4)	34(4)	-2(4)	-1(3)	-5(4)
C(12)	38(5)	53(6)	51(5)	7(5)	16(4)	4(4)
C(13)	55(6)	65(7)	63(6)	32(6)	6(5)	5(6)
C(14)	59(6)	67(7)	41(5)	-1(5)	17(5)	-15(6)
C(15)	56(6)	52(6)	57(6)	-12(5)	29(5)	-5(5)
C(16)	46(5)	39(5)	48(5)	6(4)	18(4)	-2(4)
C(21)	33(4)	25(4)	21(3)	1(3)	8(3)	3(3)
C(22)	56(6)	32(5)	27(4)	-1(4)	16(4)	4(4)
C(23)	71(7)	48(6)	37(5)	-3(4)	17(5)	-4(5)
C(24)	111(9)	27(5)	48(6)	-7(4)	20(6)	24(6)
C(25)	57(6)	48(6)	45(5)	1(5)	15(5)	27(5)
C(26)	44(5)	43(5)	31(4)	4(4)	12(4)	12(4)
C(27)	39(5)	71(7)	67(6)	2(5)	5(5)	18(5)
C(28)	44(5)	56(6)	60(6)	-20(5)	7(5)	-10(5)
C(31)	35(4)	28(4)	32(4)	8(3)	12(3)	14(4)
C(32)	35(5)	34(5)	41(5)	5(4)	12(4)	10(4)
C(33)	48(6)	50(6)	43(5)	14(4)	26(4)	17(5)
C(34)	58(6)	46(6)	84(7)	20(5)	51(6)	11(5)
C(35)	43(6)	36(5)	90(8)	-6(5)	31(5)	-8(4)
C(36)	36(5)	35(5)	62(5)	-4(4)	18(4)	8(4)
C(37)	52(6)	74(7)	64(6)	-22(5)	7(5)	-8(6)
C(38)	55(6)	78(7)	28(4)	-5(5)	9(4)	7(5)
C(41)	129(17)	128(18)	146(18)	54(15)	16(14)	-36(14)
C(42)	149(19)	52(10)	233(26)	-21(14)	88(20)	-53(11)
C(43)	160(21)	165(23)	121(16)	-78(16)	77(15)	-97(18)
C(44)	97(12)	176(20)	99(13)	33(13)	7(10)	-57(13)
C(45)	110(12)	135(14)	90(11)	-16(11)	23(10)	23(11)
C(46)	133(15)	159(18)	70(10)	-22(12)	-2(10)	16(13)

The anisotropic displacement factor exponent takes the form:
$-2\pi^2 [h^2 a^{*2} U_{11} + ... + 2 h k a^* b^* U_{12}]$

Table . Bond lengths [Å] and angles [°].

Ti-N(3)	1.977(6)	Ti-N(1)	1.979(5)
Ti-C(8)	2.121(7)	Ti-N(2)	2.126(6)
Ti-Br	2.399(2)	N(1)-C(21)	1.433(9)
N(1)-C(1)	1.458(8)	N(2)-C(2)	1.344(9)
N(2)-C(6)	1.346(9)	N(3)-C(31)	1.435(9)
N(3)-C(7)	1.473(9)	C(1)-C(2)	1.481(10)
C(2)-C(3)	1.391(10)	C(3)-C(4)	1.361(11)
C(4)-C(5)	1.385(11)	C(5)-C(6)	1.369(10)
C(6)-C(7)	1.491(10)	C(8)-C(9)	1.558(10)
C(9)-C(10)	1.490(11)	C(9)-C(11)	1.525(10)
C(9)-C(17)	1.542(10)	C(11)-C(12)	1.377(11)
C(11)-C(16)	1.380(11)	C(12)-C(13)	1.396(11)
C(13)-C(14)	1.347(13)	C(14)-C(15)	1.375(13)
C(15)-C(16)	1.386(11)	C(21)-C(22)	1.387(11)
C(21)-C(26)	1.407(10)	C(22)-C(23)	1.368(12)
C(22)-C(28)	1.507(12)	C(23)-C(24)	1.363(13)
C(24)-C(25)	1.355(13)	C(25)-C(26)	1.383(11)
C(26)-C(27)	1.498(12)	C(31)-C(36)	1.392(11)
C(31)-C(32)	1.404(10)	C(32)-C(33)	1.401(11)
C(32)-C(38)	1.498(11)	C(33)-C(34)	1.346(13)
C(34)-C(35)	1.370(13)	C(35)-C(36)	1.402(11)
C(36)-C(37)	1.498(11)	C(41)-C(46)	1.30(2)
C(41)-C(42)	1.36(2)	C(42)-C(43)	1.37(3)
C(43)-C(44)	1.34(2)	C(44)-C(45)	1.30(2)
C(45)-C(46)	1.25(2)		

N(3)-Ti-N(1)	142.1(2)	N(3)-Ti-C(8)	105.1(3)
N(1)-Ti-C(8)	102.7(3)	N(3)-Ti-N(2)	75.0(2)
N(1)-Ti-N(2)	74.7(2)	C(8)-Ti-N(2)	101.4(3)
N(3)-Ti-Br	100.3(2)	N(1)-Ti-Br	98.1(2)
C(8)-Ti-Br	102.8(2)	N(2)-Ti-Br	155.8(2)
C(21)-N(1)-C(1)	110.9(5)	C(21)-N(1)-Ti	126.8(4)
C(1)-N(1)-Ti	121.4(4)	C(2)-N(2)-C(6)	120.9(6)
C(2)-N(2)-Ti	119.4(5)	C(6)-N(2)-Ti	119.7(5)

C(31)-N(3)-C(7)	111.1(6)	C(31)-N(3)-Ti	126.5(5)
C(7)-N(3)-Ti	121.7(5)	N(1)-C(1)-C(2)	109.7(6)
N(2)-C(2)-C(3)	119.9(7)	N(2)-C(2)-C(1)	112.7(6)
C(3)-C(2)-C(1)	127.4(7)	C(4)-C(3)-C(2)	119.5(7)
C(3)-C(4)-C(5)	119.7(7)	C(6)-C(5)-C(4)	119.5(7)
N(2)-C(6)-C(5)	120.3(7)	N(2)-C(6)-C(7)	112.9(6)
C(5)-C(6)-C(7)	126.7(7)	N(3)-C(7)-C(6)	109.0(6)
C(9)-C(8)-Ti	131.2(5)	C(10)-C(9)-C(11)	113.7(7)
C(10)-C(9)-C(17)	106.4(7)	C(11)-C(9)-C(17)	107.3(6)
C(10)-C(9)-C(8)	109.8(6)	C(11)-C(9)-C(8)	111.4(6)
C(17)-C(9)-C(8)	107.9(6)	C(12)-C(11)-C(16)	116.8(7)
C(12)-C(11)-C(9)	122.3(7)	C(16)-C(11)-C(9)	120.8(7)
C(11)-C(12)-C(13)	121.7(8)	C(14)-C(13)-C(12)	120.4(9)
C(13)-C(14)-C(15)	119.2(9)	C(14)-C(15)-C(16)	120.4(9)
C(11)-C(16)-C(15)	121.4(8)	C(22)-C(21)-C(26)	119.5(7)
C(22)-C(21)-N(1)	119.5(7)	C(26)-C(21)-N(1)	121.0(7)
C(23)-C(22)-C(21)	120.1(8)	C(23)-C(22)-C(28)	119.2(8)
C(21)-C(22)-C(28)	120.7(7)	C(24)-C(23)-C(22)	120.0(9)
C(25)-C(24)-C(23)	121.2(9)	C(24)-C(25)-C(26)	120.6(9)
C(25)-C(26)-C(21)	118.5(8)	C(25)-C(26)-C(27)	120.2(8)
C(21)-C(26)-C(27)	121.3(7)	C(36)-C(31)-C(32)	120.1(7)
C(36)-C(31)-N(3)	119.1(7)	C(32)-C(31)-N(3)	120.7(7)
C(33)-C(32)-C(31)	117.8(8)	C(33)-C(32)-C(38)	120.8(7)
C(31)-C(32)-C(38)	121.5(7)	C(34)-C(33)-C(32)	122.6(8)
C(33)-C(34)-C(35)	119.6(8)	C(34)-C(35)-C(36)	120.9(9)
C(31)-C(36)-C(35)	119.0(8)	C(31)-C(36)-C(37)	121.8(7)
C(35)-C(36)-C(37)	119.2(8)	C(46)-C(41)-C(42)	120(2)
C(41)-C(42)-C(43)	117(2)	C(44)-C(43)-C(42)	118(2)
C(45)-C(44)-C(43)	122(2)	C(46)-C(45)-C(44)	120(2)
C(45)-C(46)-C(41)	124(2)		

Table . Hydrogen atom coordinates (x 10^4) and isotropic displacement parameters ($Å^2$ x 10^3).

Atom	x	y	z	U(eq)
H(1A)	4562	-291	3914	33
H(1B)	5409	223	4396	33
H(3)	5628	-1590	4982	43
H(4)	6610	-2757	4825	45
H(5)	7348	-2794	3653	43
H(7A)	7842	-1530	2496	41
H(7B)	7056	-2096	1975	41
H(8A)	4116	-382	1558	36
H(8B)	4713	-675	898	36
H(10A)	5086	-2219	711	60
H(10B)	4699	-2995	1222	60
H(10C)	5493	-2382	1657	60
H(17A)	2951	-1430	1008	62
H(17B)	3187	-2449	862	62
H(17C)	3545	-1687	317	62
H(12)	4813	-3043	2664	51
H(13)	4294	-3436	3900	68
H(14)	3245	-2557	4415	60
H(15)	2645	-1313	3655	58
H(16)	3128	-939	2404	47
H(23)	5991	3181	4080	56
H(24)	4544	3719	3737	67
H(25)	3409	2814	3101	54
H(27A)	3600	475	2673	65
H(27B)	3218	1271	2095	65
H(27C)	2898	1138	2961	65
H(27D)	2878	1448	2480	65
H(27E)	3260	651	3058	65
H(27F)	3580	785	2192	65

Atom	x	y	z	U(eq)
H(28A)	6750	1017	3608	59
H(28B)	6828	1498	4474	59
H(28C)	7094	2010	3704	59
H(28D)	7031	2000	4249	59
H(28E)	6953	1519	3383	59
H(28F)	6688	1006	4153	59
H(33)	7856	-461	-576	49
H(34)	9108	322	-19	64
H(35)	9340	683	1387	60
H(37A)	8948	632	2722	70
H(37B)	8376	-191	2937	70
H(37C)	7911	737	2714	70
H(37D)	7875	154	2860	70
H(37E)	8447	977	2645	70
H(37F)	8913	49	2868	70
H(38A)	6344	-1025	-475	59
H(38B)	6001	-1062	389	59
H(38C)	6647	-1810	146	59
H(38D)	6317	-1573	515	59
H(38E)	6660	-1536	-349	59
H(38F)	6014	-788	-106	59
H(41)	3179	5304	-246	149
H(42)	3196	5834	1107	152
H(43)	4045	5022	2197	157
H(44)	4727	3716	1865	137
H(45)	4721	3308	536	122
H(46)	3943	4069	-465	135

3 Crystallographic data for (BDPP)Ti($C_4\alpha,\beta'$-($SiMe_3$)H_2).

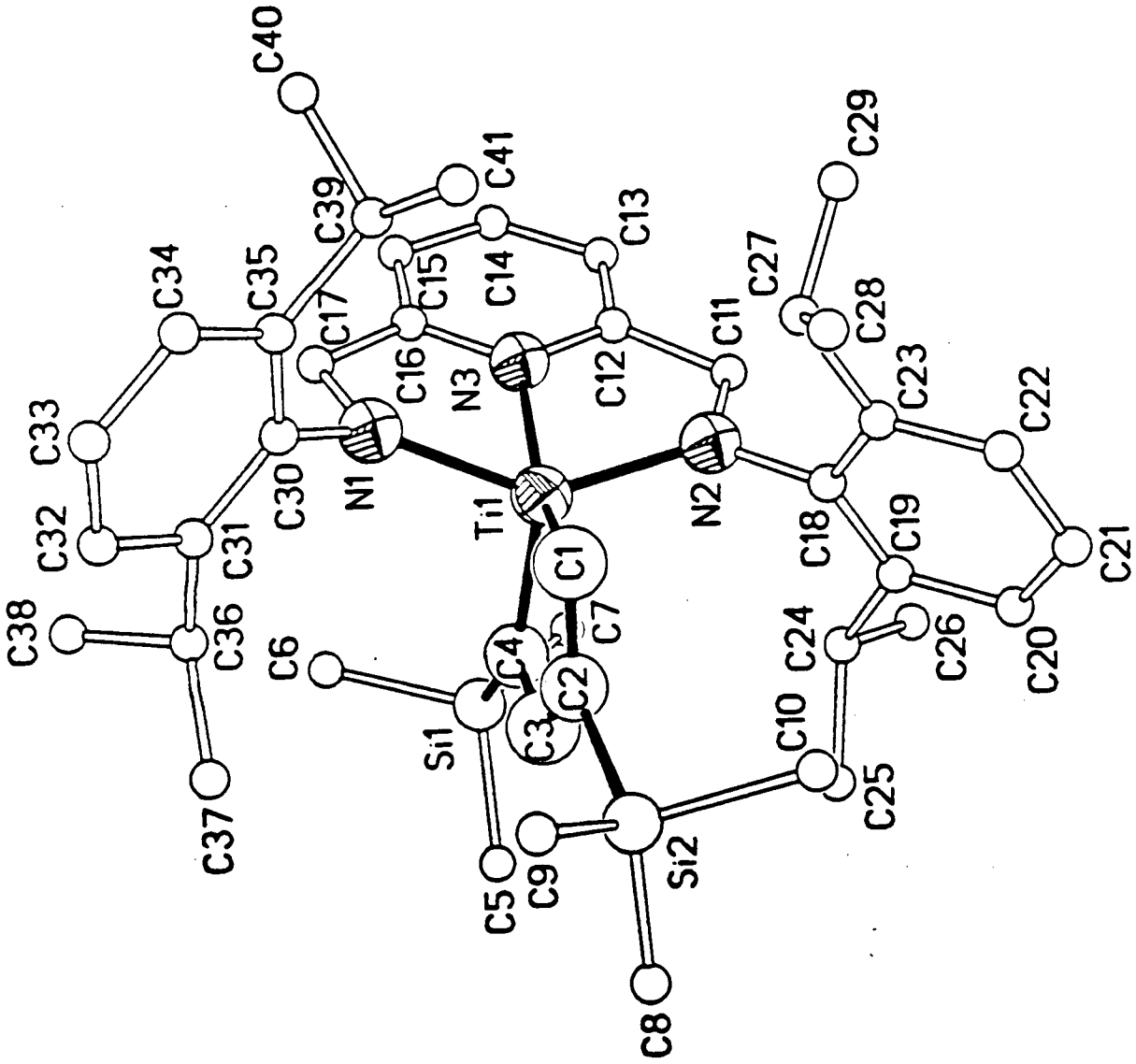

Table S1. Crystal Data and Experimental Details.

Empirical formula	$C_{41}H_{61}N_3Si_2Ti_1$
Formula weight	700.01
Temperature	25°C
Wavelength	0.71073 A
Crystal system	Monoclinic
Space group	$P2_1/n$
Unit cell dimensions	a = 10.630(3)A
	b = 36.650(9)A
	c = 12.200(4)A
	β = 110.73(2)°
Volume	4445(2) A^3
Z	4
Density, calcd.	1.046 $g.cm^{-3}$
Absorption coefficient	0.274 mm^{-1}
F(000)	1512
Reflections Collected	6646
Independent reflections	5362 [R(int) = 0.0921]
Refinement method	Full-matrix least-squares on F^2
Data/restraints/parameters	1848/127/258
Goodness-of-fit (GooF) on F^2	0.996
Final R indices [I>2sigma(I)]	R1 = 0.1017, wR2 = 0.2030
R indices (all data)	R1 = 0.2750, wR2 = 0.2733

$R1 = \Sigma(|F_o| - |F_c|)/\Sigma|F_o|$;

$wR2 = [\Sigma w(F_o^2 - F_c^2)^2/\Sigma wF_o^4]^{1/2}$

$GooF = [\Sigma w(F_o^2 - F_c^2)^2/(n-p)]^{1/2}$

where n is the number of reflections and p is the number of parameters refined.

Table S2. Atomic coordinates (x 10^4) and equivalent isotropic displacement parameters (A^2 x 10^3). U(eq) is defined as one third of the trace of the orthogonalized Uij tensor.

atom	x	y	z	Ueq
Ti(1)	5915.8(19)	1110.0(5)	2385.1(16)	47.1(6)
Si(1)	2511(4)	1474(1)	782(3)	74(1)
Si(2)	7730(4)	2171(1)	2116(4)	101(2)
N(1)	5975(8)	754(2)	1173(7)	50(2)
N(2)	5953(8)	1134(2)	4042(6)	46(2)
C(1)	7552(12)	1421(3)	2488(9)	60(3)
C(2)	6812(11)	1720(3)	2041(9)	51(3)
C(3)	5251(11)	1730(3)	1515(9)	67(4)
C(4)	4367(10)	1458(3)	1472(8)	51(3)
C(5)	1868(13)	1945(3)	279(13)	151(7)
C(6)	1970(13)	1168(4)	-527(10)	135(6)
C(7)	1715(12)	1305(3)	1820(10)	111(5)
C(8)	6598(22)	2573(6)	1634(19)	130(6)
C(9)	9014(21)	2149(7)	1462(19)	130(6)
C(10)	8683(22)	2249(6)	3792(13)	130(6)
C(8A)	6898(33)	2579(8)	2379(27)	136(9)
C(9A)	7698(34)	2198(9)	511(17)	136(9)
C(10A)	9540(20)	2153(10)	3017(25)	136(9)
C(11)	5123(11)	892(3)	4474(9)	59(3)
N(3)	4880(8)	624(2)	2634(7)	46(2)
C(12)	4562(10)	587(3)	3617(9)	53(3)
C(13)	3791(11)	294(3)	3760(10)	71(4)
C(14)	3370(12)	40(3)	2861(10)	79(4)
C(15)	3721(11)	64(3)	1866(10)	66(4)
C(16)	4508(10)	363(3)	1788(9)	54(3)
C(17)	5080(11)	437(3)	858(9)	67(4)

C(18)	6653(8)	1409(2)	4900(6)	63(3)
C(19)	5965(6)	1703(2)	5138(6)	56(3)
C(20)	6633(8)	1947(2)	6027(7)	88(4)
C(21)	7988(8)	1896(2)	6679(6)	101(5)
C(22)	8676(6)	1602(2)	6441(7)	109(5)
C(23)	8009(8)	1358(2)	5551(7)	69(4)
C(24)	4491(11)	1785(3)	4393(10)	67(4)
C(25)	4290(14)	2167(3)	3805(11)	106(5)
C(26)	3558(12)	1759(3)	5124(10)	89(4)
C(27)	8817(11)	1044(3)	5286(10)	73(4)
C(28)	10243(21)	1204(8)	5425(32)	107(10)
C(29)	8962(30)	721(7)	6095(25)	107(10)
C(28A)	10357(18)	1060(8)	5691(30)	100(10)
C(29A)	8463(31)	664(7)	5732(29)	100(10)
C(30)	6901(7)	747(2)	515(7)	58(3)
C(31)	6584(6)	929(2)	-547(7)	69(4)
C(32)	7463(9)	917(2)	-1161(5)	94(4)
C(33)	8657(8)	722(2)	-714(7)	90(4)
C(34)	8974(6)	539(2)	348(7)	89(4)
C(35)	8096(8)	551(2)	962(5)	73(4)
C(36)	5257(13)	1127(4)	-1130(11)	93(4)
C(37)	5441(18)	1533(4)	-1377(12)	172(8)
C(38)	4343(13)	926(4)	-2246(11)	135(6)
C(39)	8509(13)	353(3)	2159(10)	81(4)
C(40)	8460(17)	-68(3)	1990(14)	178(9)
C(41)	9893(13)	463(4)	3028(11)	126(6)

C(9)-Si(2)-C(8)	113.6(9)	C(9)-Si(2)-C(2)	113.1(9)
C(8A)-Si(2)-C(2)	116.6(14)	C(10A)-Si(2)-C(2)	113.9(12)
C(8)-Si(2)-C(2)	114.1(9)	C(8A)-Si(2)-C(9A)	107.3(11)
C(10A)-Si(2)-C(9A)	104.1(11)	C(2)-Si(2)-C(9A)	99.7(11)
C(9)-Si(2)-C(10)	106.0(9)	C(8)-Si(2)-C(10)	104.7(9)
C(2)-Si(2)-C(10)	104.1(8)	C(17)-N(1)-C(30)	109.8(7)
C(17)-N(1)-Ti(1)	121.8(6)	C(30)-N(1)-Ti(1)	128.3(6)
C(18)-N(2)-C(11)	112.3(7)	C(18)-N(2)-Ti(1)	125.3(6)
C(11)-N(2)-Ti(1)	122.1(6)	C(2)-C(1)-Ti(1)	93.9(8)
C(1)-C(2)-C(3)	124.8(10)	C(1)-C(2)-Si(2)	118.1(8)
C(3)-C(2)-Si(2)	117.1(8)	C(1)-C(2)-Ti(1)	53.9(6)
C(3)-C(2)-Ti(1)	71.2(6)	Si(2)-C(2)-Ti(1)	167.9(6)
C(4)-C(3)-C(2)	128.6(10)	C(4)-C(3)-Ti(1)	55.8(6)
C(2)-C(3)-Ti(1)	72.8(6)	C(3)-C(4)-Si(1)	127.4(9)
C(3)-C(4)-Ti(1)	91.3(7)	Si(1)-C(4)-Ti(1)	141.2(6)
N(2)-C(11)-C(12)	109.9(8)	C(12)-N(3)-C(16)	120.1(9)
C(12)-N(3)-Ti(1)	120.0(7)	C(16)-N(3)-Ti(1)	119.8(7)
N(3)-C(12)-C(13)	121.7(10)	N(3)-C(12)-C(11)	112.2(9)
C(13)-C(12)-C(11)	126.1(10)	C(14)-C(13)-C(12)	117.1(11)
C(13)-C(14)-C(15)	122.3(13)	C(16)-C(15)-C(14)	117.4(11)
C(15)-C(16)-N(3)	121.2(10)	C(15)-C(16)-C(17)	127.5(10)
N(3)-C(16)-C(17)	111.2(10)	N(1)-C(17)-C(16)	110.3(9)
C(19)-C(18)-N(2)	121.0(7)	C(23)-C(18)-N(2)	118.8(7)
C(20)-C(19)-C(24)	117.9(7)	C(18)-C(19)-C(24)	122.0(7)
C(22)-C(23)-C(27)	118.4(7)	C(18)-C(23)-C(27)	121.5(7)
C(19)-C(24)-C(25)	113.1(10)	C(19)-C(24)-C(26)	111.9(9)
C(25)-C(24)-C(26)	108.1(9)	C(29)-C(27)-C(23)	113(2)
C(28A)-C(27)-C(23)	121(2)	C(29)-C(27)-C(28)	110.4(14)
C(23)-C(27)-C(28)	107(2)	C(28A)-C(27)-C(29A)	106.2(14)
C(23)-C(27)-C(29A)	112(2)	C(31)-C(30)-N(1)	120.6(7)
C(35)-C(30)-N(1)	119.4(7)	C(30)-C(31)-C(36)	123.0(8)
C(32)-C(31)-C(36)	116.9(8)	C(34)-C(35)-C(39)	118.2(7)
C(30)-C(35)-C(39)	121.7(7)	C(31)-C(36)-C(37)	113.0(11)
C(31)-C(36)-C(38)	112.0(10)	C(37)-C(36)-C(38)	111.7(10)
C(41)-C(39)-C(35)	114.4(10)	C(41)-C(39)-C(40)	109.3(10)
C(35)-C(39)-C(40)	110.8(10)		

Table S3. Bond Distances (A) and Angles (°)

Ti(1)-N(1)	1.989(8)	Ti(1)-N(2)	2.009(8)
Ti(1)-N(3)	2.172(8)	Ti(1)-C(1)	2.046(11)
Ti(1)-C(4)	2.070(10)	Si(1)-C(4)	1.852(11)
Si(1)-C(5)	1.881(10)	Si(1)-C(6)	1.867(11)
Si(1)-C(7)	1.860(11)	Si(2)-C(2)	1.904(10)
Si(2)-C(8)	1.86(2)	Si(2)-C(9)	1.81(2)
Si(2)-C(10)	1.96(2)	Si(2)-C(8A)	1.82(2)
Si(2)-C(9A)	1.95(2)	Si(2)-C(10A)	1.85(2)
N(1)-C(17)	1.465(11)	N(1)-C(30)	1.474(9)
N(2)-C(11)	1.476(11)	N(2)-C(18)	1.453(9)
N(3)-C(12)	1.363(11)	N(3)-C(16)	1.359(11)
C(1)-C(2)	1.348(13)	C(2)-C(3)	1.553(14)
C(3)-C(4)	1.357(13)	C(11)-C(12)	1.502(12)
C(12)-C(13)	1.399(13)	C(13)-C(14)	1.387(14)
C(14)-C(15)	1.393(13)	C(15)-C(16)	1.400(13)
C(16)-C(17)	1.491(13)	C(19)-C(24)	1.537(11)
C(23)-C(27)	1.539(12)	C(24)-C(25)	1.554(12)
C(24)-C(26)	1.554(12)	C(27)-C(28)	1.58(2)
C(27)-C(29)	1.51(2)	C(27)-C(28A)	1.53(2)
C(27)-C(29A)	1.59(2)	C(31)-C(36)	1.520(13)
C(36)-C(37)	1.546(13)	C(36)-C(38)	1.551(13)
C(35)-C(39)	1.548(12)	C(39)-C(40)	1.557(13)
C(39)-C(41)	1.531(12)		

N(1)-Ti(1)-N(2)	141.5(3)	N(1)-Ti(1)-C(1)	99.2(4)
N(2)-Ti(1)-C(1)	101.5(4)	N(1)-Ti(1)-C(4)	103.4(4)
N(2)-Ti(1)-C(4)	104.0(4)	C(1)-Ti(1)-C(4)	100.7(4)
N(1)-Ti(1)-N(3)	73.6(3)	N(2)-Ti(1)-N(3)	74.1(3)
C(1)-Ti(1)-N(3)	155.6(4)	C(4)-Ti(1)-N(3)	103.6(4)
N(1)-Ti(1)-C(3)	111.0(3)	N(2)-Ti(1)-C(3)	106.8(3)
C(1)-Ti(1)-C(3)	68.1(4)	C(4)-Ti(1)-C(3)	32.8(3)
N(3)-Ti(1)-C(3)	136.4(3)	N(1)-Ti(1)-C(2)	110.1(3)
N(2)-Ti(1)-C(2)	104.7(3)	C(1)-Ti(1)-C(2)	32.2(3)
C(4)-Ti(1)-C(2)	68.8(4)	N(3)-Ti(1)-C(2)	172.0(3)
C(3)-Ti(1)-C(2)	36.0(3)	C(4)-Si(1)-C(7)	110.4(5)
C(4)-Si(1)-C(6)	109.1(5)	C(7)-Si(1)-C(6)	107.9(6)
C(4)-Si(1)-C(5)	112.4(6)	C(7)-Si(1)-C(5)	109.1(6)
C(6)-Si(1)-C(5)	107.8(6)	C(8A)-Si(2)-C(10A)	113.1(12)

Table S4. Anisotropic displacement parameters ($A^2 \times 10^3$). The anisotropic displacement factor exponent takes the form: $-2\pi^2[h^2a^{*2}U11 + \ldots + 2hka^*b^*U12]$

atom	U11	U22	U33	U23	U13	U12
Ti(1)	53(1)	46(1)	46(1)	3(1)	22(1)	0(1)
Si(1)	60(2)	79(3)	81(3)	13(2)	23(2)	9(2)
Si(2)	84(3)	65(3)	164(5)	25(3)	57(3)	-10(2)
C(5)	92(12)	111(13)	230(19)	75(13)	32(13)	37(11)
C(6)	80(11)	202(18)	120(13)	-68(13)	30(10)	-33(12)
C(7)	79(11)	153(14)	98(11)	12(10)	26(9)	-10(10)
C(25)	171(15)	57(9)	111(12)	16(8)	76(11)	17(10)
C(26)	94(11)	98(11)	89(10)	9(8)	49(9)	29(9)
C(37)	308(26)	116(14)	125(15)	57(12)	118(16)	48(16)
C(38)	110(13)	179(17)	90(12)	-2(12)	5(10)	21(12)
C(40)	189(20)	78(12)	199(19)	15(13)	-14(15)	7(13)
C(41)	91(12)	154(15)	102(12)	-24(11)	-4(10)	-9(11)

Table S5. Calculated hydrogen atoms positions ($\times 10^4$) and isotropic thermal parameters ($\times 10^3$).

Atom	x	y	z	Ueq
H(1A)	8470(12)	1373(3)	2748(9)	72
H(3)	4872(11)	1951(3)	1186(9)	80
H(5A)	907(19)	1938(7)	-96(99)	227
H(5B)	2265(98)	2032(14)	-267(84)	227
H(5C)	2103(110)	2106(8)	942(19)	227
H(6A)	1010(17)	1179(24)	-899(59)	203
H(6B)	2238(101)	922(6)	-287(16)	203
H(6C)	2385(93)	1247(19)	-1070(46)	203
H(7A)	1992(75)	1058(9)	2039(64)	167
H(7B)	754(12)	1314(24)	1450(31)	167
H(7C)	1988(76)	1456(16)	2507(38)	167
H(8A)	7113(35)	2793(6)	1870(145)	195
H(8B)	5921(112)	2563(27)	1986(131)	195
H(8C)	6175(149)	2569(29)	796(23)	195
H(9A)	8655(60)	2032(45)	712(74)	195
H(9B)	9769(79)	2012(43)	1964(80)	195
H(9C)	9299(131)	2391(7)	1365(146)	195
H(10A)	9067(161)	2023(12)	4154(32)	195
H(10B)	8065(46)	2338(49)	4144(33)	195
H(10C)	9386(125)	2425(39)	3902(13)	195
H(8A1)	6693(269)	2547(33)	3078(147)	203
H(8A2)	6081(154)	2619(47)	1725(121)	203
H(8A3)	7482(121)	2785(16)	2471(258)	203
H(9A1)	6784(36)	2214(82)	-19(23)	203

H(9A2)	8111(271)	1984(39)	338(87)	203
H(9A3)	8184(256)	2410(46)	424(70)	203
H(10D)	9646(20)	2106(80)	3819(52)	203
H(10E)	9953(62)	2382(29)	2965(204)	203
H(10F)	9962(62)	1962(53)	2735(165)	203
H(11A)	4392(11)	1030(3)	4573(9)	71
H(11B)	5666(11)	792(3)	5229(9)	71
H(13)	3570(11)	270(3)	4429(10)	86
H(14)	2835(12)	-154(3)	2924(10)	95
H(15)	3444(11)	-110(3)	1277(10)	80
H(17A)	5577(11)	225(3)	759(9)	80
H(17B)	4356(11)	483(3)	119(9)	80
H(20)	6172(12)	2144(2)	6187(10)	106
H(21)	8434(12)	2059(3)	7275(8)	122
H(22)	9583(6)	1568(4)	6878(9)	131
H(24)	4194(11)	1602(3)	3770(10)	81
H(25A)	4368(90)	2352(3)	4383(18)	159
H(25B)	3415(36)	2180(9)	3205(54)	159
H(25C)	4965(55)	2206(10)	3461(68)	159
H(26A)	2648(17)	1809(21)	4629(19)	134
H(26B)	3839(51)	1933(15)	5750(43)	134
H(26C)	3612(62)	1517(7)	5444(58)	134
H(28A)	10133(22)	1418(33)	4943(139)	160
H(28B)	10751(75)	1025(22)	5187(156)	160
H(28C)	10713(80)	1269(48)	6230(48)	160
H(29A)	9746(118)	754(28)	6786(85)	160
H(29B)	9053(198)	502(10)	5701(68)	160
H(29C)	8180(96)	704(31)	6312(136)	160
H(28D)	10626(20)	1290(23)	5467(155)	151
H(28E)	10676(22)	866(33)	5331(126)	151
H(28F)	10733(19)	1035(51)	6528(31)	151
H(29D)	7528(55)	610(27)	5331(132)	151
H(29E)	8646(188)	676(18)	6560(45)	151
H(29F)	9001(146)	475(10)	5573(155)	151
H(32)	7251(12)	1039(3)	-1872(6)	113
H(33)	9245(10)	714(3)	-1126(10)	108
H(34)	9774(7)	408(3)	647(10)	107
H(36)	4784(13)	1122(4)	-571(11)	111
H(37A)	6026(118)	1648(10)	-673(35)	258
H(37B)	4582(26)	1653(10)	-1636(121)	258
H(37C)	5830(136)	1552(4)	-1975(92)	258
H(38A)	3434(25)	1011(24)	-2448(61)	202
H(38B)	4376(92)	668(5)	-2100(34)	202
H(38C)	4652(73)	975(26)	-2882(28)	202
H(39)	7843(13)	416(3)	2515(10)	98
H(40A)	8490(150)	-185(4)	2703(45)	266
H(40B)	9218(82)	-145(6)	1794(126)	266
H(40C)	7643(71)	-134(5)	1368(89)	266
H(41A)	10569(17)	407(26)	2700(39)	189
H(41B)	10075(46)	330(21)	3746(34)	189
H(41C)	9902(35)	719(6)	3184(70)	189

Table S6. Selected torsion angles

50.98(96)	N2-Ti1-N1-C17	172.98(76)	C1-Ti1-N1-C17
-83.54(78)	C4-Ti1-N1-C17	16.95(71)	N3-Ti1-N1-C17
-117.08(75)	C3-Ti1-N1-C17	-155.61(71)	C2-Ti1-N1-C17
-125.48(74)	N2-Ti1-N1-C30	-3.49(82)	C1-Ti1-N1-C30
99.99(78)	C4-Ti1-N1-C30	-159.51(79)	N3-Ti1-N1-C30
66.46(80)	C3-Ti1-N1-C30	27.93(83)	C2-Ti1-N1-C30
140.97(68)	N1-Ti1-N2-C18	19.66(78)	C1-Ti1-N2-C18
-84.65(75)	C4-Ti1-N2-C18	174.90(75)	N3-Ti1-N2-C18
-50.66(75)	C3-Ti1-N2-C18	-13.27(76)	C2-Ti1-N2-C18
-46.30(94)	N1-Ti1-N2-C11	-167.60(73)	C1-Ti1-N2-C11
88.08(75)	C4-Ti1-N2-C11	-12.37(68)	N3-Ti1-N2-C11
122.07(73)	C3-Ti1-N2-C11	159.47(69)	C2-Ti1-N2-C11
113.29(68)	N1-Ti1-C1-C2	-99.33(68)	N2-Ti1-C1-C2
7.58(73)	C4-Ti1-C1-C2	-176.26(72)	N3-Ti1-C1-C2
4.29(62)	C3-Ti1-C1-C2	-7.8(1.1)	Ti1-C1-C2-C3
169.23(56)	Ti1-C1-C2-Si2	-74.90(73)	N1-Ti1-C2-C1
88.35(71)	N2-Ti1-C2-C1	-172.01(77)	C4-Ti1-C2-C1
168.8(2.1)	N3-Ti1-C2-C1	-173.23(98)	C3-Ti1-C2-C1
98.33(57)	N1-Ti1-C2-C3	-98.42(57)	N2-Ti1-C2-C3
173.23(98)	C1-Ti1-C2-C3	1.22(58)	C4-Ti1-C2-C3
-17.9(2.6)	N3-Ti1-C2-C3	-126.8(2.6)	N1-Ti1-C2-Si2
36.3(2.7)	N2-Ti1-C2-Si2	-51.9(2.4)	C1-Ti1-C2-Si2
136.0(2.7)	C4-Ti1-C2-Si2	116.7(2.9)	N3-Ti1-C2-Si2
134.7(2.9)	C3-Ti1-C2-Si2	4.4(1.8)	C1-C2-C3-C4
-172.62(93)	Si2-C2-C3-C4	-2.2(1.0)	Ti1-C2-C3-C4
6.66(97)	C1-C2-C3-Ti1	-170.40(66)	Si2-C2-C3-Ti1
82.25(72)	N1-Ti1-C3-C4	-90.02(70)	N2-Ti1-C3-C4
174.02(78)	C1-Ti1-C3-C4	-5.65(89)	N3-Ti1-C3-C4
177.9(1.0)	C2-Ti1-C3-C4	-95.66(57)	N1-Ti1-C3-C2
92.07(57)	N2-Ti1-C3-C2	-3.88(57)	C1-Ti1-C3-C2
-177.9(1.0)	C4-Ti1-C3-C2	176.45(52)	N3-Ti1-C3-C2
-177.20(77)	C2-C3-C4-Si1	-179.7(1.0)	Ti1-C3-C4-Si1
2.6(1.2)	C2-C3-C4-Ti1	-107.96(67)	N1-Ti1-C4-C3
99.27(68)	N2-Ti1-C4-C3	-5.64(74)	C1-Ti1-C4-C3
175.99(63)	N3-Ti1-C4-C3	-1.32(63)	C2-Ti1-C4-C3
71.72(90)	N1-Ti1-C4-Si1	-81.04(89)	N2-Ti1-C4-Si1
174.05(84)	C1-Ti1-C4-Si1	-4.32(94)	N3-Ti1-C4-Si1
179.6(1.3)	C3-Ti1-C4-Si1	178.37(96)	C2-Ti1-C4-Si1
-173.11(76)	C18-N2-C11-C12	13.2(1.0)	Ti1-N2-C11-C12
168.50(79)	N1-Ti1-N3-C12	9.75(71)	N2-Ti1-N3-C12
92.6(1.1)	C1-Ti1-N3-C12	-91.25(76)	C4-Ti1-N3-C12
-88.10(83)	C3-Ti1-N3-C12	-72.8(2.5)	C2-Ti1-N3-C12
-13.94(72)	N1-Ti1-N3-C16	-172.70(80)	N2-Ti1-N3-C16
-89.8(1.1)	C1-Ti1-N3-C16	86.31(79)	C4-Ti1-N3-C16
89.46(84)	C3-Ti1-N3-C16	104.7(2.3)	C2-Ti1-N3-C16
-3.3(1.5)	C16-N3-C12-C13	174.17(76)	Ti1-N3-C12-C13
176.92(87)	C16-N3-C12-C11	-5.5(1.1)	Ti1-N3-C12-C11
-4.0(1.2)	N2-C11-C12-N3	176.25(95)	N2-C11-C12-C13
0.4(1.6)	N3-C12-C13-C14	-173.44(74)	Ti1-N3-C16-C15
-173.98(87)	C12-N3-C16-C17	8.4(1.1)	Ti1-N3-C16-C17

159.13(81)	C30-N1-C17-C16	-17.9(1.1)	Ti1-N1-C17-C16
-173.20(96)	C15-C16-C17-N1	4.7(1.2)	N3-C16-C17-N1
-73.28(84)	C11-N2-C18-C19	100.06(65)	Ti1-N2-C18-C19
101.55(74)	C11-N2-C18-C23	-85.11(69)	Ti1-N2-C18-C23
174.77(71)	N2-C18-C19-C20	176.12(76)	C23-C18-C19-C24
-9.11(84)	N2-C18-C19-C24	93.18(77)	C17-N1-C30-C31
-90.02(74)	Ti1-N1-C30-C31	-86.27(76)	C17-N1-C30-C35
90.53(74)	Ti1-N1-C30-C35		

Table S7. Least-squares planes (x,y,z in crystal coordinates) and deviations from them (* indicates atom used to define plane)

- 3.704(39) x + 9.282(340) y + 11.802(30) z = 1.465(59)

*	-0.008	(0.003)	C1	* 0.016 (0.007)	C2
*	-0.017	(0.007)	C3	* 0.008 (0.003)	C4
	0.189	(0.018)	Ti1	-0.105 (0.015)	Si1
	0.184	(0.023)	Si2		

Rms deviation of fitted atoms = 0.013

7.621(30) x - 18.263(0.130) y + 2.467(37) z = 3.307(25)

Angle to previous plane (with approximate esd) = 86.33(37)

*	0.158	(0.003)	N1	* 0.156 (0.003)	N2
*	-0.077	(0.002)	N3	* -0.237 (0.004)	Ti1

Rms deviation of fitted atoms = 0.167

4 Crystallographic data for (BDEP)ZrMe$_2$.

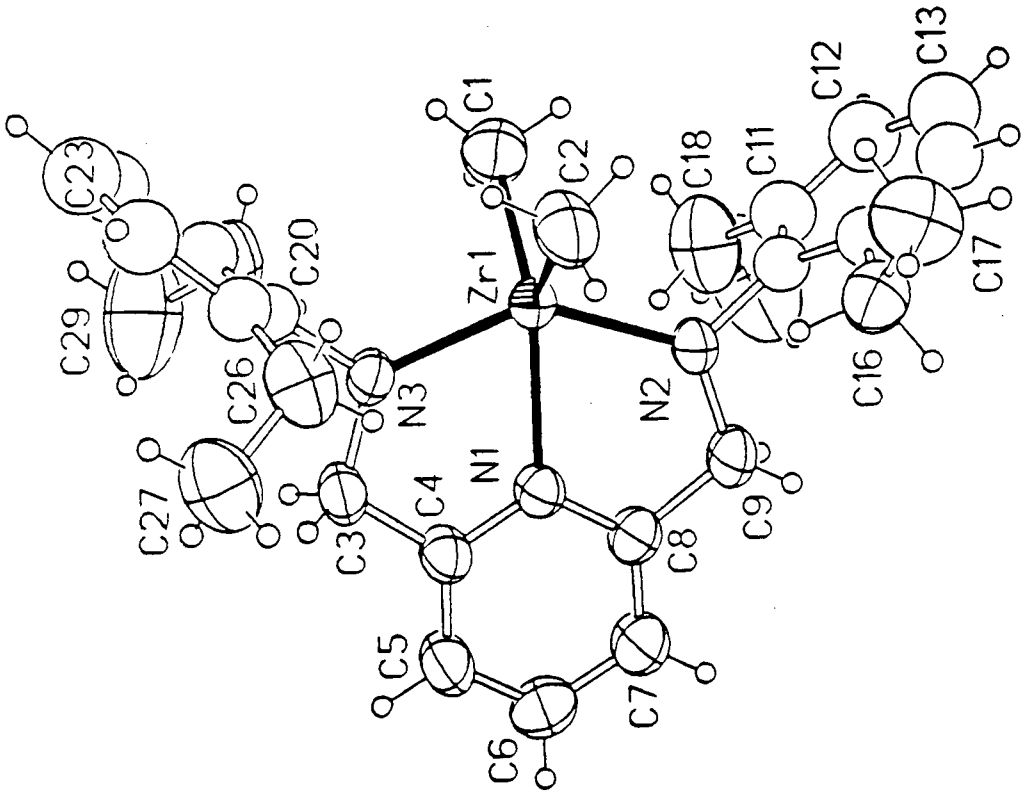

Table S1. Crystal Data and Experimental Details.

Empirical formula	$C_{29}H_{39}N_3Zr_1$
Formula weight	520.85
Temperature	25°C
Wavelength	0.71073 A
Crystal system	Monoclinic
Space group	$P2_1/c$
Unit cell dimensions	a = 12.355(2)A
	b = 15.761(2)A
	c = 15.701(3)A
	β = 111.71(1)°
Volume	2840.5(8) A^3
Z	4
Density, calcd.	1.218 $g.cm^{-3}$
Absorption coefficient	0.406 mm^{-1}
F(000)	1096
Reflections Collected	5706
Independent reflections	4950 [R(int) = 0.0322]
Refinement method	Full-matrix least-squares on F^2
Data/restraints/parameters	3011/42/244
Goodness-of-fit (GooF) on F^2	1.038
Final R indices [I>2sigma(I)]	R1 = 0.0592, wR2 = 0.1335
R indices (all data)	R1 = 0.1113, wR2 = 0.1657

$R1 = \Sigma(|F_o| - |F_c|)/\Sigma|F_o|$;

$wR2 = [\Sigma w(F_o^2 - F_c^2)^2/\Sigma wF_o^4]^{1/2}$

$GooF = [\Sigma w(F_o^2 - F_c^2)^2/(n-p)]^{1/2}$

where n is the number of reflections and p is the number of parameters refined.

Table S2. Atomic coordinates (x 10^4) and equivalent isotropic displacement parameters (A^2 x 10^3). U(eq) is defined as one third of the trace of the orthogonalized Uij tensor.

atom	x	y	z	Ueq
Zr(1)	7571.1(5)	8647.7(3)	7508.8(4)	40.8(2)
C(1)	6884(8)	8679(5)	8649(6)	85(2)
C(2)	5933(5)	8684(4)	6253(5)	71(2)
C(3)	9371(5)	10123(4)	7568(5)	52(2)
N(1)	9456(4)	8612(3)	7516(3)	42(1)
C(4)	10039(5)	9344(3)	7539(4)	48(1)
C(5)	11165(5)	9347(4)	7546(5)	67(2)
C(6)	11695(6)	8588(4)	7536(6)	74(2)
C(7)	11096(5)	7825(4)	7502(5)	64(2)
C(8)	9979(5)	7867(3)	7505(4)	50(2)
C(9)	9229(5)	7104(4)	7481(5)	56(2)
N(2)	8128(4)	7385(3)	7535(3)	47(1)
N(3)	8223(4)	9888(3)	7558(3)	43(1)
C(10)	7462(5)	6669(4)	7662(4)	46(1)
C(11)	7612(6)	6399(5)	8550(5)	68(2)
C(12)	6945(6)	5709(5)	8651(6)	80(2)
C(13)	6192(7)	5305(5)	7916(5)	78(2)
C(14)	6038(6)	5549(4)	7048(5)	63(2)
C(15)	6672(5)	6238(4)	6904(4)	53(2)
C(16)	6515(6)	6468(5)	5924(5)	71(2)
C(17)	5297(7)	6411(6)	5225(5)	98(3)
C(18)	8507(9)	6797(6)	9392(6)	106(3)
C(19)	9366(11)	6222(7)	9998(8)	177(7)
C(20)	7518(5)	10619(3)	7540(4)	45(1)
C(21)	6808(5)	10975(4)	6683(4)	53(2)
C(22)	6072(6)	11651(5)	6677(5)	72(2)
C(23)	6057(7)	11971(5)	7485(5)	79(2)
C(24)	6771(6)	11666(5)	8314(5)	74(2)
C(25)	7520(5)	10977(4)	8370(4)	59(2)
C(26)	6850(6)	10687(5)	5788(5)	72(2)
C(27)	7339(8)	11343(5)	5316(5)	87(2)
C(28)	8337(8)	10659(5)	9299(5)	86(3)

C(29)	9191(11)	11296(6)	9843(7)	158(5)

Table S3. Bond Distances (A) and Angles (°).

Zr(1)-N(2)	2.101(4)	Zr(1)-N(3)	2.104(5)
Zr(1)-C(2)	2.243(6)	Zr(1)-C(1)	2.248(7)
Zr(1)-N(1)	2.325(4)	C(3)-N(3)	1.461(7)
C(3)-C(4)	1.489(8)	N(1)-C(8)	1.344(6)
N(1)-C(4)	1.354(7)	C(4)-C(5)	1.386(8)
C(5)-C(6)	1.366(8)	C(6)-C(7)	1.403(8)
C(7)-C(8)	1.384(8)	C(8)-C(9)	1.510(8)
C(9)-N(2)	1.463(7)	N(2)-C(10)	1.453(7)
N(3)-C(20)	1.438(7)	C(10)-C(15)	1.403(8)
C(10)-C(11)	1.404(8)	C(11)-C(12)	1.409(9)
C(11)-C(18)	1.511(10)	C(12)-C(13)	1.345(9)
C(13)-C(14)	1.360(9)	C(14)-C(15)	1.405(8)
C(15)-C(16)	1.522(8)	C(16)-C(17)	1.502(10)
C(18)-C(19)	1.451(11)	C(20)-C(25)	1.419(8)
C(20)-C(21)	1.421(8)	C(21)-C(22)	1.399(9)
C(21)-C(26)	1.496(8)	C(22)-C(23)	1.373(9)
C(23)-C(24)	1.362(9)	C(24)-C(25)	1.408(9)
C(25)-C(28)	1.519(9)	C(26)-C(27)	1.522(9)
C(28)-C(29)	1.478(11)		

N(2)-Zr(1)-N(3)	139.6(2)	N(2)-Zr(1)-C(2)	102.9(2)
N(3)-Zr(1)-C(2)	102.6(2)	N(2)-Zr(1)-C(1)	102.9(2)
N(3)-Zr(1)-C(1)	101.7(2)	C(2)-Zr(1)-C(1)	102.4(3)
N(2)-Zr(1)-N(1)	70.0(2)	N(3)-Zr(1)-N(1)	69.7(2)
C(2)-Zr(1)-N(1)	125.5(2)	C(1)-Zr(1)-N(1)	132.0(3)
N(3)-C(3)-C(4)	109.7(4)	C(8)-N(1)-C(4)	119.4(5)
C(8)-N(1)-Zr(1)	120.4(4)	C(4)-N(1)-Zr(1)	120.1(4)
N(1)-C(4)-C(5)	121.7(5)	N(1)-C(4)-C(3)	114.0(5)
C(5)-C(4)-C(3)	124.3(5)	C(6)-C(5)-C(4)	118.8(6)
C(5)-C(6)-C(7)	120.1(6)	C(8)-C(7)-C(6)	118.2(6)
N(1)-C(8)-C(7)	121.8(5)	N(1)-C(8)-C(9)	113.7(5)
C(7)-C(8)-C(9)	124.4(5)	N(2)-C(9)-C(8)	109.4(4)
C(10)-N(2)-C(9)	111.0(4)	C(10)-N(2)-Zr(1)	122.7(4)
C(9)-N(2)-Zr(1)	126.2(3)	C(20)-N(3)-C(3)	112.0(4)
C(20)-N(3)-Zr(1)	121.5(3)	C(3)-N(3)-Zr(1)	126.4(3)
C(15)-C(10)-C(11)	119.4(6)	C(15)-C(10)-N(2)	120.7(5)
C(11)-C(10)-N(2)	119.8(5)	C(10)-C(11)-C(12)	118.5(6)
C(10)-C(11)-C(18)	121.9(7)	C(12)-C(11)-C(18)	119.5(7)

C(13)-C(12)-C(11)	121.1(8)	C(12)-C(13)-C(14)	121.5(8)
C(13)-C(14)-C(15)	120.0(7)	C(10)-C(15)-C(14)	119.4(6)
C(10)-C(15)-C(16)	122.0(6)	C(14)-C(15)-C(16)	118.5(6)
C(17)-C(16)-C(15)	116.3(6)	C(19)-C(18)-C(11)	115.8(8)
C(25)-C(20)-C(21)	120.2(5)	C(25)-C(20)-N(3)	120.3(5)
C(21)-C(20)-N(3)	119.5(5)	C(22)-C(21)-C(20)	118.7(6)
C(22)-C(21)-C(26)	118.2(6)	C(20)-C(21)-C(26)	123.0(6)
C(23)-C(22)-C(21)	120.3(7)	C(24)-C(23)-C(22)	121.9(8)
C(23)-C(24)-C(25)	120.7(7)	C(24)-C(25)-C(20)	118.1(6)
C(24)-C(25)-C(28)	120.1(6)	C(20)-C(25)-C(28)	121.7(6)
C(21)-C(26)-C(27)	114.2(6)	C(29)-C(28)-C(25)	114.2(7)

Table S4. Anisotropic displacement parameters ($A^2 \times 10^3$).
The anisotropic displacement factor exponent takes the form: $-2\pi^2[h^2a^{*2}U11 + \ldots + 2hka^*b^*U12]$

atom	U11	U22	U33	U23	U13	U12
Zr(1)	42(1)	31(1)	53(1)	0(1)	20(1)	0(1)
C(1)	116(6)	65(5)	106(6)	-2(5)	78(6)	-6(5)
C(2)	51(4)	54(4)	92(5)	2(4)	7(3)	-1(3)
C(3)	48(3)	34(3)	71(4)	-2(3)	17(3)	-3(3)
N(1)	40(2)	35(2)	49(3)	7(2)	15(2)	4(2)
C(4)	37(3)	40(3)	61(4)	0(3)	11(3)	-1(3)
C(5)	48(4)	43(4)	107(6)	-2(4)	27(4)	-6(3)
C(6)	46(3)	66(5)	113(6)	-2(5)	33(4)	11(4)
C(7)	52(4)	47(4)	93(5)	7(4)	27(4)	10(3)
C(8)	45(3)	38(3)	68(4)	8(3)	21(3)	11(3)
C(9)	56(4)	31(3)	81(5)	2(3)	26(3)	7(3)
N(2)	50(3)	28(2)	66(3)	3(2)	26(3)	1(2)
N(3)	42(3)	32(3)	53(3)	-3(2)	16(2)	4(2)
C(16)	81(5)	64(5)	75(5)	-7(4)	36(4)	-1(4)
C(17)	93(6)	116(8)	77(6)	0(5)	23(5)	-6(6)
C(18)	149(9)	75(6)	74(6)	19(5)	19(6)	-1(6)
C(19)	188(13)	136(11)	128(10)	47(8)	-34(9)	-21(10)
C(26)	76(5)	66(5)	59(5)	2(4)	7(4)	-9(4)
C(27)	109(6)	78(5)	70(5)	16(5)	27(4)	-9(5)
C(28)	135(7)	60(5)	62(5)	-10(4)	35(5)	-4(5)
C(29)	213(14)	107(9)	101(8)	-33(7)	-6(8)	-9(9)

H(29B)	9667(61)	11474(49)	9512(32)	238
H(29C)	9675(60)	11051(22)	10418(30)	238

Table S6. Selected torsion angles

2.02(43)	N2-Zr1-N1-C8	179.00(47)	N3-Zr1-N1-C8
-89.80(48)	C2-Zr1-N1-C8	91.46(52)	C1-Zr1-N1-C8
-177.48(46)	N2-Zr1-N1-C4	-0.51(41)	N3-Zr1-N1-C4
90.69(47)	C2-Zr1-N1-C4	-88.05(49)	C1-Zr1-N1-C4
0.41(87)	C8-N1-C4-C5	179.92(50)	Zr1-N1-C4-C5
-178.90(55)	C8-N1-C4-C3	0.61(67)	Zr1-N1-C4-C3
-0.32(73)	N3-C3-C4-N1	-179.61(62)	N3-C3-C4-C5
-0.5(1.0)	N1-C4-C5-C6	178.72(68)	C3-C4-C5-C6
1.2(1.1)	C4-C5-C6-C7	-1.7(1.1)	C5-C6-C7-C8
-1.01(91)	C4-N1-C8-C7	179.48(51)	Zr1-N1-C8-C7
179.87(55)	C4-N1-C8-C9	0.36(70)	Zr1-N1-C8-C9
1.6(1.0)	C6-C7-C8-N1	-179.31(67)	C6-C7-C8-C9
-3.51(77)	N1-C8-C9-N2	177.39(64)	C7-C8-C9-N2
-170.91(49)	C8-C9-N2-C10	6.04(76)	C8-C9-N2-Zr1
167.74(38)	N3-Zr1-N2-C10	-64.45(47)	C2-Zr1-N2-C10
41.76(49)	C1-Zr1-N2-C10	172.11(47)	N1-Zr1-N2-C10
-8.87(64)	N3-Zr1-N2-C9	118.95(53)	C2-Zr1-N2-C9
-134.84(55)	C1-Zr1-N2-C9	-4.50(49)	N1-Zr1-N2-C9
-177.16(50)	C4-C3-N3-C20	-0.13(72)	C4-C3-N3-Zr1
-178.53(40)	N2-Zr1-N3-C20	53.55(47)	C2-Zr1-N3-C20
-52.21(49)	C1-Zr1-N3-C20	177.09(46)	N1-Zr1-N3-C20
4.70(60)	N2-Zr1-N3-C3	-123.22(50)	C2-Zr1-N3-C3
131.02(52)	C1-Zr1-N3-C3	0.32(46)	N1-Zr1-N3-C3
-89.33(66)	C9-N2-C10-C15	93.60(60)	Zr1-N2-C10-C15
90.28(68)	C9-N2-C10-C11	-86.79(62)	Zr1-N2-C10-C11
90.75(59)	Zr1-N3-C20-C25	-88.47(58)	Zr1-N3-C20-C21

Table S7. Least-squares planes (x,y,z in crystal coordinates) and deviations from them (* indicates atom used to define plane)

0.036(27) x - 0.134(29) y + 14.570(13) z = 10.885(28)

*	-0.033 (0.002)	Zr1	*	-0.015 (0.001)	N1
*	0.024 (0.002)	N2	*	0.024 (0.002)	N3
	1.625 (0.010)	C1		-1.869 (0.009)	C2

Rms deviation of fitted atoms = 0.025

0.298(24) x + 15.756(3) y - 0.258(67) z = 13.657(057)

Angle to previous plane (with approximate esd) = 89.05(28)

```
*     0.000 (0.000)  Zr1        *     0.000 (0.000)  N1
*     0.000 (0.000)  C1               0.040 (0.012)  C2
     -1.974 (0.005)  N2               1.972 (0.005)  N3

Rms deviation of fitted atoms =   0.000


- 0.095(34) x - 0.380(46) y + 14.627(16) z = 10.578(47)

Angle to previous plane (with approximate esd) = 88.14(31)

*    -0.001 (0.004)  N1         *    -0.001 (0.005)  C4
*    -0.002 (0.005)  C5         *     0.007 (0.005)  C6
*    -0.008 (0.005)  C7         *     0.005 (0.005)  C8
      0.018 (0.011)  C3                0.007 (0.011)  C9

Rms deviation of fitted atoms =   0.005


- 9.646(21) x - 9.848(34) y - 4.507(42) z = 2.818(42)

Angle to previous plane (with approximate esd) = 89.37(23)

*     0.004 (0.004)  C10        *    -0.006 (0.005)  C11
*     0.004 (0.005)  C12        *     0.000 (0.005)  C13
*    -0.001 (0.005)  C14        *    -0.001 (0.004)  C15
     -0.063 (0.011)  C16              0.741 (0.014)  C17
     -0.098 (0.014)  C18             -1.220 (0.018)  C19

Rms deviation of fitted atoms =   0.003


 9.482(22) x + 10.096(33) y - 4.075(41) z = 14.796(42)

Angle to previous plane (with approximate esd) = 78.52(16)

*    -0.019 (0.004)  C20        *     0.016 (0.004)  C21
*     0.003 (0.005)  C22        *    -0.018 (0.005)  C23
*     0.014 (0.005)  C24        *     0.005 (0.005)  C25
      0.129 (0.011)  C26              1.448 (0.012)  C27
      0.081 (0.012)  C28              1.312 (0.016)  C29

Rms deviation of fitted atoms =   0.014
```

5 Crystallographic data for (BDPP')Zr(NH^{tert}Bu).

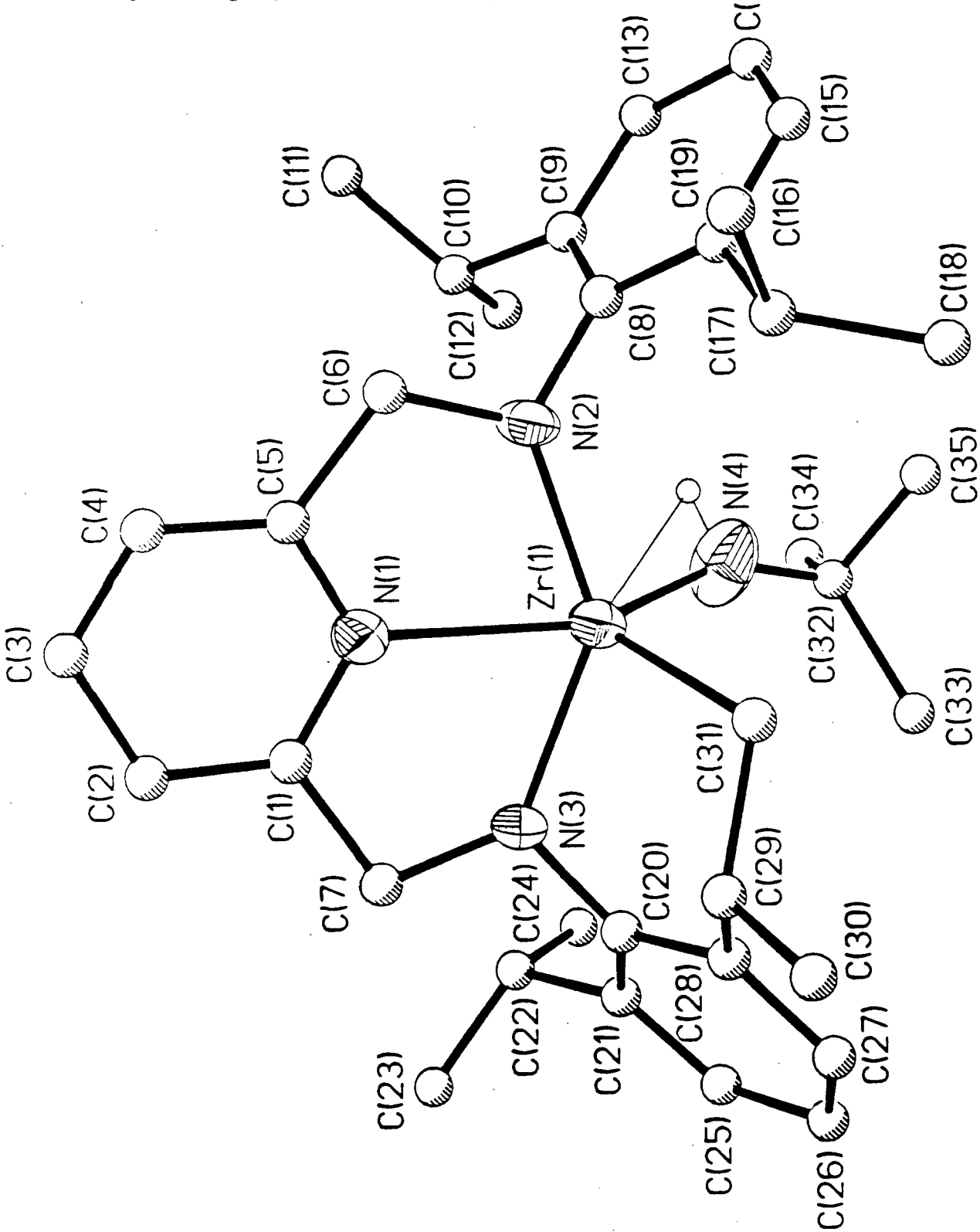

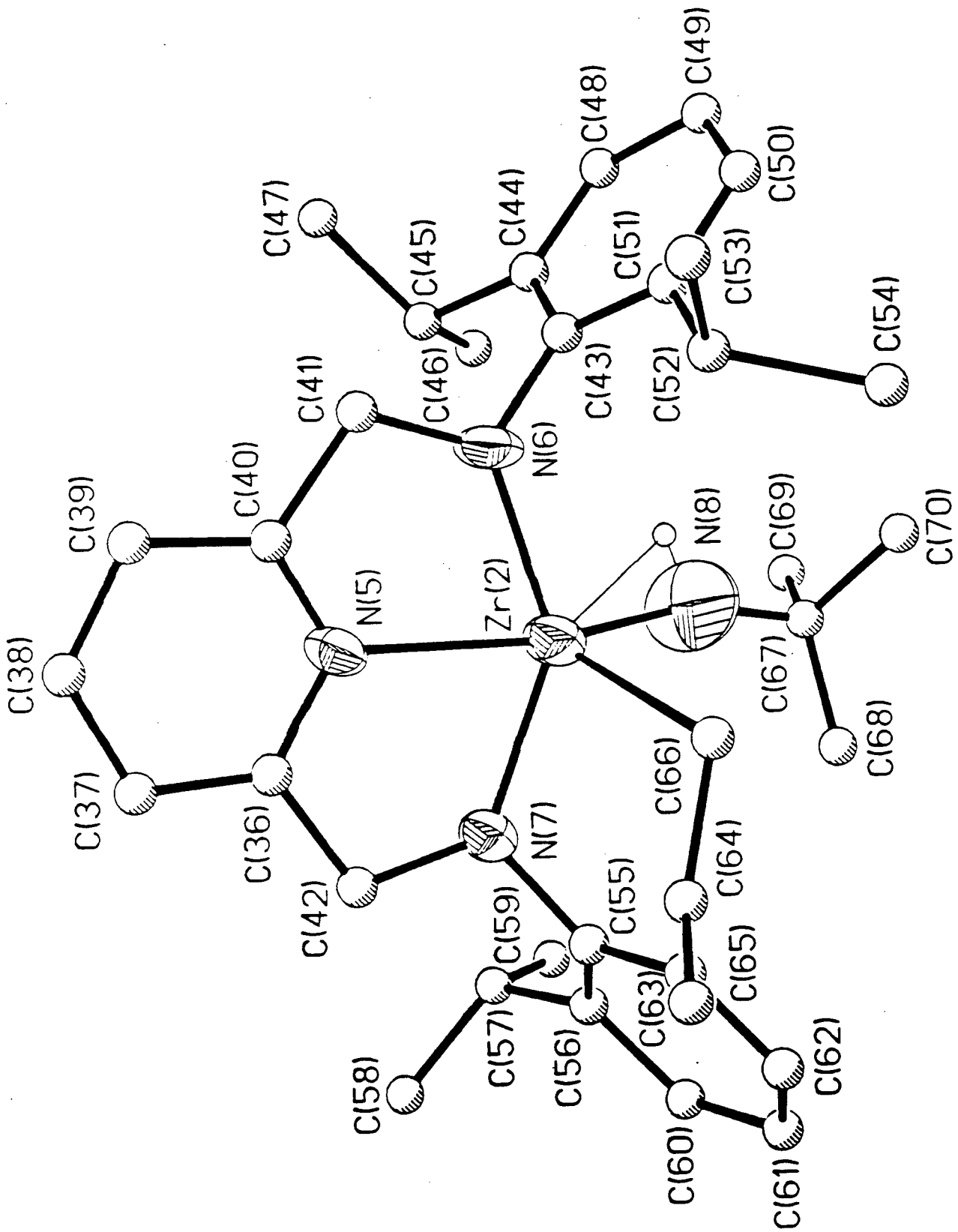
C(38)
C(39)
C(40)
C(41)
C(47)
C(45)
C(46)
C(44)
C(48)
C(49)
C(50)
C(51)
C(53)
C(52)
C(54)
N(6)
C(43)
N(5)
Zr(2)
N(8)
C(69)
C(70)
C(37)
C(36)
C(42)
N(7)
C(66)
C(67)
C(68)
C(59)
C(55)
C(64)
C(57)
C(56)
C(63)
C(65)
C(58)
C(60)
C(62)
C(61)

Table 1. Crystal data and structure refinement for [Zr(L)(HNtBu)].

Identification code	DM01
Empirical formula	$C_{35}H_{50}N_4Zr$
Formula weight	618.01
Temperature	293(2) K
Wavelength	0.71073 Å
Crystal system	Orthorhombic
Space group	*Pna2₁* (No. 33)
Unit cell dimensions	a = 29.5757(6) Å
	b = 20.0757(4) Å
	c = 11.7560(1)
Volume	6980.2(2) $Å^3$
Z	8
Density (calculated)	1.176 g/cm^3
Absorption coefficient	0.342 mm^{-1}
F(000)	2624
Crystal size	0.15 x 0.20 x 0.20 mm
Theta range for data collection	1.2 to 22.5 deg
Limiting indices	$-39 \le h \le 27, -26 \le k \le 26, -14 \le l \le 15$
Reflections collected	27501
Independent reflections	8679 (R(int) = 0.0481)
Refinement method	Full-matrix least-squares on F^2
Data / restraints / parameters	8668 / 1 / 716
Goodness-of-fit on F^2	1.064
Final R indices (I>2sigma(I))	$R_1 = 0.0734$, $wR_2 = 0.1640$
R indices (all data)	$R_1 = 0.1027$, $wR_2 = 0.1844$
Largest diff. peak and hole	0.911 and -0.764 e/$Å^3$

Table 2. Atomic coordinates (x 10^4) and equivalent isotropic displacement parameters ($Å^2$ x 10^3) for DM01.

Atom	x	y	z	U(eq)
Zr(1)	6142(1)	6472(1)	9090(1)	62(1)
Zr(2)	3714(1)	8843(1)	-14069(1)	102(1)
N(1)	6044(3)	7351(4)	7788(7)	68(2)
N(2)	5848(3)	6117(3)	7575(7)	65(2)
N(3)	6414(3)	7352(4)	9756(7)	78(3)
N(4)	6517(4)	5659(6)	9514(9)	121(4)
N(5)	3615(3)	9732(4)	-12843(8)	68(2)
N(6)	3464(4)	8497(4)	-12514(8)	100(3)
N(7)	3919(4)	9713(4)	-14844(9)	89(3)
N(8)	3955(7)	8055(8)	-14713(15)	209(8)
C(1)	6191(4)	7959(5)	8090(10)	83(3)
C(2)	6122(5)	8492(6)	7349(12)	108(4)
C(3)	5919(5)	8382(6)	6325(11)	101(4)
C(4)	5770(5)	7757(6)	6077(11)	104(4)
C(5)	5833(4)	7246(5)	6782(9)	63(3)
C(6)	5688(4)	6538(5)	6631(9)	78(3)
C(7)	6400(4)	8015(5)	9255(11)	91(3)
C(8)	5813(4)	5422(4)	7274(8)	65(3)
C(9)	6157(3)	5128(5)	6626(9)	67(3)
C(10)	6552(5)	5496(6)	6154(11)	95(4)
C(11)	6527(5)	5550(8)	4835(12)	128(5)
C(12)	7008(4)	5240(8)	6559(14)	135(6)
C(13)	6117(4)	4447(6)	6391(10)	89(3)
C(14)	5755(5)	4086(6)	6804(11)	93(4)
C(15)	5432(4)	4373(5)	7404(10)	88(3)
C(16)	5441(4)	5040(5)	7685(10)	74(3)

C(17)	5054(4)	5347(7)	8401(11)	99(4)
C(18)	4975(6)	4919(11)	9469(13)	169(8)
C(19)	4624(5)	5377(8)	7713(17)	160(7)
C(20)	6482(4)	7356(4)	10958(11)	66(3)
C(21)	6914(4)	7463(5)	11429(11)	80(3)
C(22)	7320(4)	7641(6)	10644(12)	99(4)
C(23)	7476(5)	8354(6)	10838(14)	135(5)
C(24)	7728(6)	7156(9)	10839(18)	168(7)
C(25)	6981(4)	7422(6)	12607(12)	86(3)
C(26)	6628(4)	7284(6)	13292(11)	91(4)
C(27)	6204(4)	7173(6)	12847(12)	95(4)
C(28)	6119(4)	7211(5)	11679(11)	73(3)
C(29)	5646(5)	7154(8)	11197(13)	118(5)
C(30)	5304(6)	7350(15)	11814(32)	415(32)
C(31)	5608(4)	6503(6)	10473(11)	94(4)
C(32)	6716(4)	5232(5)	10314(10)	80(3)
C(33)	6646(6)	5491(10)	11558(13)	146(6)
C(34)	7165(5)	5048(10)	10024(15)	180(9)
C(35)	6443(9)	4620(10)	10225(23)	244(13)
C(36)	3702(4)	10359(6)	-13197(9)	87(4)
C(37)	3631(4)	10911(5)	-12544(10)	90(3)
C(38)	3435(4)	10813(6)	-11496(11)	92(4)
C(39)	3330(4)	10186(6)	-11098(11)	96(4)
C(40)	3419(4)	9654(5)	-11842(12)	81(3)
C(41)	3310(6)	8930(6)	-11568(12)	143(7)
C(42)	3913(6)	10373(6)	-14355(11)	132(6)
C(43)	3412(4)	7812(5)	-12244(10)	78(3)
C(44)	3744(4)	7484(5)	-11596(10)	75(3)
C(45)	4158(5)	7860(7)	-11171(11)	106(4)
C(46)	4596(5)	7505(10)	-11581(16)	160(7)

C(47)	4152(5)	7867(8)	-9839(13)	134(5)
C(48)	3688(5)	6830(6)	-11368(11)	93(4)
C(49)	3320(5)	6478(6)	-11716(11)	97(4)
C(50)	2988(4)	6809(6)	-12358(10)	94(4)
C(51)	3029(4)	7475(5)	-12610(10)	82(3)
C(52)	2665(5)	7830(11)	-13269(14)	165(9)
C(53)	2228(5)	7875(11)	-12674(20)	202(10)
C(54)	2540(8)	7409(14)	-14443(18)	242(14)
C(55)	3963(5)	9720(5)	-16109(9)	74(3)
C(56)	4396(5)	9773(6)	-16576(11)	93(4)
C(57)	4825(4)	9898(7)	-15929(16)	112(4)
C(58)	4981(6)	10616(8)	-16054(20)	196(9)
C(59)	5183(5)	9424(10)	-16214(18)	182(9)
C(60)	4404(5)	9755(6)	-17767(13)	97(4)
C(61)	4021(5)	9657(6)	-18413(11)	93(4)
C(62)	3620(4)	9612(5)	-17904(10)	80(3)
C(63)	3561(5)	9647(6)	-16759(11)	85(3)
C(64)	3081(5)	9612(8)	-16234(14)	132(6)
C(65)	2774(6)	10070(17)	-16709(19)	280(16)
C(66)	3025(8)	8985(12)	-15490(22)	237(11)
C(67)	4103(8)	7571(6)	-15531(16)	168(9)
C(68)	4188(12)	7899(14)	-16555(21)	300(20)
C(69)	4500(13)	7209(21)	-15170(24)	441(38)
C(70)	3772(15)	7059(13)	-15542(49)	580(55)

Table 3. Bond lengths (Å) and angles (deg) for DM01.

Zr(1)-N(4)	2.036(9)
Zr(1)-N(3)	2.093(8)
Zr(1)-N(2)	2.106(7)
Zr(1)-C(31)	2.268(12)
Zr(1)-N(1)	2.352(8)
Zr(2)-N(8)	1.893(12)
Zr(2)-N(7)	2.061(9)
Zr(2)-N(6)	2.090(8)
Zr(2)-N(5)	2.313(9)
Zr(2)-C(66)	2.65(2)
N(1)-C(1)	1.343(12)
N(1)-C(5)	1.354(12)
N(2)-C(8)	1.443(11)
N(2)-C(6)	1.473(12)
N(3)-C(20)	1.428(14)
N(3)-C(7)	1.456(12)
N(4)-C(32)	1.401(14)
N(5)-C(40)	1.320(14)
N(5)-C(36)	1.350(14)
N(6)-C(43)	1.420(12)
N(6)-C(41)	1.49(2)
N(7)-C(42)	1.44(2)
N(7)-C(55)	1.49(2)
N(8)-C(67)	1.44(2)
C(1)-C(2)	1.39(2)
C(1)-C(7)	1.51(2)
C(2)-C(3)	1.36(2)
C(3)-C(4)	1.36(2)

C(4)-C(5)	1.333(14)
C(5)-C(6)	1.494(14)
C(8)-C(9)	1.401(13)
C(8)-C(16)	1.425(14)
C(9)-C(13)	1.40(2)
C(9)-C(10)	1.49(2)
C(10)-C(12)	1.52(2)
C(10)-C(11)	1.56(2)
C(13)-C(14)	1.38(2)
C(14)-C(15)	1.32(2)
C(15)-C(16)	1.381(14)
C(16)-C(17)	1.55(2)
C(17)-C(19)	1.51(2)
C(17)-C(18)	1.54(2)
C(20)-C(28)	1.40(2)
C(20)-C(21)	1.41(2)
C(21)-C(25)	1.40(2)
C(21)-C(22)	1.55(2)
C(22)-C(23)	1.52(2)
C(22)-C(24)	1.57(2)
C(25)-C(26)	1.35(2)
C(26)-C(27)	1.38(2)
C(27)-C(28)	1.40(2)
C(28)-C(29)	1.51(2)
C(29)-C(30)	1.30(3)
C(29)-C(31)	1.56(2)
C(32)-C(34)	1.42(2)
C(32)-C(35)	1.47(2)
C(32)-C(33)	1.57(2)
C(36)-C(37)	1.36(2)

C(36)-C(42)	1.50(2)
C(37)-C(38)	1.38(2)
C(38)-C(39)	1.38(2)
C(39)-C(40)	1.40(2)
C(40)-C(41)	1.52(2)
C(43)-C(51)	1.39(2)
C(43)-C(44)	1.41(2)
C(44)-C(48)	1.35(2)
C(44)-C(45)	1.52(2)
C(45)-C(46)	1.55(2)
C(45)-C(47)	1.57(2)
C(48)-C(49)	1.36(2)
C(49)-C(50)	1.40(2)
C(50)-C(51)	1.38(2)
C(51)-C(52)	1.51(2)
C(52)-C(53)	1.47(2)
C(52)-C(54)	1.66(3)
C(55)-C(56)	1.40(2)
C(55)-C(63)	1.42(2)
C(56)-C(60)	1.40(2)
C(56)-C(57)	1.50(2)
C(57)-C(59)	1.46(2)
C(57)-C(58)	1.52(2)
C(60)-C(61)	1.38(2)
C(61)-C(62)	1.33(2)
C(62)-C(63)	1.36(2)
C(63)-C(64)	1.55(2)
C(64)-C(65)	1.41(2)
C(64)-C(66)	1.54(2)
C(67)-C(68)	1.39(3)

C(67)-C(70)	1.42(3)
C(67)-C(69)	1.44(3)
N(4)-Zr(1)-N(3)	112.0(4)
N(4)-Zr(1)-N(2)	99.3(4)
N(3)-Zr(1)-N(2)	139.6(3)
N(4)-Zr(1)-C(31)	103.1(4)
N(3)-Zr(1)-C(31)	88.7(4)
N(2)-Zr(1)-C(31)	109.1(4)
N(4)-Zr(1)-N(1)	145.8(4)
N(3)-Zr(1)-N(1)	70.0(3)
N(2)-Zr(1)-N(1)	69.7(3)
C(31)-Zr(1)-N(1)	111.1(4)
N(8)-Zr(2)-N(7)	114.9(6)
N(8)-Zr(2)-N(6)	101.8(6)
N(7)-Zr(2)-N(6)	140.6(4)
N(8)-Zr(2)-N(5)	160.4(7)
N(7)-Zr(2)-N(5)	70.0(3)
N(6)-Zr(2)-N(5)	70.5(3)
N(8)-Zr(2)-C(66)	97.3(9)
N(7)-Zr(2)-C(66)	81.8(6)
N(6)-Zr(2)-C(66)	108.3(7)
N(5)-Zr(2)-C(66)	102.2(6)
C(1)-N(1)-C(5)	121.5(9)
C(1)-N(1)-Zr(1)	118.0(7)
C(5)-N(1)-Zr(1)	120.5(7)
C(8)-N(2)-C(6)	110.3(7)
C(8)-N(2)-Zr(1)	124.3(6)
C(6)-N(2)-Zr(1)	125.1(6)
C(20)-N(3)-C(7)	113.5(8)
C(20)-N(3)-Zr(1)	115.5(6)

C(7)-N(3)-Zr(1)	127.5(7)
C(32)-N(4)-Zr(1)	152.1(9)
C(40)-N(5)-C(36)	118.0(9)
C(40)-N(5)-Zr(2)	121.3(7)
C(36)-N(5)-Zr(2)	120.2(8)
C(43)-N(6)-C(41)	111.4(8)
C(43)-N(6)-Zr(2)	123.8(7)
C(41)-N(6)-Zr(2)	124.7(7)
C(42)-N(7)-C(55)	112.9(9)
C(42)-N(7)-Zr(2)	126.7(8)
C(55)-N(7)-Zr(2)	118.3(7)
C(67)-N(8)-Zr(2)	162(2)
N(1)-C(1)-C(2)	119.0(11)
N(1)-C(1)-C(7)	116.2(9)
C(2)-C(1)-C(7)	124.8(10)
C(3)-C(2)-C(1)	119.5(11)
C(4)-C(3)-C(2)	118.8(11)
C(5)-C(4)-C(3)	122.1(12)
C(4)-C(5)-N(1)	119.1(10)
C(4)-C(5)-C(6)	128.2(11)
N(1)-C(5)-C(6)	112.7(9)
N(2)-C(6)-C(5)	111.3(8)
N(3)-C(7)-C(1)	108.1(8)
C(9)-C(8)-C(16)	121.2(9)
C(9)-C(8)-N(2)	119.3(9)
C(16)-C(8)-N(2)	119.4(9)
C(13)-C(9)-C(8)	117.2(10)
C(13)-C(9)-C(10)	118.5(10)
C(8)-C(9)-C(10)	124.3(10)
C(9)-C(10)-C(12)	114.3(11)

C(9)-C(10)-C(11)	111.7(11)
C(12)-C(10)-C(11)	112.2(12)
C(14)-C(13)-C(9)	120.6(11)
C(15)-C(14)-C(13)	121.4(11)
C(14)-C(15)-C(16)	122.5(11)
C(15)-C(16)-C(8)	117.2(10)
C(15)-C(16)-C(17)	120.1(11)
C(8)-C(16)-C(17)	122.7(10)
C(19)-C(17)-C(18)	109.3(12)
C(19)-C(17)-C(16)	110.4(11)
C(18)-C(17)-C(16)	109.5(12)
C(28)-C(20)-C(21)	119.3(12)
C(28)-C(20)-N(3)	119.3(10)
C(21)-C(20)-N(3)	121.2(11)
C(25)-C(21)-C(20)	120.4(12)
C(25)-C(21)-C(22)	119.5(11)
C(20)-C(21)-C(22)	120.0(11)
C(23)-C(22)-C(21)	111.1(11)
C(23)-C(22)-C(24)	109.1(12)
C(21)-C(22)-C(24)	111.4(11)
C(26)-C(25)-C(21)	119.7(11)
C(25)-C(26)-C(27)	120.8(12)
C(26)-C(27)-C(28)	121.9(12)
C(27)-C(28)-C(20)	117.9(11)
C(27)-C(28)-C(29)	122.0(12)
C(20)-C(28)-C(29)	119.9(12)
C(30)-C(29)-C(28)	119(2)
C(30)-C(29)-C(31)	120(2)
C(28)-C(29)-C(31)	109.4(11)
C(29)-C(31)-Zr(1)	111.3(8)

N(4)-C(32)-C(34)	113.0(12)
N(4)-C(32)-C(35)	103.6(13)
C(34)-C(32)-C(35)	106(2)
N(4)-C(32)-C(33)	111.6(11)
C(34)-C(32)-C(33)	115.6(12)
C(35)-C(32)-C(33)	106(2)
N(5)-C(36)-C(37)	123.6(11)
N(5)-C(36)-C(42)	112.1(10)
C(37)-C(36)-C(42)	124.2(11)
C(36)-C(37)-C(38)	117.0(11)
C(39)-C(38)-C(37)	121.9(11)
C(38)-C(39)-C(40)	116.1(11)
N(5)-C(40)-C(39)	123.2(10)
N(5)-C(40)-C(41)	113.3(10)
C(39)-C(40)-C(41)	123.5(12)
N(6)-C(41)-C(40)	109.5(10)
N(7)-C(42)-C(36)	110.6(10)
C(51)-C(43)-C(44)	120.6(9)
C(51)-C(43)-N(6)	119.5(11)
C(44)-C(43)-N(6)	119.8(11)
C(48)-C(44)-C(43)	118.3(11)
C(48)-C(44)-C(45)	121.1(12)
C(43)-C(44)-C(45)	120.6(10)
C(44)-C(45)-C(46)	109.9(11)
C(44)-C(45)-C(47)	108.9(12)
C(46)-C(45)-C(47)	108.9(13)
C(44)-C(48)-C(49)	123.0(12)
C(48)-C(49)-C(50)	118.4(11)
C(51)-C(50)-C(49)	120.9(12)
C(50)-C(51)-C(43)	118.7(11)

C(50)-C(51)-C(52)	120.5(14)
C(43)-C(51)-C(52)	120.8(12)
C(53)-C(52)-C(51)	114.3(13)
C(53)-C(52)-C(54)	103(2)
C(51)-C(52)-C(54)	110(2)
C(56)-C(55)-C(63)	124.3(11)
C(56)-C(55)-N(7)	118.1(12)
C(63)-C(55)-N(7)	117.6(11)
C(60)-C(56)-C(55)	113.9(12)
C(60)-C(56)-C(57)	120.0(14)
C(55)-C(56)-C(57)	126.0(13)
C(59)-C(57)-C(56)	112.7(14)
C(59)-C(57)-C(58)	112.0(14)
C(56)-C(57)-C(58)	111.5(11)
C(61)-C(60)-C(56)	122.9(12)
C(62)-C(61)-C(60)	119.6(12)
C(61)-C(62)-C(63)	123.7(12)
C(62)-C(63)-C(55)	115.6(11)
C(62)-C(63)-C(64)	120.6(13)
C(55)-C(63)-C(64)	123.8(12)
C(65)-C(64)-C(66)	134(2)
C(65)-C(64)-C(63)	113.7(14)
C(66)-C(64)-C(63)	111.2(14)
C(64)-C(66)-Zr(2)	111.3(13)
C(68)-C(67)-C(70)	117(3)
C(68)-C(67)-N(8)	108.3(14)
C(70)-C(67)-N(8)	106(2)
C(68)-C(67)-C(69)	110(2)
C(70)-C(67)-C(69)	102(3)
N(8)-C(67)-C(69)	113(2)

Table 4. Anisotropic displacement parameters ($Å^2 \times 10^3$) for DM01.

Atom	U11	U22	U33	U23	U13	U12
Zr(1)	82(1)	47(1)	58(1)	-6(1)	-9(1)	-1(1)
Zr(2)	184(1)	46(1)	77(1)	5(1)	31(1)	0(1)
N(1)	92(6)	53(5)	60(6)	-2(4)	-8(5)	7(4)
N(2)	76(6)	50(4)	70(6)	-14(4)	-25(4)	6(4)
N(3)	129(8)	50(5)	56(6)	-6(4)	-31(5)	-21(5)
N(4)	132(9)	134(9)	96(8)	23(7)	10(6)	67(7)
N(5)	80(6)	47(5)	77(7)	14(4)	5(5)	-2(4)
N(6)	171(10)	53(5)	76(7)	20(5)	39(6)	-4(5)
N(7)	150(9)	46(5)	69(7)	4(5)	14(6)	-1(5)
N(8)	335(22)	129(12)	164(14)	-33(11)	86(15)	81(13)
C(1)	140(10)	41(6)	70(7)	1(5)	-17(7)	-6(6)
C(2)	169(13)	51(6)	103(10)	8(7)	-17(9)	0(7)
C(3)	156(11)	64(8)	82(9)	14(6)	-10(8)	7(7)
C(4)	157(12)	78(8)	76(9)	-2(7)	-18(8)	23(7)
C(5)	75(8)	63(7)	53(7)	-1(5)	-2(5)	16(5)
C(6)	90(8)	66(7)	78(8)	-16(6)	-32(6)	5(6)
C(7)	136(9)	62(7)	77(9)	4(6)	-17(8)	-24(6)
C(8)	88(8)	55(6)	50(6)	-5(5)	-5(5)	9(5)
C(9)	78(7)	56(6)	68(7)	-6(5)	5(6)	-8(5)
C(10)	113(10)	80(8)	92(11)	-16(7)	18(8)	-11(7)
C(11)	164(14)	124(12)	96(11)	4(9)	44(9)	-9(10)
C(12)	75(9)	183(16)	146(14)	9(11)	28(9)	-1(9)
C(13)	114(9)	68(7)	85(8)	-18(6)	4(7)	3(7)
C(14)	129(11)	51(7)	99(10)	-7(6)	4(8)	-10(7)
C(15)	120(10)	58(7)	86(9)	2(6)	-8(7)	-28(7)
C(16)	81(8)	82(8)	61(7)	-8(6)	-6(6)	-8(6)
C(17)	78(8)	129(11)	90(10)	-40(8)	12(7)	-27(7)

C(18)	176(16)	249(21)	82(13)	-12(12)	32(10)	-50(15)
C(19)	100(11)	176(16)	203(19)	-61(14)	-23(12)	11(10)
C(20)	72(7)	52(5)	74(7)	-14(6)	-15(6)	-8(5)
C(21)	109(10)	57(7)	75(9)	-8(5)	-7(7)	1(6)
C(22)	100(9)	98(9)	100(11)	0(7)	-3(7)	-15(8)
C(23)	134(11)	130(11)	140(13)	-6(11)	36(10)	-55(9)
C(24)	140(14)	177(16)	187(19)	-5(16)	71(14)	3(12)
C(25)	76(8)	100(9)	83(10)	-15(7)	-10(7)	-6(6)
C(26)	90(9)	118(10)	67(8)	-7(7)	-25(7)	-16(7)
C(27)	98(10)	100(10)	88(10)	4(8)	13(8)	-12(7)
C(28)	67(7)	62(7)	89(9)	-14(6)	-13(7)	-12(6)
C(29)	92(10)	148(13)	115(12)	-65(10)	-8(8)	-2(9)
C(30)	100(14)	440(43)	706(70)	-467(49)	-127(25)	97(19)
C(31)	86(8)	101(9)	95(9)	-17(7)	-18(6)	5(7)
C(32)	100(9)	65(7)	74(8)	4(6)	-22(6)	4(6)
C(33)	152(14)	204(18)	83(11)	7(11)	-24(10)	27(13)
C(34)	120(12)	270(24)	150(17)	52(16)	-17(11)	97(14)
C(35)	359(33)	130(17)	244(28)	-9(16)	-57(26)	-86(20)
C(36)	135(10)	65(8)	60(8)	3(6)	-2(7)	3(6)
C(37)	152(11)	56(6)	62(8)	-3(6)	-2(7)	-7(7)
C(38)	121(10)	68(8)	88(9)	-7(6)	-8(7)	15(7)
C(39)	146(10)	76(8)	65(8)	4(7)	28(8)	26(7)
C(40)	85(8)	62(7)	97(9)	10(7)	8(7)	10(6)
C(41)	260(20)	78(9)	92(10)	16(8)	62(11)	18(10)
C(42)	261(18)	57(8)	77(10)	12(6)	48(10)	-9(9)
C(43)	115(10)	46(6)	74(8)	6(5)	14(7)	6(6)
C(44)	102(9)	60(7)	64(7)	12(5)	22(6)	0(6)
C(45)	122(10)	100(9)	95(12)	-4(8)	-14(8)	-26(8)
C(46)	145(14)	184(17)	150(15)	-42(13)	20(12)	-32(13)
C(47)	155(14)	151(14)	97(11)	-14(10)	-29(10)	11(11)

C(48)	114(10)	75(9)	91(10)	16(7)	10(7)	15(7)
C(49)	132(11)	60(7)	99(9)	12(7)	19(8)	2(8)
C(50)	109(10)	90(9)	83(9)	-2(7)	-2(7)	-16(7)
C(51)	107(9)	70(8)	70(8)	23(6)	-5(7)	1(7)
C(52)	103(12)	262(23)	128(15)	106(16)	39(10)	49(13)
C(53)	104(13)	269(24)	232(22)	95(20)	-1(14)	74(14)
C(54)	252(25)	359(38)	115(18)	-3(18)	-92(18)	3(22)
C(55)	128(10)	42(5)	53(9)	16(5)	18(8)	-2(5)
C(56)	128(12)	70(7)	80(9)	22(6)	0(9)	-14(7)
C(57)	88(8)	139(11)	108(10)	25(11)	-31(10)	-18(8)
C(58)	176(15)	167(15)	245(22)	87(17)	-102(17)	-86(12)
C(59)	117(12)	225(19)	203(22)	48(17)	-21(13)	52(13)
C(60)	89(9)	100(9)	102(11)	15(8)	26(8)	0(7)
C(61)	123(11)	92(9)	65(8)	-10(7)	16(9)	-3(8)
C(62)	84(9)	86(8)	69(9)	-2(6)	-3(7)	-10(6)
C(63)	111(10)	82(8)	61(8)	16(6)	22(7)	-2(7)
C(64)	90(9)	162(13)	143(16)	65(11)	39(9)	-9(9)
C(65)	92(13)	570(50)	178(20)	35(27)	-12(13)	82(22)
C(67)	301(24)	48(7)	155(18)	8(8)	136(17)	33(10)
C(68)	517(53)	222(28)	163(22)	37(20)	160(29)	155(32)
C(69)	544(62)	588(68)	193(28)	-142(35)	-83(34)	468(62)
C(70)	679(83)	121(21)	940(126)	-97(42)	557(91)	-129(34)

6 Crystallographic data for $(BDPP)Zr(CH_2Ph)_2$.

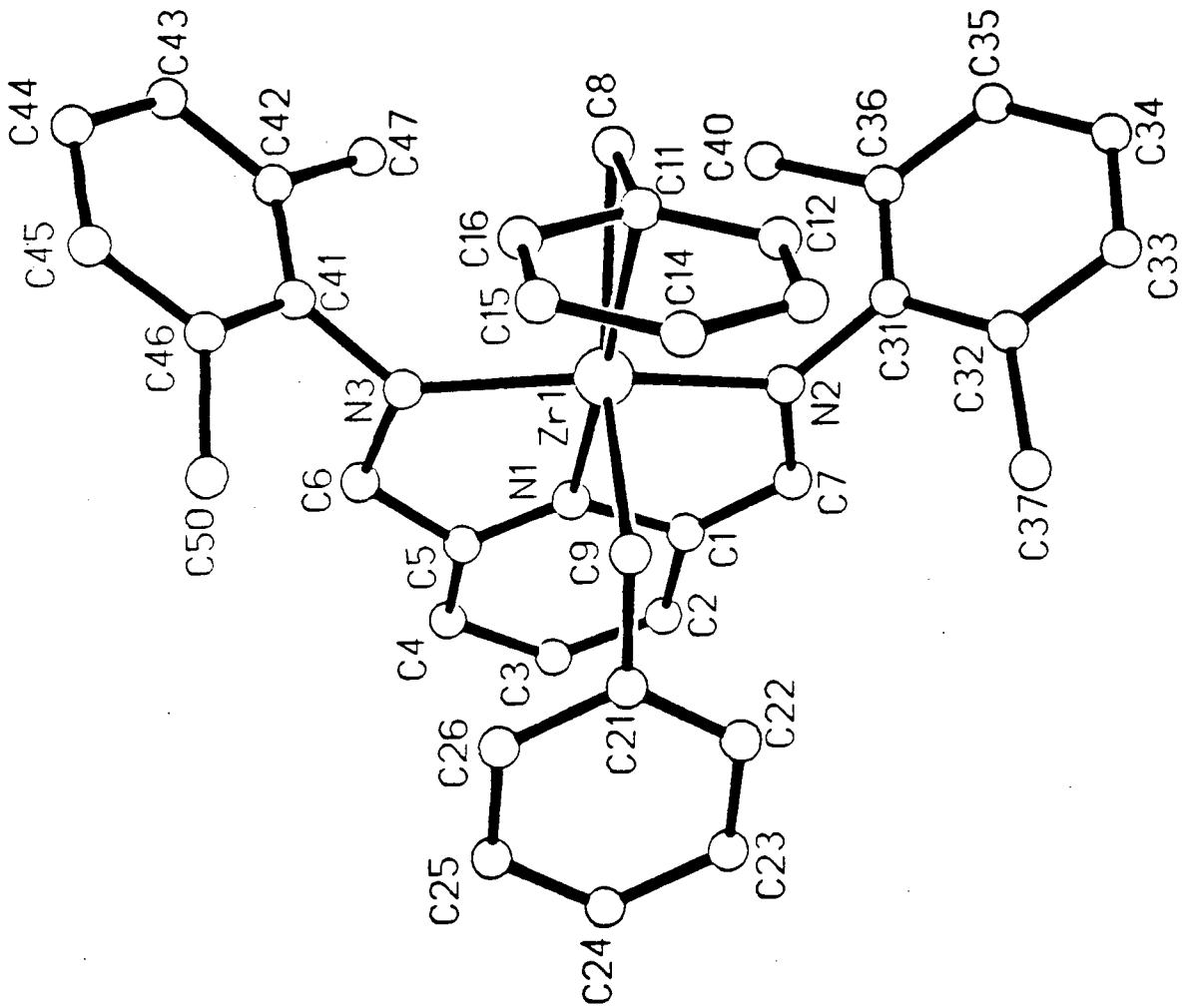

Table S1. Crystal Data and Experimental Details.

Empirical formula	$C_{45}H_{55}N_3Ti$
Formula weight	?????
Temperature	25°C
Wavelength	0.71073 Å
Crystal system	Monoclinic
Space group	$P2_1/n$
Unit cell dimensions	a = 12.535(11)Å
	b = 21.683(21)Å
	c = 14.543(18)Å
	β = 90.28(1)°
Volume	3952(7) Å^3
Z	4
Density, calcd.	1.223 g.cm^{-3}
Absorption coefficient	0.311 mm^{-1}
F(000)	1544
Reflections Collected	3654
Independent reflections	989 [R(int) = 0.0358]
Refinement method	Full-matrix least-squares on F
Data/parameters	989/ 156
Goodness-of-fit (GooF) on F^2	1.62
Final R indices [I>2sigma(I)]	R = 0.0972, wR = 0.1077
R indices (all data)	R = 0.4474, wR2 = 0.3065

$R = \Sigma(||F_o| - |F_c||)/\Sigma|F_o|$;

$wR = [\Sigma\sqrt{w}(F_o - F_c)/\Sigma\sqrt{w}F_o]$

Table S2. Atomic coordinates (x 10^4) and equivalent isotropic displacement parameters ($Å^2$ x 10^3). U(eq) is defined as one third of the trace of the orthogonalized Uij tensor.

atom	x	y	z	Ueq
Zr(1)	4123(2)	1476(1)	2508(3)	44(1)
N(2)	4146(15)	1136(12)	1139(18)	44(7)
N(3)	4164(16)	1132(12)	3846(20)	55(8)
N(1)	5019(15)	555(12)	2546(21)	37(7)
C(1)	5293(21)	363(16)	1660(27)	50(10)
C(2)	5985(24)	-209(18)	1688(35)	86(13)
C(3)	6334(24)	-411(19)	2491(31)	81(13)
C(4)	5993(25)	-201(18)	3331(33)	86(13)
C(5)	5369(23)	338(16)	3302(30)	60(10)
C(6)	4854(26)	582(18)	4079(32)	88(13)
C(7)	4883(24)	624(18)	935(30)	78(12)
C(8)	2370(17)	1895(11)	2508(22)	34(8)
C(9)	5587(15)	2115(12)	2519(22)	38(9)
C(12)	3290(14)	2780(11)	1672(15)	81(12)
C(13)	3866(14)	3330(11)	1698(15)	82(12)
C(14)	4148(14)	3592(11)	2541(15)	99(11)
C(15)	3853(14)	3304(11)	3358(15)	111(15)
C(16)	3277(14)	2753(11)	3333(15)	80(12)
C(11)	2996(14)	2491(11)	2490(15)	73(11)
C(22)	7052(16)	1609(10)	1654(15)	90(12)
C(23)	7930(16)	1213(10)	1652(15)	128(17)
C(24)	8374(16)	1015(10)	2482(15)	102(13)
C(25)	7941(16)	1212(10)	3314(15)	121(16)
C(26)	7063(16)	1607(10)	3315(15)	77(11)
C(21)	6618(16)	1806(10)	2485(15)	45(9)
C(32)	3808(10)	1691(8)	-251(14)	72(11)
C(33)	3161(10)	1828(8)	-1007(14)	60(10)
C(34)	2158(10)	1553(8)	-1092(14)	75(10)
C(35)	1804(10)	1143(8)	-422(14)	58(10)
C(36)	2451(10)	1006(8)	334(14)	68(11)
C(31)	3454(10)	1280(8)	419(14)	37(8)
C(42)	2454(11)	990(8)	4685(13)	43(9)
C(43)	1800(11)	1140(8)	5425(13)	57(10)
C(44)	2141(11)	1569(8)	6077(13)	67(10)
C(45)	3137(11)	1850(8)	5988(13)	96(13)
C(46)	3791(11)	1700(8)	5247(13)	66(11)
C(41)	3449(11)	1271(8)	4596(13)	42(9)
C(37)	4949(11)	1954(9)	-267(15)	129(17)

C(38)	5607(17)	1618(12)	-1007(24)	97(13)
C(39)	4906(22)	2648(9)	-492(32)	149(18)
C(40)	2120(14)	516(10)	1043(16)	74(11)
C(27)	2397(25)	-132(9)	679(32)	168(21)
C(28)	910(18)	558(13)	1213(28)	101(14)
C(47)	2098(13)	505(10)	3972(14)	69(11)
C(48)	905(17)	592(14)	3749(22)	103(14)
C(49)	2282(26)	-146(9)	4364(30)	211(27)
C(50)	4940(12)	1953(9)	5268(15)	87(12)
C(51)	5577(17)	1632(13)	6040(23)	119(15)
C(52)	4917(21)	2653(9)	5444(29)	162(20)

Table S3. Bond Distances (Å) and Angles (°).

Zr(1)-N(2)	2.124 (26)	Zr(1)-N(3)	2.084 (29)
Zr(1)-N(1)	2.293 (24)	Zr(1)-C(8)	2.377 (22)
Zr(1)-C(9)	2.298 (22)	Zr(1)-C(11)	2.616 (22)
N(2)-C(7)	1.474 (43)	N(2)-C(31)	1.392 (29)
N(3)-C(6)	1.510 (45)	N(3)-C(41)	1.445 (31)
N(1)-C(1)	1.397 (49)	N(1)-C(5)	1.272 (50)
C(1)-C(2)	1.514 (48)	C(1)-C(7)	1.301 (55)
C(2)-C(3)	1.321 (64)	C(3)-C(4)	1.373 (63)
C(4)-C(5)	1.406 (49)	C(5)-C(6)	1.409 (58)
C(8)-C(11)	1.513 (32)	C(9)-C(21)	1.458 (30)
C(32)-C(37)	1.540 (20)	C(36)-C(40)	1.539 (28)
C(42)-C(47)	1.541 (27)	C(46)-C(50)	1.540 (21)
C(37)-C(38)	1.542 (36)	C(37)-C(39)	1.541 (30)
C(40)-C(27)	1.540 (33)	C(40)-C(28)	1.541 (29)
C(47)-C(48)	1.540 (27)	C(47)-C(49)	1.540 (32)
C(50)-C(51)	1.541 (35)	C(50)-C(52)	1.540 (28)

N(2)-Zr(1)-N(3)	138.6(10)	N(2)-Zr(1)-N(1)	73.2(10)
N(3)-Zr(1)-N(1)	69.9(10)	N(2)-Zr(1)-C(8)	98.6(9)
N(3)-Zr(1)-C(8)	98.9(10)	N(1)-Zr(1)-C(8)	141.7(8)
N(2)-Zr(1)-C(9)	101.6(10)	N(3)-Zr(1)-C(9)	101.2(10)
N(1)-Zr(1)-C(9)	97.7(8)	C(8)-Zr(1)-C(9)	120.5(8)
N(2)-Zr(1)-C(11)	107.0(8)	N(3)-Zr(1)-C(11)	108.7(8)
N(1)-Zr(1)-C(11)	176.5(7)	C(8)-Zr(1)-C(11)	34.9(7)
C(9)-Zr(1)-C(11)	85.7(8)	Zr(1)-N(2)-C(7)	117.4(21)
Zr(1)-N(2)-C(31)	128.0(16)	C(7)-N(2)-C(31)	114.0(25)
Zr(1)-N(3)-C(6)	120.2(23)	Zr(1)-N(3)-C(41)	128.1(16)
C(6)-N(3)-C(41)	110.6(25)	Zr(1)-N(1)-C(1)	111.1(21)

Zr(1)-N(1)-C(5)	120.6(24)	C(1)-N(1)-C(5)	127.0(27)
N(1)-C(1)-C(2)	111.3(32)	N(1)-C(1)-C(7)	121.3(30)
C(2)-C(1)-C(7)	127.0(38)	C(1)-C(2)-C(3)	118.8(40)
C(2)-C(3)-C(4)	125.0(36)	C(3)-C(4)-C(5)	115.1(40)
N(1)-C(5)-C(4)	121.5(38)	N(1)-C(5)-C(6)	113.4(30)
C(4)-C(5)-C(6)	123.0(39)	N(3)-C(6)-C(5)	112.4(35)
N(2)-C(7)-C(1)	114.3(35)	Zr(1)-C(8)-C(11)	81.2(11)
Zr(1)-C(9)-C(21)	115.5(17)	Zr(1)-C(11)-C(8)	63.9(11)
Zr(1)-C(11)-C(12)	103.9(5)	C(8)-C(11)-C(12)	122.5(15)
Zr(1)-C(11)-C(16)	101.5(5)	C(8)-C(11)-C(16)	117.5(15)
C(9)-C(21)-C(22)	121.3(15)	C(9)-C(21)-C(26)	117.6(15)
C(33)-C(32)-C(37)	116.5(11)	C(31)-C(32)-C(37)	123.1(11)
C(35)-C(36)-C(40)	121.1(9)	C(31)-C(36)-C(40)	118.7(9)
N(2)-C(31)-C(32)	118.0(11)	N(2)-C(31)-C(36)	122.0(11)
C(43)-C(42)-C(47)	120.6(9)	C(41)-C(42)-C(47)	119.4(9)
C(45)-C(46)-C(50)	117.1(10)	C(41)-C(46)-C(50)	122.3(10)
N(3)-C(41)-C(42)	122.5(12)	N(3)-C(41)-C(46)	117.5(12)
C(32)-C(37)-C(38)	109.5(17)	C(32)-C(37)-C(39)	109.5(15)
C(38)-C(37)-C(39)	109.4(22)	C(36)-C(40)-C(27)	109.7(22)
C(36)-C(40)-C(28)	109.6(18)	C(27)-C(40)-C(28)	109.4(20)
C(42)-C(47)-C(48)	109.6(17)	C(42)-C(47)-C(49)	109.5(20)
C(48)-C(47)-C(49)	109.5(20)	C(46)-C(50)-C(51)	109.6(16)
C(46)-C(50)-C(52)	109.6(15)	C(51)-C(50)-C(52)	109.5(22)

Table S4. Anisotropic displacement parameters ($Å^2$ x 10^3).
The anisotropic displacement factor exponent takes the form: $-2\pi^2[h^2a^{*2}U11 + ... + 2hka^*b^*U12]$

atom	U11	U22	U33	U23	U13	U12
Zr(1)	38(1)	33(2)	62(3)	9(2)	2(1)	0(4)

7 Crystallographic data for (BDPP)Zr(C_4H_6).

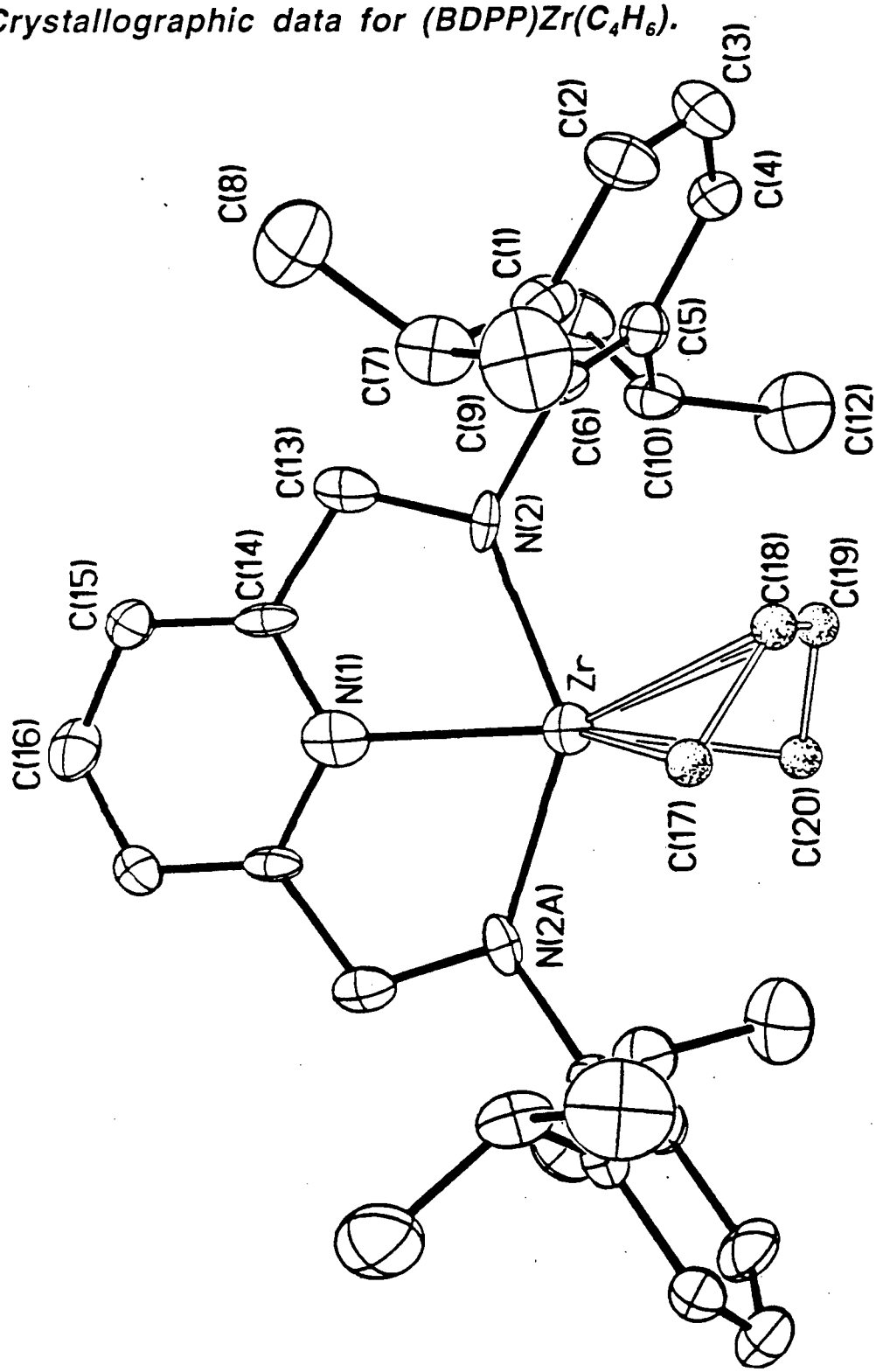

Table 1. Crystal data and structure refinement for 1.

Identification code	dm001
Empirical formula	C35.7 H48.5 N3 O0.35 Zr
Formula weight	616.49
Temperature	298(2) K
Wavelength	0.71073 A
Crystal system	Tetragonal
Space group	I-42d
Unit cell dimensions	a = 16.155(3) A alpha = 90 deg. b = 16.155(3) A beta = 90 deg. c = 26.847(6) A gamma = 90 deg.
Volume, Z	7007(2) A^3, 8
Density (calculated)	1.169 Mg/m^3
Absorption coefficient	0.336 mm^-1
F(000)	2612
Crystal size	0.20 x 0.10 x 0.10 mm
Theta range for data collection	1.47 to 21.49 deg.
Limiting indices	-20<=h<=21, -21<=k<=15, -32<=l<=35
Reflections collected	11860
Independent reflections	2019 [R(int) = 0.2999]
Refinement method	Full-matrix least-squares on F^2
Data / restraints / parameters	1998 / 6 / 186
Goodness-of-fit on F^2	1.029
Final R indices [I>2sigma(I)]	R1 = 0.0765, wR2 = 0.1635
R indices (all data)	R1 = 0.1084, wR2 = 0.1929
Absolute structure parameter	0.0(2)
Largest diff. peak and hole	0.551 and -0.489 e.A^-3

Table 2. Atomic coordinates (x 10^4) and equivalent isotropic displacement parameters (A^2 x 10^3) for 1. U(eq) is defined as one third of the trace of the orthogonalized Uij tensor.

	x	y	z	U(eq)
Zr	6917(1)	2500	1250	42(1)
N(1)	5489(8)	2500	1250	43(3)
N(2)	6469(4)	3719(5)	1336(3)	31(2)
C(1)	7142(7)	4753(7)	1890(4)	46(3)
C(2)	7629(9)	5469(8)	1952(5)	62(4)
C(3)	7901(8)	5924(8)	1544(5)	62(4)
C(4)	7740(6)	5652(7)	1067(5)	49(4)
C(5)	7261(6)	4926(7)	987(4)	43(3)
C(6)	6985(7)	4482(7)	1411(4)	36(3)
C(7)	6805(9)	4334(8)	2366(4)	60(4)
C(8)	6156(9)	4882(9)	2606(5)	84(5)
C(9)	7504(11)	4100(9)	2714(5)	92(5)
C(10)	7052(8)	4716(7)	451(4)	48(3)
C(11)	6424(10)	5346(8)	243(5)	86(5)
C(12)	7793(9)	4663(9)	118(5)	98(6)
C(13)	5615(7)	3963(6)	1342(4)	42(3)
C(14)	5080(7)	3223(6)	1287(4)	34(3)
C(15)	4201(6)	3239(6)	1293(4)	41(3)
C(16)	3805(10)	2500	1250	53(4)
C(17)	7917(15)	2166(21)	1856(9)	71(10)
C(18)	8272(13)	2945(15)	1585(9)	42(7)
C(19)	8306(13)	3069(17)	1084(9)	66(8)
C(20)	8045(15)	2386(21)	712(10)	64(8)
C(91)	10097(35)	5301(31)	1751(18)	105(18)
C(92)	10000	5000	2056(34)	75(19)
O(90)	9816(46)	4801(46)	2359(20)	82(25)

Table 3. Bond lengths [A] and angles [deg] for 1.

Zr-N(2)#1	2.111(8)
Zr-N(2)	2.111(8)
Zr-N(1)	2.307(13)
Zr-C(20)#1	2.33(2)
Zr-C(20)	2.33(2)
Zr-C(17)	2.36(2)
Zr-C(17)#1	2.36(2)
Zr-C(19)	2.47(2)
Zr-C(19)#1	2.47(2)
Zr-C(18)	2.47(2)
Zr-C(18)#1	2.47(2)
N(1)-C(14)	1.346(11)
N(1)-C(14)#1	1.346(11)
N(2)-C(13)	1.436(12)
N(2)-C(6)	1.501(13)
C(1)-C(6)	1.382(14)
C(1)-C(2)	1.41(2)
C(1)-C(7)	1.54(2)
C(2)-C(3)	1.39(2)
C(3)-C(4)	1.38(2)
C(4)-C(5)	1.42(2)
C(5)-C(6)	1.418(13)
C(5)-C(10)	1.52(2)
C(7)-C(8)	1.52(2)
C(7)-C(9)	1.51(2)
C(10)-C(12)	1.50(2)
C(10)-C(11)	1.54(2)
C(13)-C(14)	1.483(13)
C(14)-C(15)	1.420(13)
C(15)-C(16)	1.358(12)
C(16)-C(15)#1	1.358(12)
C(17)-C(18)	1.56(3)
C(18)-C(19)	1.36(3)
C(19)-C(20)	1.55(3)
C(91)-C(92)	0.97(6)
C(91)-C(91)#2	1.02(10)
C(91)-O(90)#2	1.65(6)
C(91)-O(90)	1.88(7)
C(92)-O(90)#2	0.92(7)
C(92)-O(90)	0.92(7)
C(92)-C(91)#2	0.97(6)
C(92)-O(90)#3	1.63(12)
C(92)-O(90)#4	1.63(12)
O(90)-O(90)#2	0.88(12)
O(90)-O(90)#3	0.98(8)
O(90)-O(90)#4	0.98(8)
O(90)-C(91)#2	1.65(6)
O(90)-C(92)#3	1.63(12)
N(2)#1-Zr-N(2)	140.0(4)
N(2)#1-Zr-N(1)	70.0(2)
N(2)-Zr-N(1)	70.0(2)
N(2)#1-Zr-C(20)#1	114.2(9)
N(2)-Zr-C(20)#1	97.2(8)
N(1)-Zr-C(20)#1	141.4(7)
N(2)#1-Zr-C(20)	97.2(8)

N(2)-Zr-C(20)	114.2(9)
N(1)-Zr-C(20)	141.4(7)
C(20)#1-Zr-C(20)	77.2(14)
N(2)#1-Zr-C(17)	95.5(8)
N(2)-Zr-C(17)	111.9(9)
N(1)-Zr-C(17)	133.3(6)
C(20)#1-Zr-C(17)	19.0(9)
C(20)-Zr-C(17)	82.7(9)
N(2)#1-Zr-C(17)#1	111.9(9)
N(2)-Zr-C(17)#1	95.5(8)
N(1)-Zr-C(17)#1	133.3(6)
C(20)#1-Zr-C(17)#1	82.7(9)
C(20)-Zr-C(17)#1	19.0(9)
C(17)-Zr-C(17)#1	93.3(13)
N(2)#1-Zr-C(19)	129.8(6)
N(2)-Zr-C(19)	89.1(6)
N(1)-Zr-C(19)	155.5(6)
C(20)#1-Zr-C(19)	51.0(9)
C(20)-Zr-C(19)	37.5(7)
C(17)-Zr-C(19)	65.5(9)
C(17)#1-Zr-C(19)	33.4(8)
N(2)#1-Zr-C(19)#1	89.1(6)
N(2)-Zr-C(19)#1	129.8(6)
N(1)-Zr-C(19)#1	155.5(6)
C(20)#1-Zr-C(19)#1	37.5(7)
C(20)-Zr-C(19)#1	51.0(9)
C(17)-Zr-C(19)#1	33.4(8)
C(17)#1-Zr-C(19)#1	65.5(9)
C(19)-Zr-C(19)#1	49.0(12)
N(2)#1-Zr-C(18)	127.9(6)
N(2)-Zr-C(18)	89.5(6)
N(1)-Zr-C(18)	152.3(5)
C(20)#1-Zr-C(18)	20.0(8)
C(20)-Zr-C(18)	63.7(8)
C(17)-Zr-C(18)	37.7(7)
C(17)#1-Zr-C(18)	65.0(9)
C(19)-Zr-C(18)	32.0(7)
C(19)#1-Zr-C(18)	40.3(7)
N(2)#1-Zr-C(18)#1	89.5(6)
N(2)-Zr-C(18)#1	127.9(6)
N(1)-Zr-C(18)#1	152.3(5)
C(20)#1-Zr-C(18)#1	63.7(8)
C(20)-Zr-C(18)#1	20.0(8)
C(17)-Zr-C(18)#1	65.0(9)
C(17)#1-Zr-C(18)#1	37.7(7)
C(19)-Zr-C(18)#1	40.3(7)
C(19)#1-Zr-C(18)#1	32.0(7)
C(18)-Zr-C(18)#1	55.5(11)
C(14)-N(1)-C(14)#1	121.2(13)
C(14)-N(1)-Zr	119.4(6)
C(14)#1-N(1)-Zr	119.4(6)
C(13)-N(2)-C(6)	107.9(8)
C(13)-N(2)-Zr	125.9(6)
C(6)-N(2)-Zr	126.2(6)
C(6)-C(1)-C(2)	118.1(11)
C(6)-C(1)-C(7)	124.4(11)
C(2)-C(1)-C(7)	117.4(10)
C(3)-C(2)-C(1)	121.2(11)
C(4)-C(3)-C(2)	120.3(12)
C(3)-C(4)-C(5)	120.2(11)

C(6)-C(5)-C(4)	118.0(10)
C(6)-C(5)-C(10)	125.4(10)
C(4)-C(5)-C(10)	116.6(10)
C(1)-C(6)-C(5)	121.9(10)
C(1)-C(6)-N(2)	119.2(10)
C(5)-C(6)-N(2)	118.8(8)
C(8)-C(7)-C(9)	113.5(13)
C(8)-C(7)-C(1)	109.9(11)
C(9)-C(7)-C(1)	110.9(12)
C(12)-C(10)-C(5)	113.7(11)
C(12)-C(10)-C(11)	110.4(11)
C(5)-C(10)-C(11)	110.0(10)
N(2)-C(13)-C(14)	109.8(8)
N(1)-C(14)-C(15)	120.4(10)
N(1)-C(14)-C(13)	114.9(9)
C(15)-C(14)-C(13)	124.6(9)
C(16)-C(15)-C(14)	117.0(11)
C(15)-C(16)-C(15)#1	124(2)
C(18)-C(17)-Zr	75.3(12)
C(19)-C(18)-C(17)	126(2)
C(19)-C(18)-Zr	73.7(14)
C(17)-C(18)-Zr	67.0(11)
C(18)-C(19)-C(20)	121(2)
C(18)-C(19)-Zr	74(2)
C(20)-C(19)-Zr	66.6(11)
C(19)-C(20)-Zr	76.0(11)
C(92)-C(91)-C(91)#2	58(4)
C(92)-C(91)-O(90)#2	29(3)
C(91)#2-C(91)-O(90)#2	86(3)
C(92)-C(91)-O(90)	6(3)
C(91)#2-C(91)-O(90)	61(2)
O(90)#2-C(91)-O(90)	28(4)
O(90)#2-C(92)-O(90)	57(9)
O(90)#2-C(92)-C(91)	121(4)
O(90)-C(92)-C(91)	167(7)
O(90)#2-C(92)-C(91)#2	167(7)
O(90)-C(92)-C(91)#2	121(4)
C(91)-C(92)-C(91)#2	64(8)
O(90)#2-C(92)-O(90)#3	32(5)
O(90)-C(92)-O(90)#3	32(5)
C(91)-C(92)-O(90)#3	139(4)
C(91)#2-C(92)-O(90)#3	151(5)
O(90)#2-C(92)-O(90)#4	32(5)
O(90)-C(92)-O(90)#4	32(5)
C(91)-C(92)-O(90)#4	151(5)
C(91)#2-C(92)-O(90)#4	139(4)
O(90)#3-C(92)-O(90)#4	31(6)
O(90)#2-O(90)-C(92)	62(4)
O(90)#2-O(90)-O(90)#3	63(4)
C(92)-O(90)-O(90)#3	118(9)
O(90)#2-O(90)-O(90)#4	63(4)
C(92)-O(90)-O(90)#4	118(9)
O(90)#3-O(90)-O(90)#4	53(8)
O(90)#2-O(90)-C(91)#2	91(3)
C(92)-O(90)-C(91)#2	30(3)
O(90)#3-O(90)-C(91)#2	146(8)
O(90)#4-O(90)-C(91)#2	136(8)
O(90)#2-O(90)-C(92)#3	74(3)
C(92)-O(90)-C(92)#3	136(7)
O(90)#3-O(90)-C(92)#3	30(5)

O(90)#4-O(90)-C(92)#3	30(5)
C(91)#2-O(90)-C(92)#3	163(6)
O(90)#2-O(90)-C(91)	61(3)
C(92)-O(90)-C(91)	7(3)
O(90)#3-O(90)-C(91)	114(7)
O(90)#4-O(90)-C(91)	121(7)
C(91)#2-O(90)-C(91)	33(3)
C(92)#3-O(90)-C(91)	135(4)

Symmetry transformations used to generate equivalent atoms:
#1 x+1-1,-y+1/2,-z+1/4 #2 -x+2,-y+1,z
#3 y+1/2,-x+3/2,-z+1/2 #4 -y+3/2,x-1/2,-z+1/2

Table 4. Anisotropic displacement parameters (A^2 x 10^3) for 1. The anisotropic displacement factor exponent takes the form: -2 pi^2 [h^2 a*^2 U11 + ... + 2 h k a* b* U12]

	U11	U22	U33	U23	U13	U12
Zr	36(1)	40(1)	51(1)	-2(1)	0	0
N(1)	80(10)	46(9)	13(6)	16(8)	0	0
N(2)	17(4)	55(6)	22(6)	8(5)	8(4)	9(4)
C(1)	48(9)	47(9)	43(8)	-16(6)	-17(6)	3(7)
C(2)	64(10)	58(9)	64(9)	-20(8)	-14(8)	-17(9)
C(3)	48(9)	53(9)	84(11)	-8(8)	-5(8)	-15(7)
C(4)	41(9)	37(8)	68(9)	-7(6)	-1(6)	4(6)
C(5)	33(8)	46(8)	50(8)	1(6)	-5(6)	6(6)
C(6)	44(7)	33(7)	31(7)	-9(5)	2(6)	3(6)
C(7)	77(10)	60(9)	42(7)	6(7)	-9(8)	-2(8)
C(8)	85(11)	92(12)	74(10)	1(9)	14(9)	19(10)
C(9)	94(11)	126(14)	57(9)	15(8)	-15(10)	-2(14)
C(10)	71(9)	39(8)	33(7)	-6(6)	14(7)	-9(7)
C(11)	114(13)	67(10)	77(10)	22(8)	-20(10)	-12(10)
C(12)	129(18)	115(14)	50(8)	-1(9)	29(10)	2(11)
C(13)	70(9)	31(7)	25(7)	6(6)	-3(6)	-5(6)
C(14)	67(8)	19(6)	18(6)	-4(6)	-6(7)	3(5)
C(15)	35(7)	39(7)	47(7)	0(7)	-1(7)	6(5)
C(16)	44(10)	69(13)	46(10)	-24(12)	0	0

8 Crystallographic data for (CyAP)$ZrMe_2$.

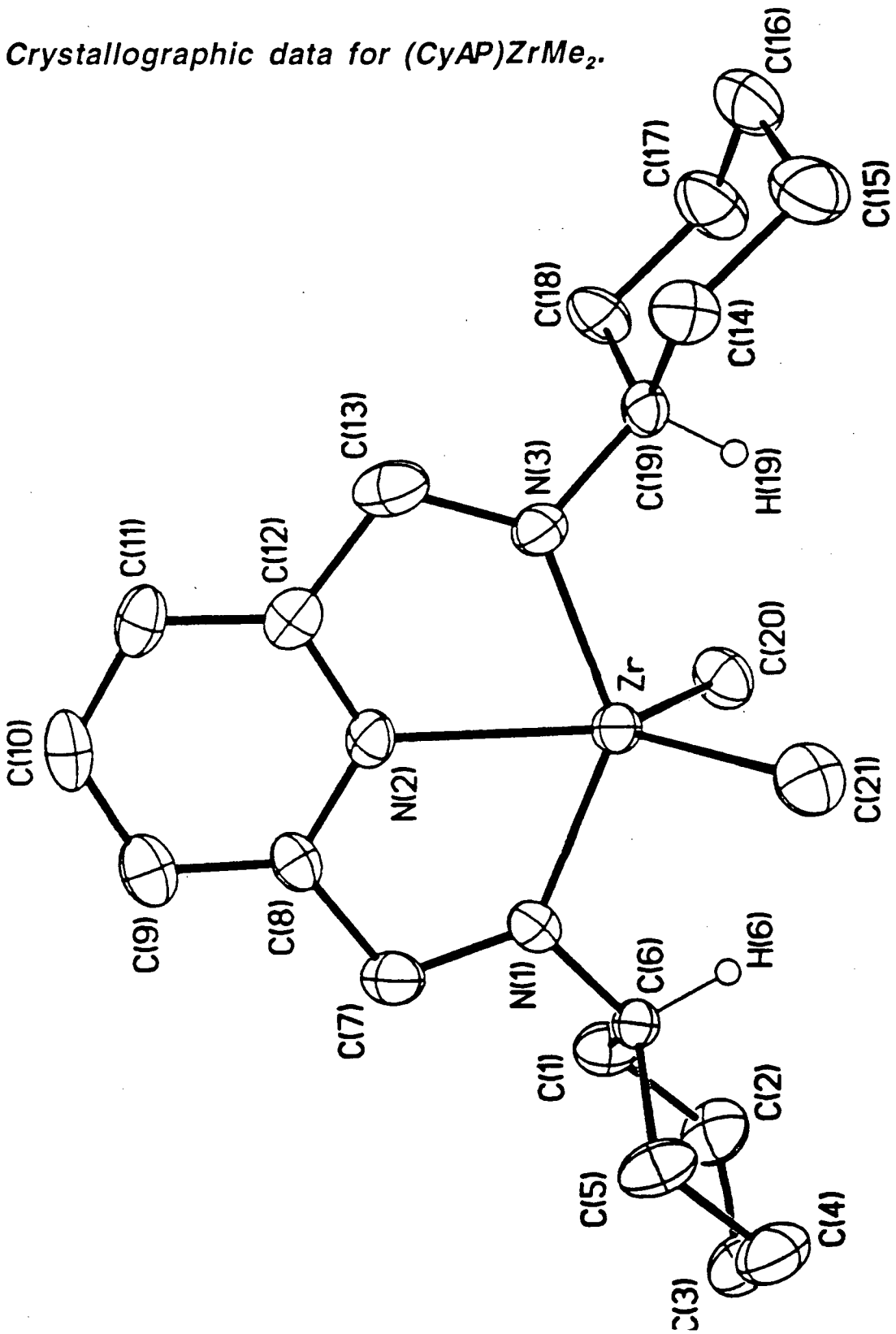

Table 1. Crystallographic data for **1**.

formula	$C_{21}H_{35}N_3Zr$
formula weight	420.74
crystal system	monoclinic
space group	$P2_1/n$
a, Å	10.4355(5)
b, Å	10.0209(5)
c, Å	21.190(1)
b, °	95.226(1)
V, Å^3	2206.6(2)
Z	4
ρ, g cm^{-1}	1.266
T_{max}/T_{min}	0.2786/0.2345
R(F), %	4.46
$R(wF^2)$, %	7.88

Quantity minimized = $R(wF^2) = \sum[w(F_o^2 - F_c^2)^2]$; $R = \sum\Delta/\sum(F_o)$, $\Delta = |(F_o - F_c)|$

Table 1. Crystal data and structure refinement for 1.

Identification code	dm004
Empirical formula	C21 H35 N3 Zr
Formula weight	420.74
Temperature	298(2) K
Wavelength	0.71073 A
Crystal system	Monoclinic
Space group	P2(1)/n
Unit cell dimensions	a = 10.4355(5) A alpha = 90 deg. b = 10.0209(5) A beta = 95.226(1) deg c = 21.190(1) A gamma = 90 deg.
Volume, Z	2206.6(2) A^3, 4
Density (calculated)	1.266 Mg/m^3
Absorption coefficient	0.506 mm^-1
F(000)	888
Crystal size	0.15 x 0.15 x 0.10 mm
Theta range for data collection	1.93 to 25.00 deg.
Limiting indices	-13<=h<=13, -12<=k<=13, -17<=l<=28
Reflections collected	10235
Independent reflections	3840 [R(int) = 0.0539]
Absorption correction	Semi-empirical from psi-scans
Max. and min. transmission	0.2786 and 0.2345
Refinement method	Full-matrix least-squares on F^2
Data / restraints / parameters	3839 / 0 / 227
Goodness-of-fit on F^2	1.014
Final R indices [I>2sigma(I)]	R1 = 0.0446, wR2 = 0.0788
R indices (all data)	R1 = 0.0844, wR2 = 0.0902
Extinction coefficient	0.0109(6)
Largest diff. peak and hole	0.439 and -0.342 e.A^-3

Table 2. Atomic coordinates (x 10^4) and equivalent isotropic displacement parameters (A^2 x 10^3) for 1. U(eq) is defined as one third of the trace of the orthogonalized Uij tensor.

	x	y	z	U(eq)
Zr	7530(1)	2201(1)	324(1)	40(1)
N(1)	7994(3)	3400(3)	1111(1)	45(1)
N(2)	9622(3)	3019(3)	328(1)	42(1)
N(3)	8354(3)	1598(3)	-483(1)	45(1)
C(1)	6433(4)	4987(4)	1556(2)	57(1)
C(2)	5289(4)	5060(5)	1955(2)	78(2)
C(3)	5635(5)	4541(5)	2621(2)	78(2)
C(4)	6189(5)	3154(5)	2619(2)	79(2)
C(5)	7329(4)	3085(4)	2216(2)	64(1)
C(6)	6968(3)	3570(4)	1543(2)	46(1)
C(7)	9191(3)	4095(4)	1295(2)	55(1)
C(8)	10106(3)	3828(4)	801(2)	46(1)
C(9)	11337(4)	4348(4)	809(2)	57(1)
C(10)	12073(4)	4020(4)	319(2)	62(1)
C(11)	11582(4)	3198(4)	-165(2)	54(1)
C(12)	10341(3)	2710(4)	-152(2)	46(1)
C(13)	9669(4)	1842(4)	-644(2)	61(1)
C(14)	7911(4)	-491(4)	-1127(2)	61(1)
C(15)	6928(5)	-1177(4)	-1605(2)	78(1)
C(16)	6665(5)	-336(5)	-2203(2)	82(2)
C(17)	6234(4)	1050(5)	-2043(2)	79(1)
C(18)	7218(4)	1729(4)	-1567(2)	59(1)
C(19)	7498(4)	908(4)	-964(2)	47(1)
C(20)	5620(4)	3071(4)	-84(2)	62(1)
C(21)	6982(4)	238(4)	764(2)	67(1)

Table 3. Bond lengths [A] and angles [deg] for 1.

Zr-N(3)	2.073(3)
Zr-N(1)	2.076(3)
Zr-C(21)	2.272(4)
Zr-C(20)	2.272(4)
Zr-N(2)	2.332(3)
N(1)-C(7)	1.453(4)
N(1)-C(6)	1.481(4)
N(2)-C(8)	1.351(4)
N(2)-C(12)	1.352(4)
N(3)-C(13)	1.464(4)
N(3)-C(19)	1.466(4)
C(1)-C(2)	1.526(5)
C(1)-C(6)	1.526(5)
C(2)-C(3)	1.517(6)
C(3)-C(4)	1.504(6)
C(4)-C(5)	1.528(5)
C(5)-C(6)	1.521(5)
C(7)-C(8)	1.503(5)
C(8)-C(9)	1.384(5)
C(9)-C(10)	1.387(5)
C(10)-C(11)	1.377(6)
C(11)-C(12)	1.387(5)
C(12)-C(13)	1.484(5)
C(14)-C(19)	1.516(5)
C(14)-C(15)	1.538(6)
C(15)-C(16)	1.525(6)
C(16)-C(17)	1.508(6)
C(17)-C(18)	1.533(5)
C(18)-C(19)	1.524(5)
N(3)-Zr-N(1)	138.36(11)
N(3)-Zr-C(21)	103.00(14)
N(1)-Zr-C(21)	102.74(14)
N(3)-Zr-C(20)	102.31(14)
N(1)-Zr-C(20)	102.46(13)
C(21)-Zr-C(20)	104.1(2)
N(3)-Zr-N(2)	69.30(11)
N(1)-Zr-N(2)	69.16(11)
C(21)-Zr-N(2)	124.99(13)
C(20)-Zr-N(2)	130.92(13)
C(7)-N(1)-C(6)	115.6(3)
C(7)-N(1)-Zr	128.7(2)
C(6)-N(1)-Zr	115.8(2)
C(8)-N(2)-C(12)	120.0(3)
C(8)-N(2)-Zr	120.0(2)
C(12)-N(2)-Zr	120.0(2)
C(13)-N(3)-C(19)	116.2(3)
C(13)-N(3)-Zr	127.7(2)
C(19)-N(3)-Zr	116.0(2)
C(2)-C(1)-C(6)	111.1(3)
C(3)-C(2)-C(1)	111.5(4)
C(4)-C(3)-C(2)	112.0(4)
C(3)-C(4)-C(5)	111.2(4)
C(6)-C(5)-C(4)	111.7(4)
N(1)-C(6)-C(5)	114.3(3)
N(1)-C(6)-C(1)	113.8(3)

C(5)-C(6)-C(1)	109.9(3)
N(1)-C(7)-C(8)	108.3(3)
N(2)-C(8)-C(9)	121.3(4)
N(2)-C(8)-C(7)	113.9(3)
C(9)-C(8)-C(7)	124.8(4)
C(8)-C(9)-C(10)	118.6(4)
C(11)-C(10)-C(9)	120.3(4)
C(10)-C(11)-C(12)	118.7(4)
N(2)-C(12)-C(11)	121.2(4)
N(2)-C(12)-C(13)	113.7(3)
C(11)-C(12)-C(13)	125.1(4)
N(3)-C(13)-C(12)	109.1(3)
C(19)-C(14)-C(15)	112.1(3)
C(16)-C(15)-C(14)	111.0(4)
C(17)-C(16)-C(15)	111.0(4)
C(16)-C(17)-C(18)	111.2(4)
C(19)-C(18)-C(17)	112.2(3)
N(3)-C(19)-C(14)	115.2(3)
N(3)-C(19)-C(18)	112.7(3)
C(14)-C(19)-C(18)	110.3(3)

Symmetry transformations used to generate equivalent atoms:

Table 4. Anisotropic displacement parameters (A^2 x 10^3) for 1. The anisotropic displacement factor exponent takes the form: -2 pi^2 [h^2 a*^2 U11 + ... + 2 h k a* b* U12]

	U11	U22	U33	U23	U13	U12
Zr	30(1)	48(1)	40(1)	-2(1)	3(1)	2(1)
N(1)	34(2)	58(2)	44(2)	-5(2)	2(2)	1(2)
N(2)	30(2)	50(2)	45(2)	3(2)	2(2)	3(1)
N(3)	35(2)	61(2)	38(2)	-6(2)	5(2)	2(2)
C(1)	61(3)	59(3)	51(3)	4(2)	6(2)	11(2)
C(2)	68(3)	88(4)	79(4)	-12(3)	22(3)	24(3)
C(3)	72(3)	98(4)	70(4)	-12(3)	32(3)	-4(3)
C(4)	101(4)	78(4)	61(3)	4(3)	29(3)	-8(3)
C(5)	78(3)	67(3)	49(3)	14(2)	17(2)	16(2)
C(6)	41(2)	52(2)	44(2)	-6(2)	5(2)	1(2)
C(7)	46(2)	70(3)	47(3)	-7(2)	-2(2)	-3(2)
C(8)	36(2)	49(2)	52(3)	2(2)	-4(2)	2(2)
C(9)	36(2)	57(3)	74(3)	-3(2)	-8(2)	-4(2)
C(10)	35(2)	61(3)	91(4)	13(3)	9(3)	-1(2)
C(11)	38(2)	58(3)	68(3)	11(2)	15(2)	6(2)
C(12)	35(2)	54(2)	47(2)	8(2)	1(2)	9(2)
C(13)	46(2)	81(3)	56(3)	-5(2)	10(2)	9(2)
C(14)	75(3)	55(3)	52(3)	3(2)	6(2)	0(2)
C(15)	103(4)	56(3)	73(4)	-10(3)	5(3)	-11(3)
C(16)	95(4)	91(4)	59(3)	-12(3)	-6(3)	-25(3)
C(17)	86(4)	81(4)	64(3)	2(3)	-26(3)	-5(3)
C(18)	64(3)	55(3)	53(3)	3(2)	-16(2)	4(2)
C(19)	45(2)	55(3)	42(2)	0(2)	5(2)	2(2)
C(20)	46(2)	65(3)	74(3)	-8(2)	0(2)	10(2)
C(21)	69(3)	61(3)	74(3)	0(3)	15(3)	-2(2)

Table 5. Hydrogen coordinates (x 10^4) and isotropic displacement parameters (A^2 x 10^3) for 1.

	x	y	z	U(eq)
H(1A)	7103(4)	5588(4)	1731(2)	68
H(1B)	6167(4)	5273(4)	1127(2)	68
H(2A)	5003(4)	5979(5)	1976(2)	93
H(2B)	4583(4)	4538(5)	1753(2)	93
H(3A)	6257(5)	5136(5)	2841(2)	94
H(3B)	4871(5)	4535(5)	2849(2)	94
H(4A)	5528(5)	2534(5)	2453(2)	95
H(4B)	6467(5)	2891(5)	3051(2)	95
H(5A)	8026(4)	3629(4)	2410(2)	77
H(5B)	7632(4)	2171(4)	2204(2)	77
H(6)	6204(3)	3034(4)	1343(2)	55
H(7A)	9557(3)	3779(4)	1705(2)	66
H(7B)	9035(3)	5046(4)	1325(2)	66
H(9A)	11662(4)	4904(4)	1137(2)	68
H(10A)	12904(4)	4356(4)	317(2)	74
H(11A)	12073(4)	2974(4)	-494(2)	65
H(13A)	9650(4)	2271(4)	-1054(2)	73
H(13B)	10124(4)	1001(4)	-665(2)	73
H(14A)	8018(4)	-1021(4)	-742(2)	73
H(14B)	8737(4)	-450(4)	-1302(2)	73
H(15A)	7255(5)	-2044(4)	-1717(2)	93
H(15B)	6130(5)	-1316(4)	-1413(2)	93
H(16A)	7441(5)	-280(5)	-2421(2)	99
H(16B)	6003(5)	-761(5)	-2485(2)	99
H(17A)	5411(4)	1000(5)	-1866(2)	95
H(17B)	6122(4)	1580(5)	-2427(2)	95
H(18A)	8012(4)	1866(4)	-1762(2)	71
H(18B)	6893(4)	2598(4)	-1457(2)	71
H(19)	6686(4)	818(4)	-786(2)	57
H(20A)	5149(4)	3387(4)	254(2)	93
H(20B)	5130(4)	2394(4)	-318(2)	93
H(20C)	5776(4)	3799(4)	-362(2)	93
H(21A)	6586(4)	412(4)	1147(2)	101
H(21B)	7740(4)	-294(4)	859(2)	101
H(21C)	6388(4)	-234(4)	472(2)	101

9 Crystallographic data for (tBAP)$ZrMe_2$.

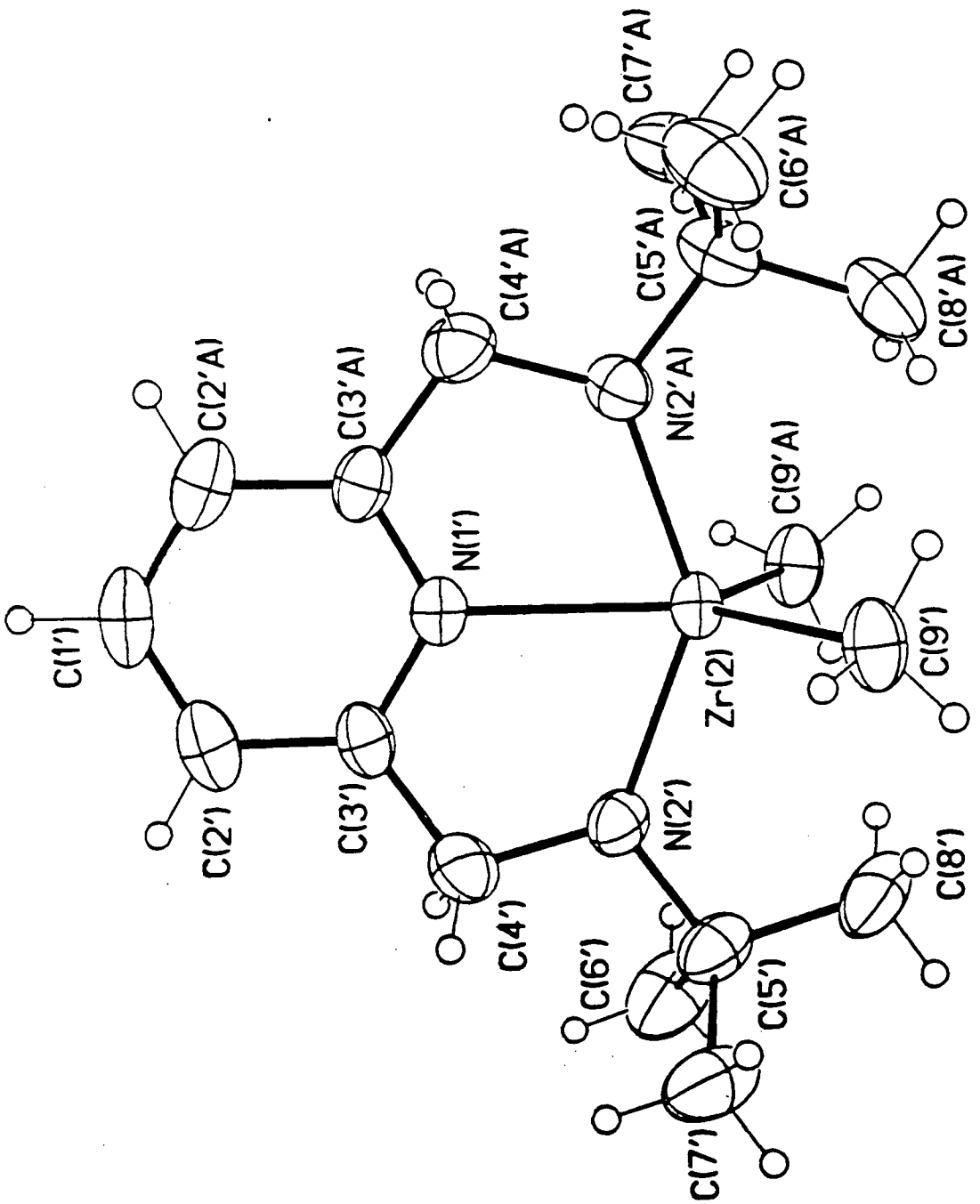

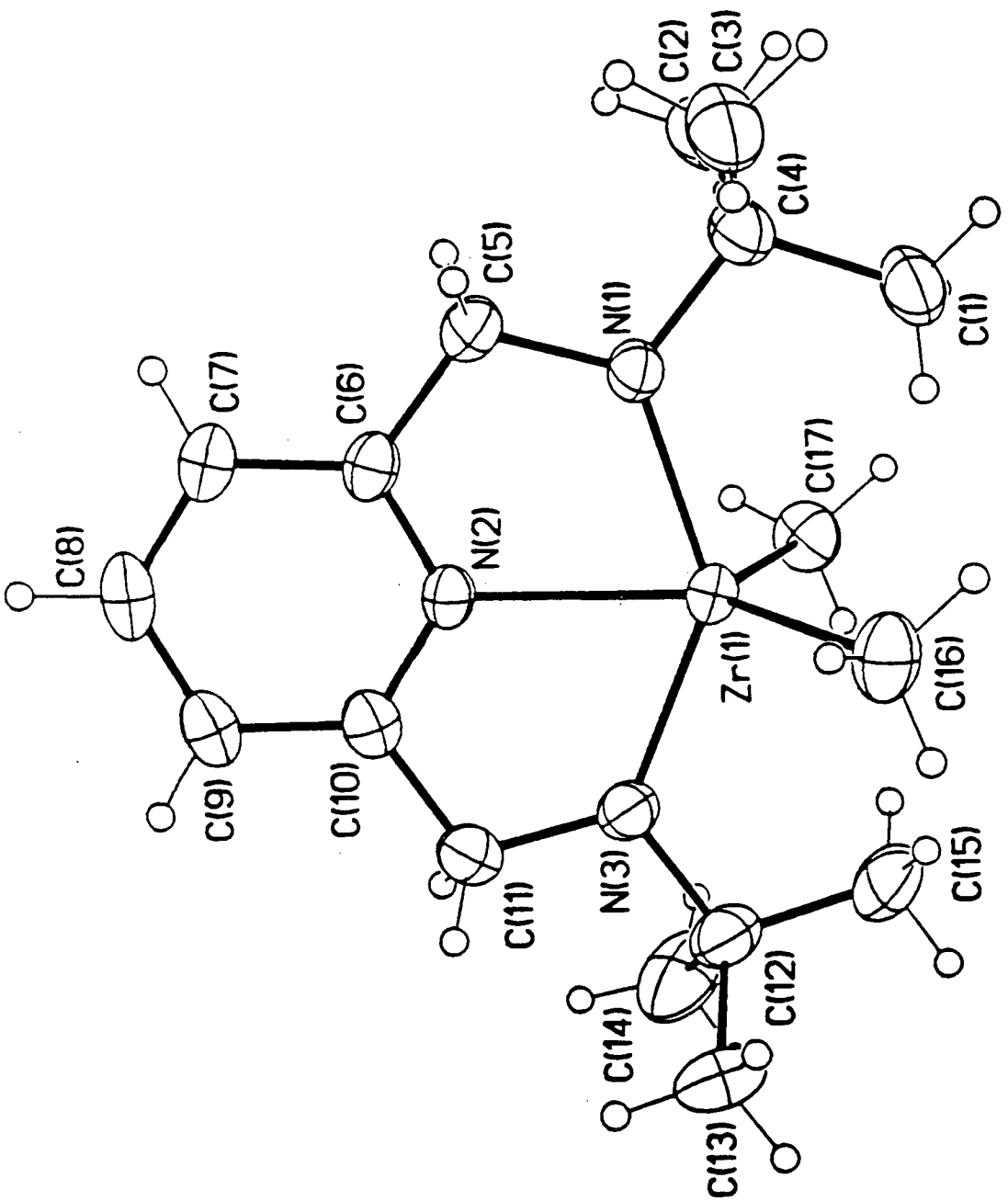
C(2)
C(3)
C(4)
C(1)
C(5)
N(1)
C(7)
C(6)
C(17)
C(8)
N(2)
Zr(1)
C(16)
C(9)
C(10)
C(11)
N(3)
C(15)
C(12)
C(14)
C(13)

Table 1. Crystal data and structure refinement for 1.

Identification code	dm005
Empirical formula	C17 H31 N3 Zr
Formula weight	368.67
Temperature	296(2) K
Wavelength	0.71073 A
Crystal system	Monoclinic
Space group	C2/c
Unit cell dimensions	a = 31.9923(9) A alpha = 90 deg. b = 9.9689(3) A beta = 93.196(1) deg. c = 17.9912(5) A gamma = 90 deg.
Volume, Z	5729.0(3) A^3, 12
Density (calculated)	1.282 Mg/m^3
Absorption coefficient	0.575 mm^-1
F(000)	2328
Crystal size	0.30 x 0.20 x 0.20 mm
Theta range for data collection	1.27 to 28.29 deg.
Limiting indices	-42<=h<=42, -5<=k<=13, -23<=l<=22
Reflections collected	17656
Independent reflections	6836 [R(int) = 0.0161]
Absorption correction	Semi-empirical from psi-scans
Max. and min. transmission	0.862128 and 0.701441
Refinement method	Full-matrix least-squares on F^2
Data / restraints / parameters	6836 / 0 / 286
Goodness-of-fit on F^2	1.059
Final R indices [I>2sigma(I)]	R1 = 0.0339, wR2 = 0.0983
R indices (all data)	R1 = 0.0416, wR2 = 0.1040
Largest diff. peak and hole	0.450 and -0.375 e.A^-3

Table 2. Atomic coordinates (x 10^4) and equivalent isotropic displacement parameters (A^2 x 10^3) for 1. U(eq) is defined as one third of the trace of the orthogonalized Uij tensor.

	x	y	z	U(eq)
Zr(1)	3352(1)	9125(1)	6577(1)	42(1)
N(1)	3379(1)	10560(2)	5712(1)	48(1)
N(2)	2736(1)	9092(2)	5866(1)	43(1)
N(3)	2953(1)	7648(2)	6994(1)	51(1)
C(1)	4079(1)	11200(3)	6236(2)	77(1)
C(2)	3961(1)	10935(5)	4875(2)	96(1)
C(3)	3651(1)	12888(3)	5528(3)	92(1)
C(4)	3757(1)	11391(3)	5586(2)	59(1)
C(5)	3043(1)	10809(3)	5154(2)	58(1)
C(6)	2681(1)	9919(2)	5278(1)	48(1)
C(7)	2312(1)	9917(3)	4835(1)	57(1)
C(8)	1999(1)	9032(3)	4995(2)	64(1)
C(9)	2056(1)	8174(3)	5599(2)	60(1)
C(10)	2430(1)	8233(2)	6029(1)	49(1)
C(11)	2531(1)	7378(3)	6691(1)	55(1)
C(12)	3070(1)	6779(3)	7649(2)	67(1)
C(13)	2776(2)	7054(6)	8285(2)	111(2)
C(14)	3059(2)	5297(4)	7432(3)	114(2)
C(15)	3518(1)	7093(4)	7934(2)	88(1)
C(16)	3435(1)	10472(3)	7605(2)	71(1)
C(17)	3893(1)	7798(3)	6263(2)	64(1)
Zr(2)	5000	6714(1)	2500	46(1)
N(1')	5000	9018(3)	2500	50(1)
N(2')	4695(1)	7419(2)	3432(1)	58(1)
C(1')	5000	11776(5)	2500	92(2)
C(2')	4820(1)	11093(3)	3055(2)	83(1)
C(3')	4823(1)	9695(3)	3047(2)	58(1)
C(4')	4644(1)	8826(3)	3616(2)	72(1)
C(5')	4510(1)	6525(4)	3994(2)	74(1)
C(6')	4033(1)	6768(5)	4000(3)	108(2)
C(7')	4717(1)	6747(5)	4769(2)	103(1)
C(8')	4576(1)	5051(4)	3775(2)	96(1)
C(9')	5526(1)	5493(3)	3081(2)	70(1)

Table 3. Bond lengths [A] and angles [deg] for 1.

Zr(1)-N(3)	2.115(2)
Zr(1)-N(1)	2.118(2)
Zr(1)-C(17)	2.274(3)
Zr(1)-N(2)	2.290(2)
Zr(1)-C(16)	2.290(3)
N(1)-C(5)	1.451(3)
N(1)-C(4)	1.494(3)
N(2)-C(10)	1.344(3)
N(2)-C(6)	1.345(3)
N(3)-C(11)	1.451(3)
N(3)-C(12)	1.494(3)
C(1)-C(4)	1.526(4)
C(2)-C(4)	1.537(5)
C(3)-C(4)	1.532(4)
C(5)-C(6)	1.484(4)
C(6)-C(7)	1.390(3)
C(7)-C(8)	1.376(4)
C(8)-C(9)	1.386(4)
C(9)-C(10)	1.389(3)
C(10)-C(11)	1.485(4)
C(12)-C(14)	1.528(5)
C(12)-C(15)	1.525(5)
C(12)-C(13)	1.545(5)
Zr(2)-N(2')	2.106(2)
Zr(2)-N(2')#1	2.106(2)
Zr(2)-C(9')	2.281(3)
Zr(2)-C(9')#1	2.281(3)
Zr(2)-N(1')	2.297(3)
N(1')-C(3')#1	1.344(3)
N(1')-C(3')	1.344(3)
N(2')-C(4')	1.452(4)
N(2')-C(5')	1.495(4)
C(1')-C(2')	1.362(5)
C(1')-C(2')#1	1.362(5)
C(2')-C(3')	1.394(4)
C(3')-C(4')	1.480(4)
C(5')-C(7')	1.527(5)
C(5')-C(8')	1.539(6)
C(5')-C(6')	1.545(5)
N(3)-Zr(1)-N(1)	141.29(8)
N(3)-Zr(1)-C(17)	99.56(10)
N(1)-Zr(1)-C(17)	98.56(10)
N(3)-Zr(1)-N(2)	70.66(7)
N(1)-Zr(1)-N(2)	70.64(7)
C(17)-Zr(1)-N(2)	119.79(9)
N(3)-Zr(1)-C(16)	99.54(11)
N(1)-Zr(1)-C(16)	100.98(11)
C(17)-Zr(1)-C(16)	119.13(12)
N(2)-Zr(1)-C(16)	121.08(10)
C(5)-N(1)-C(4)	112.0(2)
C(5)-N(1)-Zr(1)	124.4(2)
C(4)-N(1)-Zr(1)	123.5(2)
C(10)-N(2)-C(6)	119.9(2)
C(10)-N(2)-Zr(1)	120.2(2)
C(6)-N(2)-Zr(1)	119.9(2)

C(11)-N(3)-C(12)	112.1(2)
C(11)-N(3)-Zr(1)	124.3(2)
C(12)-N(3)-Zr(1)	123.6(2)
N(1)-C(4)-C(1)	109.4(2)
N(1)-C(4)-C(3)	111.9(2)
C(1)-C(4)-C(3)	108.1(3)
N(1)-C(4)-C(2)	110.4(2)
C(1)-C(4)-C(2)	107.4(3)
C(3)-C(4)-C(2)	109.5(3)
N(1)-C(5)-C(6)	110.3(2)
N(2)-C(6)-C(7)	121.3(2)
N(2)-C(6)-C(5)	114.7(2)
C(7)-C(6)-C(5)	124.0(2)
C(8)-C(7)-C(6)	119.0(3)
C(7)-C(8)-C(9)	119.7(2)
C(10)-C(9)-C(8)	118.7(3)
N(2)-C(10)-C(9)	121.4(2)
N(2)-C(10)-C(11)	114.3(2)
C(9)-C(10)-C(11)	124.4(2)
N(3)-C(11)-C(10)	110.6(2)
N(3)-C(12)-C(14)	111.0(3)
N(3)-C(12)-C(15)	109.6(2)
C(14)-C(12)-C(15)	107.0(3)
N(3)-C(12)-C(13)	110.2(3)
C(14)-C(12)-C(13)	110.8(3)
C(15)-C(12)-C(13)	108.2(3)
N(2')-Zr(2)-N(2')#1	141.01(13)
N(2')-Zr(2)-C(9')	100.11(11)
N(2')#1-Zr(2)-C(9')	100.40(11)
N(2')-Zr(2)-C(9')#1	100.40(11)
N(2')#1-Zr(2)-C(9')#1	100.11(11)
C(9')-Zr(2)-C(9')#1	115.5(2)
N(2')-Zr(2)-N(1')	70.50(6)
N(2')#1-Zr(2)-N(1')	70.50(6)
C(9')-Zr(2)-N(1')	122.24(8)
C(9')#1-Zr(2)-N(1')	122.24(8)
C(3')#1-N(1')-C(3')	119.7(3)
C(3')#1-N(1')-Zr(2)	120.1(2)
C(3')-N(1')-Zr(2)	120.1(2)
C(4')-N(2')-C(5')	111.6(2)
C(4')-N(2')-Zr(2)	124.5(2)
C(5')-N(2')-Zr(2)	123.9(2)
C(2')-C(1')-C(2')#1	120.0(4)
C(1')-C(2')-C(3')	119.3(4)
N(1')-C(3')-C(2')	120.8(3)
N(1')-C(3')-C(4')	114.0(2)
C(2')-C(3')-C(4')	125.1(3)
N(2')-C(4')-C(3')	110.8(2)
N(2')-C(5')-C(7')	111.3(3)
N(2')-C(5')-C(8')	109.3(3)
C(7')-C(5')-C(8')	108.2(3)
N(2')-C(5')-C(6')	109.9(3)
C(7')-C(5')-C(6')	110.4(3)
C(8')-C(5')-C(6')	107.6(3)

Symmetry transformations used to generate equivalent atoms:
#1 -x+1,y,-z+1/2

Table 4. Anisotropic displacement parameters (A^2 x 10^3) for 1. The anisotropic displacement factor exponent takes the form: -2 pi^2 [h^2 a*^2 U11 + ... + 2 h k a* b* U12]

	U11	U22	U33	U23	U13	U12
Zr(1)	41(1)	45(1)	40(1)	-1(1)	-5(1)	3(1)
N(1)	45(1)	47(1)	52(1)	4(1)	-5(1)	1(1)
N(2)	42(1)	46(1)	41(1)	-7(1)	-2(1)	2(1)
N(3)	57(1)	53(1)	43(1)	3(1)	2(1)	-1(1)
C(1)	53(2)	71(2)	104(2)	15(2)	-17(2)	-11(1)
C(2)	72(2)	122(4)	97(3)	3(2)	26(2)	-16(2)
C(3)	80(2)	54(2)	138(3)	16(2)	-29(2)	-6(2)
C(4)	52(1)	51(1)	72(2)	8(1)	-3(1)	-3(1)
C(5)	58(1)	59(2)	57(1)	12(1)	-9(1)	0(1)
C(6)	49(1)	50(1)	44(1)	-9(1)	-5(1)	8(1)
C(7)	55(1)	63(2)	51(1)	-9(1)	-13(1)	13(1)
C(8)	44(1)	76(2)	70(2)	-22(1)	-15(1)	9(1)
C(9)	41(1)	65(2)	73(2)	-16(1)	1(1)	-1(1)
C(10)	45(1)	51(1)	51(1)	-14(1)	3(1)	2(1)
C(11)	54(1)	55(1)	56(1)	-3(1)	9(1)	-5(1)
C(12)	84(2)	68(2)	51(1)	12(1)	3(1)	-4(2)
C(13)	117(3)	162(4)	55(2)	28(2)	18(2)	-10(3)
C(14)	171(5)	59(2)	106(3)	22(2)	-37(3)	-1(2)
C(15)	97(3)	96(3)	68(2)	28(2)	-22(2)	-2(2)
C(16)	74(2)	75(2)	62(2)	-21(2)	-11(1)	1(2)
C(17)	57(2)	58(2)	78(2)	4(1)	2(1)	13(1)
Zr(2)	38(1)	38(1)	61(1)	0	-2(1)	0
N(1')	45(1)	42(1)	61(2)	0	-5(1)	0
N(2')	53(1)	57(1)	63(1)	11(1)	6(1)	10(1)
C(1')	103(4)	38(2)	131(5)	0	-8(3)	0
C(2')	84(2)	55(2)	107(3)	-16(2)	-7(2)	15(2)
C(3')	54(1)	47(1)	73(2)	-6(1)	-7(1)	10(1)
C(4')	72(2)	70(2)	74(2)	-4(2)	12(2)	19(2)
C(5')	59(2)	87(2)	76(2)	26(2)	14(1)	9(2)
C(6')	62(2)	125(4)	140(4)	47(3)	27(2)	9(2)
C(7')	103(3)	134(4)	75(2)	32(2)	12(2)	16(3)
C(8')	99(3)	79(2)	113(3)	43(2)	20(2)	-1(2)
C(9')	57(2)	53(2)	99(2)	-3(2)	-15(2)	7(1)

Table 5. Hydrogen coordinates (x 10^4) and isotropic displacement parameters (A^2 x 10^3) for 1.

	x	y	z	U(eq)
H(1A)	4149(1)	10267(3)	6282(2)	115
H(1B)	3963(1)	11506(3)	6687(2)	115
H(1C)	4326(1)	11708(3)	6146(2)	115
H(2A)	3766(1)	11043(5)	4455(2)	145
H(2B)	4040(1)	10008(5)	4922(2)	145
H(2C)	4206(1)	11469(5)	4805(2)	145
H(3A)	3448(1)	13031(3)	5122(3)	138
H(3B)	3900(1)	13387(3)	5442(3)	138
H(3C)	3538(1)	13184(3)	5984(3)	138
H(5A)	3142(1)	10647(3)	4662(2)	70
H(5B)	2955(1)	11739(3)	5179(2)	70
H(7A)	2276(1)	10506(3)	4435(1)	68
H(8A)	1751(1)	9010(3)	4700(2)	77
H(9A)	1848(1)	7570(3)	5714(2)	72
H(11A)	2333(1)	7555(3)	7067(1)	66
H(11B)	2507(1)	6441(3)	6551(1)	66
H(13A)	2788(2)	7989(6)	8413(2)	166
H(13B)	2864(2)	6528(6)	8713(2)	166
H(13C)	2495(2)	6817(6)	8125(2)	166
H(14A)	2781(2)	5060(4)	7251(3)	170
H(14B)	3139(2)	4760(4)	7859(3)	170
H(14C)	3250(2)	5141(4)	7048(3)	170
H(15A)	3538(1)	8021(4)	8073(2)	132
H(15B)	3706(1)	6913(4)	7549(2)	132
H(15C)	3591(1)	6542(4)	8359(2)	132
H(16A)	3614(1)	11212(3)	7500(2)	107
H(16B)	3558(1)	9963(3)	8014(2)	107
H(16C)	3167(1)	10805(3)	7734(2)	107
H(17A)	4106(1)	8341(3)	6059(2)	97
H(17B)	3794(1)	7151(3)	5900(2)	97
H(17C)	4007(1)	7342(3)	6698(2)	97
H(1'A)	5000	12709(5)	2500	110
H(2'A)	4697(1)	11554(3)	3436(2)	99
H(4'A)	4783(1)	9008(3)	4098(2)	86
H(4'B)	4349(1)	9026(3)	3645(2)	86
H(6'A)	3907(1)	6626(5)	3509(3)	162
H(6'B)	3982(1)	7673(5)	4153(3)	162
H(6'C)	3914(1)	6156(5)	4341(3)	162
H(7'A)	4680(1)	7664(5)	4914(2)	155
H(7'B)	5010(1)	6548(5)	4762(2)	155
H(7'C)	4590(1)	6167(5)	5118(2)	155
H(8'A)	4448(1)	4891(4)	3288(2)	145
H(8'B)	4452(1)	4474(4)	4129(2)	145
H(8'C)	4871(1)	4868(4)	3771(2)	145
H(9'A)	5695(1)	5100(3)	2715(2)	106
H(9'B)	5407(1)	4796(3)	3372(2)	106
H(9'C)	5695(1)	6069(3)	3401(2)	106

10 Crystallographic data for (tBAP)ZrMe(Me:Cl, 60:40).

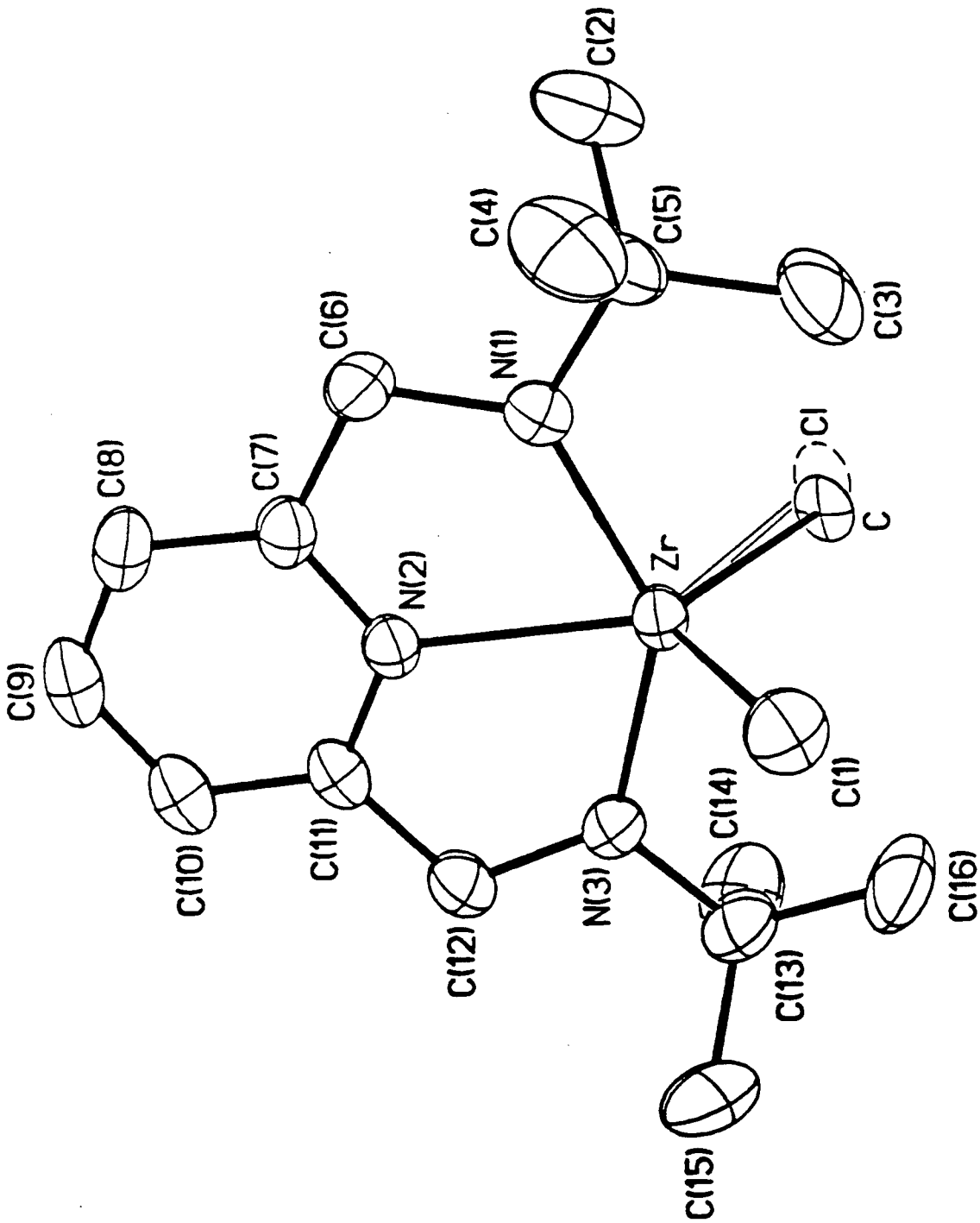

Table 1. Crystal data and structure refinement for 1.

Identification code	dm003
Empirical formula	C16.64 H29.90 Cl0.37 N3 Zr
Formula weight	376.12
Temperature	298(2) K
Wavelength	0.71073 A
Crystal system	Monoclinic
Space group	P2(1)/c
Unit cell dimensions	a = 10.4496(3) A alpha = 90 deg. b = 11.0371(3) A beta = 97.968(1) c = 16.6923(5) A gamma = 90 deg.
Volume, Z	1906.59(9) A^3, 4
Density (calculated)	1.310 Mg/m^3
Absorption coefficient	0.627 mm^-1
F(000)	788
Crystal size	0.20 x 0.10 x 0.10 mm
Theta range for data collection	1.97 to 28.26 deg.
Limiting indices	-13<=h<=7, -14<=k<=14, -21<=l<=20
Reflections collected	11760
Independent reflections	4515 [R(int) = 0.0263]
Absorption correction	Semi-empirical from psi-scans
Max. and min. transmission	0.2919 and 0.2397
Refinement method	Full-matrix least-squares on F^2
Data / restraints / parameters	4510 / 0 / 200
Goodness-of-fit on F^2	1.167
Final R indices [I>2sigma(I)]	R1 = 0.0459, wR2 = 0.1180
R indices (all data)	R1 = 0.0575, wR2 = 0.1288
Largest diff. peak and hole	0.612 and -0.333 e.A^-3

Table 2. Atomic coordinates (x 10^4) and equivalent isotropic displacement parameters (A^2 x 10^3) for 1. U(eq) is defined as one third of the trace of the orthogonalized Uij tensor.

	x	y	z	U(eq)
Zr	2205(1)	3783(1)	1163(1)	47(1)
Cl	3651(4)	3370(6)	2494(3)	54(1)
C	3312(10)	3284(13)	2353(6)	45(2)
N(1)	2133(3)	5679(3)	1238(2)	54(1)
N(2)	3001(2)	4600(2)	81(1)	46(1)
N(3)	2774(3)	2380(2)	434(2)	56(1)
C(1)	24(4)	3363(4)	1021(3)	70(1)
C(2)	2489(6)	7234(6)	2326(3)	111(2)
C(3)	1138(6)	5447(5)	2489(3)	107(2)
C(4)	335(5)	7036(5)	1493(3)	106(2)
C(5)	1540(4)	6349(4)	1874(2)	69(1)
C(6)	2649(4)	6503(3)	676(2)	60(1)
C(7)	3078(3)	5806(3)	6(2)	53(1)
C(8)	3547(4)	6324(4)	-653(2)	67(1)
C(9)	3918(4)	5595(4)	-1238(2)	72(1)
C(10)	3845(4)	4354(4)	-1160(2)	66(1)
C(11)	3385(3)	3874(3)	-487(2)	53(1)
C(12)	3273(4)	2556(3)	-327(2)	63(1)
C(13)	2746(5)	1057(3)	662(3)	76(1)
C(14)	4134(6)	611(5)	943(4)	115(2)
C(15)	2141(7)	295(5)	-55(4)	126(2)
C(16)	1960(6)	901(4)	1357(4)	105(2)

Table 4. Anisotropic displacement parameters (A^2 x 10^3) for 1. The anisotropic displacement factor exponent takes the form: -2 pi^2 [h^2 a*^2 U11 + ... + 2 h k a* b* U12]

	U11	U22	U33	U23	U13	U12
Zr	52(1)	49(1)	42(1)	5(1)	13(1)	-2(1)
Cl	47(3)	79(2)	32(2)	14(2)	-6(2)	-5(2)
C	30(4)	73(4)	25(3)	8(3)	-19(2)	-4(3)
N(1)	64(2)	51(2)	48(1)	-4(1)	12(1)	1(1)
N(2)	45(1)	53(1)	41(1)	4(1)	5(1)	-3(1)
N(3)	66(2)	46(1)	56(2)	-1(1)	15(1)	-4(1)
C(1)	53(2)	83(3)	74(2)	0(2)	8(2)	-3(2)
C(2)	126(5)	121(4)	86(3)	-49(3)	14(3)	-5(4)
C(3)	150(5)	103(4)	83(3)	-6(3)	67(3)	20(4)
C(4)	98(4)	123(4)	98(3)	-14(3)	20(3)	47(3)
C(5)	81(3)	70(2)	56(2)	-12(2)	12(2)	12(2)
C(6)	70(2)	49(2)	59(2)	3(2)	5(2)	-4(2)
C(7)	51(2)	58(2)	48(2)	11(1)	2(1)	-4(2)
C(8)	65(2)	72(2)	62(2)	25(2)	3(2)	-9(2)
C(9)	62(2)	103(3)	51(2)	23(2)	13(2)	-3(2)
C(10)	62(2)	93(3)	46(2)	4(2)	14(2)	7(2)
C(11)	48(2)	70(2)	41(1)	0(1)	9(1)	4(2)
C(12)	75(2)	65(2)	53(2)	-7(2)	18(2)	3(2)
C(13)	92(3)	49(2)	88(3)	3(2)	16(2)	0(2)
C(14)	124(5)	80(3)	142(5)	35(3)	24(4)	30(3)
C(15)	181(7)	60(3)	134(5)	-15(3)	12(5)	-33(3)
C(16)	141(5)	57(2)	127(4)	24(3)	60(4)	-6(3)

Table 5. Hydrogen coordinates (x 10^4) and isotropic displacement parameters (A^2 x 10^3) for 1.

	x	y	z	U(eq)
H(0A)	3406(10)	2420(13)	2386(6)	67
H(0B)	2856(10)	3563(13)	2780(6)	67
H(0C)	4150(10)	3655(13)	2407(6)	67
H(1A)	-105(4)	2503(4)	977(3)	105
H(1B)	-401(4)	3749(4)	541(3)	105
H(1C)	-330(4)	3661(4)	1484(3)	105
H(2A)	2756(6)	7811(6)	1953(3)	167
H(2B)	3230(6)	6800(6)	2584(3)	167
H(2C)	2081(6)	7650(6)	2729(3)	167
H(3A)	536(6)	4875(5)	2217(3)	161
H(3B)	738(6)	5874(5)	2890(3)	161
H(3C)	1888(6)	5025(5)	2747(3)	161
H(4A)	-267(5)	6477(5)	1206(3)	158
H(4B)	576(5)	7634(5)	1123(3)	158
H(4C)	-61(5)	7428(5)	1909(3)	158
H(6A)	3372(4)	6952(3)	959(2)	72
H(6B)	1987(4)	7078(3)	462(2)	72
H(8A)	3607(4)	7162(4)	-695(2)	80
H(9A)	4219(4)	5932(4)	-1688(2)	86
H(10A)	4102(4)	3846(4)	-1553(2)	80
H(12A)	2697(4)	2182(3)	-763(2)	76
H(12B)	4114(4)	2176(3)	-302(2)	76
H(14A)	4644(6)	707(5)	511(4)	172
H(14B)	4114(6)	-228(5)	1091(4)	172
H(14C)	4508(6)	1078(5)	1402(4)	172
H(15A)	2636(7)	386(5)	-495(4)	189
H(15B)	1271(7)	561(5)	-223(4)	189
H(15C)	2136(7)	-542(5)	102(4)	189
H(16A)	2339(6)	1375(4)	1811(4)	157
H(16B)	1956(6)	62(4)	1509(4)	157
H(16C)	1090(6)	1168(4)	1189(4)	157

Table 3. Bond lengths [A] and angles [deg] for 1.

Zr-N(1)	2.099(3)
Zr-N(3)	2.105(3)
Zr-C	2.225(9)
Zr-N(2)	2.277(2)
Zr-C(1)	2.305(4)
Zr-Cl	2.549(4)
N(1)-C(6)	1.462(4)
N(1)-C(5)	1.497(5)
N(2)-C(7)	1.341(4)
N(2)-C(11)	1.345(4)
N(3)-C(12)	1.452(4)
N(3)-C(13)	1.511(5)
C(2)-C(5)	1.516(7)
C(3)-C(5)	1.530(6)
C(4)-C(5)	1.531(6)
C(6)-C(7)	1.478(5)
C(7)-C(8)	1.388(5)
C(8)-C(9)	1.364(6)
C(9)-C(10)	1.379(6)
C(10)-C(11)	1.387(5)
C(11)-C(12)	1.486(5)
C(13)-C(16)	1.520(7)
C(13)-C(15)	1.526(7)
C(13)-C(14)	1.542(7)
N(1)-Zr-N(3)	141.56(10)
N(1)-Zr-C	102.2(4)
N(3)-Zr-C	100.4(4)
N(1)-Zr-N(2)	70.88(10)
N(3)-Zr-N(2)	70.69(10)
C-Zr-N(2)	127.2(3)
N(1)-Zr-C(1)	99.43(14)
N(3)-Zr-C(1)	98.45(14)
C-Zr-C(1)	115.2(3)
N(2)-Zr-C(1)	117.55(12)
N(1)-Zr-Cl	98.5(2)
N(3)-Zr-Cl	101.0(2)
N(2)-Zr-Cl	121.64(13)
C(1)-Zr-Cl	120.8(2)
C(6)-N(1)-C(5)	111.9(3)
C(6)-N(1)-Zr	124.2(2)
C(5)-N(1)-Zr	123.9(2)
C(7)-N(2)-C(11)	119.9(3)
C(7)-N(2)-Zr	120.1(2)
C(11)-N(2)-Zr	120.1(2)
C(12)-N(3)-C(13)	111.8(3)
C(12)-N(3)-Zr	124.9(2)
C(13)-N(3)-Zr	123.3(2)
N(1)-C(5)-C(2)	111.4(4)
N(1)-C(5)-C(3)	109.4(3)
C(2)-C(5)-C(3)	107.8(4)
N(1)-C(5)-C(4)	110.3(3)
C(2)-C(5)-C(4)	109.4(4)
C(3)-C(5)-C(4)	108.4(5)
N(1)-C(6)-C(7)	109.9(3)
N(2)-C(7)-C(8)	121.0(4)

N(2)-C(7)-C(6)	114.7(3)
C(8)-C(7)-C(6)	124.3(3)
C(9)-C(8)-C(7)	119.4(4)
C(8)-C(9)-C(10)	119.6(3)
C(9)-C(10)-C(11)	119.1(4)
N(2)-C(11)-C(10)	121.0(3)
N(2)-C(11)-C(12)	114.7(3)
C(10)-C(11)-C(12)	124.4(3)
N(3)-C(12)-C(11)	109.6(3)
N(3)-C(13)-C(16)	109.5(3)
N(3)-C(13)-C(15)	110.8(4)
C(16)-C(13)-C(15)	109.1(5)
N(3)-C(13)-C(14)	109.5(4)
C(16)-C(13)-C(14)	108.4(5)
C(15)-C(13)-C(14)	109.4(5)

Symmetry transformations used to generate equivalent atoms:

11 Crystallographic data for (iPAP)ZrCl^{i}Pr.

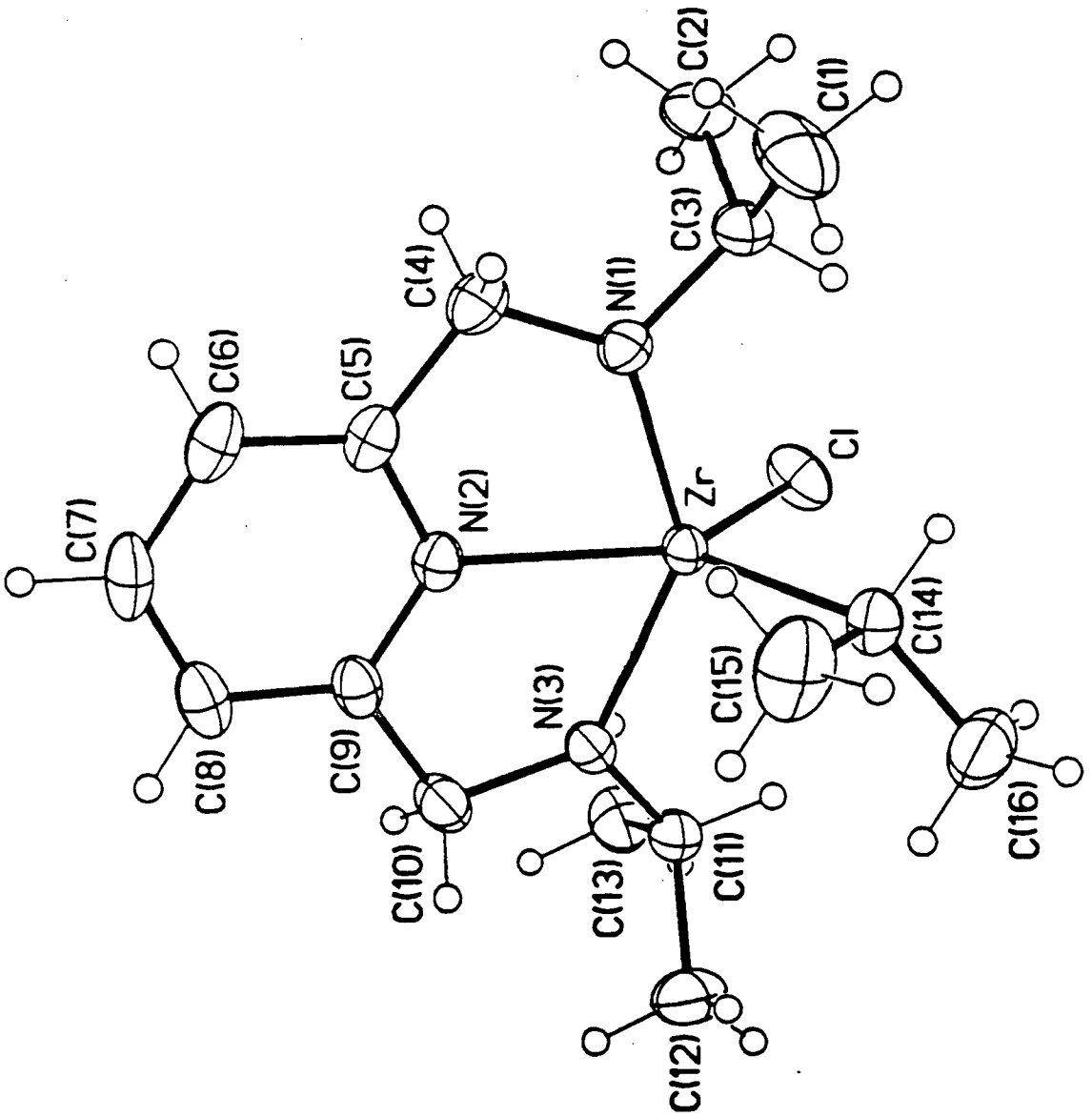

Table 1. Crystal data and structure refinement for 1.

Identification code	dm006
Empirical formula	C16 H28 Cl N3 Zr
Formula weight	389.08
Temperature	296(2) K
Wavelength	0.71073 A
Crystal system	Orthorhombic
Space group	Pbca
Unit cell dimensions	a = 13.9320(3) A alpha = 90 deg. b = 15.0145(3) A beta = 90 deg. c = 18.2507(2) A gamma = 90 deg.
Volume, Z	3817.7(1) A^3, 8
Density (calculated)	1.354 Mg/m^3
Absorption coefficient	0.714 mm^-1
F(000)	1616
Crystal size	0.20 x 0.20 x 0.20 mm
Theta range for data collection	2.23 to 25.00 deg.
Limiting indices	-18<=h<=18, -17<=k<=19, -24<=l<=12
Reflections collected	18143
Independent reflections	3355 [R(int) = 0.0353]
Absorption correction	Semi-empirical from psi-scans
Max. and min. transmission	0.801475 and 0.724184
Refinement method	Full-matrix least-squares on F^2
Data / restraints / parameters	3355 / 0 / 190
Goodness-of-fit on F^2	1.055
Final R indices [I>2sigma(I)]	R1 = 0.0293, wR2 = 0.0624
R indices (all data)	R1 = 0.0433, wR2 = 0.0671
Largest diff. peak and hole	0.285 and -0.338 e.A^-3

Table 2. Atomic coordinates (x 10^4) and equivalent isotropic displacement parameters (A^2 x 10^3) for 1. U(eq) is defined as one third of the trace of the orthogonalized Uij tensor.

	x	y	z	U(eq)
Zr	6084(1)	6563(1)	1385(1)	32(1)
Cl	7404(1)	7375(1)	809(1)	58(1)
N(1)	4881(1)	7143(1)	944(1)	40(1)
N(2)	4989(1)	5491(1)	1045(1)	38(1)
N(3)	6644(2)	5312(1)	1557(1)	41(1)
C(1)	4089(3)	8560(2)	1317(2)	91(1)
C(2)	4973(3)	8449(2)	113(2)	79(1)
C(3)	4903(2)	8120(2)	898(2)	50(1)
C(4)	4020(2)	6713(2)	673(2)	50(1)
C(5)	4138(2)	5736(2)	751(1)	43(1)
C(6)	3469(2)	5101(2)	550(2)	56(1)
C(7)	3685(2)	4217(2)	642(2)	60(1)
C(8)	4559(2)	3969(2)	934(2)	55(1)
C(9)	5200(2)	4625(2)	1130(1)	42(1)
C(10)	6180(2)	4461(2)	1436(2)	51(1)
C(11)	7663(2)	5269(2)	1770(2)	48(1)
C(12)	7845(2)	4678(2)	2438(2)	77(1)
C(13)	8307(2)	5001(2)	1129(2)	61(1)
C(14)	5909(2)	7066(2)	2542(2)	50(1)
C(15)	5054(3)	6575(2)	2868(2)	92(1)
C(16)	6785(3)	7009(2)	3039(2)	80(1)

Table 3. Bond lengths [A] and angles [deg] for 1.

Zr-N(1)	2.053(2)
Zr-N(3)	2.059(2)
Zr-C(14)	2.255(3)
Zr-N(2)	2.304(2)
Zr-Cl	2.4445(7)
N(1)-C(4)	1.449(3)
N(1)-C(3)	1.470(3)
N(2)-C(9)	1.342(3)
N(2)-C(5)	1.353(3)
N(3)-C(10)	1.449(3)
N(3)-C(11)	1.473(3)
C(1)-C(3)	1.518(4)
C(2)-C(3)	1.520(4)
C(4)-C(5)	1.483(4)
C(5)-C(6)	1.382(4)
C(6)-C(7)	1.371(4)
C(7)-C(8)	1.380(4)
C(8)-C(9)	1.378(4)
C(9)-C(10)	1.495(4)
C(11)-C(12)	1.529(4)
C(11)-C(13)	1.528(4)
C(14)-C(16)	1.523(4)
C(14)-C(15)	1.523(4)
N(1)-Zr-N(3)	139.10(8)
N(1)-Zr-C(14)	97.86(9)
N(3)-Zr-C(14)	101.76(9)
N(1)-Zr-N(2)	69.50(8)
N(3)-Zr-N(2)	69.74(8)
C(14)-Zr-N(2)	114.48(8)
N(1)-Zr-Cl	103.57(6)
N(3)-Zr-Cl	103.63(6)
C(14)-Zr-Cl	108.48(7)
N(2)-Zr-Cl	137.00(5)
C(4)-N(1)-C(3)	116.2(2)
C(4)-N(1)-Zr	128.4(2)
C(3)-N(1)-Zr	115.4(2)
C(9)-N(2)-C(5)	120.2(2)
C(9)-N(2)-Zr	120.0(2)
C(5)-N(2)-Zr	119.8(2)
C(10)-N(3)-C(11)	115.5(2)
C(10)-N(3)-Zr	127.8(2)
C(11)-N(3)-Zr	116.4(2)
N(1)-C(3)-C(1)	113.0(2)
N(1)-C(3)-C(2)	112.3(2)
C(1)-C(3)-C(2)	112.4(3)
N(1)-C(4)-C(5)	108.4(2)
N(2)-C(5)-C(6)	120.5(3)
N(2)-C(5)-C(4)	113.8(2)
C(6)-C(5)-C(4)	125.6(3)
C(7)-C(6)-C(5)	119.2(3)
C(6)-C(7)-C(8)	120.2(3)
C(9)-C(8)-C(7)	118.6(3)
N(2)-C(9)-C(8)	121.3(3)
N(2)-C(9)-C(10)	113.8(2)
C(8)-C(9)-C(10)	124.8(3)

N(3)-C(10)-C(9)	108.5(2)
N(3)-C(11)-C(12)	113.3(2)
N(3)-C(11)-C(13)	112.1(2)
C(12)-C(11)-C(13)	111.1(2)
C(16)-C(14)-C(15)	111.5(3)
C(16)-C(14)-Zr	116.9(2)
C(15)-C(14)-Zr	106.7(2)

Symmetry transformations used to generate equivalent atoms:

Table 4. Anisotropic displacement parameters (A^2 x 10^3) for 1. The anisotropic displacement factor exponent takes the form: -2 pi^2 [h^2 a*^2 U11 + ... + 2 h k a* b* U12]

	U11	U22	U33	U23	U13	U12
Zr	31(1)	30(1)	37(1)	0(1)	-1(1)	-4(1)
Cl	46(1)	44(1)	83(1)	6(1)	18(1)	-9(1)
N(1)	35(1)	42(1)	43(1)	1(1)	-4(1)	-1(1)
N(2)	37(1)	42(1)	34(1)	-2(1)	3(1)	-9(1)
N(3)	43(1)	32(1)	47(1)	2(1)	-3(1)	-2(1)
C(1)	70(2)	61(2)	141(4)	-20(2)	10(2)	17(2)
C(2)	96(3)	57(2)	84(3)	27(2)	-24(2)	-6(2)
C(3)	44(2)	43(2)	62(2)	0(1)	-8(1)	6(1)
C(4)	35(1)	61(2)	53(2)	-2(1)	-5(1)	-1(1)
C(5)	36(1)	58(2)	34(1)	-4(1)	3(1)	-10(1)
C(6)	41(2)	79(2)	48(2)	-9(2)	-1(1)	-20(2)
C(7)	60(2)	67(2)	53(2)	-17(2)	8(2)	-34(2)
C(8)	66(2)	44(2)	55(2)	-7(1)	14(2)	-20(2)
C(9)	49(2)	39(1)	38(1)	-3(1)	8(1)	-12(1)
C(10)	57(2)	35(1)	60(2)	3(1)	0(1)	-4(1)
C(11)	46(2)	39(2)	57(2)	2(1)	-11(1)	2(1)
C(12)	79(2)	76(2)	76(2)	22(2)	-25(2)	4(2)
C(13)	42(2)	53(2)	87(2)	-7(2)	0(2)	6(1)
C(14)	56(2)	51(2)	45(2)	-8(1)	-3(1)	-2(1)
C(15)	99(3)	116(3)	59(2)	-11(2)	20(2)	-34(2)
C(16)	83(2)	88(3)	67(2)	-21(2)	-20(2)	13(2)

Table 5. Hydrogen coordinates (x 10^4) and isotropic displacement parameters (A^2 x 10^3) for 1.

	x	y	z	U(eq)
H(1A)	4073(3)	8333(2)	1808(2)	109
H(2A)	3491(3)	8434(2)	1078(2)	109
H(3A)	4190(3)	9193(2)	1329(2)	109
H(2A)	5495(3)	8153(2)	-130(2)	95
H(2B)	5084(3)	9080(2)	112(2)	95
H(2C)	4385(3)	8321(2)	-140(2)	95
H(3A)	5497(2)	8307(2)	1141(2)	60
H(4A)	3919(2)	6866(2)	163(2)	59
H(4B)	3467(2)	6912(2)	951(2)	59
H(6A)	2880(2)	5271(2)	356(2)	67
H(7A)	3242(2)	3784(2)	506(2)	72
H(8A)	4711(2)	3371(2)	998(2)	66
H(10A)	6132(2)	4136(2)	1894(2)	61
H(10B)	6554(2)	4106(2)	1095(2)	61
H(11A)	7851(2)	5874(2)	1910(2)	57
H(12A)	7430(2)	4858(2)	2831(2)	116
H(12B)	8502(2)	4737(2)	2589(2)	116
H(12C)	7716(2)	4068(2)	2313(2)	116
H(13A)	8178(2)	5379(2)	717(2)	91
H(13B)	8180(2)	4393(2)	998(2)	91
H(13C)	8968(2)	5061(2)	1270(2)	91
H(14A)	5731(2)	7696(2)	2509(2)	60
H(15A)	4514(3)	6625(2)	2543(2)	137
H(15B)	4893(3)	6832(2)	3333(2)	137
H(15C)	5214(3)	5958(2)	2932(2)	137
H(16A)	7309(3)	7327(2)	2820(2)	119
H(16B)	6961(3)	6396(2)	3105(2)	119
H(16C)	6636(3)	7268(2)	3507(2)	119

12 Crystallographic data for (BDPP)TaCl(η^2-oct-4-yne).

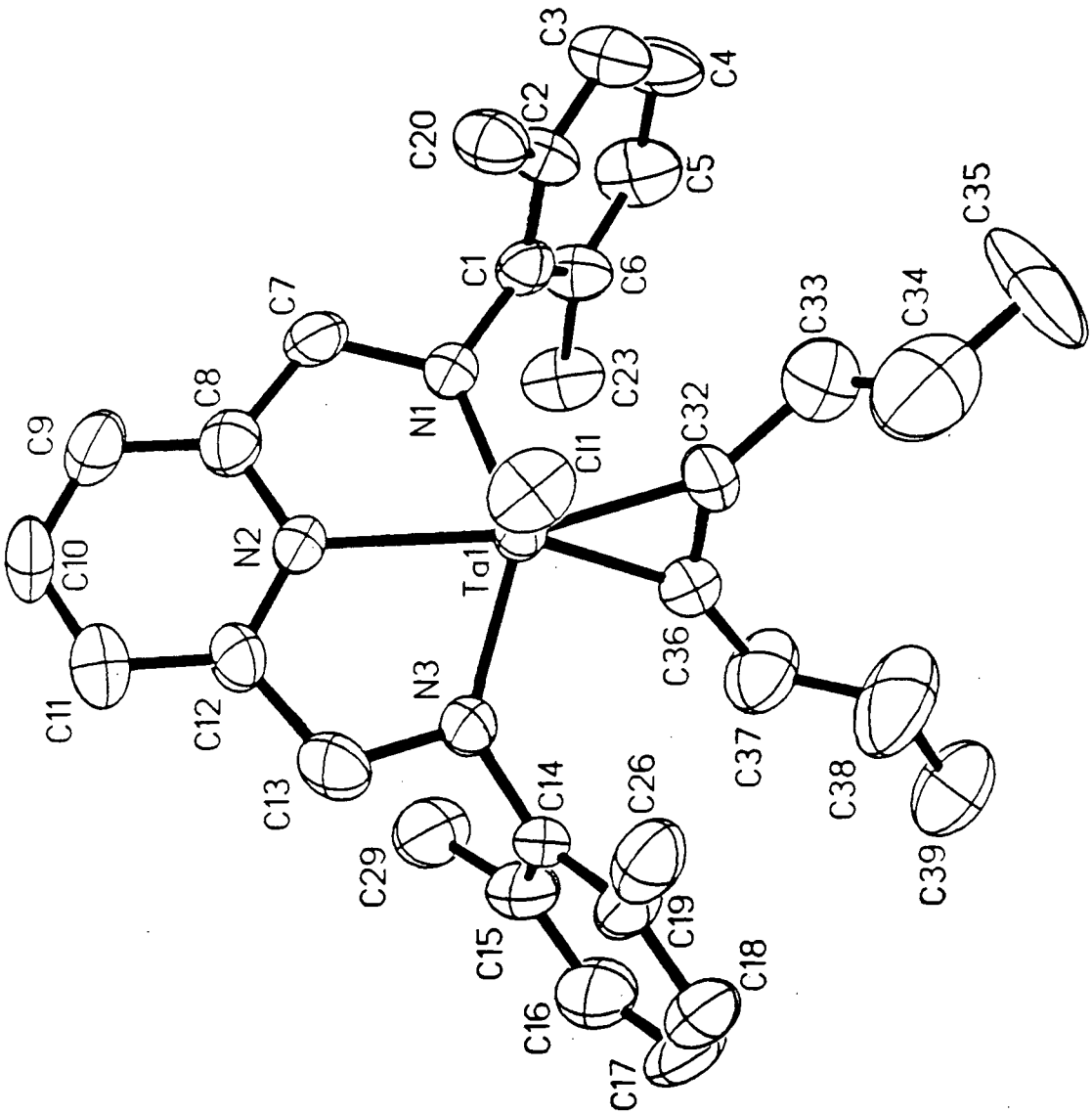

Table S1. Crystal Data and Experimental Details.

Empirical formula	$C_{39}H_{65}C\ell_3N_3Ta_1$
Formula weight	792.36
Temperature	23°C
Wavelength	0.71073 Å
Crystal system	Triclinic
Space group	$P\bar{1}$
Unit cell dimensions	a = 9.936(2)Å
	b = 11.558(1)Å
	c = 17.689(2)Å
	α = 74.997(6)°
	β = 87.424(10)°
	γ = 75.372(9)°
Volume	1898.0(5) Å^3
Z	2
Density, calcd.	1.386 g.cm^{-3}
Absorption coefficient	2.995 mm^{-1}
F(000)	820
Reflections Collected	6078
Independent reflections	5179 [R(int) = 0.0284]
Refinement method	Full-matrix least-squares on F^2
Data/restraints/parameters	5179/90/408
Goodness-of-fit (GooF) on F^2	1.037
Final R indices [I>2sigma(I)]	R1 = 0.0401, wR2 = 0.0946
R indices (all data)	R1 = 0.0519, wR2 = 0.1011

$R1 = \Sigma(\|F_o\| - \|F_c\|)/\Sigma|F_o|$;

$wR2 = [\Sigma w(F_o^2 - F_c^2)^2/\Sigma wF_o^4]^{1/2}$

$GooF = [\Sigma w(F_o^2 - F_c^2)^2/(n-p)]^{1/2}$

where n is the number of reflections and p is the number of parameters refined.

Table S2. Atomic coordinates (x 10^4) and equivalent isotropic displacement parameters ($Å^2$ x 10^3). U(eq) is defined as one third of the trace of the orthogonalized Uij tensor.

atom	x	y	z	Ueq
Ta(1)	2183.0(3)	2065.6(3)	7998.6(2)	33.1(1)
Cl(1)	3823(2)	573(2)	8902(1)	60(1)
N(1)	1164(6)	3359(5)	8572(3)	37(1)
C(1)	1591(8)	4434(6)	8626(4)	39(2)
C(2)	2398(8)	4353(7)	9276(5)	45(2)
C(3)	2773(10)	5399(8)	9339(5)	61(2)
C(4)	2383(12)	6499(8)	8792(5)	75(3)
C(5)	1597(11)	6566(7)	8157(5)	67(3)
C(6)	1197(9)	5552(7)	8049(4)	48(2)
C(7)	-15(8)	3232(7)	9086(4)	46(2)
N(2)	346(6)	1452(5)	8610(3)	38(1)
C(8)	-436(8)	2078(7)	9089(4)	47(2)
C(9)	-1532(9)	1679(9)	9483(5)	61(2)
C(10)	-1801(10)	629(9)	9379(5)	70(3)
C(11)	-1043(10)	24(9)	8872(5)	66(3)
C(12)	34(9)	448(7)	8487(5)	47(2)
C(13)	919(9)	-23(7)	7874(5)	57(2)
N(3)	1675(6)	879(5)	7456(3)	42(2)
C(14)	2003(8)	699(7)	6682(4)	42(2)
C(15)	972(10)	1276(8)	6083(5)	60(2)
C(16)	1347(12)	1123(10)	5336(6)	79(3)
C(17)	2631(11)	436(11)	5188(6)	82(3)
C(18)	3567(11)	-142(9)	5780(6)	70(3)
C(19)	3280(9)	-53(8)	6544(5)	56(2)
C(20)	2925(7)	3157(7)	9898(4)	49(2)
C(21)	4518(7)	2765(9)	9945(6)	85(3)
C(22)	2351(9)	3251(9)	10705(4)	75(3)
C(23)	346(8)	5707(7)	7325(4)	62(3)
C(24)	1045(11)	6236(10)	6570(5)	99(4)
C(25)	-1130(9)	6518(10)	7344(6)	100(4)
C(26)	4350(8)	-762(6)	7183(5)	63(3)
C(27)	5639(9)	-251(8)	7133(6)	83(3)
C(28)	4791(12)	-2149(7)	7234(7)	101(4)
C(29)	-476(9)	2035(8)	6226(5)	72(3)
C(30)	-1572(53)	1505(51)	5947(39)	94(20)
C(31)	-771(76)	3428(19)	5845(45)	94(20)
C(30A)	-1496(36)	1248(32)	6198(26)	87(12)
C(31A)	-1002(45)	3330(18)	5682(25)	87(12)
C(30B)	-1643(39)	1801(39)	5792(28)	83(14)
C(31B)	-463(54)	3406(16)	5940(33)	83(14)
C(32)	3559(8)	3116(8)	7526(5)	59(2)
C(33)	4530(9)	3933(9)	7569(7)	96(4)
C(34)	6025(9)	3252(11)	7634(8)	121(5)
C(35)	6931(11)	4095(13)	7659(9)	148(7)
C(36)	2943(8)	2957(7)	6951(4)	49(2)
C(37)	2932(9)	3376(10)	6061(4)	77(3)
C(38)	4336(10)	3205(14)	5718(5)	119(5)
C(39)	4258(13)	3554(12)	4845(5)	111(5)

Table S3. Bond Distances (Å) and Angles (°)

Ta(1)-N(3)	2.033(6)	Ta(1)-N(1)	2.053(6)
Ta(1)-C(32)	2.062(7)	Ta(1)-C(36)	2.085(7)
Ta(1)-N(2)	2.255(6)	Ta(1)-Cl(1)	2.361(2)
N(1)-C(1)	1.436(9)	N(1)-C(7)	1.463(9)
C(1)-C(6)	1.401(10)	C(1)-C(2)	1.401(10)
C(2)-C(3)	1.383(11)	C(2)-C(20)	1.515(10)
C(3)-C(4)	1.361(11)	C(4)-C(5)	1.370(12)
C(5)-C(6)	1.388(11)	C(6)-C(23)	1.512(11)
C(7)-C(8)	1.494(11)	N(2)-C(12)	1.345(9)
N(2)-C(8)	1.348(9)	C(8)-C(9)	1.379(11)
C(9)-C(10)	1.365(12)	C(10)-C(11)	1.363(12)
C(11)-C(12)	1.369(11)	C(12)-C(13)	1.491(11)
C(13)-N(3)	1.464(9)	N(3)-C(14)	1.449(9)
C(14)-C(19)	1.396(11)	C(14)-C(15)	1.415(11)
C(15)-C(16)	1.399(12)	C(15)-C(29)	1.532(12)
C(16)-C(17)	1.376(14)	C(17)-C(18)	1.348(14)
C(18)-C(19)	1.393(11)	C(19)-C(26)	1.506(12)
C(20)-C(22)	1.532(5)	C(20)-C(21)	1.532(5)
C(23)-C(25)	1.533(5)	C(23)-C(24)	1.533(5)
C(26)-C(27)	1.530(5)	C(26)-C(28)	1.531(5)
C(29)-C(31A)	1.531(6)	C(29)-C(30)	1.533(6)
C(29)-C(31)	1.533(6)	C(29)-C(30A)	1.533(6)
C(29)-C(30B)	1.534(6)	C(29)-C(31B)	1.536(6)
C(30A)-C(30B)	0.82(6)	C(31A)-C(31B)	0.76(5)
C(32)-C(36)	1.287(11)	C(32)-C(33)	1.527(9)
C(33)-C(34)	1.489(8)	C(34)-C(35)	1.494(8)
C(36)-C(37)	1.522(8)	C(37)-C(38)	1.483(8)
C(38)-C(39)	1.492(8)		

N(3)-Ta(1)-N(1)	137.2(2)	N(3)-Ta(1)-C(32)	122.1(3)
N(1)-Ta(1)-C(32)	91.5(3)	N(3)-Ta(1)-C(36)	90.0(3)
N(1)-Ta(1)-C(36)	109.2(3)	C(32)-Ta(1)-C(36)	36.2(3)
N(3)-Ta(1)-N(2)	71.9(2)	N(1)-Ta(1)-N(2)	71.4(2)
C(32)-Ta(1)-N(2)	162.6(3)	C(36)-Ta(1)-N(2)	146.2(3)
N(3)-Ta(1)-Cl(1)	96.9(2)	N(1)-Ta(1)-Cl(1)	106.6(2)
C(32)-Ta(1)-Cl(1)	94.5(3)	C(36)-Ta(1)-Cl(1)	117.1(2)
N(2)-Ta(1)-Cl(1)	93.7(2)	C(1)-N(1)-C(7)	108.7(5)
C(1)-N(1)-Ta(1)	126.3(5)	C(7)-N(1)-Ta(1)	124.5(5)
C(6)-C(1)-C(2)	120.1(7)	C(6)-C(1)-N(1)	121.1(7)
C(2)-C(1)-N(1)	118.8(6)	C(3)-C(2)-C(1)	118.7(7)
C(3)-C(2)-C(20)	118.4(7)	C(1)-C(2)-C(20)	122.8(7)
C(4)-C(3)-C(2)	122.1(8)	C(3)-C(4)-C(5)	118.7(8)
C(4)-C(5)-C(6)	122.4(8)	C(5)-C(6)-C(1)	117.9(7)
C(5)-C(6)-C(23)	118.8(7)	C(1)-C(6)-C(23)	123.2(7)
N(1)-C(7)-C(8)	110.6(6)	C(12)-N(2)-C(8)	120.2(7)
C(12)-N(2)-Ta(1)	118.8(5)	C(8)-N(2)-Ta(1)	121.0(5)
N(2)-C(8)-C(9)	121.0(8)	N(2)-C(8)-C(7)	112.1(7)
C(9)-C(8)-C(7)	126.8(8)	C(10)-C(9)-C(8)	118.3(8)
C(11)-C(10)-C(9)	120.6(8)	C(10)-C(11)-C(12)	119.6(9)
N(2)-C(12)-C(11)	120.2(8)	N(2)-C(12)-C(13)	111.7(6)
C(11)-C(12)-C(13)	127.9(8)	N(3)-C(13)-C(12)	110.6(6)
C(14)-N(3)-C(13)	109.3(6)	C(14)-N(3)-Ta(1)	130.2(5)

C(13)-N(3)-Ta(1)	120.4(5)	C(19)-C(14)-C(15)	121.6(7)
C(19)-C(14)-N(3)	120.6(7)	C(15)-C(14)-N(3)	117.7(7)
C(16)-C(15)-C(14)	116.1(9)	C(16)-C(15)-C(29)	120.9(9)
C(14)-C(15)-C(29)	123.0(7)	C(17)-C(16)-C(15)	122.5(10)
C(18)-C(17)-C(16)	119.7(9)	C(17)-C(18)-C(19)	121.8(9)
C(18)-C(19)-C(14)	118.1(9)	C(18)-C(19)-C(26)	119.1(8)
C(14)-C(19)-C(26)	122.8(7)	C(2)-C(20)-C(22)	111.8(6)
C(2)-C(20)-C(21)	111.6(7)	C(22)-C(20)-C(21)	109.7(5)
C(6)-C(23)-C(25)	112.1(7)	C(6)-C(23)-C(24)	112.3(7)
C(25)-C(23)-C(24)	109.4(5)	C(19)-C(26)-C(27)	113.7(7)
C(19)-C(26)-C(28)	112.9(8)	C(27)-C(26)-C(28)	109.8(5)
C(31A)-C(29)-C(15)	118(2)	C(30)-C(29)-C(15)	109(3)
C(30)-C(29)-C(31)	109.7(6)	C(15)-C(29)-C(31)	115(3)
C(31A)-C(29)-C(30A)	109.7(6)	C(15)-C(29)-C(30A)	107(2)
C(15)-C(29)-C(30B)	113(2)	C(15)-C(29)-C(31B)	107(2)
C(30B)-C(29)-C(31B)	109.1(6)	C(36)-C(32)-C(33)	132.6(8)
C(36)-C(32)-Ta(1)	72.9(4)	C(33)-C(32)-Ta(1)	153.3(7)
C(34)-C(33)-C(32)	112.9(7)	C(33)-C(34)-C(35)	110.8(8)
C(32)-C(36)-C(37)	137.2(8)	C(32)-C(36)-Ta(1)	71.0(4)
C(37)-C(36)-Ta(1)	151.7(6)	C(38)-C(37)-C(36)	114.1(7)
C(37)-C(38)-C(39)	111.7(8)		

Table S4. Anisotropic displacement parameters ($Å^2 \times 10^3$).
The anisotropic displacement factor exponent takes the form: $-2\pi^2[h^2a^{*2}U11 + \ldots + 2hka^*b^*U12]$

atom	U11	U22	U33	U23	U13	U12
Ta(1)	35(1)	31(1)	34(1)	-10(1)	6(1)	-9(1)
Cl(1)	60(1)	54(1)	51(1)	-6(1)	-6(1)	5(1)
N(1)	37(4)	39(3)	36(3)	-11(3)	5(3)	-11(3)
C(1)	44(5)	34(4)	41(4)	-15(3)	9(4)	-6(3)
C(2)	47(5)	36(4)	55(5)	-16(4)	-11(4)	-8(4)
C(3)	73(7)	57(5)	59(5)	-19(4)	-13(5)	-20(5)
C(4)	128(10)	41(5)	70(6)	-19(5)	-12(6)	-37(6)
C(5)	104(8)	28(4)	62(6)	-4(4)	-6(6)	-10(5)
C(6)	60(5)	40(4)	45(5)	-12(4)	-9(4)	-7(4)
C(7)	46(5)	54(5)	41(4)	-24(4)	7(4)	-10(4)
N(2)	41(4)	41(3)	34(3)	-12(3)	10(3)	-13(3)
C(8)	43(5)	57(5)	39(4)	-9(4)	0(4)	-14(4)
C(9)	54(6)	82(7)	50(5)	-21(5)	21(4)	-24(5)
C(10)	70(7)	90(7)	61(6)	-13(5)	28(5)	-51(6)
C(11)	68(6)	68(6)	65(6)	-10(5)	18(5)	-36(5)
C(12)	56(5)	37(4)	50(5)	-7(4)	13(4)	-22(4)
C(13)	66(6)	36(4)	75(6)	-20(4)	9(5)	-18(4)
N(3)	45(4)	37(3)	47(4)	-15(3)	11(3)	-16(3)
C(14)	49(5)	46(4)	43(4)	-24(4)	12(4)	-23(4)
C(15)	64(6)	72(6)	55(5)	-33(5)	2(5)	-22(5)
C(16)	80(8)	111(9)	63(6)	-41(6)	-1(6)	-33(7)
C(17)	73(7)	134(10)	64(6)	-69(7)	20(6)	-27(7)
C(18)	61(6)	89(7)	76(7)	-49(6)	21(6)	-18(6)
C(19)	61(6)	54(5)	59(5)	-27(4)	23(5)	-15(5)
C(20)	59(6)	43(4)	46(5)	-8(4)	-10(4)	-15(4)
C(21)	69(7)	78(7)	100(8)	-18(6)	-31(6)	-3(6)
C(22)	98(8)	80(7)	51(5)	-18(5)	-8(5)	-27(6)
C(23)	86(7)	40(5)	47(5)	-4(4)	-13(5)	-1(5)
C(24)	129(11)	102(8)	48(6)	-6(6)	-5(7)	-8(8)
C(25)	80(8)	115(9)	93(8)	-39(7)	-24(7)	13(7)
C(26)	65(6)	52(5)	66(6)	-16(4)	23(5)	-7(5)
C(27)	69(7)	83(7)	93(8)	-16(6)	1(6)	-19(6)
C(28)	114(10)	59(6)	127(10)	-35(7)	41(8)	-14(7)
C(29)	45(6)	106(8)	78(7)	-47(6)	-3(5)	-14(5)
C(32)	64(6)	78(6)	53(5)	-22(5)	15(5)	-47(5)
C(33)	97(9)	134(11)	80(8)	-42(7)	23(7)	-58(8)
C(34)	99(11)	155(13)	95(9)	-38(9)	-4(8)	-1(10)
C(35)	97(11)	187(16)	192(16)	-39(13)	-33(10)	-98(11)
C(36)	53(5)	55(5)	45(5)	-19(4)	8(4)	-21(4)
C(37)	73(7)	107(8)	46(5)	-13(5)	7(5)	-22(6)
C(38)	97(10)	200(15)	52(6)	-20(8)	19(7)	-39(10)
C(39)	135(12)	150(12)	59(7)	-28(7)	43(7)	-58(10)

Table S5. Calculated Hydrogen Atom Coordinates (x 10^4) and Thermal Parameters (x 10^3)

atom	x	y	y	Ueq
H(3)	3310(10)	5348(8)	9769(5)	73
H(4)	2644(12)	7191(8)	8847(5)	90
H(5)	1320(11)	7320(7)	7786(5)	80
H(7A)	-794(8)	3943(7)	8907(4)	55
H(7B)	240(8)	3207(7)	9614(4)	55
H(9)	-2073(9)	2115(9)	9810(5)	73
H(10)	-2509(10)	323(9)	9657(5)	84
H(11)	-1255(10)	-672(9)	8789(5)	79
H(13A)	1578(9)	-796(7)	8117(5)	68
H(13B)	339(9)	-184(7)	7506(5)	68
H(16)	704(12)	1500(10)	4925(6)	95
H(17)	2853(11)	371(11)	4682(6)	99
H(18)	4427(11)	-614(9)	5675(6)	84
H(20)	2599(7)	2508(7)	9754(4)	59
H(21A)	4816(7)	2003(37)	10341(30)	128
H(21B)	4863(8)	3395(32)	10075(42)	128
H(21C)	4872(8)	2651(66)	9449(14)	128
H(22A)	2719(57)	3833(49)	10879(18)	112
H(22B)	2621(62)	2455(17)	11071(10)	112
H(22C)	1355(10)	3525(62)	10670(10)	112
H(23)	266(8)	4885(7)	7311(4)	74
H(24A)	1982(31)	5747(50)	6567(24)	149
H(24B)	1056(82)	7074(29)	6543(25)	149
H(24C)	534(53)	6219(74)	6127(5)	149
H(25A)	-1634(30)	6591(66)	6877(24)	150
H(25B)	-1083(9)	7325(26)	7374(50)	150
H(25C)	-1597(31)	6147(41)	7793(28)	150
H(26)	3908(8)	-675(6)	7678(5)	75
H(27A)	6286(34)	-754(40)	7547(26)	124
H(27B)	5370(14)	583(24)	7185(42)	124
H(27C)	6068(43)	-262(62)	6637(18)	124
H(28A)	5348(75)	-2573(12)	7700(28)	151
H(28B)	5322(78)	-2283(9)	6784(27)	151
H(28C)	3978(12)	-2460(17)	7250(51)	151
H(33A)	4385(9)	4618(9)	7103(7)	115
H(33B)	4295(9)	4274(9)	8018(7)	115
H(34A)	6266(9)	2901(11)	7189(8)	145
H(34B)	6183(9)	2578(11)	8105(8)	145
H(35A)	6755(91)	4775(60)	7199(36)	221
H(35B)	7891(11)	3648(32)	7676(71)	221
H(35C)	6732(88)	4404(88)	8116(39)	221
H(37A)	2411(9)	2918(10)	5853(4)	92
H(37B)	2450(9)	4244(10)	5897(4)	92
H(38A)	4846(10)	2347(14)	5902(5)	143
H(38B)	4841(10)	3709(14)	5893(5)	143
H(39A)	5180(15)	3376(83)	4643(5)	167
H(39B)	3830(92)	4422(22)	4659(5)	167
H(39C)	3715(85)	3090(66)	4671(5)	167

13 Crystallographic data for (BDPP)Ta(CPh=CHCPr=CPrC≡CPh).

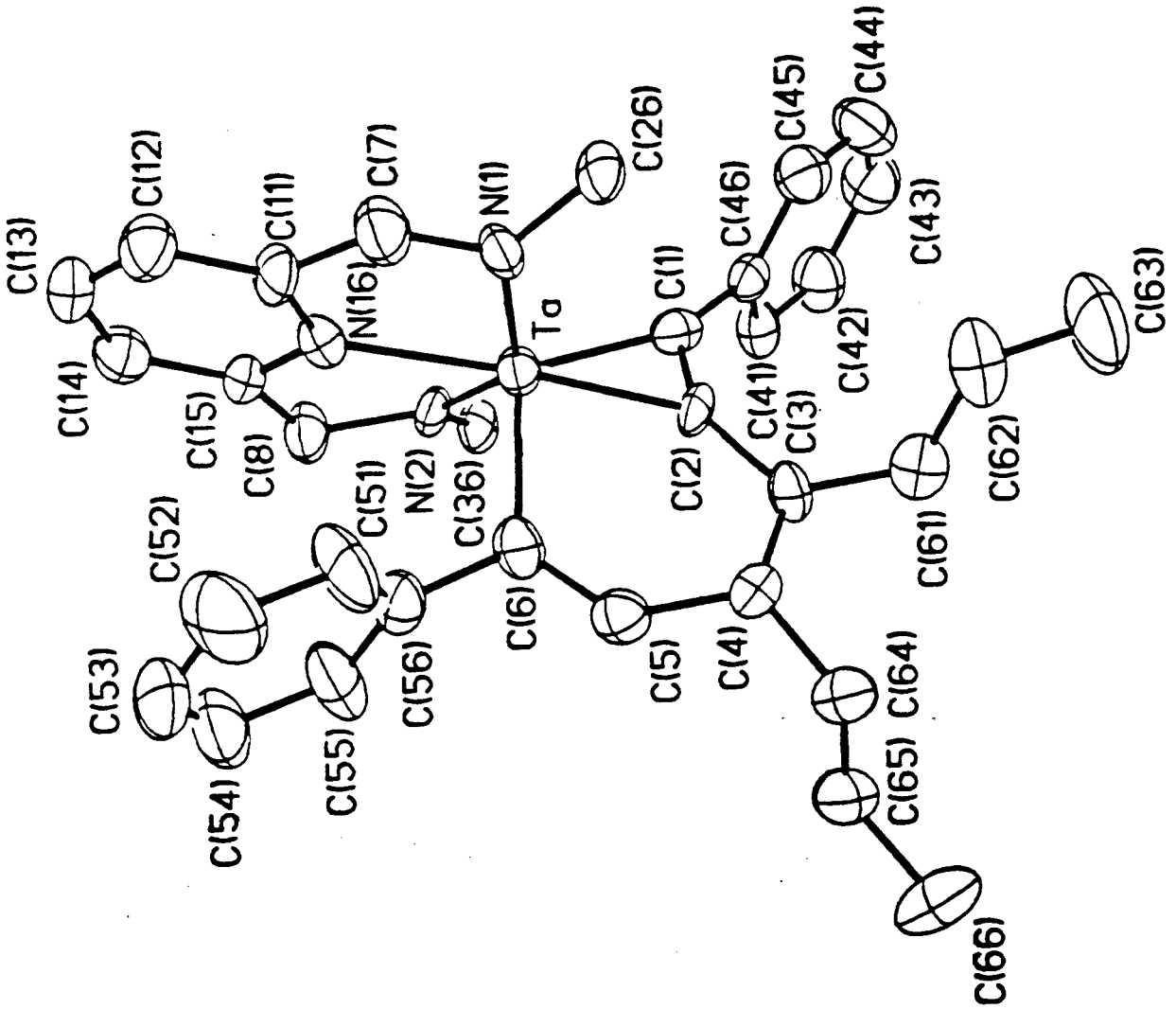

Table 1. Crystal data and structure refinement for 1.

Identification code	dm002
Empirical formula	C58 H73 N3 Ta
Formula weight	993.14
Temperature	293(2) K
Wavelength	0.71073 A
Crystal system	Monoclinic
Space group	P2(1)/c
Unit cell dimensions	a = 13.530(2) A alpha = 90 deg. b = 18.389(2) A beta = 102.98(1) deg. c = 21.604(3) A gamma = 90 deg.
Volume, Z	5238(1) A^3, 4
Density (calculated)	1.259 Mg/m^3
Absorption coefficient	2.136 mm^-1
F(000)	2060
Crystal size	0.10 x 0.10 x 0.10 mm
Theta range for data collection	1.47 to 21.00 deg.
Limiting indices	-17<=h<=17, -11<=k<=23, -28<=l<=27
Reflections collected	18018
Independent reflections	5624 [R(int) = 0.0902]
Absorption correction	None
Refinement method	Full-matrix least-squares on F^2
Data / restraints / parameters	5575 / 3 / 500
Goodness-of-fit on F^2	1.230
Final R indices [I>2sigma(I)]	R1 = 0.0794, wR2 = 0.1458
R indices (all data)	R1 = 0.1099, wR2 = 0.1593
Extinction coefficient	0.0033(3)
Largest diff. peak and hole	0.667 and -0.634 e.A^-3

Table 2. Atomic coordinates (x 10^4) and equivalent isotropic displacement parameters (A^2 x 10^3) for 1. U(eq) is defined as one third of the trace of the orthogonalized Uij tensor.

	x	y	z	U(eq)
Ta	-2885(1)	5671(1)	-2871(1)	51(1)
C(1)	-1329(10)	5602(7)	-2786(6)	54(3)
N(1)	-3131(8)	6643(6)	-2512(5)	60(3)
C(2)	-1575(9)	5336(7)	-2285(6)	49(3)
N(2)	-3284(7)	5147(6)	-3704(5)	50(3)
C(3)	-1135(10)	4920(8)	-1723(7)	59(4)
C(4)	-1777(12)	4553(8)	-1457(7)	70(4)
C(5)	-2907(11)	4559(7)	-1731(7)	65(4)
C(6)	-3457(10)	4910(8)	-2255(7)	63(4)
C(7)	-4135(11)	6965(9)	-2588(8)	84(5)
C(8)	-4352(10)	5105(8)	-4075(7)	72(4)
C(11)	-4855(7)	6657(5)	-3126(4)	67(4)
C(12)	-5792(7)	6916(5)	-3455(5)	83(5)
C(13)	-6307(6)	6564(6)	-4002(5)	86(5)
C(14)	-5886(7)	5953(6)	-4221(4)	76(5)
C(15)	-4949(7)	5694(4)	-3892(4)	64(4)
N(16)	-4434(5)	6046(5)	-3345(4)	55(3)
C(21)	-2156(8)	7075(5)	-1474(5)	72(4)
C(22)	-1437(9)	7540(7)	-1119(5)	98(6)
C(23)	-928(7)	8033(6)	-1423(7)	127(8)
C(24)	-1137(8)	8061(6)	-2082(7)	113(7)
C(25)	-1856(9)	7596(6)	-2438(5)	82(5)
C(26)	-2366(6)	7103(5)	-2134(5)	63(4)
C(31)	-2237(8)	5111(4)	-4481(5)	59(4)
C(32)	-1629(7)	4742(7)	-4817(4)	78(5)
C(33)	-1441(6)	4004(7)	-4713(5)	91(6)
C(34)	-1860(8)	3635(4)	-4272(5)	75(5)
C(35)	-2468(7)	4004(5)	-3935(4)	57(4)
C(36)	-2656(6)	4742(5)	-4040(4)	57(4)
C(41)	-37(8)	5106(5)	-3337(5)	68(4)
C(42)	857(9)	5175(6)	-3546(5)	90(5)
C(43)	1433(7)	5806(8)	-3418(6)	99(6)
C(44)	1113(9)	6368(6)	-3079(6)	99(6)
C(45)	219(9)	6299(5)	-2870(5)	84(5)
C(46)	-356(6)	5668(7)	-2998(4)	56(3)
C(51)	-5128(11)	5304(7)	-2090(6)	123(7)
C(52)	-6175(10)	5233(8)	-2190(8)	175(12)
C(53)	-6667(6)	4661(10)	-2554(8)	155(11)
C(54)	-6111(11)	4159(8)	-2818(6)	134(9)
C(55)	-5065(11)	4230(7)	-2718(6)	108(6)
C(56)	-4573(6)	4802(8)	-2354(6)	76(5)
C(61)	18(12)	4891(9)	-1495(8)	84(5)
C(62)	442(12)	5597(12)	-1212(9)	115(7)
C(63)	1602(14)	5633(14)	-1080(13)	191(12)
C(64)	-1465(12)	4080(8)	-853(7)	81(5)
C(65)	-1402(13)	3290(9)	-1016(9)	107(6)
C(66)	-1063(17)	2828(11)	-413(11)	160(10)
C(211)	-2708(14)	6576(9)	-1120(8)	93(6)
C(212)	-2016(17)	6138(12)	-564(9)	143(8)
C(213)	-3538(14)	6960(11)	-869(10)	127(7)

C(251)	-2036(17)	7640(10)	-3169(10)	110(7)
C(252)	-2932(18)	8051(20)	-3492(12)	238(19)
C(253)	-1138(17)	7912(11)	-3394(12)	167(10)
C(311)	-2390(14)	5930(8)	-4616(9)	89(5)
C(312)	-3173(18)	6058(13)	-5234(14)	224(17)
C(313)	-1428(14)	6339(10)	-4634(9)	127(8)
C(351)	-2903(12)	3607(7)	-3444(8)	78(5)
C(352)	-2093(16)	3270(10)	-2933(9)	126(7)
C(353)	-3647(16)	3000(11)	-3766(11)	152(9)
C(93)	-5486(33)	8521(29)	-4598(24)	358(37)
C(92)	-5709(30)	9159(27)	-4901(29)	351(37)
C(91)	-4983(55)	9641(11)	-4939(28)	356(44)

Table 3. Bond lengths [A] and angles [deg] for 1.

Ta-N(2)	2.005(10)
Ta-N(1)	2.006(11)
Ta-C(2)	2.030(12)
Ta-C(1)	2.075(14)
Ta-C(6)	2.19(2)
Ta-N(16)	2.225(6)
C(1)-C(2)	1.30(2)
C(1)-C(46)	1.49(2)
N(1)-C(7)	1.46(2)
N(1)-C(26)	1.440(12)
C(2)-C(3)	1.45(2)
N(2)-C(36)	1.442(12)
N(2)-C(8)	1.49(2)
C(3)-C(4)	1.33(2)
C(3)-C(61)	1.53(2)
C(4)-C(5)	1.51(2)
C(4)-C(64)	1.55(2)
C(5)-C(6)	1.37(2)
C(6)-C(56)	1.49(2)
C(7)-C(11)	1.45(2)
C(8)-C(15)	1.46(2)
C(11)-C(12)	1.39
C(11)-N(16)	1.39
C(12)-C(13)	1.39
C(13)-C(14)	1.39
C(14)-C(15)	1.39
C(15)-N(16)	1.39
C(21)-C(22)	1.39
C(21)-C(26)	1.39
C(21)-C(211)	1.50(2)
C(22)-C(23)	1.39
C(23)-C(24)	1.39
C(24)-C(25)	1.39
C(25)-C(26)	1.39
C(25)-C(251)	1.55(2)
C(31)-C(32)	1.39
C(31)-C(36)	1.39
C(31)-C(311)	1.54(2)
C(32)-C(33)	1.39
C(33)-C(34)	1.39
C(34)-C(35)	1.39
C(35)-C(36)	1.39
C(35)-C(351)	1.51(2)
C(41)-C(42)	1.39
C(41)-C(46)	1.39
C(42)-C(43)	1.39
C(43)-C(44)	1.39
C(44)-C(45)	1.39
C(45)-C(46)	1.39
C(51)-C(52)	1.39
C(51)-C(56)	1.39
C(52)-C(53)	1.39
C(53)-C(54)	1.39
C(54)-C(55)	1.39
C(55)-C(56)	1.39
C(61)-C(62)	1.49(2)

C(62)-C(63)	1.53(2)
C(64)-C(65)	1.50(2)
C(65)-C(66)	1.54(2)
C(211)-C(213)	1.52(2)
C(211)-C(212)	1.57(2)
C(251)-C(252)	1.46(3)
C(251)-C(253)	1.49(2)
C(311)-C(313)	1.51(2)
C(311)-C(312)	1.52(2)
C(351)-C(352)	1.50(2)
C(351)-C(353)	1.56(2)
C(93)-C(92)	1.35(4)
C(92)-C(91)	1.34(4)
C(91)-C(91)#1	1.35(4)

N(2)-Ta-N(1)	137.9(4)
N(2)-Ta-C(2)	115.8(5)
N(1)-Ta-C(2)	103.1(5)
N(2)-Ta-C(1)	96.5(4)
N(1)-Ta-C(1)	105.9(5)
C(2)-Ta-C(1)	36.8(5)
N(2)-Ta-C(6)	100.2(5)
N(1)-Ta-C(6)	102.8(5)
C(2)-Ta-C(6)	78.7(5)
C(1)-Ta-C(6)	113.3(5)
N(2)-Ta-N(16)	72.6(4)
N(1)-Ta-N(16)	71.4(4)
C(2)-Ta-N(16)	169.0(4)
C(1)-Ta-N(16)	153.1(4)
C(6)-Ta-N(16)	93.0(4)
C(2)-C(1)-C(46)	134.1(12)
C(2)-C(1)-Ta	69.7(8)
C(46)-C(1)-Ta	156.1(9)
C(7)-N(1)-C(26)	111.0(10)
C(7)-N(1)-Ta	123.3(8)
C(26)-N(1)-Ta	125.6(7)
C(1)-C(2)-C(3)	140.0(13)
C(1)-C(2)-Ta	73.5(8)
C(3)-C(2)-Ta	145.3(10)
C(36)-N(2)-C(8)	108.3(9)
C(36)-N(2)-Ta	129.0(7)
C(8)-N(2)-Ta	122.7(8)
C(4)-C(3)-C(2)	116.4(12)
C(4)-C(3)-C(61)	124.3(14)
C(2)-C(3)-C(61)	119.2(13)
C(3)-C(4)-C(5)	122.1(13)
C(3)-C(4)-C(64)	124.7(14)
C(5)-C(4)-C(64)	113.3(13)
C(6)-C(5)-C(4)	129.9(13)
C(5)-C(6)-C(56)	113.6(13)
C(5)-C(6)-Ta	127.2(10)
C(56)-C(6)-Ta	118.9(10)
N(1)-C(7)-C(11)	111.9(12)
C(15)-C(8)-N(2)	110.3(10)
C(12)-C(11)-N(16)	120.0
C(12)-C(11)-C(7)	130.2(9)
N(16)-C(11)-C(7)	109.5(9)
C(13)-C(12)-C(11)	120.0
C(14)-C(13)-C(12)	120.0
C(15)-C(14)-C(13)	120.0

C(14)-C(15)-N(16)	120.0
C(14)-C(15)-C(8)	127.9(8)
N(16)-C(15)-C(8)	111.9(8)
C(15)-N(16)-C(11)	120.0
C(15)-N(16)-Ta	119.2(5)
C(11)-N(16)-Ta	120.7(5)
C(22)-C(21)-C(26)	120.0
C(22)-C(21)-C(211)	117.5(10)
C(26)-C(21)-C(211)	122.5(10)
C(21)-C(22)-C(23)	120.0
C(24)-C(23)-C(22)	120.0
C(23)-C(24)-C(25)	120.0
C(26)-C(25)-C(24)	120.0
C(26)-C(25)-C(251)	122.5(10)
C(24)-C(25)-C(251)	117.5(10)
C(25)-C(26)-C(21)	120.0
C(25)-C(26)-N(1)	119.0(9)
C(21)-C(26)-N(1)	121.0(9)
C(32)-C(31)-C(36)	120.0
C(32)-C(31)-C(311)	116.6(11)
C(36)-C(31)-C(311)	123.3(11)
C(31)-C(32)-C(33)	120.0
C(32)-C(33)-C(34)	120.0
C(35)-C(34)-C(33)	120.0
C(36)-C(35)-C(34)	120.0
C(36)-C(35)-C(351)	120.0(10)
C(34)-C(35)-C(351)	120.0(10)
C(35)-C(36)-C(31)	120.0
C(35)-C(36)-N(2)	122.0(9)
C(31)-C(36)-N(2)	118.0(9)
C(42)-C(41)-C(46)	120.0
C(43)-C(42)-C(41)	120.0
C(42)-C(43)-C(44)	120.0
C(45)-C(44)-C(43)	120.0
C(46)-C(45)-C(44)	120.0
C(45)-C(46)-C(41)	120.0
C(45)-C(46)-C(1)	120.0(10)
C(41)-C(46)-C(1)	120.0(10)
C(52)-C(51)-C(56)	120.0
C(51)-C(52)-C(53)	120.0
C(52)-C(53)-C(54)	120.0
C(55)-C(54)-C(53)	120.0
C(56)-C(55)-C(54)	120.0
C(55)-C(56)-C(51)	120.0
C(55)-C(56)-C(6)	121.5(11)
C(51)-C(56)-C(6)	118.5(11)
C(62)-C(61)-C(3)	111.9(14)
C(61)-C(62)-C(63)	113(2)
C(65)-C(64)-C(4)	111.5(14)
C(64)-C(65)-C(66)	111(2)
C(21)-C(211)-C(213)	113.0(14)
C(21)-C(211)-C(212)	115(2)
C(213)-C(211)-C(212)	109(2)
C(252)-C(251)-C(253)	109(2)
C(252)-C(251)-C(25)	116(2)
C(253)-C(251)-C(25)	113(2)
C(313)-C(311)-C(312)	109(2)
C(313)-C(311)-C(31)	114.3(14)
C(312)-C(311)-C(31)	110.8(14)
C(35)-C(351)-C(352)	112.3(14)

C(35)-C(351)-C(353)	110.3(14)
C(352)-C(351)-C(353)	109.0(14)
C(91)-C(92)-C(93)	121(5)
C(92)-C(91)-C(91)#1	132(10)

Symmetry transformations used to generate equivalent atoms:
#1 -x-1,-y+2,-z-1

Table 4. Anisotropic displacement parameters (A^2 x 10^3) for 1. The anisotropic displacement factor exponent takes the form: -2 pi^2 [h^2 a*^2 U11 + ... + 2 h k a* b* U12]

	U11	U22	U33	U23	U13	U12
Ta	44(1)	51(1)	53(1)	-4(1)	2(1)	0(1)
C(1)	74(10)	46(8)	40(8)	-1(7)	7(7)	-3(8)
N(1)	35(7)	57(7)	83(9)	-10(6)	2(6)	-5(6)
C(2)	49(8)	56(9)	31(8)	1(7)	-12(7)	10(7)
N(2)	39(7)	64(8)	41(6)	12(5)	-4(5)	10(6)
C(3)	32(8)	83(11)	61(10)	-4(8)	9(8)	0(8)
C(4)	64(11)	67(11)	73(11)	18(8)	3(9)	5(8)
C(5)	65(11)	67(11)	69(10)	5(8)	24(9)	-1(8)
C(6)	45(9)	80(11)	68(11)	-5(9)	19(8)	4(8)
C(7)	64(11)	81(12)	96(13)	-19(10)	-4(9)	0(10)
C(8)	52(10)	78(11)	74(11)	-11(9)	-8(8)	1(8)
C(11)	37(9)	63(10)	98(12)	-9(9)	8(9)	17(8)
C(12)	71(12)	73(11)	99(13)	-12(10)	5(10)	14(10)
C(13)	51(10)	90(13)	107(15)	8(11)	-2(10)	7(10)
C(14)	73(12)	63(11)	86(12)	-12(9)	6(10)	-3(9)
C(15)	43(9)	53(9)	88(11)	13(9)	-2(8)	5(8)
N(16)	47(7)	63(8)	53(7)	-6(6)	7(6)	-8(6)
C(21)	68(11)	60(11)	83(13)	-39(10)	5(10)	-2(9)
C(22)	85(14)	97(15)	93(14)	-32(12)	-18(11)	-2(11)
C(23)	76(14)	120(19)	178(25)	-62(18)	12(15)	-9(13)
C(24)	95(15)	90(14)	158(21)	-45(15)	40(14)	-28(12)
C(25)	72(12)	55(11)	120(16)	-41(11)	22(11)	-26(9)
C(26)	45(10)	59(10)	78(12)	-17(9)	4(9)	17(8)
C(31)	55(9)	85(12)	39(9)	-16(8)	12(7)	7(8)
C(32)	73(12)	106(14)	52(10)	19(10)	7(9)	-15(11)
C(33)	69(12)	134(18)	59(12)	-19(11)	-6(9)	-2(12)
C(34)	77(12)	54(10)	79(12)	-15(9)	-16(9)	27(9)
C(35)	59(10)	36(9)	71(10)	-12(8)	8(8)	1(7)
C(36)	54(9)	66(11)	43(9)	-7(8)	-7(8)	2(8)
C(41)	54(10)	96(13)	49(9)	-2(9)	2(8)	-1(9)
C(42)	64(12)	123(17)	84(13)	4(11)	20(10)	1(11)
C(43)	70(12)	125(17)	108(15)	24(13)	32(11)	3(13)
C(44)	82(14)	91(15)	122(16)	-5(12)	21(12)	-27(11)
C(45)	62(11)	89(14)	103(14)	14(10)	20(10)	2(10)
C(46)	49(9)	66(10)	47(8)	15(8)	1(7)	0(9)
C(51)	44(11)	161(20)	171(21)	-15(16)	39(12)	-18(12)
C(52)	85(19)	164(25)	292(37)	17(24)	81(21)	4(16)
C(53)	54(14)	184(27)	218(30)	84(23)	14(16)	13(16)
C(54)	75(16)	189(25)	118(17)	35(16)	-18(13)	-40(16)
C(55)	66(13)	155(19)	98(14)	-12(13)	5(10)	-37(13)
C(56)	50(11)	111(14)	70(11)	28(10)	20(9)	5(10)
C(61)	78(13)	91(13)	80(12)	2(10)	12(10)	4(10)
C(62)	69(12)	165(21)	102(15)	-17(15)	0(10)	-2(14)
C(63)	71(15)	263(33)	215(28)	19(24)	-20(16)	-41(18)
C(64)	91(12)	68(12)	83(12)	11(9)	15(10)	-3(9)
C(65)	82(13)	79(14)	152(19)	38(13)	11(12)	-4(10)
C(66)	189(23)	112(18)	162(22)	74(16)	0(18)	11(16)
C(211)	110(15)	84(13)	78(13)	-44(11)	7(11)	13(11)
C(212)	184(22)	169(21)	71(13)	8(14)	19(14)	55(18)
C(213)	125(17)	116(16)	141(19)	-23(14)	33(14)	16(14)

C(251)	132(18)	94(14)	125(18)	-29(13)	73(16)	-42(13)
C(252)	123(21)	457(56)	128(22)	37(29)	16(17)	111(30)
C(253)	184(23)	109(17)	243(29)	65(19)	124(22)	24(17)
C(311)	113(15)	57(11)	105(14)	7(9)	38(12)	-19(10)
C(312)	156(23)	152(22)	287(37)	118(24)	-111(24)	-59(18)
C(313)	144(18)	114(16)	102(15)	44(12)	-17(13)	-55(14)
C(351)	101(13)	28(9)	97(13)	-8(8)	4(11)	-5(9)
C(352)	153(19)	109(16)	123(18)	32(13)	43(15)	19(14)
C(353)	165(21)	125(18)	177(23)	-23(17)	63(18)	-46(17)
C(93)	317(67)	527(90)	250(52)	103(55)	107(45)	255(62)
C(92)	149(37)	501(108)	376(81)	13(80)	3(44)	106(55)
C(91)	300(57)	300(82)	505(80)	-247(90)	166(58)	-78(73)

15 Design of polymerization reactor

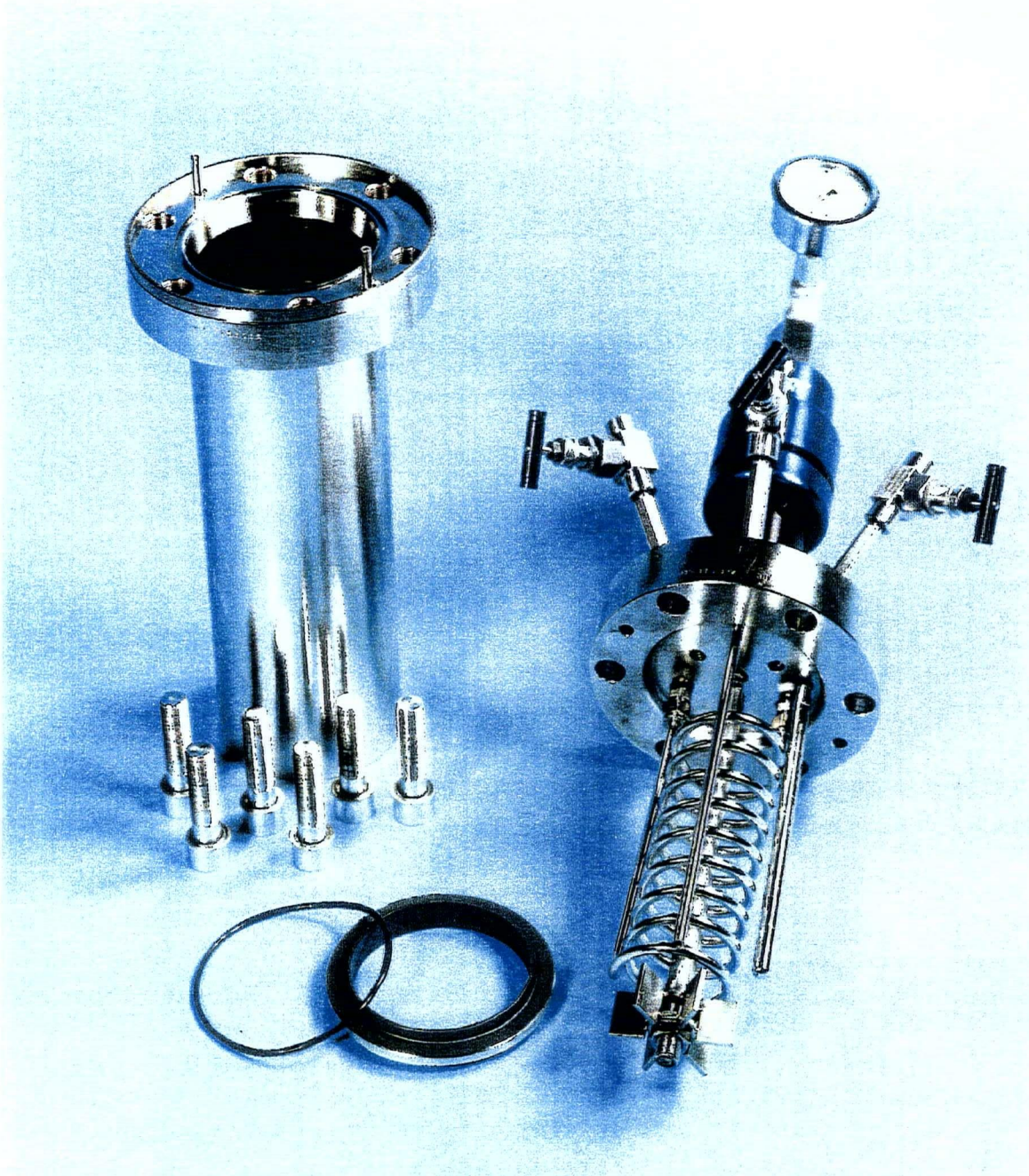

1000 mL LC SERIES STIRRED REACTOR
WITH INTERNAL COMPONENTS DISPLAYED
RATED FOR 138 BAR AT 350 C IN STAINLESS STEEL

500 mL LC SERIES STIRRED REACTOR
IN BENCH TOP FURNACE STAND
RATED FOR 138 BAR AT 350 C IN STAINLESS STEEL
SIDE VIEW

CP-F-14 CONTROL PACKAGE
PID TEMPERATURE CONTROL WITH
DIGITAL TACHOMETER, DIGITAL PRESSURE INDICATION,
AND HIGH SKIN TEMPERATURE SHUTDOWN